SANDIA REPORT

SAND92—0094 • UC—713
Unlimited Release
Printed November 1993

SNL RML Recommended Dosimetry Cross Section Compendium

Patrick J. Griffin, John (Jake) G. Kelly, Theodore F. Luera, Jason VanDenburg

Prepared by
Sandia National Laboratories
Albuquerque, New Mexico 87185 and Livermore, California 94550
for the United States Department of Energy
under Contract DE-AC04-94AL85000

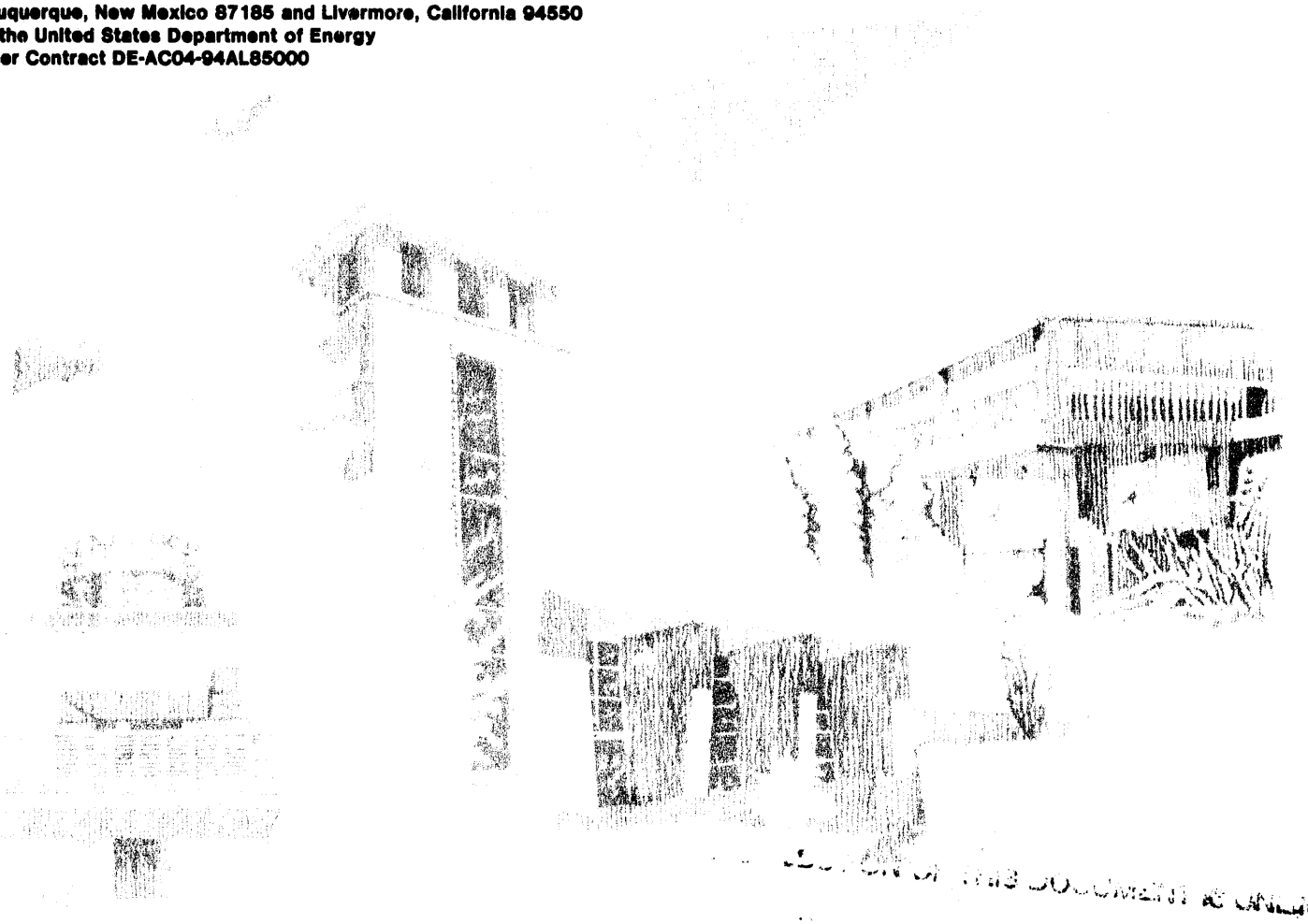

Issued by Sandia National Laboratories, operated for the United States Department of Energy by Sandia Corporation.

Available to DOE and DOE contractors from
Office of Scientific and Technical Information
PO Box 62
Oak Ridge, TN 37831

Prices available from (615) 576-8401, FTS 626-8401

Available to the public from
National Technical Information Service
US Department of Commerce
5285 Port Royal Rd
Springfield, VA 22161

NTIS price codes
Printed copy: A17
Microfiche copy: A01

SAND92-0094
Unlimited Release
November 1993

Distribution
Category UC-713

SNL RML Recommended Dosimetry Cross Section Compendium

Patrick J. Griffin, John (Jake) G. Kelly
Nuclear Systems Research Department
Sandia National Laboratories
Albuquerque, NM 87185

Theodore F. Luera
Reactor Engineering Technology Center
Sandia National Laboratories
Albuquerque, NM 87185

Jason VanDenburg
Science and Engineering Associates, Inc.
Albuquerque, NM 87190

Abstract

A compendium of dosimetry cross sections is presented for use in the characterization of fission reactor spectrum and fluence. The contents of this cross section library are based upon the ENDF/B-VI and IRDF-90 cross section libraries and are recommended as a replacement for the DOSCROS84 multigroup library that is widely used by the dosimetry community. Documentation is provided on the rationale for the choice of the cross sections selected for inclusion in this library and on the uncertainty and variation in cross sections presented by state-of-the-art evaluations.

Acknowledgment

The authors thank David W. Vehar, supervisor of the Radiation Metrology Laboratory, for consultation and advice in making the format and content of this cross section compendium support both the dosimetrist and the reactor experimenter. We also thank Charles V. Holm for providing the highest quality foil activities and experimental support for fielding dosimetry sensors. High quality dosimetry sensor readings were critical in allowing the authors to judge the consistency and accuracy of the cross sections provided in this compendium.

Contents

Contents (Continued)

Contents (Continued)

Figures

Tables

Summary

The SNLRML cross section compendium has been prepared by taking the latest and most consistent dosimetry-oriented cross sections from all available evaluations. The contents of the library include all dosimetry sensors (activation reactions, threshold reactions, fission reactions, and special damage sensors) that are in general use by the dosimetry community for the characterization of fission neutron spectra. The cross section compendium has been interfaced with spectrum determination codes and found to produce consistent spectrum "unfolds" with more sensors than were possible with previous libraries. The SNLRML library is being made available to the general dosimetry community in order to encourage the use of a consistent cross section library for spectrum determination. The authors plan on updating the library as part of the RML quality assurance program. This document provides part of the QA audit trail for the selection and choice of sensor response functions that are used in the spectrum determination of the SNL reactor facilities.

Nomenclature

Spectrum Descriptors

$\Delta\sigma/\sigma$ cross section standard deviation, typically expressed as a percentage.

$\phi(E)$ differential number distribution of the fluence. Typical units are $n/(cm^2 \cdot MeV)$.

Φ neutron fluence. Typical units are n/cm^2.

$\sigma(E)$ microscopic neutron cross section. Typical units are b.

$\langle\sigma\rangle_x$ spectrum averaged cross section, where the neutron spectrum denoted by "x" is used as a weighting function.

Nuclear Particle and State Identification

α an alpha particle, ${}_2He^4$.

β a beta particle or electron.

β^+ a positron, a particle with the same mass as an electron and a positive electrical charge.

d a deuteron, ${}_1H^2$.

γ a photon.

t a triton, ${}_1H^3$.

λ decay constant, $\lambda = \ln(2)/\tau_{1/2}$.

$\tau_{1/2}$ isotope half-life, he time lapse during which a radioactive species decays to one half its initial number of atoms.

^{aam}X a metastable state of ^{aa}X.

^{aa}X the element "X" with atomic mass "aa".

${}_{zz}X^{aa}$ the element "X" with atomic mass, or M, "aa" and atomic number, or Z, "zz".

Reaction Designators

(n,abs) an absorption process where an a neutron is incident on a target nucleus, but no neutron is present in the exit channel.

(n,f) a fission reaction.

(n,n') an inelastic scattering process where a neutron is incident on a target nucleus and scatters leaving the target nucleus in an excited nuclear state. The target nucleus typically returns to the ground state accompanied with the emission of photon(s).

(n,X) a neutron induced reaction where a neutron is incident on a target nucleus and any number of particles can appear in the exit channel (denoted by the X). If a residual nucleus is specified, some constraints are implied on X.

Miscellaneous Abbreviations

amu	atomic mass unit, equals 931501.6 keV.
dpa	displacement per atom in a crystal lattice produced by interactions of a primary particle with the lattice material.
F.P.	Fission Product
RC	cumulative fission yield, expressed as a percent. In the ENDF-6 format this quantity has an MT = 459.
RI	independent fission yield, expressed as a percent. In the ENDF-6 format this quantity has an MT = 454.
RML	Radiation Metrology Laboratory
SNL	Sandia National Laboratories
SNLRML	Sandia National Laboratories' Radiation Metrology Library
SNL RML	Sandia National Laboratories' Radiation Metrology Laboratory

This page intentionally left blank.

SNL RML Recommended Dosimetry Cross Section Compendium

1. Introduction

Several new cross section libraries have been made available to the dosimetry community. These include the ENDF/B-VI [1,2], the International Reactor Dosimetry File (IRDF-90) [3], the Japanese Evaluated Nuclear Data Library (JENDL-3) [4], the USSR Evaluated Neutron Data Library (BROND) [5], the Joint Evaluated File (JEF-2.2) [6], an updated ORNL GLUCS [7] evaluation, and the International Library of Neutron Activation Cross Section Data for Fusion Reactor applications (FENDL-2) [8]. Through their use as activation sensors for determining neutron spectra and fluence, these new dosimetry cross sections affect the characterization of neutron radiation damage facilities, the use of monitor foils to relate a given device irradiation to the specified environment, the comparison of device damage between reactor facilities, and the comparison of radiation-hardening test environments with anticipated operating environments.

The Sandia National Laboratories (SNL) Radiation Metrology Laboratory (RML) has worked with versions of these cross sections since pre-release data were available. These new cross sections have been compared with each other and evaluated with respect to their accuracy and consistency for spectrum unfolding applications. A compendium of dosimetry cross sections was assembled for use within the SNL Radiation Metrology Laboratory. This library, referred to as the SNLRML library [9], was empirically tested for use in fission spectra determination and in the fluence and energy characterization of 14-MeV neutron sources [10]. The library has been prepared in a format that can be readily interfaced with both iterative spectrum unfolding codes, such as SAND-II [11], and least-square codes, such as LSL-M2 [12].

2. Scope of Compendium

The SNLRML library contains a set of 66 dosimetry sensors (and 3 special dosimeters unique to the RML sensor inventory) drawn from the most recent cross section evaluations. Table 1 summarizes the cross section libraries examined in the preparation of this compendium. The FENDL-2 and CENDL libraries have not been completely analyzed at this time, but will be reflected in future updates to the SNLRML library. Covariance matrices are included to support the requirements of least-squares unfolding codes. In cases where covariance data were not available for the selected cross section evaluation, an alternate source for the covariance data has sometimes been used temporarily to estimate the data covariance matrix. Table 2 shows the contents of the library and indicates the source of the cross sections and covariance data. The SNLRML library has been tested by

Table 1. Sources of Evaluated Cross Sections

Library	Comment	Year
ENDF/B-VI	319 evaluations, replaced ENDF/B-V general purpose and dosimetry tape.	June 1990, mod 0 Sept. 1991, mod 1 mod 2 tbd ~ July 1993
IRDF-90	Replaced IRDF-82, 44 partial evaluations for reactor dosimetry.	1990 1993 mod tbd
GLUCS	ORNL dosimetry set, 14 reactions with cross isotope correlations, source for new ENDF/B-VI, update covariance in 1993.	1990 1993
JENDL-3	171 element Japanese Evaluated Library.	1990
JENDL-DOS	42 element JENDL Dosimetry Library.	1992
JEF-2.2	344 element Joint Evaluated File by NEA.	Jan. 1993
BROND	76 USSR evaluated cross sections.	1987/1990 mod tbd
CENDL	50 element Chinese Evaluated Nuclear Data Library [57, 58].	1992
ENDF/B-V	Evaluated Nuclear Data File by CSEWG.	1979-81
IRDF-82	40 element International Reactor Dosimetry File.	1982
ENDL	LLNL Evaluated Cross Sections [13].	1978-84
DOSCROS84	74 element multi-group compendium of ENDF/B-V and IRDF-82 [14].	1984
Private Evaluations	Includes pre-ENDF evaluations [15], partial dosimetry-oriented evaluations [16, 17].	----
FENDL-2	International Library of Neutron Activation Cross Section Data for Fusion Reactor Applications.	1992

Table 2. Contents of SNLRML Library

	Dosimetry Reactions	Source Library	Cov.+	SNL Experimental Verification		Comment
				Fission	14-MeV	
1.	$^{10}B(n,abs)$	ENDF/B-VI	--- ●	---	---	Very useful as a cover material to push neutron sensor response above thermal region. Uses covariance from (n,α) reaction.
2.	$^{10}B(n,X)^{4}He$	ENDF/B-VI	--- ●	---	---	Used in LWR PV surveillance material damage studies. Uses covariance from (n,α) component.
3.	$^{11}B(n,abs)$	ENDF/B-VI	---	---	---	Often mixed with ^{10}B in cover material.
4.	$^{Nat}B(n,abs)$	ENDF/B-VI	--- ●	---	---	Typical boron cover material is ^{nat}B (19.9% ^{10}B, 80.1% ^{11}B). Uses covariance from $^{10}B(n,\alpha)$ reaction.
5.	$^{enrich}B_4C(n,abs)$	ENDF/B-VI	---- ●	✓		Standard SNL B_4C boron ball. Uses covariance from $^{10}B(n,\alpha)$ reaction.
6.	$^{6}Li(n,X)^{4}He$	ENDF/B-VI	---- ●			Used in LWR PV surveillance. Uses covariance from $^{6}Li(n,t)^{4}He$ reaction.
7.	$^{19}F(n,2n)^{18}F$	IRDF-90	●	---	---	Disagrees with recent ENDF/B-VI evaluation. Analysis of recommended source is pending.
8.	$^{23}Na(n,\gamma)^{24}Na$	ENDF/B-VI	●	✓	---	No recent dosimetry evaluation available. The JENDL-3 cross section is under consideration for selection.
9.	$^{24}Mg(n,p)^{24}Na$	IRDF-90	●	✓	✓	ENDF/B-VI is format translation of ENDF/B-V.
10.	$^{27}Al(n,p)^{27}Mg$	GLUCS/IRDF-90	●	---	✓	ENDF/B-VI is format translation of ENDF/B-V. Uses updated GLUCS covariance.
11.	$^{27}Al(n,\alpha)^{24}Na$	IRDF-90	●	✓	✓	ENDF/B-VI is format translation of ENDF/B-V.
12.	$^{Nat}Si(n,X)1MEV$	private, ORNL	---	✓	✓	Expected to be in ENDF/B-VI release 4, ASTM E-722-93 standard.
13.	$^{31}P(n,p)^{31}Si$	IRDF-90	●	---	---	No recent dosimetry evaluation.
14.	$^{32}S(n,p)^{32}P$	GLUCS/IRDF-90	●	✓	---	Incorporates latest ORNL analysis, large std. dev. Uses updated 1993 GLUCS covariance.

+Legend: ● = Cov. obtained from same library as cross section ✓ = Verified; ? = Caution; --- = No Data

Table 2. Contents of SNLRML Library (Continued)

	Dosimetry Reactions	Source Library	Cov.+	SNL Experimental Verification		Comment
				Fission	14-MeV	
15.	$^{45}Sc(n,\gamma)^{46}Sc$	ENDF/B-VI	●	✓	---	No recent dosimetry evaluation.
16.	$^{46}Ti(n,p)^{46}Sc$	GLUCS/IRDF-90	●	✓	---	ENDF/B-VI is a format translation of ENDF/B-V. Uses updated 1993 GLUCS covariance matrix.
17.	$^{47}Ti(n,p)^{47}Sc$	IRDF-90	GLUCS	✓	---	ENDF/B-VI is a format translation of ENDF/B-V. Incorporates latest Mannhart analysis. Uses 1993 GLUCS updated covariance matrix.
18.	$^{47}Ti(n,np)^{46}Sc$	ENDF/B-VI	●	---	---	No recent dosimetry evaluation.
19.	$^{Nat}Ti(n,X)^{46}Sc$	private	---	✓	✓	IRDF-90 (n,p) and re-normalized ENDF/B-VI (n,np) component.
20.	$^{48}Ti(n,p)^{48}Sc$	GLUCS/IRDF-90	GLUCS	✓	✓	ENDF/B-VI is a format translation of ENDF/B-V. IRDF-90 covariance processing error. Uses updated 1993 GLUCS covariance.
21.	$^{48}Ti(n,np)^{47}Sc$	ENDF/B-VI	●	---	---	No recent dosimetry evaluation.
22.	$^{Nat}Ti(n,X)^{47}Sc$	private	---	✓	---	IRDF-90 (n,p) and re-normalized ENDF/B-VI (n,np).
23.	$^{55}Mn(n,\gamma)^{56}Mn$	ENDF/B-V	E6	✓	---	Specifically reject ENDF/B-VI resonance height for iterative unfolds.
24.	$^{55}Mn(n,2n)^{54}Mn$	ENDF/B-VI	●	---	---	
25.	$^{54}Fe(n,p)^{54}Mn$	ENDF/B-VI	GLUCS	✓	✓	Same as GLUCS but with some smoothing of unphysical features. Covariance updated with 1993 GLUCS, ENDF will follow.
26.	$^{56}Fe(n,p)^{56}Mn$	ENDF/B-VI	GLUCS	✓	---	Same as GLUCS. Covariance replaced by 1993 GLUCS, ENDF will follow.
27.	$^{58}Fe(n,\gamma)^{59}Fe$	ENDF/B-VI	●	?	---	Does not fit SNL fast fission data, OK for pool-type reactors. The JENDL-3 cross section is under consideration for selection.
28.	$^{Nat}Fe(n,X)dpa$	ASTM E 693	---	---	---	Used as a common exposure function. ASTM standard E693-79.
29.	$^{59}Co(n,p)^{59}Fe$	ENDF/B-VI	●	---	---	Significant differences with E5a above 10 MeV.

+Legend: ● = Cov. obtained from same library as cross section ✓ = Verified; ? = Caution; --- = No Data

Table 2. Contents of SNLRML Library (Continued)

	Dosimetry Reactions	Source Library	Cov.+	SNL Experimental Verification		Comment
				Fission	14-MeV	
30.	$^{59}Co(n,\gamma)^{60}Co$	ENDF/B-VI	E5	✓	---	
31.	$^{59}Co(n,\alpha)^{56}Mn$	ENDF/B-VI	●	---	---	
32.	$^{59}Co(n,2n)^{58}Co$	IRDF-90	●	---	---	
33.	$^{58}Ni(n,p)^{58}Co$	ENDF/B-VI	GLUCS	✓	✓	Same as GLUCS with some smoothing. Covariance updated with 1993 GLUCS, ENDF will follow.
34.	$^{58}Ni(n,2n)^{57}Ni$	ENDF/B-VI	●	---	✓	
35.	$^{60}Ni(n,p)^{60}Co$	ENDF/B-VI	●	---	---	Significant change from ENDF/B-V dosimetry tape.
36.	$^{63}Cu(n,\gamma)^{64}Cu$	ENDF/B-VI	●	---	---	
37.	$^{63}Cu(n,2n)^{62}Cu$	IRDF-90	●	---	---	Investigation of GLUCS and IRDF-90 differences is pending.
38.	$^{63}Cu(n,\alpha)^{60}Co$	ENDF/B-VI	GLUCS	---	---	Significant change from ENDF/B-V dosimetry tape. Covariance updated with 1993 GLUCS, ENDF will follow. Does not fit SNL fast fission unfolds.
39.	$^{65}Cu(n,2n)^{64}Cu$	ENDF/B-VI	GLUCS	---	✓	Same as GLUCS with some smoothing. Covariance updated with 1993 GLUCS, ENDF will follow.
40.	$^{64}Zn(n,p)^{64}Cu$	IRDF-90	●	✓	✓	
41.	$^{90}Zr(n,2n)^{89}Zr$	IRDF-90	●	✓	✓	ENDF/B-VI is format translation of ENDF/B-V.
42.	GaAs(n,X)1MeV	Private	----	---	---	PKA-dependent damage efficiency required to match device damage data. Used in ASTM standard E-722-93.
43.	$^{93}Nb(n,\gamma)^{94}Nb$	ENDF/B-VI	●	---	---	
44.	$^{93}Nb(n,2n)^{92m}Nb$	IRDF-90	●	---	✓	Cross section to metastable state not in ENDF/B-VI.
45.	$^{93}Nb(n,n')^{93m}Nb$	IRDF-90	●	---	---	Cross section to metastable state not in released ENDF/B-VI, but private communication indicates that it will be added. Analysis of effect of private communication instead of IRDF-90 is pending.

+Legend: ● = Cov. obtained from same library as cross section ✓ = Verified; ? = Caution; --- = No Data

Table 2. Contents of SNLRML Library (Continued)

	Dosimetry Reactions	Source Library	Cov.+	SNL Experimental Verification		Comment
				Fission	14-MeV	
46.	$^{98}Mo(n,\gamma)^{99}Mo$	JENDL-3	----	✓	---	No recent dosimetry-oriented evaluation.
47.	$^{103}Rh(n,n')^{103m}Rh$	IRDF-90	●	---	---	Cross section to metastable state not in ENDF/B-VI.
48.	$^{109}Ag(n,\gamma)^{110m}Ag$	DOSCROS84	----	---	---	DOSCROS84 is the only library that includes a ratio to metastable state.
49.	$^{Nat}Cd(n,abs)$	JENDL-3	----	✓	---	No new ENDF/B-VI evaluation.
50.	$^{115}In(n,\gamma)^{116m}In$	ENDF/B-VI	●	?	---	New evaluation, identical to ENDF/B-V dosimetry tape. Thermal response conflicts with $^{197}Au(n,\gamma)^{198}Au$.
51.	$^{115}In(n,n')^{115m}In$	IRDF-90	●	?	---	Slight difference between IRDF-90 and ENDF/B-VI, cause is inadvertent absence of latest update to metastable cross section in ENDF/B-VI library. Often this sensor conflicts with fission foils.
52.	$^{127}I(n,2n)^{126}I$	ENDF/B-VI	E5	---	---	
53.	$^{197}Au(n,p)^{197}Pt$	ENDF/B-VI	----	---	---	
54.	$^{197}Au(n,\gamma)^{198}Au$	ENDF/B-VI	IRDF-90	✓	---	ENDF/B-VI deleted covariance matrix pending additional review.
55.	$^{197}Au(n,2n)^{196}Au$	IRDF-90	●	---	---	
56.	$^{197}Au(n,3n)^{195}Au$	ENDF/B-VI	----	---	---	Significant change from ENDF/B-V dosimetry tape.
57.	$^{Nat}Au(n,abs)$	ENDF/B-VI	---- ●	✓	---	Covariance for $^{197}Au(n,\gamma)$ reaction used.
58.	$^{232}Th(n,\gamma)^{233}Th$	ENDF/B-VI	●	---	---	No recent dosimetry-oriented evaluation.
59.	$^{232}Th(n,2n)^{231}Th$	ENDF/B-VI	----	---	---	No recent dosimetry-oriented evaluation.
60.	$^{232}Th(n,f)F.P.$	ENDF/B-VI	●	---	---	No recent dosimetry-oriented evaluation.
61.	$^{235}U(n,f)F.P.$	ENDF/B-VI	IRDF90	✓	---	Covariance deleted from ENDF/B-VI pending additional review.
62.	$^{238}U(n,f)F.P.$	ENDF/B-VI	IRDF90	✓	---	Covariance deleted from ENDF/B-VI pending additional review.
63.	$^{237}Np(n,f)F.P.$	ENDF/B-VI	E5d	✓	---	

+Legend: ● = Cov. obtained from same library as cross section ✓ = Verified; ? = Caution; --- = No Data

Table 2. Contents of SNLRML Library (Continued)

	Dosimetry Reactions	Source Library	Cov.+	SNL Experimental Verification		Comment
				Fission	14-MeV	
64.	^{239}Pu(n,f)F.P.	ENDF/B-VI	JENDL-3d	✓	---	Error in processing ENDF/B-VI covariance due to ratio technique, JENDL-3d used instead.
65.	^{241}Am(n,f)F.P.	ENDF/B-VI	●	---	---	Significant difference with IRDF-82. Processing error in covariance due to ratio technique, JENDL-3d (which was taken from ENDF/B-V and is identical to ENDF/B-VI) used instead.
66.	RML Enriched Uranium Fission Foil	ENDF/B-VI	IRDF90	✓	---	Includes ^{234}U, ^{236}U, ^{238}U contaminants, normalized to one atom of elemental uranium.
67.	RML Depleted Uranium Fission Foil	ENDF/B-VI	IRDF90	✓	---	Includes ^{234}U, ^{235}U, ^{236}U contaminants, normalized to one atom of elemental uranium. ^{235}U is a major thermal fission contaminant.
68.	RML Plutonium Fission Foil	ENDF/B-VI	JENDL-3d	✓	---	Includes ^{238}Pu, ^{240}Pu, ^{241}Pu, ^{242}Pu, ^{235}U, ^{237}Np contaminants, normalized to one atom of elemental plutonium. ^{240}Pu causes a shape change in dosimeter cross section.
69.	^{32}S-3MeV	GLUCS/IRDF-90	●	✓	---	Sensor for flux transfer calibration of ^{32}S(n,p)^{32}P activities. This sensor can only be used when sulfur is calibrated with the ^{252}Cf fluence greater than 3 MeV.

+Legend: ● = Cov. obtained from same library as cross section ✓ = Verified; ? = Caution; --- = No Data

unfolding over twenty-five reactor neutron spectra and comparing the resulting spectra with previous determinations. This comparison has been presented to the dosimetry community and peer-reviewed [9, 10].

There are significant differences between the ENDF/B-V and new ENDF/B-VI dosimetry cross sections for some reactions. Many dosimetry reactions were found to differ in the region above 7 MeV. The $^{63}Cu(n,\alpha)^{60}Co$ reaction, shown in Figure A-38a, is one example. In this case, despite the significant change in the shape of the cross section, folding the cross section in with a fission reactor spectrum results in very little (2-5%) difference in the resulting activity. For most dosimetry reactions, the ENDF/B-V and ENDF/B-VI cross sections were in very good agreement below 7 MeV. The $^{58}Fe(n,\gamma)^{59}$ Fe reaction, shown in Figure A-27a, was an exception. When this cross section is folded with typical fission reactor spectra, the resulting calculated activities from ENDF/B-V and ENDF/B-VI cross sections differ by 30-60%.

3. CROSS SECTIONS

3.1 Comparison of Cross Section Evaluations

Appendix A summarizes the cross section libraries that provided evaluations for each of the sensors included in the SNLRML library. Comparison plots for all reaction cross sections from the various dosimetry libraries are also provided in Appendix A. The cross section selected for inclusion in the SNLRML is highlighted in the Appendix tables. Section 5 provides some comments of the selection criteria used for each dosimetry sensor. Covariance plots for the reaction evaluations in the SNLRML library are provided in Appendix B.

The SNLRML library includes all dosimetry-quality sensors that the RML expects to use for routine dosimetry applications. The library also includes some damage measures, such as the GaAs 1-MeV-equivalent damage and the ^{Nat}Fe displacement per atom (dpa) cross section, that are not recommended for use as dosimetry sensors but are widely used as exposure parameters.

The selection of dosimetry-related cross sections for inclusion in the SNLRML library, in cases where the authors did not have extensive experience with the specific reaction and its consistency with other dosimetry sensors, has been biased in favor of the IRDF-90 library over the JENDL-3 Dosimetry Library. This approach was due to several considerations. First, the authors of the JENDL-3 Dosimetry Library did not perform a detailed analysis of the covariance matrix for the specific reaction; rather they adopted the IRDF-85 covariance matrix. This decision may not correctly reflect the covariance in cases where new experimental data have resulted in significant changes in the evaluation. Second, the IRDF-90 library evaluations were often based on the application of a statistical methodology with careful selection/renormalization of experimental data [17, 18], while the JENDL-3 Dosimetry Library was often based on fitting of theoretical model calculations to the experimental data [19].

3.2 Sensor Sensitive Region

The RML supports neutron dosimetry for a wide range of environments. The range in neutron spectra are fairly well bracketed by considering the Sandia Pulsed Reactor (SPR-III) central cavity and the Annular Core Research Reactor (ACRR) central cavity. Figure 1 compares the differential number spectra for these two well characterized benchmark fields. The SPR-III reactor is an unmoderated fast-burst reactor with a cylindrical fuel assembly of uranium enriched to 93% ^{235}U. The central cavity spectrum represents a very hard fission neutron spectrum (E_{avg} = 1.25 MeV), moderated only by the reactor fuel. The ACRR is a pool-type reactor with BeO:UO_2 fuel enriched to 35% ^{235}U and with 21.5% UO_2. The central cavity spectrum represents a soft water-moderated neutron spectrum (E_{avg} = 0.66 MeV).

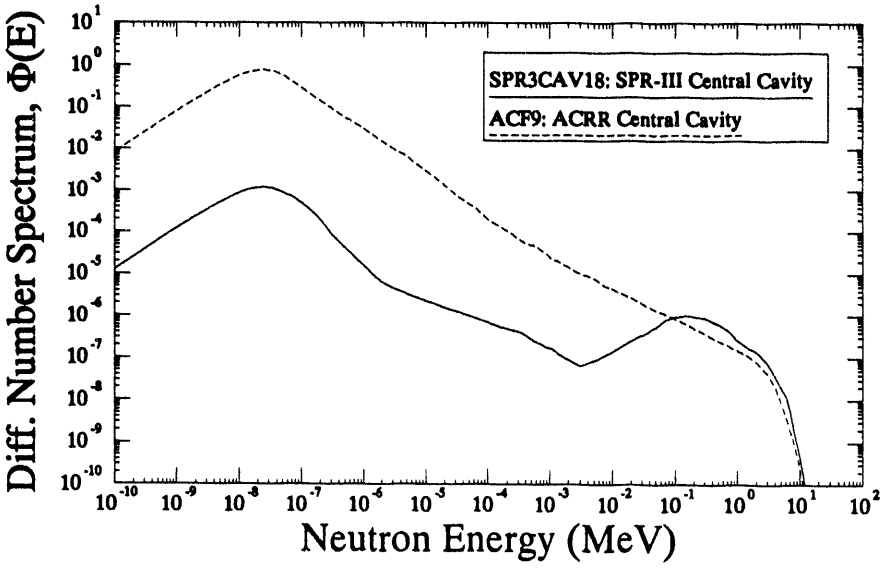

Figure 1. Representative Neutron Spectra Available at SNL Radiation Facilities

A good neutron spectrum determination requires the use of dosimetry sensors that span the complete energy range of the source. The usefulness of specific dosimetry sensors for spectrum determination and the energy region over which they are sensitive is, however, very dependent upon the spectrum in which they are irradiated and on the presence of cover materials that are typically used to reduce the sensor sensitivity to thermal neutrons. This coupling between a good sensor set (which has full energy coverage) and the spectrum itself that is to be determined can greatly complicate the job of spectrum unfolding. A good spectrum characterization at SNL may utilize 30 different sensors to ensure good energy coverage and sensor consistency.

In choosing the sensors to use in a spectrum characterization, the sensor energy sensitivity, reaction half-life, and reaction cross section must be considered. Appendix C provides the

recommended reaction half-lives for all sensors in the SNLRML library. Appendix D provides guidelines to the energy sensitivity of the sensors. Table D-1 provides spectrum-averaged cross sections and 95% response regions for bare and B_4C-covered foils in the SPR-III central cavity spectrum (spectrum SPRCAV18). Table D-2 provides the same data for the ACRR central cavity (spectrum ACF9). These tables show that the sensitive region in soft spectra can be very dependent upon the presence of sensor covers. The energy-range sensitivity shown in these tables should bracket that found from most fission spectra used in the testing/characterization of radiation-hardened electronic parts. Similar data are available for thermal neutron spectra (such as that typically used in neutron radiography) and for 14-MeV D-T sources.

3.3 Evaluation-Dependence of Calculated Activities

The first question that a user of the SNLRML library may ask is "How will use of this new cross section library change my dosimetry?" The second question is, "How sure are you of these new data?" The answers to these questions will require a detailed discussion of the particular application and the dosimetry sensors involved. The covariance data in Appendix B should provide information on the reliability of the new data. Table 3 shows the effects of the new cross sections on the spectrum-averaged activity for the two representative spectra, the SPR-III central cavity and the ACRR central cavity. Table 3 does not include all of the reactions in the SNLRML library since some of the sensors are closely related to another sensor, some of the cross sections did not have a recent evaluation and did not change, and some of the library sensors are not commonly used by the community.

Table 4 provides a comparison of the spectrum-averaged cross section for many of the sensors included in the SNLRML library with other recent dosimetry-quality evaluations (usually the JENDL-3 Dosimetry Library) available within the dosimetry community.

Table 3. Effect of New Cross Sections on Reaction Activities

Dosimetry Reactions		Cross Section Library		Ratio of Spectrum-Averaged Cross Section (General/SNLRML)	
		General Usage	SNLRML Recommended	FBR (SPR3CAV18)	Pool-Type (ACF9)
1.	$^{19}F(n,2n)^{18}F$	ENDF/B-Va	IRDF-90	1.1533	1.1553
2.	$^{23}Na(n,\gamma)^{24}Na$	ENDF/B-Vd	ENDF/B-VI	1.0003	0.9997
3.	$^{24}Mg(n,p)^{24}Na$	ENDF/B-Va	IRDF-90	0.9728	0.9723
4.	$^{27}Al(n,p)^{27}Mg$	ENDF/B-Vd	GLUCS	1.0695	1.0674
All cross sections are for bare foils					

Table 3. Effect of New Cross Sections on Reaction Activities (Continued)

Dosimetry Reactions		Cross Section Library		Ratio of Spectrum-Averaged Cross Section (General/SNLRML)	
		General Usage	SNLRML Recommended	FBR (SPR3CAV18)	Pool-Type (ACF9)
5.	$^{27}Al(n,\alpha)^{24}Na$	ENDF/B-Vd	IRDF-90	0.9967	0.9982
6.	$^{Nat}Si(n,X)1MEV$	ASTM E722-85	Private ASTM E722-93	1.0973	1.0829
7.	$^{31}P(n,p)^{31}Si$	ENDF/B-Va	IRDF-90	1.184	1.1926
8.	$^{32}S(n,p)^{32}P$	ENDF/B-Vd	GLUCS	1.0836	1.08296
9.	$^{45}Sc(n,\gamma)^{46}Sc$	ENDF/B-Vd	ENDF/B-VI	1.0 (exact)	1.0 (exact)
10.	$^{Nat}Ti(n,X)^{46}Sc$	ENDF/B-Vd	Private	1.0718	1.0731
11.	$^{48}Ti(n,p)^{48}Sc$	ENDF/B-Vd	GLUCS	1.033	1.03549
12.	$^{Nat}Ti(n,X)^{47}Sc$	ENDF/B-Vd	Private	1.235	1.2332
13.	$^{55}Mn(n,\gamma)^{56}Mn$	ENDF/B-Va	ENDF/B-Va	1.0 (exact)	1.0 (exact)
14.	$^{55}Mn(n,2n)^{54}Mn$	ENDF/B-Vd	ENDF/B-VI	0.9536	0.9523
15.	$^{54}Fe(n,p)^{54}Mn$	ENDF/B-Vd	ENDF/B-VI	1.0006	1.00062
16.	$^{56}Fe(n,p)^{56}Mn$	ENDF/B-Vd	ENDF/B-VI	1.0013	1.0032
17.	$^{58}Fe(n,\gamma)^{59}Fe$	ENDF/B-Vd	ENDF/B-VI	0.6239	0.9458
18.	$^{59}Co(n,p)^{59}Fe$	ENDF/B-Va	ENDF/B-VI	1.080	1.0939
19.	$^{59}Co(n,\gamma)^{60}Co$	ENDF/B-Vd	ENDF/B-VI	1.0686	0.9954
20.	$^{59}Co(n,\alpha)^{56}Mn$	ENDF/B-Vd	ENDF/B-VI	0.9747	0.9704
21.	$^{59}Co(n,2n)^{58}Co$	ENDF/B-Vd	IRDF-90	1.0032	1.0021
22.	$^{58}Ni(n,p)^{58}Co$	ENDF/B-Vd	ENDF/B-VI	0.9873	0.9856
23.	$^{58}Ni(n,2n)^{57}Ni$	ENDF/B-Vd	ENDF/B-VI	0.89325	0.8933
24.	$^{60}Ni(n,p)^{60}Co$	ENDF/B-Vd	ENDF/B-VI	1.332	1.3249
25.	$^{63}Cu(n,\gamma)^{64}Cu$	ENDF/B-Vd	ENDF/B-VI	0.9272	1.0435
All cross sections are for bare foils					

Table 3. Effect of New Cross Sections on Reaction Activities (Continued)

Dosimetry Reactions		Cross Section Library		Ratio of Spectrum-Averaged Cross Section (General/SNLRML)	
		General Usage	SNLRML Recommended	FBR (SPR3CAV18)	Pool-Type (ACF9)
26.	$^{63}Cu(n,2n)^{62}Cu$	IRDF-82	IRDF-90	0.9774	0.9783
27.	$^{63}Cu(n,\alpha)^{60}Co$	ENDF/B-Vd	ENDF/B-VI	1.0535	1.0652
28.	$^{65}Cu(n,2n)^{64}Cu$	ENDF/B-Vd	ENDF/B-VI	0.990	0.9912
29.	$^{64}Zn(n,p)^{64}Cu$	IRDF-82	IRDF-90	0.9313	0.93029
30.	$^{90}Zr(n,2n)^{89}Zr$	ENDF/B-Va	IRDF-90	1.0413	1.04117
31.	$^{93}Nb(n,\gamma)^{94m}Nb$	ENDF/B-Va	ENDF/B-VI	0.970	0.9577
32.	$^{93}Nb(n,2n)^{92m}Nb$	DOSCROS84	IRDF-90	1.143	1.1335
33.	$^{93}Nb(n,n')^{93m}Nb$	IRDF-82	IRDF-90	1.147	1.1517
34.	$^{98}Mo(n,\gamma)^{99}Mo$	ENDF/B-Va	JENDL-3	0.7947	1.042
35.	$^{103}Rh(n,n')^{103m}Rh$	IRDF-82	IRDF-90	1.0017	1.0017
36.	$^{115}In(n,\gamma)^{116m}In$	ENDF/B-Vd	ENDF/B-VI	1.0 (exact)	1.0 (exact)
37.	$^{115}In(n,n')^{115m}In$	ENDF/B-Vd	IRDF-90	0.9652	0.9644
38.	$^{127}I(n,2n)^{126}I$	ENDF/B-Vd	ENDF/B-VI	1.0 (exact)	1.0 (exact)
39.	$^{197}Au(n,\gamma)^{198}Au$	ENDF/B-Vd	ENDF/B-VI	1.002	0.9999
40.	$^{197}Au(n,2n)^{196}Au$	ENDF/B-Va	IRDF-90	0.9650	0.968
41.	RML $^{Enriched}U$ $^{235}U(n,f)F.P.$	^{235}U ENDF/B-Vd ENDF/B-Vd	ENDF/B-VI ENDF/B-VI	1.075 1.015	1.071 0.9961
42.	RML $^{Depleted}U$ $^{238}U(n,f)F.P.$	^{238}U ENDF/B-Vd ENDF/B-Vd	ENDF/B-VI ENDF/B-VI	0.9879 1.0024	0.4996 1.00199
43.	$^{237}Np(n,f)F.P.$	ENDF/B-Vd	ENDF/B-VI	1.027	1.0307
44.	RML Pu $^{239}Pu(n,f)F.P.$	^{239}Pu ENDF/B-Vd ENDF/B-Vd	ENDF/B-VI ENDF/B-VI	1.070 1.0071	1.1286 0.99586
All cross sections are for bare foils					

Table 4. Effect of Alternate Cross Sections Selections on Reaction Activities

	Dosimetry Reactions	Cross Section Library		Ratio of Spectrum-Averaged Cross Section (Alt./SNLRML)	
		Alternate	SNLRML Recommended	FBR (SPR3CAV18)	Pool-Type (ACF9)
1.	$^{19}F(n,2n)^{18}F$	JENDL-3d	IRDF-90	1.137	1.146
2.	$^{23}Na(n,\gamma)^{24}Na$	JENDL-3d	ENDF/B-VI	0.79719	1.0026
3.	$^{24}Mg(n,p)^{24}Na$	JENDL-3d	IRDF-90	1.0656	1.060
4.	$^{27}Al(n,p)^{27}Mg$	JENDL-3d	GLUCS	1.0756	1.071
5.	$^{27}Al(n,\alpha)^{24}Na$	JENDL-3d	IRDF-90	0.9552	0.9563
6.	$^{31}P(n,p)^{31}Si$	JENDL-3d	IRDF-90	1.294	1.303
7.	$^{32}S(n,p)^{32}P$	JENDL-3d Fu	GLUCS	1.0735 1.039	1.0705 1.037
8.	$^{45}Sc(n,\gamma)^{46}Sc$	JENDL-3d	ENDF/B-VI	1.21	0.9993
9.	$^{Nat}Ti(n,X)^{46}Sc$	JENDL-3d	Private	1.0805	1.082
10.	$^{48}Ti(n,p)^{48}Sc$	JENDL-3d	GLUCS	1.0221	1.023
11.	$^{Nat}Ti(n,X)^{47}Sc$	JENDL-3d	Private	1.071	1.071
12.	$^{55}Mn(n,\gamma)^{56}Mn$	JEF 2.2	ENDF/B-Va	1.2167	1.023
13.	$^{55}Mn(n,2n)^{54}Mn$	JENDL-3d	ENDF/B-VI	0.99927	0.9992
14.	$^{54}Fe(n,p)^{54}Mn$	JENDL-3d	ENDF/B-VI	0.994	0.9909
15.	$^{56}Fe(n,p)^{56}Mn$	JENDL-3d	ENDF/B-VI	1.0185	1.0241
16.	$^{58}Fe(n,\gamma)^{59}Fe$	JENDL-3d JEF 2.2	ENDF/B-VI	0.968 0.8818	1.106 1.041
17.	$^{59}Co(n,p)^{59}Fe$	JENDL-3	ENDF/B-VI	1.377	1.0442
18.	$^{59}Co(n,\gamma)^{60}Co$	JENDL-3d	ENDF/B-VI	1.039	1.002
19.	$^{59}Co(n,\alpha)^{56}Mn$	JENDL-3d	ENDF/B-VI	1.0815	1.072
All cross sections are for bare foils					

Table 4. Effect of Alternate Cross Sections Selections on Reaction Activities (Continued)

Dosimetry Reactions		Cross Section Library		Ratio of Spectrum-Averaged Cross Section (Alt./SNLRML)	
		Alternate	SNLRML Recommended	FBR (SPR3CAV18)	Pool-Type (ACF9)
20.	$^{59}Co(n,2n)^{58}Co$	JENDL-3d	IRDF-90	0.9947	0.9942
21.	$^{58}Ni(n,p)^{58}Co$	JENDL-3d	ENDF/B-VI	1.0025	1.004
22.	$^{58}Ni(n,2n)^{57}Ni$	JENDL-3d	ENDF/B-VI	0.962	0.9617
23.	$^{60}Ni(n,p)^{60}Co$	JENDL-3d	ENDF/B-VI	1.338	1.337
24.	$^{63}Cu(n,\gamma)^{64}Cu$	JENDL-3d	ENDF/B-VI	0.8024	0.9988
25.	$^{63}Cu(n,2n)^{62}Cu$	JENDL-3d	IRDF-90	1.057	1.057
26.	$^{63}Cu(n,\alpha)^{60}Co$	JENDL-3d	ENDF/B-VI	1.0566	1.068
27.	$^{65}Cu(n,2n)^{64}Cu$	JENDL-3d	ENDF/B-VI	1.0336	1.0337
28.	$^{64}Zn(n,p)^{64}Cu$	JENDL-3d	IRDF-90	1.1075	1.1096
29.	$^{90}Zr(n,2n)^{89}Zr$	JENDL-3d	IRDF-90	1.0395	1.041
30.	$^{93}Nb(n,\gamma)^{94m}Nb$	JENDL-3	ENDF/B-VI	1.0143	0.975
31.	$^{93}Nb(n,2n)^{92m}Nb$	JENDL-3d	IRDF-90	1.154	1.1447
32.	$^{93}Nb(n,n')^{93m}Nb$	JENDL-3d	IRDF-90	1.0503	1.052
33.	$^{127}I(n,2n)^{126}I$	JENDL-3d	ENDF/B-VI	1.202	1.2035
34.	$^{197}Au(n,\gamma)^{198}Au$	JENDL-3d	ENDF/B-VI	0.995	1.001
35.	$^{197}Au(n,2n)^{196}Au$	JENDL-3d	IRDF-90	1.0317	1.0254
36.	$^{235}U(n,f)F.P.$	JENDL-3d	ENDF/B-VI	1.007	0.9883
37.	$^{238}U(n,f)F.P.$	JENDL-3d	ENDF/B-VI	1.013	1.0135
38.	$^{237}Np(n,f)F.P.$	JENDL-3d	ENDF/B-VI	1.011	1.011
39.	$^{239}Pu(n,f)F.P.$	JENDL-3d	ENDF/B-VI	0.9999	1.0015
All cross sections are for bare foils					

3.4 Nuclear Constants

The nuclear, atomic, and reaction constants were taken from the best available references and are presented in the tables in Appendix B. In the case of the emission gamma energies and emission gamma probabilities, the data came from the on-line (as the library existed in November 1992) Evaluated Nuclear Structure Data File (ENSDF) [20] at the National Nuclear Data Center (NNDC) at Brookhaven National Laboratory (BNL). In the case of the reaction half-lives, the data came from the nuclear data file derived from Evaluated Nuclear Structure Data File (ENSDF) and Nuclear Wallet Cards (NUDAT), an on-line database at the NNDC. In a few cases (e.g. ^{23}Na) the data were superceded by data taken from community standards databases, such as Lemmel's detector calibration standards [21], instead of ENSDF. When this happened, a notation is made in the section 5 discussion of the reaction. Unit time conversions were performed assuming 1 yr (tropical) = 365.24220 d = 31556926 s. The conversion data were taken from Zijp [22] and are consistent with 24 h = 1 d.

The target atom atomic weight and the isotopic number abundance were taken from the Nuclear Wallet Cards [23]. The isotopic abundance data in the Nuclear Wallet Cards was, in turn, derived from Holden [24]. The isotopic mass excesses were taken from Firestone [25].

The fission yield data in Table 2 comes from the initial ENDF/B-VI release. These data are the same as the ENDF/B-V data. Modified ENDF/B-VI data are still under development by Tal England. These new data will be adopted as soon as they are available. The independent fission yield is taken from the MT=454 ENDF data and is designated as RI. The cumulative fission yield is taken from the MT=459 ENDF data and is designated as RC. All fission yield data given in Table 2 are associated with an incident neutron energy of 0.5 MeV and corresponds to a fast fission event. If the user of this cross section compendium is concerned about fission events induced by thermal neutrons or by 14-MeV neutrons, he should refer to the ENDF fission yield tapes for the recommended data.

4. USE IN SPECTRUM DETERMINATIONS

4.1 Fission Spectrum Determination

Spectrum adjustment at Sandia National Laboratories is done primarily with an enhanced version of the SAND-II methodology [11, 26]. When the new cross section library was assembled for the reactions in use at the Sandia RML, 15 previously determined spectra [27] were re-analyzed. Integral parameters, such as the spectral index (SI) and hardness parameter (HP) (defined by Kelly [27]), were not significantly altered by the updated cross sections. The quality of the fits, in terms of smoothness and standard deviation of experimental versus calculated activity, was slightly worse for the updated cross sections, but acceptable. Some problems were seen with resonances in specific reactions. This may be due to the fact that experience has led to the exclusion of certain ENDF/B-V dosimetry reactions that do not fit a large body of data. This process of "weeding out" poorly defined reactions is just beginning for the ENDF/B-VI cross sections.

This work has indicated that the $^{47}Ti(n,p)$ reaction, which had previously been excluded from the Sandia foil set based on a poor match with ENDF/B-V data for almost all reactor spectra, is now in acceptable agreement with the other reactions in that energy region. However, the resonances in the 0.3 to 2.0 keV energy region for the $^{55}Mn(n,\gamma)^{56}Mn$ reaction, that previously was consistent with other reactions in this region, produced anomalous "bumps" in the spectrum. This happened in each of the spectra studied. In 14 of the 15 spectra the conflict could not be resolved through the elimination of only one of the other foils. The "bumps" were introduced in the very first iteration of the spectral fit. This indicates that the poor agreement is not due to the tendency of iterative unfolding methods to "over-fit" the data, but rather is a problem with the cross sections.

4.2 14-MeV Spectrum Characterization

The new cross sections were empirically tested for consistency [10] by using fourteen foils/ reactions to characterize the spectrum and fluence of the Sandia DT neutron generator. The characterization of 14-MeV neutron sources was found to be very dependent upon the consistent application of a given cross section set. The most recent evaluations (updated ENDF/B-VI and IRDF-90 evaluations) result in a decrease of about 0.3 MeV in the neutron energy from DT sources when compared to previous results based on ENDF/B-V data. DT neutron fluence estimates from the SNLRML library cross section evaluations are at least as tightly clustered as those from previous ENDF/B-V data. Results based solely on new evaluations within the SNLRML library are more tightly clustered than ENDF/B-V results.

5. NOTES ON INDIVIDUAL REACTIONS

Several of the dosimetry reactions in Table 2 require some additional comments to fully understand the library comparison and the rationale behind the choices reflected in the contents of the SNLRML library. Full understanding of the derivation of these cross sections is critical if the dosimetry cross sections are to be used at another facility. The following subsections will provide the rationale for the choice of the cross section evaluations that were included in the SNLRML library. In addition, sufficient details on the derivation of any special cross section are provided to allow a reader to duplicate the data provided in this document.

5.1 $^{10}B(n,abs)$

^{10}B is used as the active material in boron covers. The large (over 10^4 b at thermal energies) long 1/v (n,γ) absorption cross section can be used to shift the response of a dosimetry sensor from the thermal energies into the keV energy region. Boron covers are almost always used with fission foils. They can also be combined with foils such as $^{197}Au(n,\gamma)^{198}Au$, which are typically used to define the thermal energy spectrum, to provide better sensor coverage of the keV energy region.

The ENDF/B-VI library (revision 1) provides the most recent ^{10}B cross section evaluation. This cross section was adopted by the JEF-2 library. ^{10}B covariance data for all of the absorption channels are not provided by any available cross section compilation.

The absorption cross section, as included in the SNLRML library, includes all absorption processes [(n,γ), (n,p), (n,α), (n,d), (n,t2α)] and not just the (n,γ) component. This is a significant modification over the previous community standard boron cover cross section that was distributed in the DOSDAM84 [14] library and usually interfaced with the SAND-II spectrum unfolding code. The other absorption processes are not important for sensors in the thermal and keV energy region, but the details of the high energy cover cross section are important for some reactions, such as $^{237}Np(n,f)F.P.$, that have a significant high energy response. The effect of the high energy cover cross section can also be important in the application/interpretation of monitor foils [such as $^{58}Ni(n,p)^{58}Co$ or $^{32}S(n,p)^{32}P$] that are used to combine activities from several different irradiations to obtain a spectrum.

It should be noted that most spectrum unfolding codes that use cover cross sections only treat the effect of the cover material as an exponential attenuation. If boron covers are used in a case where high energy scattering processes are important, then a true sensor response and not an exponentially attenuated cross section may be needed. The true sensor response can be obtained by doing an adjoint radiation transport calculation through the cover material using the dosimetry sensor cross section as the adjoint transport source.

5.2 $^{10}B(n,X)^4He$

This is a frequently used damage sensor in the light-water pressure vessel surveillance community. The data were derived by combining the ENDF/B-VI reactions that produced helium as a sum of the $^{10}B(n,\alpha)^7Li$ (MT=107) and twice the $^{10}B(n,t\alpha)^4He$ (MT=113) cross sections.

An inspection of the plots in Figures A-2a and A-2b shows a considerable difference in the ^4He production for high energy neutrons. This difference is usually not of practical concern since the production of ^4He by low energy neutron interaction typically dominates. The IRDF-90 helium production cross section only considers the direct (n,α) reaction as extracted from the ENDF/B-VI evaluation. The actual ENDF/B-VI cross section includes the (n,t2α) breakup interaction. The JENDL-3 and ENDF/B-VI cross sections agree very well in their cross sections for these two reactions. However, the JENDL-3 cross section also indicates which (n,n') inelastic scattering reactions result in a ^{10}B nucleus that breaks up into a deuteron and two alphas. While the ENDF/B-VI cross section models the inelastic scattering cross section to discrete states as well as to the continuum, it does not indicate which excited states will result in breakup.

Figure A-2b also shows the ENDF/B-V dosimetry tape evaluation of the ^{10}B helium production cross section. This cross section is identical to the ENDF/B-V ^{10}B gas production tape. The new ENDF/B-VI evaluation was done by the same laboratory and the

comments indicate that the evaluators incorporated new data and adjusted the (n,α) cross section above the standard region (thermal to 100 keV) for better consistency with other cross sections.

Since the $^{10}B(n,\alpha)$ reaction is considered an ENDF/B-VI standard cross section, ENDF/B-VI data were adopted for this element in the SNLRML library. The activation Handbook [28] indicates that the recommended range for use of this reaction as a standard cross section is thermal to 250 keV [29, 30]. The reader is warned, as discussed above, that the helium contribution from the inelastic excitation and subsequent breakup of ^{10}B is not included in this term. Future versions of this library may remedy this omission.

The phase 1 reviewers of the ENDF/B-VI standard cross sections have expressed concern that the uncertainties resulting from the combination of R-matrix and simultaneous evaluations might have led to uncertainties that are too small. As a result, detailed covariance data will be added to the ENDF/B-VI files at a later time. The Standards Subcommittee (at the May 1990 CSEWG meeting) has produced a set of expanded covariance estimates for the standard cross section reactions. These uncertainties are estimates such that if a modern-day experiment were performed on a given standard cross section using the best techniques, approximately 2/3 of the results should fall within these expanded uncertainties. These estimates can be found in the comment section of the ENDF/B-VI evaluation. A recent publication [30] documents the final ENDF/B-VI CSEWG-endorsed standard cross sections and uncertainties. The Activation Handbook [28] also includes comments that indicate the uncertainty estimates for this reaction may be too low. Poenitz [31] recommends that the $^{6}Li(n,\alpha)$ cross section be used as a reference cross section below 100-150 keV until a more reasonable data base for the ^{10}B+n interactions becomes available.

Since a complete covariance matrix is required for the SNLRML library, the covariance matrix is taken from the IRDF-90 library and represents the covariance matrix for the (n,α) reaction, which was drawn from a pre-release version of the original ENDF/B-VI evaluation. As such, this covariance matrix is not endorsed by the phase 1 reviewers of the ENDF/B-VI standard cross sections as mentioned above.

5.3 $^{11}B(n,abs)$

Various enrichments of boron are used in boron covers. ^{11}B absorption cross section is included in the library to allow users to combine the absorption cross section for ^{10}B and ^{11}B in a ratio reflective of the enrichment in their cover boron material.

The ENDF/B-VI library (revision 1) provides the most recent ^{11}B cross section evaluation and is consistent with the ^{10}B cross section selection. Significant differences in the keV to MeV energy region are noted between the JENDL-3 and the ENDF/B-VI absorption cross sections.

See section 5.1 for cautions in the application of cover cross sections.

5.4 $^{Nat}B(n,abs)$

Natural boron is a common cover material. Natural boron is composed of 19.9% ^{10}B and 80.1% ^{11}B. The ^{Nat}B absorption cross section is a combination of the cross sections discussed in sections 5.1 and 5.3 and are taken from the ENDF/B-VI library. The ^{10}B cross section dominates at all energies and the differences between cross section evaluations was found to be small.

See section 5.1 for cautions in the application of cover cross sections.

5.5 $^{Enriched}B_4C(n,abs)$

The SNL RML uses a 91.67% ^{10}B-enriched B_4C ball to cover fission foils. The boron absorption of low energy neutrons is often used to move the response of sensors from the thermal into the resonance region. A comparison of the ^{10}B, ^{11}B, and ^{Nat}C absorption cross sections in Figures A-5a and A-5b shows that the ^{10}B absorption is the dominant influence at all energies. Note that if B_4C is specified as the cover material, then the cover thickness, typically expressed in atoms per barn, must correspond to the B_4C atom thickness and is not the same as an equivalent ^{10}B atom thickness. The SNLRML library B_4C cover is mixed with the atom number fractions and normalized to a single atom. Thus, the input SAND-II cover thickness for B_4C must be relative to the number of atoms in the cover material and not the number of B_4C molecules. For example, the SNL RML uses a B_4C ball (77.08% weight fraction of boron or 80.0025% number fraction using exact isotopic weights for the conversion), which has a thickness of 1.03 cm and a density of 2.5 gm/cm^3, to cover its fission foils. This corresponds to a cover thickness of 0.14808 atoms/barn of B_4C. If the cover material is modeled as pure ^{10}B, then an atom thickness of 0.10863 atoms/barn of ^{10}B must be used.

5.6 $^6Li(n,X)^4He$

This is a frequently-used damage sensor in the light-water pressure vessel surveillance community. The data were derived by combining the ENDF/B-VI reactions that produced helium as a product from the $^6Li(n,t)^4He$ reaction (MT=105) and the inelastic cross section that results in an excited state of ^6Li that decays into a deuteron and an alpha particle (MT=4 minus MT=57).

An inspection of Figures A-6a and A-6b shows a moderate difference in the ^4He production for high energy neutrons. This difference is usually not of practical concern since the production of ^4He by low energy neutrons typically dominates. The IRDF-90 helium production cross section only considers the $^6Li(n,t)^4He$ reaction. The ENDF/B-VI and

JENDL-3 cross sections include the contribution from the (n,n') inelastic reactions that result in an unstable nucleus that subsequently breaks up into a deuteron and an alpha particle.

See section 5.2 for a discussion of the covariance matrix for ENDF/B-VI standard cross sections. The activation Handbook [28] indicates that the recommended energy range for use of this reaction as a standard is thermal to 100 keV [29]. A recent publication [30] recommends the $^{6}Li(n,t)^{4}He$ reaction as a CSEWG standard for energies below 1 MeV.

The covariance matrix included with this library was taken from the IRDF-90 library and represents the covariance data for the $^{6}Li(n,t)^{4}He$ reaction drawn from a pre-release version of the ENDF/B-VI cross section. As such, the covariance matrix is not endorsed by the phase 1 reviewers of the ENDF/B-VI standard cross sections.

5.7 $^{19}F(n,2n)^{18}F$

The $^{19}F(n,2n)^{18}F$ reaction is not typically used at the RML because it decays by β emission and has no strong gamma line. Thus, we have no validation data for this reaction. The high energy threshold for this reaction makes it useful primarily for fusion spectra.

The most recent cross section evaluation came from the ENDF/B-VI library, but the (n,2n) component of this evaluation was based on calculations (with the TNG code) rather than measurements. The European dosimetry community, which had access to the ENDF/B-VI cross sections, chose to incorporate an IRK $^{19}F(n,2n)^{18}F$ evaluation in the IRDF-90 Library. Furthermore, the ENDF/B-VI cross section curve in Figure A-7a shows a piece-wise segmented structure that is not thought to be physical and would cause problems if this cross section was applied to the energy characterization of a 14-MeV neutron source [10]. Since the IRDF-90 library is tailored towards dosimetry applications, in the absence of more information on the evaluations, the IRDF-90 cross section was chosen for inclusion in this dosimetry compendium. A new IRK evaluation has been done [17] and will be adopted by the upcoming IRDF-93 revision to IRDF-90. This evaluation was not yet available to the authors, but will be adopted in the next version of the SNLRML Library.

5.8 $^{23}Na(n,\gamma)^{24}Na$

There are no recent cross section evaluations for $^{23}Na(n,\gamma)^{24}Na$ that emphasize dosimetry applications. The ENDF/B-VI cross section is merely a format translation of the ENDF/B-V cross section. There is also no significant disagreement in the cross sections from the available libraries (except in a resonance near 10 keV). In the absence of better dosimetry-oriented evaluations and since the ENDF/B-V $^{23}Na(n,\gamma)^{24}Na$ dosimetry cross section has been fairly well validated for a wide range of fission spectra at SNL, for which its sensitivity range extends down to 30 keV, the ENDF/B-VI evaluation was selected for inclusion in the compendium.

The JENDL-3 Dosimetry Library includes a $^{23}Na(n,\gamma)^{24}Na$ cross section and covariance matrix. The cross section for this reaction is identical to that contained in the JEF 2.2 library and the JENDL-3 general purpose library. The covariance data were taken from the IRDF-85 ^{23}Na evaluation. Since the JENDL-3 Dosimetry Library (as opposed to the JENDL-3 General Purpose Library) only recently became available to the authors, a careful evaluation of the internal consistency of the dosimetry library cross sections is still underway. The JENDL-3 Dosimetry $^{23}Na(n,\gamma)^{24}Na$ cross section appears to be consistent with other cross sections in spectrum unfolds performed at SNL and may indeed be better than the ENDF/B-VI data. Concern about the JENDL library adopting the IRDF-85 covariance matrix, rather than performing a careful evaluation of the covariance consistent with their new evaluation, leads us to include the JENDL-3 data in the library as an alternative cross section rather than adopting it as a recommendation at this time.

The $^{23}Na(n,\gamma)^{24}Na$ evaluation must be used with care. Work at SNL has indicated that the cross section is consistent for spectrum determinations of pool-type reactors, such as the ACRR central cavity, where the majority of the sensor response comes from the resonance region. However, for fast burst reactor spectra, such as the SPR-III central cavity, much of the sensor response is moved into the 0.100 to 2.9 MeV region and shows moderate disagreement with other foils in this region. This cross section has self-consistency problems between the resonance region and the high energy region. Self-consistency between the resonance and MeV energy region of the $^{23}Na(n,\gamma)^{24}Na$ reaction is an issue for all of the available cross section libraries, JENDL-3 and ENDF.

The ^{24}Na decay half-life and gamma emission probabilities were taken from Lemmel [21] rather than the ENSDF compilation.

5.9 $^{24}Mg(n,p)^{24}Na$

The ENDF/B-VI $^{24}Mg(n,p)^{24}Na$ cross section is just a format translation of the ENDF/B-V data and exhibits a piece-wise discontinuous representation for this reaction. The IRDF-90 data provides the most recent dosimetry-oriented evaluation and was chosen for inclusion in the SNLRML library. The differences in spectrum-averaged cross sections between the IRDF-90 and the ENDF/B-VI cross sections is minimal for both fission and 14-MeV sources. The IRDF-90 evaluation provides a smooth representation of the cross section at high energies.

The JENDL-3 Dosimetry Library is identical to the JENDL-3 General Purpose Library cross section. The JENDL-3 covariance matrix is taken from the IRDF-85.

The ^{24}Na decay half-life and gamma emission probabilities were taken from Lemmel [21] rather than the ENSDF compilation.

5.10 $^{27}Al(n,p)^{27}Mg$

The ENDF/B-VI $^{27}Al(n,p)^{27}Mg$ cross section is just a format translation of the ENDF/B-V data. The most recent dosimetry-oriented cross section is from the GLUCS library. The GLUCS cross section was incorporated into the IRDF-90 library. Since the IRDF-90 library is more readily obtained than the GLUCS library, the SNLRML library cross section reference is given as IRDF-90. For energies between 7 and 15 MeV there are significant differences in the cross sections from different libraries. The JENDL-3 library $^{27}Al(n,p)^{27}Mg$ cross section lacks some of the low energy structure that is found in the other evaluations and this difference may be important in a spectrum determination.

H. Vonach discovered that some of the GLUCS covariance matrices were singular. D. Hetrick traced the problem to the use of a ENDF/B-V covariance matrix that was not positive definite. The 1993 update to the GLUCS data provided new positive definite covariance matrices. The SNLRML library covariance matrix is taken from the 1993 GLUCS results.

The difference between the ENDF/B-VI (ENDF/B-V) and IRDF-90 (GLUCS) fission-spectrum-averaged cross section is very small.

5.11 $^{27}Al(n,\alpha)^{24}Na$

The ENDF/B-VI cross section is just a format translation of the ENDF/B-V data. The most recent dosimetry-oriented evaluations are from the GLUCS and IRDF-90 library. The differences between these evaluations are very small for fission spectrum unfolding applications.

The IRDF-90 evaluation was chosen for inclusion in this compendium. This decision is based on maintaining a reference consistency between the (n,p) and (n,α) dosimetry components and the fact that the European dosimetry community had access to the GLUCS cross sections when they chose to use an IRK evaluation. If users are sensitive to cross section differences in the 7 to 13 MeV region, the GLUCS library should be re-examined.

The Activation Handbook [28] indicates that this reaction is widely employed as a standard for dosimetry and activation measurements [32]. The recommended energy region for use of this reaction as a standard is from 11 to 20 MeV.

The ^{24}Na decay half-life and gamma emission probabilities were taken from Lemmel [21] rather than the ENSDF compilation.

5.12 $^{Nat}Si(n,X)1MeV$

Silicon has recently gained attention as a dosimetry sensor because it has response in the energy region between 200 keV and 1 MeV that is not covered by widely used dosimetry foils. Fission foils or some reactions with soft gammas, such as the $^{93}Nb(n,n')^{93m}Nb$, have response in this same region, but are not available at most dosimetry laboratories. The

silicon damage is typically measured as resistivity changes in Van der Pauw samples due to changes in the carrier removal rate, degradation in carrier lifetime or total light output in LEDs, and as gain changes due to minority-carrier-lifetime degradation in bipolar devices (such as 2N2222 transistors). The silicon response function is displacement damage, which has been found to correspond to the silicon displacement kerma. Damage ratios for 14-MeV spectra and a wide variety of fission spectra have validated [33] this correspondence to within experimental uncertainty (~ 6%).

The silicon displacement kerma was calculated with the NJOY code [34], version 91.38. RECONR was used to do resonance reconstruction at 0 K, BROADR was used to include doppler resonance broadening at 300 K, and GROUPR was used to collapse the kerma components to a 640 group energy structure using a weighting function (IWT=4) that included a thermal Maxwellian tail (with a 0.1 eV thermal break and a 0.025 eV thermal temperature), a 1/E scattering component, and a fission component (with a fission break point of 0.1 MeV and a fission temperature of 1.4 MeV).

A ORNL silicon evaluation [15] was used for ^{28}Si. This is the cross section that is expected to be incorporated in release 4 of the ENDF/B-VI library. Silicon displacement kerma from this evaluation was chosen because it was used to establish the correlation between observed device damage and silicon displacement kerma and because this response function has been adopted by the ASTM community for inclusion in the E 722-93 standard on 1-MeV equivalent damage [35].

5.13 ^{31}P(n,p)^{31}Si

The recommended ^{31}P(n,p)^{31}Si cross section for dosimetry applications is the 1980 IRDF-90 evaluation. The JENDL-3 evaluation is more recent (1987), but this library does not have a dosimetry orientation and does not show cross section structure that is reflected in both the IRDF and ENDF evaluations. The JENDL-3 Dosimetry Library ^{31}P cross section is identical to the JENDL-3 data and shows a piece-wise segmentation. The ENDF/B-VI cross section is a format translation of ENDF/B-V, which, in turn, was a format translation of the 1977 ENDL cross sections.

This is not a reaction that SNL has used in any of its spectrum unfolds. The ^{31}Si isotope decays through β decay and does not have a good gamma signature (only 0.07% of the decays result in a 1.2662 MeV gamma). Since this reaction was supported in the DOSCROS84 library it is included in this compilation as an aid to the dosimetry community.

5.14 ^{32}S(n,p)^{32}P

The sulfur (n,p) dosimetry cross section has a very complicated and confusing history. There are three ENDF/B-V evaluations, one full evaluation, one in the activation library, and one in the dosimetry library. The activation and full evaluations are very similar, differing only near the reaction threshold energy. The dosimetry cross section differs significantly from the other two and shows considerable structure in the threshold region

between 2 and 5 MeV. The ENDF/B-VI library required full evaluations and thus adopted the older ENDF/B-V full evaluation.

The most recent careful dosimetry cross section evaluation was done as part of the GLUCS cross-correlation study at ORNL. The ORNL cross section was adopted by the IRDF-90 community and is included in the SNLRML library. The reference for the sulfur (n,p) dosimetry cross section in the SNLRML library is given as IRDF-90 even though the original work was done as part of the ORNL GLUCS library. This choice was made because the IRDF-90 library is more readily available to the dosimetry and radiation effects community for checking and validation purposes.

The use of new cross sections for the $^{32}S(n,p)^{32}P$ reaction is complicated since this reaction is typically read with a beta counting system that uses a transfer calibration with a NIST ^{252}Cf irradiation. The fission spectrum-averaged cross section changes about the same amount as the ^{252}Cf spectrum-averaged cross section; thus, the calibration procedure cancels out (to a large extent) the effect of the change in cross section. However, the calibration procedure introduces additional uncertainty related to the exact shape of the ^{252}Cf fission spectrum. Mannhart [36] has suggested changes in the ^{252}Cf spectrum relative to that currently employed by NIST for calibration purposes. The Mannhart ^{252}Cf fission neutron spectrum has been adopted by the ENDF/B-VI library and appears in Tape 200, MAT=9861, MT=18, MF=5. See section 5.69 for further discussion of the importance of correlating the sulfur activity with the β-counting system calibration.

Some work on the $^{32}S(n,p)^{32}P$ reaction by Fu [37] at ORNL differs from the ORNL/ GLUCS/IRDF data at high energies (> 4.5 MeV). The difference in the Fu cross section at high energies can couple with the ^{252}Cf transfer calibration procedure to affect the fission spectrum-averaged cross section by a couple of percent. There is some indication that the Fu cross section, when properly related to the Sandia/NIST transfer calibration procedure, may provide better agreement with the SNL $^{58}Ni(n,p)^{58}Co$ monitor foil. The situation is not completely clear at this time since the effect is small and difficult to separate from fluctuations in counting statistics and transfer calibrations. Since the dosimetry community tends to favor the GLUCS/IRDF shape, that is what is currently incorporated into the SNLRML library. The Fu cross section is under additional study for foil consistency.

H. Vonach discovered that some of the GLUCS covariance matrices were singular. D. Hetrick traced the problem to the use of a ENDF/B-V covariance matrix that was not positive definite. The 1993 update to the GLUCS data provided new positive definite covariance matrices. The SNLRML library covariance matrix is taken from the 1993 GLUCS results.

5.15 $^{45}Sc(n,\gamma)^{46}Sc$

There are no recent dosimetry-oriented evaluations of this reaction. The ENDF/B-VI cross section, which was adopted from the ENDF/B-V evaluation, is adopted for inclusion in the SNLRML library. The JENDL-3 cross section, which did not emphasize dosimetry applications, will be monitored since it is more recent and shows some disagreements with ENDF at high neutron energies (> 0.1 MeV). The response to this cross section is generally driven by epithermal-energy neutrons.

The ^{46}Sc decay half-life and gamma emission probabilities were taken from Lemmel [21] rather than the ENSDF compilation.

5.16 $^{46}Ti(n,p)^{46}Sc$

The latest dosimetry-oriented cross section data come from the ORNL GLUCS and were incorporated in the IRDF-90 library. These data were adopted by the SNLRML library.

H. Vonach discovered that some of the GLUCS covariance matrices were singular. D. Hetrick traced the problem to the use of an ENDF/B-V covariance matrix that was not positive definite. The 1993 update to the GLUCS data provided new positive definite covariance matrices. The SNLRML library covariance matrix is taken from the 1993 GLUCS results.

The ^{46}Sc decay half-life and gamma emission probabilities were taken from Lemmel [21] rather than the ENSDF compilation

5.17 $^{47}Ti(n,p)^{47}Sc$

The SNL RML has not been able to use this dosimetry sensor for many years because it could not be made consistent with other foils. This has been confirmed, informally, by other laboratories. Mannhart [38] has shown that the disagreement related to difficulties in normalizing differential and integral data. He proposed a normalization change to the ENDF/B-V data which was found to make this reaction consistent with other dosimetry sensors in SNL spectrum unfolds. His analysis has been incorporated and extended in the GLUCS-90 release (which considers cross reaction correlations). The GLUCS/ORNL data have been, in turn, incorporated in the IRDF-90 library and has been adopted by the SNLRML library.

The IRDF-90 cross section file for ^{47}Ti indicates that the data were taken from ENDF/B-VI. This is an error in documentation. There is no new ENDF/B-VI ^{47}Ti evaluation; the ENDF/B-V data were adopted for ENDF/B-VI. New $^{47}Ti(n,p)^{47}Sc$ data should have appeared in the ENDF/B-VI cross sections, but was left out due to a miscommunication with the evaluators. The IRDF-90 library compilers went directly to the ENDF material evaluator for a pre-release version of the cross section and were not aware of the miscommunications. This situation should be remedied in release 2 of ENDF/B-VI.

The data in the IRDF-90 library is presented in a different numerical form than GLUCS, but the resulting cross section is nearly identical to the GLUCS-90 data.

H. Vonach discovered that some of the GLUCS covariance matrices were singular. D. Hetrick traced the problem to the use of a ENDF/B-V covariance matrix that was not positive definite. The 1993 update to the GLUCS data provided new positive definite covariance matrices. The SNLRML library covariance matrix is taken from the 1993 GLUCS results.

5.18 ^{47}Ti(n,np)^{46}Sc

There is no recent dosimetry-oriented evaluation of the ^{47}Ti(n,np)^{46}Sc reaction. Some data exist for energies near 14 MeV, but no complete energy-dependent evaluations were available. The JENDL-3 and JENDL-3 Dosimetry Libraries include this reaction, but have covariance matrices taken from the IRDF-85 library. The ENDF/B-V data, which were incorporated in ENDF/B-VI, were adopted in the SNLRML library pending further analysis of the JENDL-3 Dosimetry Library.

The ^{46}Sc decay half-life and gamma emission probabilities were taken from Lemmel [21] rather than the ENSDF compilation.

5.19 ^{Nat}Ti(n,X)^{46}Sc

An important consideration for many experimenters who use natural titanium foils is that the ^{47}Ti(n,np)^{46}Sc reaction produces the same activation product as ^{46}Ti(n,p)^{46}Sc. This (n,np) contribution to the observed activity can be important for spectra with a high energy (>12 MeV) component. Meadows and others [39] have advocated characterizing the ^{Nat}Ti(n,X)^{46}Sc reaction while retaining a normalization to a per ^{46}Ti atom in elemental titanium. A similar reporting convention has been adopted in the JENDL-3 Dosimetry Library; however, they report the cross section per elemental Ti atom and not per isotopic atom.

Since the ^{47}Ti(n,np)^{46}Sc reaction is not well characterized (it has a large standard deviation), this component has been added with a normalization factor to the ^{47}Ti(n,p)^{47}Sc cross section so that the ^{Nat}Ti(n,X)^{46}Sc cross section matches evaluations and experiments at 14.7 MeV [39].

The ^{46}Sc decay half-life and gamma emission probabilities were taken from Lemmel [21] rather than the ENSDF compilation

5.20 $^{48}Ti(n,p)^{48}Sc$

The most recent dosimetry-oriented $^{48}Ti(n,p)^{48}Sc$ cross section evaluation is from the ORNL GLUCS library. These data were incorporated into the IRDF-90 and adopted by the SNLRML library.

H. Vonach discovered that some of the GLUCS covariance matrices were singular. D. Hetrick traced the problem to the use of an ENDF/B-V covariance matrix that was not positive definite. The 1993 update to the GLUCS data provided new positive definite covariance matrices. The SNLRML library covariance matrix is taken from the 1993 GLUCS results.

5.21 $^{48}Ti(n,np)^{47}Sc$

There is no recent dosimetry-oriented evaluation of the $^{48}Ti(n,np)^{47}Sc$ reaction. Some data exist for energies near 14 MeV, but no complete energy-dependent evaluations were available. The ENDF/B-V data, which were incorporated in ENDF/B-VI, were adopted in the SNLRML library. The flat top on the $^{48}Ti(n,np)^{47}Sc$ cross section above 18 MeV raises questions about the fidelity of the cross section shape in this region. The JENDL-3 representation is probably a better shape and may be adopted when further analysis of the titanium cross sections is completed.

5.22 $^{Nat}Ti(n,X)^{47}Sc$

An important consideration for many experimenters who use natural titanium foils is that the $^{48}Ti(n,np)^{47}Sc$ reaction produces the same activation product as $^{47}Ti(n,p)^{47}Sc$. This (n,np) contribution to the observed activity can be important for spectra with a high energy (>12 MeV) component. Meadows and others [39] have advocated characterizing the $^{Nat}Ti(n,X)^{47}Sc$ reaction while retaining a normalization to a per ^{47}Ti atom in elemental titanium. A similar reporting convention has been adopted in the JENDL-3 Dosimetry Library, however, they report the cross section per elemental Ti atom and not per isotopic atom.

Since the $^{48}Ti(n,np)^{47}Sc$ reaction is not well characterized, this component has been added with a normalization factor to the $^{47}Ti(n,p)^{47}Sc$ cross section so that the $^{Nat}Ti(n,X)^{47}Sc$ cross section matches evaluations and experiments at 14.7 MeV [39].

5.23 $^{55}Mn(n,\gamma)^{56}Mn$

Resonance reactions are very useful in determining the unfolded spectrum in the 10^{-3} to 10 keV energy region. However, the resonances in the 0.3 to 2.0 keV energy region for the $^{55}Mn(n,\gamma)^{56}Mn$ reaction, which previously was consistent with other reactions in this region, produced anomalous "bumps" in the spectrum when ENDF/B-VI cross sections are used. This happened in each of the spectra studied. In 14 of the 15 spectra the conflict could

not be resolved by eliminating only one of the other foils. The "bumps" were introduced in the very first iteration of the spectral fit. This indicates that the poor agreement is not due to the tendency of iterative unfolding methods to "over-fit" the data, but rather is a problem with these cross sections. The difference in cross section shape is rather minor, and only involves the resonance peaks. The difference between evaluations probably relates to the ratio of the resonance cross sections to the cross section above 100 keV (where most of the sensor response is for fast neutron spectra). The typical $^{55}Mn(n,\gamma)^{56}Mn$ spectrum-averaged cross section only differs by 2 to 3% between the ENDF/B-V and ENDF/B-VI evaluations for fission spectra. This difference in cross sections may only be important when unfolds are performed with fine energy structures in iterative unfolding codes, such as SAND-II. Because of this problem, the default $^{55}Mn(n,\gamma)^{56}Mn$ cross section in the SNLRML library was taken from ENDF/B-V. The ENDF/B-VI $^{55}Mn(n,\gamma)^{56}Mn$ cross section is included so that knowledgeable users can further address reaction consistency in the resonance region.

The $^{55}Mn(n,\gamma)^{56}Mn$ evaluation must be used with great caution. Work at SNL has indicated that the cross section is consistent for spectrum determinations of pool-type reactors, such as the ACRR central cavity, where the majority of the sensor response comes from the resonance region. However, for fast burst reactor spectra, such as the SPR-III central cavity, much of the sensor response is moved into the 0.100 to 2.4 MeV region and shows moderate disagreement with other foils in this region. The ENDF/B-V cross section is more consistent than the ENDF/B-VI or JENDL data, but it still has self-consistency problems between the resonance region and the high energy region for the $^{55}Mn(n,\gamma)^{56}Mn$ reaction.

5.24 $^{55}Mn(n,2n)^{54}Mn$

The ENDF/B-VI $^{55}Mn(n,2n)^{54}Mn$ cross section represents a new evaluation and has been adopted in the IRDF-90 library. It was chosen for inclusion as a baseline cross section in the SNLRML library.

The ^{54}Mn decay half-life and gamma emission probabilities were taken from Lemmel [21] rather than the ENSDF compilation

5.25 $^{54}Fe(n,p)^{54}Mn$

The latest dosimetry-oriented $^{54}Fe(n,p)^{54}Mn$ cross section evaluation has been done by ORNL. Their evaluations have been included in the ENDF/B-VI library which has been, in turn, adopted by the IRDF-90. There are some slight differences between the ORNL GLUCS evaluations and the ORNL contribution to ENDF/B-VI. The differences arose in smoothing out unphysical features that resulted from the cross-reaction correlations used in the GLUCS evaluation. The SNLRML library will follow the IRDF-90 and ENDF/B-VI standards in its recommended cross section.

H. Vonach discovered that some of the GLUCS covariance matrices were singular. D. Hetrick traced the problem to the use of an ENDF/B-V covariance matrix that was not positive definite. The 1993 update to the GLUCS data provided new positive definite covariance matrices. The SNLRML library covariance matrix is taken from the 1993 GLUCS results. The next ENDF/B-VI release is expected to update the covariance matrix to the GLUCS 1993 results.

The ^{54}Mn decay half-life and gamma emission probabilities were taken from Lemmel [21] rather than the ENSDF compilation.

5.26 ^{56}Fe(n,p)^{56}Mn

The latest dosimetry-oriented ^{56}Fe(n,p)^{56}Mn cross section evaluation has been done by ORNL. This cross section appears in the GLUCS library and was adopted by the ENDF/B-VI and the IRDF-90 libraries. The SNLRML library reflects this community consensus.

This reaction is frequently used to measure fast-neutron fluences, especially near 14 MeV. This is the same energy range covered by the ^{27}Al(n,α) reaction. Use of the ^{56}Fe(n,p)^{56}Mn cross section is recommended in the energy range from 11 to 20 MeV [28]. The Activation Handbook 29 details some of the controversy over the ENDF/B-V cross section evaluation for this reaction. There was a belief that the uncertainty data may have been too low. The ENDF/B-VI evaluation appears to have answered most of the communities' concern. Since the ENDF/B-VI evaluation agrees with the GLUCS simultaneous evaluation and has been accepted in the IRDF-90 library, it appears that this reaction can be used as a reference.

H. Vonach discovered that some of the GLUCS covariance matrices were singular. D. Hetrick traced the problem to the use of a ENDF/B-V covariance matrix that was not positive definite. The 1993 update to the GLUCS data provided new positive definite covariance matrices. The SNLRML library covariance matrix is taken from the 1993 GLUCS results. The next ENDF/B-VI release is expected to update the covariance matrix to the GLUCS 1993 results.

5.27 ^{58}Fe(n,γ)^{59}Fe

The latest dosimetry-oriented ^{58}Fe(n,γ)^{59}Fe cross section has been evaluated by ORNL. This cross section was adopted by the ENDF/B-VI and the IRDF-90 libraries. The SNLRML library reflects this community consensus.

The previous ENDF/B-V dosimetry library evaluation for this reaction was inconsistent with other dosimetry sensors in the resonance energy region and could not typically be used in spectrum unfolding. The new ENDF/B-VI evaluation must still be used with great caution. Work at SNL has indicated that the ENDF/B-VI cross section is consistent for spectrum determinations of pool-type reactors, such as the ACRR central cavity, where the majority of the sensor response comes from the resonance region. However, for fast burst reactor spectra, such as the SPR-III central cavity, the sensor response is moved into the 0.200 to 2.5 MeV region and disagrees by 15%-30% with other foils in this region. The

new cross section is a significant improvement over the ENDF/B-V dosimetry data, but it still has problems in the high energy region and should not be used for routine dosimetry.

The consistency of the JENDL-3 $^{58}Fe(n,\gamma)^{59}Fe$ cross section with other dosimetry sensors is being evaluated. Initial examinations suggest that it has the same problem in fitting hard neutron spectra from fast-burst assemblies. A CENDL-2 evaluation exists but has not yet been analyzed.

5.28 $^{Nat}Fe(n,X)dpa$

This reaction is a commonly used exposure unit in the light-water reactor industry and is used in pressure vessel surveillance programs. The response data are taken directly from the ASTM E 693-79 standard [40]. As specified in the ASTM standard, these data are based on the ENDF/B-IV cross sections, the use of the Lindhard model of energy partition between atoms and electrons [41], and the IAEA recommended conversion of damage energy to displacements [42].

No covariance matrix is currently available for this reaction. If this sensor is treated as an exposure parameter and the response function is held constant by all users, then no uncertainty is attributed to the use of this response function. The uncertainty remains with regard to establishing a correlation between this exposure parameter and a particular damage mechanism.

5.29 $^{59}Co(n,p)^{59}Fe$

The new ENDF/B-VI cross section has been adopted in the SNLRML library. This cross section differs significantly from the previous ENDF/B-V activation library data for neutron energies above 10 MeV. The JENDL-3 cross section is very similar to the ENDF/B-VI evaluation.

5.30 $^{59}Co(n,\gamma)^{60}Co$

The ENDF/B-VI data were adopted by the IRDF-90 library and are used in the SNLRML library. Figure A-30b shows that there is some disagreement between the ENDF/B-VI and JENDL-3 libraries in resonance location and magnitude in the 3 - 10 keV energy region and significant disagreement above 1 MeV. Since most of the response to fission reactor spectra comes from the 0.1 keV resonance, which is identical in all evaluations, validation work from spectrum unfolding does not aid in choosing between these evaluations.

The ^{60}Co decay half-life and gamma emission probabilities were taken from Lemmel [21] rather than the ENSDF compilation.

5.31 $^{59}Co(n,\alpha)^{56}Mn$

The ENDF/B-VI data were adopted by the IRDF-90 library and are used in the SNLRML library. The ENDF/B-VI cross section is very similar to the ENDF/B-V cross section, but

deviates from the JENDL-3 evaluations near 14-MeV. Because of the low activity and high reaction threshold this reaction is not typically used at the SNL RML.

5.32 $^{59}Co(n,2n)^{58}Co$

The IRDF-90 cross section is adopted in the SNLRML library. There are small differences between recent ENDF/B-VI, JENDL-3 Dosimetry, and IRDF-90 evaluations. This reaction is not generally used at the SNL RML due to low activity; thus, we have adopted the IRDF recommendation.

Figure A-32b shows that the reaction threshold energy is significantly different in the JENDL-3 as compared to the IRDF-90 and ENDF/B-VI libraries.

The ^{58}Co decay half-life and gamma emission probabilities were taken from Lemmel [21] rather than the ENSDF compilation.

5.33 $^{58}Ni(n,p)^{58}Co$

The $^{58}Ni(n,p)^{58}Co$ reaction is very commonly used as a monitor for irradiations. The most recent dosimetry-oriented evaluation is from the ORNL GLUCS work. The low-energy (up to 6 MeV) GLUCS results were adopted by the ENDF/B-VI community. From 6 to 13 MeV, there was disagreement among the experimental data, and a compromise was adopted by the ORNL evaluators and the ENDF community. Above 13 MeV, calculations, confirmed by some measurements, were used. The IRDF-90 adopted the ENDF/B-VI evaluations. The JENDL-3 evaluation is very close to the ENDF/B-VI data.

There is a significant difference between the GLUCS work and the ENDF/B-VI at energies above 13 MeV. This is because the GLUCS work used a trial cross section taken from the ENDF/B-V Dosimetry File and had no sensors or cross-reaction correlation data to perturb the trial cross section.

H. Vonach discovered that some of the GLUCS covariance matrices were singular. D. Hetrick traced the problem to the use of a ENDF/B-V covariance matrix that was not positive definite. The 1993 update to the GLUCS data provided new positive definite covariance matrices. The SNLRML library covariance matrix is taken from the 1993 GLUCS results. The next ENDF/B-VI release is expected to update the covariance matrix to the GLUCS 1993 results.

The ^{58}Co decay half-life and gamma emission probabilities were taken from Lemmel [21] rather than the ENSDF compilation.

5.34 $^{58}Ni(n,2n)^{57}Ni$

The ENDF/B-VI cross section was adopted for use in the SNLRML library. This cross section is indistinguishable from that adopted by the IRDF-90 community. The JENDL-3 cross section is very close to ENDF/B-VI evaluation. Both JENDL-3 and ENDF/B-VI

have significantly larger cross sections above 14-MeV than is found in the ENDF/B-V Dosimetry Library.

5.35 $^{60}Ni(n,p)^{60}Co$

The ENDF/B-VI data were chosen for use in the SNLRML library. This cross section was also adopted for the IRDF-90 library. These data represent a significant shape change from the ENDF/B-V Dosimetry data and from the recently evaluated JENDL-3 data.

The ^{60}Co decay half-life and gamma emission probabilities for the 1925.5 d ground-state were taken from Lemmel [21] rather than the ENSDF compilation.

5.36 $^{63}Cu(n,\gamma)^{64}Cu$

The ENDF/B-VI evaluations were used in the SNLRML Library. The IRDF-90 community also adopted this evaluation. This represents only a small change from ENDF/B-V data. Both the ENDF/B-VI and ENDF/B-V evaluations were performed at ORNL. The high energy (above 0.1 MeV) JENDL-3 cross section shows significant deviations from the ENDF/B-VI data.

5.37 $^{63}Cu(n,2n)^{62}Cu$

The most recent dosimetry-oriented cross section evaluation for the $^{63}Cu(n,2n)^{62}Cu$ reaction is found in the GLUCS work. This evaluation was adopted by the ENDF/B-VI. Figure A-37b shows that the IRDF-90 recommendation differs only slightly from the ENDF/B-VI evaluation. The IRDF-90 release contains the ENDF/B-VI $^{63}Cu(n,2n)^{62}Cu$ evaluation as well as the IRK recommendation.

5.38 $^{63}Cu(n,\alpha)^{60}Co$

The most recent dosimetry-oriented evaluation of the $^{63}Cu(n,\alpha)^{60}Co$ reaction is found in the GLUCS work. The GLUCS evaluation was adopted by ENDF/B-VI and IRDF-90 communities. This cross section represents a significant shape change over the ENDF/B-V Dosimetry cross section.

Data at SNL for fast fission spectra conflict with this measured activity. The reaction is currently being studied.

H. Vonach discovered that some of the GLUCS covariance matrices were singular. D. Hetrick traced the problem to the use of an ENDF/B-V covariance matrix that was not positive definite. The 1993 update to the GLUCS data provided new positive definite covariance matrices. The SNLRML library covariance matrix is taken from the 1993 GLUCS results. The next ENDF/B-VI release is expected to update the covariance matrix to the GLUCS 1993 results.

The ^{60}Co decay half-life and gamma emission probabilities were taken from Lemmel [21] rather than the ENSDF compilation.

5.39 $^{65}Cu(n,2n)^{64}Cu$

The most recent dosimetry-oriented evaluation of the $^{65}Cu(n,2n)^{64}Cu$ reaction is found in the GLUCS work. The GLUCS (n,2n) reaction evaluation was adopted by ENDF/B-VI with some smoothing near 20 MeV. The JENDL-3 and ENDF/B-V Dosimetry data are nearly identical to the ENDF/B-VI results.

H. Vonach discovered that some of the GLUCS covariance matrices were singular. D. Hetrick traced the problem to the use of an ENDF/B-V covariance matrix that was not positive definite. The 1993 update to the GLUCS data provided new positive definite covariance matrices. The SNLRML library covariance matrix is taken from the 1993 GLUCS results. The next ENDF/B-VI release is expected to update the covariance matrix to the GLUCS 1993 results.

5.40 $^{64}Zn(n,p)^{64}Cu$

The most recent dosimetry-oriented evaluation comes from the IRDF-90 community. There is no ENDF ^{64}Zn evaluation. The JEF-2.2 and JENDL-3 reaction evaluations show a significantly different shape in the 5 to 10 MeV energy region.

The IRDF-90 cross section is similar to the IRDF-82 data. The $^{64}Zn(n,p)^{64}Cu$ reaction is routinely used in spectrum unfolds at SNL and is consistent with other high energy (sensitive in the 2 to 7 MeV region) reactions.

5.41 $^{90}Zr(n,2n)^{89}Zr$

ENDF/B-VI adopted the older ENDF/B-V zirconium cross section evaluation. The recommended dosimetry cross section comes from the IRDF-90 library. The JENDL-3, ENDF/B-V, IRDF-82, and IRDF-90 cross sections for $^{90}Zr(n,2n)^{89}Zr$ are all very similar.

5.42 GaAs(n,X)1MeV

GaAs 1-MeV equivalent damage is frequently requested as an exposure parameter in the testing of radiation-hardened electronics. The ASTM E 722-93 standard [35] has recently adopted a GaAs damage function. This damage function is not identical to the GaAs displacement kerma, but includes a semi-empirical primary knock-on atom (PKA) energy-dependent efficiency factor that was determined from comparisons of device damage in fission, DD, and DT neutron spectra. The SNLRML library has adopted the ASTM recommended damage factor. The origin of this damage factor is discussed by Griffin [43].

The GaAs displacement kerma was calculated with the NJOY code [34], version 91.38. RECONR was used to do resonance reconstruction at 300 K, and GROUPR was used to collapse the kerma components to a 640 group energy structure using a weighting function

(IWT=4) that included a thermal Maxwellian tail (with a 0.1 eV thermal break and a 0.025 eV thermal temperature), a 1/E scattering component, and a fission component (with a fission break point of 0.1 MeV and a fission temperature of 1.4 MeV). A 10 eV threshold damage energy was used to partition the displacement and electronic damage energies. Modifications were made to the NJOY code to incorporate the PKA-energy dependent damage efficiency term in the DF function subroutine. This damage efficiency function is shown in Figure 2.

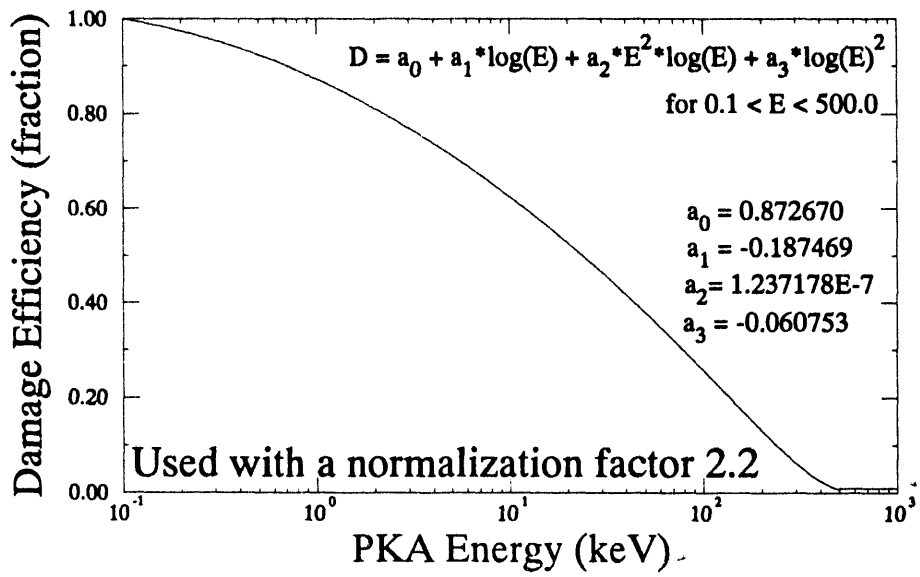

Figure 2. GaAs PKA-Energy-Dependent Damage Efficiency Function

The ENDF/B-VI ^{Nat}Ga cross section was used for gallium. The ENDL ^{75}As cross section evaluation was used for arsenic. The ENDF/B-VI ^{75}As file does not contain the gamma production data. In order to subtract out the energy that goes into gammas from that available for atomic displacements, the ENDL evaluation was used. Figure A-42c shows the differences between the ENDF/B-VI and ENDL displacement kermas. Figure A-42d compares the displacement kerma and the kinematic kerma limit for ENDF/B-VI and ENDL evaluations of ^{75}As. Some problems are seen with the energy balance for ENDL evaluation at low neutron energies (as evidenced by the displacement kerma exceeding the kinematic kerma limit). However, the importance of subtracting the photon energy is seen by the difference between the kinematic kerma limit and the displacement kerma for energies above 100 keV. The SNLRML library cross section selection preserves the fidelity of the high energy displacement kerma since the major part of the GaAs device damage for typical fission spectra comes from neutron energies above 100 keV.

5.43 $^{93}Nb(n,\gamma)^{94}Nb$

The ENDF/B-VI $^{93}Nb(n,\gamma)^{94}Nb$ evaluation was chosen for inclusion in the SNLRML library. This is not a reaction used at the SNL RML for routine spectrum unfolds. The major difference between the ENDF/B-VI, ENDF/B-V, JEF-2.2, and JENDL-3 evaluations is in the depth of the resonances in the 0.01 to 1 keV region. The resonance peaks are very similar.

5.44 $^{93}Nb(n,2n)^{92m}Nb$

The IRDF-90 cross section for the $^{93}Nb(n,2n)^{92m}Nb$ reaction was adopted in the SNLRML library. The IRDF-90 cross section is based on Strohmaier's work [16] and shows considerable differences from the earlier DOSCROS84 cross sections.

The ENDF, JENDL-3, and BROND evaluations give the total reaction cross section but do not separate the component that populates the metastable state. The DOSCROS84 results used the ENDF/B-V data and a population ratio of 0.4 to describe the excitation of the metastable state. It was not felt that this excitation ratio could be separated from the cross section for which it was derived.

The JENDL-3 Dosimetry Library does identify the (n,2n) cross section that populates the ^{92m}Nb state and is very similar to the IRDF-90 cross section.

An updated $^{93}Nb(n,2n)^{93m}Nb$ cross section evaluation has been performed by Wagner [17]. This new evaluation changes the cross section below 13 MeV, so that it more closely agrees with the JENDL Dosimetry evaluation, but leaves the cross section above 13 MeV very similar to the IRDF-90 evaluation. As soon as the cross section evaluation becomes available to the authors it will replace the IRDF-90 entry in the SNLRML library. It is expected that the new Wagner evaluation will be incorporated in the IRDF-93 library.

5.45 $^{93}Nb(n,n')^{93m}Nb$

The ENDF/B-VI cross section did not initially include the (n,n') contribution to the metastable state. The cross sections to the individual inelastic excited states were given, but a unique branching ratio to the metastable state is not given. Figure A-45b compares the (n,n') cross section for the first inelastic state for several cross section evaluations. Figure A-45c shows that even if the ENSDF nuclear structure information is used to provide the metastable state branching ratios for the ENDF/B-VI-modeled discrete inelastic states, the inelastic continuum contribution to the metastable state cannot be properly modeled. A pre-release ENDF/B-VI cross section is available that contains the cumulative (n,n') contribution to the metastable state in a comment section. These data are expected to be incorporated into File 8 in the next ENDF/B-VI release.

The IRDF-90 cross section was selected as the recommended description of this cross section. This decision is based on the discussion of the $^{93}Nb(n,n')^{93m}Nb$ cross section

by Strohmaier [44]. Figure A-45a shows that the IRDF-82 cross section is very close to the ENDF/B-VI pre-release cross section and the JENDL-3 Dosimetry cross section.

The ^{93m}Nb decay half-life and the K_α x-ray decay energy and yield were taken from Lemmel [21] rather than the ENSDF compilation. Note that, in accordance with Lemmel [21], the K_α x-ray line includes both the $K_{\alpha 1}$ and $K_{\alpha 2}$ lines. The gamma decay energy and yield were taken from the ENSDF.

5.46 ^{98}Mo(n,γ)^{99}Mo

The ^{98}Mo(n,γ)^{99}Mo reaction is not typically used at SNL for spectrum unfolds. Previous attempts to use this reaction have shown that it did not agree with other dosimetry reactions. This reaction is not typically considered a dosimetry-quality cross section and covariance matrices for this reaction are not available to the authors.

The ENDF/B-VI library adopted the ENDF/B-V activation tape evaluation. The SNLRML library adopted the most recent evaluation, the JENDL-3 evaluation completed in August 1989, for inclusion in the library.

5.47 ^{103}Rh(n,n')^{103m}Rh

The ^{103}Rh(n,n')^{103m}Rh reaction decays with a very soft gamma that requires a thin window on the gamma counter. This reaction is not used at the SNL RML.

The IRDF-90 library provides the recommended cross section information. These data were incorporated into the SNLRML library. The ENDF/B-VI library adopted the ENDF/B-V fission product data and does not provide branching ratios for determining the final metastable state population. The JENDL-3 Dosimetry evaluation is adopted from the IRDF-85 data.

5.48 ^{109}Ag(n,γ)^{110m}Ag

The ENDF/B-VI data were adopted from the ENDF/B-V fission product tape. None of the standard evaluations report the branching ratios to the metastable state. The DOSCROS84 library is based on the ENDF/B-V activation tape cross section and uses a branching ratio of 5.299×10^{-2} from Zijp [45]. The DOSCROS84 data for this reaction are used in the SNLRML library. A new CENDL-2 evaluation of this reaction is available [57] but has not yet been analyzed. This evaluation will be considered in future versions of the SNLRML Library.

5.49 ^{Nat}Cd(n,abs)

Cadmium is used as an activation foil cover material. The thermal cross section below 0.2 eV is largely eliminated when a foil is covered with this material. The ENDF/B-VI cross section was taken from the ENDF/B-V library and only includes the (n,γ), (n,p), and (n,α) reactions. The JENDL-3 elemental cadmium evaluation was used in preparing the SNLRML library cover cross section since it includes many other absorption cross section

components. The (n,γ) contribution provides all of the significant thermal-energy attenuation. The other reactions have a significant contribution only for high neutron energies and are typically not important. Figures A-49b and A-49c show the JENDL-3 absorption cross section components.

See section 5.1 for cautions in the application of cover cross sections.

5.50 $^{115}In(n,\gamma)^{116m}In$

The ENDF/B-VI $^{115}In(n,\gamma)^{116m}In$ cross sections were chosen for inclusion in the SNLRML library. This cross section is identical to the ENDF/B-V Dosimetry Library cross section.

The JENDL-3 Dosimetry Library cross section is seen in Figure A-50a to differ slightly from the ENDF/B-VI. The data below 2 keV were calculated from resonance parameters determined by experiment and reported in the JENDL-3 Fission Product nuclear data file.

The SNL RML had stopped using this reaction because it conflicts with other well known cross sections, such as that for the $^{197}Au(n,\gamma)^{198}Au$ reaction, in the thermal energy region. Self-shielding effects in indium may be the cause of the disagreements. The SNL RML has not found a readily available source for dilute indium foils.

5.51 $^{115}In(n,n')^{115m}In$

The SNLRML library has incorporated the $^{115}In(n,n')^{115m}In$ cross section from the IRDF-90. This cross section is identical to a private communication* from the ENDF/B-VI evaluators. The officially released ENDF/B-VI data shows slight differences from these two cross sections.

New $^{115}In(n,n')^{115m}In$ data should have appeared in the ENDF/B-VI cross sections, but were left out due to a miscommunication with the evaluators. The IRDF-90 library compilers went directly to the ENDF material evaluator for a pre-release version of the cross section and were not aware of the miscommunications. This situation should be remedied in release 3 of ENDF/B-VI.

As is shown in Figure A-51a, an analyst must be careful in determining all inelastic contributions to a metastable state. The ENDF/B-V Fission Product Data Tape reports cross sections for several discrete inelastic states but does not report branching ratios to the metastable state. If one took the cross section for excitation to any single discrete inelastic state, the population of the metastable state would be severely underestimated.

*D. L. Smith, Argonne National Laboratory, private communication to P. J. Griffin in October 1992. Contents included a letter and a floppy disk.

5.52 $^{127}I(n,2n)^{126}I$

The $^{127}I(n,2n)^{126}I$ cross section in the SNLRML library was taken from the ENDF/B-VI cross sections. The ENDF/B-VI cross section was adopted from the ENDF/B-V data. This cross section was also used in the IRDF-82 library.

JEF 2.2 and JENDL-3 Dosimetry cross sections are shown in Figure A-52a. The JENDL-3 Dosimetry cross section was calculated from preequilibrium and multi-step evaporation models and normalized to experimental data at 14.5 MeV. A CENDL-2 evaluation is also available, but has not yet been analyzed.

Most of the $^{127}I(n,2n)^{126}I$ response comes from neutrons with energies above 10 MeV. The work at SNL with fission neutron spectra has not used this dosimetry reaction.

5.53 $^{197}Au(n,p)^{197}Pt$

The $^{197}Au(n,p)^{197}Pt$ cross section is taken from the ENDF/B-VI library. The (n,p) reaction in ENDF/B-VI was taken from the ENDF/B-V evaluations. The DOSCROS84 library used the ENDF/B-V cross section. This is not a commonly used dosimetry cross section and is not found in the IRDF-90 or JENDL-3 Dosimetry libraries.

5.54 $^{197}Au(n,\gamma)^{198}Au$

The ENDF/B-VI $^{197}Au(n,\gamma)^{198}Au$ cross section is considered a standard cross section for energies below 2.5 MeV. Above 2.5 MeV, calculations and experimental data were used to determine the cross section. Since this is considered an ENDF community standard, it was adopted in the SNLRML library. The IRDF-90 library uses the ENDF/B-VI data. The Activation Handbook [28] recommends use of this reaction as a standard in the energy range from 0.2 to 3.5 MeV. A recent publication [30] recommends use of this reaction as a CSEWG standard for energies from 0.2 to 2.5 MeV.

The JEF 2.2 library states that it used the ENDF/B-V MAT=1379 (n,γ) cross section and replaced it by the ENDF/B-VI data in May 1989. Despite this comment, the cross section above 2 MeV disagrees with the ENDF/B-VI revision 1 data. The JEF 2.2 cross section appears identical to the ENDF/B-V Dosimetry library at high energies.

The covariance matrix used in the SNLRML library is that from the pre-release ENDF/B-VI library. This is also what is reported in the IRDF-90 library. See section 5.2 for a discussion of covariances for ENDF standard cross sections.

The ^{198}Au decay half-life and 411.8044 keV decay yield were taken from Lemmel [21] rather than the ENSDF compilation

5.55 $^{197}Au(n,2n)^{196}Au$

The IRDF-90 $^{197}Au(n,2n)^{196}Au$ cross section was incorporated into the SNLRML library. These data differ slightly from the ENDF/B-V Activation Library data and significantly from the ENDF/B-VI data. This choice in cross section was made based on the cross section evaluation date. The IRDF-90 evaluation cites an April 1990 evaluation date, while the main ENDF/B-VI evaluation cites a January 1984 evaluation date with a minor revision of a Q-value in July 1991. The ENDF/B-VI cross section shape is largely determined by calculations.

5.56 $^{197}Au(n,3n)^{195}Au$

The $^{197}Au(n,3n)^{195}Au$ cross section from the ENDF/B-VI evaluation was incorporated into the SNLRML library. This cross section shows significant changes in magnitude near threshold when compared to the ENDF/B-V Activation File data.

5.57 $^{Nat}Au(n,abs)$

The ENDF/B-VI ^{197}Au evaluation was used to determine the gold cover absorption cross section. The (n,γ), (n,p) and (n,α) cross section components were included in the absorption term. Figure A-57b shows many of the high threshold cross section components for ^{197}Au.

See section 5.1 for cautions in the application of cover cross sections

5.58 $^{232}Th(n,\gamma)^{233}Th$

The $^{232}Th(n,\gamma)^{233}Th$ cross section from ENDF/B-VI is used in the SNLRML library. The IRDF-90 library adopted the same ENDF/B-VI cross section. Figure A-58a compares the ENDF/B-VI cross section with that used in the JEF 2.2 and JENDL-3 libraries.

5.59 $^{232}Th(n,2n)^{231}Th$

The $^{232}Th(n,2n)^{231}Th$ cross section from ENDF/B-VI is used in the SNLRML library. The IRDF-90 library does not include this reaction. Figure A-59a compares the ENDF/B-VI cross section with that used in the JEF 2.2 and JENDL-3 libraries.

5.60 $^{232}Th(n,f)F.P.$

The ENDF/B-VI thorium fission cross section has been included in the SNLRML library. The IRDF-90 library also uses the ENDF/B-VI fission cross section. Figure A-60a shows that there are moderate differences in the threshold energy for thorium fission.

5.61 $^{235}U(n,f)F.P.$

The ENDF/B-VI ^{235}U fission cross section is considered a standard cross section at thermal energies and in the energy region from 0.1 to 20 MeV [29]. A recent publication [30]

recommends this reaction as a standard for energies above 150 keV. Since this is considered an ENDF community standard, it was adopted in the SNLRML library. The IRDF-90 library also uses the ENDF/B-VI data.

See the discussion in section 5.2 on the use of a covariance matrix for ENDF/B-VI standard cross sections.

5.62 ^{238}U(n,f)F.P.

The ENDF/B-VI ^{238}U fission cross section is considered a standard cross section. The data from 0.3 to 20 MeV were taken from the simultaneous standards analysis [46]. Since this is considered an ENDF community standard, it was adopted in the SNLRML library. The IRDF-90 library also uses the ENDF/B-VI data.

The ENDF/B-VI ^{238}U fission cross section is indistinguishable from the GLUCS results at high energy (above 2 MeV). The GLUCS results do not extend to low energy. Figures A-62b and A-62c show that there is considerable variation in the various evaluations for resonance region and thermal energy fission cross sections.

See the discussion in section 5.2 on the use of covariance matrix for ENDF/B-VI standard cross sections.

5.63 ^{237}Np(n,f)F.P.

The SNLRML library incorporated the ENDF/B-VI ^{237}Np fission cross section. The IRDF-90 library also incorporated this fission cross section evaluation. Substantial differences in the resonance region cross section (0.1 eV to 10 keV) can be seen in Figure A-63b. A new fission cross section evaluation is underway at Los Alamos National Laboratory and may be available for future versions of the SNLRML Library. A CENDL-2 evaluation also exists, but has not been analyzed at this time.

5.64 ^{239}Pu(n,f)F.P.

The ENDF/B-VI ^{239}Pu fission cross section has been incorporated into the SNLRML library. This cross section evaluation is also used in the IRDF-90 library.

Covariance matrices for the ^{239}Pu fission reaction are only found in the ENDF/B-V and JENDL-3 Dosimetry libraries. Unfortunately, the covariance matrix in the ENDF/B-V library is presented as a ratio to a standard material covariance matrix and the NJOY processing system has a problem handling the data. The SNLRML library has incorporated the JENDL-3 Dosimetry library covariance matrix which is based on the IRDF-85 covariance matrix.

5.65 ^{241}Am(n,f)F.P.

The ENDF/B-VI ^{241}Am fission cross section has been incorporated into the SNLRML library. The IRDF-90 library no longer contains this reaction for dosimetry applications.

Covariance matrices for the ^{241}Am fission reaction are only found in the ENDF/B-VI and JENDL-3 Dosimetry libraries. The JENDL-3 Dosimetry cross section is taken from ENDF/B-VI. Since this ENDF/B-VI covariance matrix is stored as a ratio to a standard material, ^{235}U, and since the ^{235}U covariance matrix has been eliminated from the ENDF/B-VI cross section pending further study (see section 5.2 on a covariance matrix for standard materials), the SNLRML library took the data from the JENDL-3 Dosimetry library. Note that this covariance matrix is presumably based on the ^{235}U standard material uncertainty which is currently under review by the CSWEG community and should be treated with caution.

5.66 RML Enriched Uranium Fission Foil

The RML enriched uranium fission foil sensor is very similar to the ^{235}U fission cross section in section 5.61. This sensor is intended to model the exact fission foil composition in use at the SNL RML for dosimetry applications. The ^{234}U, ^{236}U, and ^{238}U contaminant fission cross sections are modeled. The contaminant fission reactions only have a small effect which is shown in Figure A-66b.

Note that the atom fractions (primary isotope and contaminants) shown in Table A-66 are all normalized to one atom of elemental uranium. It is expected that the dosimetry counting laboratory also reports fissions per uranium atom rather than per ^{235}U atom.

The correct fission yields for interpreting the dosimetry of this foil depend upon the relative fissions produced in each fissionable component of the dosimeter. Tables 5 and 6 show the relative division of fissions between the dosimeter components for the SPR-III central cavity (spectrum SPR3CAV18) and the Annular Core Research Reactor central cavity (spectrum ACF9) for bare and covered foils. The B_4C-covered numbers were used to weight the isotopic fission yields and to derive the dosimeter fission yields reported in Table C-1 of Appendix C.

Table 5. Fission in RML Enriched Fission Foil

Fissionable Isotope	SPR3CAV18		ACF9	
	Fission Cross Section (barns)*	Relative Fission Density (%)	Fission Cross Section (barns)*	Relative Fission Density (%)
^{235}U	1.31674	98.492%	42.95543	99.972%
^{234}U	8.9154E-3	0.667%	5.20369E-3	0.012%
^{236}U	1.2784E-3	0.096%	1.238854E-3	0.003%
^{238}U	9.9631E-3	0.745%	5.46716E-3	0.013%
Total	1.3368969	100%	42.9673397	100%

*results normalized to one atom of the predominant isotope and averaged over the indicated fission spectrum.

Table 6. Fission in B_4C-Covered RML Enriched Fission Foil

Fissionable Isotope	SPR3CAV18		ACF9	
	Fission Cross Section (barns)*	Relative Fission Density (%)	Fission Cross Section (barns)*	Relative Fission Density (%)
^{235}U	1.14300	98.344%	0.89079	99.883%
^{234}U	8.5014E-3	0.7315%	0.45261E-3	0.0507%
^{236}U	1.22495E-3	0.1054%	0.68585E-4	0.0077%
^{238}U	9.51989E-3	0.8191%	0.52187E-3	0.0586%
Total	1.62246	100%	0.89183	100.%

*results normalized to one atom of the predominant isotope and averaged over the indicated fission spectrum.

5.67 RML Depleted Uranium Fission Foil

The RML depleted uranium fission foil sensor is very similar to the ^{238}U fission cross section in section 5.62. This sensor is intended to model the exact fission foil composition in use at the SNL RML for dosimetry applications. The ^{234}U, ^{236}U, and ^{238}U contaminant fission cross sections are modeled. The contaminant fission reactions are important for neutrons with an energy less than 0.5 MeV as shown in Figures A-67a and A-67b. Since the SNL RML typically fields fission foils in a boron ball, the thermal fission cross section is suppressed and thus the effect of the ^{235}U contaminant is suppressed.

Note that the atom fractions (primary isotope and contaminants) shown in Table A-67 are all normalized to one atom of elemental uranium. It is expected that the dosimetry counting laboratory also reports fissions per uranium atom rather than per ^{238}U atom.

The correct fission yields for interpreting the dosimetry of this foil depend upon the relative fissions produced in each fissionable component of the dosimeter. Tables 7 and 8 show the relative division of fissions between the dosimeter components for the SPR-III central cavity (spectrum SPR3CAV18) and the Annular Core Research Reactor central cavity (spectrum ACF9) for bare and covered foils. The B_4C-covered numbers were used to weight the isotopic fission yields and to derive the dosimeter fission yields reported in Table C-1 of Appendix C.

Table 7. Fission in RML Depleted Fission Foil

Fissionable Isotope	SPR3CAV18		ACF9	
	Fission Cross Section (barns)*	Relative Fission Density (%)	Fission Cross Section (barns)*	Relative Fission Density (%)
^{235}U	2.705E-3	1.624%	0.088243	49.523%
^{234}U	8.469E-6	0.005%	4.943E-6	0.003%
^{236}U	1.327E-5	0.008%	1.2864E-5	0.007%
^{238}U	0.16386	98.363%	0.899247E-1	50.467%
Total	0.166586739	100%	0.178185507	100%

*results normalized to one atom of the predominant isotope and averaged over the indicated fission spectrum.

Table 8. Fission in B_4C-Covered RML Depleted Fission Foil

Fissionable Isotope	SPR3CAV18		ACF9	
	Fission Cross Section (barns)*	Relative Fission Density (%)	Fission Cross Section (barns)*	Relative Fission Density (%)
^{235}U	2.3481E-3	1.477%	0.182995E-3	0.2127%
^{234}U	8.0757E-6	0.005%	4.2994E-6	0.005%
^{236}U	1.2714E-5	0.008%	0.712174E-5	0.0083%
^{238}U	0.15657	98.510%	0.85839E-1	99.774%
Total	0.158939	100%	0.860334E-1	100%

*results normalized to one atom of the predominant isotope and averaged over the indicated fission spectrum.

5.68 RML Plutonium Fission Foil

The RML plutonium fission foil sensor is very similar to the ^{239}Pu fission cross section in section 5.64. This sensor is intended to model the exact fission foil composition in use at the SNL RML for dosimetry applications. The ^{239}Pu, ^{238}Pu, ^{240}Pu, ^{241}Pu, ^{242}Pu, ^{235}U, and ^{237}Np contaminant fission cross sections are modeled. The ^{240}Pu contaminant fission reaction has a moderate effect which is shown in Figure A-68b.

Note that the atom fractions (primary isotope and contaminants) shown in Table A-68 are all normalized to one atom of elemental plutonium. It is expected that the dosimetry counting laboratory also reports fissions per plutonium atom rather than per ^{239}Pu atom.

The correct fission yields for interpreting the dosimetry of this foil depend upon the relative fissions produced in each fissionable component of the dosimeter. Tables 9 and 10 show the relative division of fissions between the dosimeter components for the SPR-III central cavity (spectrum SPR3CAV18) and the Annular Core Research Reactor central cavity (spectrum ACF9) for the bare and covered foils. The B_4C-covered numbers were used to weight the isotopic fission yields and to derive the dosimeter fission yields reported in Table C-1 of Appendix C.

Table 9. Fission in RML Plutonium Fission Foil

Fissionable Isotope	SPR3CAV18		ACF9	
	Fission Cross Section (barns)*	Relative Fission Density (%)	Fission Cross Section (barns)*	Relative Fission Density (%)
^{239}Pu	1.80643	92.478%	94.43105	98.599%
^{238}Pu	1.2477E-3	0.064%	1.800E-3	0.002%
^{240}Pu	0.12096	6.192%	7.6616E-2	0.080%
^{241}Pu	2.25035E-2	1.152%	1.2549396	1.310%
^{242}Pu	1.9687E-3	0.101%	1.089468E-3	0.001%
^{235}U	2.3237E-4	0.012%	7.580559E-3	0.008%
^{237}Np	2.3138E-5	0.001%	1.2607E-5	0.000%
Total	1.953365408	100%	95.77308823	100%

*results normalized to one atom of the predominant isotope and averaged over the indicated fission spectrum.

Table 10. Fission in B_4C-Covered RML Plutonium Fission Foil

Fissionable Isotope	SPR3CAV18		ACF9	
	Fission Cross Section (barns)*	Relative Fission Density (%)	Fission Cross Section (barns)*	Relative Fission Density (%)
^{239}Pu	1.55678	92.9058%	1.01725	92.7119%
^{238}Pu	1.1689E-3	0.0698%	0.68259E-3	0.0622%
^{240}Pu	0.11540	6.8869%	6.3513E-2	5.7886%
^{241}Pu	0.189223E-2	0.1129%	1.45695E-2	1.3279%
^{242}Pu	0.188506E-3	0.0113%	1.031693E-3	0.0940%
^{235}U	2.0171E-4	0.0120%	1.57202E-4	0.0143%
^{237}Np	2.21268E-5	0.0013%	1.19159E-5	0.0011%
Total	1.67565	100%	1.097216	100%

*results normalized to one atom of the predominant isotope and averaged over the indicated fission spectrum.

5.69 ^{32}S-3MEV as Measured In ^{252}Cf Field

The $^{32}S(n,p)^{32}P$ activity is typically measured on a β counting system that was calibrated with a flux transfer from an NIST ^{252}Cf irradiation. If the dosimetry counting laboratory reports an activity rather than a ^{252}Cf equivalent neutron fluence exposure, it has assumed a $^{32}S(n,p)^{32}P$ dosimetry cross section and a ^{252}Cf fission neutron spectrum. If the counting laboratory did not assume the same dosimetry cross section in calculating its activity as is used in a spectrum unfold/adjustment, then a systematic bias of up to 10% can be introduced. To avoid this problem, this ^{252}Cf 3-MeV equivalent fluence was introduced into the SNLRML library.

The cross section and covariance matrix for this sensor are identical to that for $^{32}S(n,p)^{32}P$. When this dosimetry library is interfaced with a spectrum unfold/adjustment code, the computer code should use the spectrum averaged $^{32}S(n,p)^{32}P$ cross section for ^{252}Cf fission neutrons and the fraction of the ^{252}Cf neutron spectrum which has a neutron energy greater than 3 MeV to convert the $^{32}S(n,p)^{32}P$ cross section into a fluence sensor. If the reader is using the ^{252}Cf fission spectrum that is recommended in the ENDF/B-VI library (ENDF/B-VI Tape 200, MAT=9861, MT=18, MF=5), then these values are:

$$\langle\sigma\rangle_{252Cf\text{-}avg} = \quad 0.070229 \text{ b}$$

$$\Phi(> 3\text{-MeV}) = \quad 0.2368 \text{ n/cm}^2$$

The true sensor response is given by the $^{32}S(n,p)^{32}P$ cross section presented in this library multiplied by the Φ(>3-MeV) and divided by $\langle\sigma\rangle_{252Cf\text{-}avg}$. For the above values, the true sensor response is given by the SNLRML library tabulated values multiplied by 3.3718. The ENDF/B-VI ^{252}Cf fission neutron spectrum is shown in Figure A-69b.

6. LIBRARY FORMAT

The following subsections define the format of the SNLRML library. All information is provided in ASCII format to facilitate library portability. The library format was designed to provide all of the information required by either iterative unfolding codes, such as SAND-II, or least-squares adjustment codes, such as LSL-M2. This library should be easily interfaced with either type of code. The input format consists of blank-delimited free-field quantities compatible with the SAND-II VIF input processor. The following subsections give a recommended fixed-format description of the fields (e.g. F15.7 or I10), but this fixed-format is a recommendation and not a requirement for the library format.

6.1 Card Set 1: Title Cards

All title cards have the letter "t" in column 1. The cards are read with a character A80 format. The title cards provide information on the version of the library, the latest revision

date, and information on what has been changed in the library. There is no limit to the number of title cards in the library. The title/comment cards must all appear at the beginning of the file.

6.2 Card Set 2: Cover Cross Sections

This set of cards describes the cross sections for the cover materials available within the SNLRML library. The order of cards within this card-set is one card of type 2-1, followed by N_c sets of cards, where N_c is defined by the type 2-1 card. Each of the N_c sets of cards consists of one card of type 2-2, one of 2-3, one of 2-4, one set of type 2-A, and one card set of type 2-5.

6.2.1 Card 2-1: Number of Covers

Card appearance: N_c COVERS

Card variables: N_c = number of cover materials.

Card read format: free format integer field (I5) followed by keyword.

6.2.2 Card 2-2: Cover ID

Card appearance: *cov_name, library, MAT, t* K

Card variables:

cov_name	=	4 letter abbreviation for cover cross section.
library	=	cross section library from which the evaluation was drawn.
MAT	=	cross section material number.
t	=	NJOY processing temperature in degrees Kelvin.

Card read format: free format mixed fields (Hollerith string, Hollerith string, integer, integer).

6.2.3 Card 2-3: Cover Label

Card appearance: *reaction_name, elemental_mass, decay_time, abundance, fission_fraction*

Card variables:

reaction_name	=	4 letter abbreviation for cover cross section.
elemental_mass	=	mass of naturally occurring element (in amu).
decay_time	=	dummy field for cover materials, set equal to 1.0.
abundance	=	naturally occurring abundance of isotope. In the case of special damage sensors this field represents the 1-MeV(material) reference displacement kerma.
fission_fraction	=	dummy field for cover materials, set equal to 1.0.

Card read format: blank delimited Hollerith field (4A4).
free format floating point field (F10.5).
free format floating point field (F10.5).
free format floating point field (F10.5).
free format floating point field (F10.5).

6.2.4 Card 2-4: Energy Grid

Card appearance: *Elow, Ehigh*

Card variables:
- *Elow* = number of first non-zero cross section value in SAND-II 640 energy group structure (from low to high energy).
- *Ehigh* = number of last non-zero cross section value in SAND-II 640 energy group structure.

Card read format: free format integer fields (2I5).

6.2.5 Card Set 2-A: Cover Cross Section

Card appearance: $xsec_i$, $i = Elow, Ehigh$

Card variables:
- $xsec_i$ = value of cross section at the i^{th} energy point in the SAND-II 640 energy group structure.

Card read format: free format floating point fields (5E15.7).

6.2.6 Card Set 2-5: Covariance Data Label

Card appearance: COR *library, MAT, t* K

Card variables:
- *library* = cross section library from which the evaluation was drawn. If *library* = NULL, covariance matrix is not available and this card set is finished.
- *MAT* = cross section material number.
- *t* = NJOY processing temperature in degrees Kelvin.

Card read format: free format fields (A8, I4, I2).

Covariance matrix is not typically given for the cover materials in the SNLRML library. If the *library* field is not NULL, then see Card Set 3-B for the cards that will follow this header card.

6.3 Card Set 3: Sensor Cross Sections

This set of cards describes the cross sections for the sensors available within the SNLRML library. The order of cards within this card-set is one card of type 3-1, followed by N_c sets of cards, where N_c is defined by the type 3-1 card. Each of the N_c sets of cards consists of one card of type 3-2, one of 3-3, one of 3-4, one set of type 3-A, one card set of type 3-5, and one set of type 3-B. The type 3-B card set consists of a 3-6, 3-7, 3-8, 3-9, 3-10 card set.

6.3.1 Card 3-1: Number of Dosimetry Sensors

Card appearance: N_c FOILS

Card variables: N_c = number of sensors.

Card read format: free format integer field (I5).

6.3.2 Card 3-2: Reaction ID

Card appearance: *cov_name, library, MAT, t* K

Card variables:

cov_name	=	4 letter abbreviation for sensor cross section.
library	=	cross section library from which the evaluation was drawn.
MAT	=	cross section material number.
t	=	NJOY processing temperature in degrees Kelvin.

Card read format: free format (character string, character string, integer, integer).

6.3.3 Card 3-3: Reaction Label and Nuclear Data

Card appearance: *reaction_name, elemental_mass, decay_time, abundance, fission_fraction*

Card variables:

reaction_name	=	16 character abbreviation for the reaction.
elemental_mass	=	mass of naturally occurring element.
decay_time	=	decay constant, λ, in units of sec^{-1}. If value is negative, then the *decay_time* represents a half-life in units of hours.
abundance	=	naturally occurring abundance of isotope. In the case of special damage sensors this field represents the 1-MeV(material) reference displacement kerma.
fission_fraction	=	fission fraction for the material modeled. Since the RML reports all fission foil sensors in units of fissions per atom of primary sensor material and since this is the way the SNLRML library cross sections are constructed, this quantity is 1.0 for all current sensors.

Card read format: blank delimited Hollerith field (4A4).
free format floating point field (F10.5).
free format floating point field (F10.5).
free format floating point field (F10.5).
free format floating point field (F10.5).

6.3.4 Card 3-4: Energy Grid

This card set defines the energy grid used to provide cross section data. See section 6.2.4 for a description of the format and content of this field.

6.3.5 Card Set 3-A: Cross Section

This card set defines the cross section for the dosimetry sensor. See section 6.2.5 for a description of the format and content of this field.

6.3.6 Card Set 3-5: Covariance Data Label

Card appearance: COR *library, MAT, t* K

Card variables:

library	=	cross section library from which the evaluation was drawn. If *library* = NULL, covariance matrix is not available.
MAT	=	cross section material number.
t	=	NJOY processing temperature in degrees Kelvin.

Card read format: free format fields (A8, I4, I2).

6.3.7 Card Set 3-B: Covariance Data

The cards described in sections 6.3.7.1 through 6.3.7.5 (Card Sets 3-6 through 3.10) describe the covariance matrix for this cross section. Each card set contains a header card that identifies the following card field and a card data set. If the *library* field in Card Set 3-5 in "NULL" then this field is skipped for the given cross section.

6.3.7.1 Card Set 3-6: Covariance Energy Bin Number

Card appearance: * Number of Energies plus 1.

Card variables: - comment/header card, no variables -.

Card read format: character (A1, A79).

Card appearance: *number*

Card variables:

number	=	number of energy points plus 1.

Card read format: free format (I5).

6.3.7.2 Card Set 3-7: Covariance Energy Bin Boundaries

Card appearance: *Energy Grid (eV)

Card variables: - comment/header card, no variables -.

Card read format: character (A1, A79).

Card appearance: $energy_i$, i=1, *number*

Card variables: $energy_i$ = energy bin boundary (upper bin boundary of bin i).

Card read format: free format floating point field (5G15.7).

6.3.7.3 *Card Set 3-8: Cross Section in Covariance Bin Structure*

Card appearance: *Cross Section (barns)

Card variables: - comment/header card, no variables -.

Card read format: character (A1, A79).

Card appearance: sig_i, i=1,*number*-1

Card variables: sig_i = cross section in bin number i.

Card read format: free format floating point field (5G15.7).

6.3.7.4 *Card Set 3-9: Standard Deviation*

Card appearance: *% Standard Deviation

Card variables: - comment/header card, no variables -.

Card read format: character (A1, A79).

Card appearance: sd_i = 1,*number*-1

Card variables: sd_i = standard deviation expressed as a percentage. of the i^{th} bin cross section value.

Card read format: free format floating point field (5G15.7).

6.3.7.5 *Card Set 3-10: Correlation Coefficient Matrix*

Card appearance: *Correlation Coefficient - Upper Triangular

Card variables: - comment/header, no variables -.

Card read format: character (A1, A79).

Card appearance: ((cor_{ij}, i=1,*number*-1),j=i,*number*-1)

Card variables: cor_{ij} = correlation coefficient normalized to the interval from -100 to +100. This can be converted into a covariance value using the standard deviations, sd_i and sd_j.

Card read format: free format integer (10I5). Each new row starts on a new card.

7. LIBRARY AVAILABILITY

The SNLRML library cross section compendium has been submitted to the Radiation Shielding Information Center (RSIC) operated by Oak Ridge National Laboratory and should be readily available to the dosimetry community.

Prior to the public availability of this library through RSIC, potential users of the library who are willing to provide feedback on the accuracy, consistency, and completeness of the library are invited to contact the authors to receive a beta-test version for cooperative evaluation purposes.

This cross section library is being distributed to the dosimetry community; however, the QA assessment of the library has been restricted to the environments and sensors in use at the SNL RML. Neither the authors, nor Sandia National Laboratories, nor the Department of Energy makes any warranty, expressed or implied; or assumes any legal liability or responsibility for the accuracy, completeness, usefulness or functioning of any information, code/data and related material; or represents that its use would not infringe privately owned rights.

A version of the SAND-II iterative spectrum unfolding code has been interfaced with the SNLRML library cross section compendium. This code is currently undergoing testing and is expected to be made available through RSIC by January 1994. A version of the LSL-M2 least-square spectrum adjustment code is currently being interfaced with the SNLRML library cross section compendium. This code will also be made available to the dosimetry community when the cross section interface is completed, validated, and documented.

The SNLRML library cross sections are readily interfaced to existing codes for spectrum determination. Codes such as STAY'SL [47], DANTA [48], FERRET [49], BAYES [50], and UFO [51] should be easily interfaced to the SNLRML library using the library format documentation provided in section 6.

8. Conclusion

The SNLRML library cross section compendium has been prepared by taking the latest and most consistent dosimetry-oriented cross sections from all available evaluations. The contents of the library include all dosimetry sensors (activation reactions, threshold reactions, fission reactions, and special damage sensors) that are in general use by the dosimetry community for the characterization of fission neutron spectra. The cross section compendium has been interfaced with spectrum determination codes and found to produce consistent spectrum "unfolds" with more sensors than were possible with previous libraries. The SNLRML library is being made available to the general dosimetry community in order to encourage the use of a consistent cross section library for spectrum determination. The authors plan on updating the library as part of the RML quality assurance program. This document provides part of the QA audit trail for the selection and choice of sensor response functions that is used in the spectrum determination of the SNL reactor facilities.

9. References

[1] "ENDF-201, ENDF/B-VI Summary Documentation," edited by P. F. Rose, Brookhaven National Laboratory Report BNL-NCS-1741, 4th Edition, October 1991. The cross section libraries are distributed by the National Nuclear Data Center, Brookhaven National Laboratory. The file format is described in reference 2.

[2] "ENDF-102, Data Formats and Procedures for the Evaluated Nuclear Data File ENDF-6," edited by P. F. Rose and C. L. Dunford, Brookhaven National Laboratory Report BNL-NCS-44945, July 1990, revised October 1991.

[3] "International Reactor Dosimetry File (IRDF-90)," assembled by N. P. Kocherov et al., International Atomic Energy Agency, Nuclear Data Section, IAEA-NDS-141 Rev. 0, August 1990. This dosimetry library is available within the United Stated by contacting the National Nuclear Data Center at Brookhaven National Laboratory.

[4] T. Asami, T. Nakagawa, M. Mizumoto, T. Narita, K. Shibata, S. Chiba, T. Fukahori, A. Hasegawa, S. Igarasi, "Status of Japanese Evaluated Nuclear Data Library Version 3," Nuclear Data for Science and Technology (1988 MITO), pp. 533-536, JAERI, 1988.

[5] V. N. Manokhin, "BROND, USSR Evaluated Neutron Data Library," International Atomic Energy Agency Nuclear Data Services, Documentation Series of the IAEA Nuclear Data Section, IAEA-NDS-90, Rev. 2, October 1989.

[6] C. Nordborg, H. Gruppelaar, M. Salvatores, "Status of the JEF and EFF Projects," pp. 782 in Nuclear Data for Science and Technology, editor S. Qaim, Springer-Verlag, Berlin, 1992.

[7] C. Y. Fu, D. M. Hetrick, "Experience in Using the Covariances of Some ENDF/B-V Dosimetry Cross Sections: Proposed Improvements and Addition of Cross-Reaction Covariance," Proceedings of the Fourth ASTM-Euratom Symposium on Reactor Dosimetry: Radiation Metrology Techniques, Data Bases, and Standardization, Volume II, conference held at the National Bureau of Standards, Gaithersburg, Maryland on March 22-26, 1982, pp. 877 - 887, Report number NUREG/CP-0029, CONF-820321/V2. The latest GLUCS library contains 14 dosimetry reactions, was updated in January 1993, and is available from D. Hetrick at Oak Ridge National Laboratory.

[8] A. B. Pashchenko et al., "FENDL-2 and Associated Benchmark Calculations," International Atomic Energy Agency (Austria), International Nuclear Data Committee, report INDC(NDS)-260/LF, March 1992.

[9] P. J. Griffin, J. G. Kelly, T. F. Luera, "Effect of New Cross Section Evaluations on Spectrum Determinations," SAND92-0093, Sandia National Laboratories, presented at the 29th International Nuclear and Space Radiation Effects Conference held on July 13-17, 1992 in New Orleans, Louisiana. Conference proceedings are

published in IEEE Transactions on Nuclear Science, Vol. 39, No. 6, pp. 2078-2085, Dec. 1992.

[10] P. J. Griffin, J. G. Kelly, T. F. Luera, "Effect of ENDF/B-VI Cross Sections on Neutron Dosimetry," Proceedings of the Seventh ASTM-Euratom Symposium on Reactor Dosimetry, held in Strassbourg, France on August 27-31, 1990, G. Tsotridis, R. Dierckx, P. D'Hondt editors, Kluwer Academic Publishers, 1990, pp. 669-675.

[11] W. N. McElroy, S. Berg, T. Crockett, and R. Hawkins, "A Computer-Automated Iterative Method for Neutron Flux Spectral Determination by Foil Activation," AFWL-TR-67-41, Vol. 1, Air Force Weapons Laboratory, Kirtland AFB, New Mexico, July 1967.

[12] F. W. Stallman, "LSL-M2: A Computer Program for Least-Squares Logarithmic Adjustment of Neutron Spectra," NUREG/CR-4349, ORNL/TM-9933, March 1985.

[13] R. J. Howerton, D. E. Cullen, R. C. Haight, M. H. MacGregor, S. T. Perkins, and E. F. Plechaty, "The LLL Evaluated Nuclear Data Library (LENDL): Evaluation Techniques, Reaction Index, and Description of Individual Evaluations," Lawrence Livermore Laboratory report UCRL-50400, Vol. 15, Part A, September 1975.

[14] W. L. Zijp, H. J. Nolthenius, G. C. H. M. Verhaag, "Cross-Section Library DOSCROS84 (in a 640 group structure of the SAND-II type)," Netherlands Energy Research Foundation ECN, Petten, report ECN-160, October 1984.

[15] D. C. Larson, D. M. Hetrick, S. J. Epperson. N. M. Larson, "Evaluation of ^{28,29,30}Si Neutron Induced Cross Sections for ENDF/B-VI," Oak Ridge National Laboratory, Report ORNL-TM-11825, to be published. This cross section is likely to be considered for inclusion in the next ENDF/B-VI release.

[16] B. Strohmaier, "New Issue of Nuclear Model Calculations of Cross Sections for Neutron-Induced Reactions on ^{93}Nb to 20 MeV," Ann. Nucl. Energy, Vol. 16, No. 9, pp. 461-470, 1989.

[17] M. Wagner, "Update of the Evaluation of the Cross Sections for the Neutron-Dosimetry Reactions ^{19}F(n,2n)^{18}F and ^{93}Nb(n,2n)^{92m}Nb," Institut fur Radiumforschung und Kernphysik der Universitat Wien, International Atomic Agency report INDC(AUS)-014, October 1991.

[18] S. Iwasaki, M. Sakuma, N. Odano, H. Suda, K. Sugiyama, "Ratio Tests of Dosimetry Cross-Sections for ^{93}Nb(n,2n)^{92m}Nb and ^{197}Au(n,2n)^{196}Au to ^{27}Al(n,α)^{24}Na Reactions," Progress in Nuclear Energy, Vol. 26, No. 3, pp. 231-247, 1991.

[19] M. Nakazawa, K. Kobayashi, S. Iwasaki, T. Iguchi, K. Sakurai, Y. Ikeda, T. Nakagawa, JAERI 1325, Japan Atomic Energy Research Institute, Tokai, Japan, 1992.

[20] Evaluated Nuclear Structure Data File (ENSDF), a computer file of evaluated nuclear structure and radioactive decay data, which is maintained by the National Nuclear Data Center (NNDC), Brookhaven National Laboratory (BNL), on behalf

of The International Network for Nuclear Structure Data Evaluation, which functions under the auspices of the Nuclear Data Section of the International Atomic Energy Agency (IAEA).

[21] H. D. Lemmel, "X-ray and Gamma-ray Standards for Detector Calibration," International Atomic Energy Agency, IAEA-TECDOC-619, September 1991.

[22] W. L. Zijp, J. H. Baard, "Nuclear Data Guide for Reactor Neutron Metrology. Part 1. Activation Reactions (1979 Edition)," Report ECN-70, Netherlands Energy Research Foundation ECN, Petten, August 1979. Also issued as report EUR-7164 EN, Luxembourg, 1981.

[23] Nuclear Wallet Cards, compiled by Jagdish K. Tuli, National Nuclear Data Center, July 1990.

[24] N. E. Holden, "Review of Thermal Cross Sections and Isotopic Composition of the Elements," BNL-NCS-42224, March 1989.

[25] E. Browne, R. B.Firestone, Table of Radioactive Isotopes, edited by V. S. Shirley, John Wiley & Sons, New York, 1986.

[26] J. G. Kelly, "Neutron Spectrum Adjustment with SANDII Using Arbitrary Trial Functions," Reactor Dosimetry: Methods, Applications, and Standardization, ASTM STP 1001, Harry Farrar IV and E. P. Lippincott, Eds., American Society for Testing and Materials, Philadelphia, 1989, pp. 460-468.

[27] J. G. Kelly, D. W. Vehar, "Measurement of Neutron Spectra in Varied Environments by the Foil-Activation Method With Arbitrary Trials," SAND87-1330, Sandia National Laboratories, December 1987.

[28] Handbook on Nuclear Activation Data, Technical Reports Series No. 273, Part 1-2 "Standard Monitor Reactions for Neutrons," by Z. Brody, International Atomic Energy Agency, Vienna, 1987,

[29] A. J. Deruytter, "Requirements for Nuclear Standard Reference Data From the Users' Point of View," Nuclear Standard Reference Data, IEAE-TECDOC-335, IAEA, Vienna, 1985, p. 65.

[30] A. D. Carlson, W. P. Poenitz, G. M. Hale, R. W. Peelle, D. C. Dodder, C. Y. Fu, W. Mannhart, "The ENDF/B-VI Neutron Cross Section Measurement Standards," U. S. Department of Commerce Technology Administration National Institute of Standards and Technology report NISTIR 5177, May 1993.

[31] W. P. Poenitz, "The Data for the Neutron Interations with ^{6}Li and ^{10}B," Nuclear Standard Reference Data, IAEA-TEC-335, IAEA, Vienna, 1985, p. 112.

[32] H. Vonach, "The $^{27}Al(n,\alpha)$ Cross Section," Nuclear Data Standards for Nuclear Measurement, Technical Reports Series No. 227, IAEA, Vienna, 1983, p. 59.

[33] J. G. Kelly, P. J.Griffin, "Comparison of Measured Silicon Displacement Damage Ratios with ASTM E-722 and NJOY Calculated Damage," Proceedings of the Seventh ASTM-Euratom Symposium on Reactor Dosimetry, held in Strasbourg,

France, 27-31 August 1990, G. Tsotridis, R. Dierckx, P. D'Hondt editors, Kluwer Academic Publishers, 1990, pp. 711-718.

[34] R. E. MacFarlane, D. W. Muir, R. M. Boicourt, "The NJOY Nuclear Data Processing System, Volume 1: User's Manual," LA-9303-M, ENDF-324, May 1982. The code is available as PSR-171 from the Oak Ridge National Laboratory (ORNL) Radiation Shielding Information Center (RSIC).

[35] "Standard Practice for Characterizing Neutron Energy Fluence Spectra in Terms of an Equivalent Monoenergetic Neutron Fluence for Radiation-Hardness Testing of Electronics," Designation E 722-93, Annual Book of ASTM Standards, Vol. 12.02, 1993.

[36] W. Mannhart, "Status of CF-252 Neutron Spectrum as a Standard," Reactor Dosimetry: Methods, Applications, and Standardization, ASTM STP 1001, Harry Farrar IV and E. P. Lippincott, Eds., American Society for Testing and Materials, Philadelphia, 1989, pp. 340-347.

[37] C. Y. Fu, "A Re-Evaluation of $^{32}S(n,p)$ Cross Sections From Threshold to 5 MeV," in the proceedings from the American Nuclear Society Proceedings on a Topical Meeting on Advances in Nuclear Engineering Computation and Radiation Shielding, Santa Fe, New Mexico April 9-13, 1989, University of New Mexico Publications, Ed. M. L. Hall.

[38] W. Mannhart, D. L. Smith, J. W. Meadows, "The Discrepancy Between Differential and Integral Data on Ti-47(n,p)," in the proceedings from the American Nuclear Society Proceedings on a Topical Meeting on Advances in Nuclear Engineering Computation and Radiation Shielding, Santa Fe, New Mexico, April 9-13, 1989, University of New Mexico Publications, Ed. M. L. Hall, pp. 577-580.

[39] J. W. Meadows, D. L. Smith, M. M. Bretscher, S. A. Cox, "Measurement of 14.7 MeV Neutron-Activation Cross Sections for Fusion," Ann. Nucl. Energy, Vol. 14, No. 9, pp. 489-497, 1987.

[40] "Standard Practice for Characterizing Neutron Exposures in Ferritic Steels in Terms of Displacements Per Atom (DPA), E706(ID)," Designation E 693-79, Annual Book of ASTM Standards, Vol. 12.02, 1991.

[41] J. Lindhard, M. Scharff, H. E. Schiasott, "Range Concepts and Heavy Ion Ranges," Matematisk-fysiske Meddelelser-Kongelige Danske Videnskaberns Selskab, KDVSA, Vol. 33, No. 14, 1963.

[42] "Recommendations for Displacement Calculations for Reactor/Accelerator Studies in Austenitic Steel," Nuclear Engineering and Design, Vol. 33, 1975, pp. 91.

[43] P. J. Griffin, J. G.Kelly, T. F. Luera, "Neutron Damage Equivalence in GaAs," IEEE Trans. on Nuclear Science, Vol. 38, No. 6, pp. 1216-1224, December 1991.

[44] B. Strohmaier, "Letter to the Editors: Status of the Evaluated Excitation Functions for the Neutron-Dosimetry Reaction $^{93}Nb(n,n')^{93m}Nb$," Ann. Nucl. Energy, Vol. 19, No. 8, p. 477, 1992.

[45] J. H. Baard, W. L. Zijp, H. J. Nolthenius, Nuclear Data Guide for Reactor Neutron Metrology, EUR 12354 EN, Netherlands Energy Research Foundation ECN, Petter, The Netherlands, Kluwer Academic Publishers, 1989. This work has been presented at the 54th meeting of the Euratom Working Group on Reactor Dosimetry (EWGRD) at JRC Petten, April 12, 1989.

[46] A. Carlson et al., Nuclear Data for Basic & Applied Science, Santa Fe, NM, p. 1429, 1985.

[47] F. G. Perey, "Least-Squares Dosimetry Unfolding: The Program STAY'SL," ORNL/TM-6062, Oak Ridge National Laboratory, also report ENDF-254, October 1977.

[48] M. Petilli, "DANTA: Unfolding Code for Energy Spectra Evaluations," CNEN-RT/FI(79)7,8, 1979.

[49] F. Schmittroh, "FERRET Data Analysis Code," report HEDL-TME 79-40, Hanford Engineering Development Laboratory, Richland, WA, September 1979.

[50] N. M. Larson, "User's Guide for BAYES: A General Purpose Computer Code for Fitting a Functional Form to Experimental Data," ORNL/TM-8185, Oak Ridge National Laboratory, August 1982.

[51] L. Kissel, F. Biggs, T. R. Marking, "UFO (Unfold Operator) USER GUIDE: PART 1 - Overview and Brief Command Descriptions," report SAND82-0396, Sandia National Laboratories, Albuquerque, NM, June 1991.

[52] S. Blow, AERE-R6540, Jan. 1971.

[53] A. H. Wapstra, R. Hoekstra, Atomic and Nuclear Data Tables, Vol. 39, pp. 281, 1988.

[54] D. M. Hetrick, Oak Ridge National Laboratory, private communication to P. J. Griffin on December 4, 1991 and on January 13, 1992. Contents included a letter and a floppy disk.

[55] T. F. Luera, J. G. Kelly, H. J. Stein, M. S. Lazo, C. E. Lee, L. R. Dawson, "Neutron Damage Equivalence for Silicon, Silicon Dioxide, and Gallium Arsenide," IEEE Trans. on Nuclear Science, Vol. NS-34, No. 6, pp. 1557 - 1563, December 1987.

[56] W. L. Zijp, H. J. Nolthenius, G. C. H. M. Verhaag, "Damage Cross-Section Library DAMSIG84 (in a 640 group structure of the SAND-II type)," Netherlands Energy Research Foundation ECN, Petten, report ECN-159, October 1984.

[57] C. Dunjui, "Evaluation of Cross Sections for Dosimetry Reactions," Chinese Nuclear Data Centre, Institute of Atomic Energy, International Atomic Energy Agency report INDC(CPR)-024, October 1991.

[58] T. Guoyou, F. Jihong, C. Wentian, B. Shanglian, "Evaluation of Neutron Nuclear Data of Np-237 For CENDL-2," Physics Department, Nankai University, P. R. of China, International Atomic Energy Agency report INDC(CPR)-023, October 1991.

Intentionally Left Blank

APPENDIX A

Comparison of Dosimetry Cross Sections

Table A-1a
Alternative Cross Section Sources for the $^{10}B(n,abs)$ Reaction

$^{10}B(n,abs)$			Comment
Cross Section Library	Material Number	Covariance Data	
ENDF/B-VI	525	No	LANL, Eval. Nov. 1989, revision 1, tape b-10a, components 102, 103, 104, 107, 113.
ENDF/B-V	1305	No	LANL Eval. Dec. 1976, tape 511.
JENDL-3	3051	No	JAERI, Eval. Mar. 1987, tape 23.
JEF 2.2	525	No	LANL, Eval. Mar. 1989, taken from ENDF/B-VI, tape jef-1.
BROND	511	No	Taken from ENDF/B-V mat 1305, tape ma242.51.
SAND-II	----	No	Absorption cross section with DOSDAM84 code distribution by RSIC, taken from ENDF/B-V revision 2 and only includes the MT=107 component.

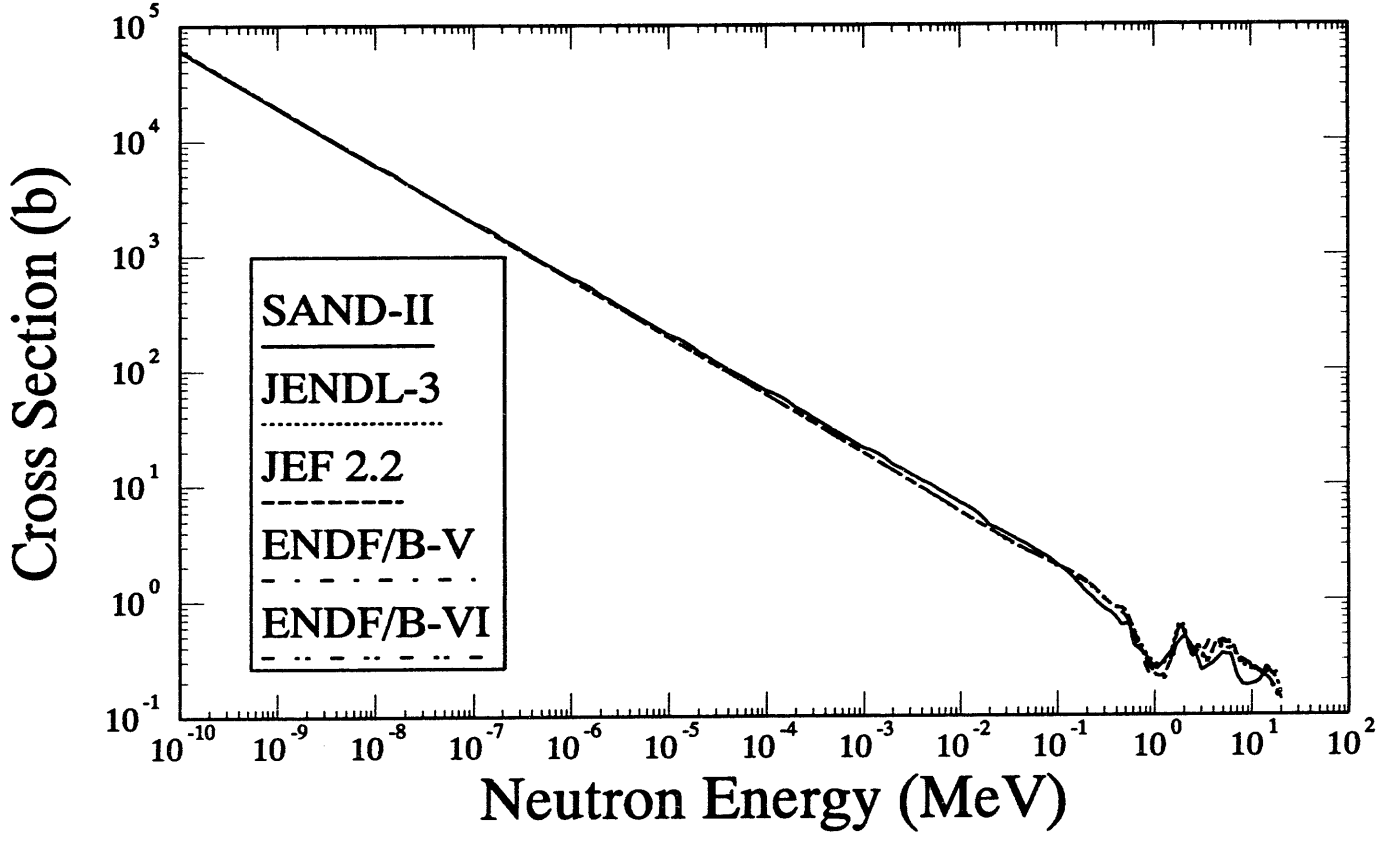

Figure A-1a: ^{10}B(n,abs) Cross Section

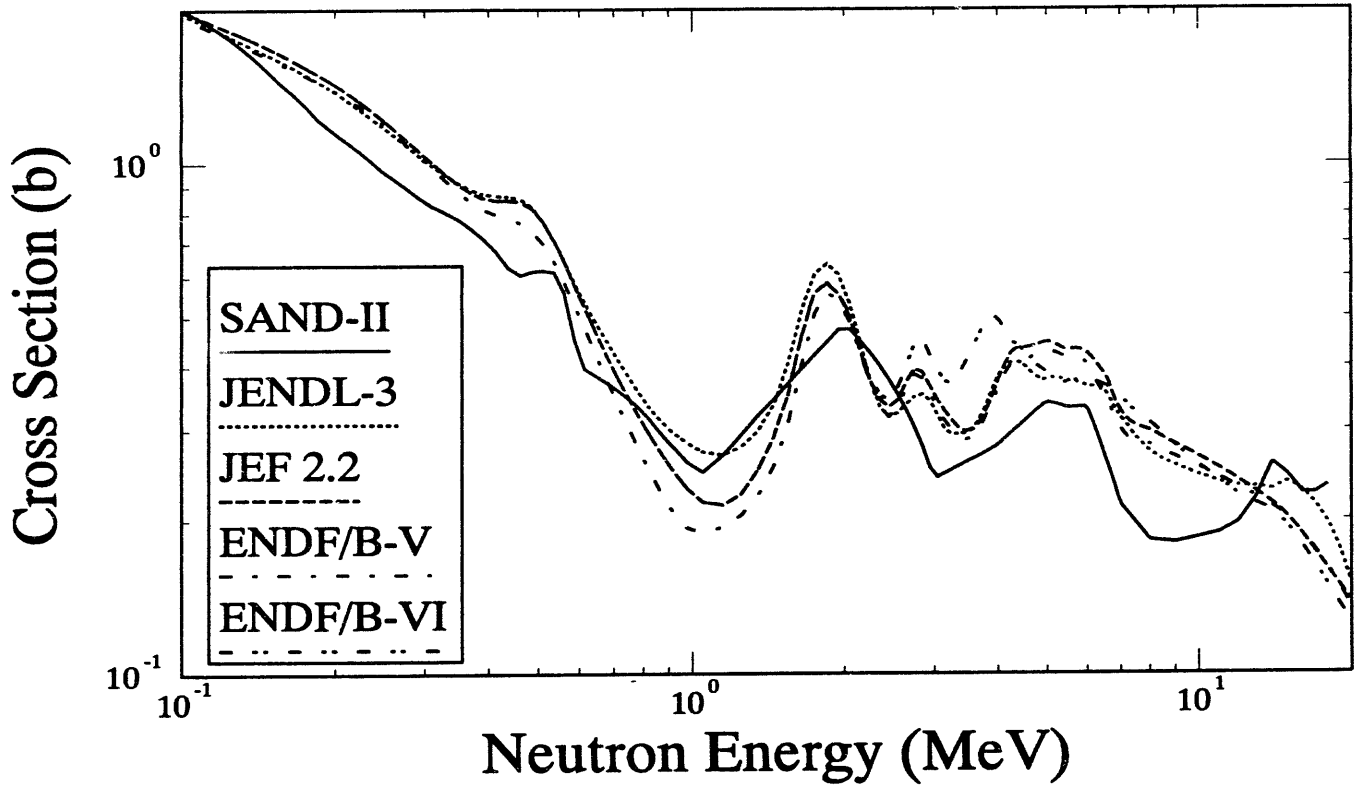

Figure A-1b: ^{10}B(n,abs) Cross Section

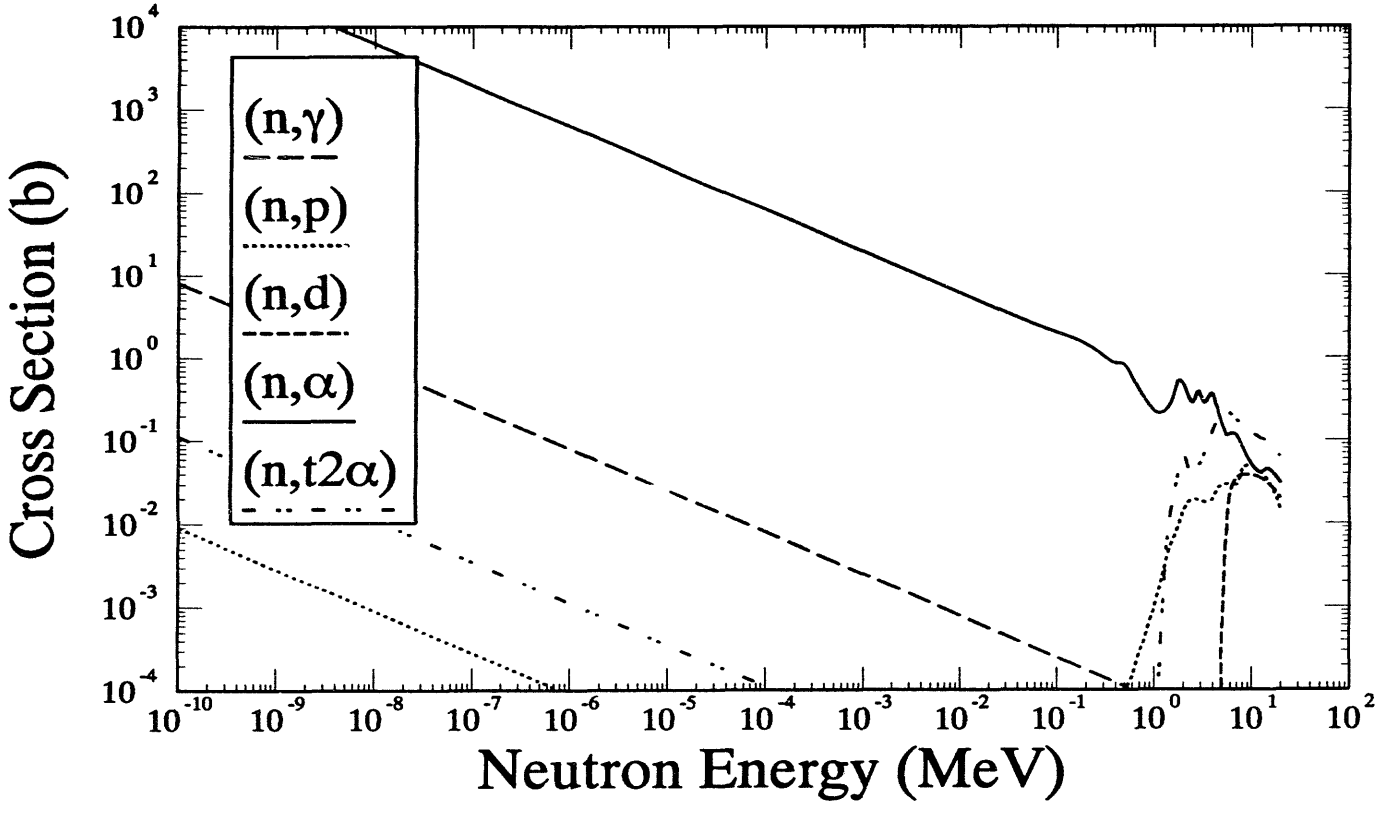

Figure A-1c: ^{10}B(n,abs) Components

Table A-2a
Alternative Cross Section Sources for the $^{10}B(n,X)^{4}He$ Reaction

$^{10}B(n,X)^{4}He$			Comment
Cross Section Library	Material Number	Covariance Data	
ENDF/B-VI	525	No	LANL, Eval. Nov. 1989, revision 1, tape b-10a, components MT=107 and twice MT=113.
ENDF/B-V	1305	No	LANL Eval. Dec. 1976, tape 511.
ENDF/B-V	5305	No	LASL, Eval. January 1979, Tape 533, gas production, MT=207, sum of (n,α), (n,nα), and twice (nt2α), (n,nd2α) and (n,2n).
ENDF/B-V	6425	Yes	LANL, Eval. Jan. 1979, Tape 531, dosimetry. MT=207, same as ENDF/B-V gas production.
IRDF-90	525	Yes	References the MT=107 component from ENDF/B-VI.
JENDL-3	3051	No	JAERI, Eval. Mar. 1987, tape 23, includes (n,α) MT=107, twice the (n,2n) MT=16, twice the (nt2α) MT=113, and twice the (n,nd2α) MT=60, 63, 67-89.
JEF 2.2	525	No	LANL, Eval. Mar. 1989, taken from ENDF/B-VI, tape jef-1.
BROND	511	No	Taken from ENDF/B-V mat 1305, tape ma242.51.
SAND-II	----	No	Absorption cross section with DOSDAM84 code distribution by RSIC, taken from ENDF/B-V revision 2 and only includes the 107 component.

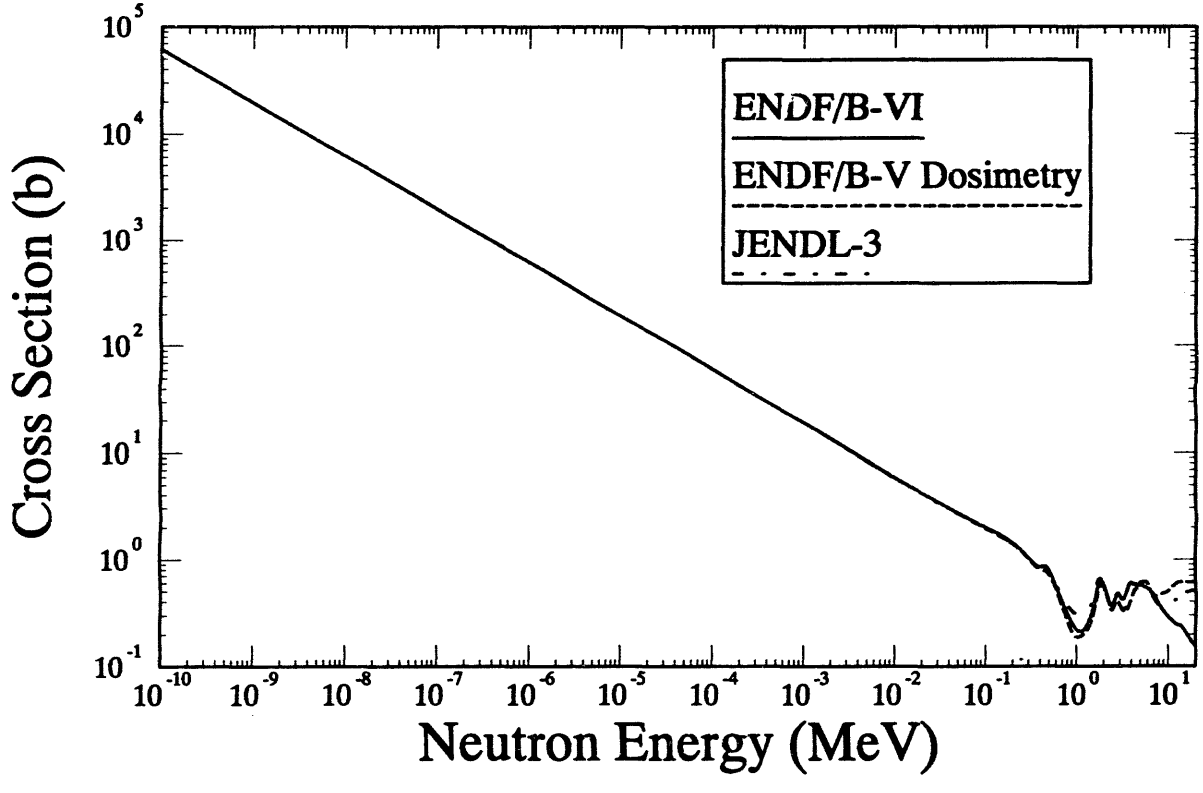

Figure A-2a: $^{10}B(n,X)^{4}He$ Cross Section

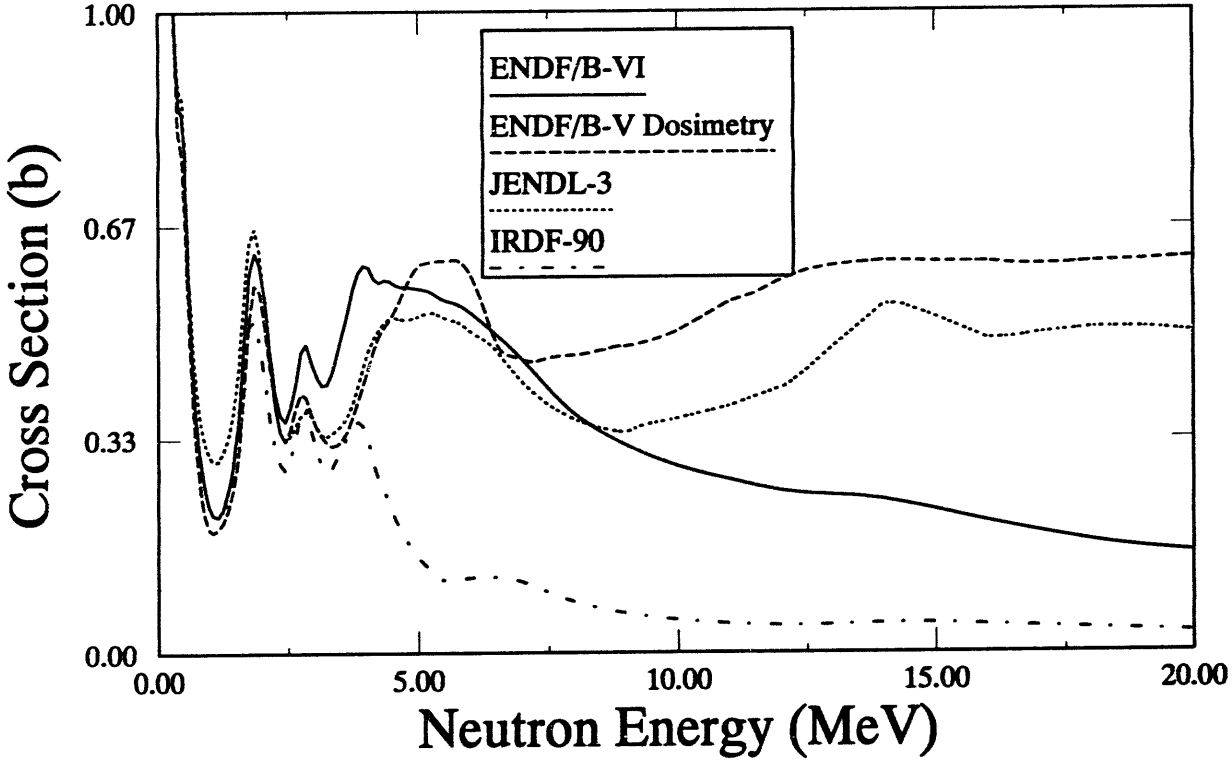

Figure A-2b: $^{10}B(n,X)^{4}He$ Cross Section

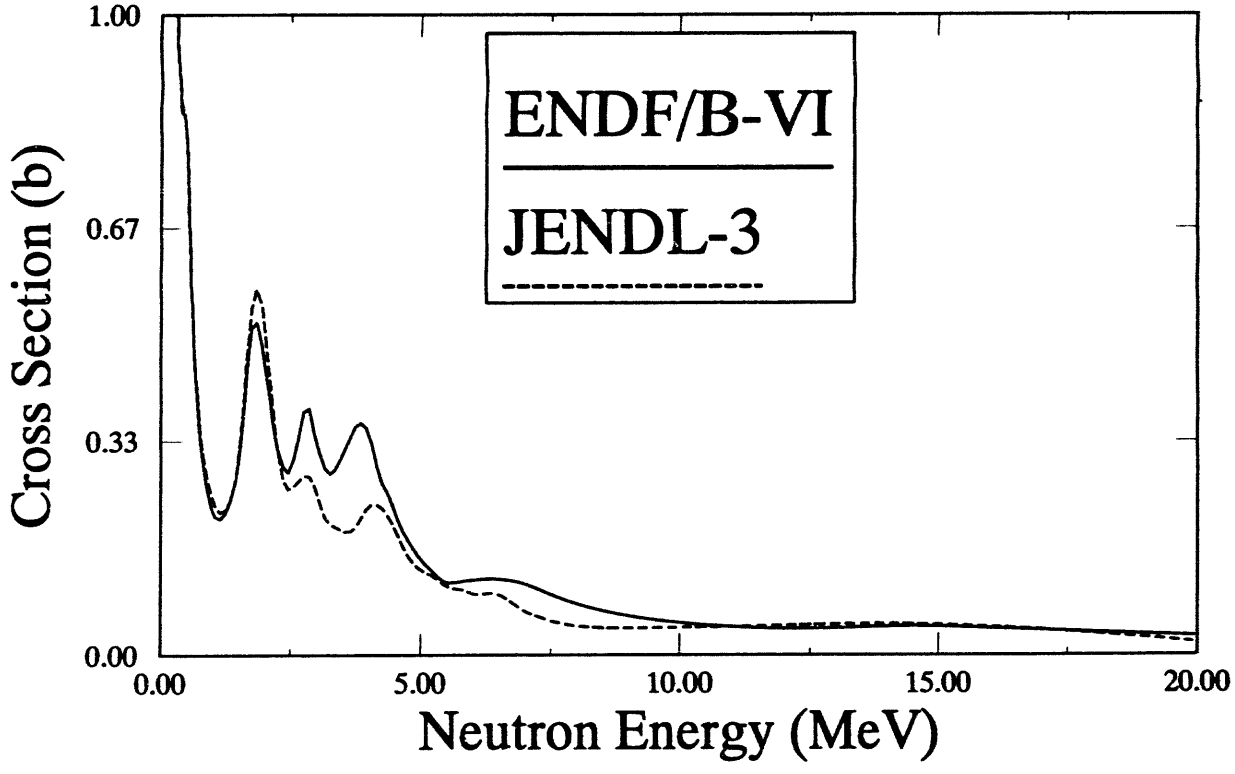

Figure A-2c: $^{10}B(n,\alpha)^{6}Li$ Cross Section

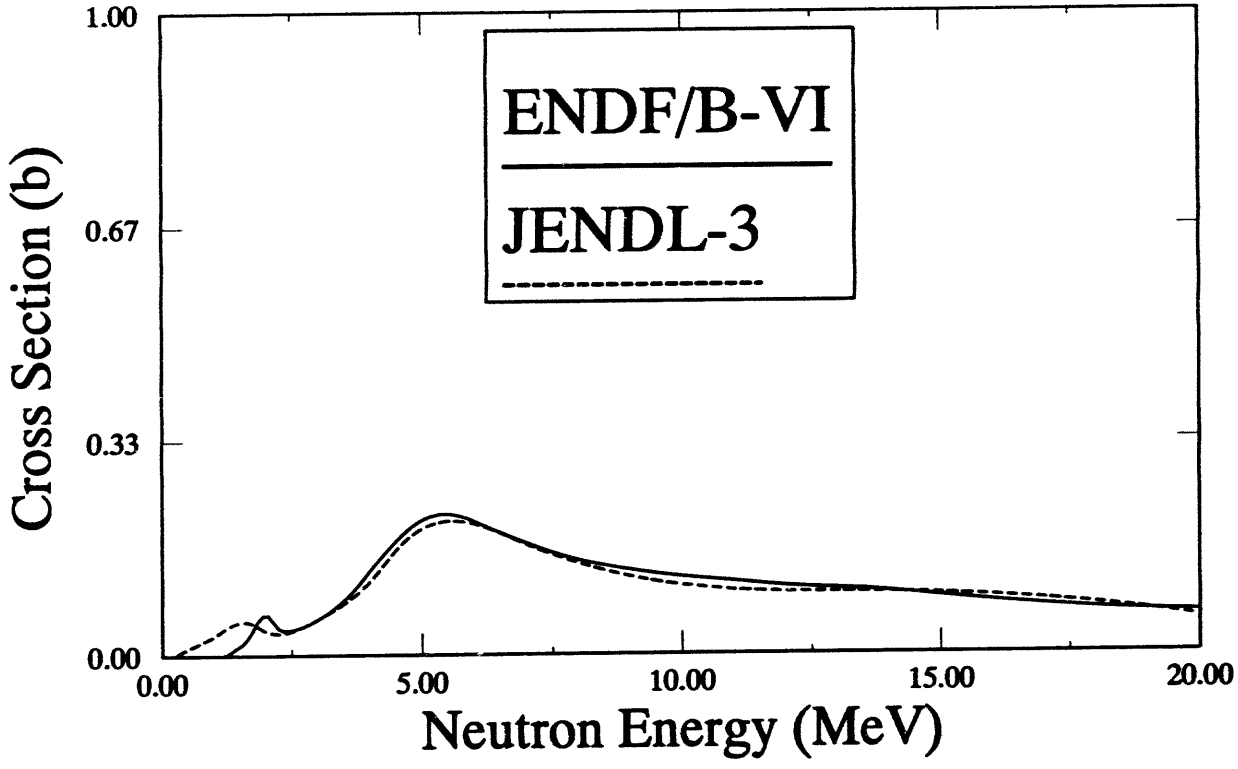

Figure A-2d: $^{10}B(n,t2\alpha)$ Cross Section

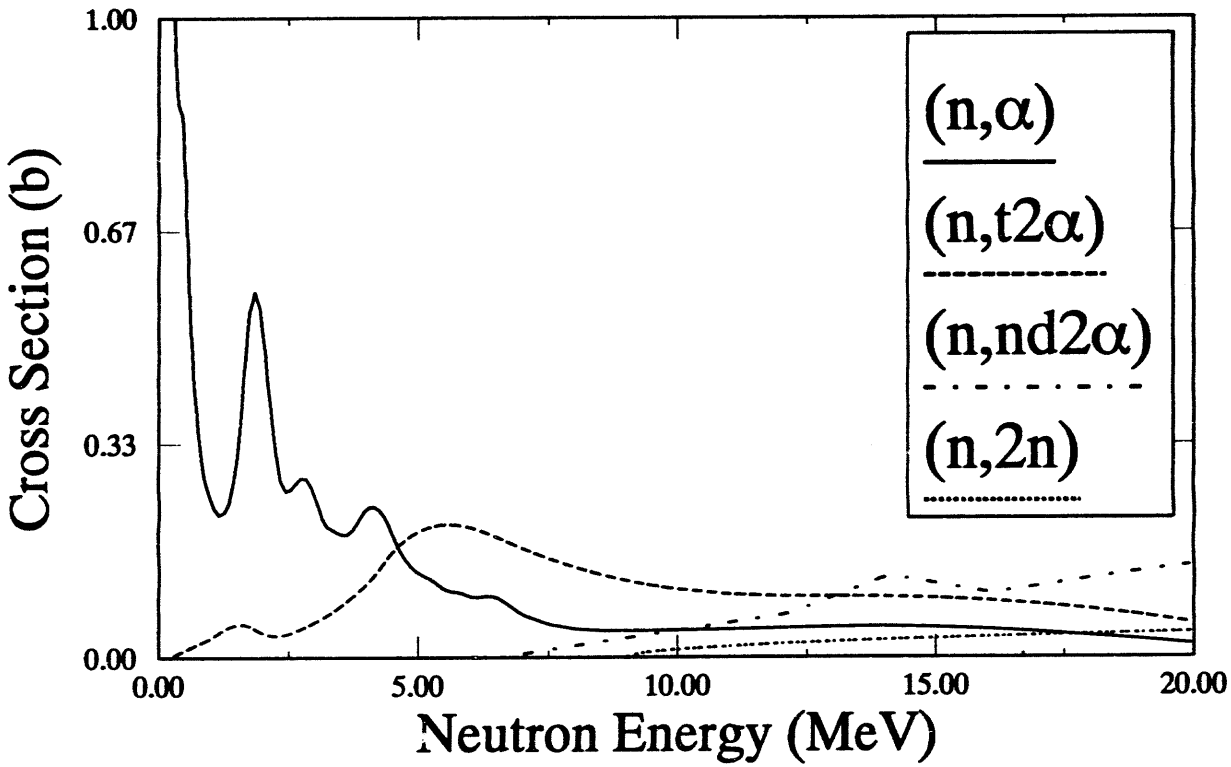

Figure A-2e: $^{10}B(n,X)^{4}He$ Cross Section Components for the JENDL-3 Library

Table A-3a
Alternative Cross Section Sources for the ^{11}B(n,abs) Reaction

^{11}B(n,abs)			Comment
Cross Section Library	Material Number	Covariance Data	
ENDF/B-VI	528	No	LANL, Eval. May 1989, components 102, 103, 105, 107.
ENDF/B-V	1160	No	GE/BNL, Eval. Sept. 1971, tape 501.
JENDL-3	3052	No	JAERI, Eval. May 1988, tape 23, includes component 104 in addition to base set.
JEF 2.2	528	No	LANL, Eval. May 1989, tape jef-1.
BROND	NA	No	No ^{11}B cross section given.

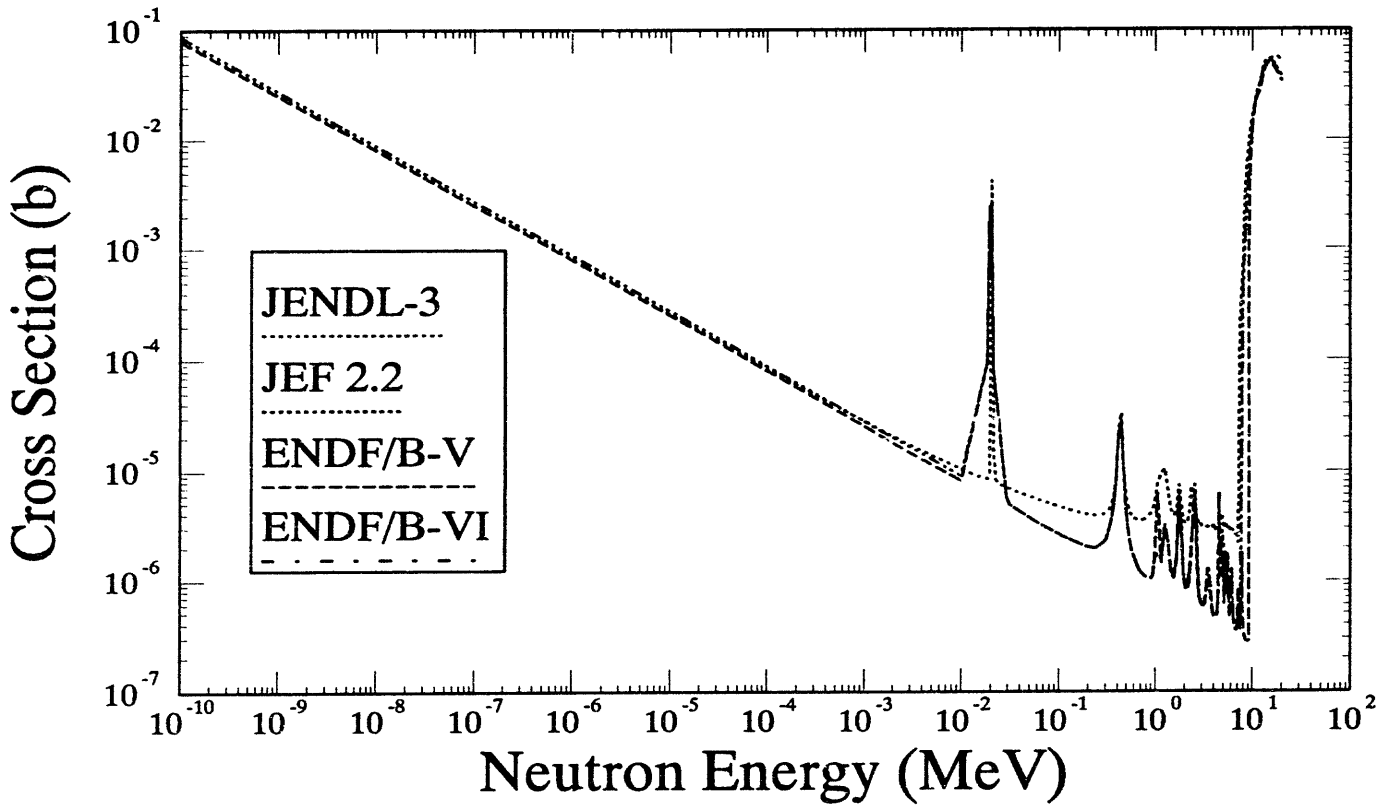

Figure A-3a: ^{11}B(n,abs) Cross Section

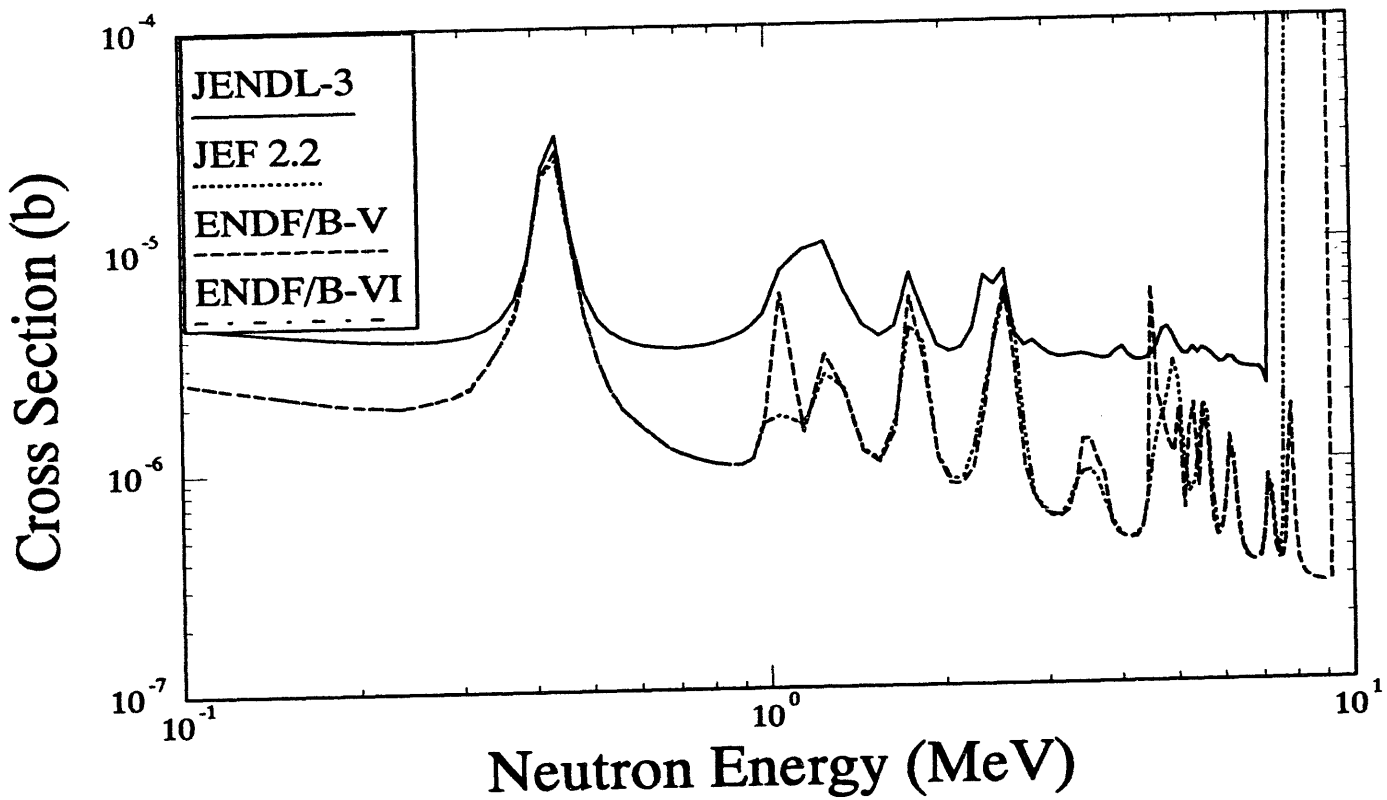

Figure A-3b: ^{11}B(n,abs) Cross Section

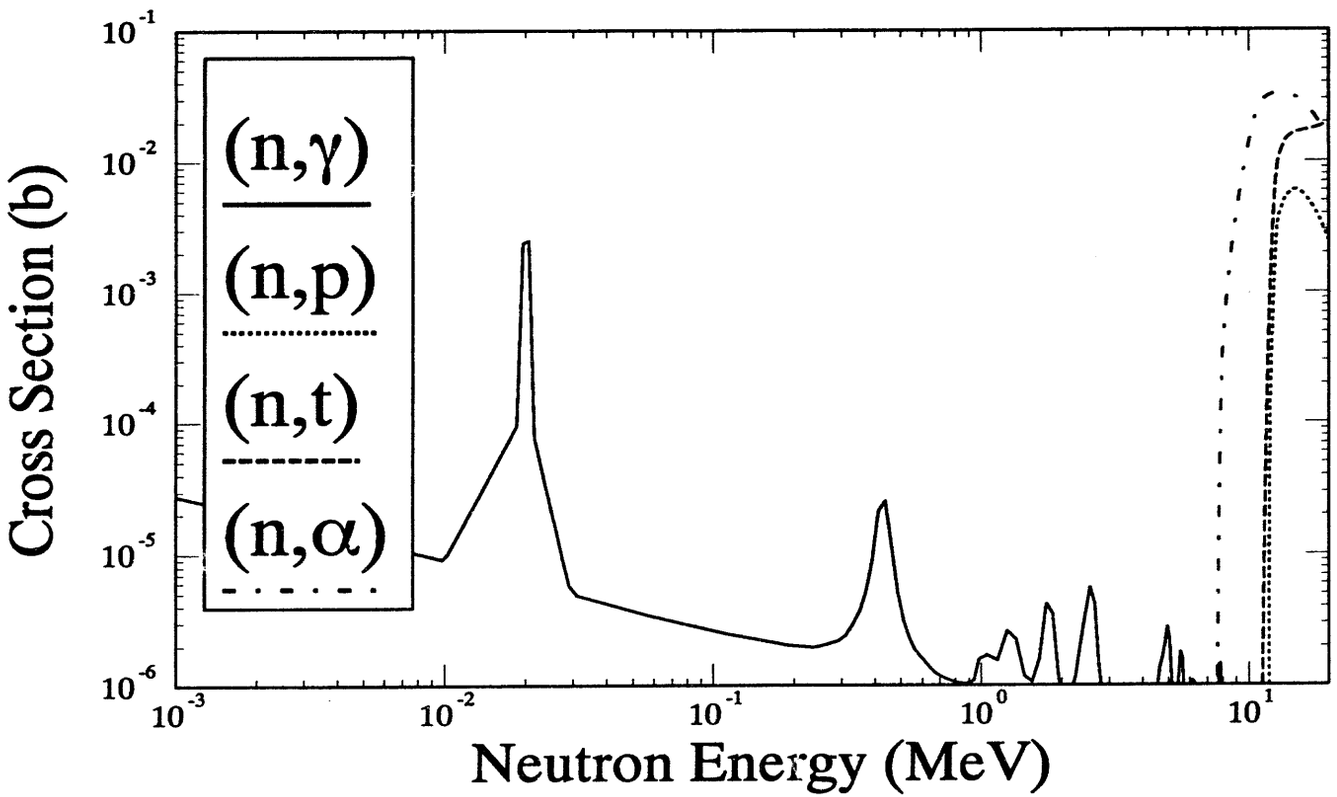

Figure A-3c: ^{11}B(n,abs) Components

Table A-4a
Alternative Cross Section Sources for the $^{Nat}B(n,abs)$ Reaction

$^{Nat}B(n,abs)$			Comment
Cross Section Library	Material Number	Covariance Data	
ENDF/B-VI	525/528	No	LANL, Eval. Nov. 1989, revision 1, tape b-10a, components 102, 103, 104, 107, 113.
ENDF/B-V	1305/1160	No	LANL Eval., see Table A-1a and A-2a.
JENDL-3	3051/3052	No	JAERI, Eval., see Table A-1a and A-2a.
JEF 2.2	525/528	No	LANL, Eval. Mar. 1989, taken from ENDF/B-VI.

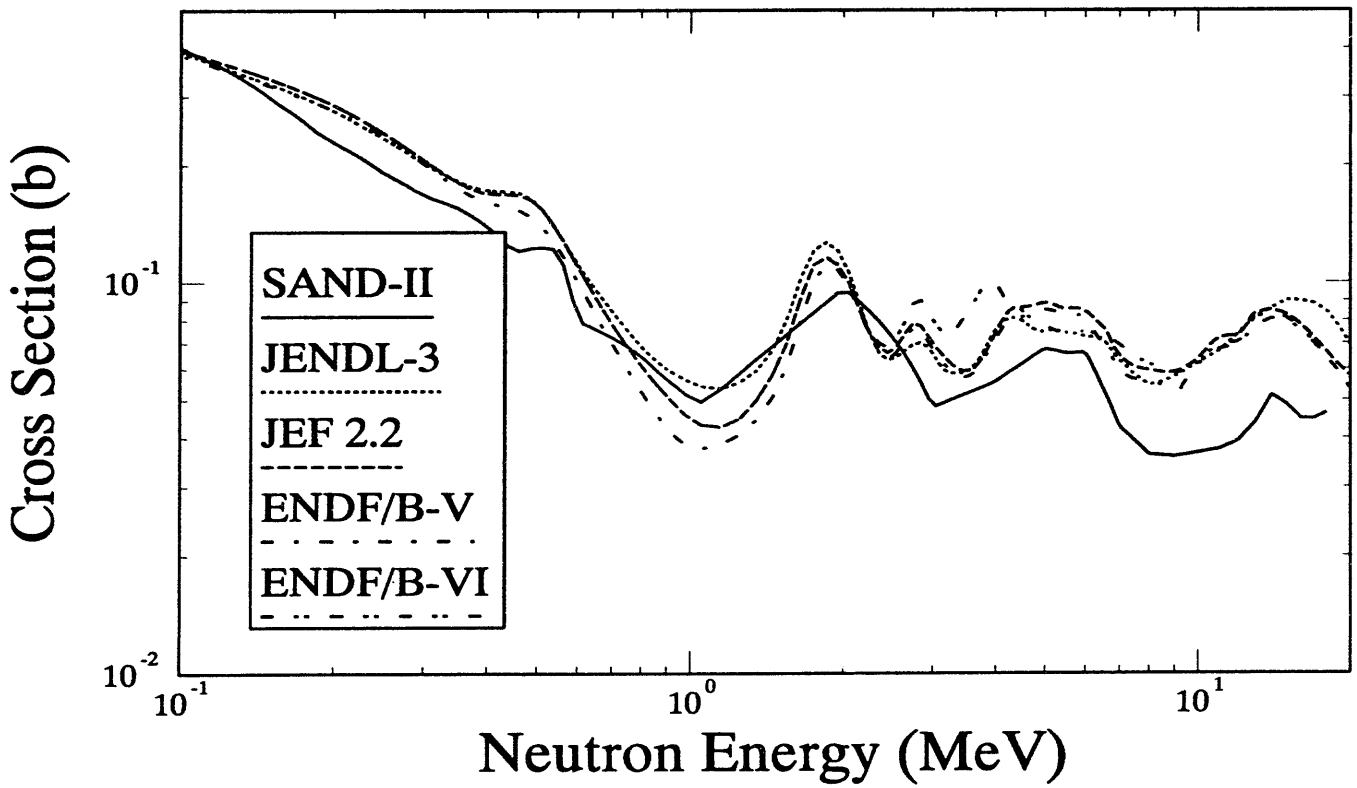

Figure A-4a: ^{Nat}B(n,abs) Cross Section

Table A-5a
Alternative Cross Section Sources for the $^{Enriched}B_4C$(n,abs) Reaction

$^{Enriched}B_4C$(n,abs)			Comment (91.67% enrichment ^{10}B)
Cross Section Library	Material Number	Covariance Data	
ENDF/B-VI	525/528 600	No	Boron from LANL, Eval. Nov. 1989, revision 1, tape b-10a, components 102, 103, 104, 107, 113. Natural carbon from ORNL, Eval. August 1989, components 102, 103, 104, 105, 107, 111, 112, 115, 116.
ENDF/B-V	1305/1160 1306	No	Boron from LANL Eval., see Table A-1a and A-2a. Natural carbon from ENDF/B-V.
JENDL-3	3051/3052 3061	No	Boron from JAERI, Eval. see Table A-1a and A-2a. Carbon-12 from tape ma257.23, JAERI Eval. August 1983, components 102, 103, 104, and 107.
JEF 2.2	525/528 600	No	Boron from LANL, Eval. Mar. 1989, taken from ENDF/B-VI. Carbon from tape jef-1, taken from ENDF/B-V, updated from ENDF/B-VI

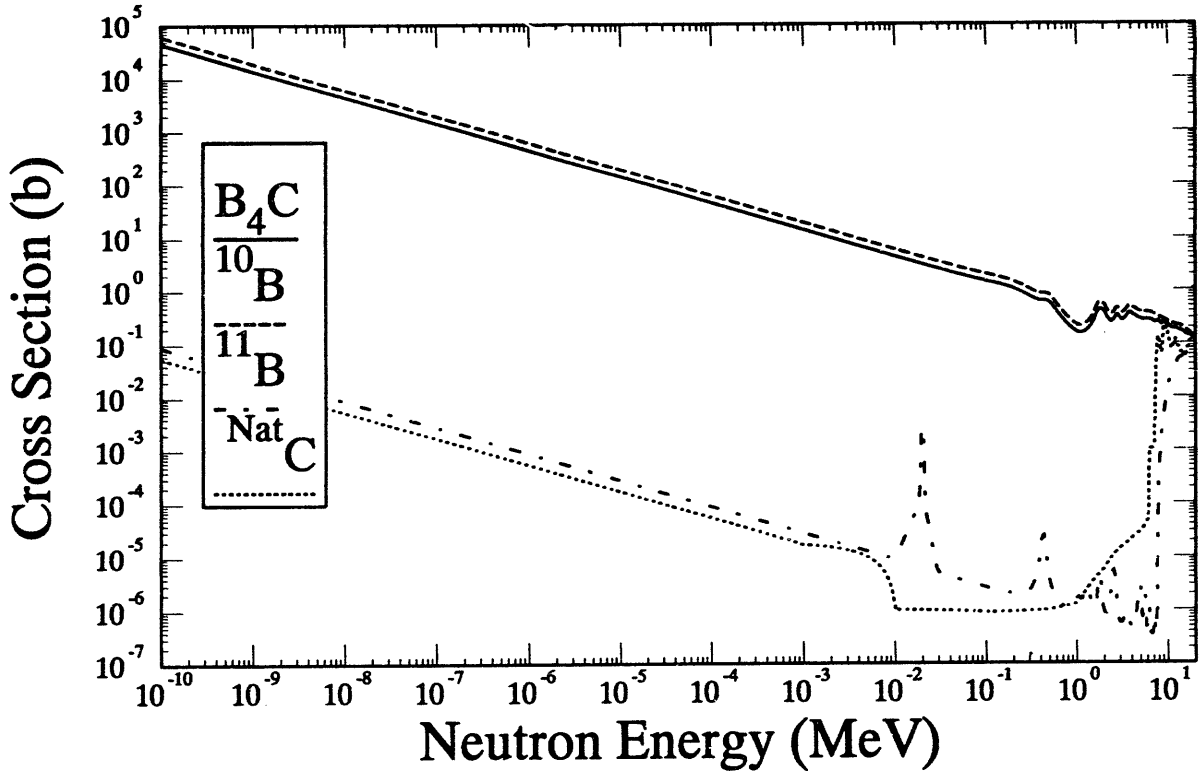

Figure A-5a: $^{\text{Enriched}}B_4C$(n,abs) Cross Section

Figure A-5b: Enriched B_4C(n,abs) Cross Section

Table A-6a
Alternative Cross Section Sources for the $^{6}Li(n,X)^{4}He$ Reaction

$^{6}Li(n,X)^{4}He$			Comment
Cross Section Library	Material Number	Covariance Data	
ENDF/B-VI	325	No	LANL, Eval. April 1989. Includes $^{6}Li(n,t)^{4}He$ reaction (MT=105) and the $^{6}Li(n,n')^{6}Li$ cross section that decays into a deuteron and alpha particle (MT=4 minus MT=57).
ENDF/B-V	1303	No	LASL, Eval. Sept.1977, Tape 511.
ENDF/B-V	5303	No	LASL, Eval. Dec. 1978, Tape 533, gas production, MT=207, sum of (n,tα), (n,nα),and (n,2n).
ENDF/B-V	6424	Yes	LANL, Eval. December 1978, Tape 531, dosimetry, MT=207, same as main ENDF/B-V file.
ENDF/B-V	7036	No	Tape 532, activation, only includes the (n,t) term.
IRDF-82	6424	Yes	Taken from ENDF/B-V gas production tape.
IRDF-90	325	Yes	References the MT=105 contribution from the ENDF/B-VI evaluation.
JENDL-3	3031	No	JAERI, Eval. March 1985, tape ma257.23, MT=51, 52, 54-56, 58, 60-62, 64-86, 105.
JEF 2.2	325	No	Rcom. June 1982, tape jef-1, taken from ENDF/B-V MAT=1303, (n,t) cross section modified to ENDF/V-VI.
BROND	361	No	Tape ma242.51CJD-FEI, Eval. May 1984.

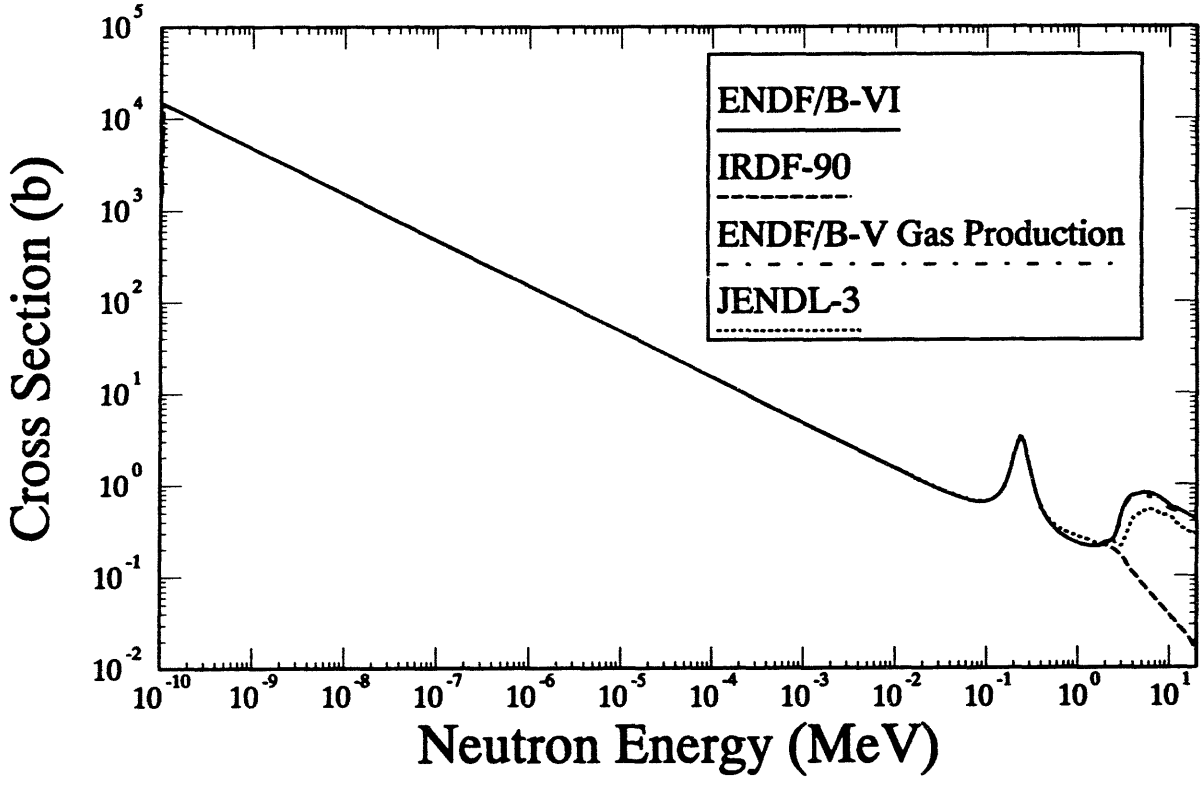

Figure A-6a: $^{6}Li(n,X)^{4}He$ Cross Section

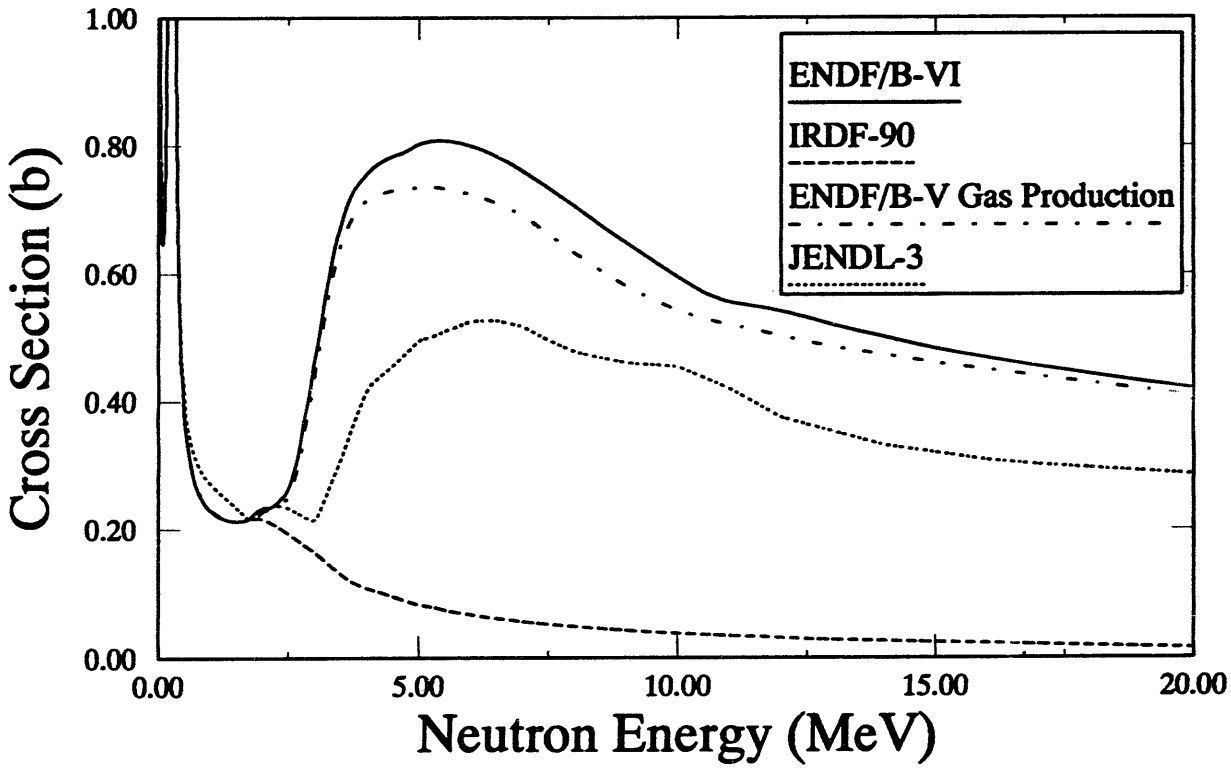

Figure A-6b: $^{6}Li(n,X)^{4}He$ Cross Section

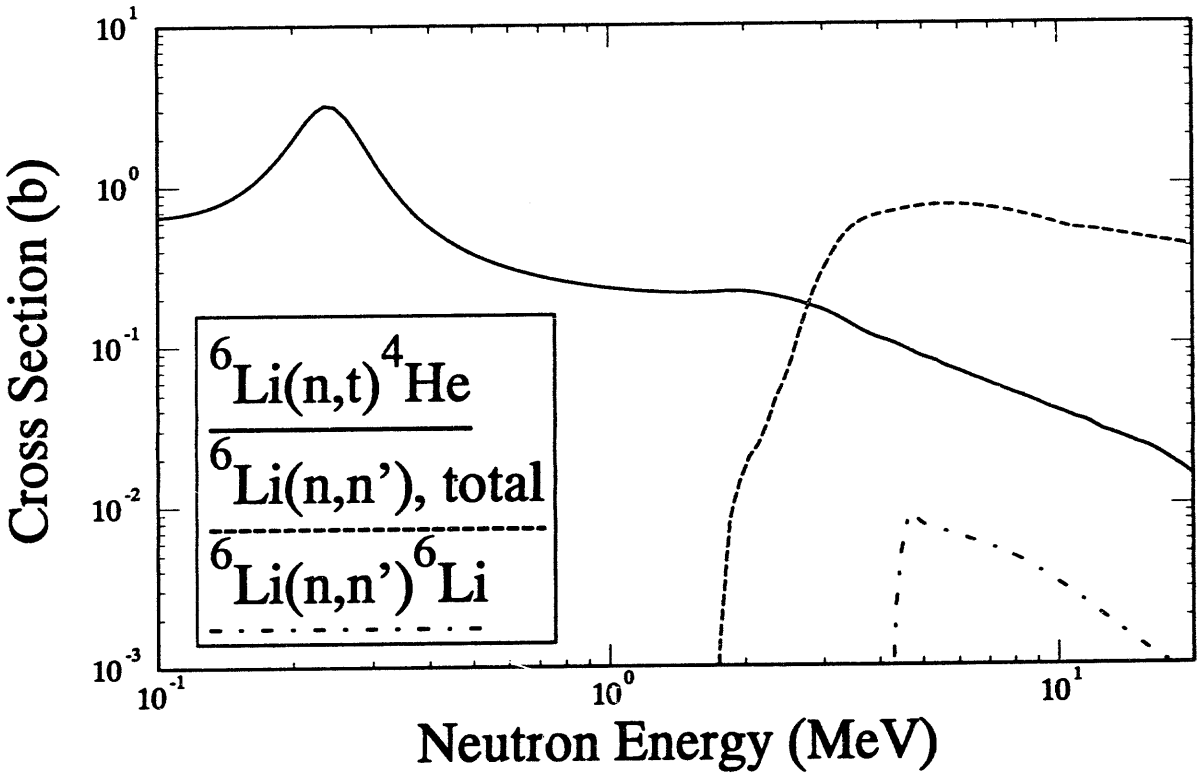

Figure A-6c: $^{6}Li(n,X)^{4}He$ Cross Section Components

Table A-7a
Alternative Cross Section Sources for the $^{19}F(n,2n)^{18}F$ Reaction

$^{19}F(n,2n)^{18}F$			
Cross Section Library	Material Number	Covariance Data	Comment
ENDF/B-VI	925	Yes	CNDC, ORNL, June 1990.
ENDF/B-V	1309	Yes	ORNL, July 1974, Tape 556, release 2, based on ENDF/B-IV evaluation.
ENDF/B-V	7099	Yes	ORNL, Nov. 1979, Activation Tape 532b.
IRDF-90	925	Yes	IRK, June 1980.
IRDF-82	920	Yes	AUSIRK, 1979.
JENDL-3	3091	No	JAERI, July 1989, ma257.23.
JEF 2.2	925	No	RCOM, June 1982, taken from ENDF/B-IV, jef-1.
BROND	-- NA --	----	A 1990 evaluation is reported, but not in NNDC distribution.

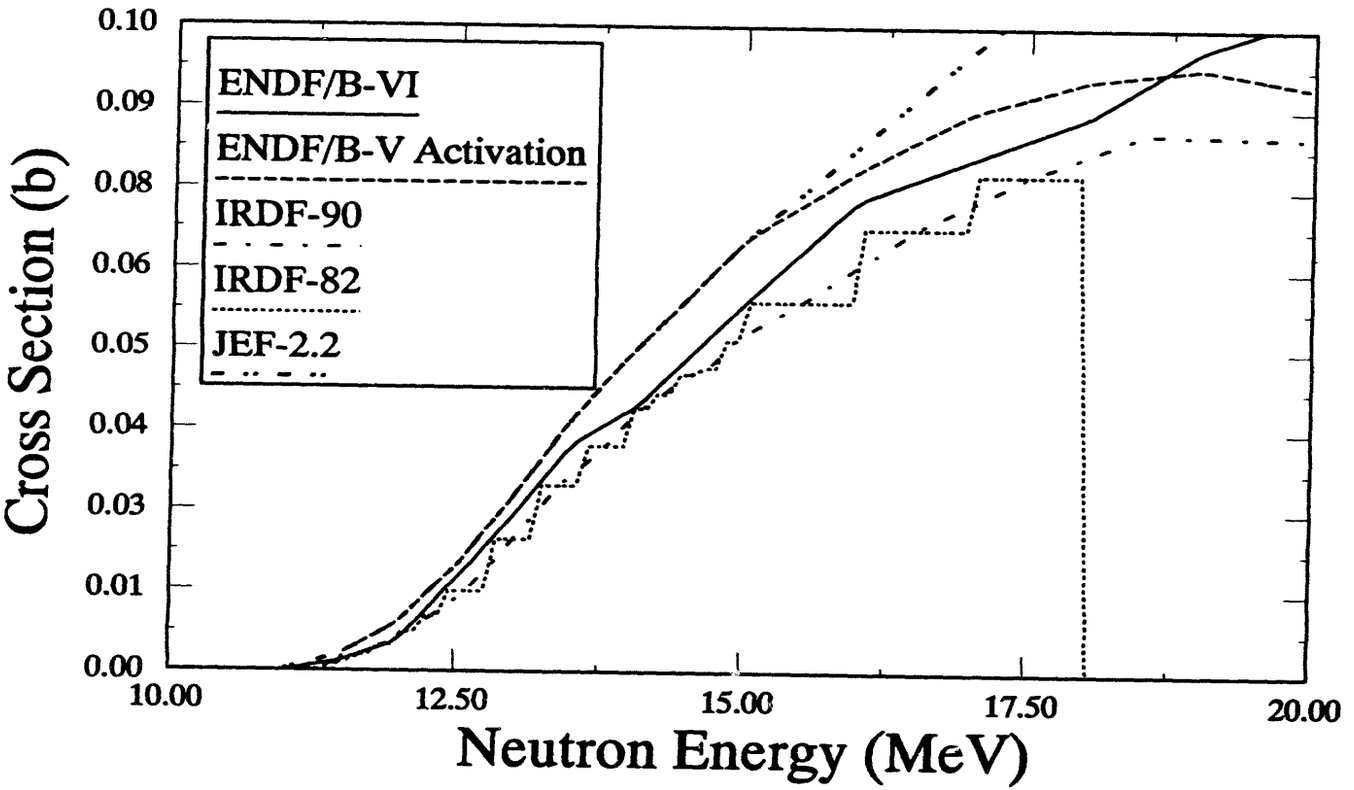

Figure A-7a: $^{19}F(n,2n)^{18}F$ Cross Section

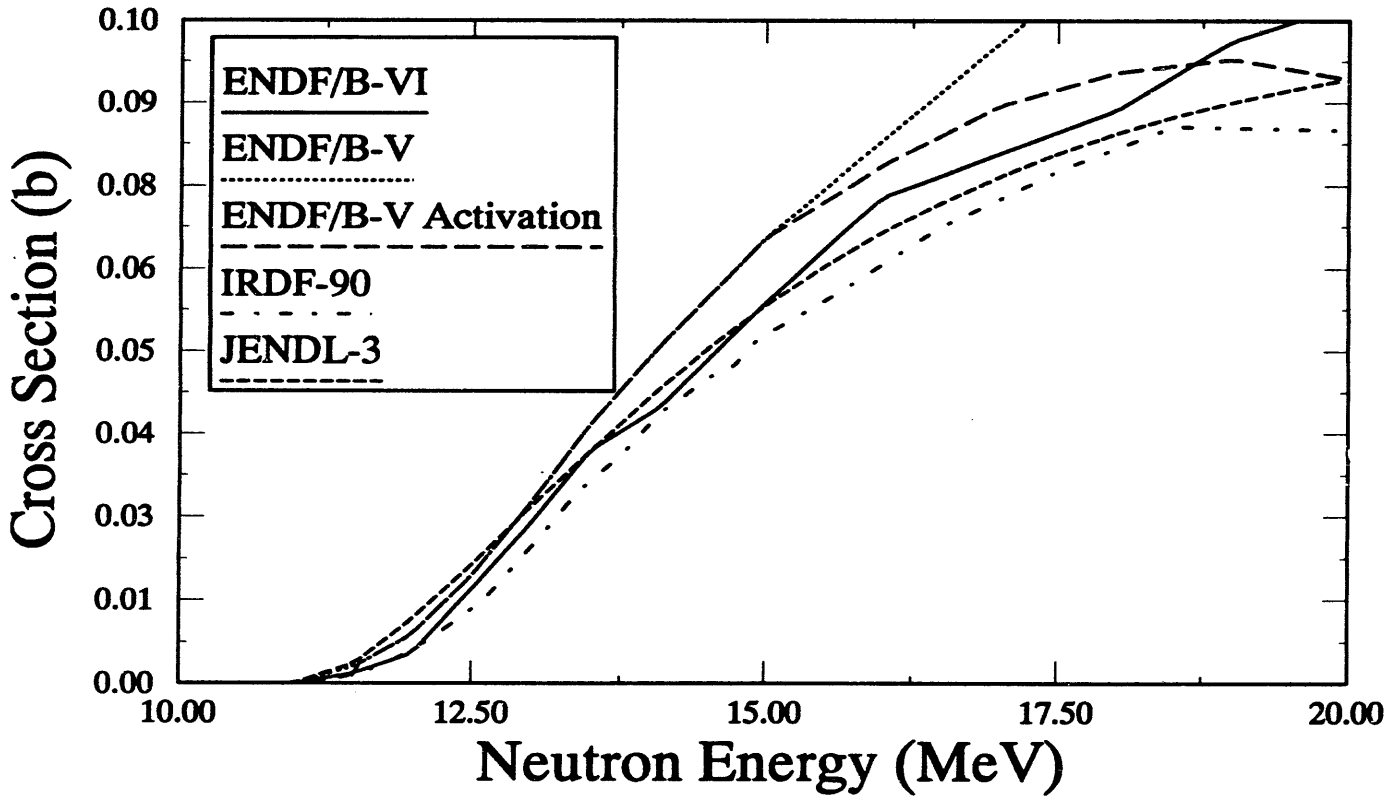

Figure A-7b: $^{19}F(n,2n)^{18}F$ Cross Section

Table A-8a
Alternative Cross Section Sources for the $^{23}Na(n,\gamma)^{24}Na$ Reaction

$^{23}Na(n,\gamma)^{24}Na$			Comment
Cross Section Library	Material Number	Covariance Data	
ENDF/B-VI	1125	Yes	Format translation of ENDF/B-V.
ENDF/B-V	6311	Yes	Dosimetry Tape, ORNL, Dec 77.
ENDF/B-V	7113	No	Activation Tape, ORNL, Nov 79.
ENDF/B-V	1311	Yes	Complete Evaluation, ORNL, Dec 77.
JENDL-3	3111	No	SRI, Mar, 87.
JENDL-3 Dos.	1131	Yes	Identical to JENDL-3, covariance adopted from IRDF-85.
JEF 2.2	1125	No	Taken over from JENDL-3, 1987, tape jef-1.
BROND	1111	No	1978, Obninsk, tape ma242.51.

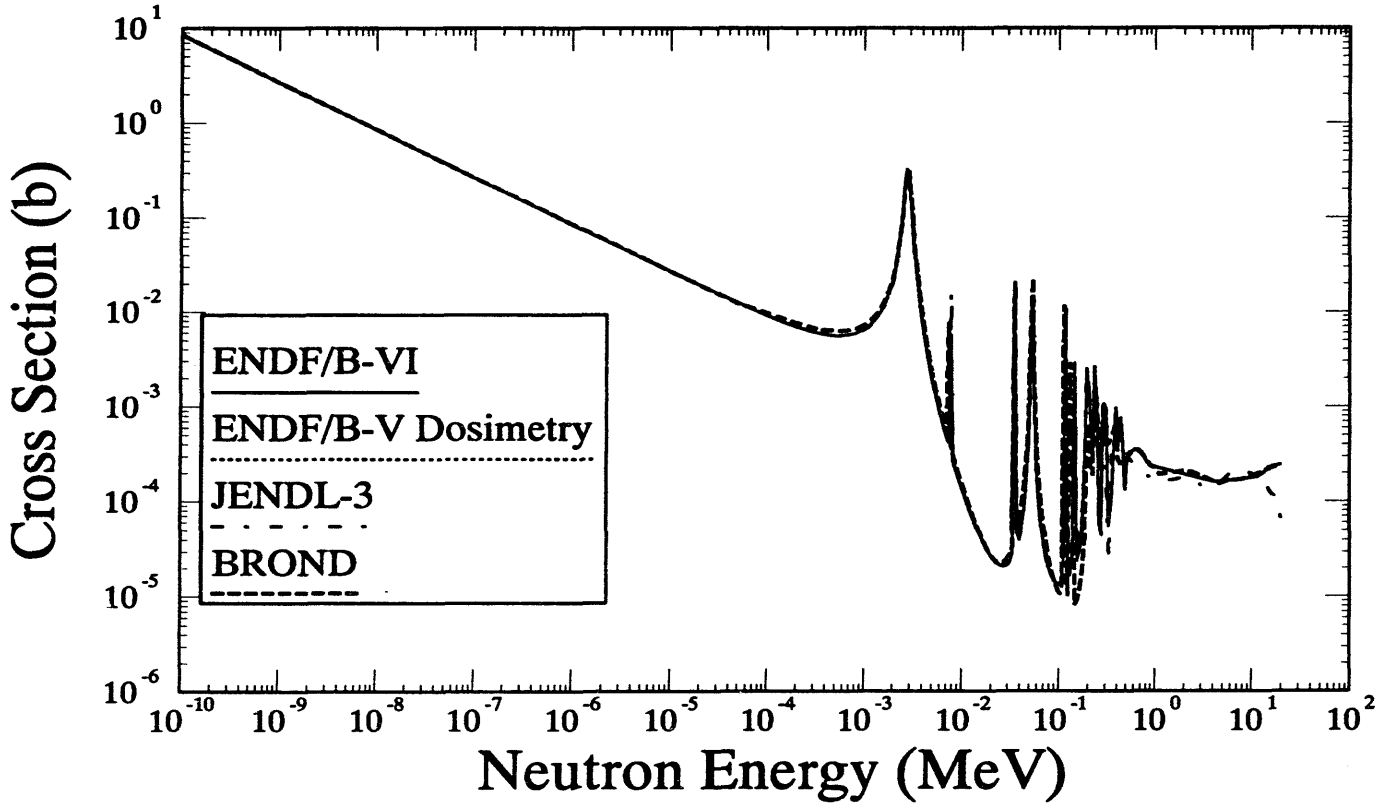

Figure A-8a: $^{23}Na(n,\gamma)^{24}Na$ Cross Section

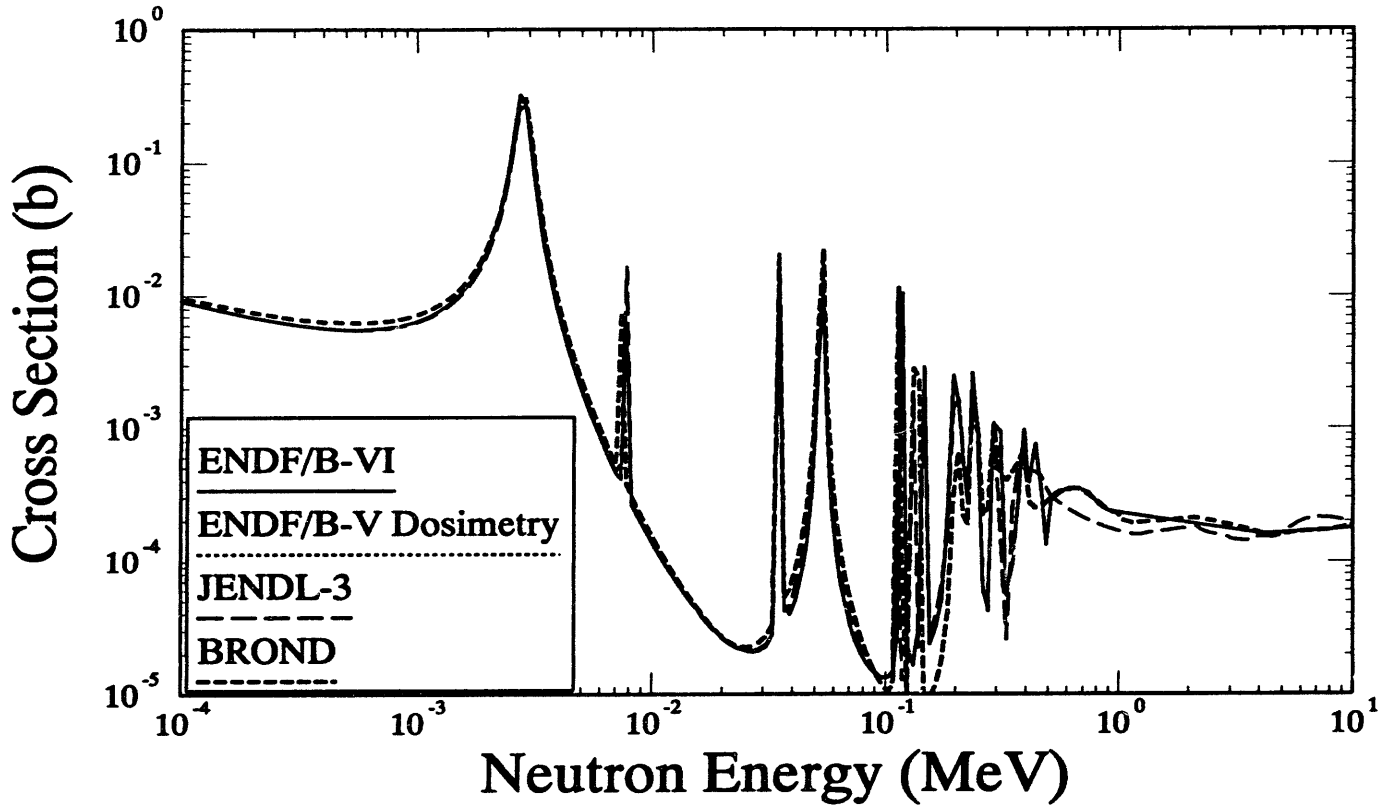

Figure A-8b: $^{23}Na(n,\gamma)^{24}Na$ Cross Section

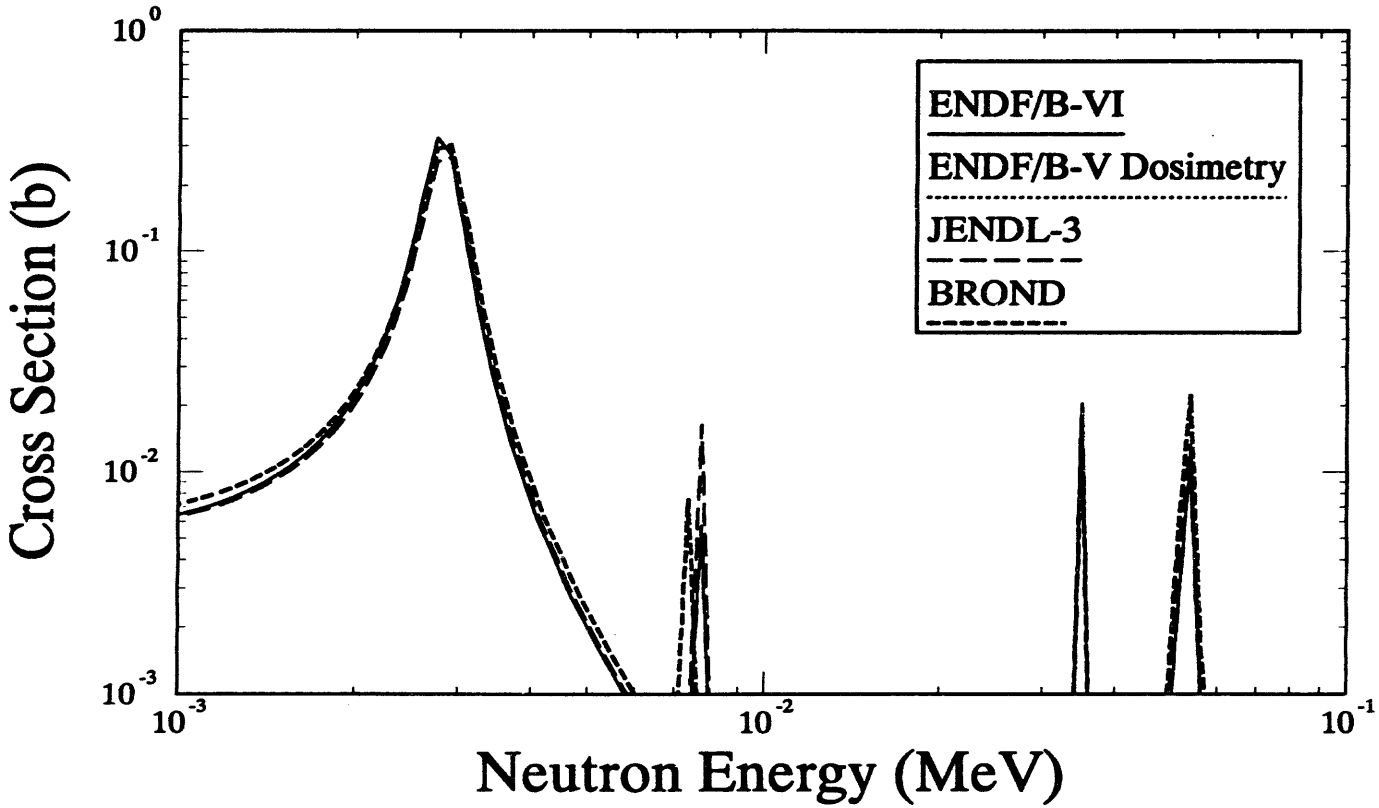

Figure A-8c: $^{23}Na(n,\gamma)^{24}Na$ Cross Section

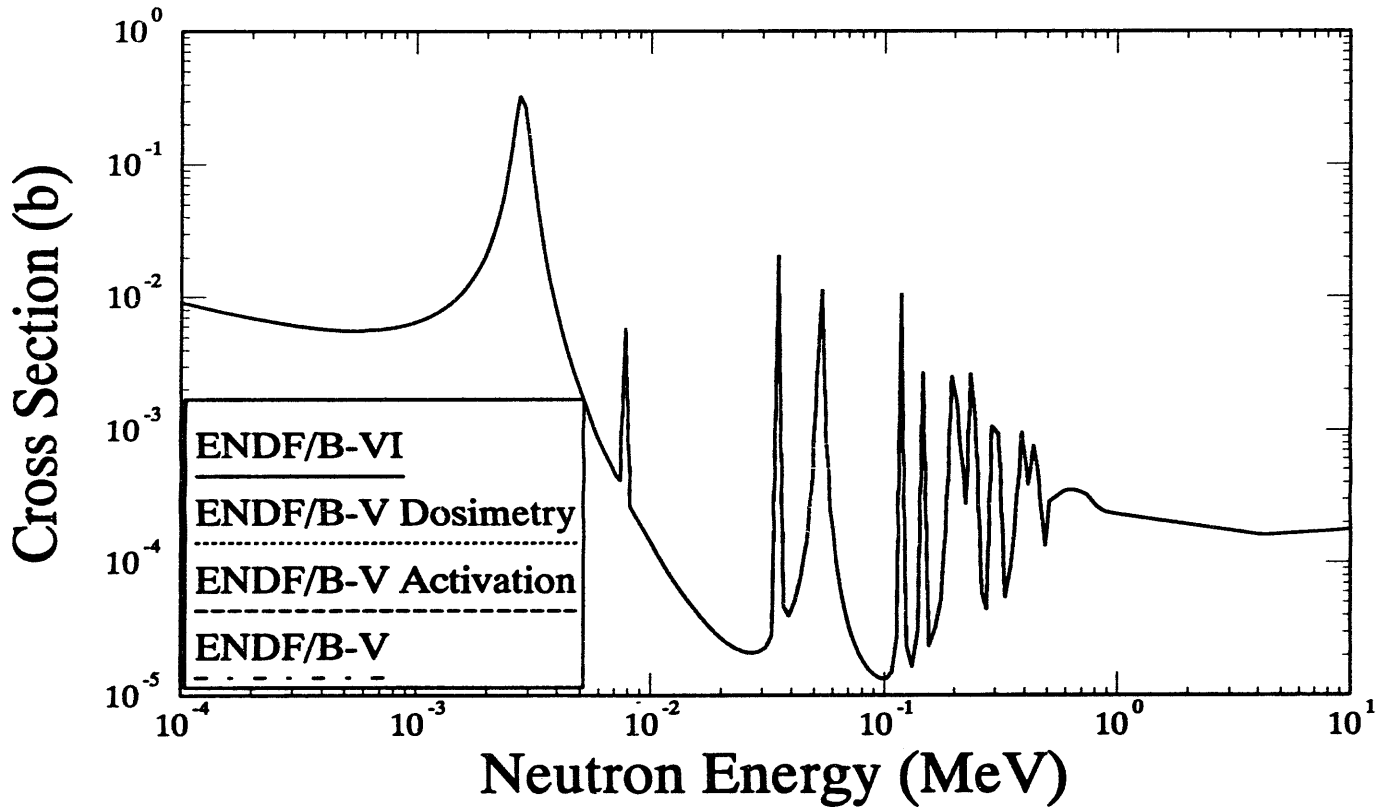

Figure A-8d: $^{23}Na(n,\gamma)^{24}Na$ Cross Section

Table A-9a
Alternative Cross Section Sources for the $^{24}Mg(n,p)^{24}Na$ Reaction

$^{24}Mg(n,p)^{24}Na$			
Cross Section Library	Material Number	Covariance Data	Comment
ENDF/B-VI	1225	No	Format translation of ENDF/B-V.
IRDF-90	1225	Yes	IRK, 1990.
ENDF/B-V	7124	No	Activation Tape, HEDL, ORNL, Mar, 80.
IRDF-82	1220	Yes	AUSIRK, 1979.
JENDL-3	3121	No	NEDAC, Sept., 89.
JENDL-3 Dos.	1231	Yes	Cross section identical to JENDL-3, covariance taken from IRDF-85.

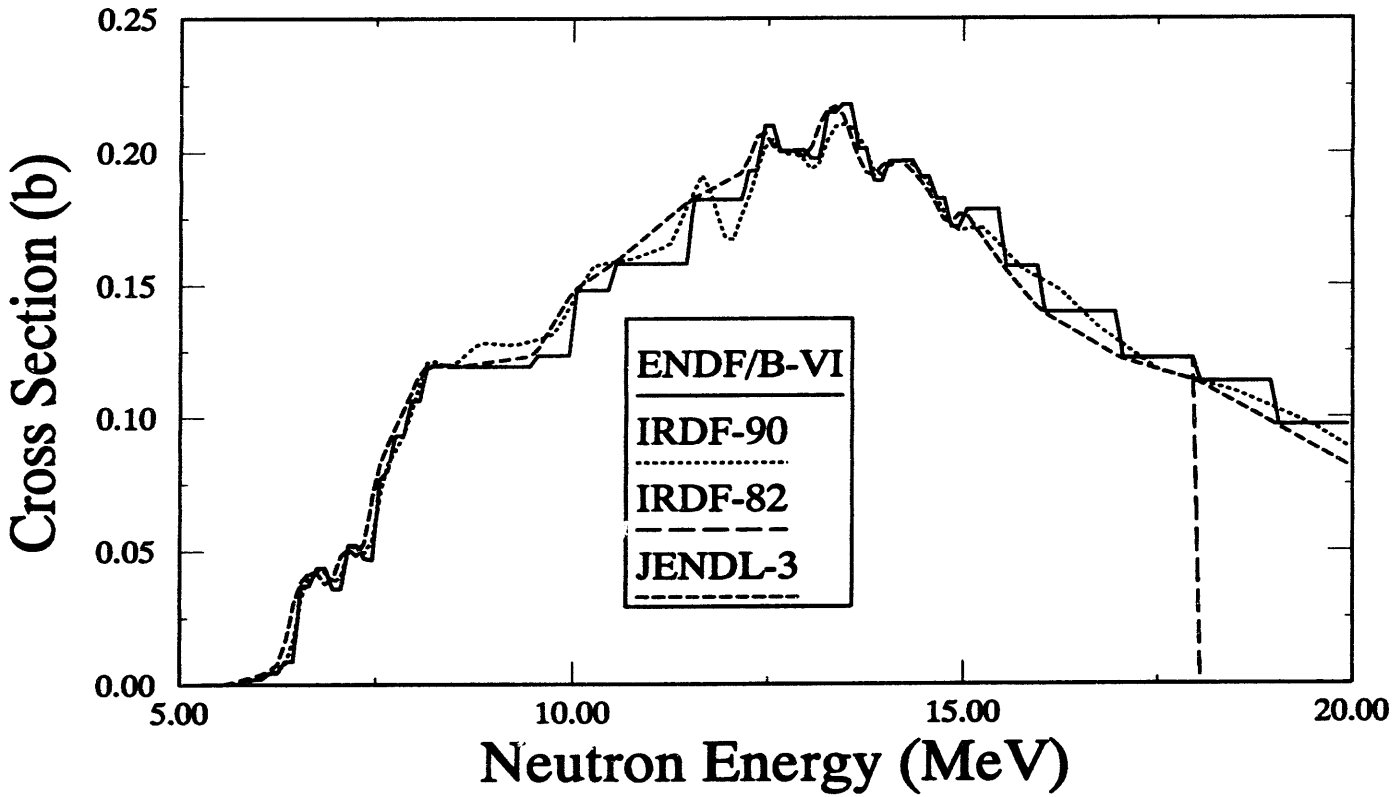

Figure A-9a: $^{24}Mg(n,p)^{24}Na$ Cross Section

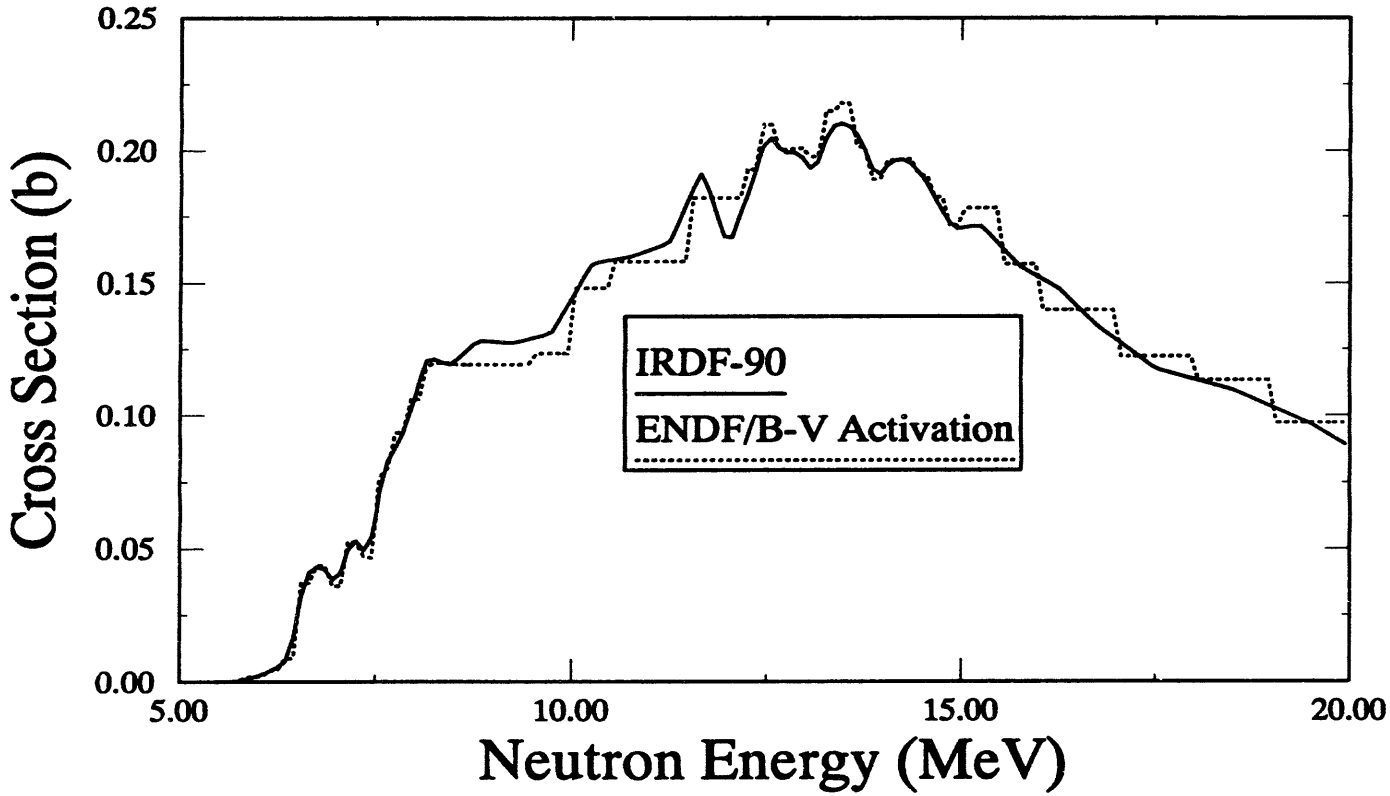

Figure A-9b: $^{24}Mg(n,p)^{24}Na$ Cross Section

Table A-10a
Alternative Cross Section Sources for the $^{27}Al(n,p)^{27}Mg$ Reaction

$^{27}Al(n,p)^{27}Mg$			Comment
Cross Section Library	Material Number	Covariance Data	
ENDF/B-VI	1325	Yes	Format translation of ENDF/B-V.
IRDF-90	1325	Yes	ORNL, 1990.
GLUCS	6313	Yes	ORNL.
ENDF/B-V	6313	Yes	Dosimetry Tape, LANL 1973, Rev. 1977, taken from ENDF/B-IV.
ENDF/B-V	7137	No	Activation Tape, LANL, 1973, Rev. 1977, taken from ENDF/B-IV.
ENDF/B-V	1313	Yes	Complete evaluation, LANL, 1973, Rev.1977, taken from ENDF/B-IV.
IRDF-82	6313	Yes	Adopted from ENDF/B-V, LANL, 1973.
JENDL-3	3131	No	TIT & JAERI, Evaluation Mar. 1988.
JEF 2.2	1325	No	Recom. July 1986, taken from ENDF/B-IV, revised by ENEA.

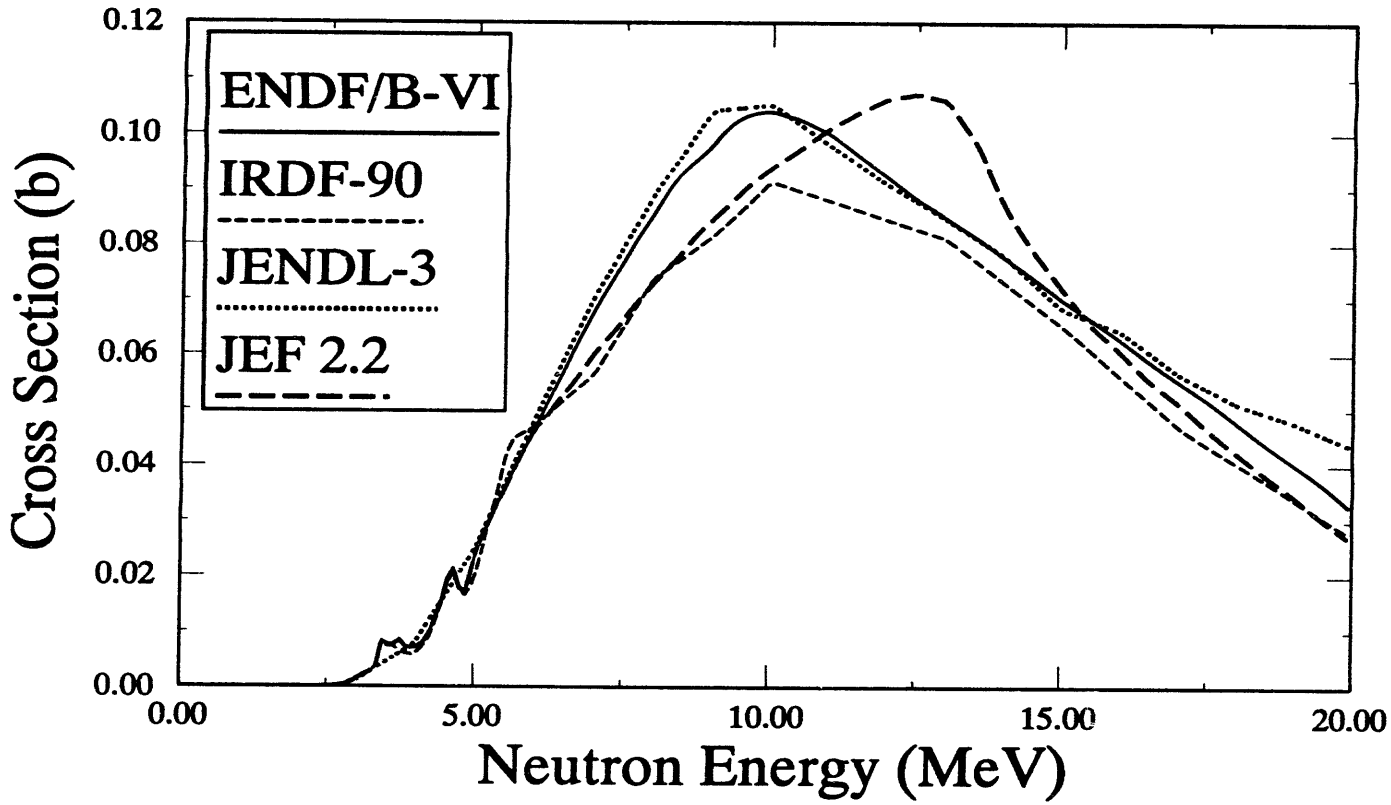

Figure A-10a: $^{27}Al(n,p)^{27}Mg$ Cross Section

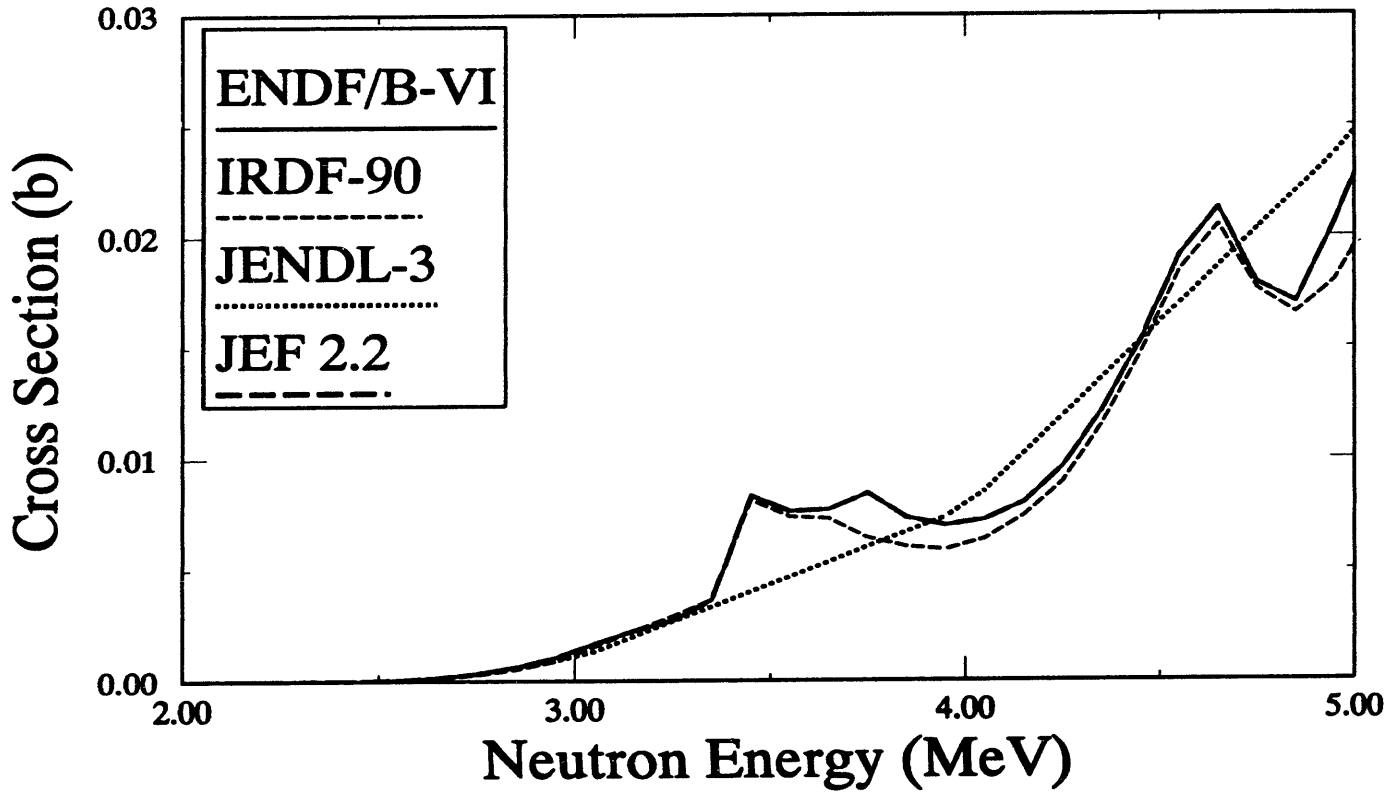

Figure A-10b: $^{27}Al(n,p)^{27}Mg$ Cross Section

Table A-11a
Alternative Cross Section Sources for the $^{27}Al(n,\alpha)^{24}Na$ Reaction

$^{27}Al(n,\alpha)^{24}Na$			
Cross Section Library	Material Number	Covariance Data	Comment
ENDF/B-VI	1325	Yes	Format translation of ENDF/B-V.
IRDF-90	1325	Yes	IRK, Vienna, 1990.
GLUCS	6313	Yes	ORNL.
ENDF/B-V	6313	Yes	Dosimetry Tape, LANL 1973, Rev. 1977, taken from ENDF/B-IV.
ENDF/B-V	7137	No	Activation Tape, LANL, 1973, Rev. 1977, taken from ENDF/B-IV.
ENDF/B-V	1313	Yes	Complete evaluation, LANL, 1973, Rev. 1977, taken from ENDF/B-IV.
IRDF-82	6313	Yes	Adopted from ENDF/B-V, LANL, 1973.
JENDL-3	3131	No	TIT & JAERI, Evaluation Mar. 1988.
JEF 2.2	1325	No	Recom. July 1986, taken from ENDF/B-IV, revised by ENEA.

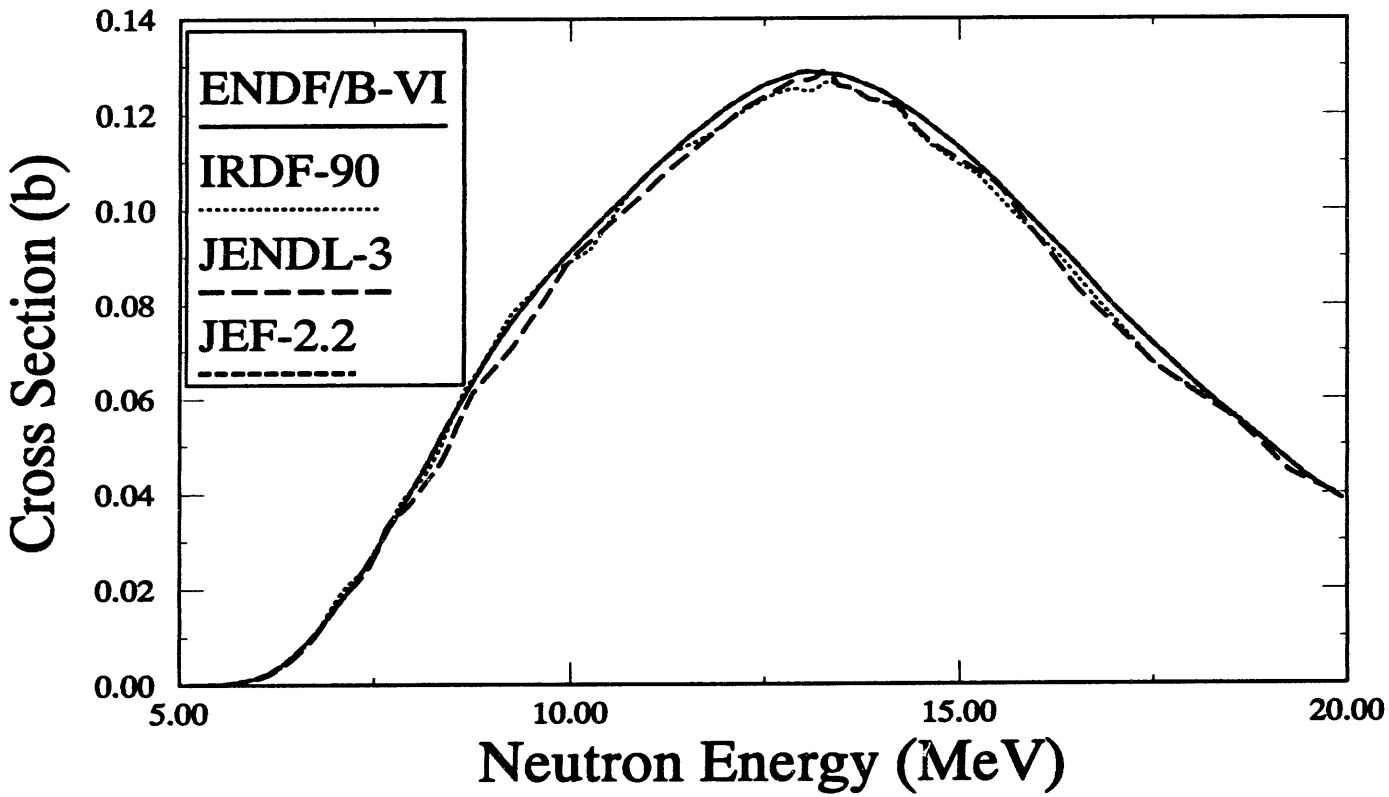

Figure A-11a: $^{27}Al(n,\alpha)^{24}Na$ Cross Section

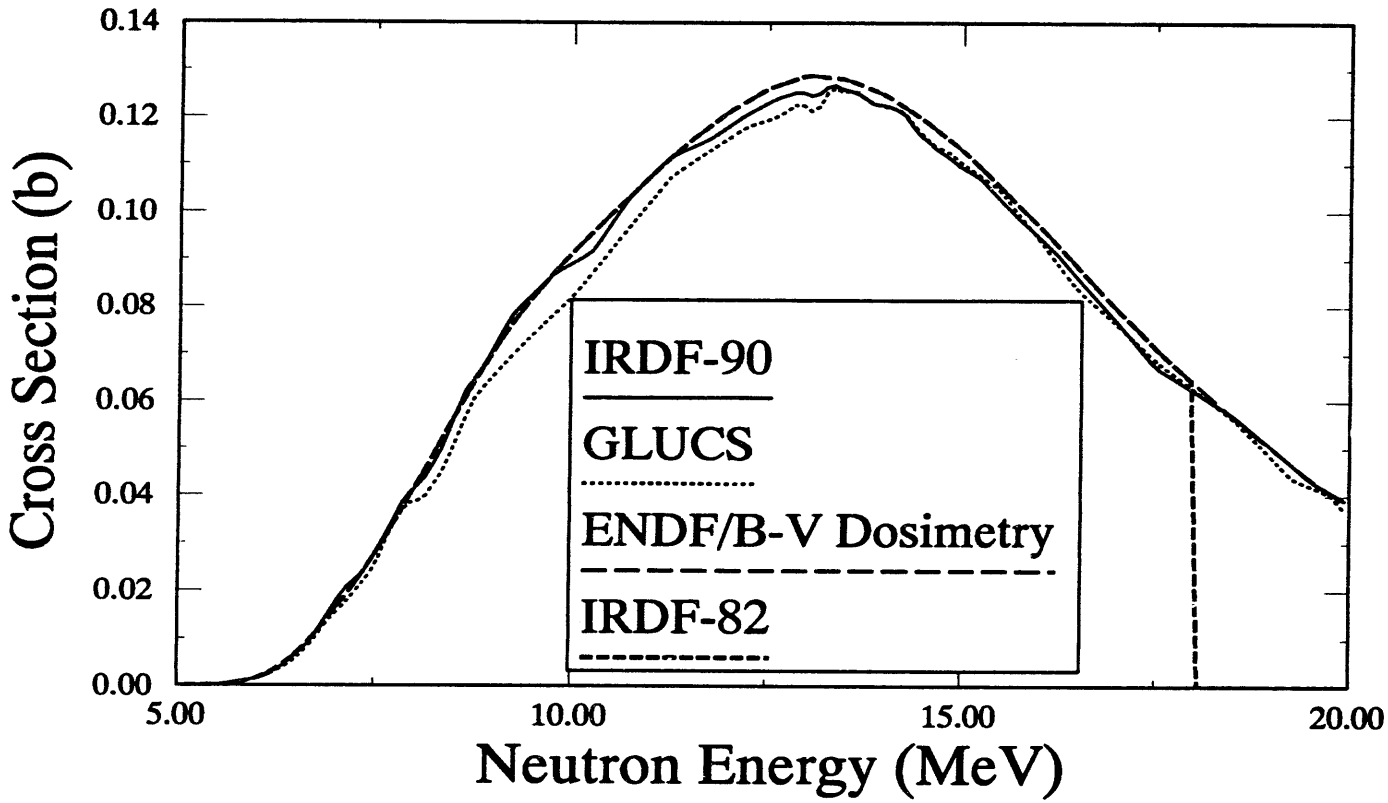

Figure A-11b: $^{27}Al(n,\alpha)^{24}Na$ Cross Section

Table A-12a
Alternative Cross Section Sources for the ^{Nat}Si(n,X)1MeV

^{Nat}S(n,X)1MeV			Comment
Cross Section Library	Material Number	Covariance Data	
ENDF/B-VI	1400	No	^{Nat}Si, Format translation of ENDF/B-V data.
ENDF/B-V	1314	No	ORNL Feb 1974 evaluation, revised Oct 1980, tape 556, revision 2.
JENDL-3	3140	No	^{Nat}Si, and ^{28}Si, ^{29}Si, ^{30}Si, JAERI Eval. Mar 1988, tape 23. NJOY/CONBAR processing error.
JEF 2.2	1400	No	Recom. July 1986, taken from ENDF/B-IV, revised by ENEA, tape jef-1.
BROND	1402	No	TUD/CJD Eval. May 1985. Inadequate (n,2n) γ-production data.
private	1428	No	ORNL Sept. 1989 evaluation [15], submitted for ENDF/B-VI release 2. incorporated into ASTM E 722-93
ENDF/B-IV	1194	No	ORNL eval. Feb. 1974, tape 405.
ASTM	----	No	ASTM E 722-85, pre-1992 standard.
LENDL-V	7820	No	Howerton, NJOY processing error.

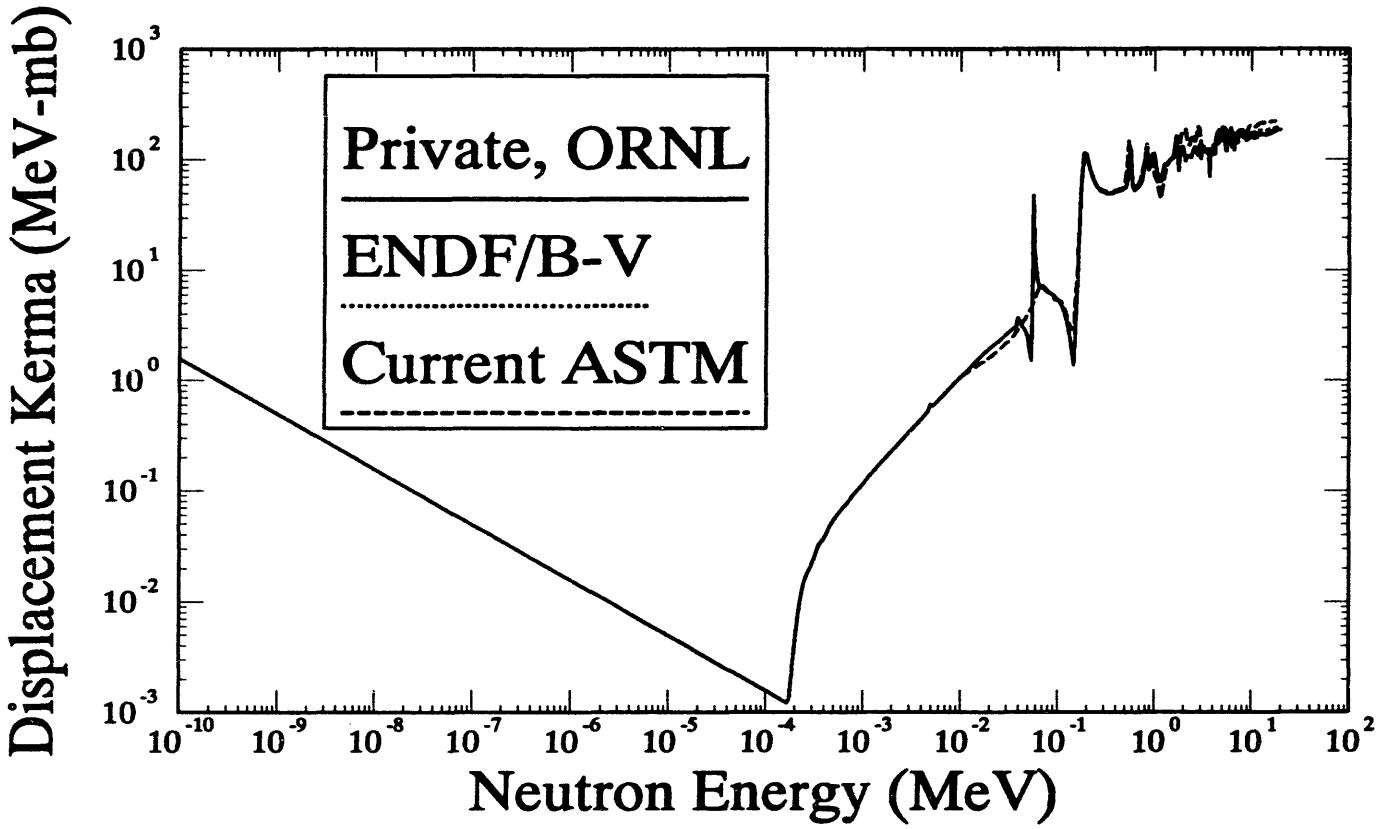

Figure A-12a: $^{Nat}Si(n,X)1MeV$ Damage Function

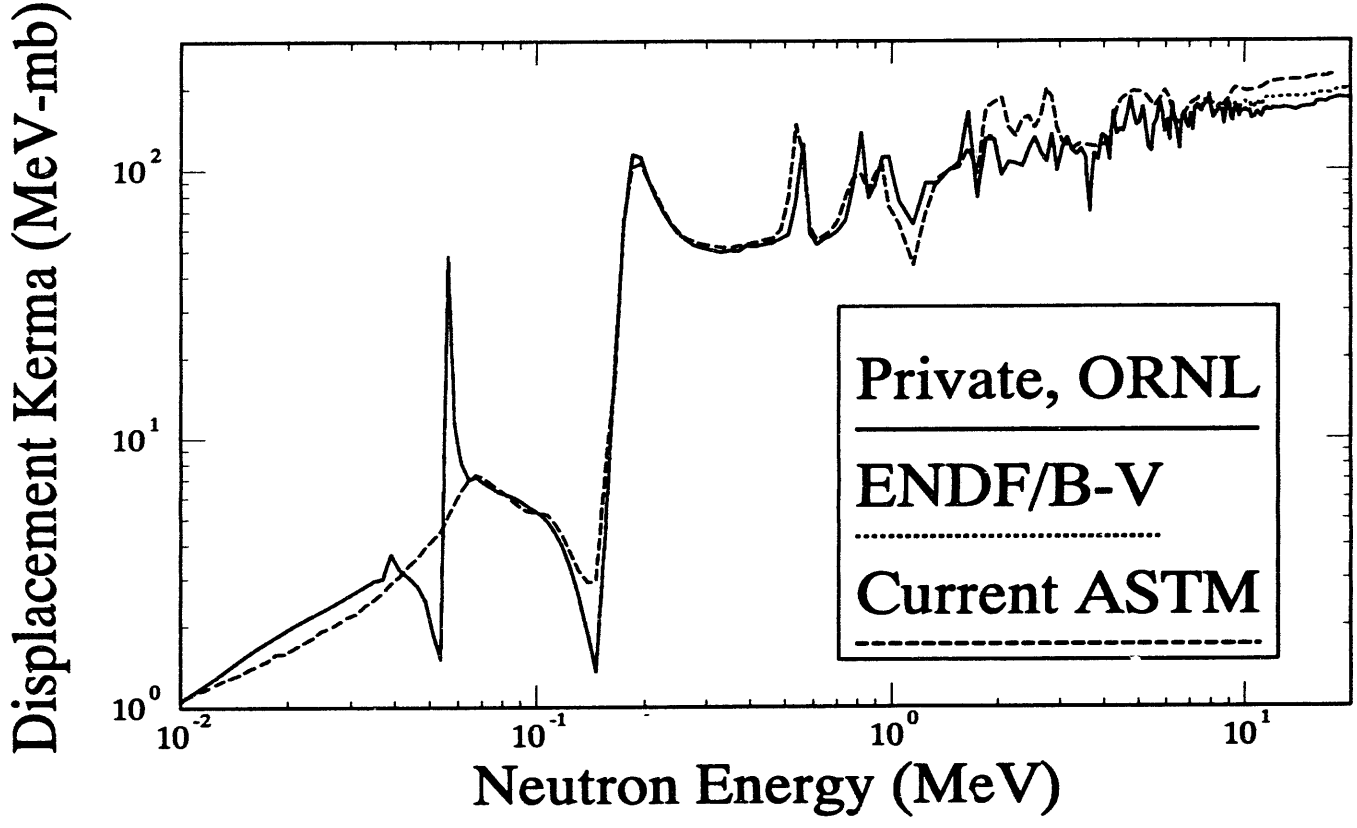

Figure A-12b: ^{Nat}Si(n,X)1MeV Damage Function

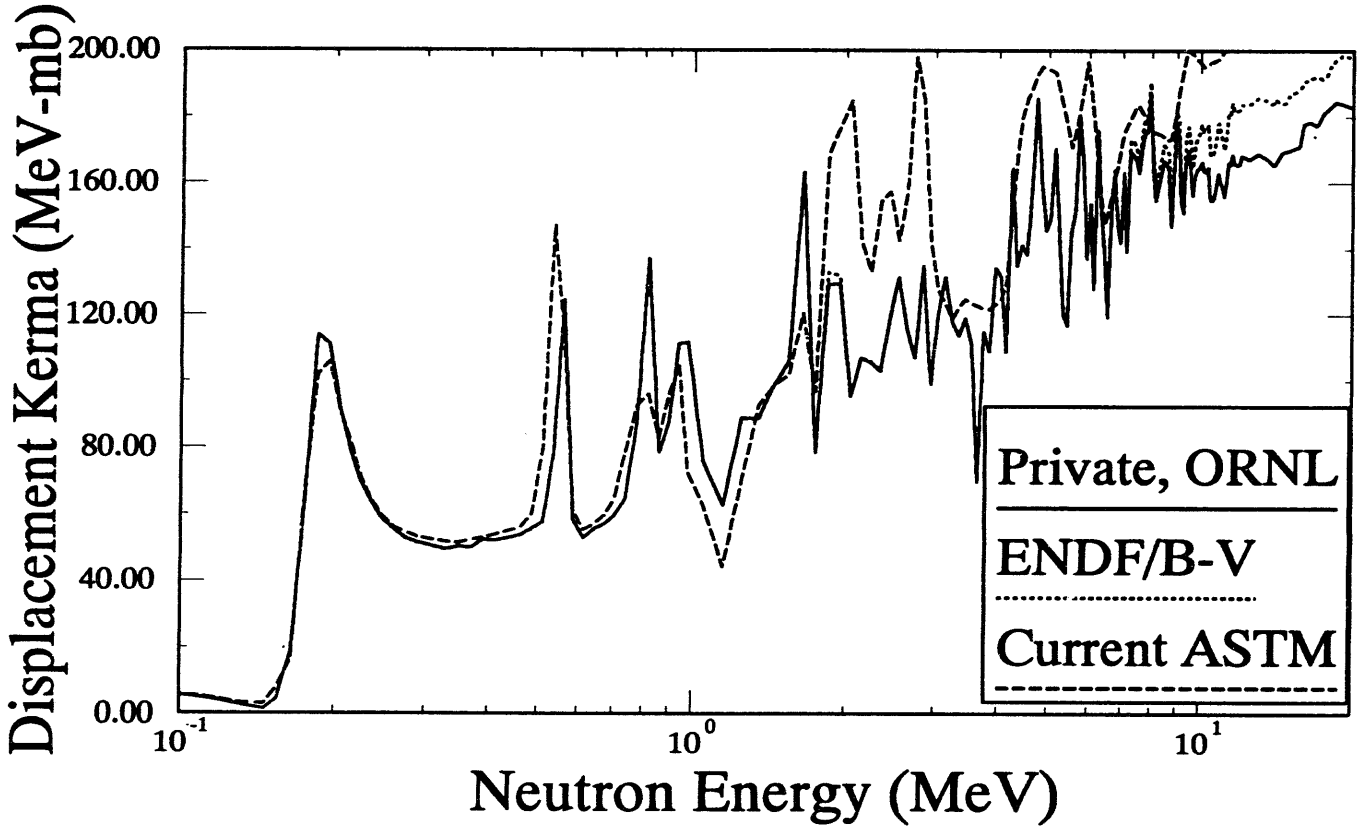

Figure A-12c: ^{Nat}Si(n,X)1MeV Damage Function

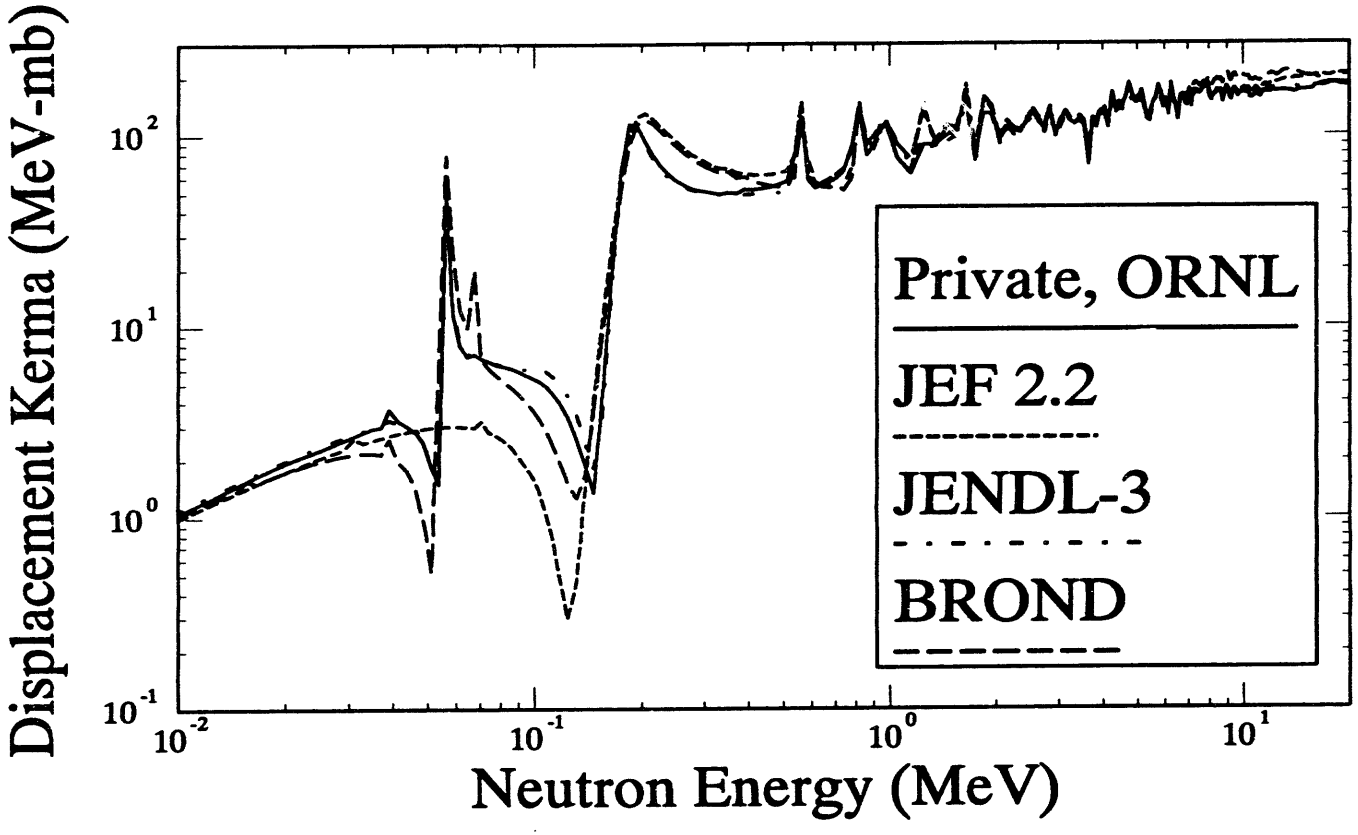

Figure A-12d: ^{Nat}Si(n,X)1MeV Damage Function

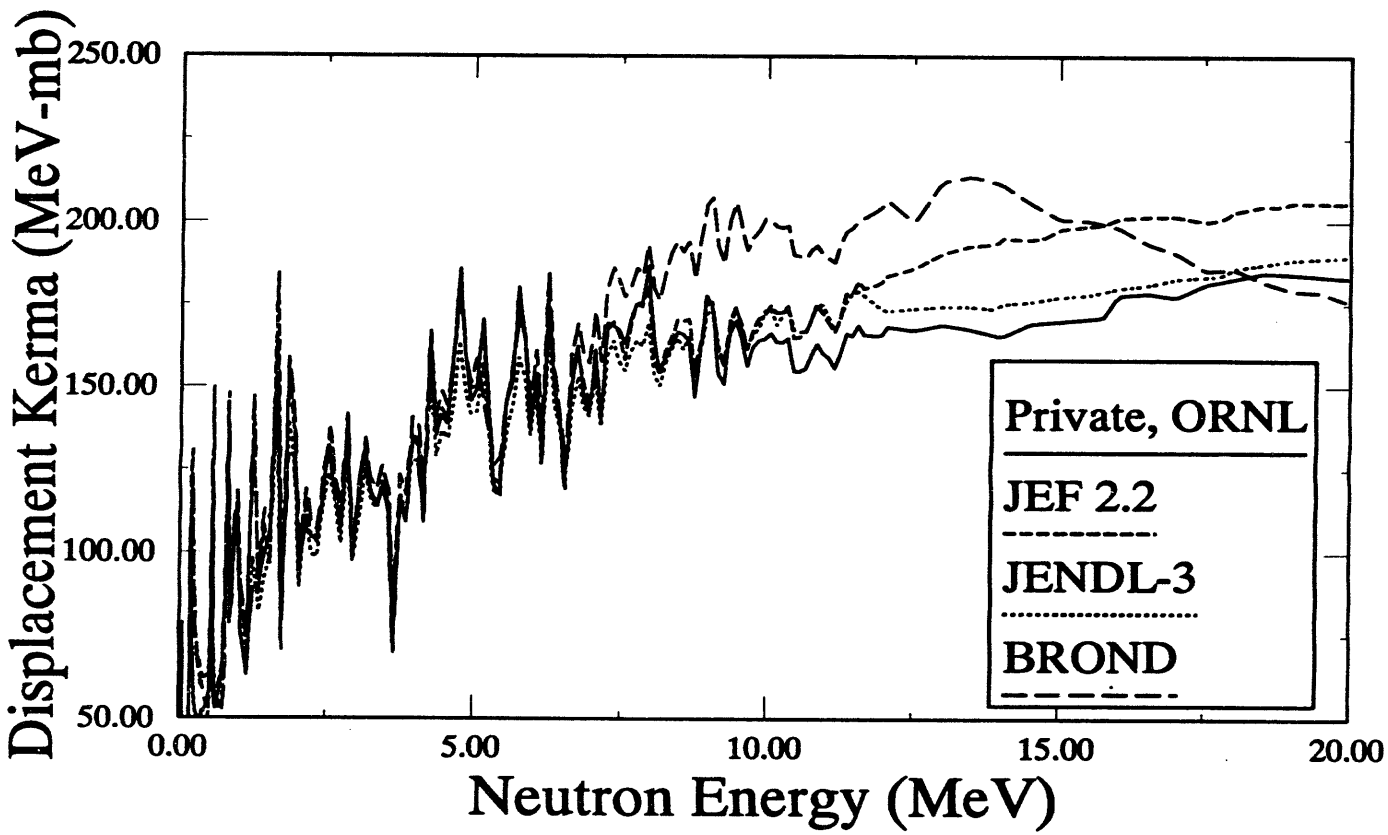

Figure A-12e: ^{Nat}Si(n,X)1MeV Damage Function

Table A-13a
Alternative Cross Section Sources for the $^{31}P(n,p)^{31}Si$

$^{31}P(n,p)^{31}Si$			Comment
Cross Section Library	Material Number	Covariance Data	
ENDF/B-VI	1525	No	Taken from ENDL Howerton eval., Oct. 1977, also in ENDF/B-V.
ENDF/B-V	1315	No	Taken from ENDL Howerton eval. Oct. 1977, tape 503.
ENDF/B-V	7151	No	ENDL Howerton, eval. 1977, Activation Tape 532b.
JENDL-3	3151	No	FUJI E. C., May 1987, tape ma257.23.
JENDL-3 Dos.	1531	Yes	Cross section identical to JENDL-3, covariance from IRDF-85.
JEF 2.2	1525	No	Taken from JENDL-3, jef-1 tape.
IRDF-82	1520	Yes	AUSIRK, Eval. 1979.
IRDF-90	1525	Yes	IRK, Eval. June 1980.

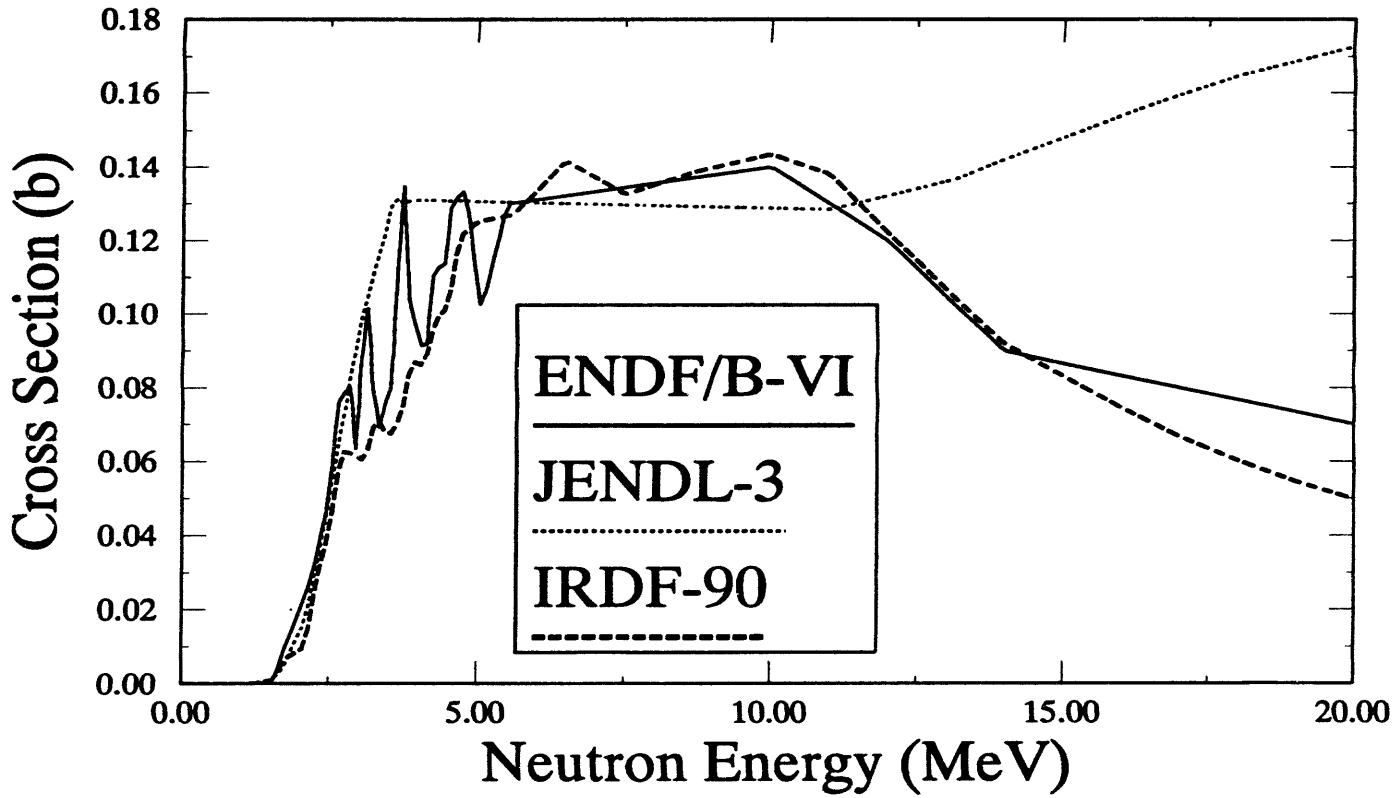

Figure A-13a: $^{31}P(n,p)^{31}Si$ Cross Section

Table A-14a
Alternative Cross Section Sources for the $^{32}S(n,p)^{32}P$ Reaction

$^{32}S(n,p)^{32}P$			Comment
Cross Section Library	Material Number	Covariance Data	
ENDF/B-VI	1625	No	Format translation of ENDF/B-V.
IRDF-90	1625	Yes	ORNL, 1989.
GLUCS	32	Yes	ORNL, 1993 update to GLUC library. New std. dev. data larger due to inclusion of additional data.
ENDF/B-V	6439	Yes	Dosimetry Tape, BNL, Mar 84.
ENDF/B-V	7162	No	Activation Tape, LLL, Mar 84, identical to ENDF/B-V full evaluation except near the threshold.
ENDF/B-V	1316	No	Complete evaluation, LLL May 78.
IRDF-82	6439	Yes	Adopted from ENDF/B-V, LANL, 1973.
JENDL-3	3161	No	Fuji E. C. L, Evaluation Mar. 1987.
JEF 2.2	1625	No	Taken from JENDL-3, May, 1987.
private	7439	No	ORNL, Fu ANS presentation Apr 89, Re-evaluation from threshold to 5 MeV. Used as an input to the GLUCS analysis.

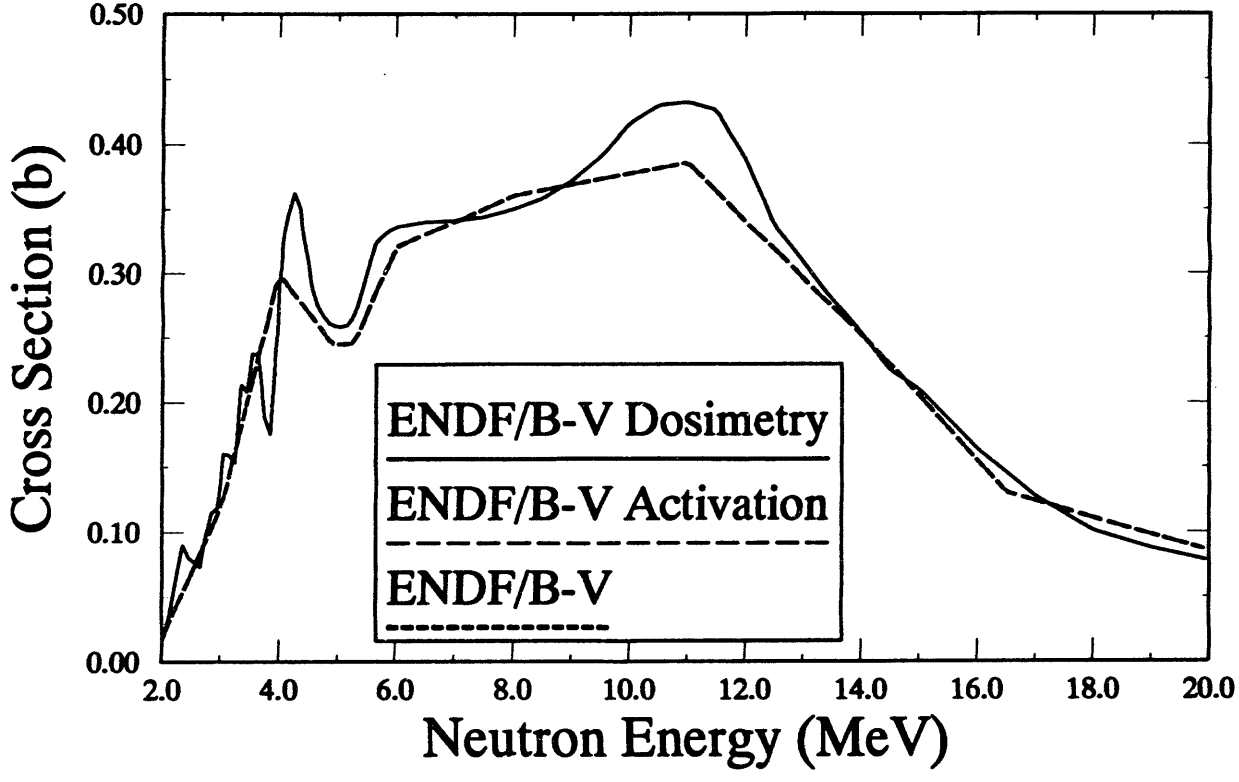

Figure A- 14a: $^{32}S(n,p)^{32}P$ Cross Section

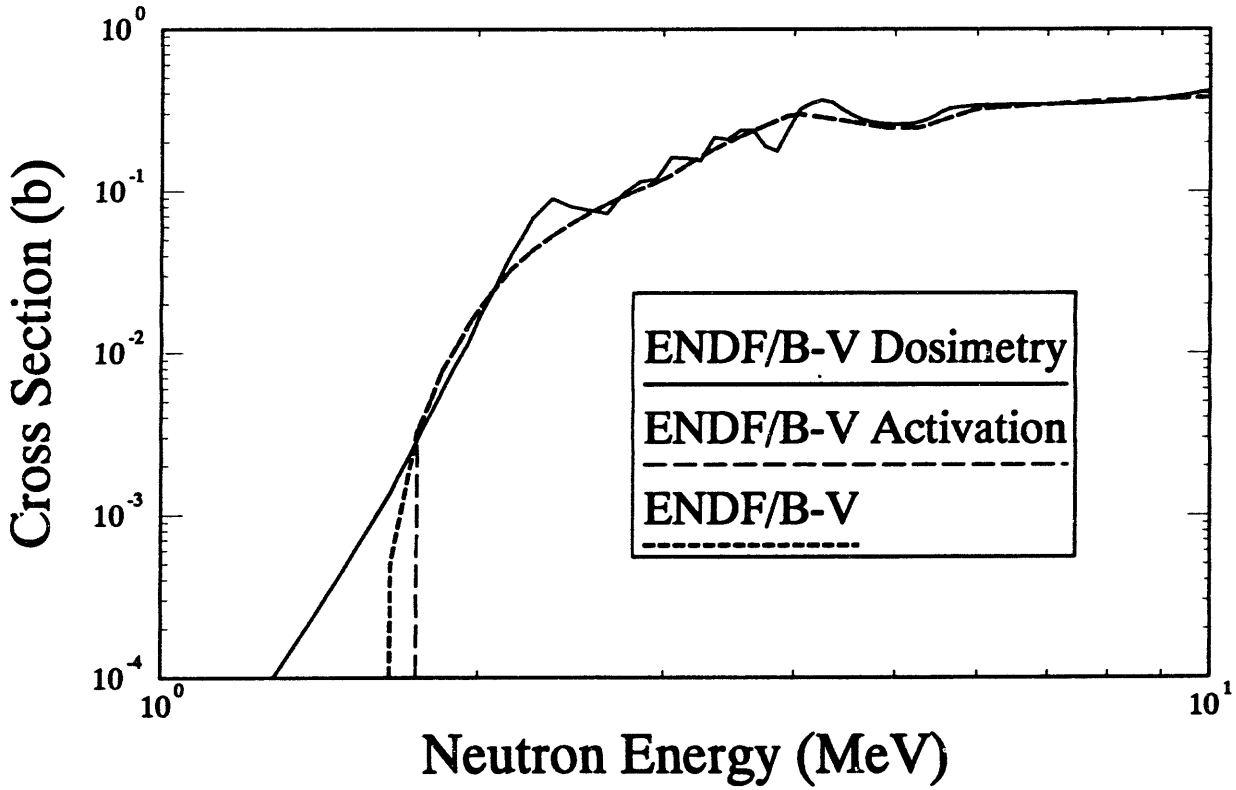

Figure A-14b: $^{32}S(n,p)^{32}P$ Cross Section

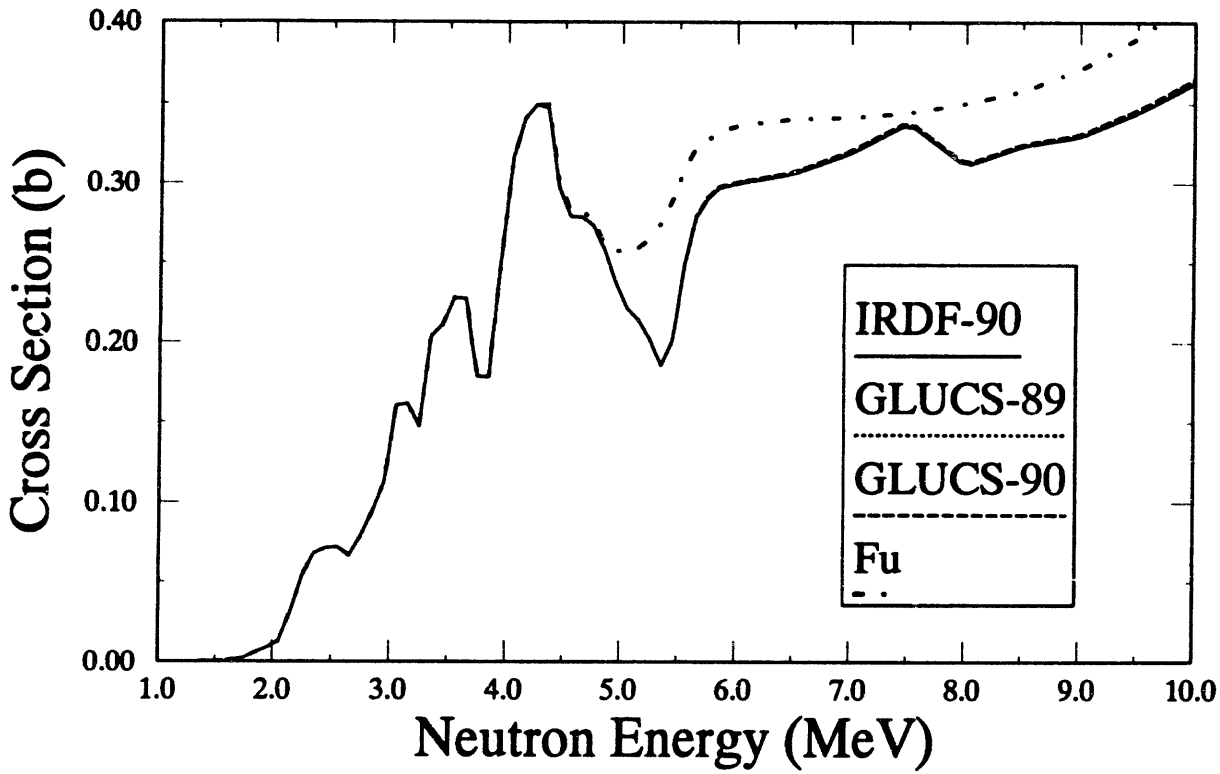

Figure A-14c: $^{32}S(n,p)^{32}P$ Cross Section

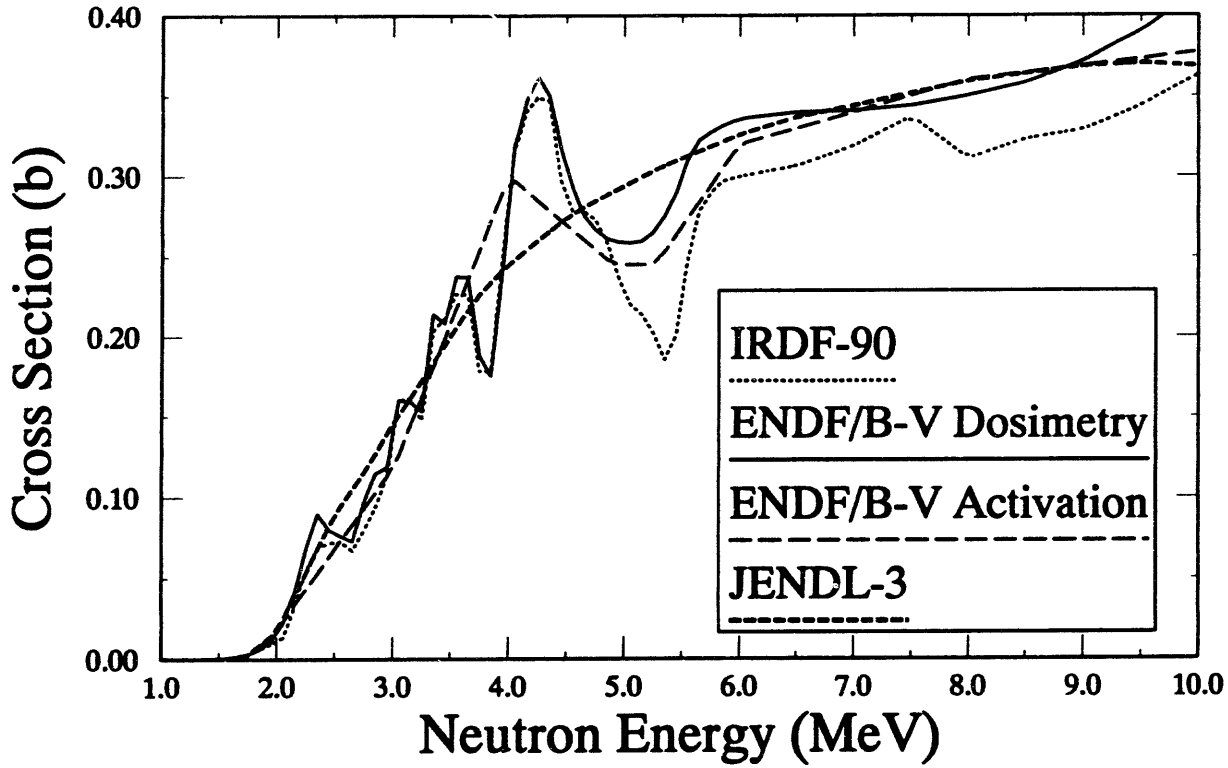

Figure A-14d: $^{32}S(n,p)^{32}P$ Cross Section

Table A-15a
Alternative Cross Section Sources for the $^{45}Sc(n,\gamma)^{46}Sc$ Reaction

$^{45}Sc(n,\gamma)^{46}Sc$			Comment
Cross Section Library	Material Number	Covariance Data	
ENDF/B-VI	2125	Yes	BNL, Eval. July 1979, taken from ENDF/B-V evaluation.
IRDF-90	2125	Yes	Taken from ENDF.
ENDF/B-V	6426	Yes	BNL, Eval. July 1979, Dosimetry Tape 531a.
ENDF/B-V	7215	No	BNL, Eval. July 1979, Activation Tape, 532b.
JENDL-3	3211	No	KHI, Eval. Aug. 1988, tape 23.
JENDL-3 Dos.	2131	Yes	Identical to JENDL-3, covariance from IRDF-85.

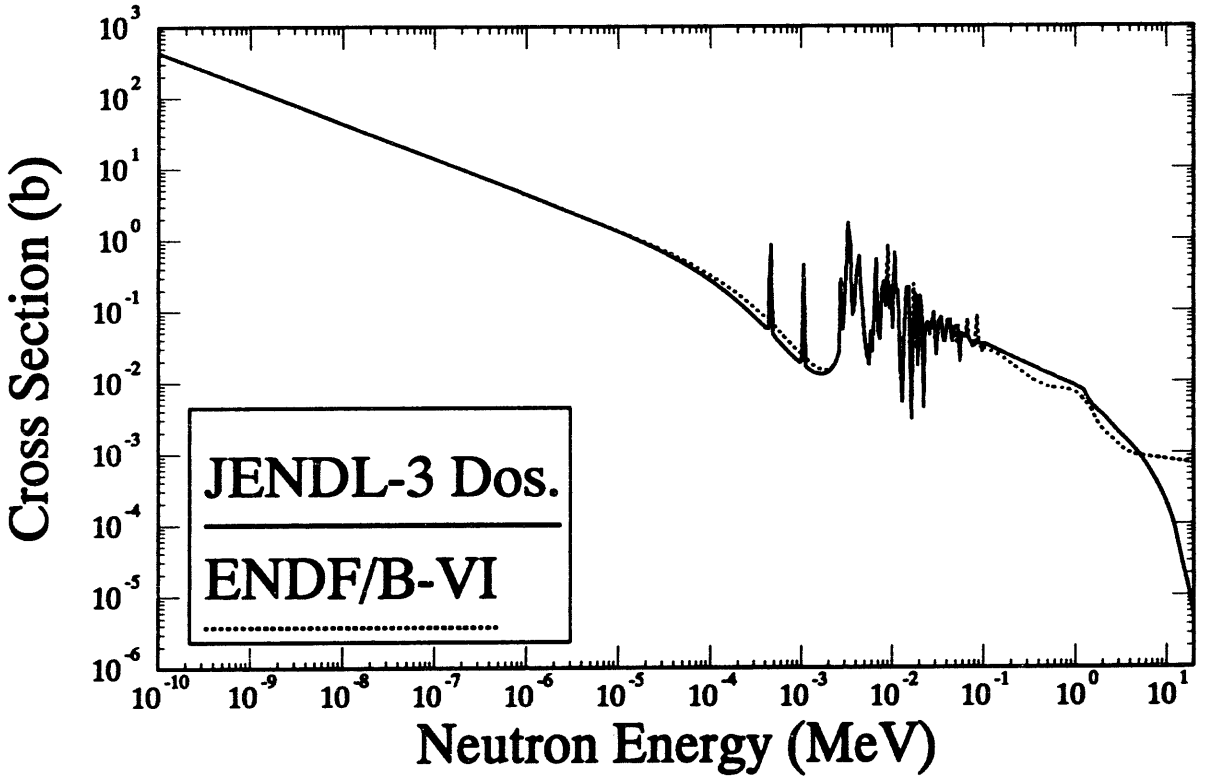

Figure A-15a: $^{45}Sc(n,\gamma)^{46}Sc$ Cross Section

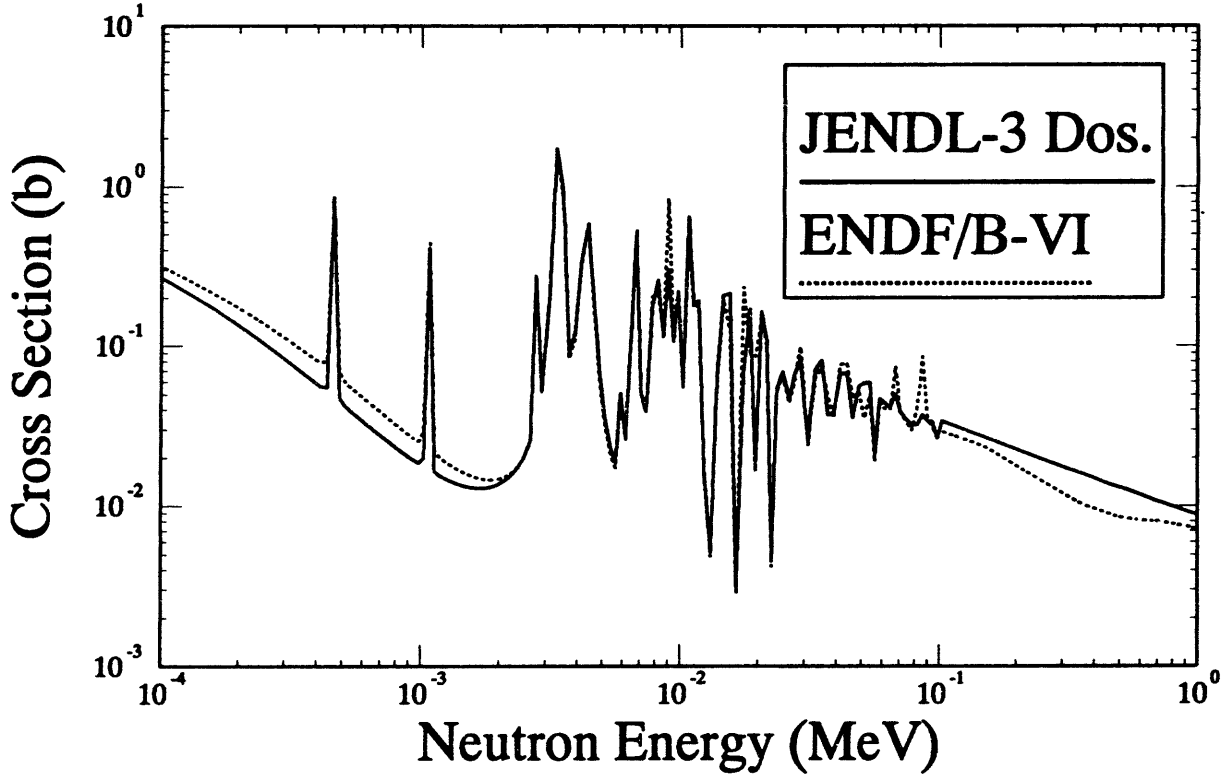

Figure A-15b: $^{45}Sc(n,\gamma)^{46}Sc$ Cross Section

Table A-16a
Alternative Cross Section Sources for the $^{46}Ti(n,p)^{46}Sc$ Reaction

$^{46}Ti(n,p)^{46}Sc$			Comment
Cross Section Library	Material Number	Covariance Data	
ENDF/B-VI	2225	Yes	Format translation of ENDF/B-V.
IRDF-90	2225	Yes	ORNL, identical to GLUCS.
GLUCS	3222	Yes	ORNL, 1990 update to GLUC library.
ENDF/B-V	6427	Yes	Dosimetry Tape, ANL, 1977.
ENDF/B-V	7226	No	Activation Tape, ANL, 1977.
IRDF-82	6427	Yes	Adopted from ENDF/B-V, ANL, 1977.
JENDL-3	3221	No	KUR, 1989.

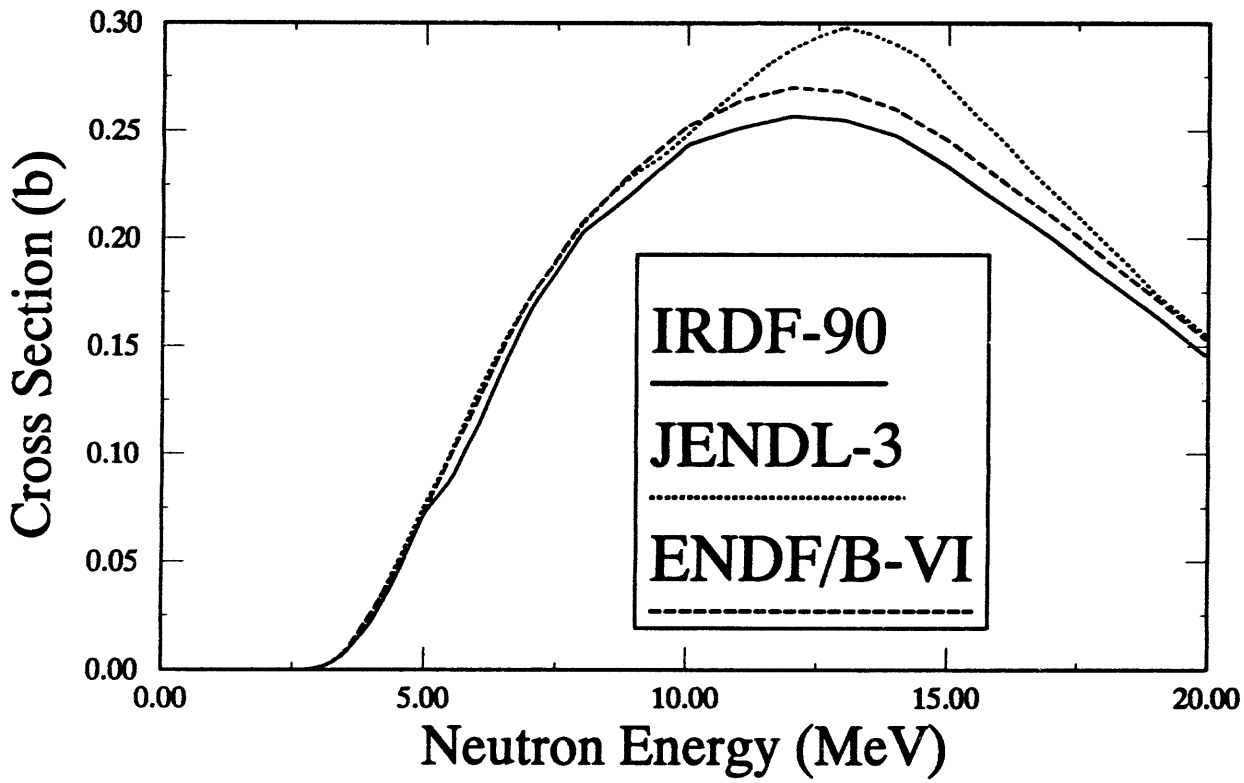

Figure A-16a: $^{46}Ti(n,p)^{46}Sc$ Cross Section

Table A-17a
Alternative Cross Section Sources for the $^{47}Ti(n,p)^{47}Sc$ Reaction

$^{47}Ti(n,p)^{47}Sc$			Comment
Cross Section Library	Material Number	Covariance Data	
ENDF/B-VI	2228	Yes	Format translation of ENDF/B-V.
IRDF-90	2228	Yes	File header states taken from ANL ENDF/B-VI, numerical contents and library printed documents identify as from ORNL. Data very similar to GLUCS-90 data. Incorporates Mannhart ^{252}Cf data.
GLUCS-89	2228	Yes	ORNL, 1989, original GLUCS.
GLUCS-90	3222	Yes	ORNL, 1990 update to GLUCS library.
ENDF/B-V	6428	Yes	Dosimetry Tape, ANL, 1977.
ENDF/B-V	7227	No	Activation Tape, ANL, 1977.
IRDF-82	6428	Yes	Adopted from ENDF/B-V, ANL, 1977.
JENDL-3	3222	No	KUR, 1989.
private	-- NA --	use ENDF/B-V data	PTB, Mannhart&Smith, ANS presentation at Santa Fe, NM, re-normalization of Smith 1975 data by 0.8208 to fit ^{252}Cf integral data.

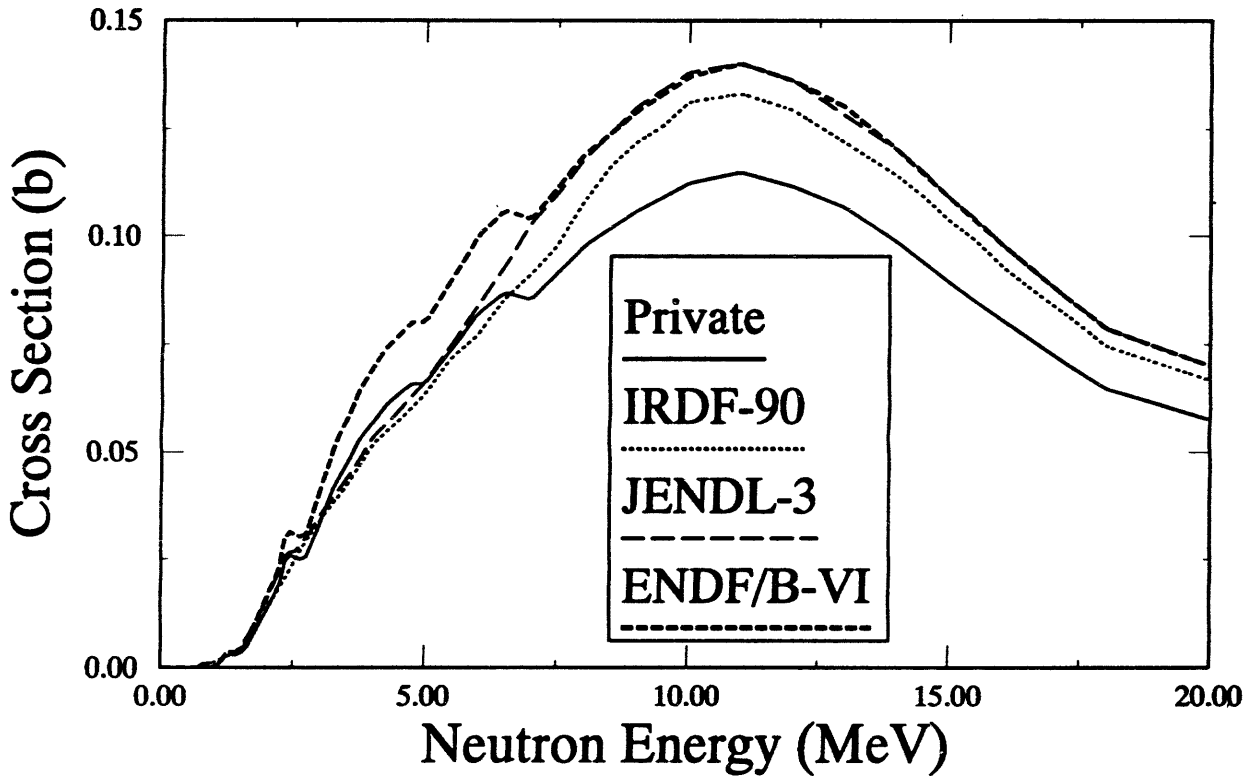

Figure A-17a: $^{47}Ti(n,p)^{47}Sc$ Cross Section

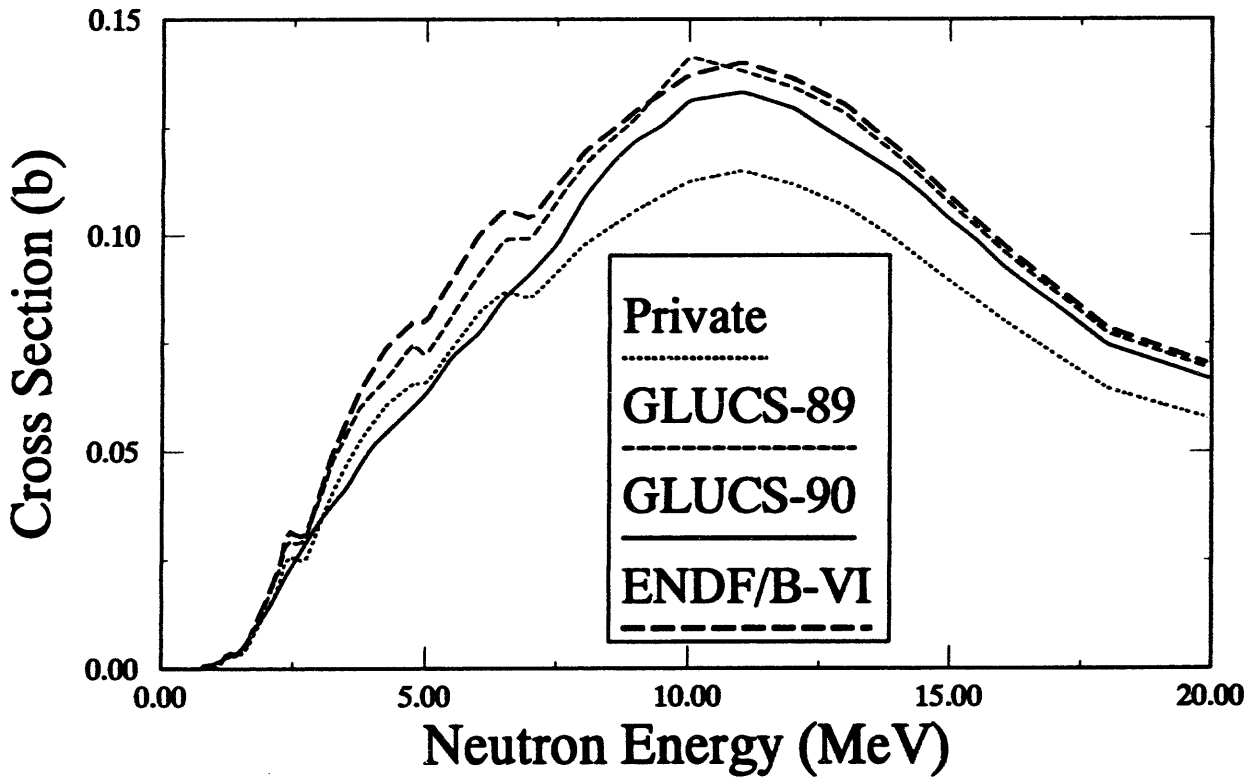

Figure A-17b: $^{47}Ti(n,p)^{47}Sc$

Table A-18a
Alternative Cross Section Sources for the $^{47}Ti(n,np)^{46}Sc$ Reaction

$^{47}Ti(n,np)^{46}Sc$			Comment
Cross Section Library	Material Number	Covariance Data	
ENDF/B-VI	2228	Yes	Format translation of ENDF/B-V.
IRDF-90	2228 -- NA	----	ORNL, present in data file, not listed in documentation, identical to ENDF/B-VI.
GLUCS	-- NA --	----	ORNL, 1990 update to GLUC library, reaction not included.
ENDF/B-V	6428	Yes	Dosimetry Tape, ANL, 1977.
ENDF/B-V	7227	No	Activation Tape, ANL, 1977.
IRDF-82	6428	Yes	Adopted from ENDF/B-V, ANL, 1977.
JENDL-3	3222	No	KUR, 1989.

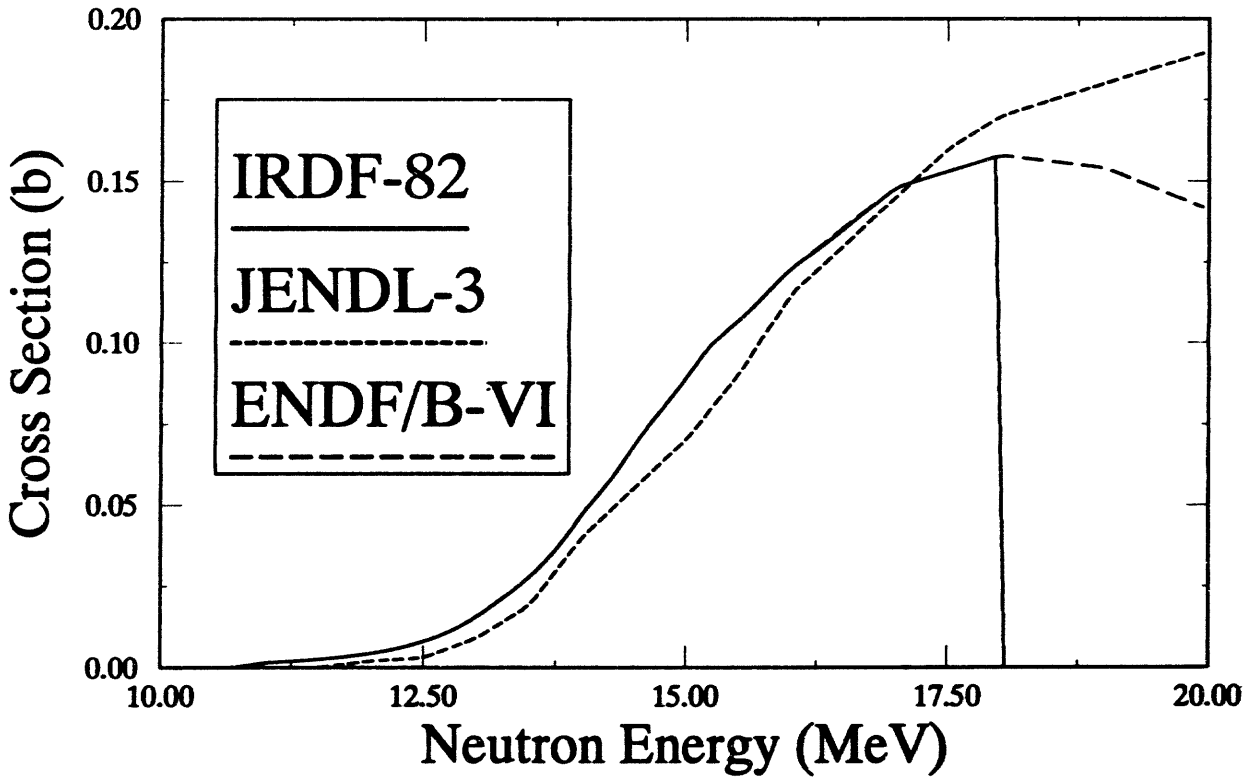

Figure A-18a: $^{47}Ti(n,np)^{46}Sc$ Cross Section

Table A-19a
Alternative Cross Section Sources for the $^{Nat}Ti(n,X)^{46}Sc$ Reaction

$^{Nat}Ti(n,X)^{46}Sc$			Comment
Cross Section Library	Material Number	Covariance Data	
ENDF/B-VI	2225 2228	Yes but not coupled	Format conversion of ENDF/B-V.
IRDF-90	2225 2228	Yes but not coupled	ORNL, (n,p) identical to early GLUCS, (n,np) identical to ENDF/B-VI.
ENDF/B-V	6427 6428	Yes but not coupled	Dosimetry tape, 531a.
ENDF/B-V	7226 7227	No	Activation Tape 532b.
JENDL-3	3221 3222	No	KUR, Eval. 1989.
JEF-2	2200 - NA	----	Natural Ti only, no way to separate a single product.
private	NA	use ENDF/B-VI data	IRDF-90 with $^{47}Ti(n,np)$ component renormalized to fit Smith's total 14.7 MeV value of 294.8 mb.

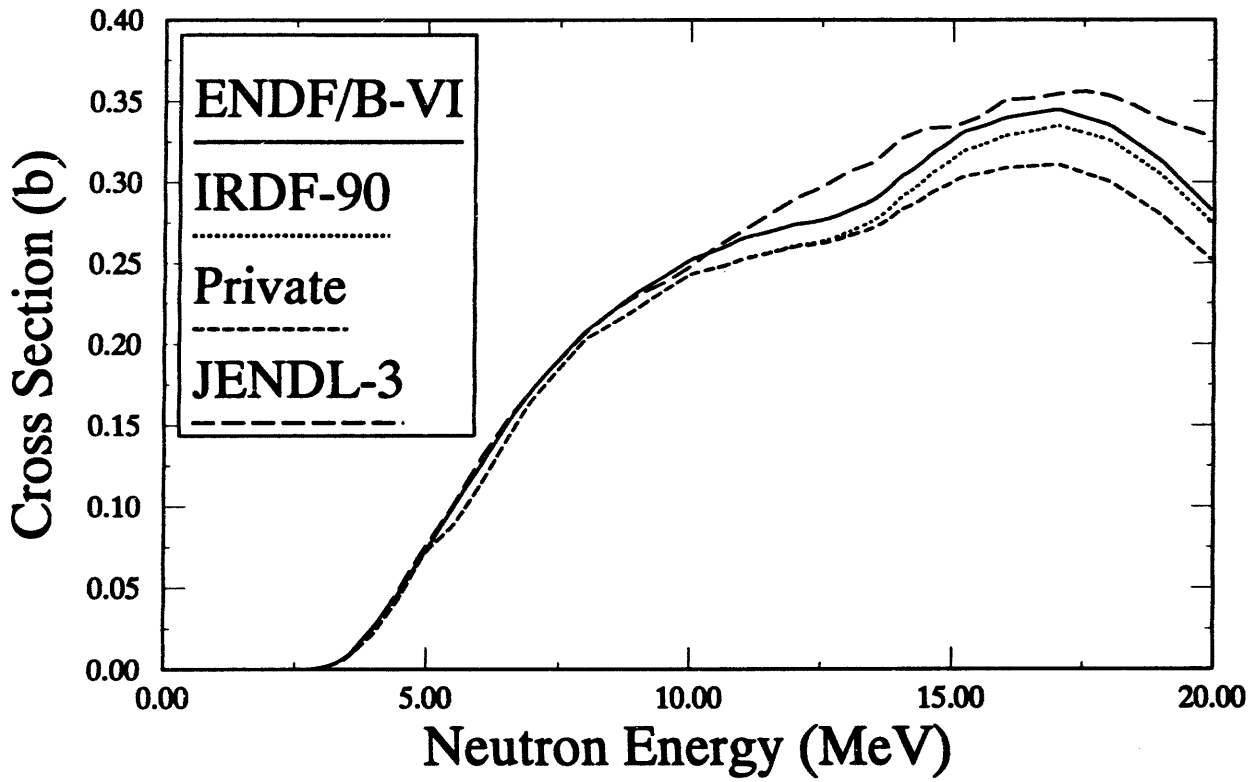

Figure A-19a: $^{Nat}Ti(n,X)^{46}Sc$ Cross Section

Table A-20a
Alternative Cross Section Sources for the $^{48}Ti(n,p)^{48}Sc$ Reaction

$^{48}Ti(n,p)^{47}Sc$			Comment
Cross Section Library	Material Number	Covariance Data	
ENDF/B-VI	2231	Yes	Format translation of ENDF/B-V.
IRDF-90	2231	Yes, GLUCS	ORNL, identical to GLUCS, NJOY processing error in covariance data.
GLUCS	6429	Yes	ORNL, 1990 GLUC library.
ENDF/B-V	6429	Yes	Dosimetry Tape, ANL, 1977.
ENDF/B-V	7228	No	Activation Tape, ANL, 1977.
IRDF-82	6429	Yes	Adopted from ENDF/B-V, ANL, 1977.
JENDL-3	3223	No	KUR, 1989.
JENDL-3 Dos.	2233	Yes	Identical to JENDL-3, covariance adopted from IRDF-85.

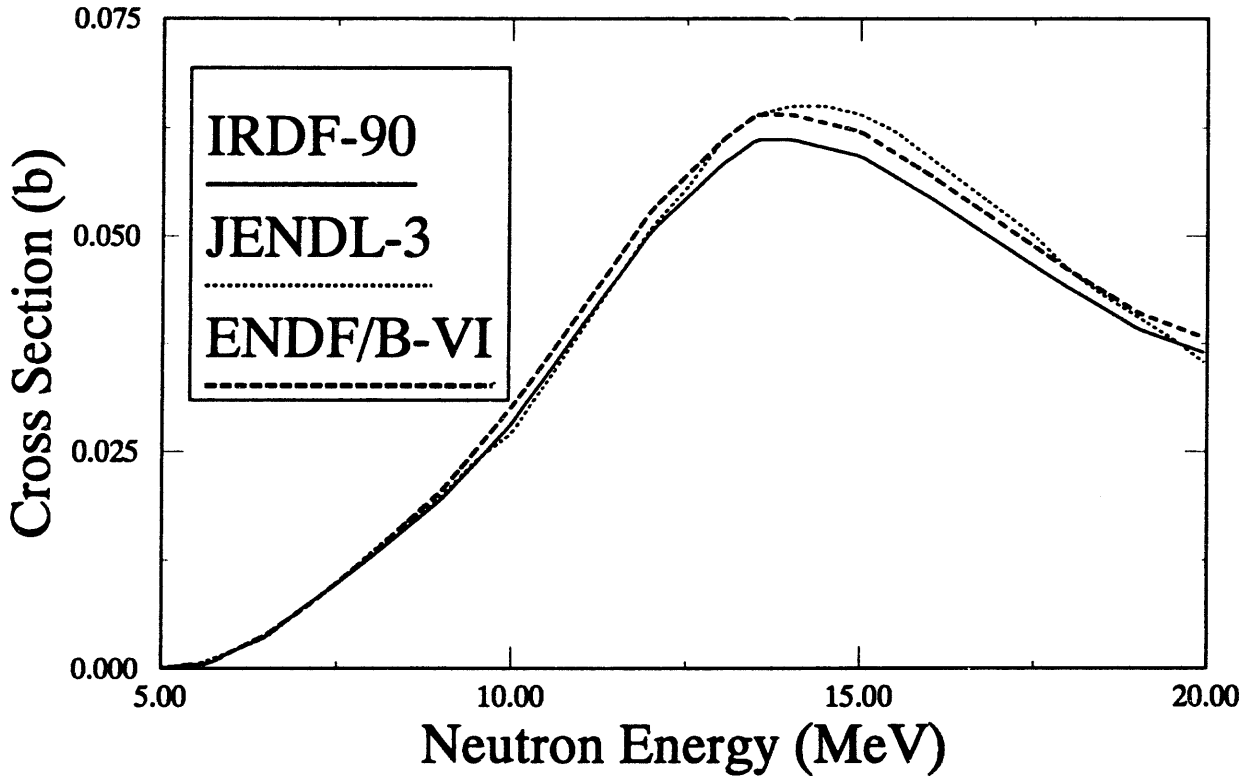

Figure A-20a: ^{48}Ti(n,p)^{48}Sc Cross Section

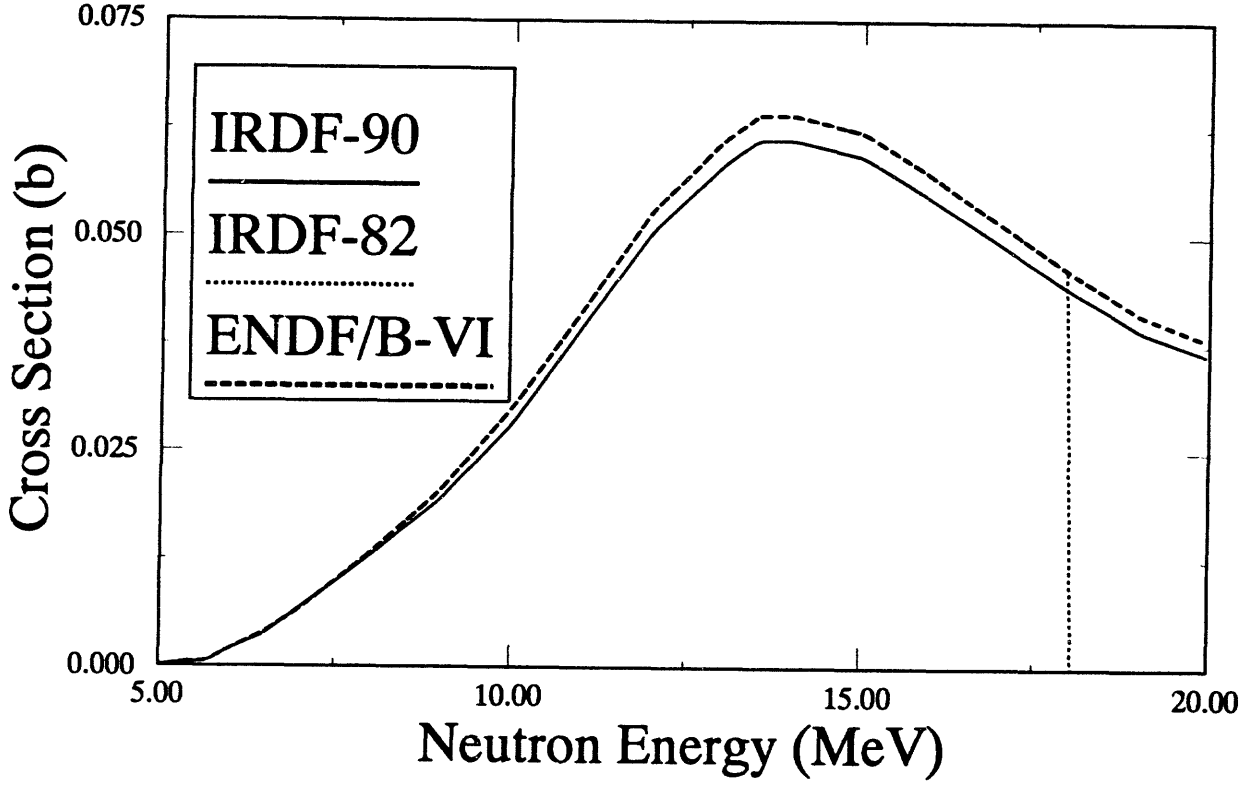

Figure A-20b: $^{48}Ti(n,p)^{48}Sc$ Cross Section

Table A-21a
Alternative Cross Section Sources for the $^{48}Ti(n,np)^{47}Sc$ Reaction

$^{48}Ti(n,np)^{47}Sc$			Comment
Cross Section Library	Material Number	Covariance Data	
ENDF/B-VI	2231	Yes	Format translation of ENDF/B-V.
IRDF-90	2231	Yes	Taken from ENDF/B-VI.
GLUCS	-- NA --	----	This reaction not part of GLUCS database.
ENDF/B-V	6429	Yes	Dosimetry Tape, ANL, 1977.
ENDF/B-V	7228	No	Activation Tape, ANL, 1977.
IRDF-82	6429	Yes	Adopted from ENDF/B-V, ANL, 1977.
JENDL-3	3223	No	KUR, 1989.

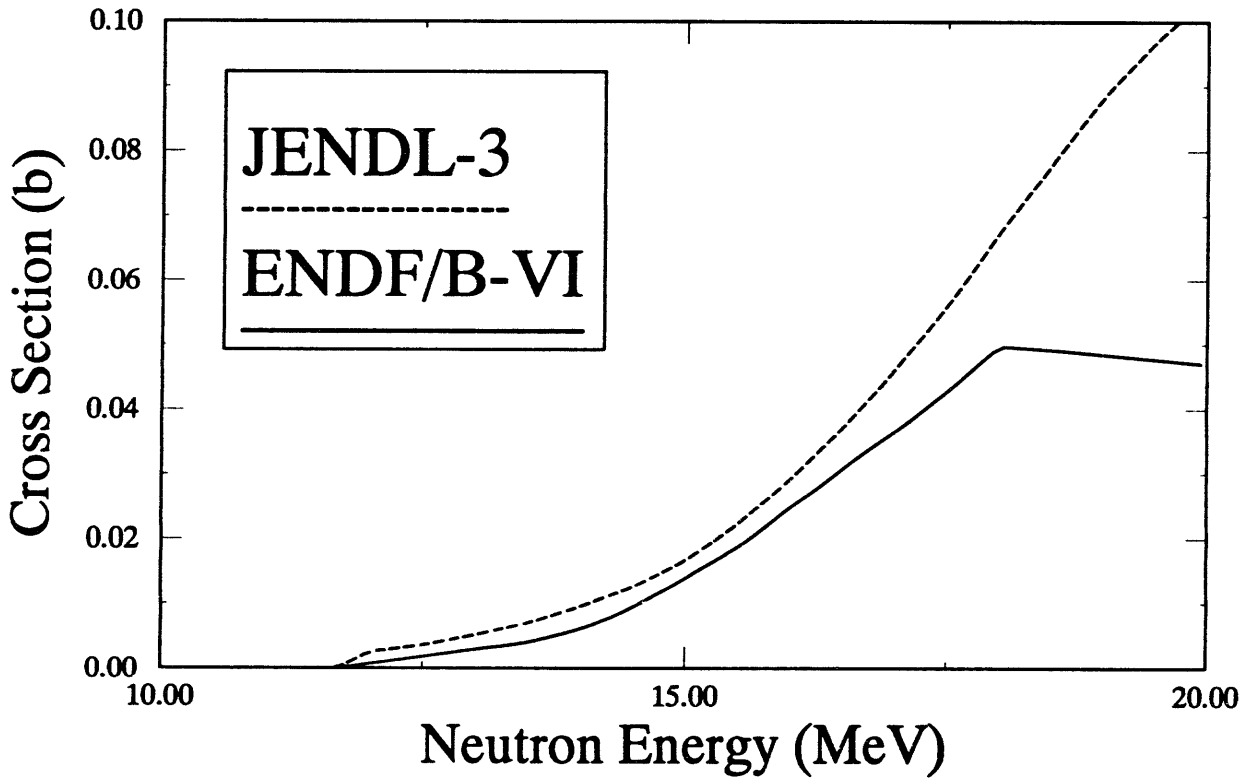

Figure A-21a: $^{48}Ti(n,np)^{47}Sc$

Table A-22a
Alternative Cross Section Sources for the $^{Nat}Ti(n,X)^{47}Sc$ Reaction

$^{Nat}Ti(n,X)^{47}Sc$			Comment
Cross Section Library	Material Number	Covariance Data	
ENDF/B-VI	2225 2228	Yes but not coupled	Format conversion of ENDF/B-V.
IRDF-90	2228 2231	Yes but not coupled	ORNL, (n,p) identical to early GLUCS, (n,np) identical to ENDF/B-VI.
ENDF/B-V	6428 6429	Yes but not coupled	Dosimetry tape, 531a.
ENDF/B-V	7227 7228	No	Activation Tape 532b.
JENDL-3	3221 3222	No	KUR, Eval. 1989.
JEF-2	2200 - NA	----	Natural Ti only, no way to separate a single product.
private	-- NA --	use ENDF/B-VI data	IRDF-90 $^{47}Ti(n,p)$ with ENDF $^{48}Ti(n,np)$ component renormalized to fit Smith's total 14.7 MeV value of 223.1 mb.

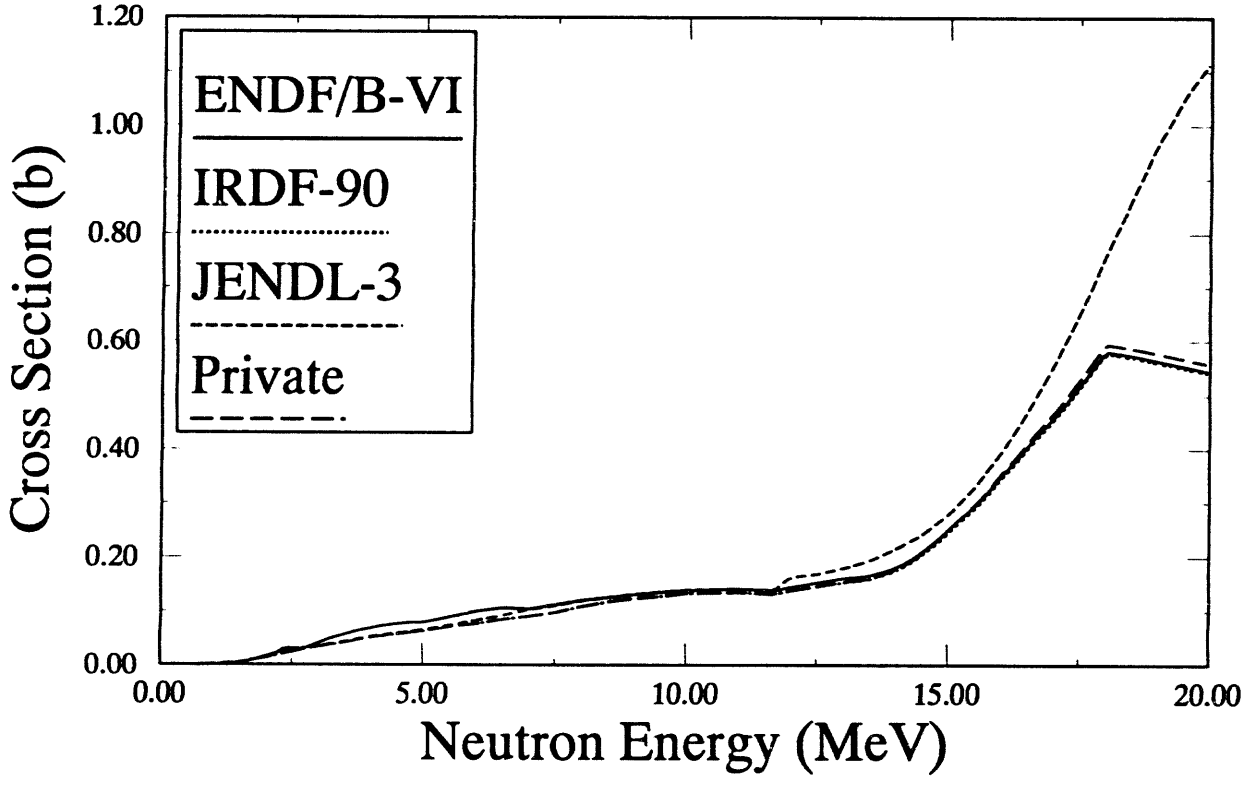

Figure A-22a: $^{Nat}Ti(n,X)^{47}Sc$

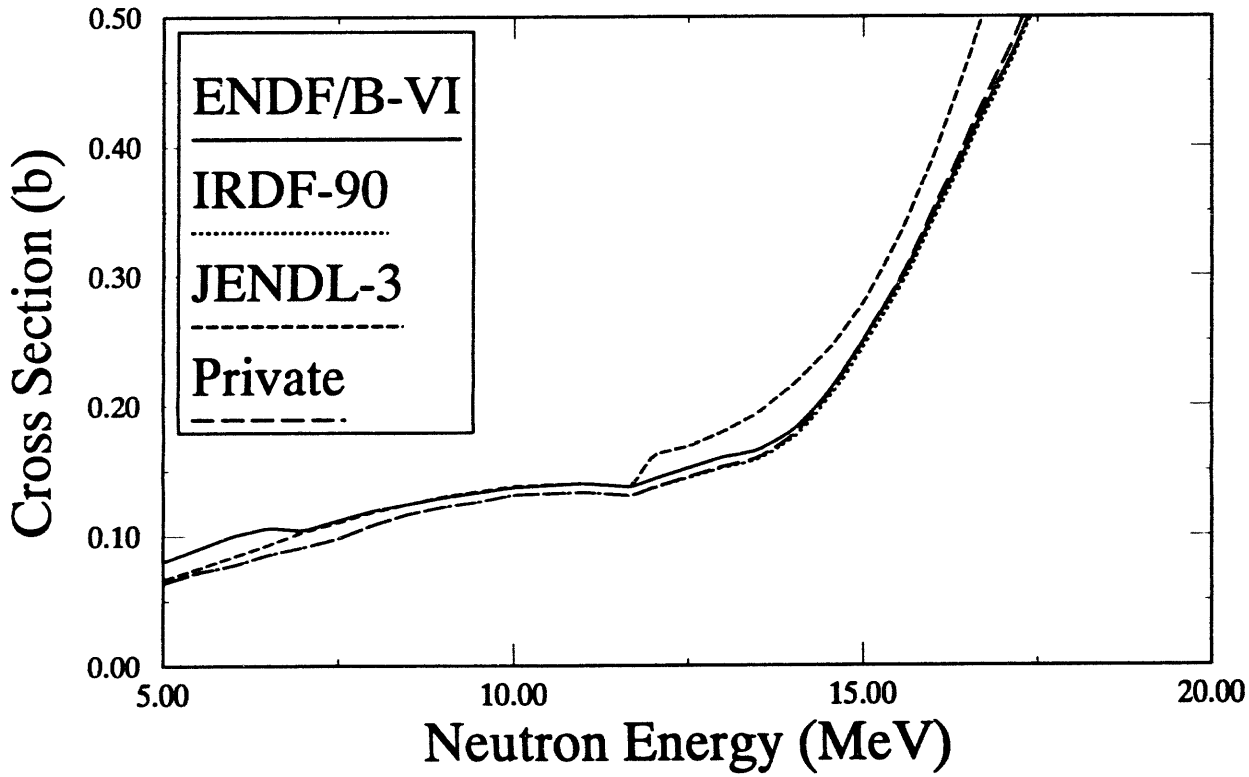

Figure A-22b: $^{Nat}Ti(n,X)^{47}Sc$

Table A-23a
Alternative Cross Section Sources for the $^{55}Mn(n,\gamma)^{56}Mn$ Reaction

$^{55}Mn(n,\gamma)^{56}Mn$			Comment
Cross Section Library	Material Number	Covariance Data	
ENDF/B-VI	2525	Yes	JAERI, ORNL Eval March 1988.
IRDF-90	2525 - NA	Yes	Taken from ENDF/B-VI, only includes (n,2n) NOT (n.,γ).
ENDF/B-V	1325	No	BNL, March 1977, Tape 553, revision 1.
ENDF/B-V	6325 -NA	No	BNL, March 1977, Dosimetry Tape 531, includes (n,2n), NOT (n,γ).
ENDF/B-V	7255	No	BNL, March 1977, Activation tape 532.
JENDL-3	3251	Yes	JAERI March 1987 eval., tape 24, same as ENDF/B-VI.
BROND	--- NA ---	----	Advertised as part of the 1989 update, but not in author's 1989 version.
JEF 2.2	2525	No	NEA, Recom. June 1982, taken from ENDF/B-IV mat 1197.

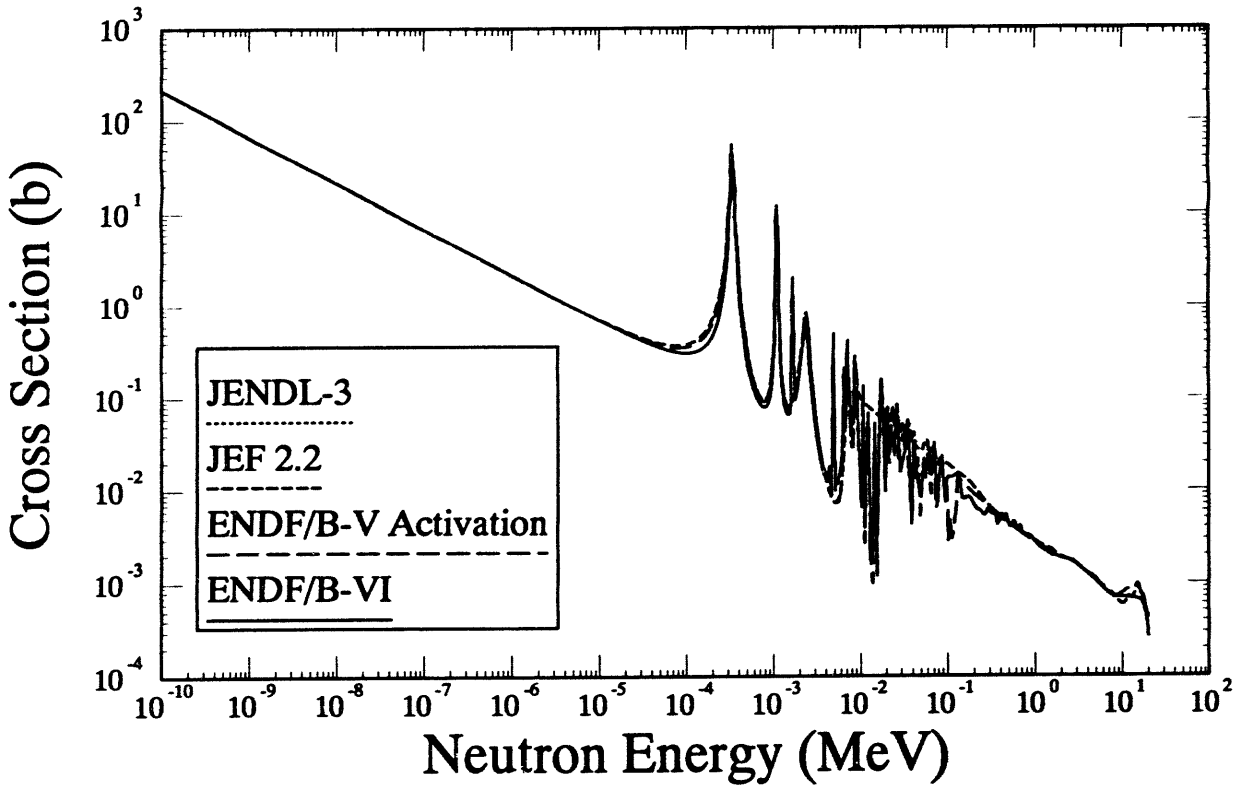

Figure A-23a: $^{55}Mn(n,\gamma)^{56}Mn$ Cross Section

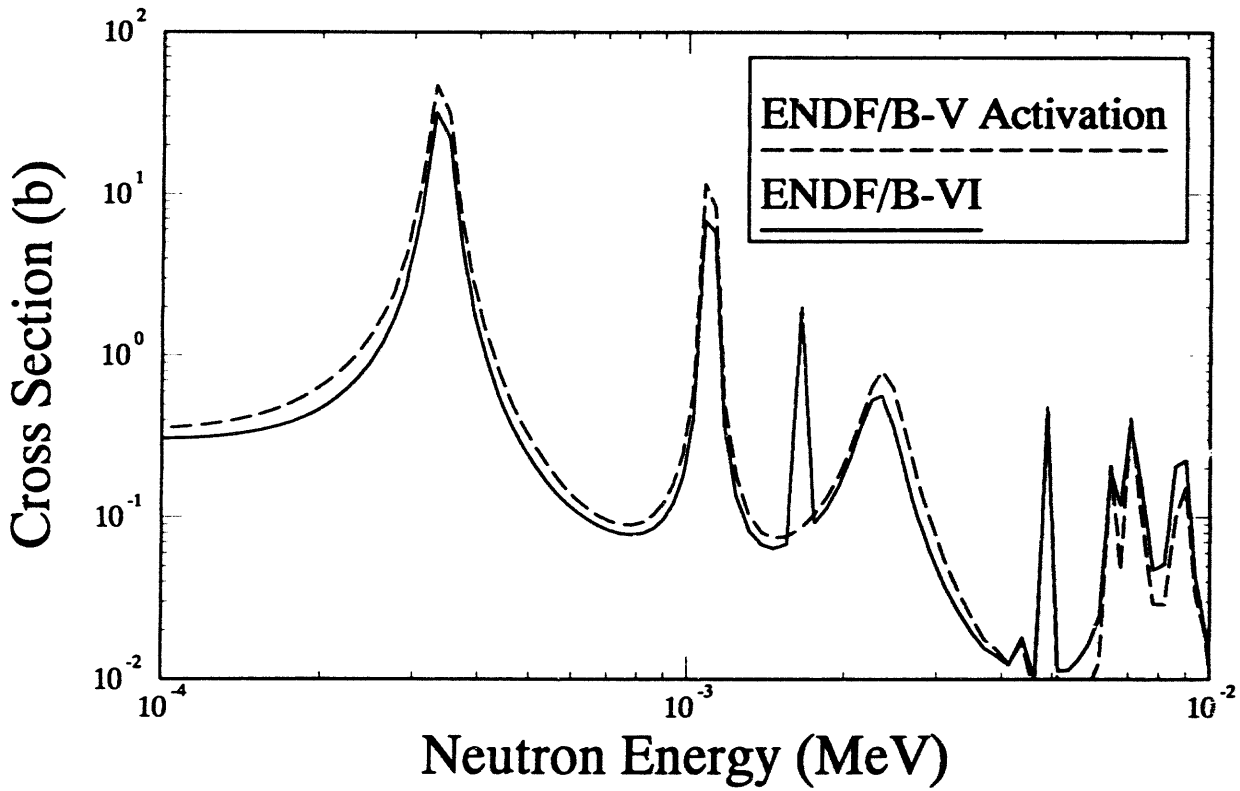

Figure A-23b: $^{55}Mn(n,\gamma)^{56}Mn$ Cross Section

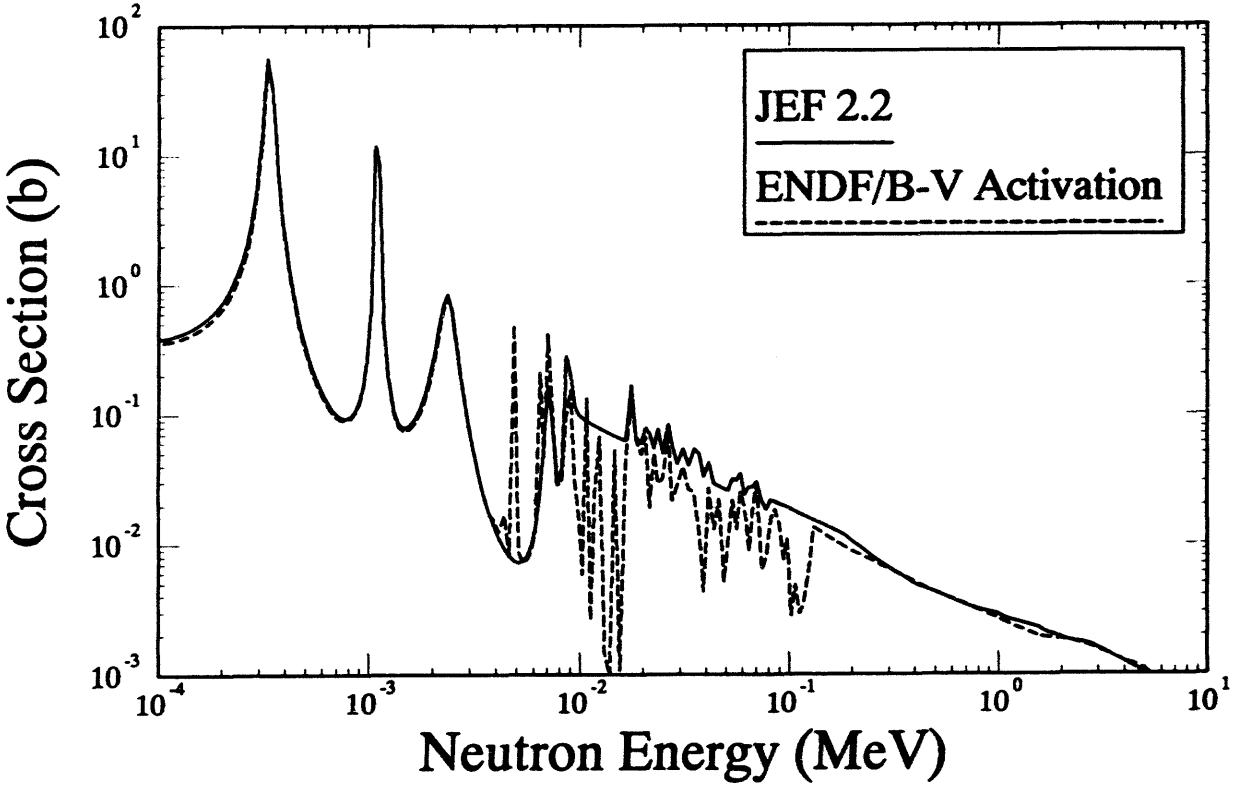

Figure A-23c: $^{55}Mn(n,\gamma)^{56}Mn$ Cross Section

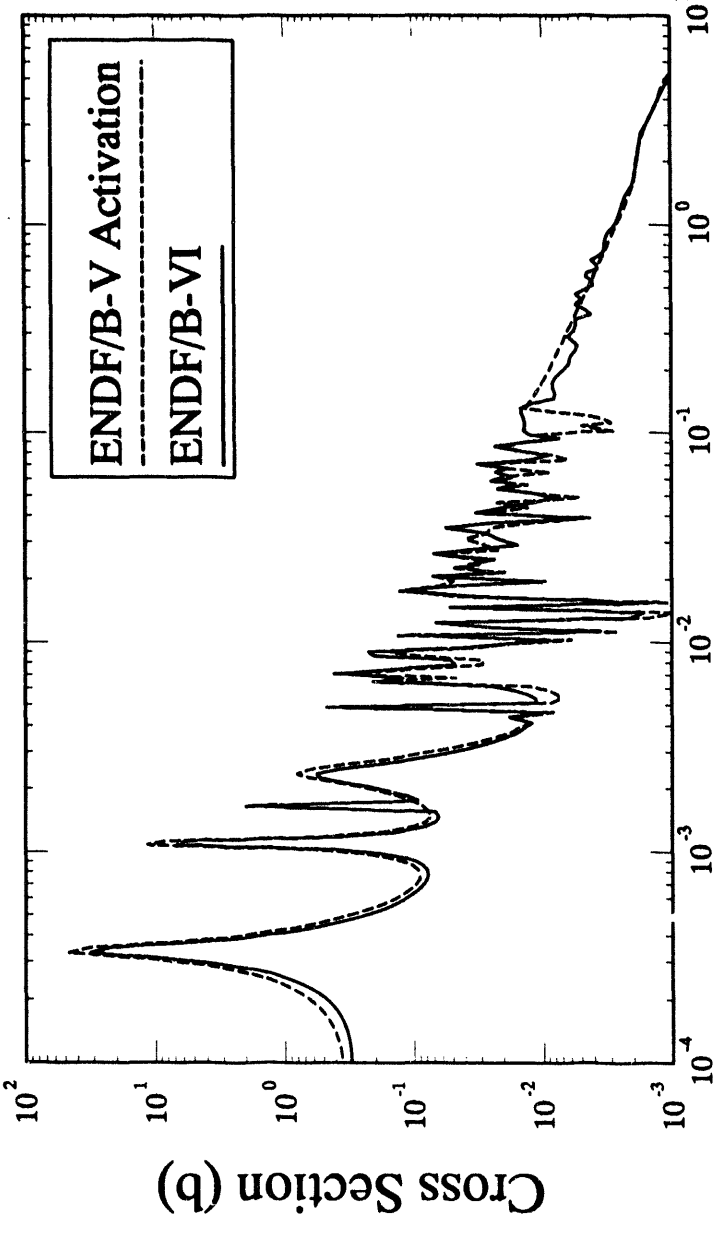

Figure A-23d: $^{55}Mn(n,\gamma)^{56}Mn$ Cross Section

Table A-24a
Alternative Cross Section Sources for the $^{55}Mn(n,2n)^{54}Mn$ Reaction

$^{55}Mn(n,2n)^{54}Mn$			Comment
Cross Section Library	Material Number	Covariance Data	
ENDF/B-VI	2525	Yes	JAERI, ORNL Eval. March 1988, (n,2n) calculated with TNG.
IRDF-90	2525	Yes	Taken from ENDF/B-VI, only includes (n,2n) NOT (n,γ).
ENDF/B-V	1325	Yes	BNL, March 1977, Tape 553, revision 1.
ENDF/B-V	6325	Yes	BNL, March 1977, Dosimetry Tape 531a, includes (n,2n), NOT (n,γ).
ENDF/B-V	7255	No	BNL, March 1977, Activation Tape 532b.
JENDL-3	3251	Yes	JAERI March 1987 Eval.., tape 24, (n,2n) calculated with TNG, same as ENDF/B-VI.
BROND	--- NA ---	----	Advertised as part of the 1989 update, but not in my 1989 version.
JEF 2.2	2525	No	NEA, Recom. June 1982, taken from ENDF/B-IV mat 1197, tape jef-2.
IRDF-82	6325	Yes	BNL, Eval. March 1977, taken from ENDF/B-V.

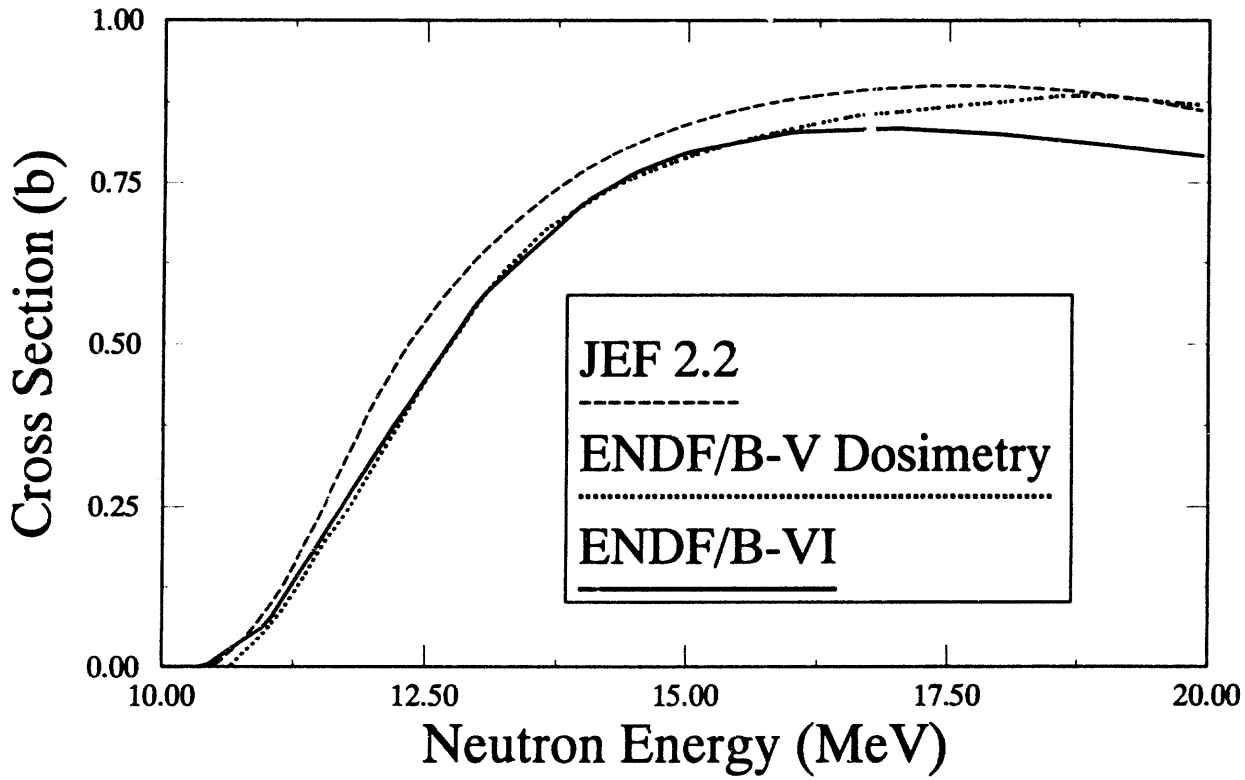

Figure A-24a: $^{55}Mn(n,2n)^{54}Mn$

Table A-25a
Alternative Cross Section Sources for the $^{54}Fe(n,p)^{54}Mn$ Reaction

$^{54}Fe(n,p)^{56}Mn$			Comment
Cross Section Library	Material Number	Covariance Data	
ENDF/B-VI	2625	Yes	ORNL, Nov. 1989, taken from GLUCS with some smoothing.
IRDF-90	2625	Yes	ORNL, Nov. 1989, same as ENDF/B-VI.
GLUCS	6430	Yes	ORNL, 1990 distribution.
ENDF/B-V	6430	Yes	HEDL, Eval. June 1979, Dosimetry Tape, 531a.
ENDF/B-V	7264	No	HEDL, ORNL, June 1979, Activation Tape, 532b.
JENDL-3	3261	No	JNDC, Eval. March 1987, Tape 24.
BROND	2611	No	CCPFEI, Eval. Nov. 1985, tape ma242.51.
JEF 2.2	2625	No	KFK/ENEA, Eval. May 1990.

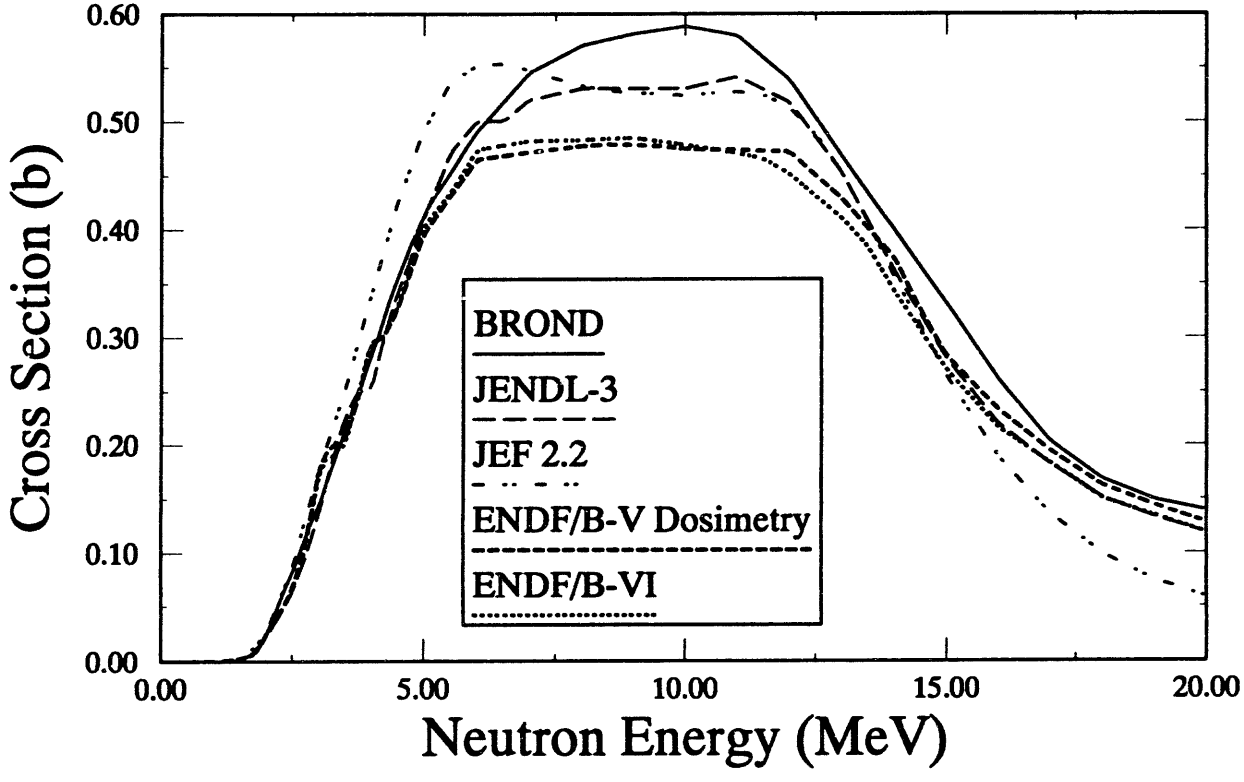

Figure A-25a: $^{54}Fe(n,p)^{54}Mn$ Cross Section

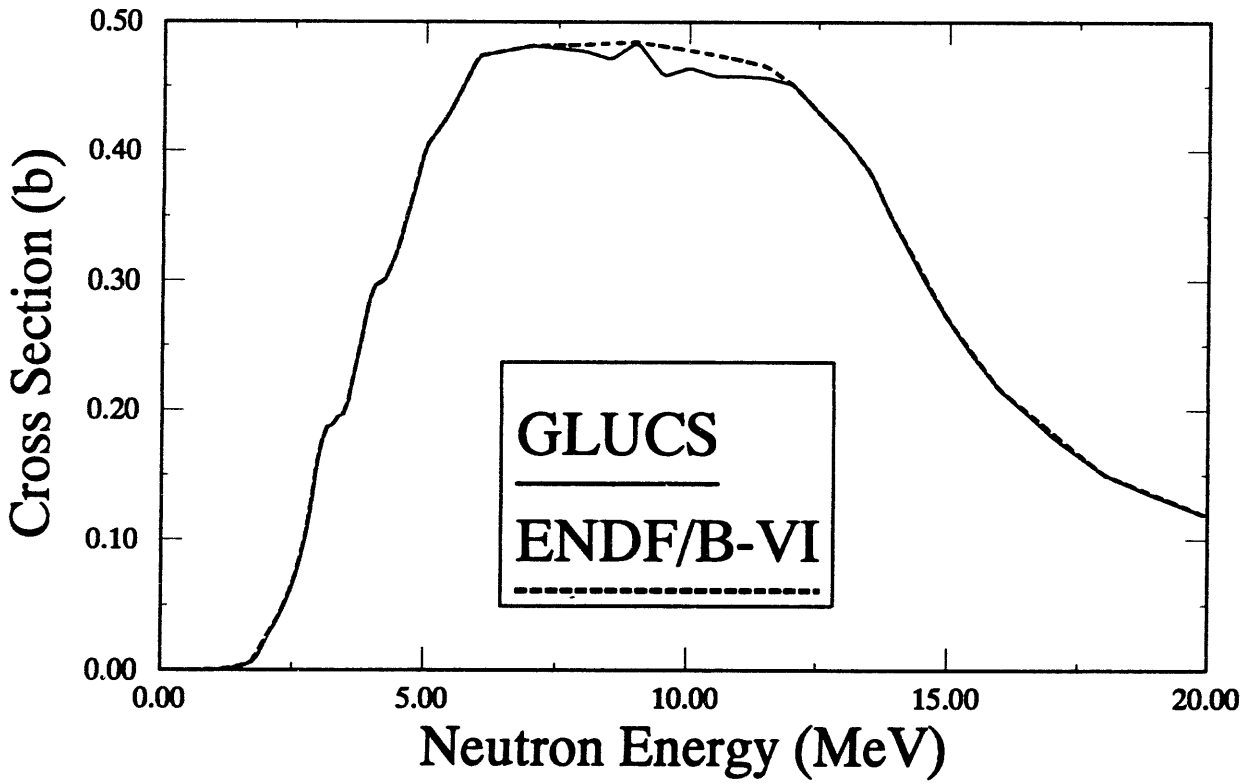

Figure A-25b: $^{54}Fe(n,p)^{54}Mn$ Cross Section

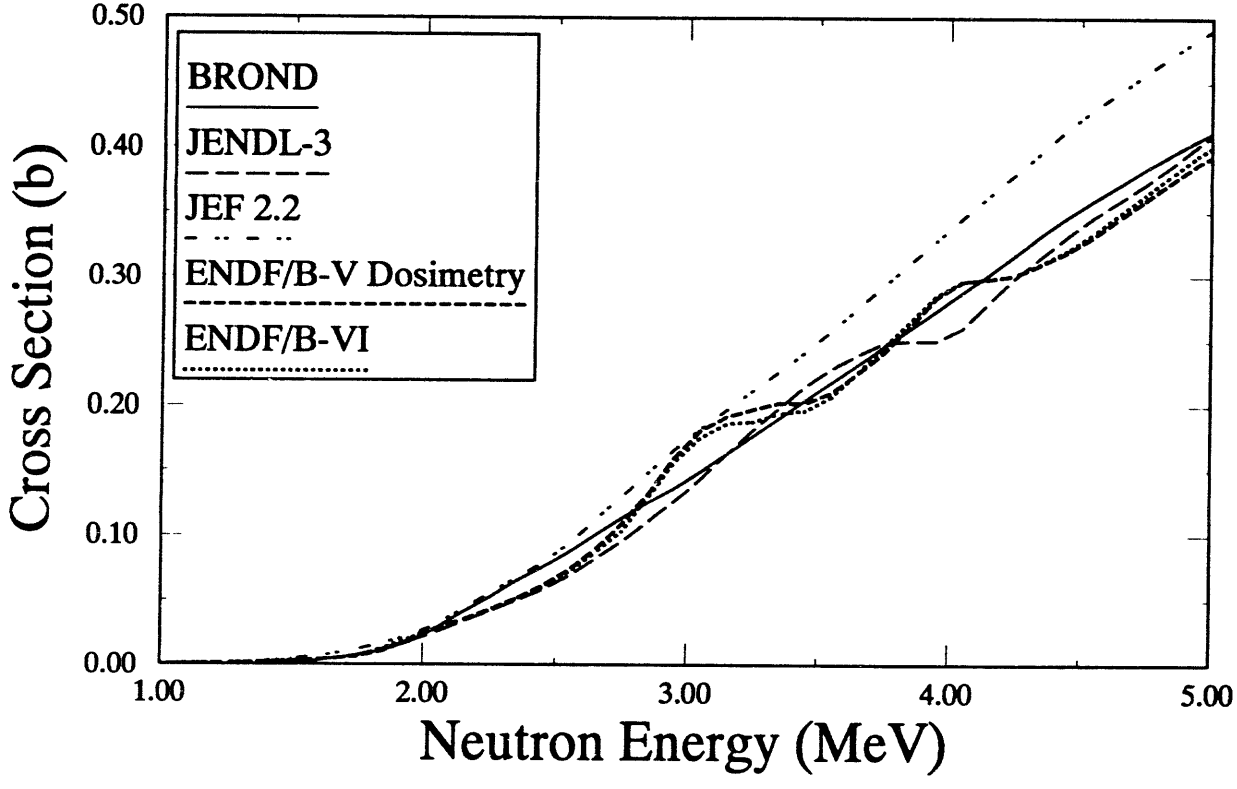

Figure A-25c: $^{54}Fe(n,p)^{54}Mn$ Cross Section

Table A-26a
Alternative Cross Section Sources for the $^{56}Fe(n,p)^{56}Mn$ Reaction

$^{56}Fe(n,p)^{56}Mn$			Comment
Cross Section Library	Material Number	Covariance Data	
ENDF/B-VI	2631	Yes	ORNL, Eval. March 1989.
IRDF-90	2631	Yes	Taken from ENDF/B-VI.
GLUCS	561	Yes	ORNL, 1990 distribution, same as ENDF/B-VI.
ENDF/B-V	6431	Yes	ORNL, Eval. July 1978, Dosimetry Tape, 531a.
ENDF/B-V	7266	No	ORNL, Eval. July 1978, Activation Tape, 532b.
JENDL-3	3262	No	JNDC, Eval. March 1987.
BROND	2621	No	CCPFEI, Eval. Nov. 1985, tape ma242.51.
JEF 2.2	2631	No	KFK/ENEA, Eval. Dec. 1989.

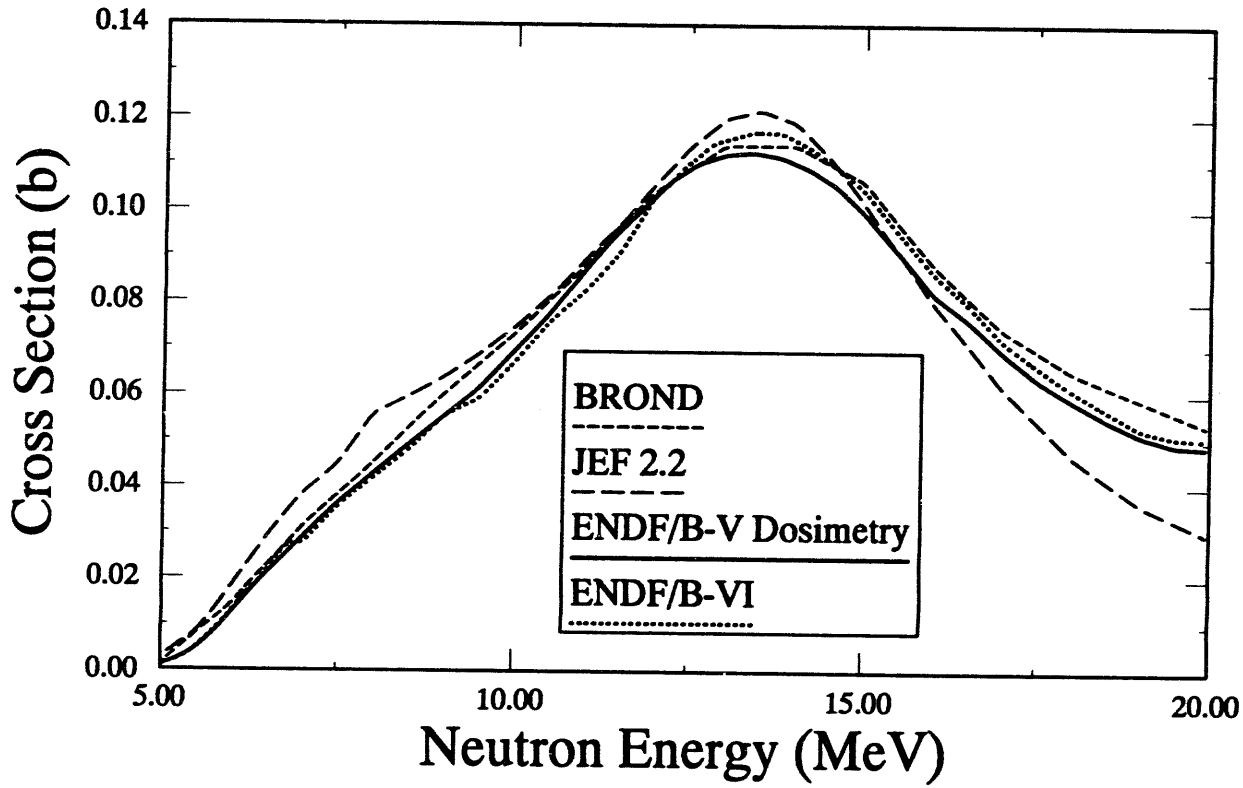

Figure A-26a: $^{56}Fe(n,p)^{56}Mn$ Cross Section

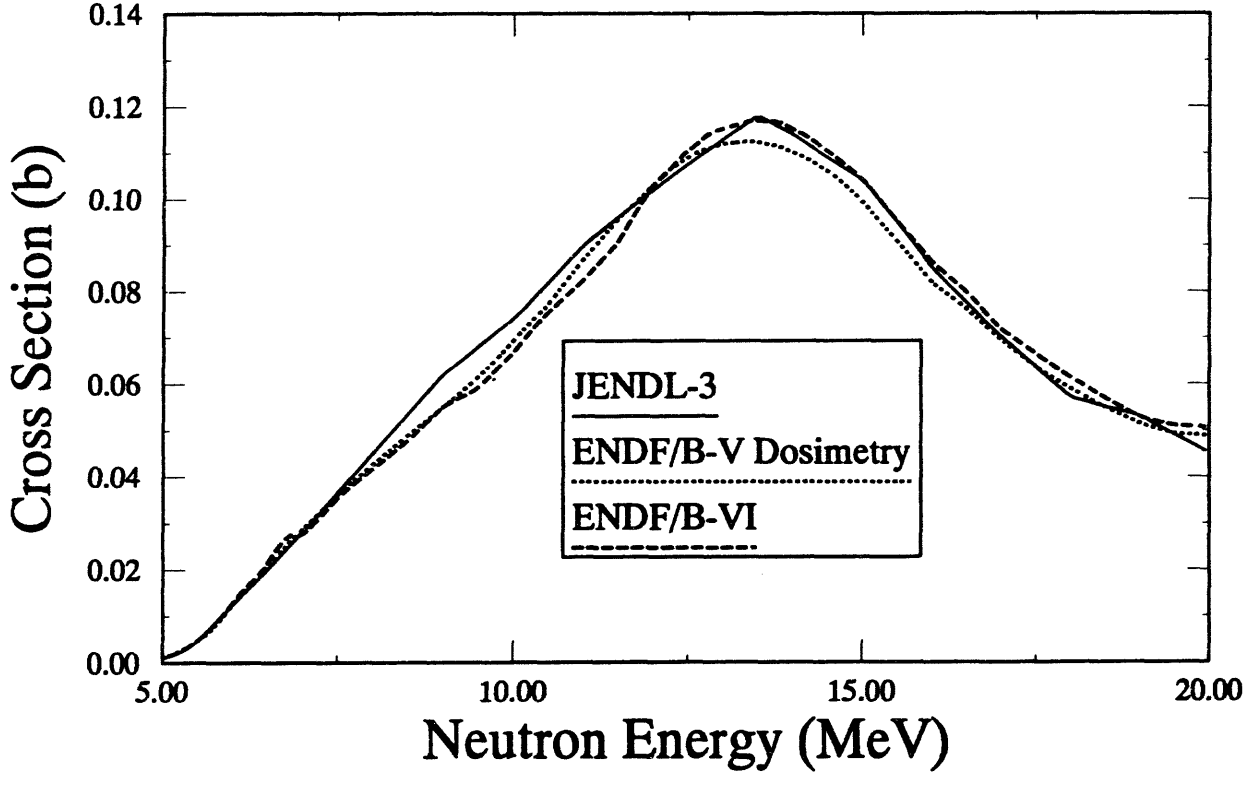

Figure A-26b: $^{56}Fe(n,p)^{56}Mn$ Cross Section

Table A-27a
Alternative Cross Section Sources for the $^{58}Fe(n,\gamma)^{59}Fe$ Reaction

$^{58}Fe(n,\gamma)^{59}Fe$			Comment
Cross Section Library	Material Number	Covariance Data	
ENDF/B-VI	2637	Yes	ORNL, Eval. Nov. 1989.
IRDF-90	2637	No	Taken from ENDF/B-VI.
ENDF/B-V	6432	Yes	HEDL, Eval. June 1979, Dosimetry Tape, 531a.
ENDF/B-V	7268	No	HEDL, June 1979, Activation Tape, 532b.
JENDL-3	3264	No	JNDC, Eval. March 1987, Tape 24.
JENDL-3 Dos.	2634	Yes	Identical to JENDL-3, covariance adopted from IRDF-85.
BROND	2641	No	CCPFEI, Eval. Nov. 1985.
JEF 2.2	2637	No	KFK/ENEA, Eval. Dec. 1989, tape jef-2.

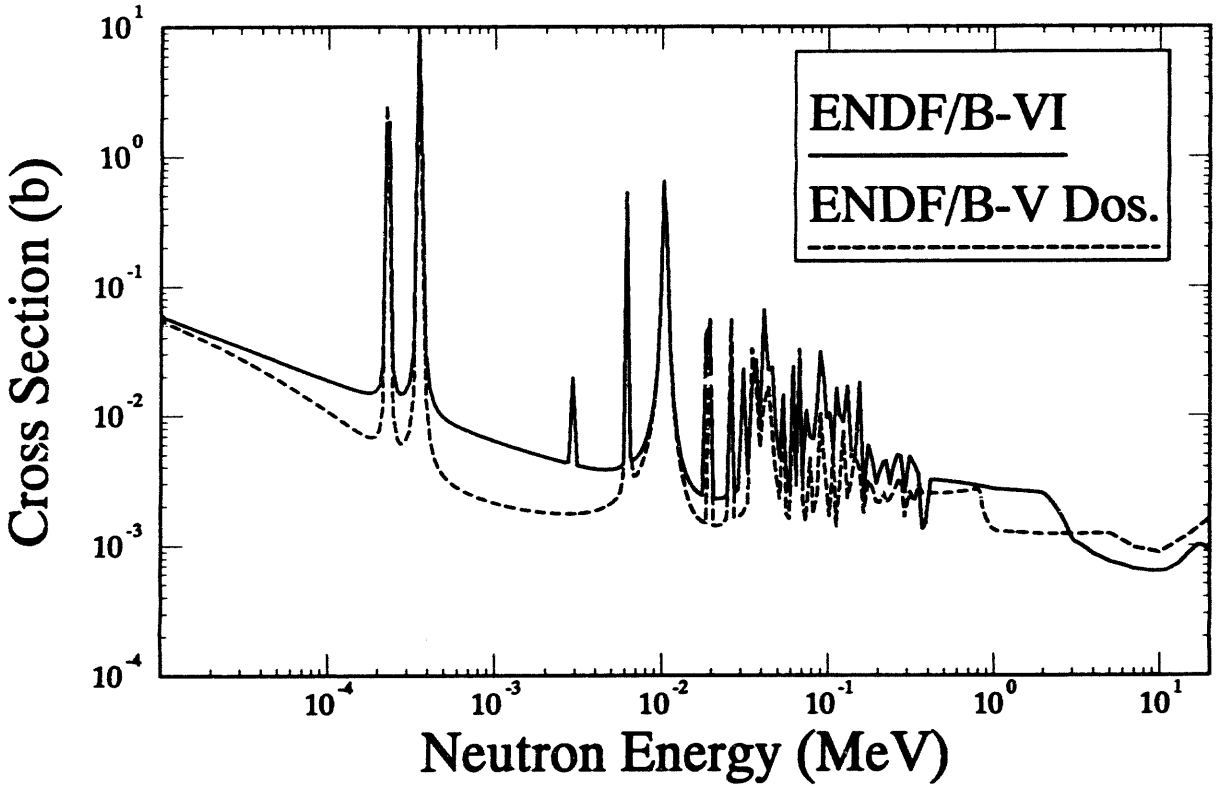

Figure A-27a: $^{58}Fe(n,\gamma)^{59}Fe$ Cross Section

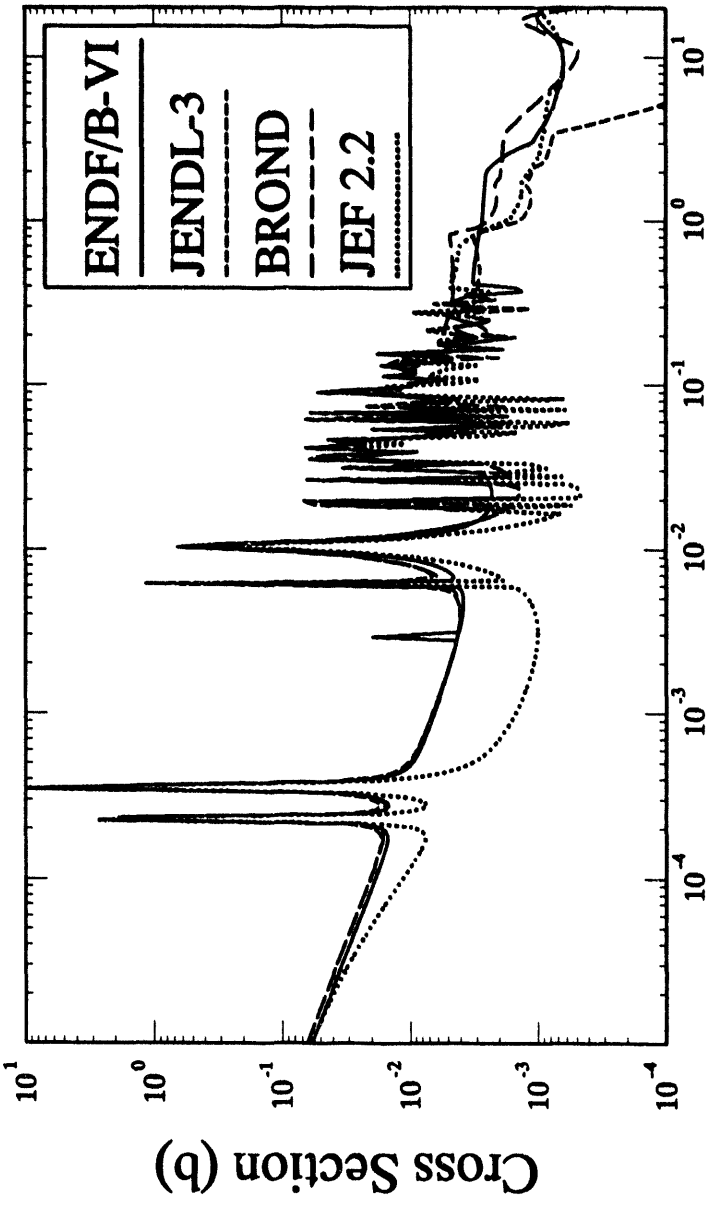

Figure A-27b: $^{58}Fe(n,\gamma)^{59}Fe$ Cross Section

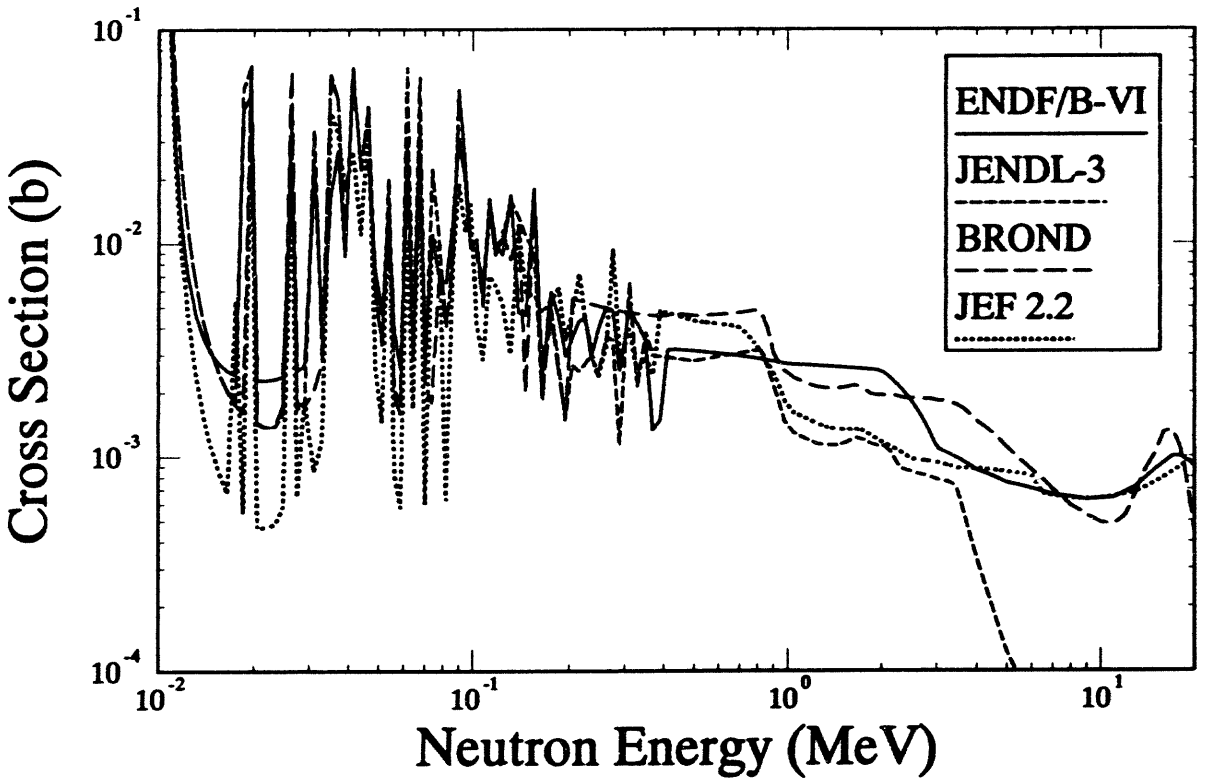

Figure A-27c: $^{58}Fe(n,\gamma)^{59}Fe$ Cross Section

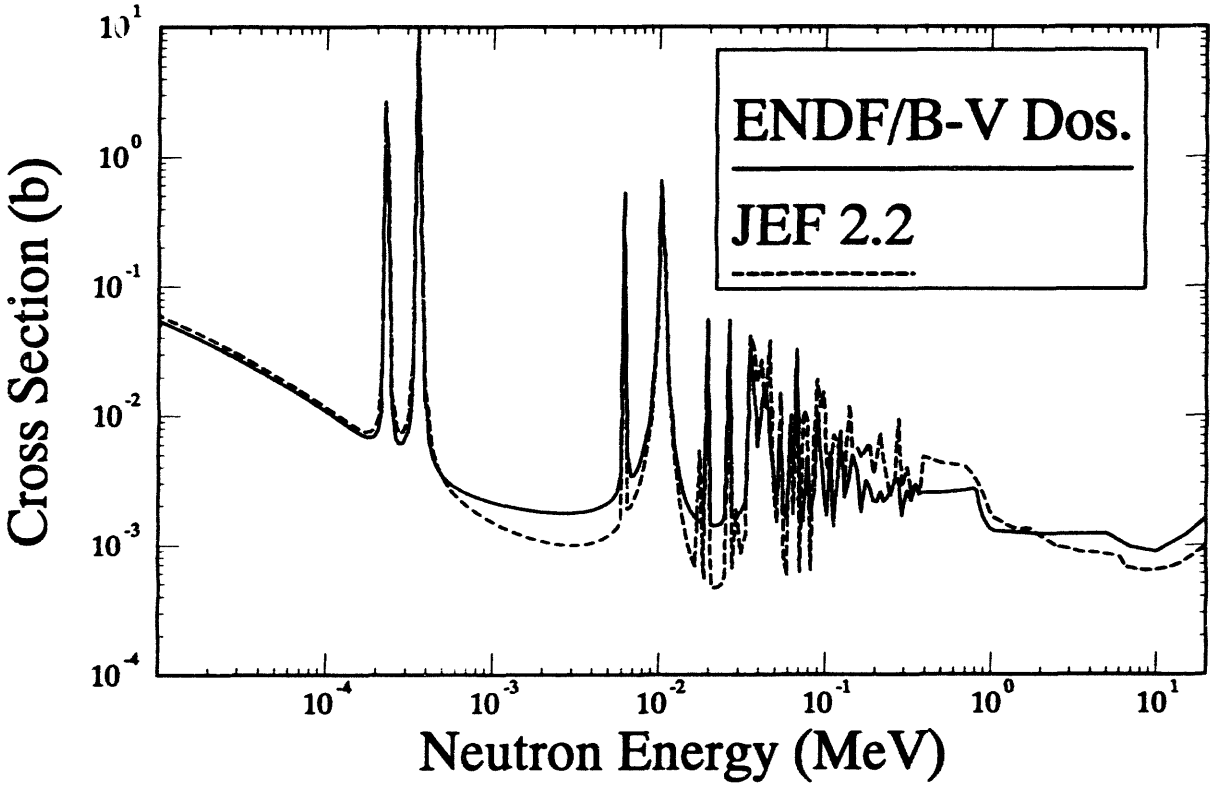

Figure A-27d: $^{58}Fe(n,\gamma)^{59}Fe$ Cross Section

Table A-28a
Alternative Cross Section Sources for the ^{Nat}Fe(n,X)dpa Reaction

^{nat}Fe(n,X)dpa			Comment
Cross Section Library	Material Number	Covariance Data	
ASTM E 693-79	---	No	A standard exposure parameter.

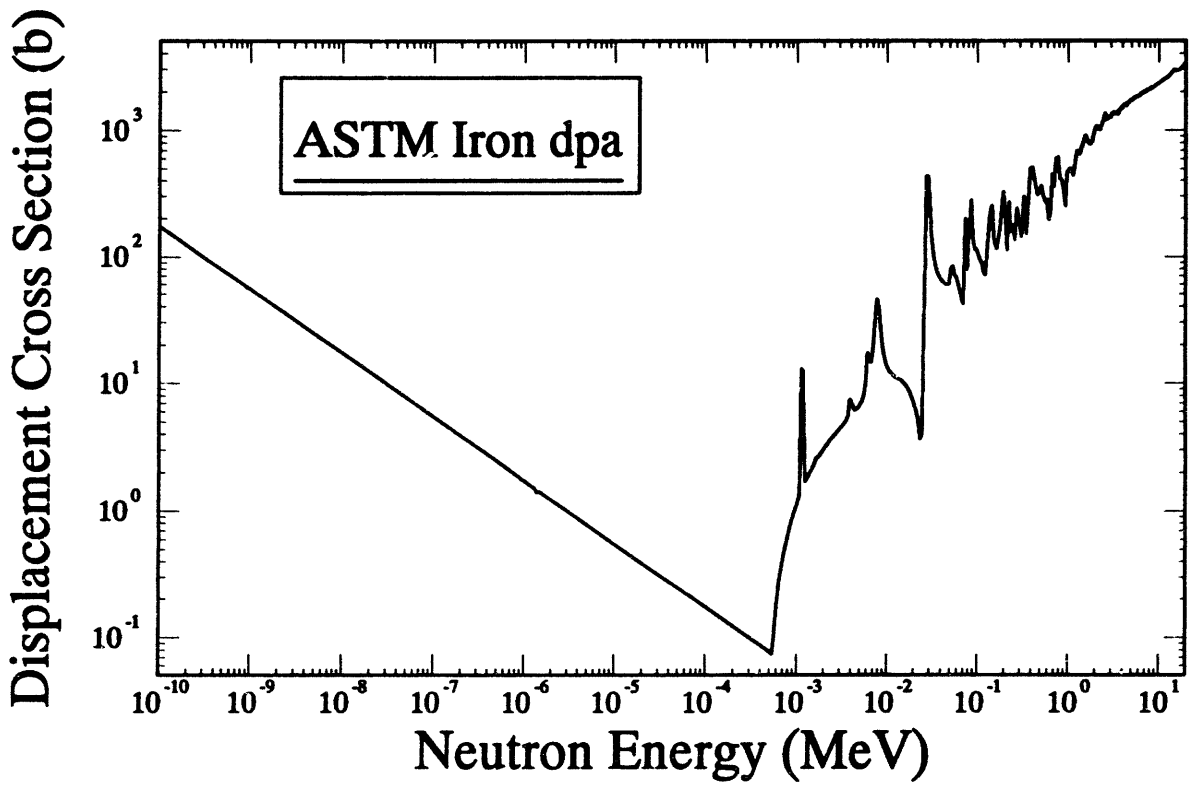

Figure A-28a: ^{Nat}Fe(n,X)dpa Cross Section

Table A-29a
Alternative Cross Section Sources for the $^{59}Co(n,p)^{59}Fe$ Reaction

$^{59}Co(n,p)^{59}Fe$			Comment
Cross Section Library	Material Number	Covariance Data	
ENDF/B-VI	2725	Yes	ANL, Eval. July 1989.
IRDF-90	NA -- 2725	--	Taken from ENDF/B-VI, file co-59b, does not include (n,p) reaction, just (n,α) and (n,2n).
ENDF/B-V	1327	No	BNL, Eval. June 1977, tape 561, revision 2, based on ENDF/B-IV, a wide variation in experimental values was noted.
ENDF/B-V	NA--6327	--	BNL, Eval. June 1977, Dosimetry Tape 531a, this reaction not included.
ENDF/B-V	7279	No	BNL, Eval. June 1977, Activation Tape, 532b, based on ENDF/B-IV.
JENDL-3	3271	No	KHI, Eval. Aug. 1988, tape 24.
BROND	NA	----	Reported to be in library, but not in part available through BNL.
JEF 2.2	2725	Yes	ANL, Eval. July 1988, tape jef-2, same as ENDF/B-VI.

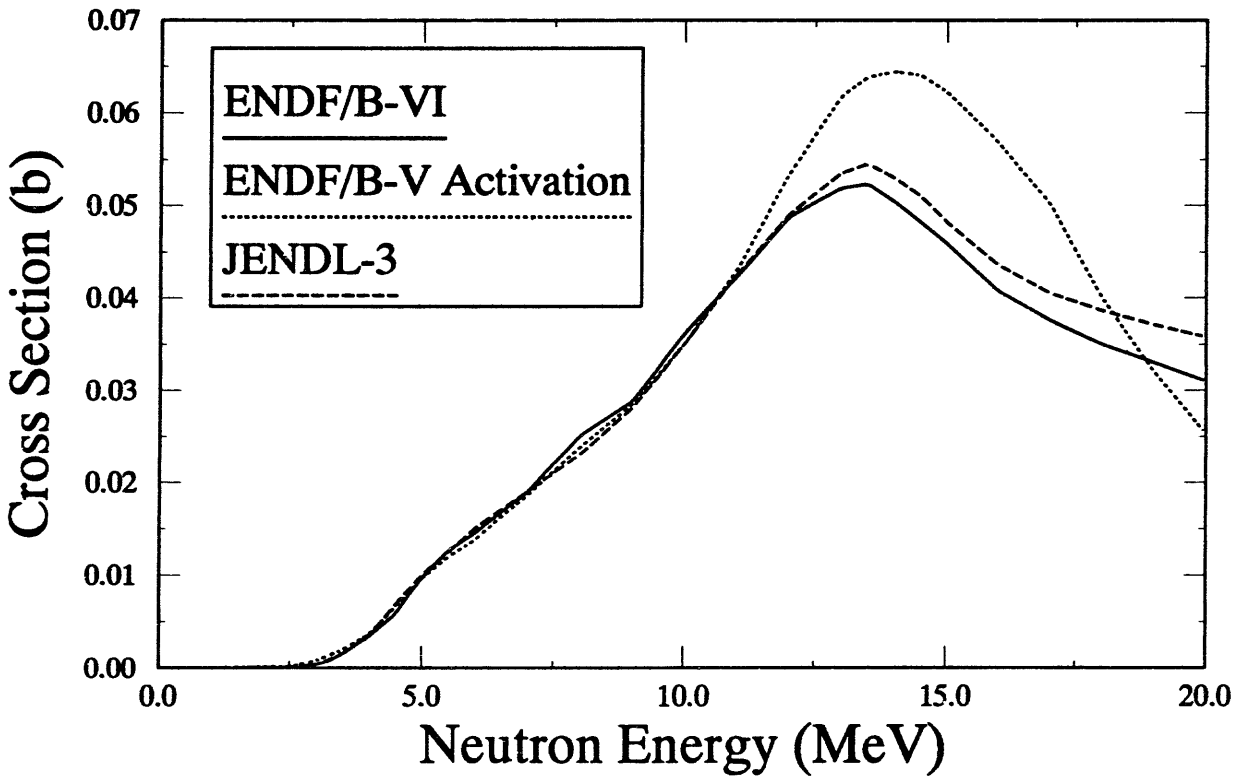

Figure A-29a: $^{59}Co(n,p)^{59}Fe$ Cross Section

Table A-30a
Alternative Cross Section Sources for the $^{59}Co(n,\gamma)^{60}Co$ Reaction

$^{59}Co(n,\gamma)^{60}Co$			Comment
Cross Section Library	Material Number	Covariance Data	
ENDF/B-VI	2725	No	ANL, Eval. July 1989.
IRDF-90	2725	No	Taken from ENDF/B-VI, file co-59b.
ENDF/B-V	1327	Yes	BNL, Eval. June 1977, tape 561, revision 2, based on ENDF/B-IV.
ENDF/B-V	6327	Yes	BNL, Eval. June 1977, Dosimetry Tape 531a.
ENDF/B-V	7279	No	BNL, Eval. June 1977, Activation Tape, 532b, based on ENDF/B-IV.
JENDL-3	3271	No	KHI, Eval. Aug. 1988, tape 24.
BROND	NA	----	Reported to be in library, but not in part available through BNL.
JEF 2.2	2725	No	ANL, Eval. July 1988, tape jef-2.

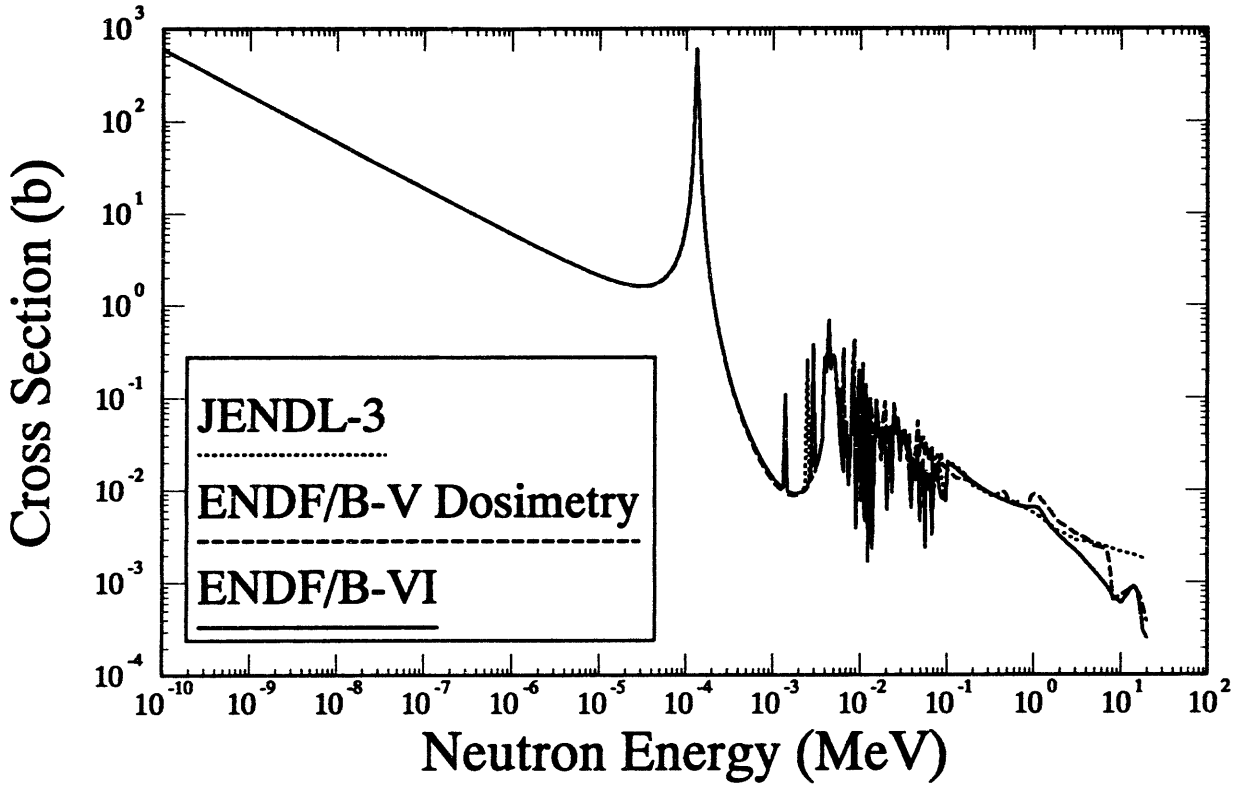

Figure A-30a: $^{59}Co(n,\gamma)^{60}Co$ Cross Section

Figure A-30b: $^{59}Co(n,\gamma)^{60}Co$ Cross Section

Table A-31a
Alternative Cross Section Sources for the $^{59}Co(n,\alpha)^{56}Mn$ Reaction

$^{59}Co(n,\alpha)^{56}Mn$			Comment
Cross Section Library	Material Number	Covariance Data	
ENDF/B-VI	2725	Yes	ANL, Eval. July 1989.
IRDF-90	2725	Yes	Taken from ENDF/B-VI, file co-59b.
ENDF/B-V	1327	Yes	BNL, Eval. June 1977, tape 561, revision 2, based on ENDF/B-IV, a wide variation in experimental values was noted.
ENDF/B-V	6327	Yes	BNL, Eval. June 1977, Dosimetry Tape 531a.
ENDF/B-V	NA --7279	---	BNL, Eval. June 1977, Activation Tape, 532b, based on ENDF/B-IV, does not include (n,α) reaction.
JENDL-3	3271	No	KHI, Eval. Aug. 1988, tape 24.
BROND	NA	----	Reported to be in library, but not in part available through BNL.
JEF 2.2	2725	Yes	ANL, Eval. July 1988, tape jef-2.

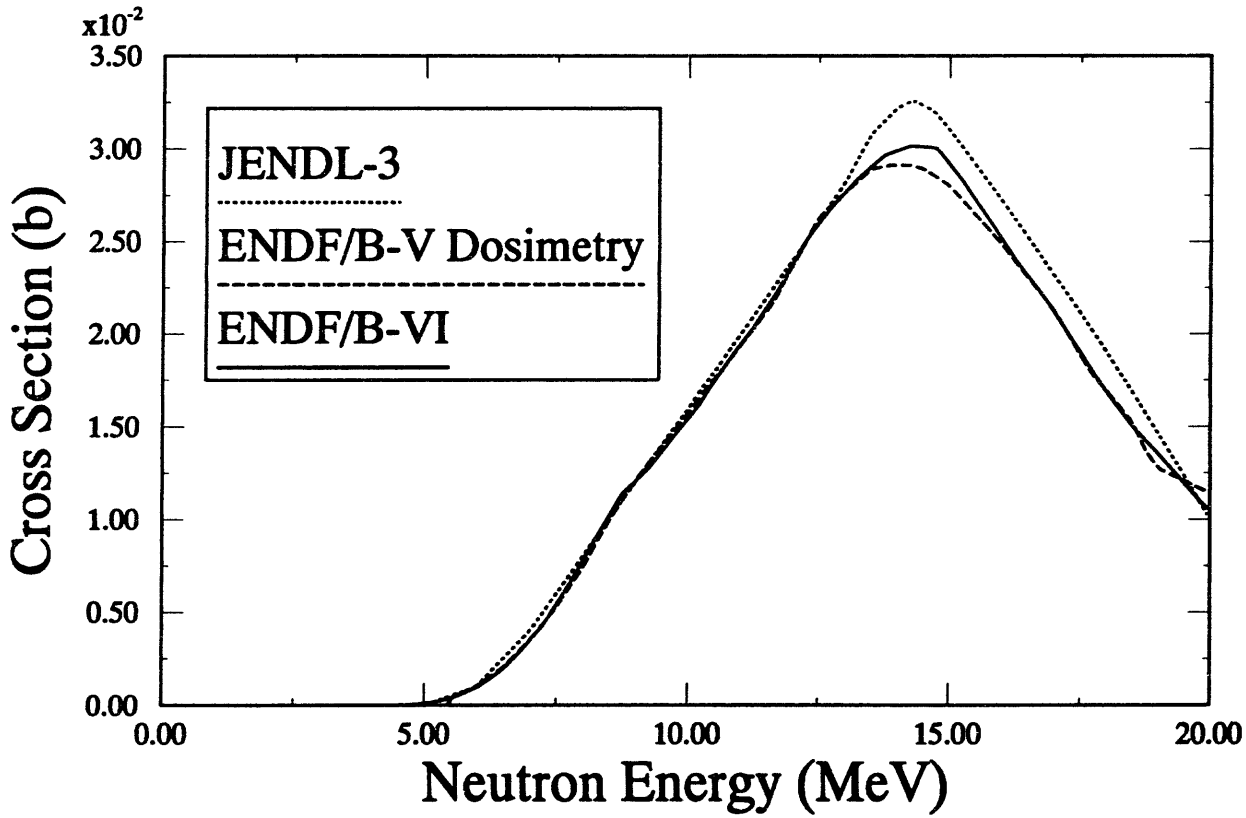

Figure A-31a: $^{59}Co(n,\alpha)^{56}Mn$ Cross Section

Table A-32a
Alternative Cross Section Sources for the $^{59}Co(n,2n)^{58}Co$ Reaction

$^{59}Co(n,2n)^{58}Co$			Comment
Cross Section Library	Material Number	Covariance Data	
ENDF/B-VI	2725	Yes	ANL, Eval. July 1989.
IRDF-90	2725	Yes	IRK-Vienna, eval. April 1990, file co-59a.
ENDF/B-V	1327	No	BNL, Eval. June 1977, tape 561, revision 2, based on ENDF/B-IV, a wide variation in experimental values was noted.
ENDF/B-V	6327	Yes	BNL, Eval. June 1977, Dosimetry Tape 531a.
ENDF/B-V	7279	No	BNL, Eval. June 1977, Activation Tape, 532b, based on ENDF/B-IV.
JENDL-3	3271	No	KHI, Eval. Aug. 1988, tape 24, same as ENDF/B-VI.
BROND	NA	----	Reported to be in library, but not in part available through BNL.
JEF 2.2	2725	Yes	ANL, Eval. July 1988, tape jef-2.

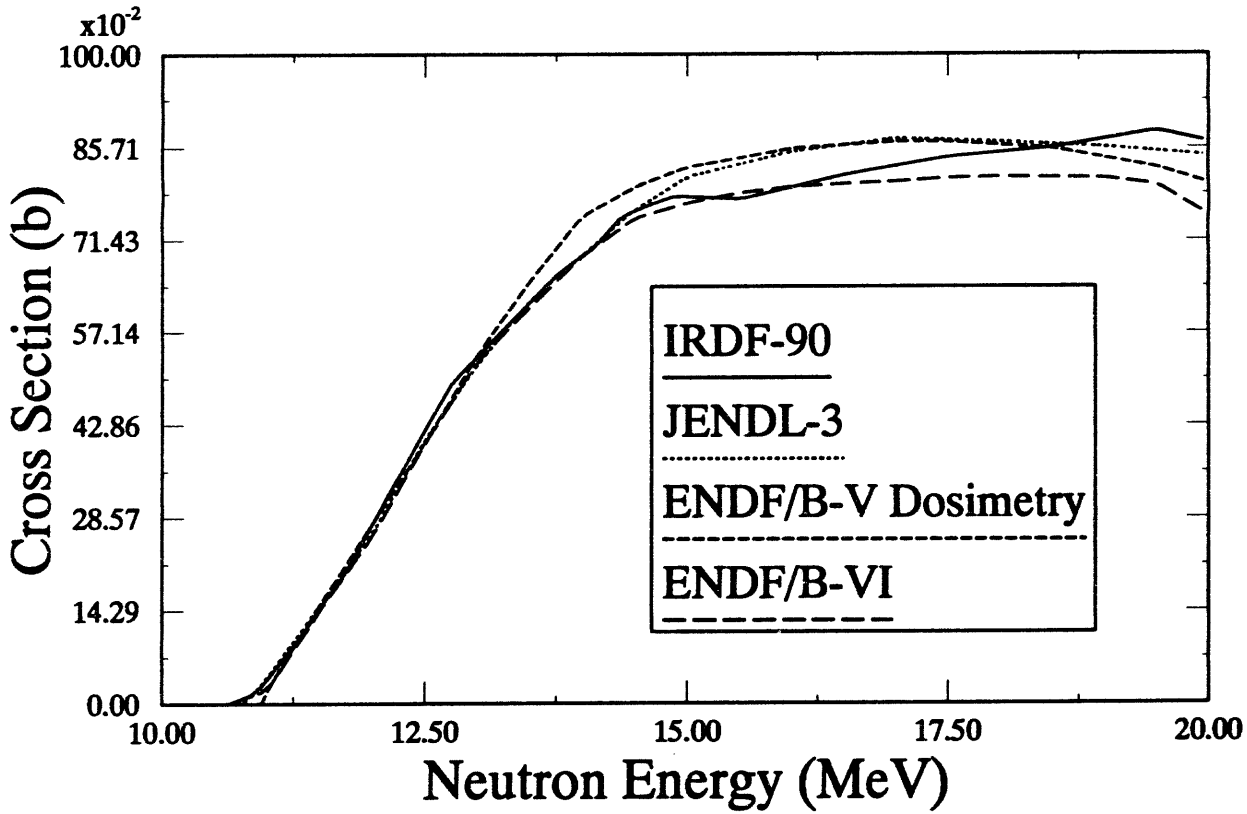

Figure A-32a: $^{59}Co(n,2n)^{58}Co$ Cross Section

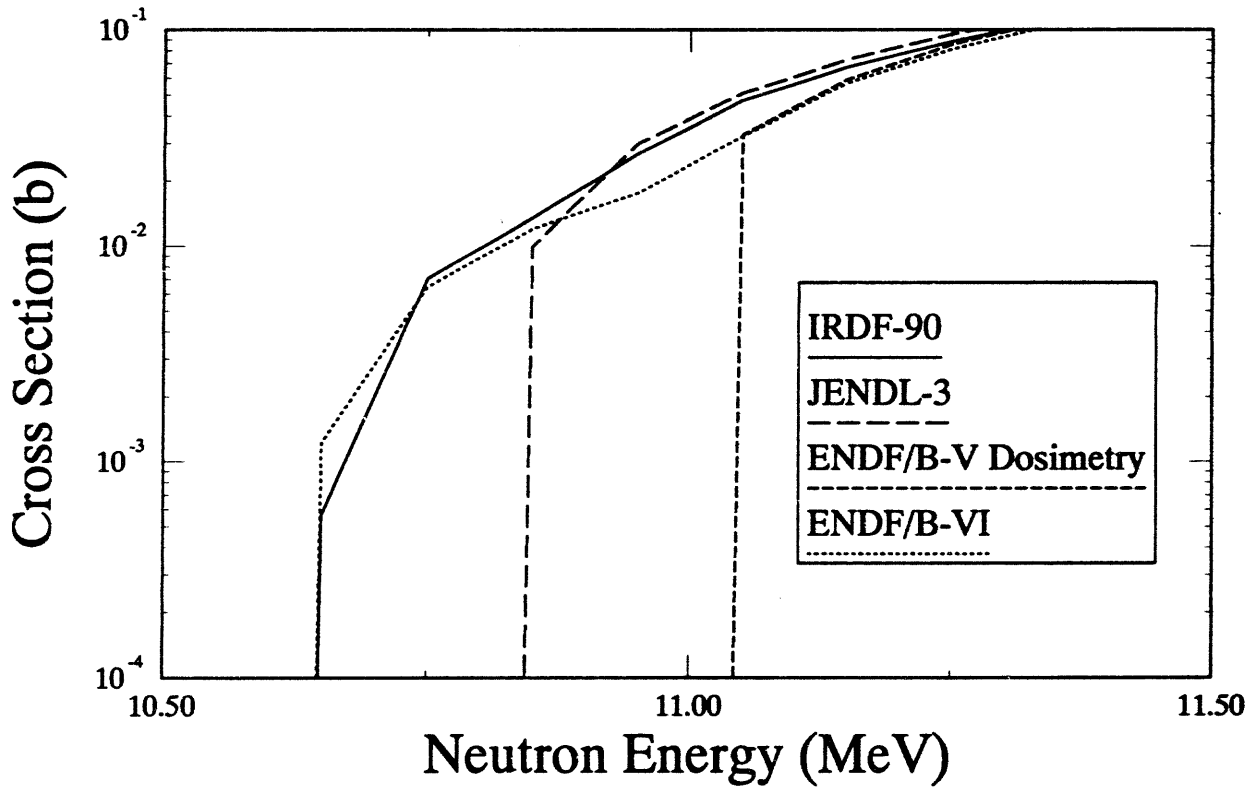

Figure A-32b: $^{59}Co(n,2n)^{58}Co$ Cross Section

Table A-33a
Alternative Cross Section Sources for the $^{58}Ni(n,p)^{58}Co$ Reaction

$^{58}Ni(n,p)^{58}Co$			Comment
Cross Section Library	Material Number	Covariance Data	
ENDF/B-VI	2825	Yes	ORNL, Eval. Oct. 1989, taken from GLUCS with some smoothing.
IRDF-90	2825	Yes	Taken from ENDF/B-VI.
ENDF/B-V	6433	Yes	BNL, Eval. March 1977, Dosimetry Tape, 531a.
ENDF/B-V	7288	No	BNL, Eval. May 1978, Activation Tape, 532b.
GLUCS	6433	Yes	ORNL, 1990 distribution.
JENDL-3	3281	No	NAIG, Eval. March 1987, Tape 24.
BROND	2811	No	FEI-CID, Eval. May 1985.
JEF 2.2	2825	Yes	NEA, Recom. Jun 1991, taken from ENDF/B-VI, tape jef-2.

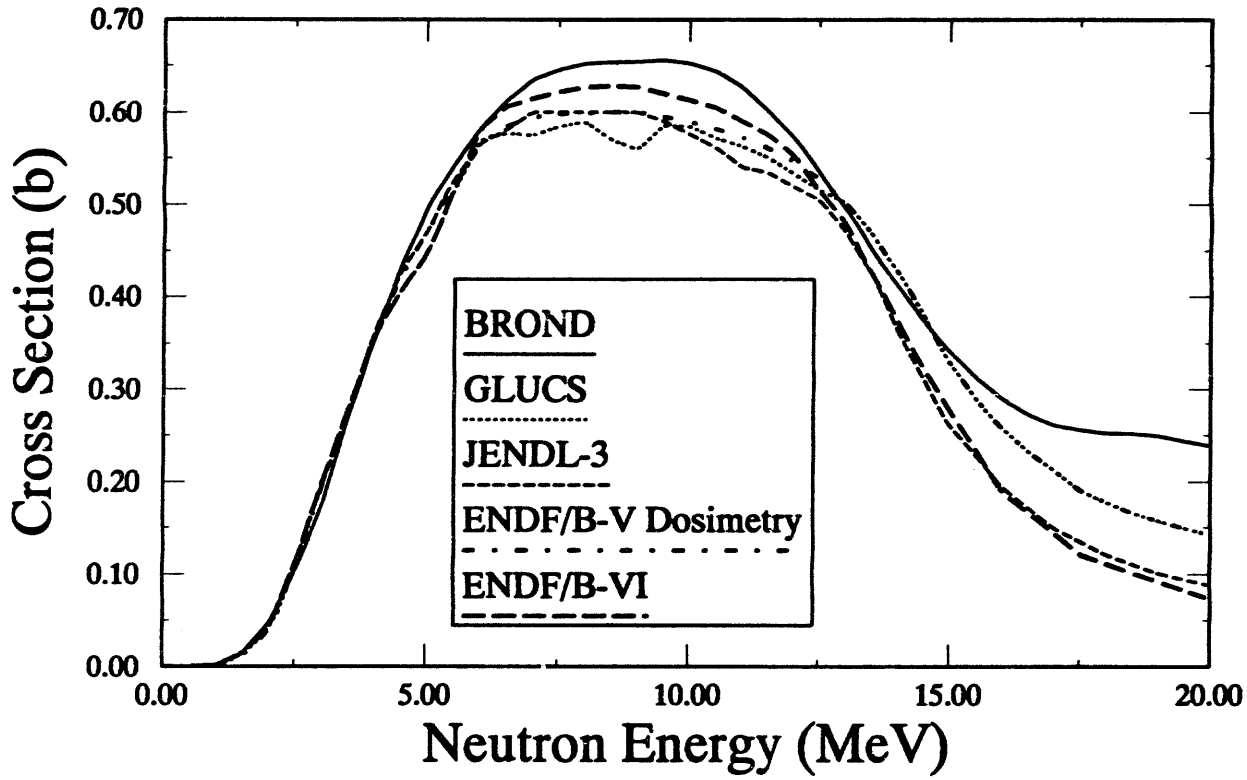

Figure A-33a: $^{58}Ni(n,p)^{58}Co$ Cross Section

Table A-34a
Alternative Cross Section Sources for the $^{58}Ni(n,2n)^{57}Ni$ Reaction

$^{58}Ni(n,2n)^{57}Ni$			Comment
Cross Section Library	Material Number	Covariance Data	
ENDF/B-VI	2825	Yes	ORNL, Eval. Oct. 1989.
IRDF-90	2825	Yes	IRK-Vienna, Eval. April 1990, file ni-58b, indistinguishable from ENDF/B-VI.
IRDF-90	2825	Yes	NOT IRDF Recommended file, but present on release tape, file ni-58a, taken from ENDF/B-VI.
ENDF/B-V	6433	Yes	BNL, Eval. March 1977, Dosimetry Tape, 531a.
ENDF/B-V	7288	No	BNL, Eval. May 1978, Activation Tape, 532b.
GLUCS	6433 - NA	---	ORNL, 1990 distribution, does not include (n,2n) reaction.
JENDL-3	3281	No	NAIG, Eval. March 1987, Tape 24.
BROND	2811	No	FEI-CID, Eval. May 1985.
JEF 2.2	2825	Yes	NEA, Recom. June 1991, taken from ENDF/B-VI, tape jef-2.

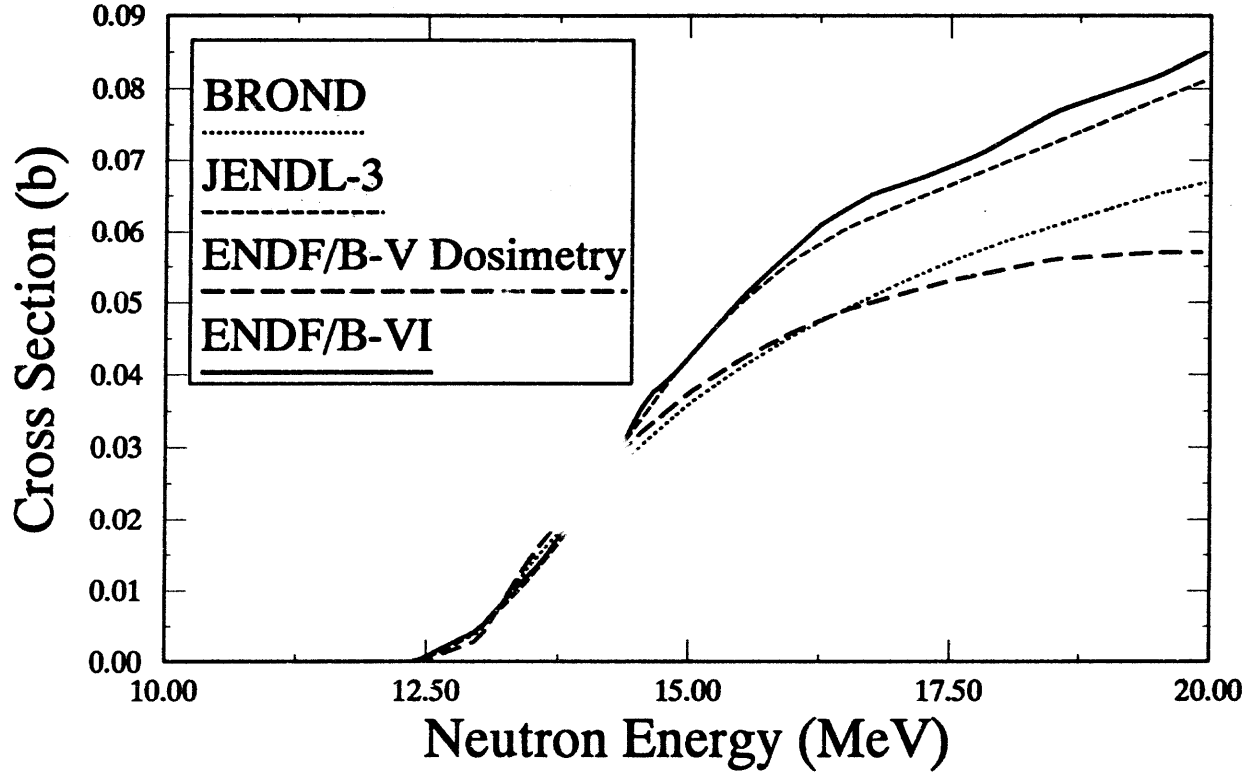

Figure A-34a: $^{58}Ni(n,2n)^{57}Ni$ Cross Section

Table A-35a
Alternative Cross Section Sources for the $^{60}Ni(n,p)^{60}Co$ Reaction

$^{60}Ni(n,p)^{60}Co$			Comment
Cross Section Library	Material Number	Covariance Data	
ENDF/B-VI	2831	Yes	ORNL, Eval. Oct. 1989.
IRDF-90	2831	Yes	Taken from ENDF/B-VI, format mod.
ENDF/B-V	6434	Yes	BNL, Eval. March 1977, Dosimetry tape 531a.
ENDF/B-V	7280	No	BNL, Eval. May 1978, Activation Tape 532b, includes population of 1st ES and GS in file 9.
JENDL-3	3282	No	NAIG, Eval. March 1987, Tape 24.
BROND	2821	No	FEI-CJD, Eval. May 1985.
JEF 2.2	2831	Yes	NEA, Rcom. June 1991, tape jef-2, taken from ENDF/B-VI.

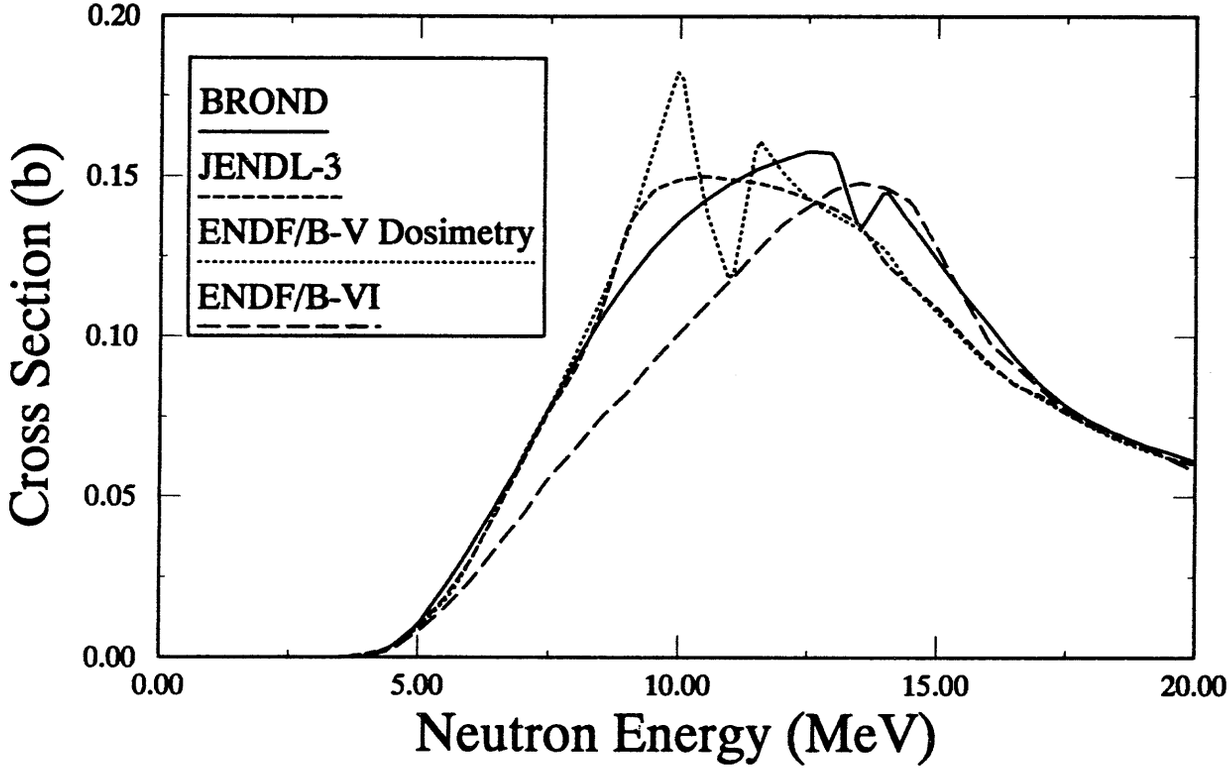

Figure A-35a: $^{60}Ni(n,p)^{60}Co$ Cross Section

Table A-36a
Alternative Cross Section Sources for the $^{63}Cu(n,\gamma)^{64}Cu$ Reaction

$^{63}Cu(n,\gamma)^{64}Cu$			Comment
Cross Section Library	Material Number	Covariance Data	
ENDF/B-VI	2925	Yes	ORNL, Eval. Nov. 1989.
IRDF-90	2925	No	ORNL, Eval. Nov. 1989, taken from ENDF/B-VI.
ENDF/B-V	6435	Yes	ORNL, Eval. July 1978, Dosimetry Tape 531a.
ENDF/B-V	7293	No	ORNL, Eval. July 1978, Activation Tape 532b.
JENDL-3	3291	No	NAIG/MAPI, Eval. March 1987, Tape 25.
BROND	-- NA --	----	Advertised as part of library, Eval. 1986, but not in my files.
JEF 2.2	2900 - NA	---	Only includes ^{Nat}Cu, $^{63}Cu(n,\gamma)$ component taken from experimental data.

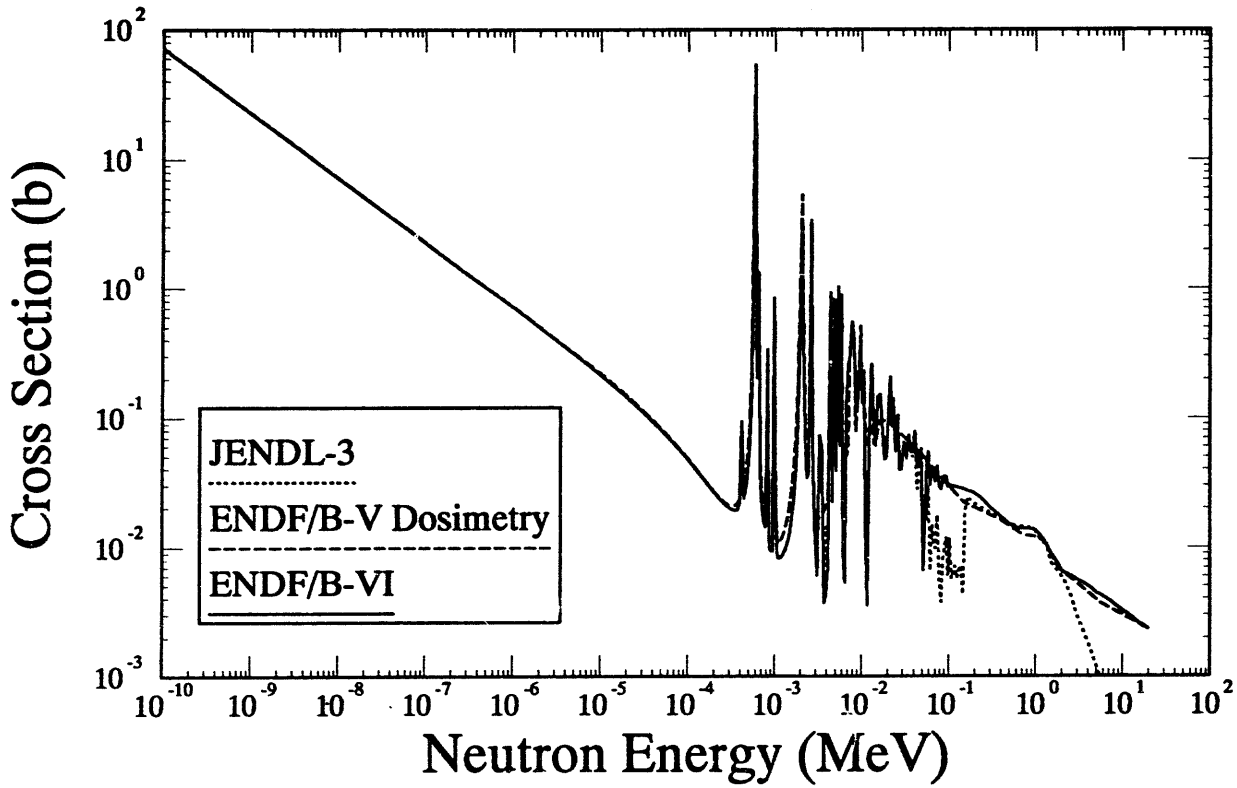

Figure A-36a: $^{63}Cu(n,\gamma)^{64}Cu$ Cross Section

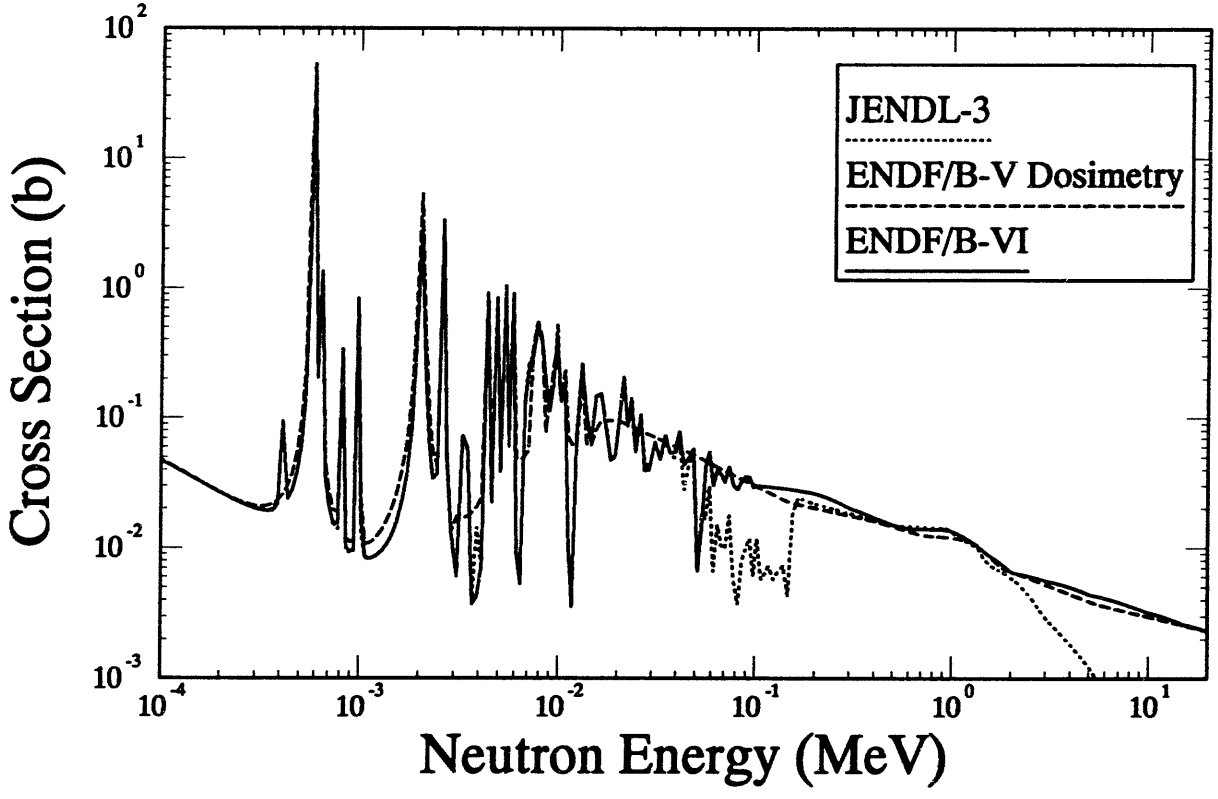

Figure A-36b: $^{63}Cu(n,\gamma)^{64}Cu$ Cross Section

Table A-37a
Alternative Cross Section Sources for the $^{63}Cu(n,2n)^{62}Cu$ Reaction

$^{63}Cu(n,2n)^{62}Cu$			Comment
Cross Section Library	Material Number	Covariance Data	
ENDF/B-VI	2925	Yes	ORNL, Eval. Nov. 1989.
IRDF-90	2925	Yes	NOT IRDF recommended file, but present on released tape. ORNL, Eval. Nov. 1989, file cu-63b, taken from ENDF/B-VI.
GLUCS	6435	Yes	ORNL, 1990 distribution, same as ENDF/B-VI.
IRDF-90	2925	Yes	IRK-Vienna, Eval. June. 1979, file cu-63a.
IRDF-82	2920	Yes	AUSIRK, Eval. 1979.
ENDF/B-V	6435 - NA	---	ORNL, Eval. July 1978, Dosimetry Tape 531a. (n,2n) reaction NOT on tape.
ENDF/B-V	7293 - NA	--	ORNL, Eval. July 1978, Activation Tape 532b. (n,2n) reaction NOT on tape.
JENDL-3	3291	No	NAIG/MAPI, Eval. March 1987, Tape 25.
BROND	-- NA --	----	Advertised as part of library, Eval. 1986, but not in my files.
JEF 2.2	2900 - NA	---	Only includes ^{Nat}Cu, $^{63}Cu(n,2n)$ component taken from experimental data and renormalized with the ^{65}Cu data to fit total measurements.

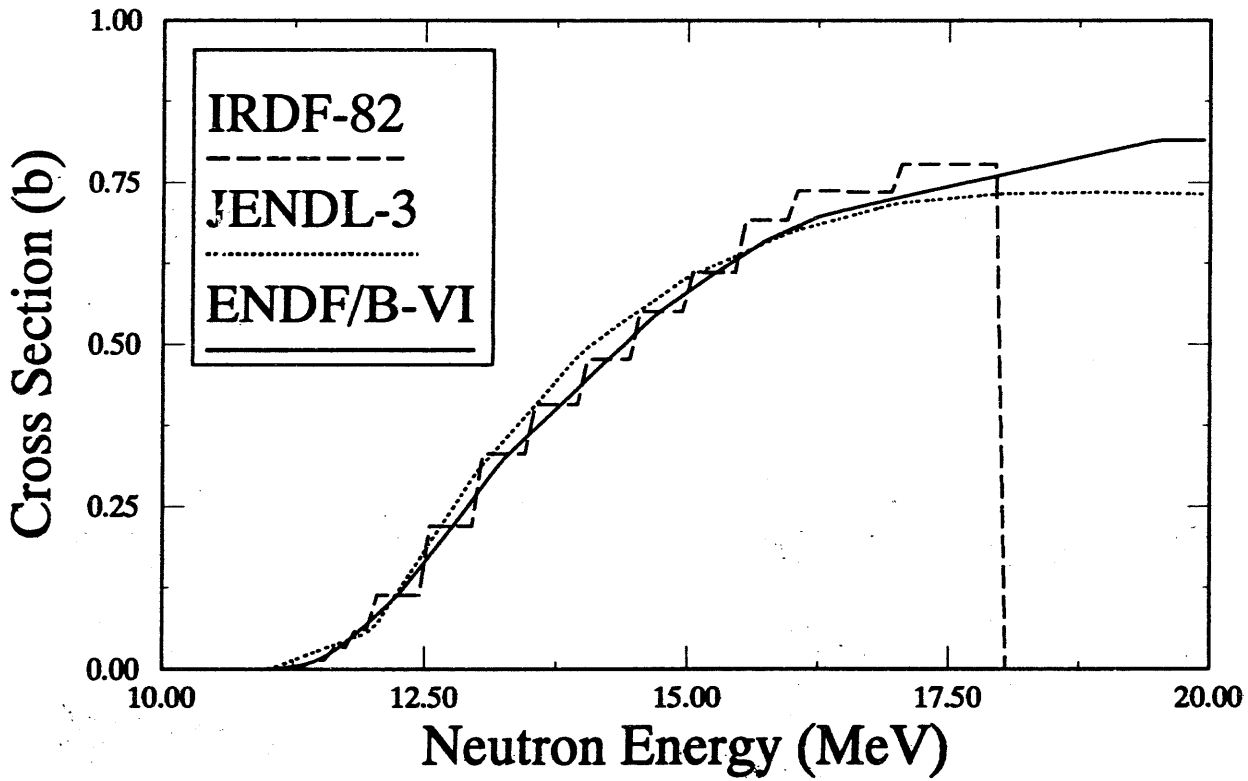

Figure A-37a: $^{63}Cu(n,2n)^{62}Cu$ Cross Section

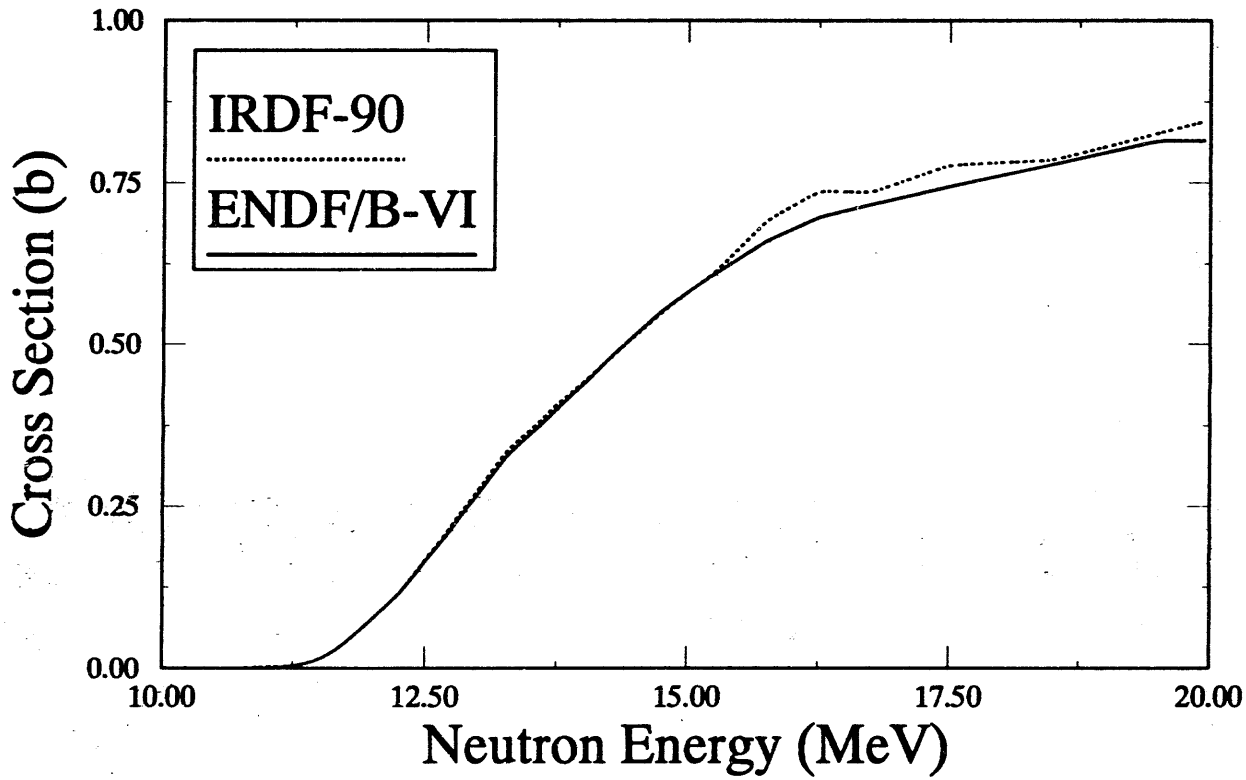

Figure A-37b: $^{63}Cu(n,2n)^{62}Cu$ Cross Section

Table A-38a
Alternative Cross Section Sources for the $^{63}Cu(n,\alpha)^{60}Co$ Reaction

$^{63}Cu(n,\alpha)^{602}Co$			Comment
Cross Section Library	Material Number	Covariance Data	
ENDF/B-VI	2925	Yes	ORNL, Eval. Nov. 1989.
IRDF-90	2925	Yes	ORNL, Eval. Nov. 1989, file cu-63b, taken from ENDF/B-VI.
GLUCS	6435	Yes	ORNL, 1990 distribution.
ENDF/B-V	6435	Yes	ORNL, Eval. July 1978, Dosimetry Tape 531a.
ENDF/B-V	7293	No	ORNL, Eval. July 1978, Activation Tape 532b.
JENDL-3	3291	No	NAIG/MAPI, Eval. March 1987, Tape 25.
BROND	-- NA --	----	Advertised as part of library, Eval. 1986, but not in my files.
JEF 2.2	2900 - NA	---	Only includes ^{Nat}Cu, $^{63}Cu(n,\alpha)$ component taken from ENDF/B-V dosimetry library.

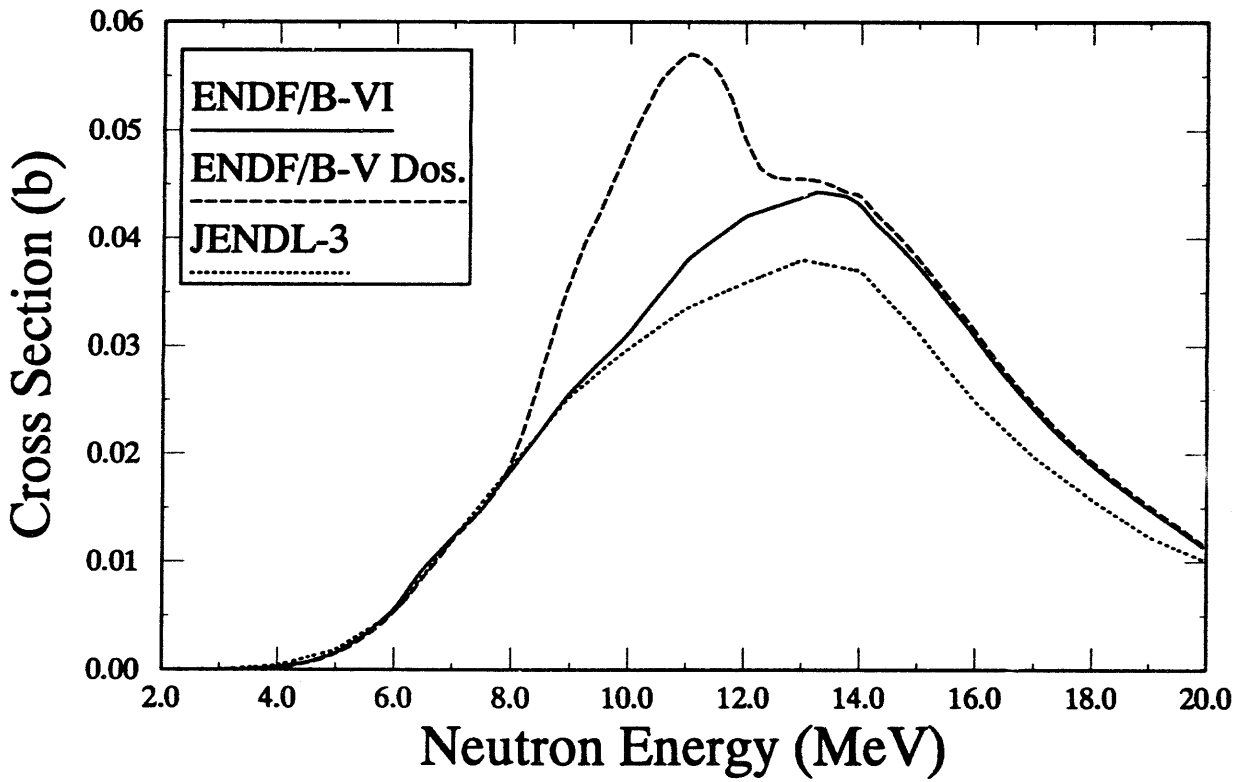

Figure A-38a: $^{63}Cu(n,\alpha)^{60}Co$ Cross Section

Table A-39a
Alternative Cross Section Sources for the $^{65}Cu(n,2n)^{64}Cu$ Reaction

$^{65}Cu(n,2n)^{64}Cu$			Comment
Cross Section Library	Material Number	Covariance Data	
ENDF/B-VI	2931	Yes	ORNL, Eval. Nov. 1989, taken from GLUCS with some smoothing.
IRDF-90	2931	Yes	Taken from ENDF/B-VI.
GLUCS	6436	Yes	ORNL, 1990 release, slightly different from ENDF/B-VI.
ENDF/B-V	6436	Yes	ORNL, Eval. July 1978, Dosimetry Tape 531a.
ENDF/B-V	7295	No	ORNL, Eval. July 1978, Activation Tape, 532b.
JENDL-3	3292	No	NAIG/MAPI, Eval. Mar. 1987, tape 25.
BROND	NA	----	Reported to part of the library, but no included in the release to the NNDC.
JEF 2.2	2900 - NA	---	Only includes ^{Nat}Cu, $^{65}Cu(n,2n)$ component taken from ENDF/B-V dosimetry library.

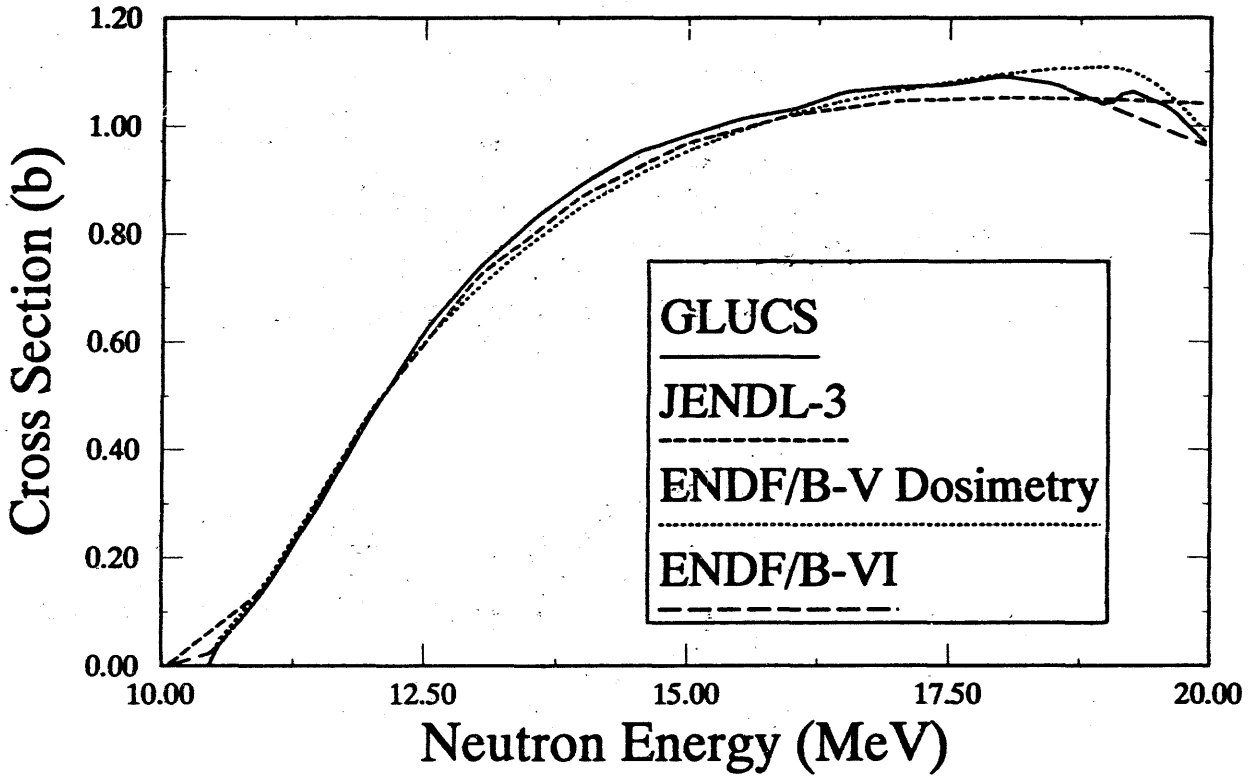

Figure A-39a: $^{65}Cu(n,2n)^{64}Cu$ Cross Section

Table A-40a
Alternative Cross Section Sources for the $^{64}Zn(n,p)^{64}Cu$ Reaction

$^{64}Zn(n,p)^{64}Cu$			Comment
Cross Section Library	Material Number	Covariance Data	
ENDF/B-VI	NA	----	No ENDF/B evaluation exists.
IRDF-90	3025	Yes	IRK Eval. April 1990.
IRDF-82	3020	Yes	AUSIRK, Eval. 1979.
JEF 2.2	3025	No	NEA, Rcom. June 1983, taken from RCN-2 evaluation, tape jef-2.
JENDL-3 Dos.	3031	Yes	DE, Eval. March 1990, covariance taken from IRDF-85.

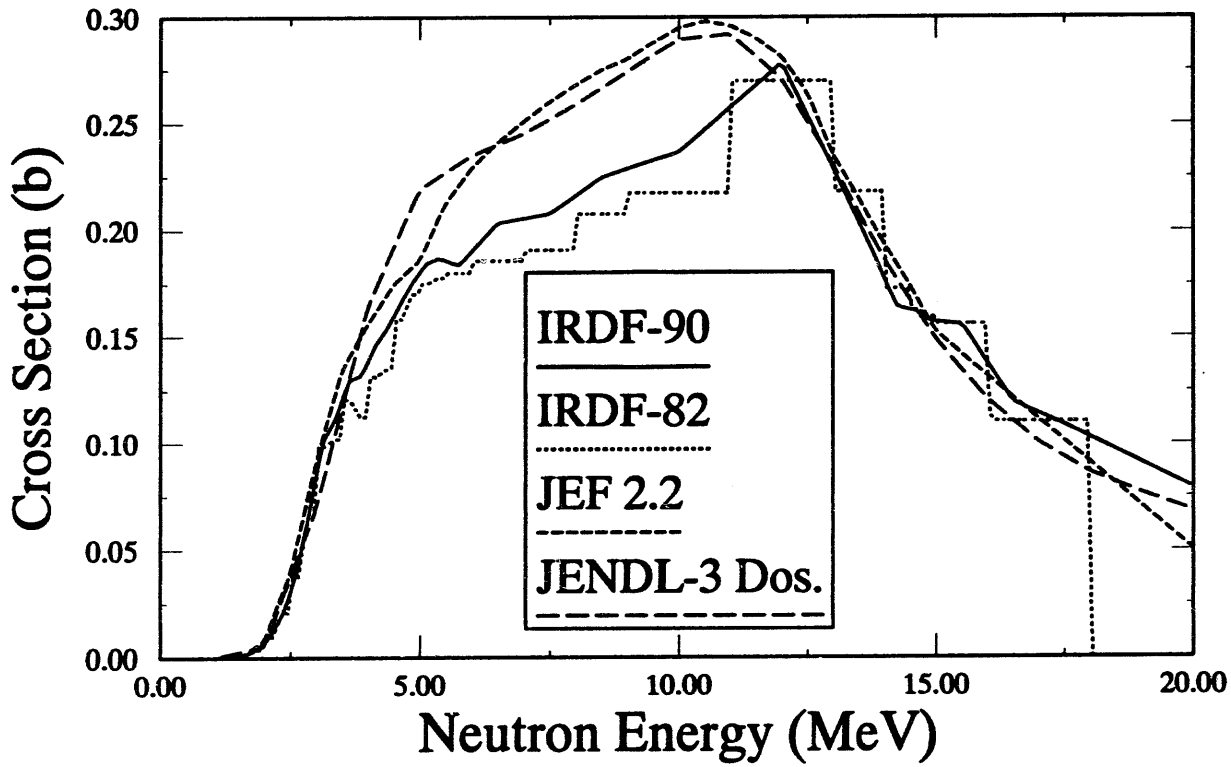

Figure A-40a: $^{64}Zn(n,p)^{64}Cu$ Cross Section

Table A-41a
Alternative Cross Section Sources for the $^{90}Zr(n,2n)^{89}Zr$ Reaction

$^{90}Zr(n,2n)^{89}Zr$			Comment
Cross Section Library	Material Number	Covariance Data	
ENDF/B-VI	4025	No	SAI/BNL, Eval. April 1976, tape 104, taken from ENDF/B-V.
IRDF-90	4025	Yes	IRK, Eval. April 1990.
IRDF-82	4020	Yes	AUSIRK, Eval. 1979.
ENDF/B-V	1385	No	SAI, Eval. April 1976, tape 558, revision 2.
ENDF/B-V	7400	No	SAI, Eval. April 1976, Activation Tape, 532b.
JENDL-3	3401	No	JNDC, Eval. Aug. 1989, tape 25.
BROND	NA	----	Reported to be part of the library, but not in tapes delivered to NNDC.
JEF 2.2	4025 - NA	---	Recom. July 1983, tape jef-3, taken from JENDL-1, mat 4090. Does not include (n,2n) reaction.

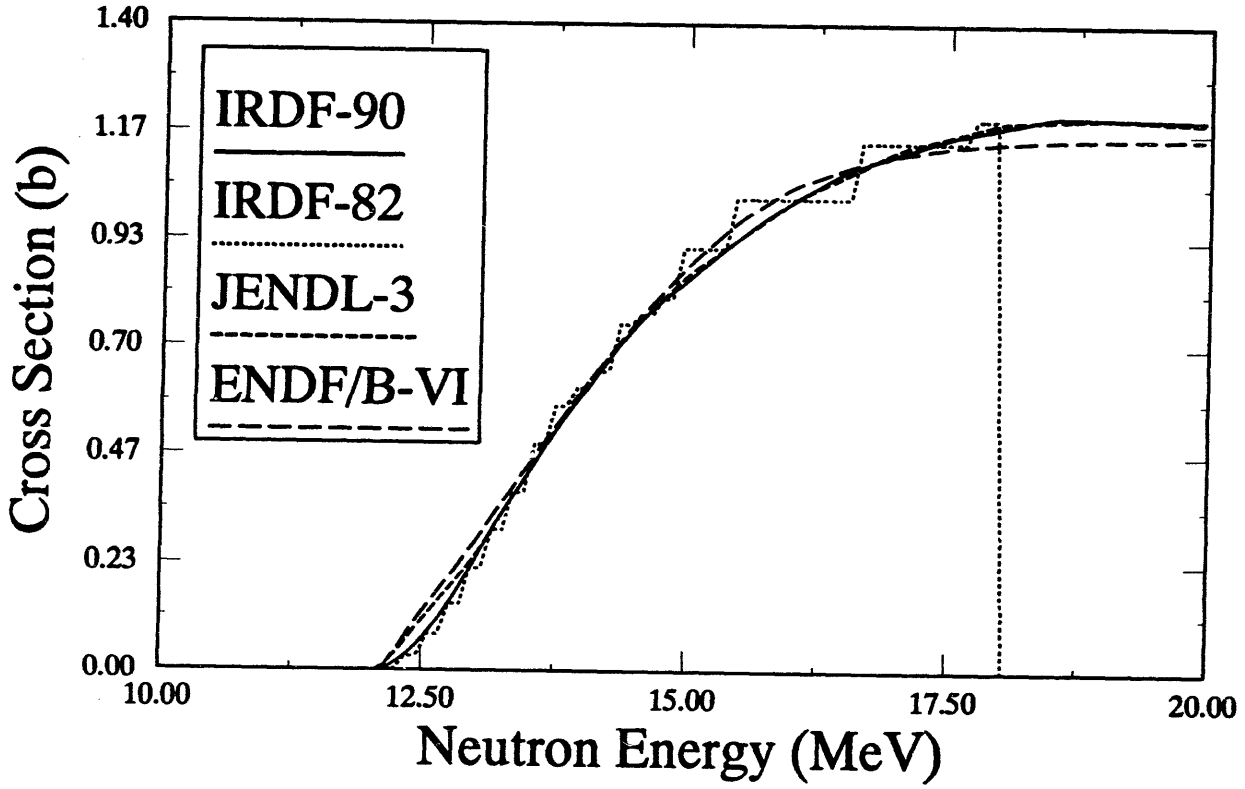

Figure A-41a: $^{90}Zr(n,2n)^{89}Zr$ Cross Section

Table A-42a
Alternative Cross Section Sources for the GaAs(n,X)1MeV Reaction

GaAs(n,X)1MeV			Comment
Cross Section Library	Material Number	Covariance Data	
ENDF/B-VI	3100 3325	No	LLNL Howerton LENDL evaluation modified by Young (LANL), converted from ENDF/B-V. Uses 10 eV for displacement damage threshold. HEDL, April 1974 eval, taken from ENDF/B-V. Uses 10 eV for displacement damage threshold.
ENDF/B-V	1358 9071	No	LLL Howerton LENDL with LANL Young mod, May 1980, tape 517. HEDL, April 1974, partial fission product tape 541.
JEF 2.2	3100 3325	No	Recom. July 1982, taken from LENDL, tape jef-3. Recom. July 1982, taken from ENDF/B-V, tape jef-3.
MIX	3100 8302	No	ENDF/B-VI for Ga, ENDL original for As-75. The original ENDL contains information on photons to allow their subtraction from kerma, as well as (n,p), (n,2n), (n,3n), and (n,α) reactions.
Private	3100 8302	No	Same as MIX, but processed with NJOY using a PKA energy dependent displacement damage efficiency factor.

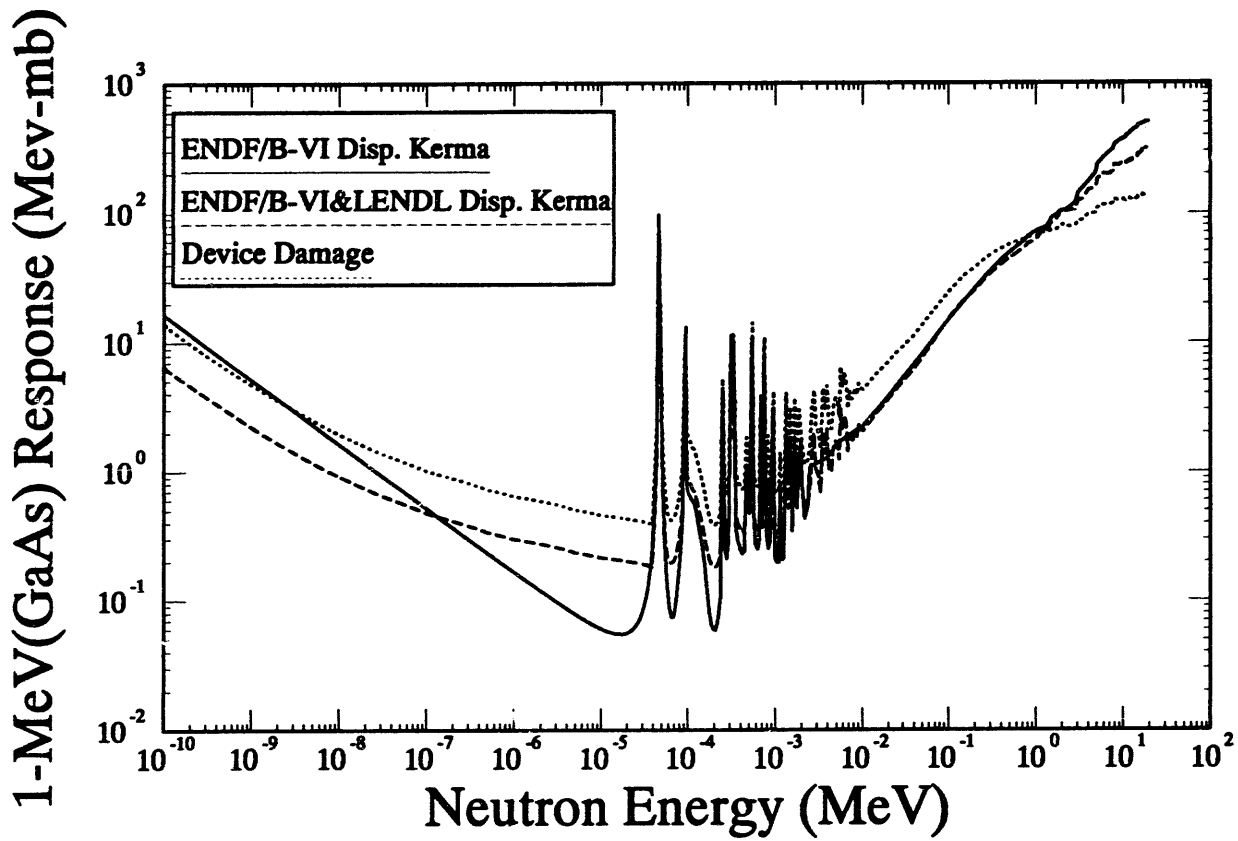

Figure A-42a: GaAs(n,X)1MeV Displacement Damage

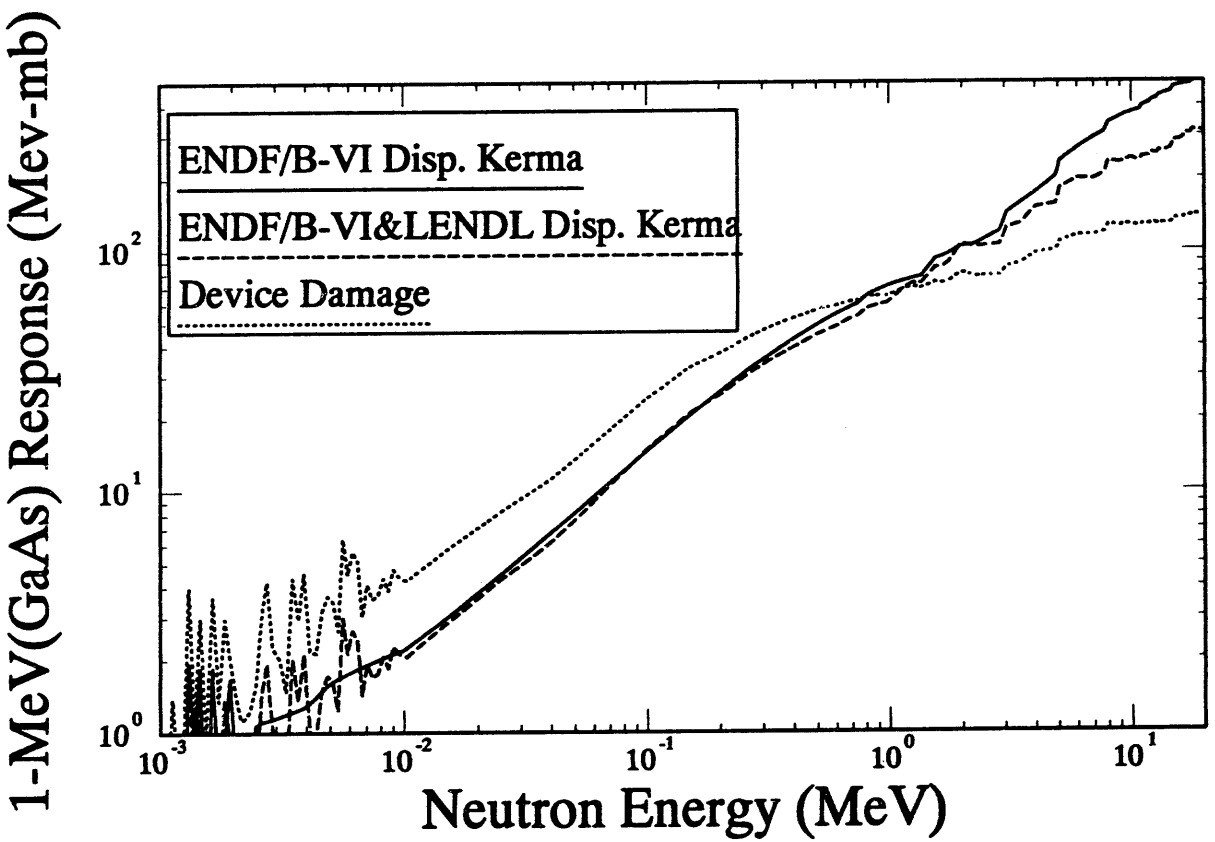

Figure A-42b: GaAs(n,X)1MeV Displacement Damage

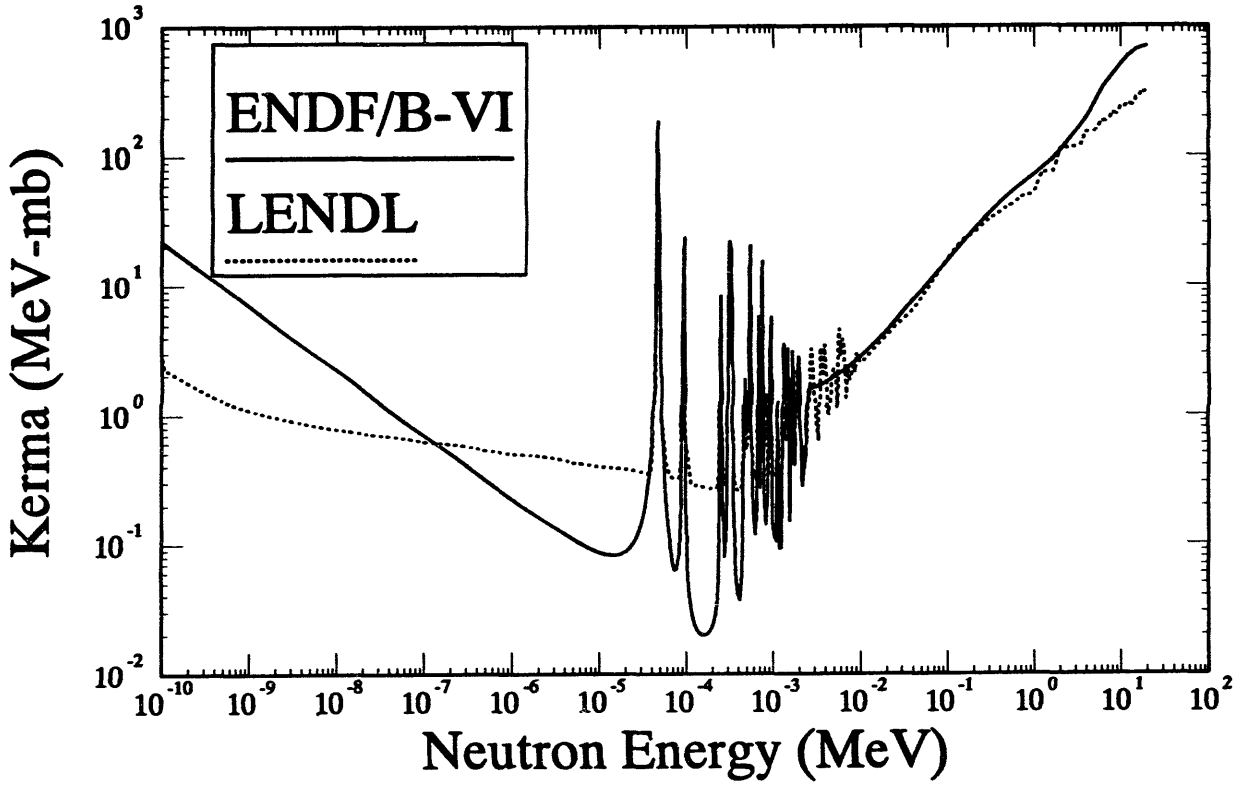

Figure A-42c: ^{75}As Displacement Kerma

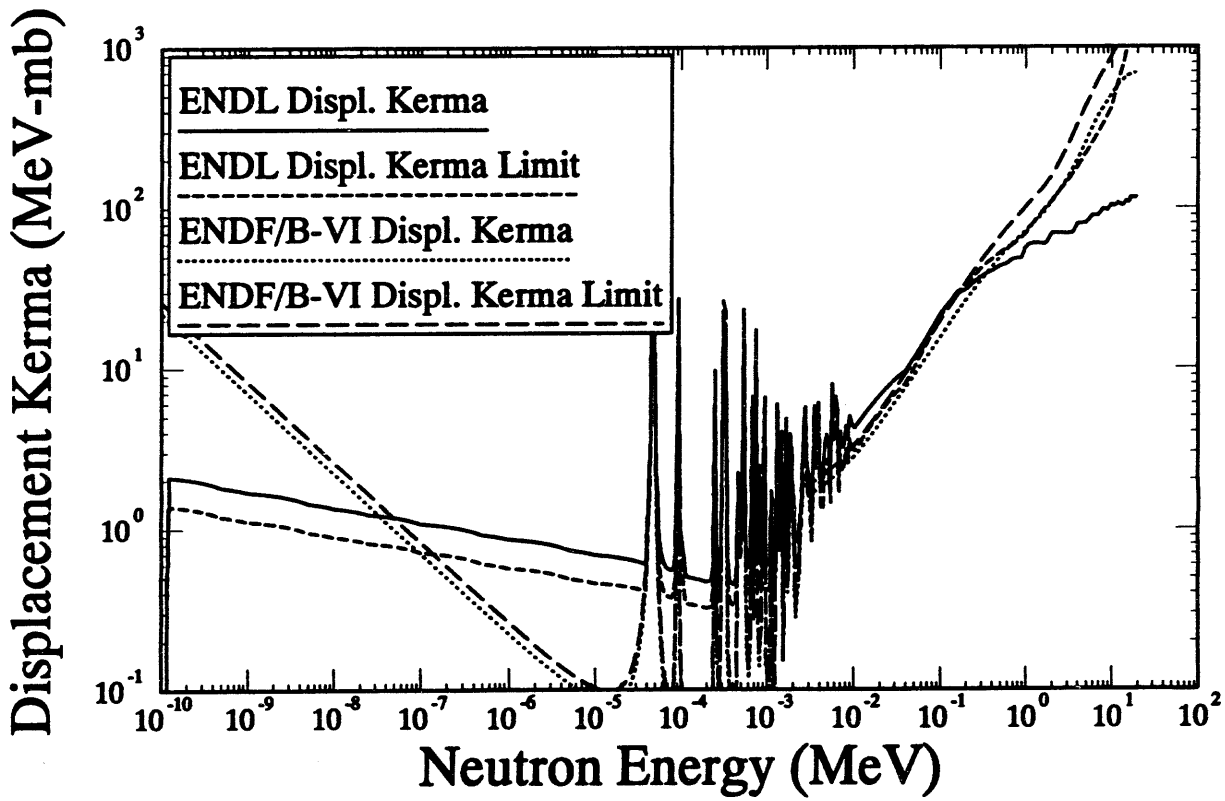

Figure A-42d: ^{75}As Displacement Kerma

Figure A-42e: ^{Nat}Ga Displacement Kerma

Table A-43a
Alternative Cross Section Sources for the $^{93}Nb(n,\gamma)^{94m}Nb$ Reaction

$^{93}Nb(n,\gamma)^{94m}Nb$			Comment
Cross Section Library	Material Number	Covariance Data	
ENDF/B-VI	4125	Yes	ANL/LLL Eval. March 1990.
IRDF-90	4125 - NA	---	IRK Eval April 1990. Does not include (n,γ) reaction.
IRDF-82	4120 - NA	---	AUSIRK, Eval. 1979. Does not include (n,γ).
ENDF/B-V	1189	No	ANL/LLL, Eval. May 1974, Tape 510.
ENDF/B-V	7413	No	ANL/LLL, Eval. May 1974, Activation Tape, 532b.
JENDL-3	3411	No	NAIG, Eval Nov. 1988, Tape 25.
BROND	4193	No	CCPFEI, Eval. 1988, tape 77, updated of 4111.
JEF 2.2	4125	No	Taken from ENDF/B-V, mat 1189, tape jef-3. Resonance parameters revised.

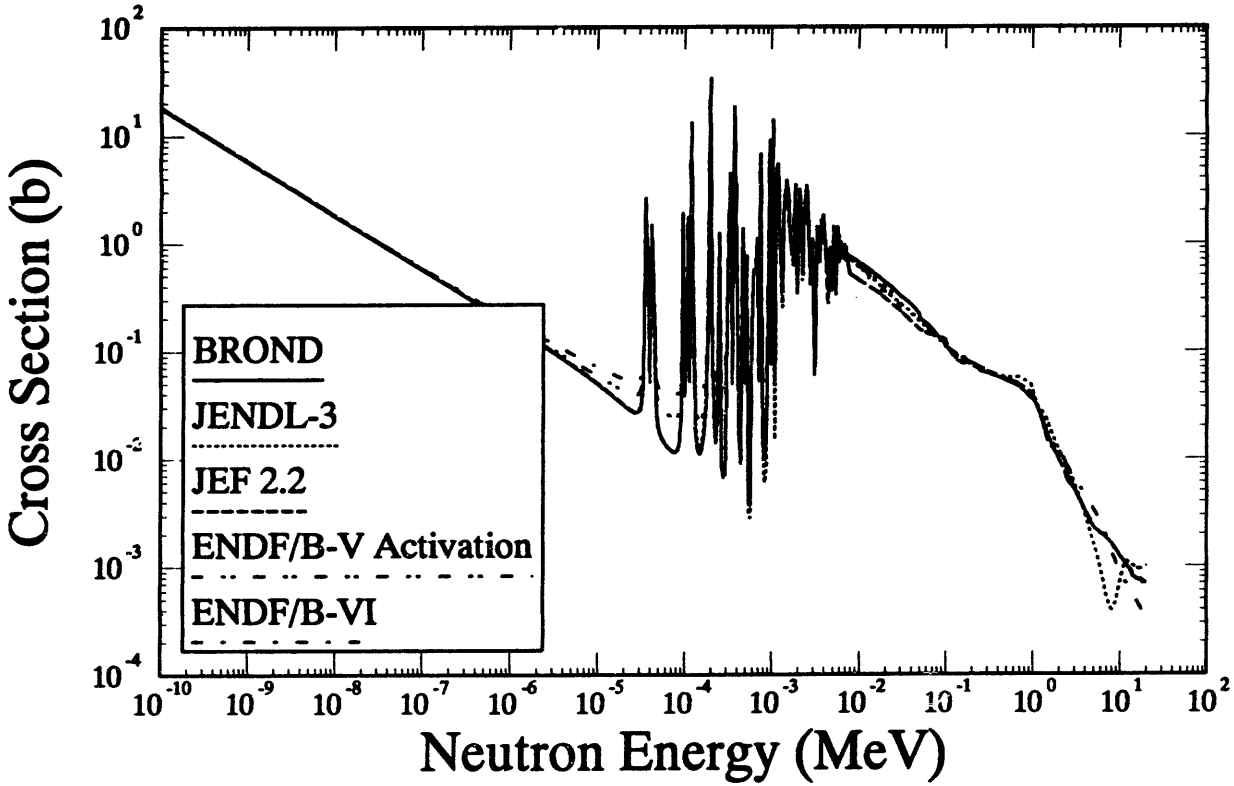

Figure A-43a: $^{93}Nb(n,\gamma)^{94m}Nb$ Cross Section

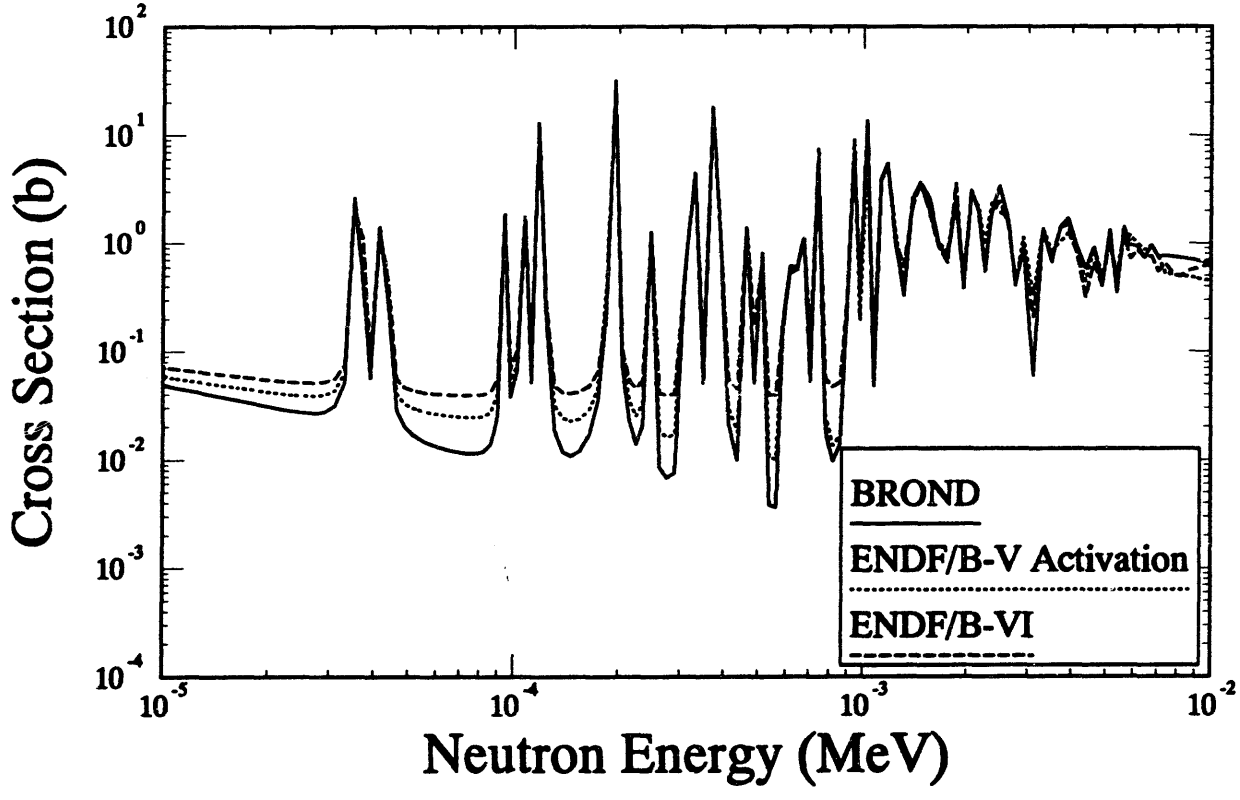

Figure A-43b: $^{93}Nb(n,\gamma)^{94m}Nb$ Cross Section

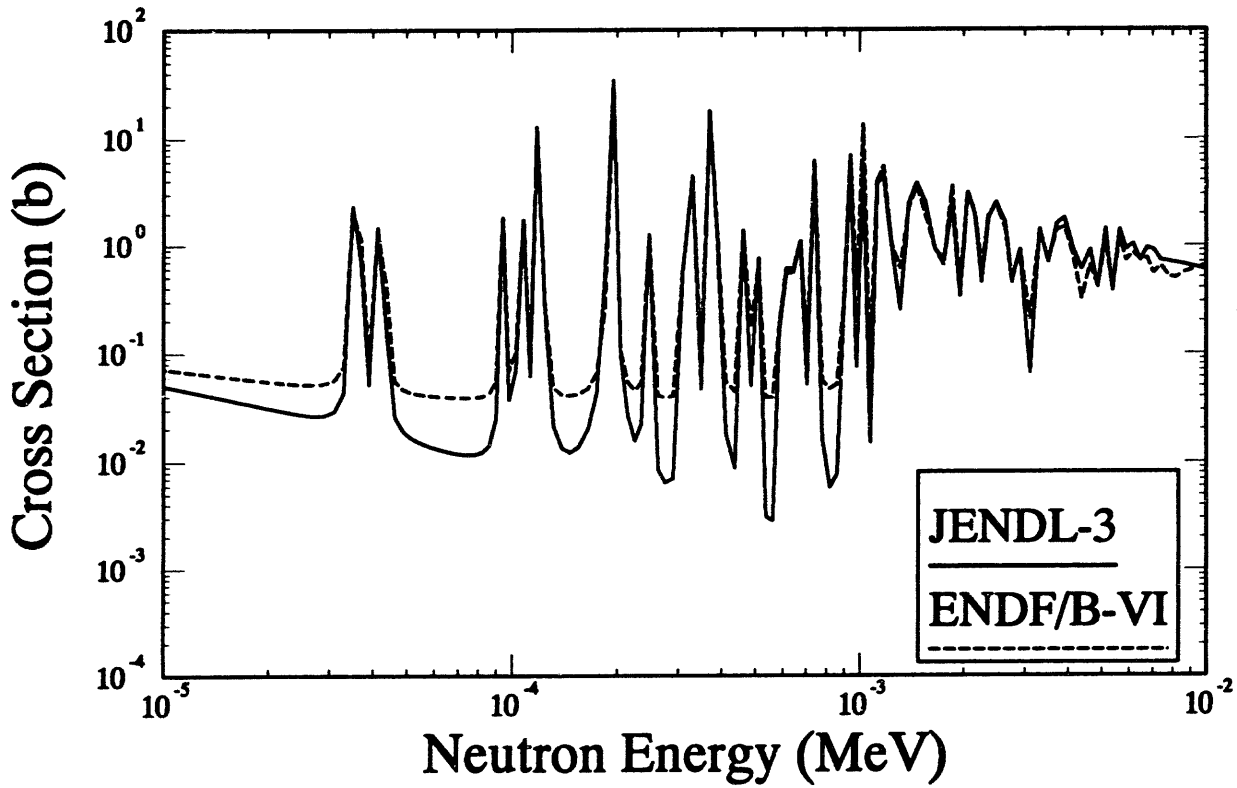

Figure A-43c: $^{93}Nb(n,\gamma)^{94m}Nb$ Cross Section

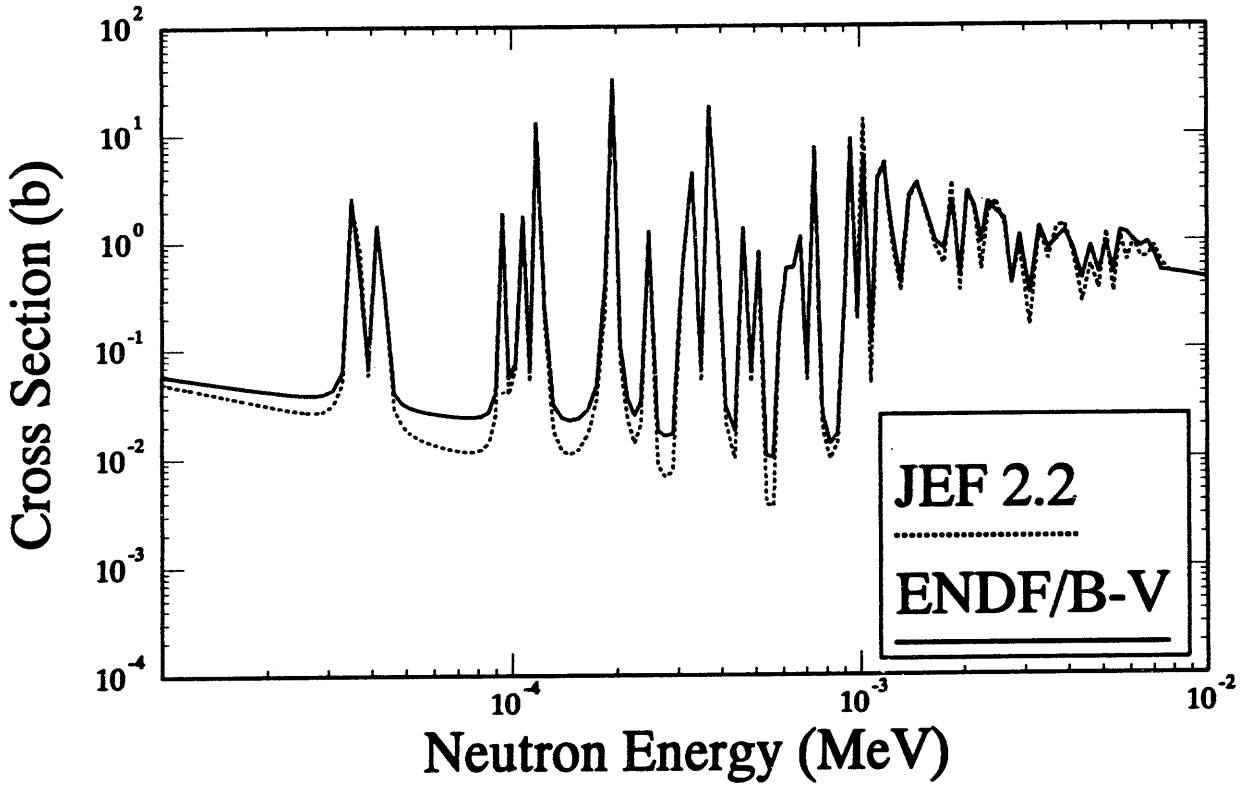

Figure A-43d: $^{93}Nb(n,\gamma)^{94m}Nb$ Cross Section

Table A-44a
Alternative Cross Section Sources for the $^{93}Nb(n,2n)^{92m}Nb$ Reaction

$^{93}Nb(n,2n)^{92m}Nb$			Comment
Cross Section Library	Material Number	Covariance Data	
ENDF/B-VI	4125	Yes	ANL/LLL Eval. March 1990.
IRDF-90	4125	Yes	IRK Eval April 1990.
IRDF-82	4120 - NA	---	AUSIRK, Eval. 1979. Does not include (n,2n).
ENDF/B-V	1189	No	ANL/LLL, Eval. May 1974, Tape 510.
ENDF/B-V	7413	No	ANL/LLL, Eval. May 1974, Activation Tape, 532b.
JENDL-3	3411	No	NAIG, Eval Nov. 1988, Tape 25.
JENDL-3 Dos.	4131	Yes	JAERI,DE, Eval. Mar. 1990. Covariance data taken from IRDF-85.
BROND	4193	No	CCPFEI, Eval. 1988, tape 77. Updated of 4111.
JEF 2.2	4125	No	Taken from ENDF/B-V, mat 1189.
DOSCROS84	7413	No	ENDF/B-V with modified ratio = 0.4 from S. Blow, AERE-R6540, Jan. 1971 [51].
Strohmaier	-----	No	Strohmaier, private communication 1990. See ref. 17 and 19. This work formed one input to the IRDF-90 cross section.

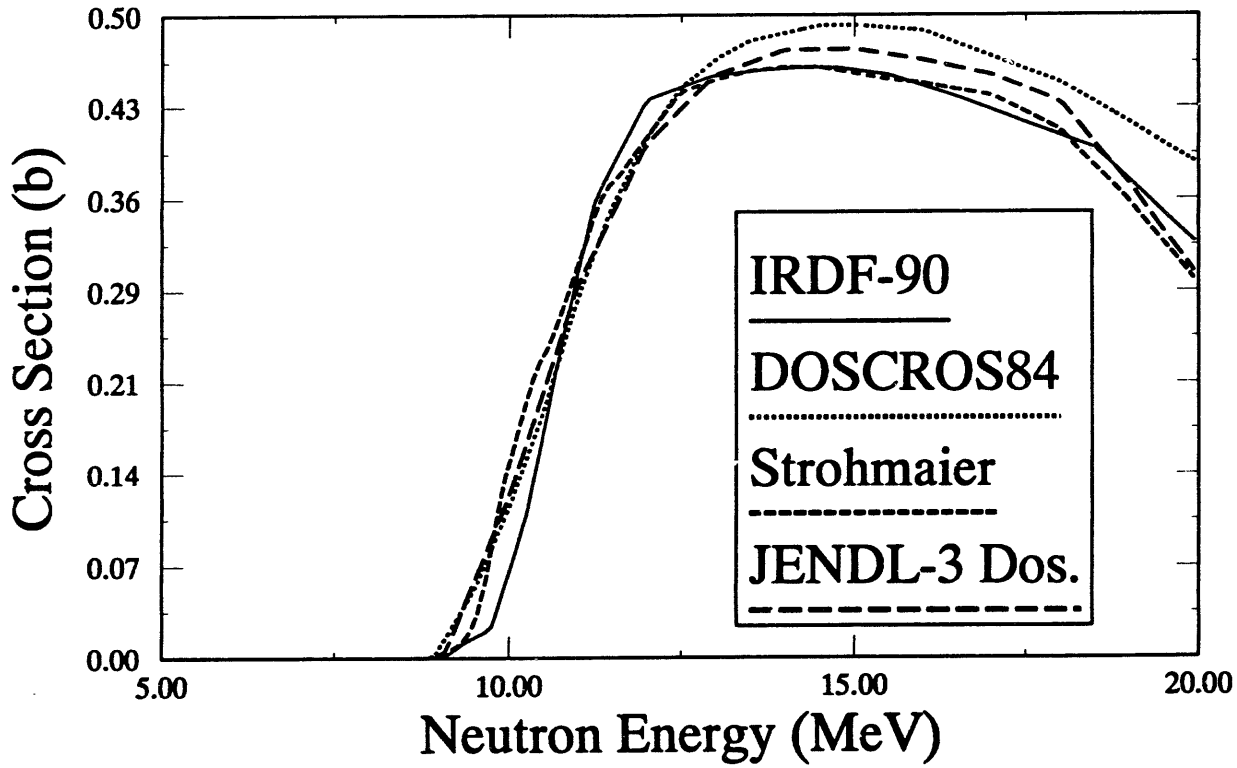

Figure A-44a: $^{93}Nb(n,2n)^{92m}Nb$ Cross Section

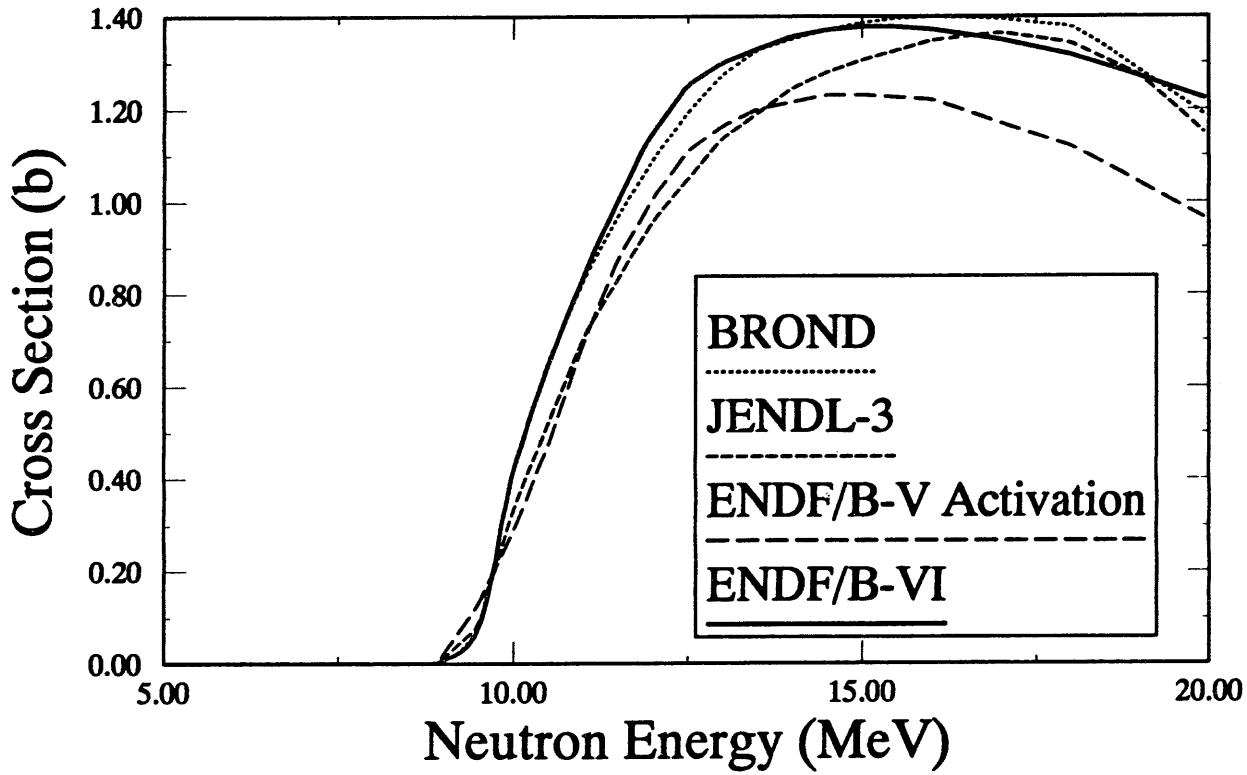

Figure A-44b: ^{93}Nb(n,2n)^{92}Nb Cross Section

Table A-45a
Alternative Cross Section Sources for the $^{93}Nb(n,n')^{93m}Nb$ Reaction

$^{93}Nb(n,n')^{93m}Nb$			Comment
Cross Section Library	Material Number	Covariance Data	
ENDF/B-VI	4125	Yes	ANL/LLL Eval. March 1990.
IRDF-90	4125	Yes	IRK Eval. April 1990.
IRDF-82	4120	Yes	AUSIRK, Eval. 1979.
ENDF/B-V	1189	No	ANL/LLL, Eval. May 1974, Tape 510.
ENDF/B-V	7413	---	ANL/LLL, Eval. May 1974, Activation Tape, 532b, MT=4, obtained by subtraction.
JENDL-3	3411	No	NAIG, Eval. Nov. 1988, Tape 25.
JENDL-3 Dos.	4131	Yes	JAERI,DE, Eval. March 1990. Covariance matrix from IRDF-85.
BROND	4193	No	CCPFEI, Eval. 1988, tape 77. Updated of 4111.
JEF 2.2	4125	No	Taken from ENDF/B-V, mat 1189.
Pre-ENDF-VI	4125	Yes	Pre-release version contains cumulative (n,n') contribution in comment section, not permitted in official ENDF format. Nearly identical to IRDF-82 evaluation.
Private, Smith	4125	Yes	Smith private communication [16], should be in official ENDF/B-VI version, initial format problem because it must appear in File 8 not 3.

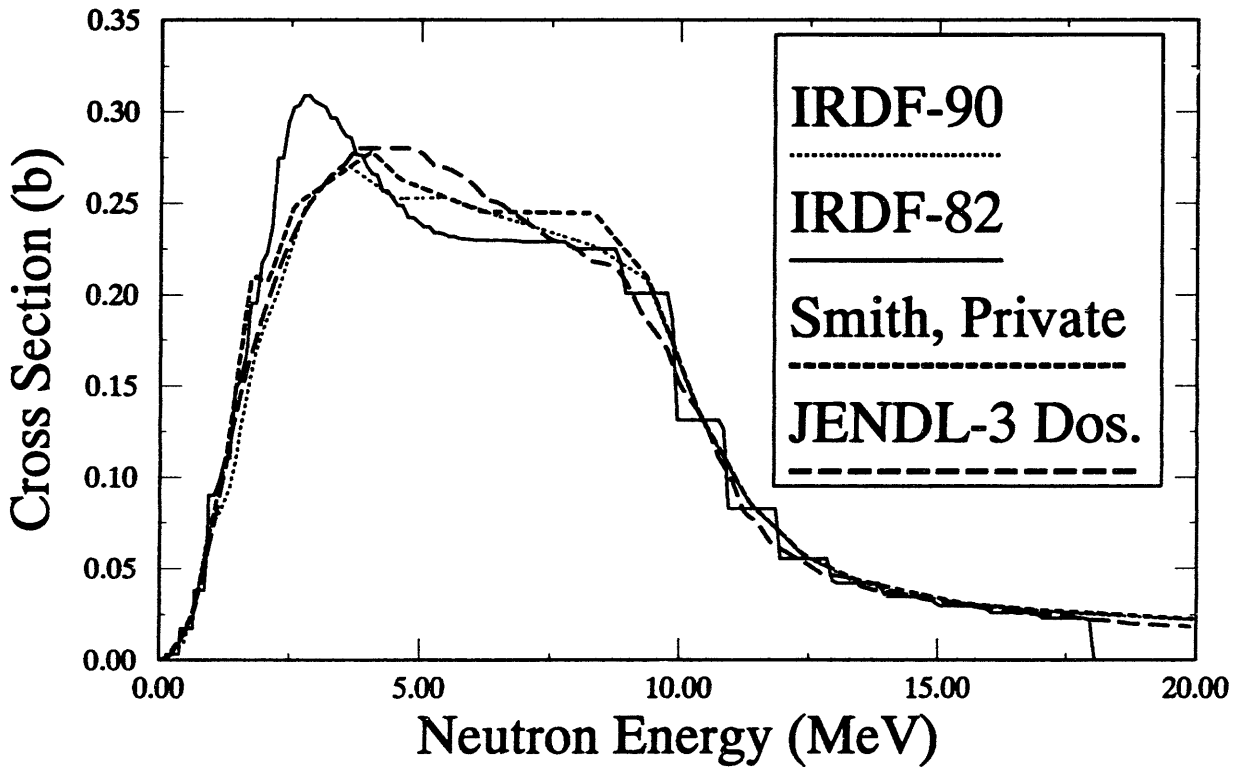

Figure A-45a: $^{93}Nb(n,n')^{93m}Nb$ Cross Section

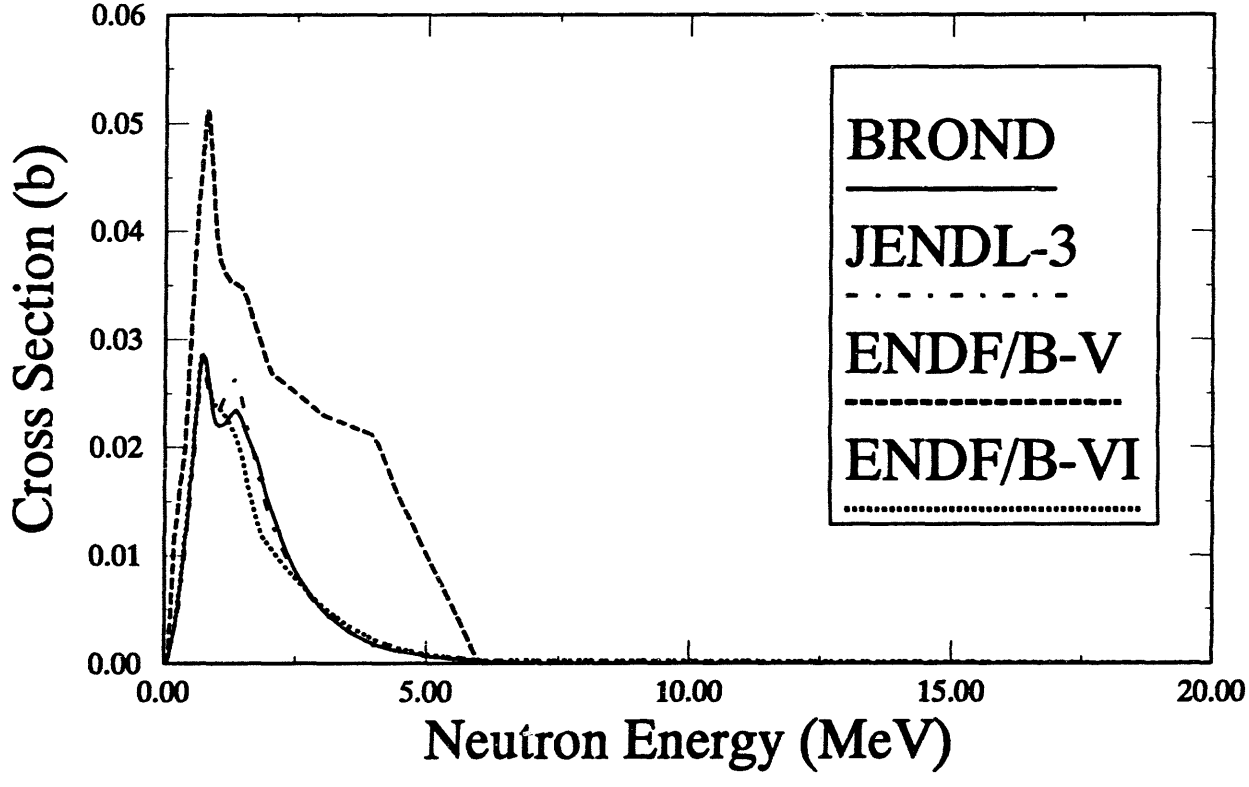

Figure A-45b: ^{93}Nb(n,n')^{93}Nb Cross Sections for 1st Excited State

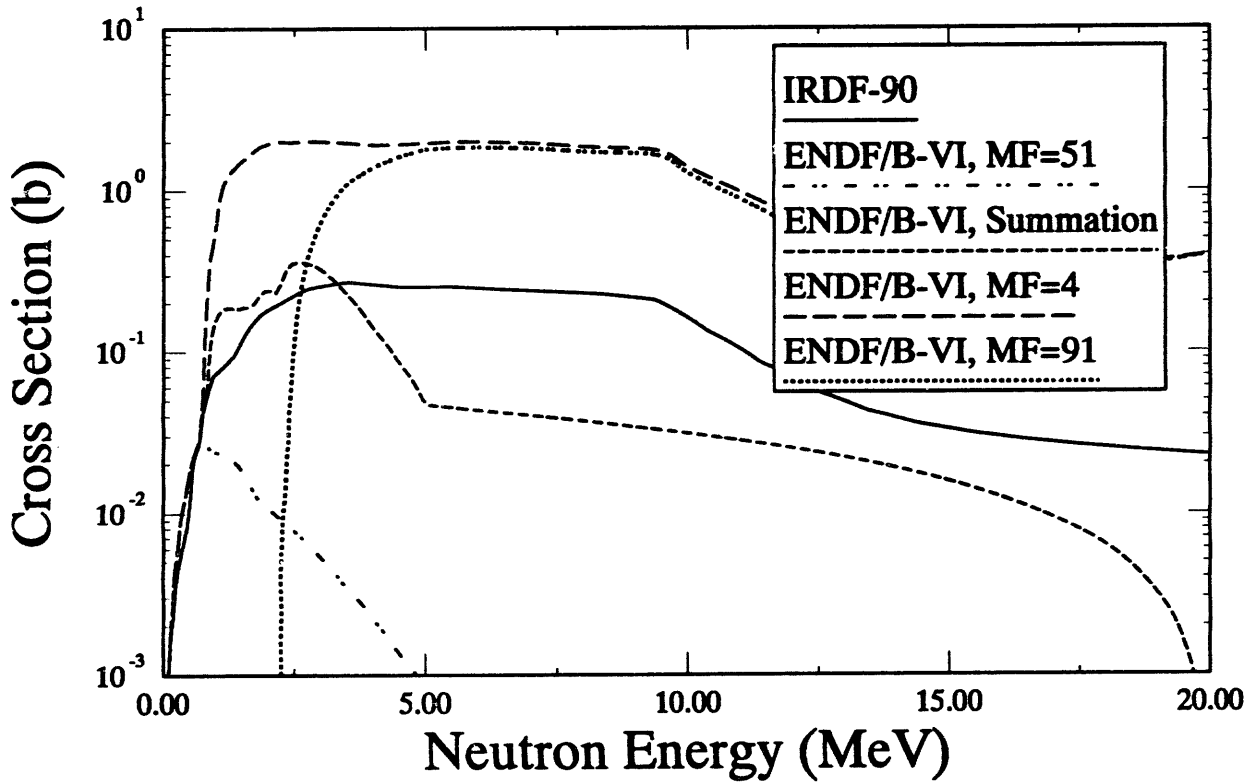

Figure A-45c: ^{93}Nb(n,n')^{93}Nb Cross Section Components

Table A-46a
Alternative Cross Section Sources for the $^{98}Mo(n,\gamma)^{99}Mo$ Reaction

$^{98}Mo(n,\gamma)^{99}Mo$			Comment
Cross Section Library	Material Number	Covariance Data	
ENDF/B-VI	4243	No	Accepted from ENDF/B-V fission product tape.
ENDF/B-V	7428	No	HEDL, Eval. Feb. 1980, Activation Tape, 532b.
JENDL-3	3426	No	JNDC, Eval. Aug. 1989, Tape 25.
BROND	4231	No	CJD/FEI, Exam. Oct. 1985.
JEF 2.2	4243	No	NEA, Rcom. July 1982, tape jef-3.

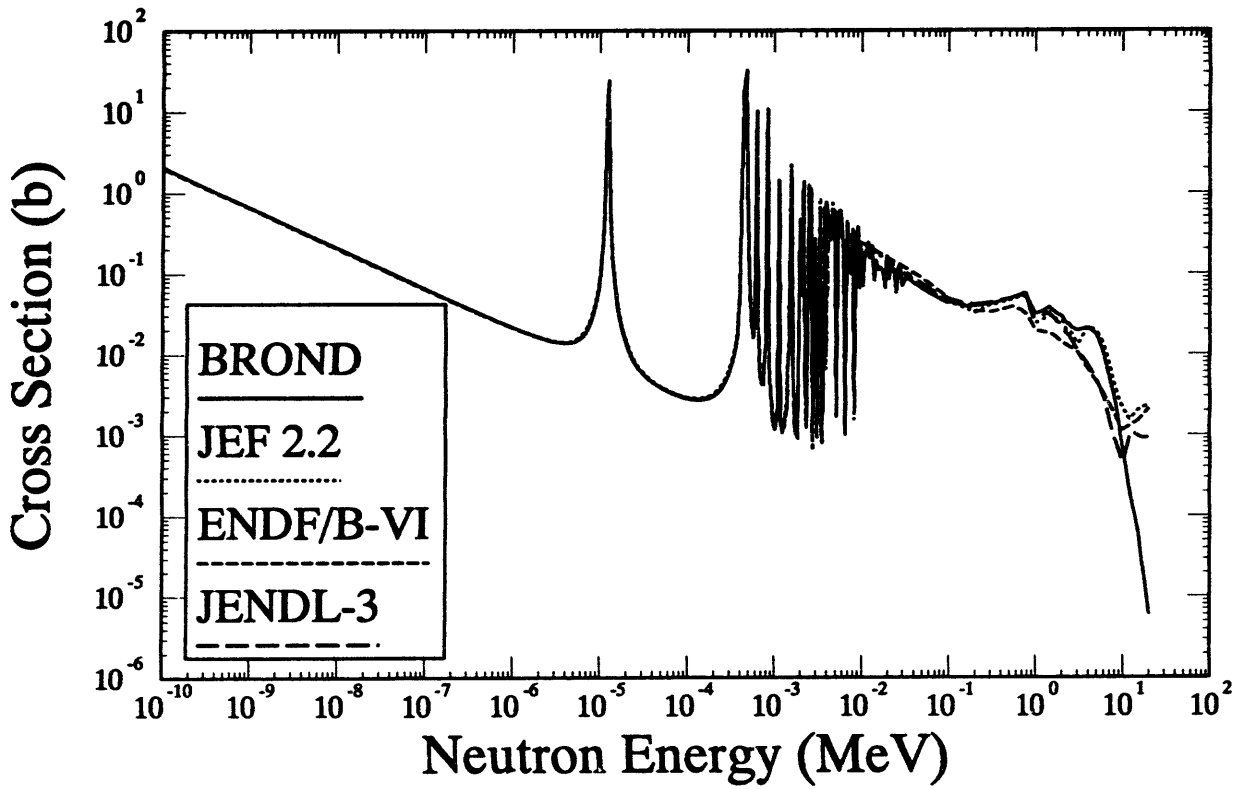

Figure A-46a: $^{98}Mo(n,\gamma)^{99}Mo$ Cross Section

Figure A-46b: $^{98}Mo(n,\gamma)^{99}Mo$ Cross Section

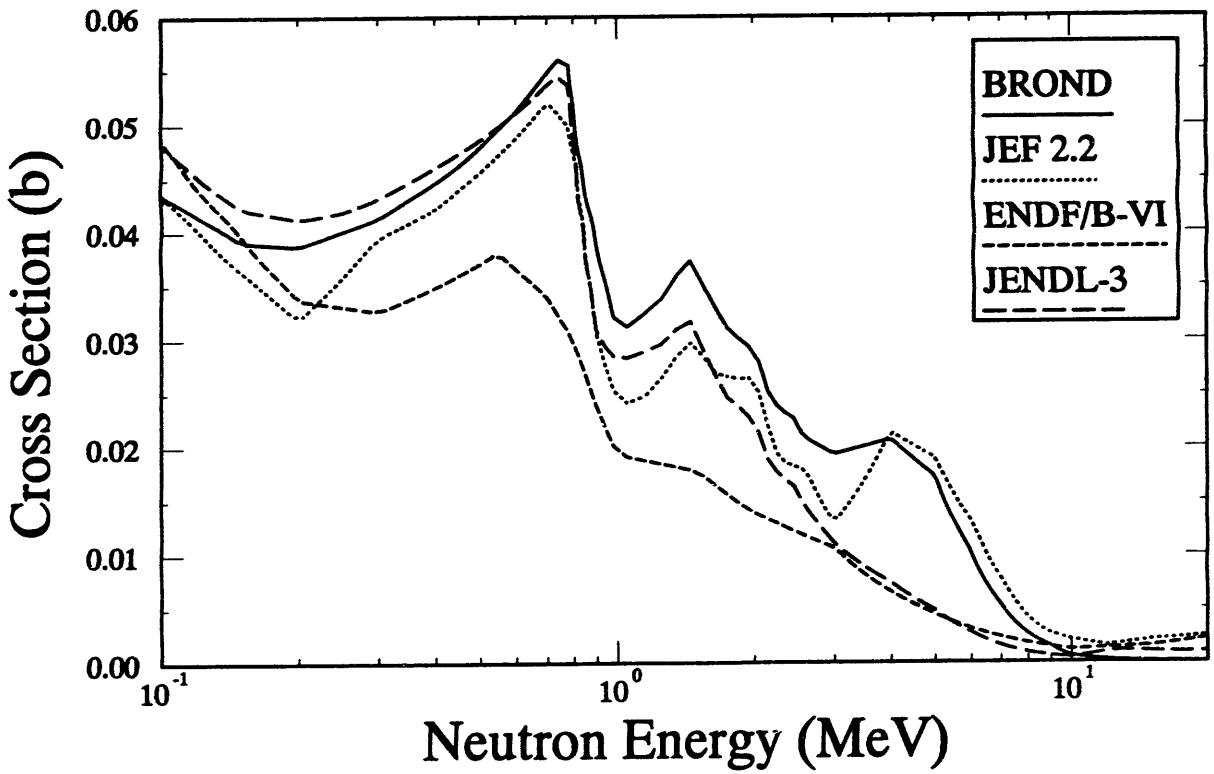

Figure A-46c: $^{98}Mo(n,\gamma)^{99}Mo$ Cross Section

Table A-47a
Alternative Cross Section Sources for the $^{103}Rh(n,n')^{103m}Rh$ Reaction

$^{103}Rh(n,n')^{103m}Rh$			Comment
Cross Section Library	Material Number	Covariance Data	
ENDF/B-VI	4525	No	HEDL, BAW, Nov. 1978. Taken from ENDF/B-V fission product library, inelastic states 51-64&91 exist.
ENDF/B-V	1310	No	HEDL, BAW, Nov. 1978, tape 510 fission product tape.
IRDF-90	4525	Yes	IRK, Eval. June 1980.
IRDF-82	4520	Yes	AUSIRK, Eval. 1979.
JENDL-3 Dos.	4531	Yes	Cross section and covariance data taken from IRDF-85.
JEF 2.2	4525	No	NEA, Rcom. July 1983, tape jef-3. Taken from RCN-3 evaluation (MAT=4503), inelastic states 51-74&91.
BROND	4501	No	CJD-FEI, Eval. Sept. 1984, tape ma242.51, states 51-63&91.

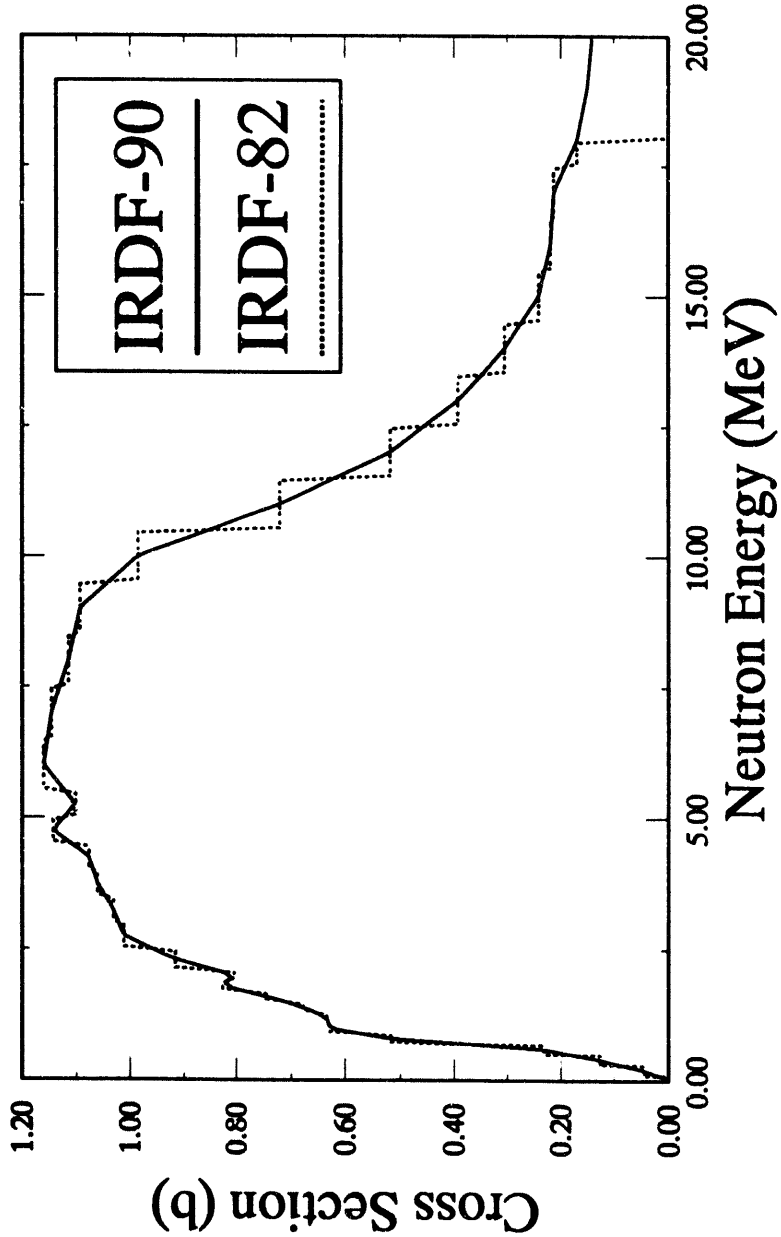

Figure A-47a: $^{103}Rh(n,n')^{103m}Rh$ Cross Section

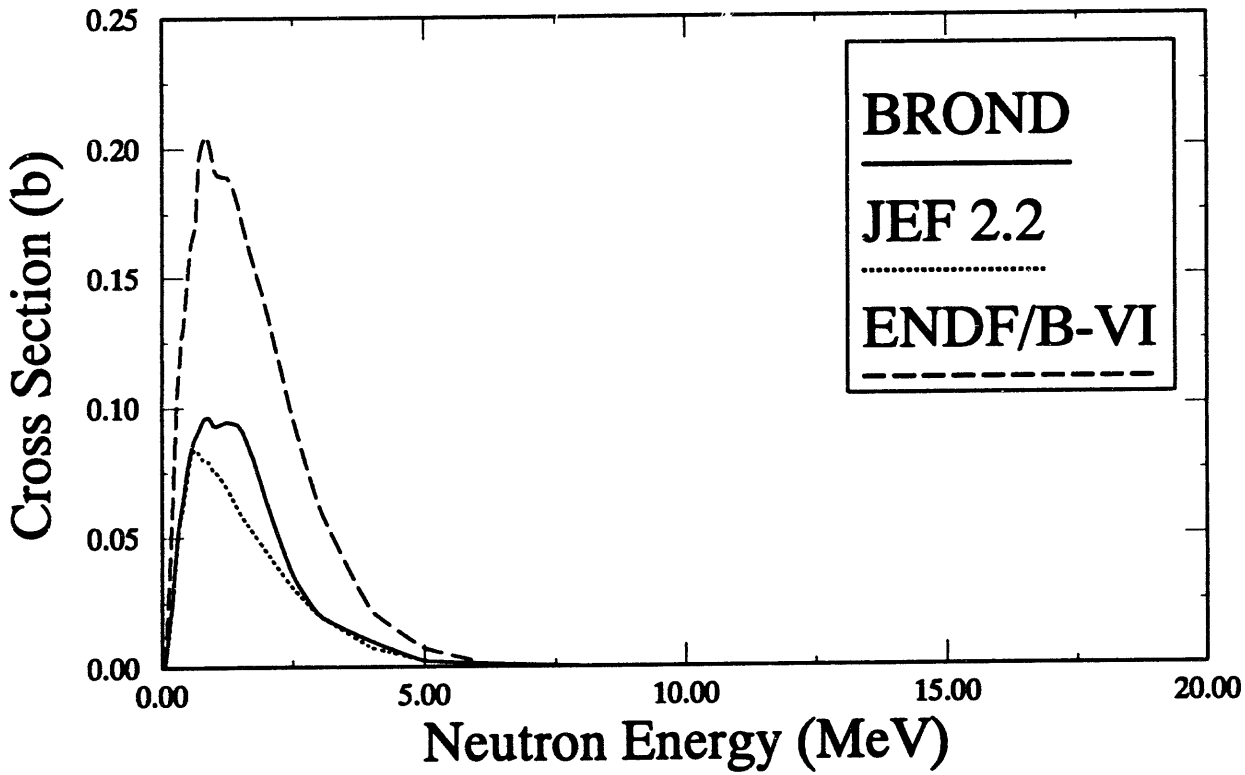

Figure A-47b: $^{103}Rh(n,n')^{103m}Rh$ Cross Section for 1st Excited State

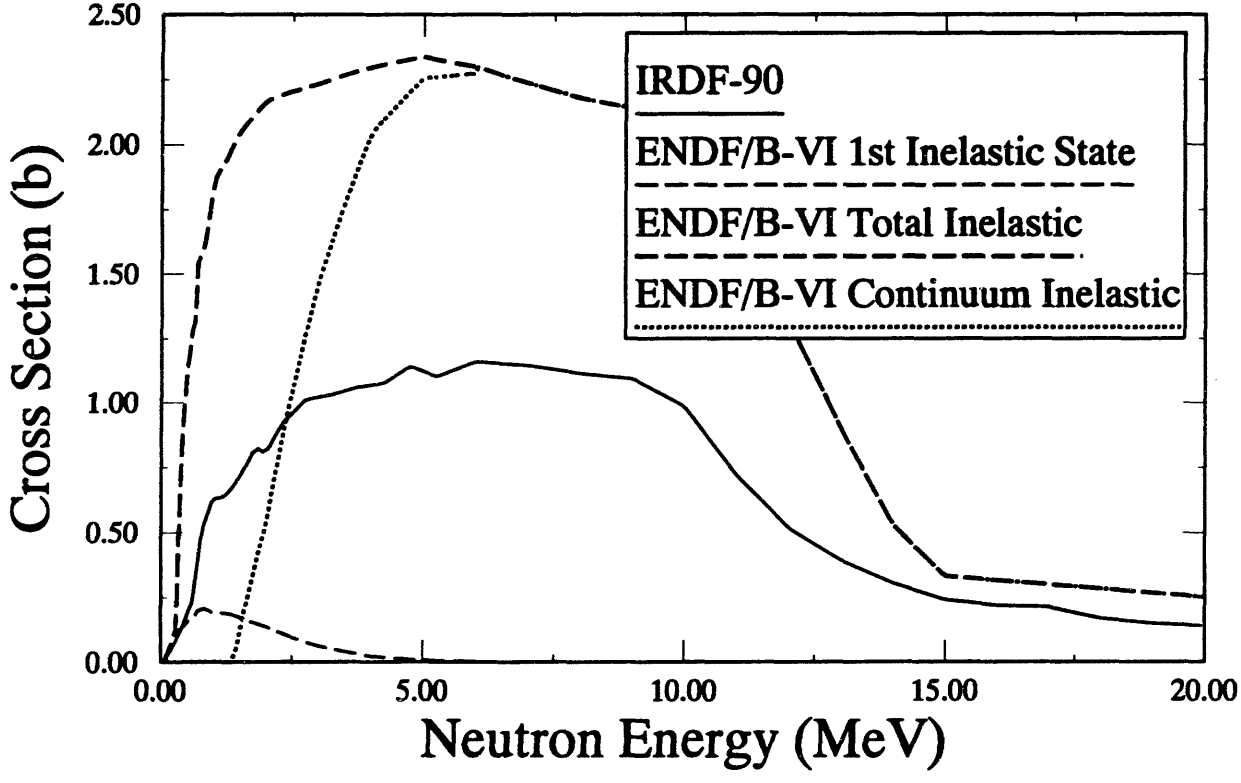

Figure A-47c: $^{103}Rh(n,n')^{103m}Rh$ Cross Section Components

Table A-48a
Alternative Cross Section Sources for the $^{109}Ag(n,\gamma)^{110m}Ag$ Reaction

$^{109}Ag(n,\gamma)^{110m}Ag$			Comment
Cross Section Library	Material Number	Covariance Data	
ENDF/B-VI	4731	No	BNL, HEDL, Eval. June 1983. Taken from ENDF/B-V fission -product tape, also from ENDF/B-IV.
ENDF/B-V	1373	No	HEDL, BNL, Eval. Nov. 1978, tape 510 fission product tape.
ENDF/B-V	1409	No	BNL, HEDL, Eval. June 1983, revision 2, tape 563, supersedes 1373.
ENDF/B-V	7479	No	HEDL, BNL, Eval. Nov. 1978, Activation Tape 532. Note this evaluation was NOT updated in 1983 when the full evaluation was changed.
JENDL-3	3472	No	JAERI, Eval. March 1987, tape ma257.25.
BROND	4711	No	CJD-FEI, Eval. May 1984, tape NDS1. Quoted in BROND documentation as 4791, difference unknown, tape ma242.51.
JEF 2.2	4731	No	NEA, Rcom. July 1983. Taken from RCN-3 evaluation (MAT=4709), tape jef-3.
DOSCROS84	7479	No	Taken from ENDF/B-V Activation Tape with a branching ratio of 5.299E-2 (referenced by Zijp [14]).

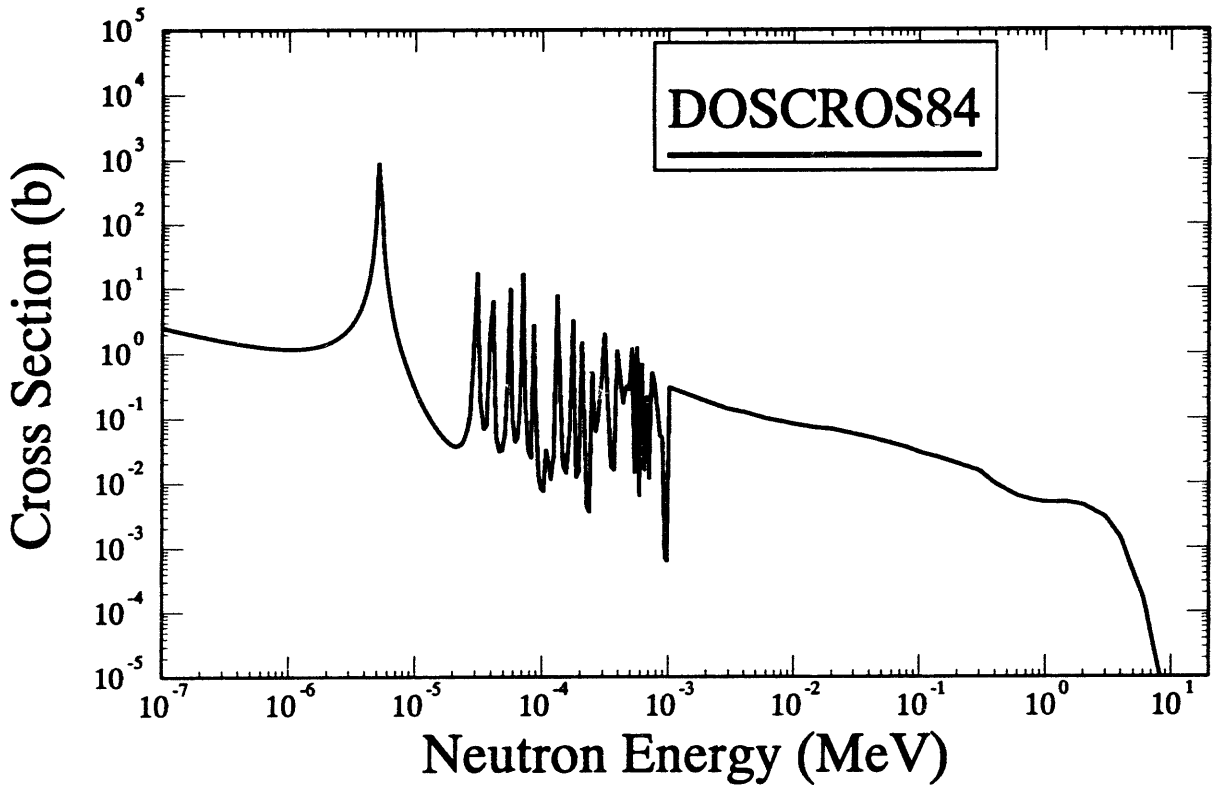

Figure A-48a: $^{109}Ag(n,\gamma)^{110m}Ag$ Cross Section

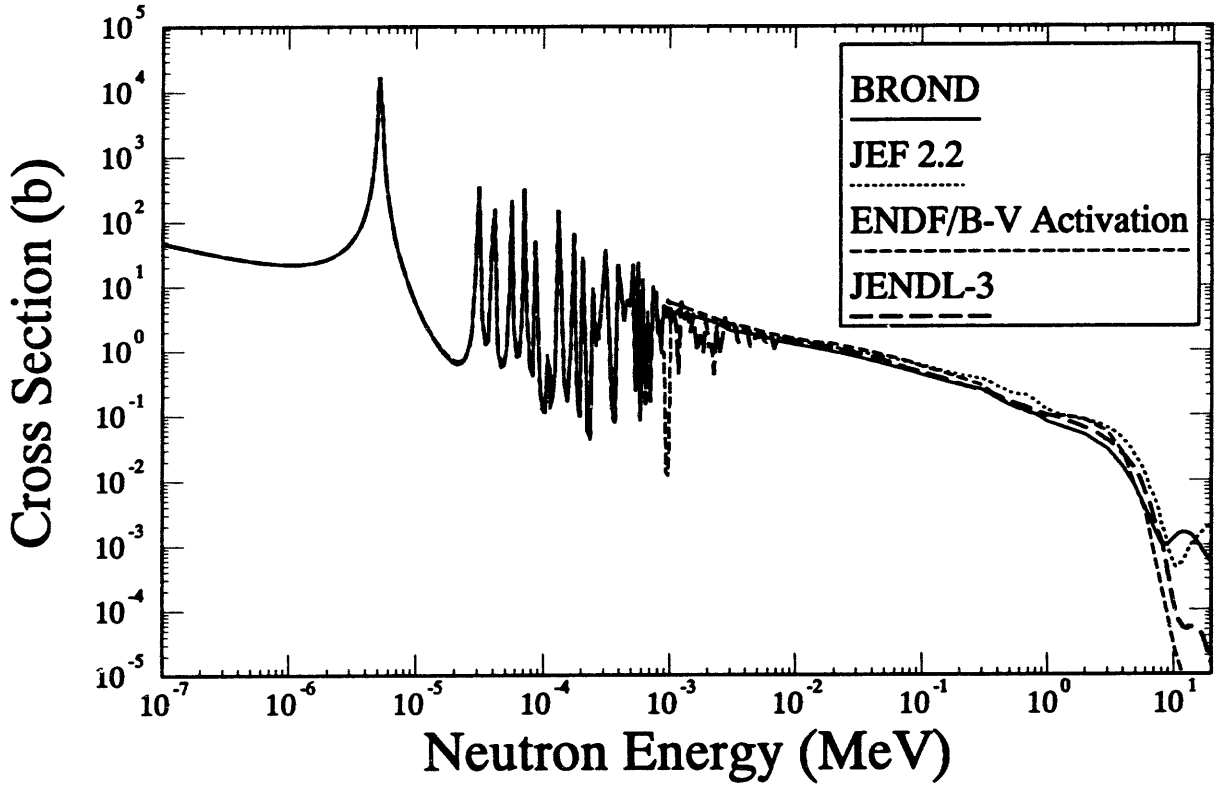

Figure A-48b: $^{109}Ag(n,\gamma)^{110m}Ag$ Cross Section

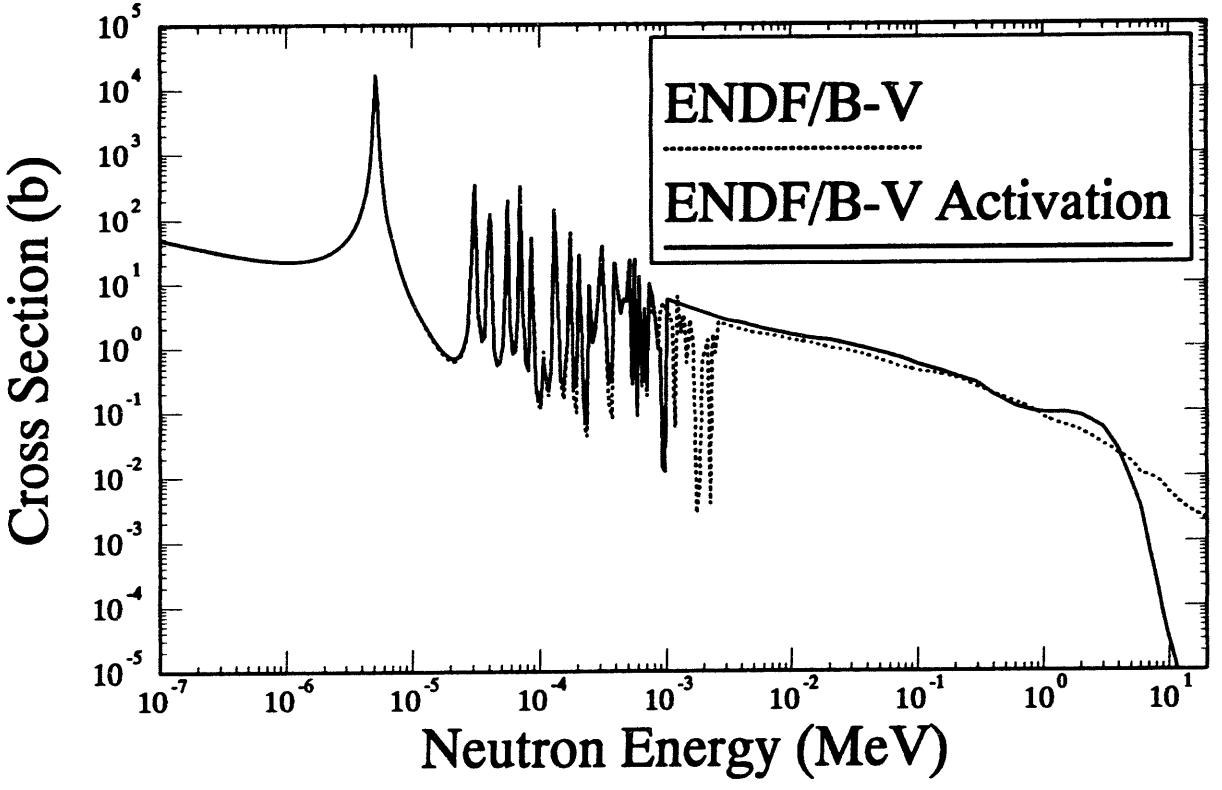

Figure A-48c: $^{109}Ag(n,\gamma)^{110m}Ag$ Cross Section

Table A-49a
Alternative Cross Section Sources for the ^{Nat}Cd(n,abs) Reaction

^{Nat}Cd(n,abs)			Comment
Cross Section Library	Material Number	Covariance Data	
ENDF/B-VI	4800	No	BNL, Eval. May 1974, taken from ENDF/B-V, components 102,103, 107.
ENDF/B-V	1281	No	BNL, Eval. May 1974, tape 501, translation of UKNDL file.
JENDL-3	3480	No	JNDC, Eval. March 1989, tape 25, components 102, 103, 104, 105, 106, 107, 111.
JEF 2.2	4800	No	Rcom. July 1982, NEA, tape jef-4. Taken from ENDF/B-IV, mat=1281. Same as ENDF/B-VI.

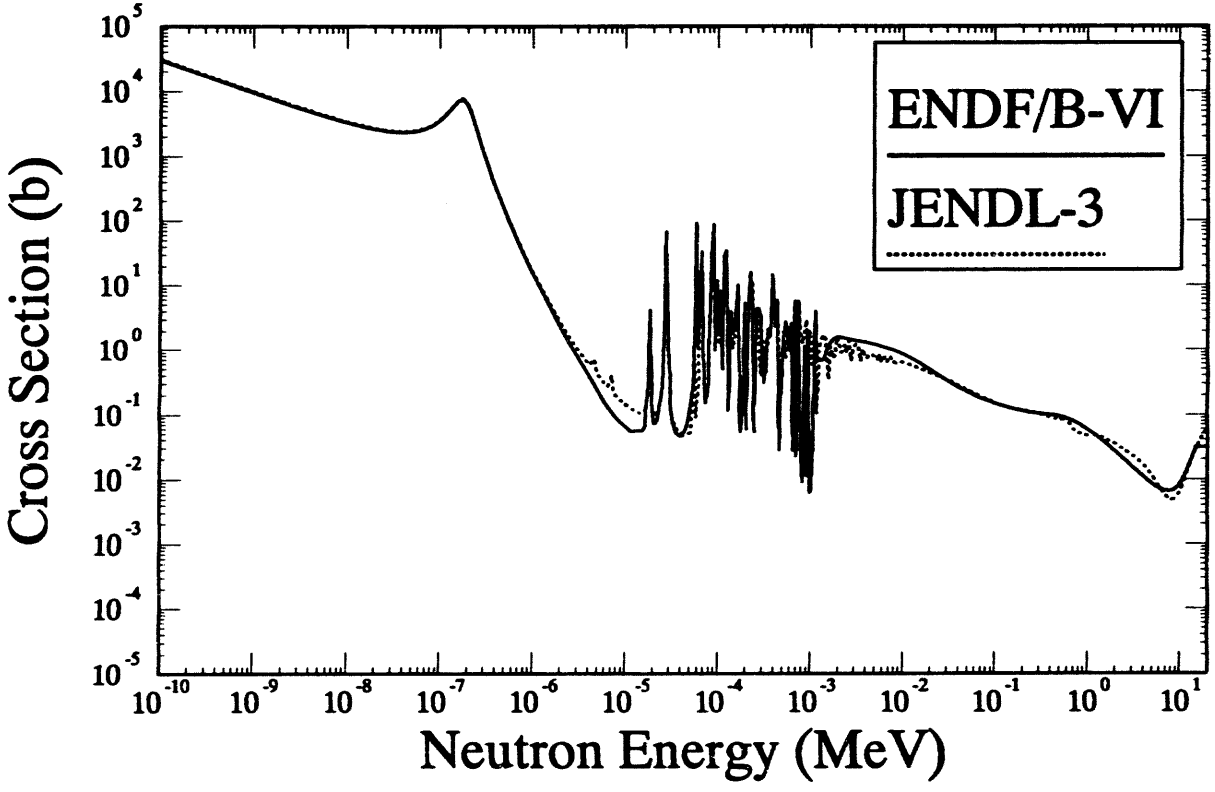

Figure A-49a: ^{Nat}Cd(n,abs) Cross Section

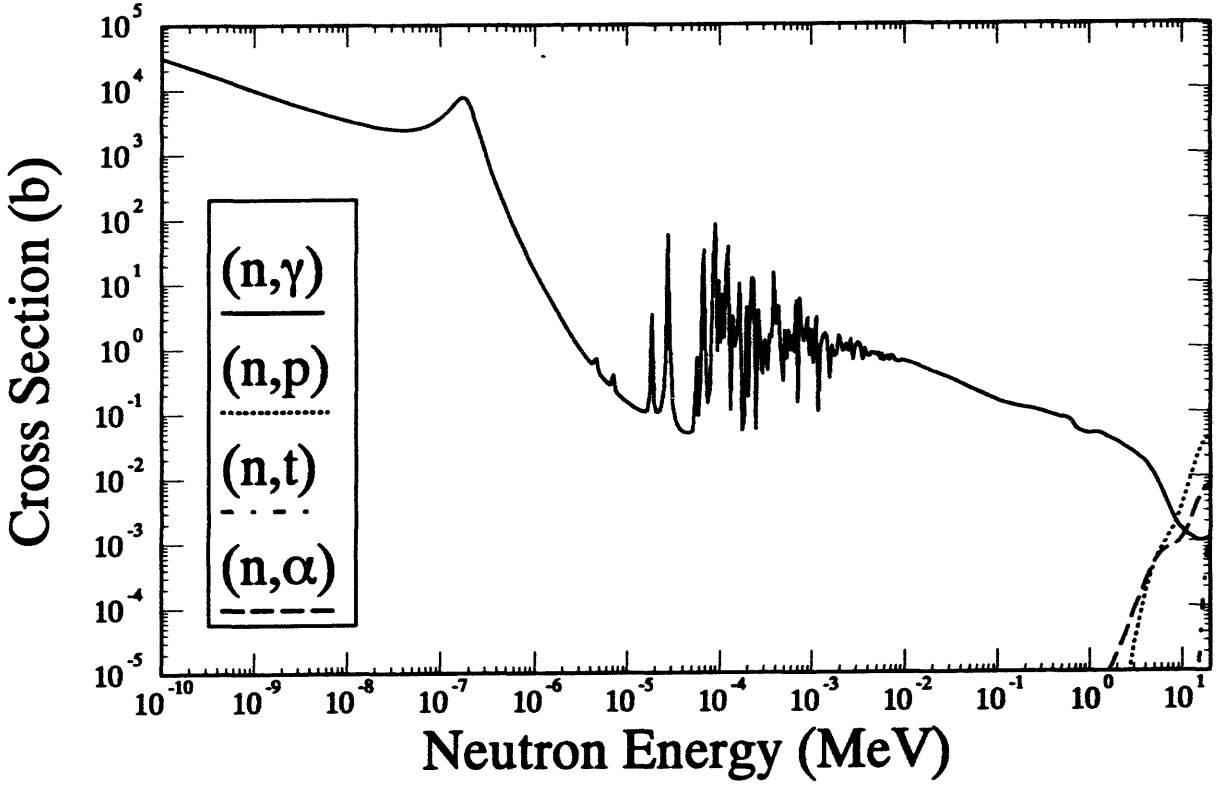

Figure A-49b: ^{Nat}Cd(n,abs) Cross Section Components

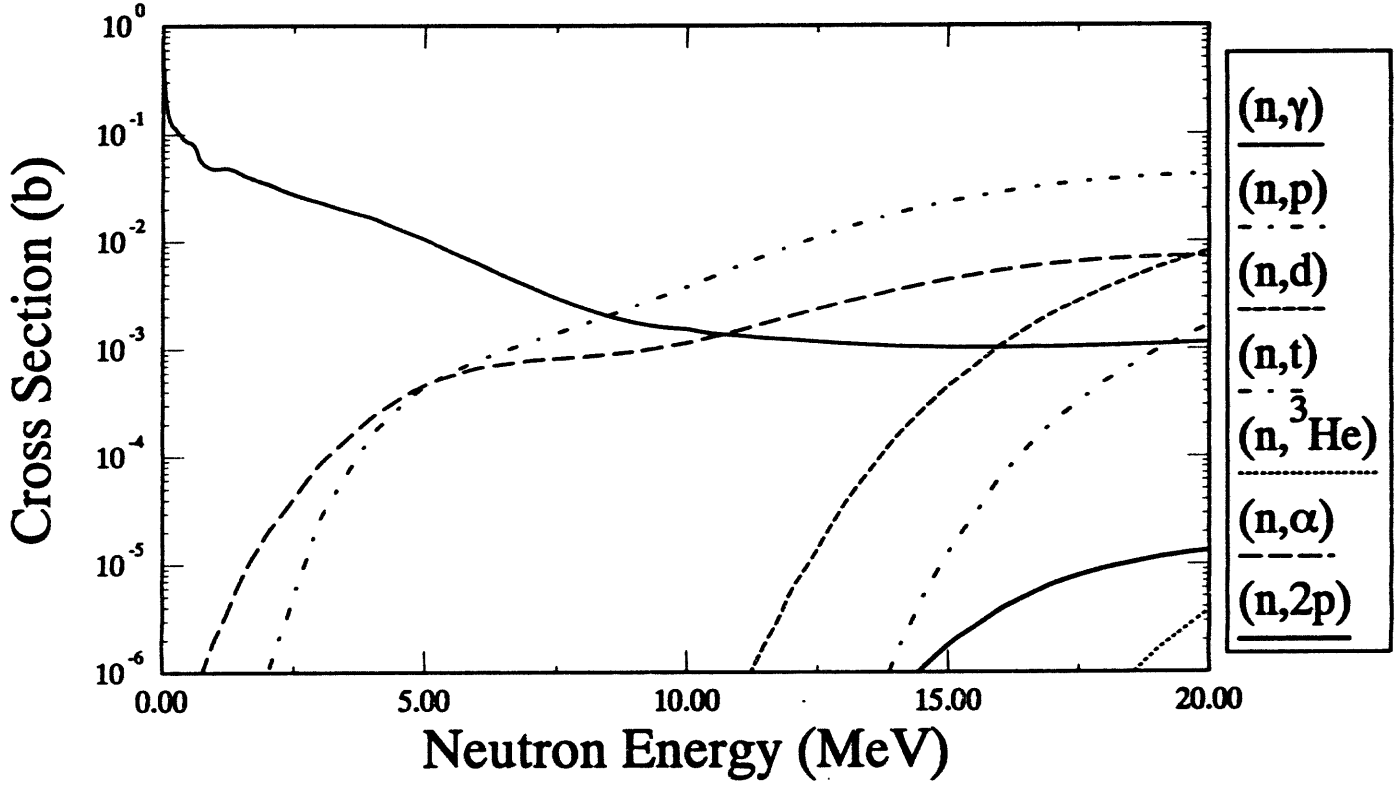

Figure A-49c: ^{Nat}Cd(n,abs) Cross Section Components

Table A-50a
Alternative Cross Section Sources for the $^{115}In(n,\gamma)^{116m}In$ Reaction

$^{115}In(n,\gamma)^{116m}In$			Comment
Cross Section Library	Material Number	Covariance Data	
ENDF/B-VI	4931	Yes	HEDL/ANL, Eval. March 1990.
IRDF-90	NA -- 4931	---	Taken from ENDF/B-VI, ANL, Eval. Jan. 1990. (n,γ) not in evaluation.
ENDF/B-V	6437	Yes	HEDL/ANL, Eval. Jan. 1978, Dosimetry Tape 531a.
ENDF/B-V	7495	No	HEDL/ANL, Eval. Jan. 1978, Activation Tape, 532b.
ENDF/B-V	9477	No	HEDL, INEL, Eval. Dec. 1979, Fission Product Tape. (n,γ) calculated by NCAP code.
JEF 2.2	4931	No	Documentation states taken from ENDF/B-V mat 9477, a fission product tape, tape jef-4.
private	NA -- 0909	Yes	ANL, Smith, Eval. Jan. 1990, only contains the (n,n') reaction.

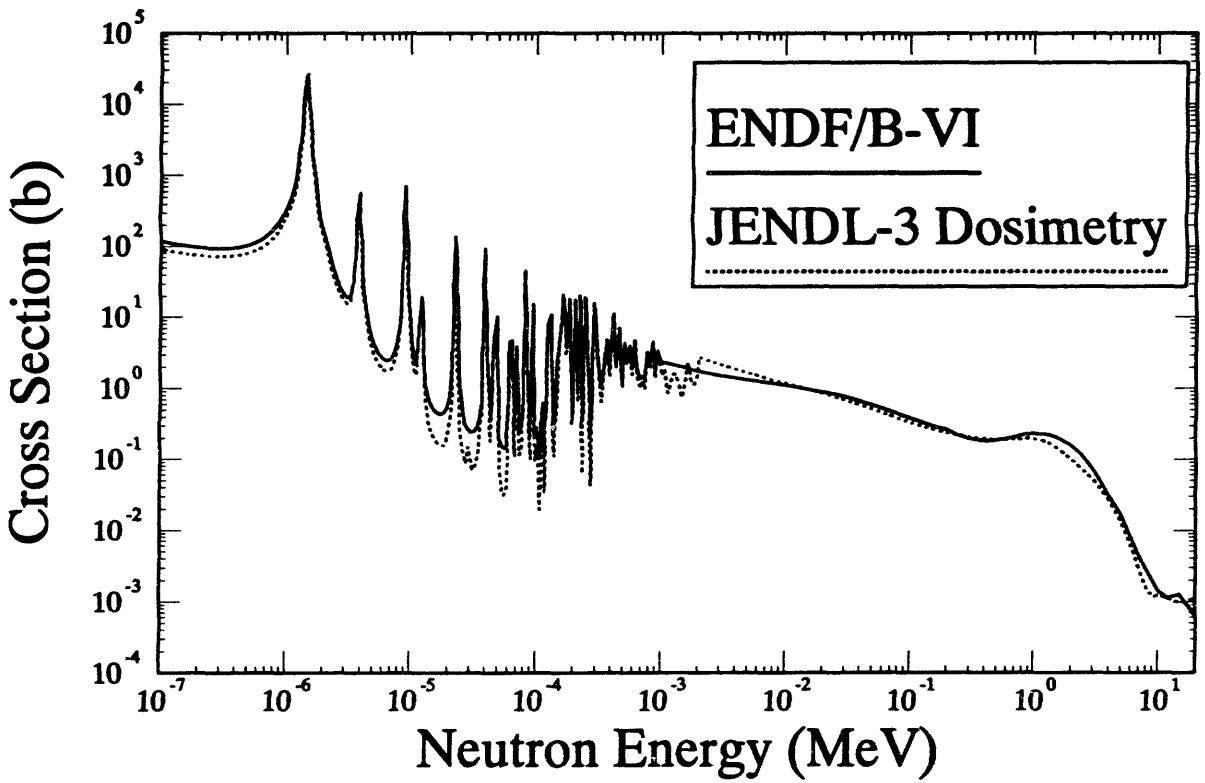

Figure A-50a: $^{115}In(n,\gamma)^{115m}In$ Cross Section

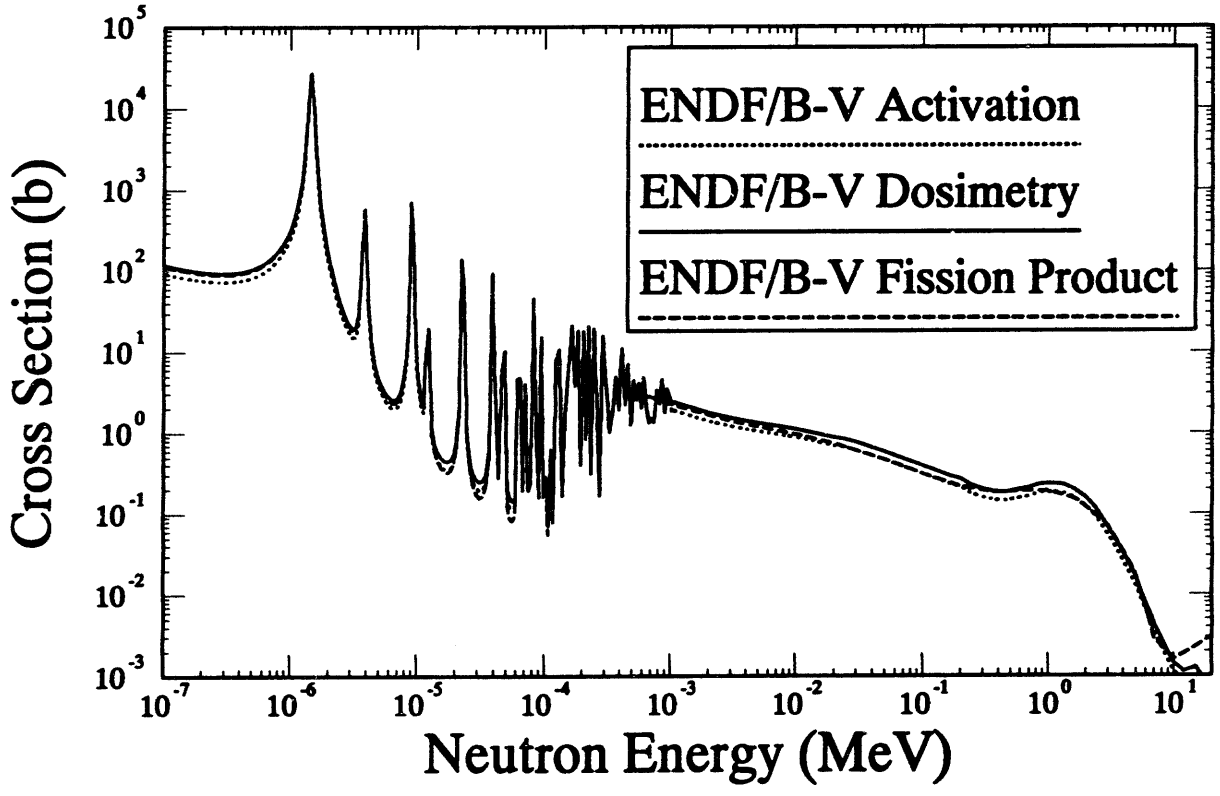

Figure A-50b: $^{115}In(n,\gamma)^{115m}In$ Cross Section

Table A-51a
Alternative Cross Section Sources for the $^{115}In(n,n')^{115m}In$ Reaction

$^{115}In(n,n')^{115m}In$			Comment
Cross Section Library	Material Number	Covariance Data	
ENDF/B-VI	4931	Yes	HEDL/ANL, Eval. March 1990. Revision from D. Smith did not make original release, will be modified, see private entry.
IRDF-90	4931	Yes	File states that it is taken from ENDF/B-VI, ANL, Eval. Jan. 1990, however the plots differ.
ENDF/B-V	6437	Yes	HEDL/ANL, Eval. Jan. 1978, Dosimetry Tape 531a.
ENDF/B-V	7495	No	HEDL/ANL, Eval. Jan. 1978, Activation Tape, 532b.
ENDF/B-V	9477	No	HEDL, INEL, Eval. Dec. 1979, Fission Product Tape 543. Calculated with COMNUC-3 code. This file has several inelastic components.
JEF 2.2	4931	No	Taken from ENDF/B-V mat 9477, tape jef-4
private	0909	Yes	Private communication of pre-ENDF/B-6 evaluation [16]. ANL, Smith, Eval. Jan. 1990, same as IRDF-90. Will be incorporated into ENDF/B-VI. Confirmation from D. Smith on 10/26/92.

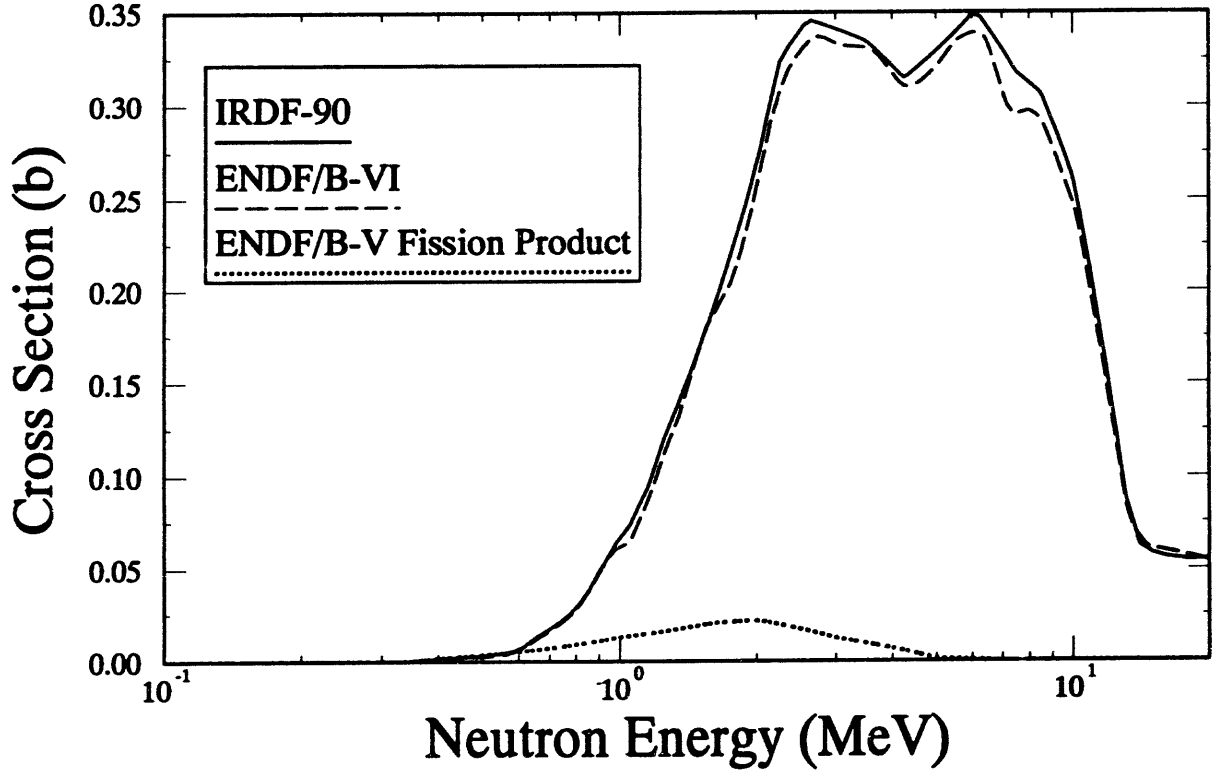

Figure A-51: $^{115}In(n,n')^{115m}In$ Cross Section

Table A-52a
Alternative Cross Section Sources for the $^{127}I(n,2n)^{126}I$ Reaction

$^{127}I(n,2n)^{126}I$			Comment
Cross Section Library	Material Number	Covariance Data	
ENDF/B-VI	5325	No	HEDL, RCN, Eval. Feb. 1980, taken from ENDF/B-V Fission Product Tape.
ENDF/B-V	6438	Yes	Stanford, Eval. Aug. 1972, Dosimetry Tape 531a.
ENDF/B-V	7537	No	HEDL, Feb. 1980, Activation Tape 532b.
JEF 2.2	5325	No	NEA, Rcom. July 1983, tape jef-4, taken from RCN-3 eval. (MAT=4533).
JENDL-3 Dos.	5331	Yes	Covariance taken from IRDF-85.
IRDF-82	6438	Yes	Taken from ENDF/B-V Dosimetry Tape.

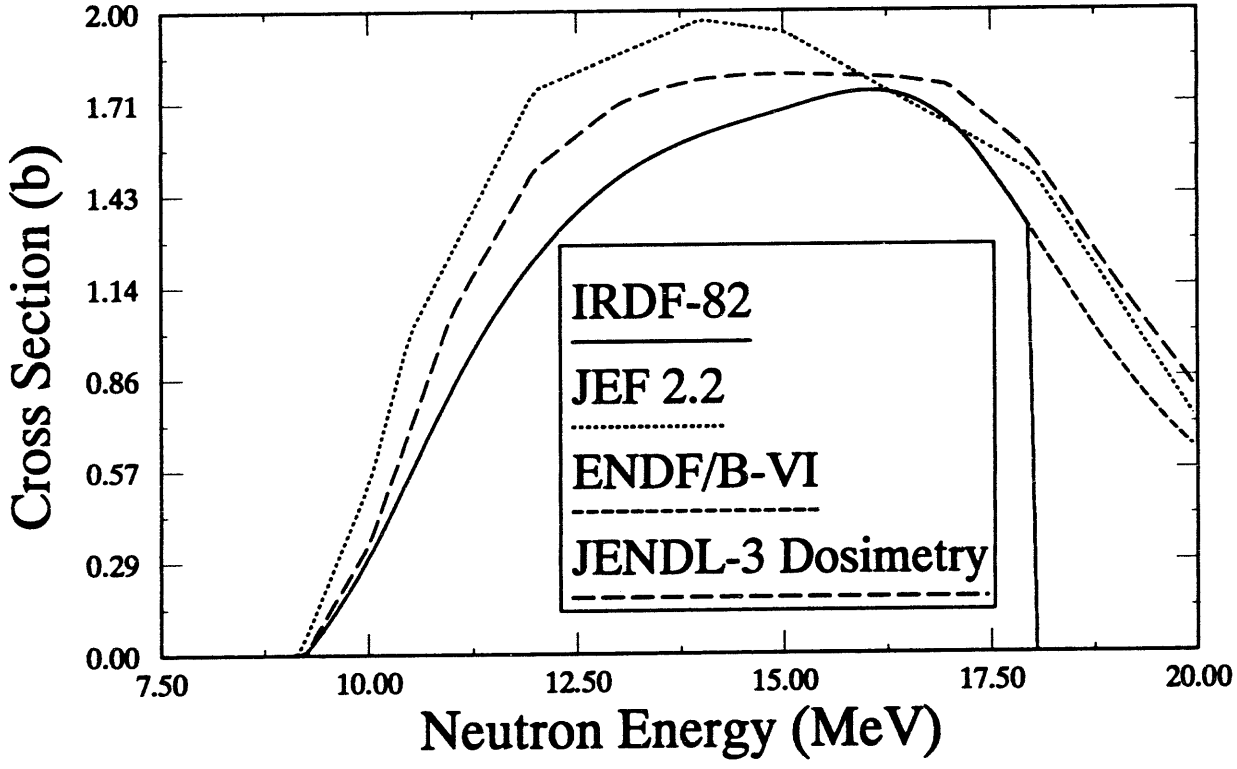

Figure A-52a: $^{127}I(n,2n)^{126}I$ Cross Section

Table A-53a
Alternative Cross Section Sources for the $^{197}Au(n,p)^{197}Pt$ Reaction

$^{197}Au(n,p)^{197}Pt$			Comment
Cross Section Library	Material Number	Covariance Data	
ENDF/B-VI	7925	No	LANL, Eval. Jan. 1984. Q-value revised July 1991. This is ENDF/B-VI revision 1, file au-197a. The (n,p) reaction adopted from ENDF/B-V.
IRDF-90	NA -- 7925	---	Reaction not in either file au-197a or au-197b.
ENDF/B-V	1379	No	BNL, Eval. Feb. 1977, Tape 554.
ENDF/B-V	NA -- 6379	---	BNL, Eval. Feb. 1977, Dosimetry Tape 531a. Does not include (n,p) reaction.
ENDF/B-V	NA -- 7797	---	BNL, Eval. Feb. 1977, Activation Tape, 532b. Does not include reaction.
JEF 2.2	7925	No	RCOM June 1982, taken from ENDF/B-V, mat=1379. (n,γ) replaced by ENDF/B-VI on May 1989, tape jef-6.
DOSCROS84	7797	No	Listed as taken from ENDF/V Activation Tape 532, but not in my version of 532 tape. Taken directly from DOSDAM84 tape. Identical to ENDF/B-VI.

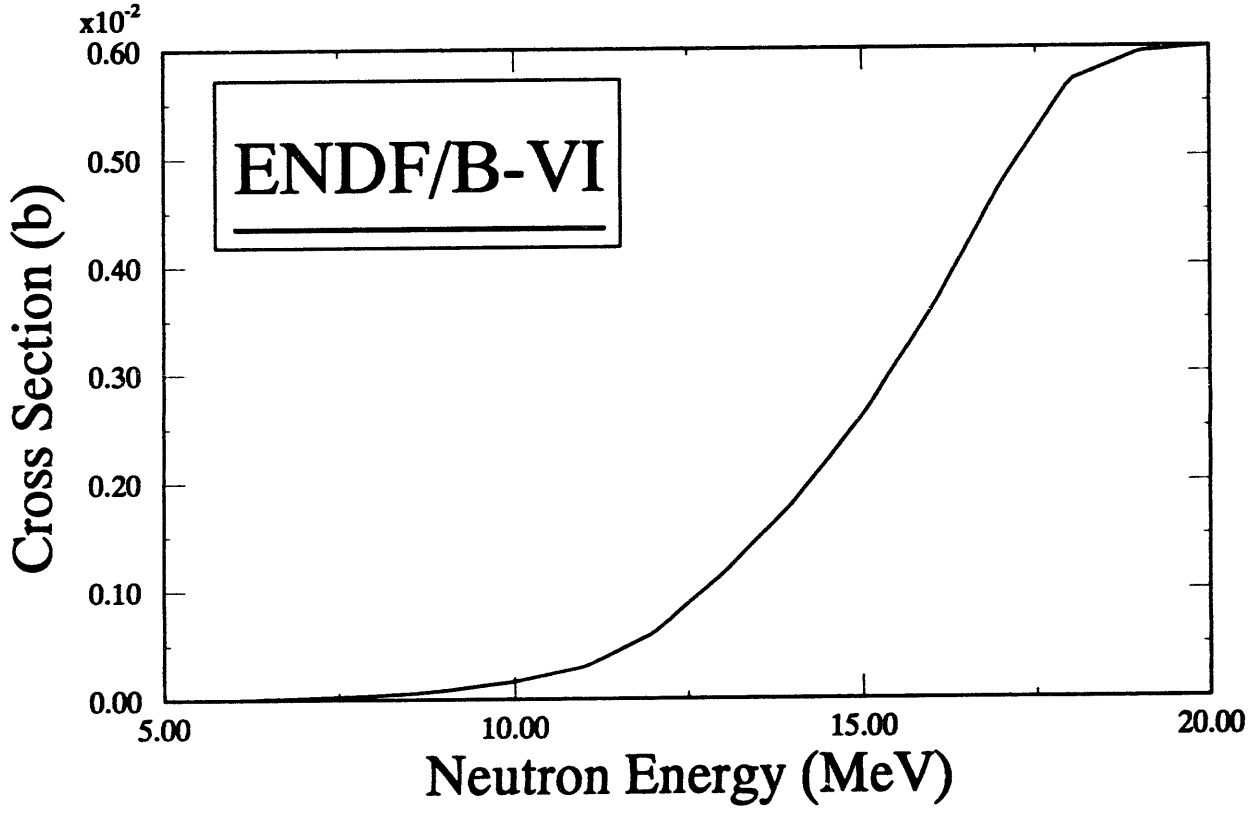

Figure A-53a: $^{197}Au(n,p)^{197}Pt$ Cross Section

Table A-54a
Alternative Cross Section Sources for the $^{197}Au(n,\gamma)^{198}Au$ Reaction

$^{197}Au(n,\gamma)^{198}Au$			Comment
Cross Section Library	Material Number	Covariance Data	
ENDF/B-VI	7925	No (addressed in file comments)	LANL, Eval. Jan. 1984. Q-value revised July 1991. Uses Version VI standard cross section for (n,γ). This is ENDF/B-VI revision 1. Both ENDF/B-VI versions say they adopted the ENDF/B-VI standard cross section below 2.5 MeV. Uses calculation and experimental data above this energy.
IRDF-90	7925	Yes	Taken from ENDF/B-VI.
ENDF/B-V	1379	Yes	BNL, Eval. Feb. 1977, Tape 554.
ENDF/B-V	6379	Yes	BNL, Eval. Feb. 1977, Dosimetry Tape 531a.
ENDF/B-V	7797	No	BNL, Eval. Feb. 1977, Activation Tape, 532b.
JEF 2.2	7925	Yes	RCOM. June 1982, Tape jef-6, taken from ENDF/B-V, mat=1379. (n,γ) replaced by ENDF/B-VI on May 1989. Despite this comment in file, data agrees with ENDF/B-V and NOT with ENDF/B-VI. See note under ENDF/B-VI on use of ENDF/B-VI standard cross section.

Figure A-54a: $^{197}Au(n,\gamma)^{198}Au$ Cross Section

Table A-55a
Alternative Cross Section Sources for the $^{197}Au(n,2n)^{196}Au$ Reaction

$^{197}Au(n,2n)^{196}Au$			Comment
Cross Section Library	Material Number	Covariance Data	
ENDF/B-VI	7925	No	LANL, Eval. Jan. 1984. Q-value revised July 1991. This is ENDF/B-VI revision 1, file au-197a.
IRDF-90	7925	Yes	IRK, Eval. April 1990, file au-197b.
ENDF/B-V	1379	Yes	BNL, Eval. Feb. 1977, Tape 554. (n,2n) same as ENDF/B-IV.
ENDF/B-V	NA -- 6379	---	BNL, Eval. Feb. 1977, Dosimetry Tape 531a, not in reaction list.
ENDF/B-V	7797	No	BNL, Eval. Feb. 1977, Activation Tape, 532b.
JEF 2.2	7925	No	RCOM. June 1982. Taken from ENDF/B-V, mat=1379, tape jef-6.

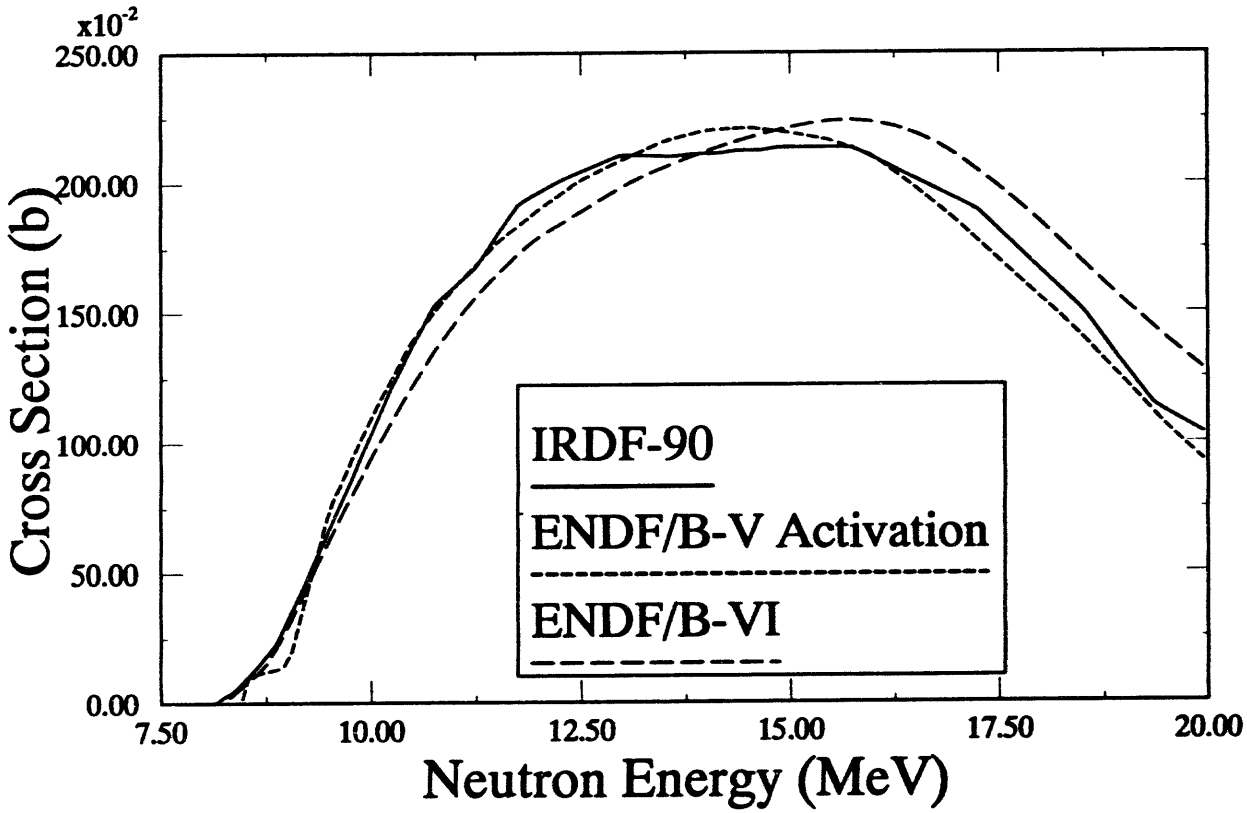

Figure A-55a: $^{197}Au(n,2n)^{196}Au$ Cross Section

Table A-56a
Alternative Cross Section Sources for the $^{197}Au(n,3n)^{195}Au$ Reaction

$^{197}Au(n,3n)^{195}Au$			Comment
Cross Section Library	Material Number	Covariance Data	
ENDF/B-VI	7925	No	LANL, Eval. Jan. 1984. Q-value revised July 1991. This is ENDF/B-VI revision 1.
IRDF-90	NA -- 7925	--	Reaction not in either au-197a or au-197b.
ENDF/B-V	1379	No	BNL, Eval. Feb. 1977, Tape 554.
ENDF/B-V	NA -- 6379	--	BNL, Eval. Feb. 1977, Dosimetry Tape 531a, not in reaction list.
ENDF/B-V	7797	No	BNL, Eval. Feb. 1977, Activation Tape, 532b.
JEF 2.2	7925	No	RCOM. June 1982. Taken from ENDF/B-V, mat=1379, tape jef-6.

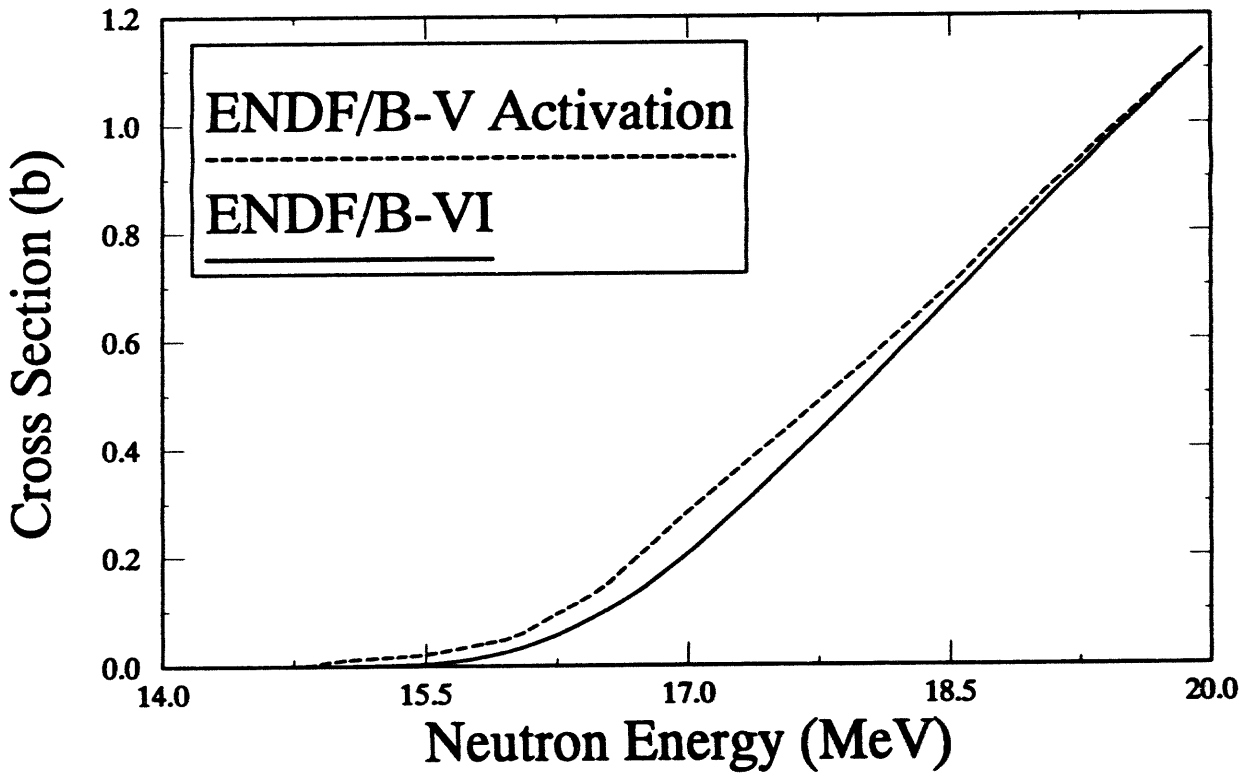

Figure A-56a: $^{197}Au(n,3n)^{196}Au$ Cross Section

Table A-57a
Alternative Cross Section Sources for the ^{197}Au(n,abs) Reaction

^{197}Au(n,abs)			Comment
Cross Section Library	Material Number	Covariance Data	
ENDF/B-VI	7925	Only on total	LANL, Eval. Jan. 1984, components 102, 103, 107.
ENDF/B-V	1379	No	BNL Eval. Feb. 1977, tape 554.
JEF 2.2	7925	No	Rcom. June 1982. Taken from ENDF/B-V, mat=1379. (n,γ) replaced by ENDF/B-VI on May 1989, tape jef-6.

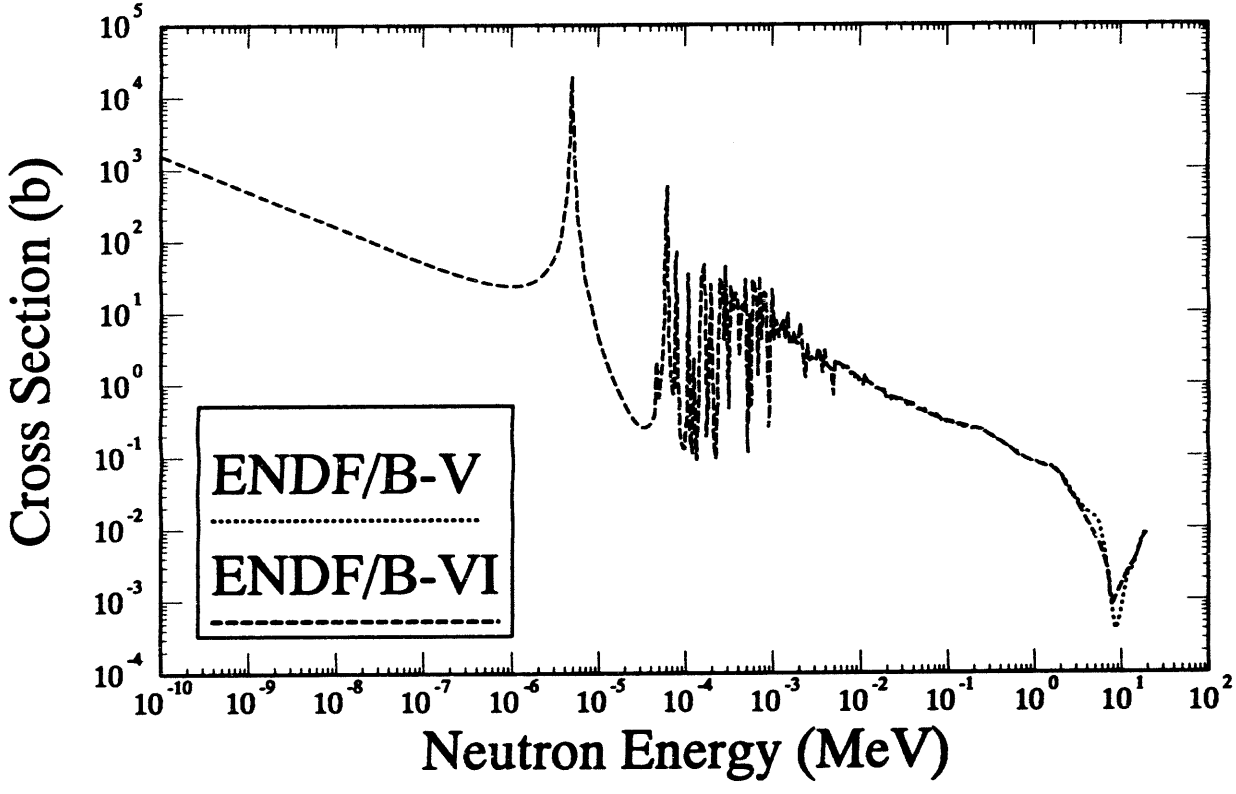

Figure A-57a: ^{197}Au(n,abs) Cross Section

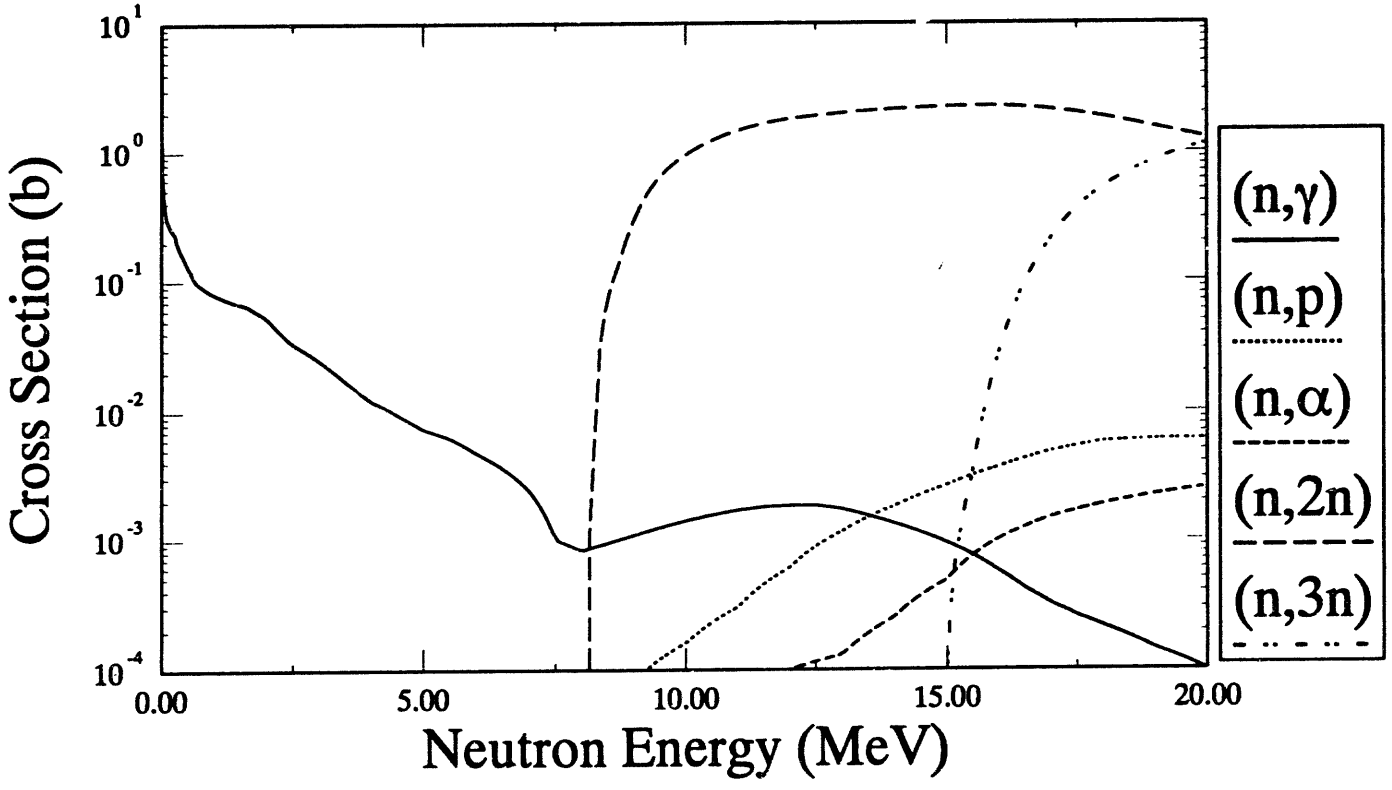

Figure A-57b: ^{197}Au(n,abs) Cross Section Components

Table A-58a
Alternative Cross Section Sources for the $^{232}Th(n,\gamma)^{233}Th$ Reaction

$^{232}Th(n,\gamma)^{233}Th$			Comment
Cross Section Library	Material Number	Covariance Data	
ENDF/B-VI	9040	Yes	BNL, ANL, Eval. Dec. 1977. Taken form ENDF/B-V.
IRDF-90	9040	Yes	Taken from ENDF/B-VI.
ENDF/B-V	1390	Yes	BNL, Eval. Dec. 1977, rev. March 1982, tape 561, revision 2.
ENDF/B-V	6390	Yes	BNL, Eval. Dec. 1977, Dosimetry Tape 531a.
ENDF/B-V	7902	No	BNL, Eval. 1977, Activation Tape 532b.
JEF 2.2	9040	No	NEA, Rcom. June 1982. Taken from ENDF/B-IV (MAT=1296), tape jef-7.
JENDL-3	3905	No	Kinki U., Eval. March 1987, tape ma257.27.

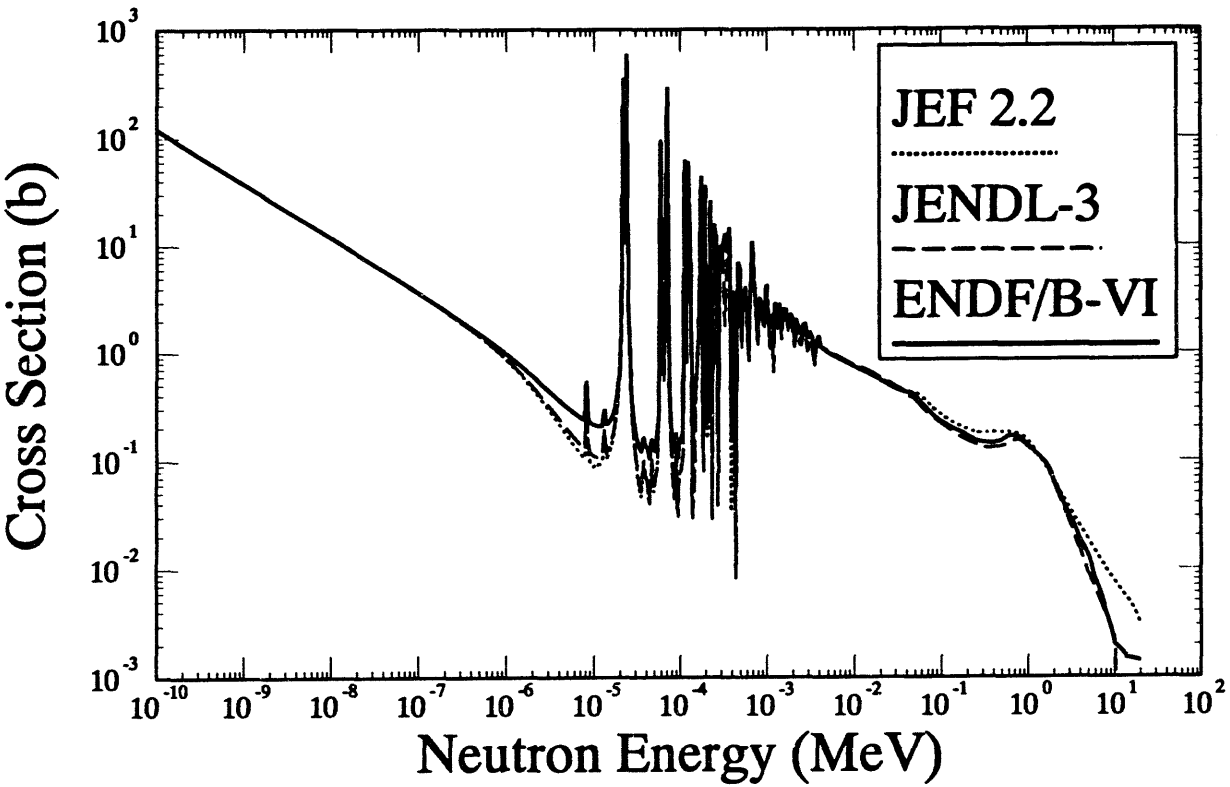

Figure A-58a: $^{232}Th(n,\gamma)^{233}Th$ Cross Section

Table A-59a
Alternative Cross Section Sources for the $^{232}Th(n,2n)^{231}Th$ Reaction

$^{232}Th(n,2n)^{231}Th$			Comment
Cross Section Library	Material Number	Covariance Data	
ENDF/B-VI	9040	No	BNL, ANL, Eval. Dec. 1977. Taken form ENDF/B-V.
IRDF-90	NA -- 9040	---	Taken from ENDF/B-VI, reaction not in file.
ENDF/B-V	1390	No	BNL, Eval. Dec. 1977, rev. March 1982, tape 561, revision 2.
ENDF/B-V	NA -- 6390	---	BNL, Eval. Dec. 1977, Dosimetry Tape 531a, reaction not in file.
ENDF/B-V	7902	No	BNL, Eval. 1977, Activation Tape 532b.
JEF 2.2	9040	No	NEA, Rcom. June 1982. Taken from ENDF/B-IV (MAT=1296), tape jef-7.
JENDL-3	3905	No	Kinki U., Eval. March 1987, tape ma257.27.

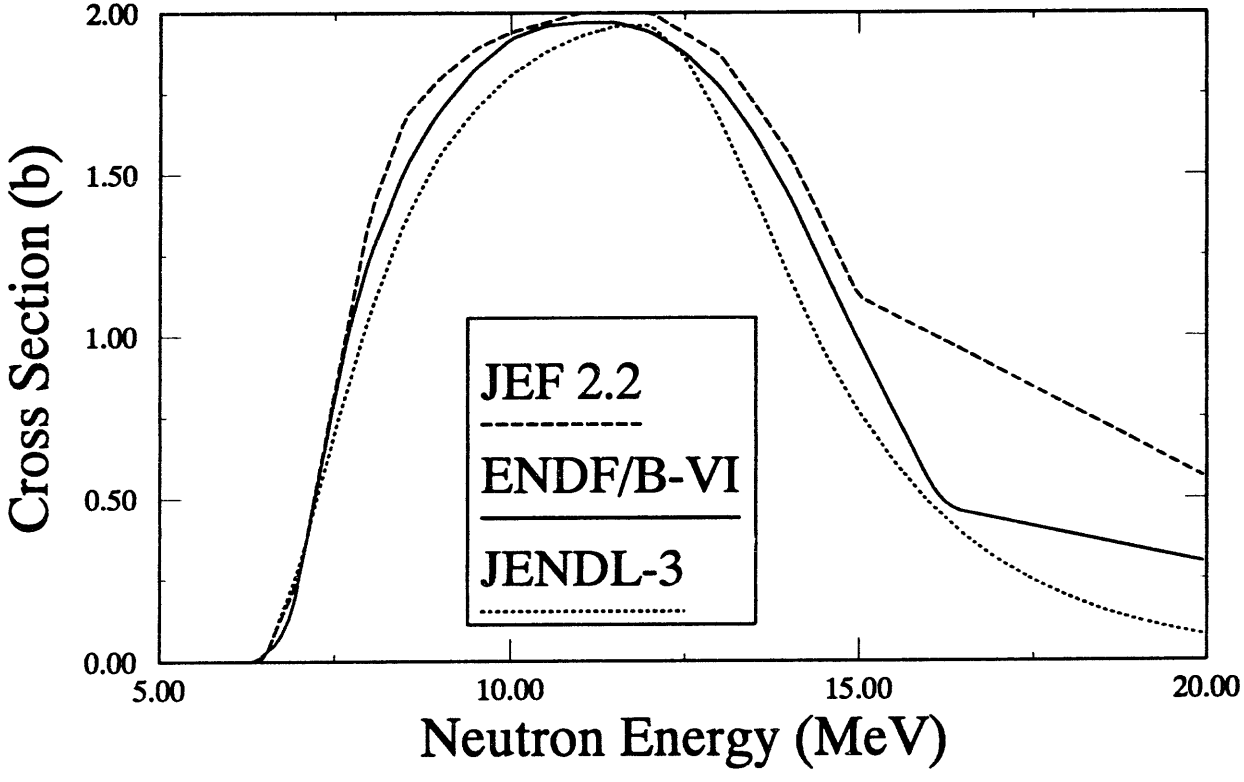

Figure A-59a: ^{232}Th(n,2n)^{231}Th Cross Section

Table A-60a
Alternative Cross Section Sources for the ^{232}Th(n,f)F.P. Reaction

^{232}Th(n,f)F.P.			Comment
Cross Section Library	Material Number	Covariance Data	
ENDF/B-VI	9040	Yes	BNL, ANL, Eval. Dec. 1977. Taken form ENDF/B-V.
IRDF-90	9040	Yes	Taken from ENDF/B-VI.
ENDF/B-V	1390	Yes	BNL, Eval. Dec. 1977, rev. March 1982, tape 561, revision 2.
ENDF/B-V	6390	Yes	BNL, Eval. Dec. 1977, Dosimetry Tape 531a.
ENDF/B-V	NA - 7902	No	BNL, Eval. 1977, Activation Tape 532b, reaction not on tape.
JEF 2.2	9040	No	NEA, Rcom. June 1982. Taken from ENDF/B-IV (MAT=1296), tape jef-7.
JENDL-3	3905	No	Kinki U., Eval. March 1987, tape ma257.27.

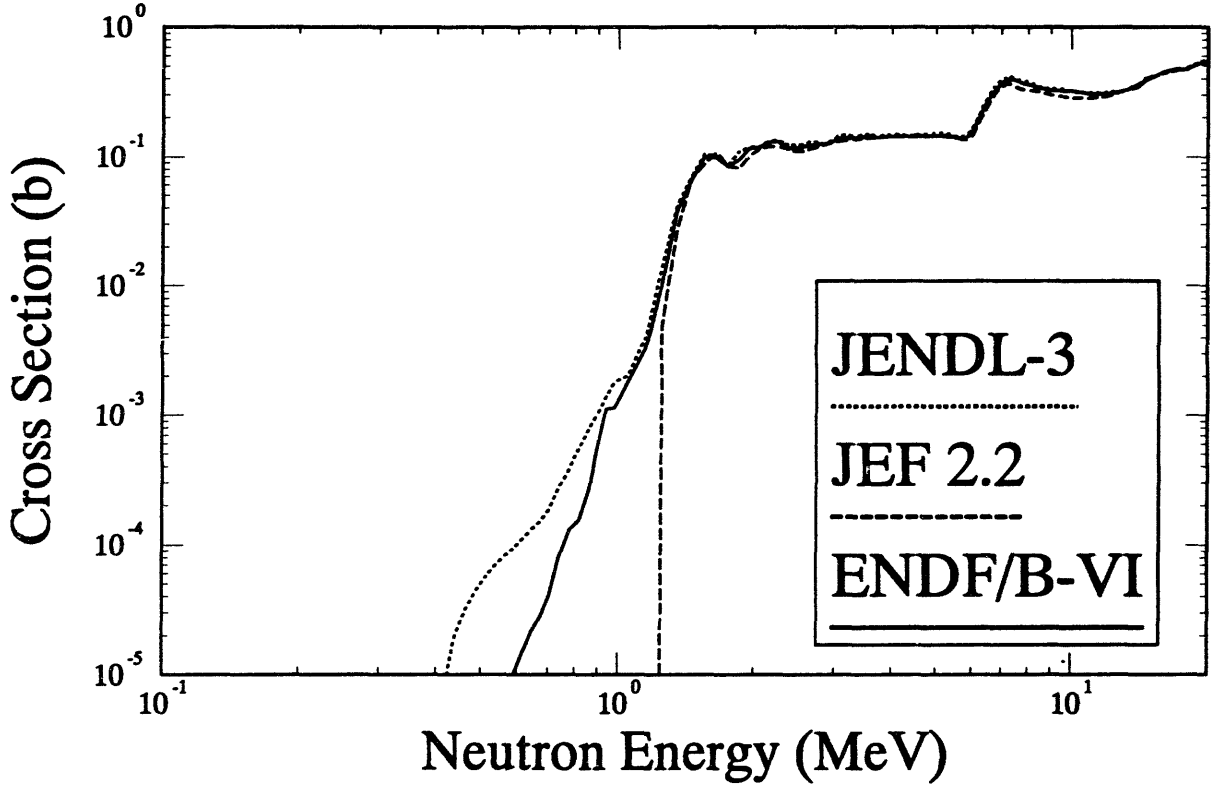

Figure A-60a: ^{232}Th(n,f)F.P. Cross Section

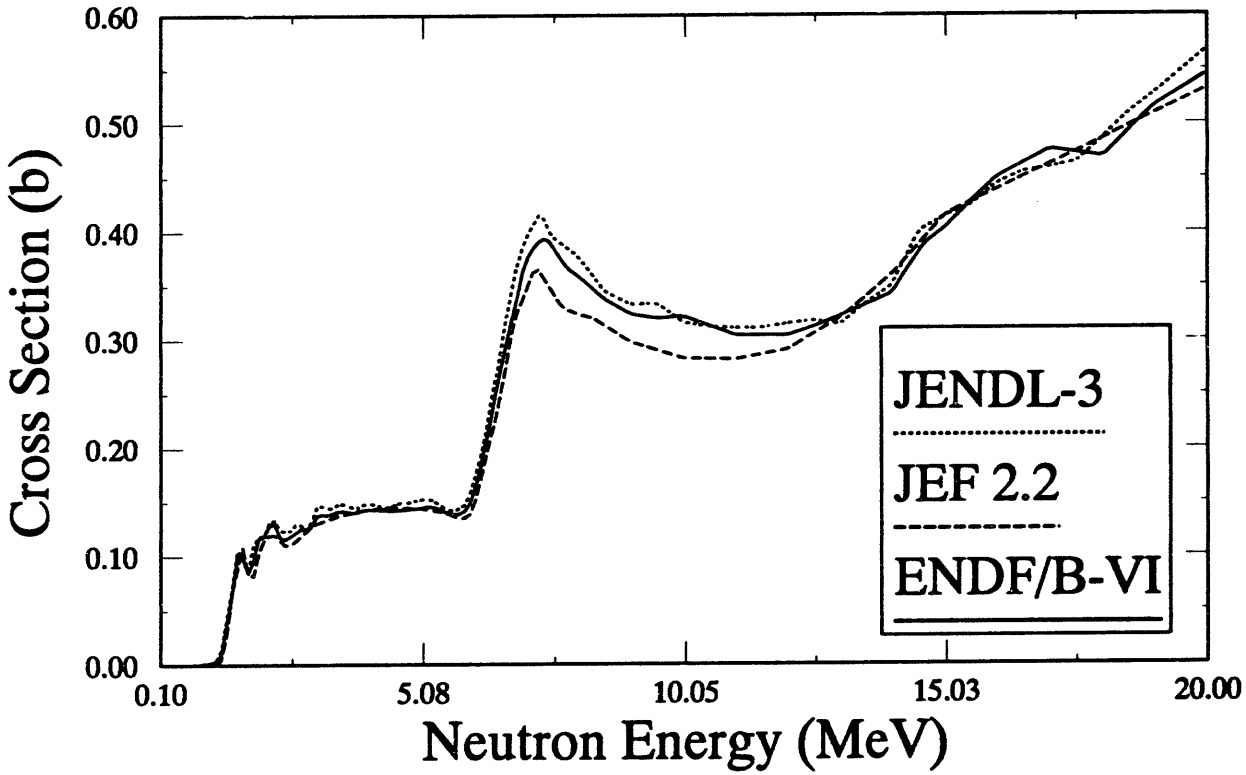

Figure A-60b: ^{232}Th(n,f)F.P. Cross Section

Table A-61a
Alternative Cross Section Sources for the $^{235}U(n,f)F.P.$ Reaction

$^{235}U(n,f)F.P.$			Comment
Cross Section Library	Material Number	Covariance Data	
ENDF/B-VI	9228	tbd	ORNL/LANL, Eval. Nov. 1989, Tape 121, release 1. Covariance data removed from early version pending further analysis.
pre-ENDF/B-VI	9228	Yes	ORNL/LANL, Eval. Apr. 1989, u-235o.
GLUCS	9228	Yes	ORNL, 1990 release.
IRDF-90	9228	Yes	Taken from ENDF/B-VI.
ENDF/B-V	1395	Yes	BNL, Eval. April 1977, Release 2, Tape 562.
ENDF/B-V	6395	Yes	BNL, April 1977, Dosimetry Tape 531a.
JENDL-3	3924	No	SAEI, Eval. Mar. 1987, Tape 27.
BROND	2021	No	CCPIJE, Eval. April 1985, Dec. 1989 revision, tape ma257.77.
JEF 2.2	9228	Yes	Based on ENDF/B-VI, Recom. Aug. 1990, tape jef-2.

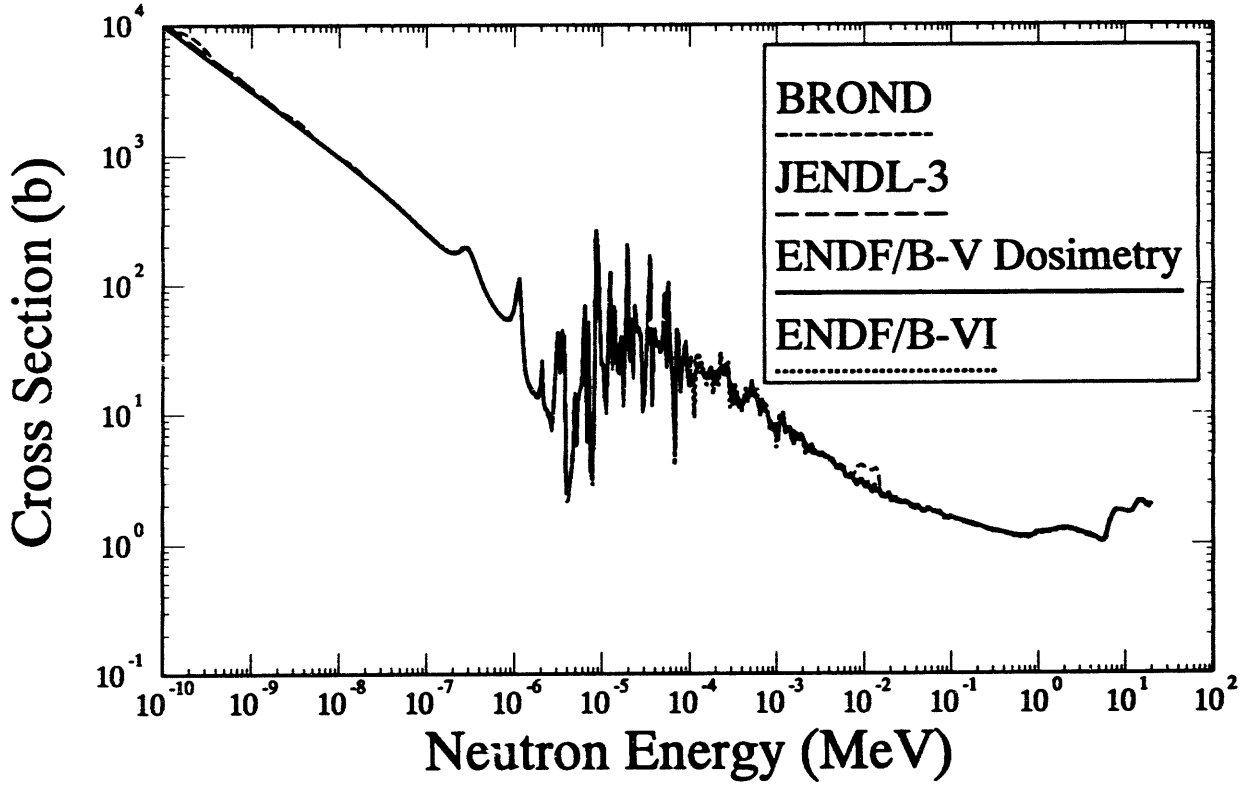

Figure A-61a: ^{235}U(n,f)F.P. Cross Section

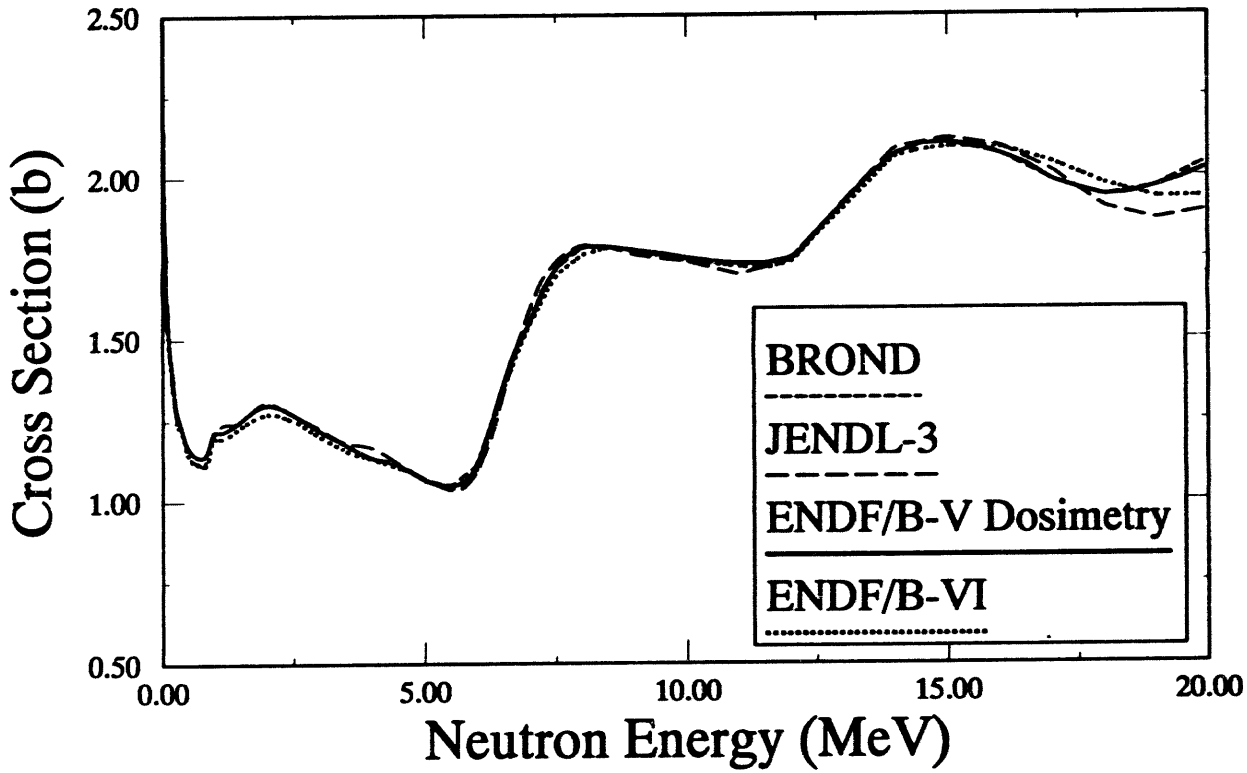

Figure A-61b: ^{235}U(n,f)F.P. Cross Section

Table A-62a
Alternative Cross Section Sources for the $^{238}U(n,f)F.P.$ Reaction

$^{238}U(n,f)F.P.$			Comment
Cross Section Library	Material Number	Covariance Data	
ENDF/B-VI	9237	tbd	ORNL/LANL, Eval. Nov. 1989, revision 1, tape 121. Covariance data removed from early version pending review by the community.
IRDF-90	9237	Yes	Taken from ENDF/B-VI.
GLUCS	9237	Yes	ORNL, 1990 Release, high energy identical to ENDF/B-VI.
ENDF/B-V	1398	Yes	ANL, Eval. June 1977, Revision 2, tape 562.
ENDF/B-V	6398	Yes	ANL, Eval. June 1977, Dosimetry Tape 531a.
ENDF/B-V	NA - 7928	No	ANL, Eval. June 1977, Activation Tape, 532b. Does not include (n,f) reaction.
JENDL-3	3926	No	KYU, JAERI, Eval. April 1987, tape 27.
BROND	9271	No	Eval. Feb. 1978 revision 1 Dec. 1981, tape ma242.51.
JEF 2.2	9237	Yes	JEF Collab., Eval. June 1989. High energy identical to ENDF/B-VI.

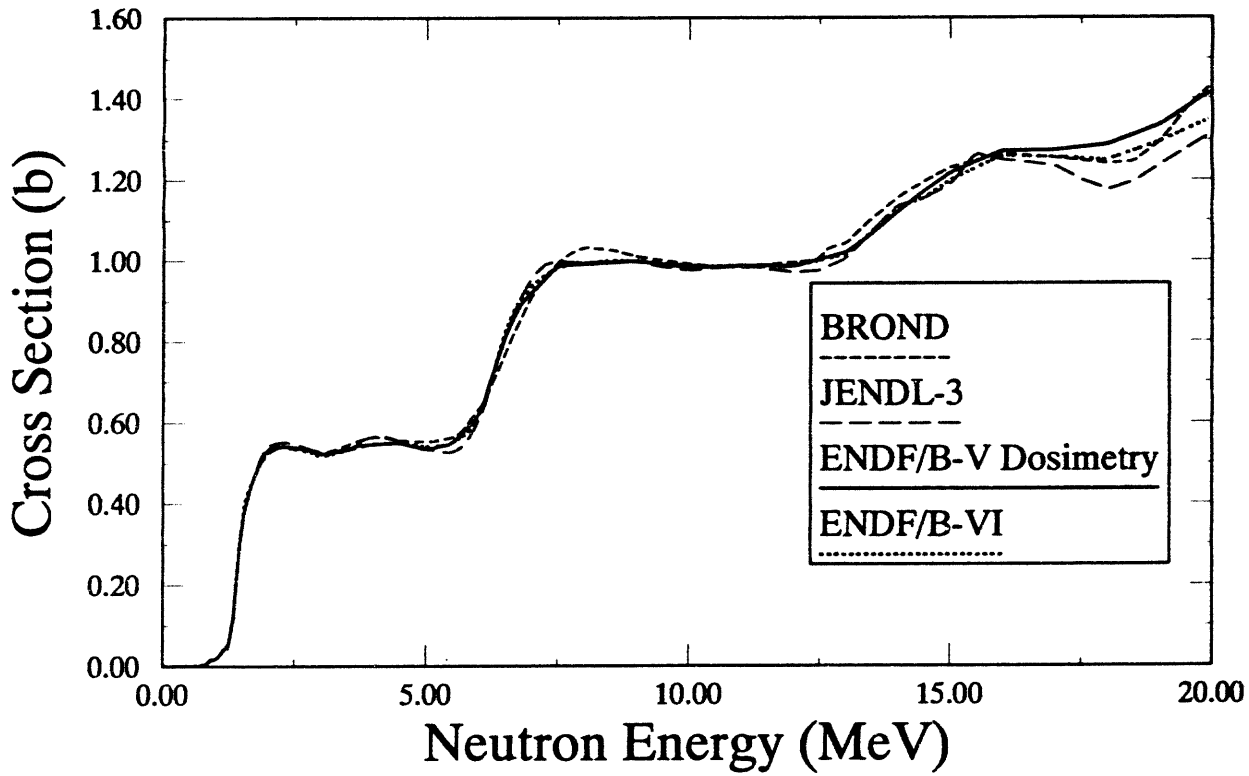

Figure A-62a: ^{238}U(n,f)F.P. Cross Section

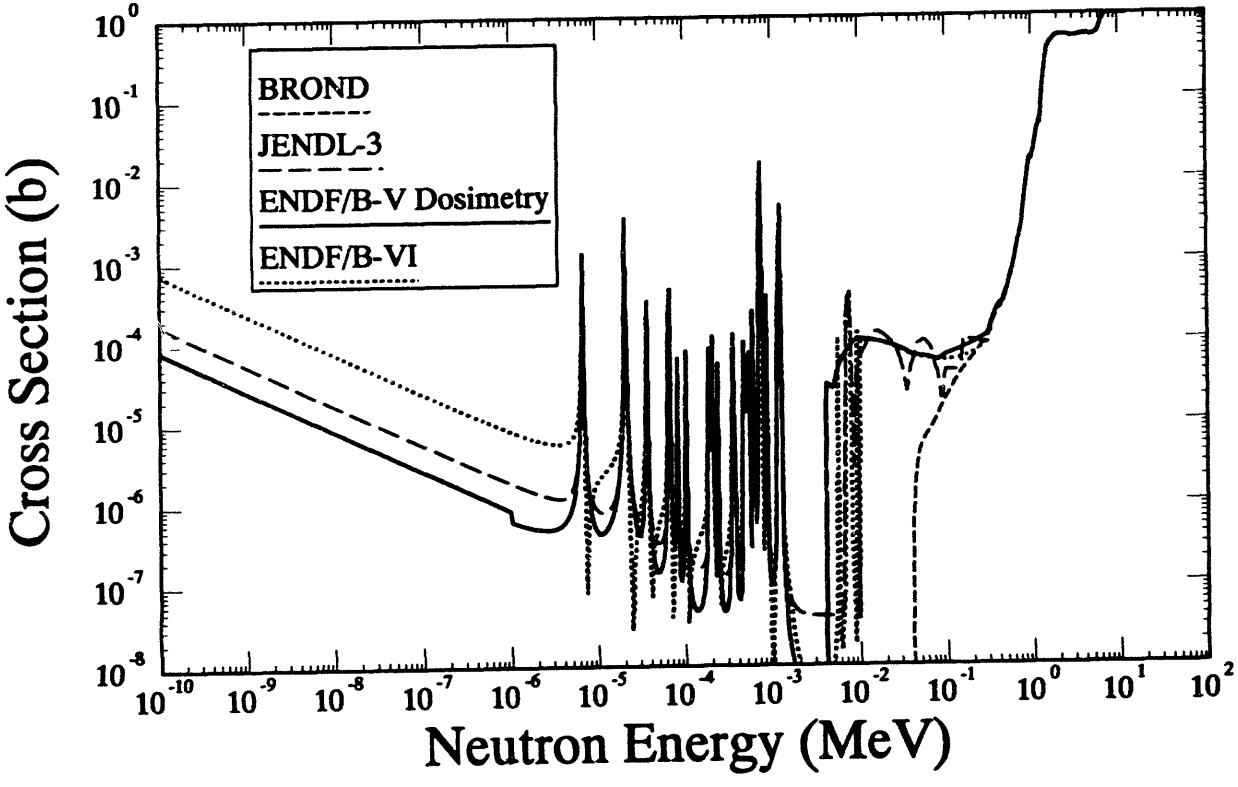

Figure A-62b: ^{238}U(n,f)F.P. Cross Section

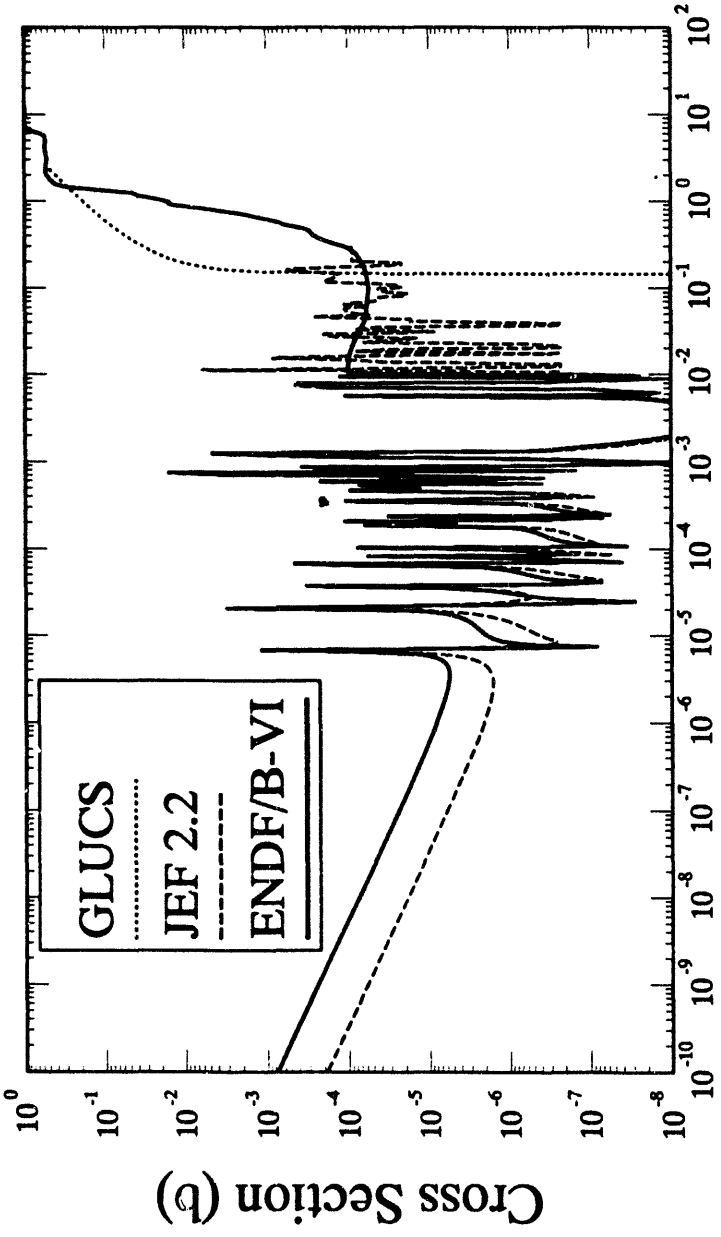

Figure A-62c: $^{238}U(n,f)F.P.$ Cross Section

Table A-63a
Alternative Cross Section Sources for the ^{237}Np(n,f)F.P. Reaction

^{237}Np(n,f)F.P.			Comment
Cross Section Library	Material Number	Covariance Data	
ENDF/B-VI	9346	No	LANL, Eval. April 1990, revision 1.
IRDF-90	9346	No	Taken from ENDF/B-VI.
ENDF/B-V	1337	Yes	HEDL/SRL, Eval. April 1978, tape 560, revision 2.
ENDF/B-V	6337	Yes	HEDL/SRL, Eval. April 1978, Dosimetry Tape 531a.
JENDL-3	3931	No	KYUSHU, Eval. Nov. 1987, NJOY processing error.
BROND	9311	No	FR/CAD, Eval. Mar. 1981, tape ma242.51. Based on INDC eval., revised Nov. 1982.
JEF 2.2	9346	No	NEA, Recom. June 1982. Taken from Derrien eval. tape jef-8.
IRDF-82	6337	Yes	Taken from ENDF/B-V.
private	NA	Yes	A new fission cross section is being prepared by LANL. Preliminary analysis of new experimental data indicates that there may be significant differences from previous evaluations. This evaluation will be examined in future releases of the SNLRM L library.

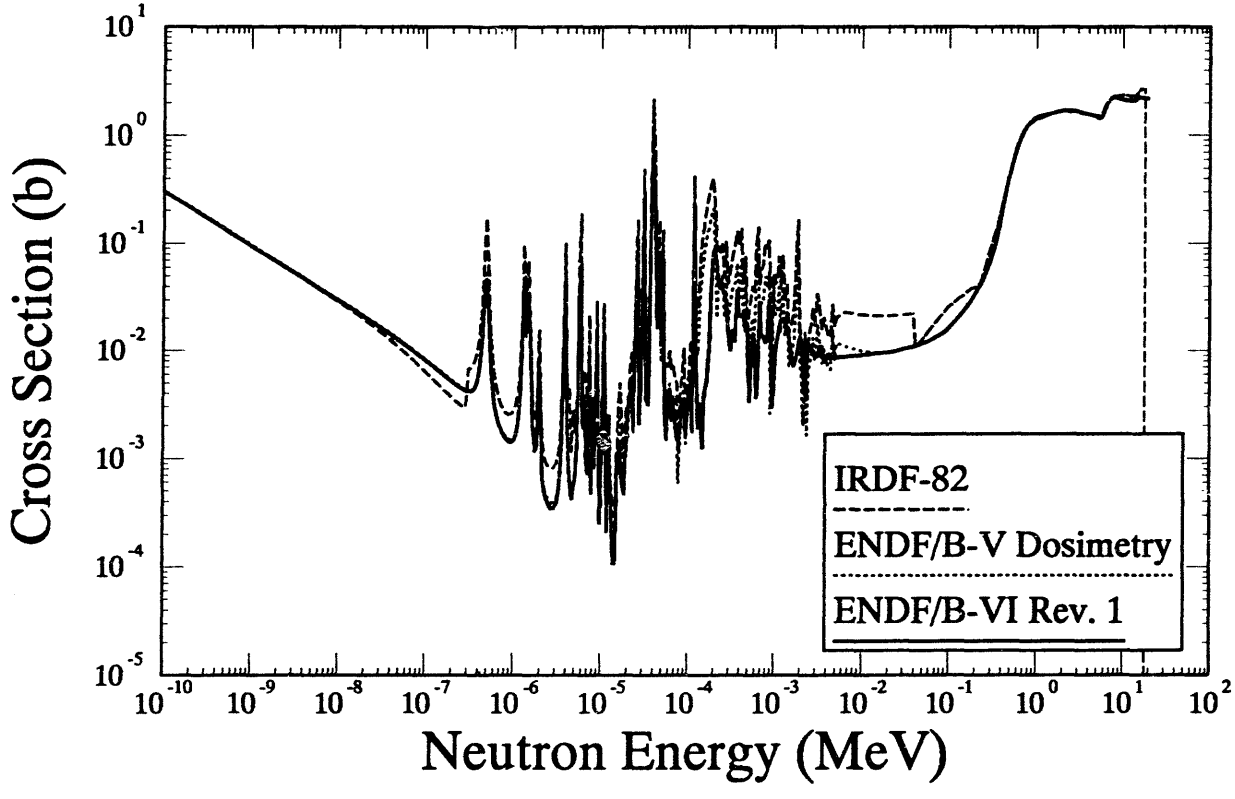

Figure A-63a: ^{237}Np(n,f)F.P. Cross Section

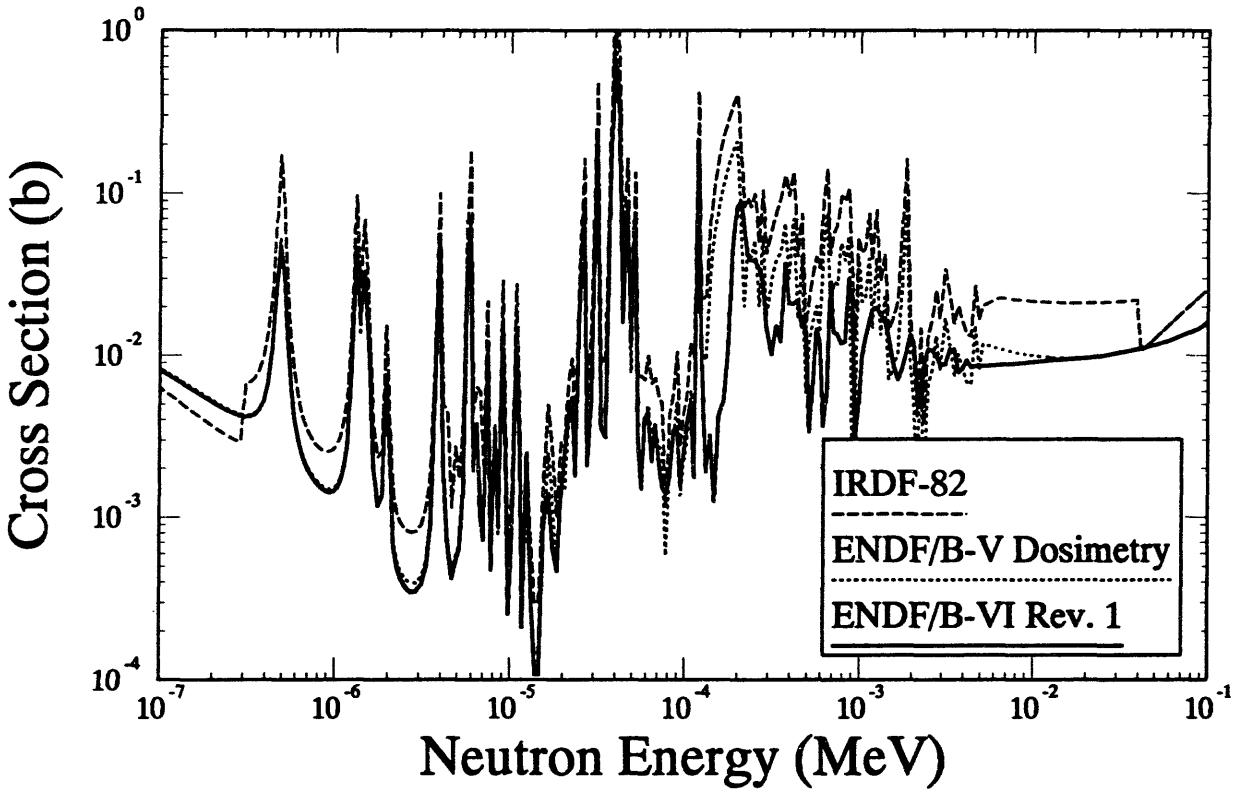

Figure A-63b: ^{237}Np(n,f)F.P. Cross Section

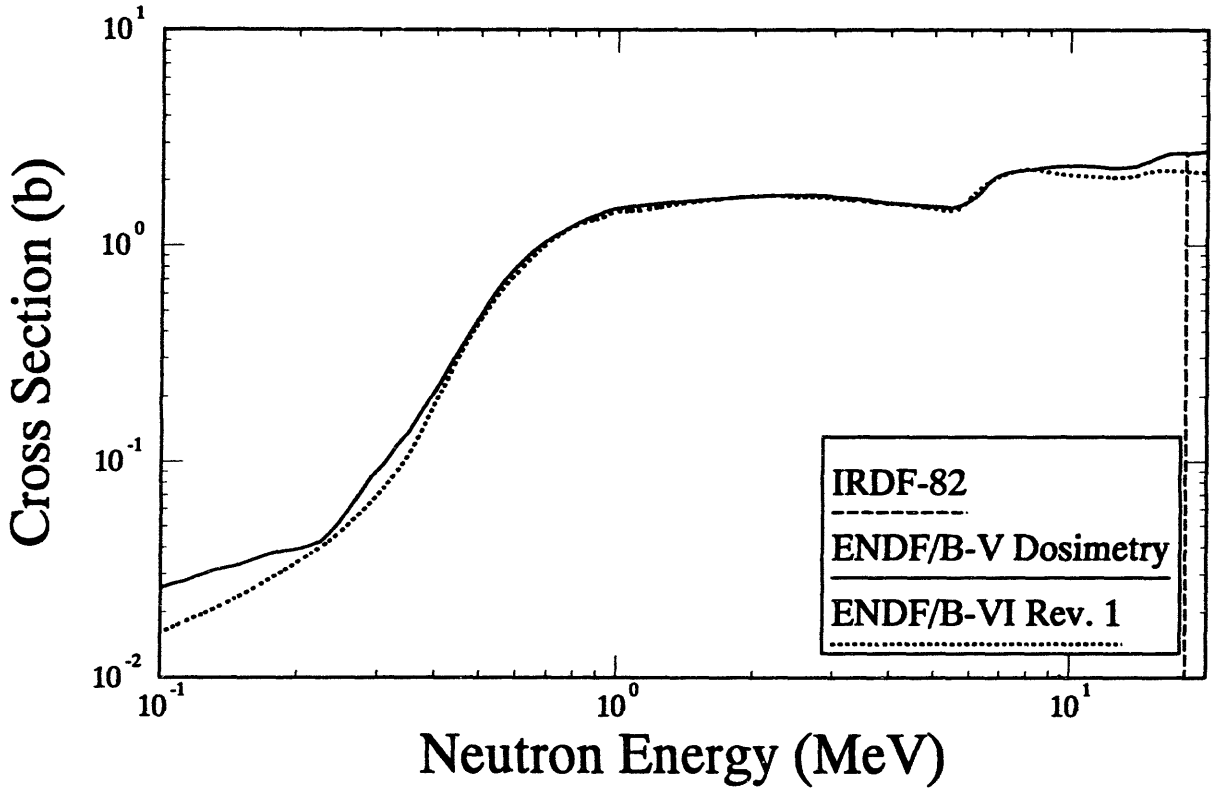

Figure A-63c: ^{237}Np(n,f)F.P. Cross Section

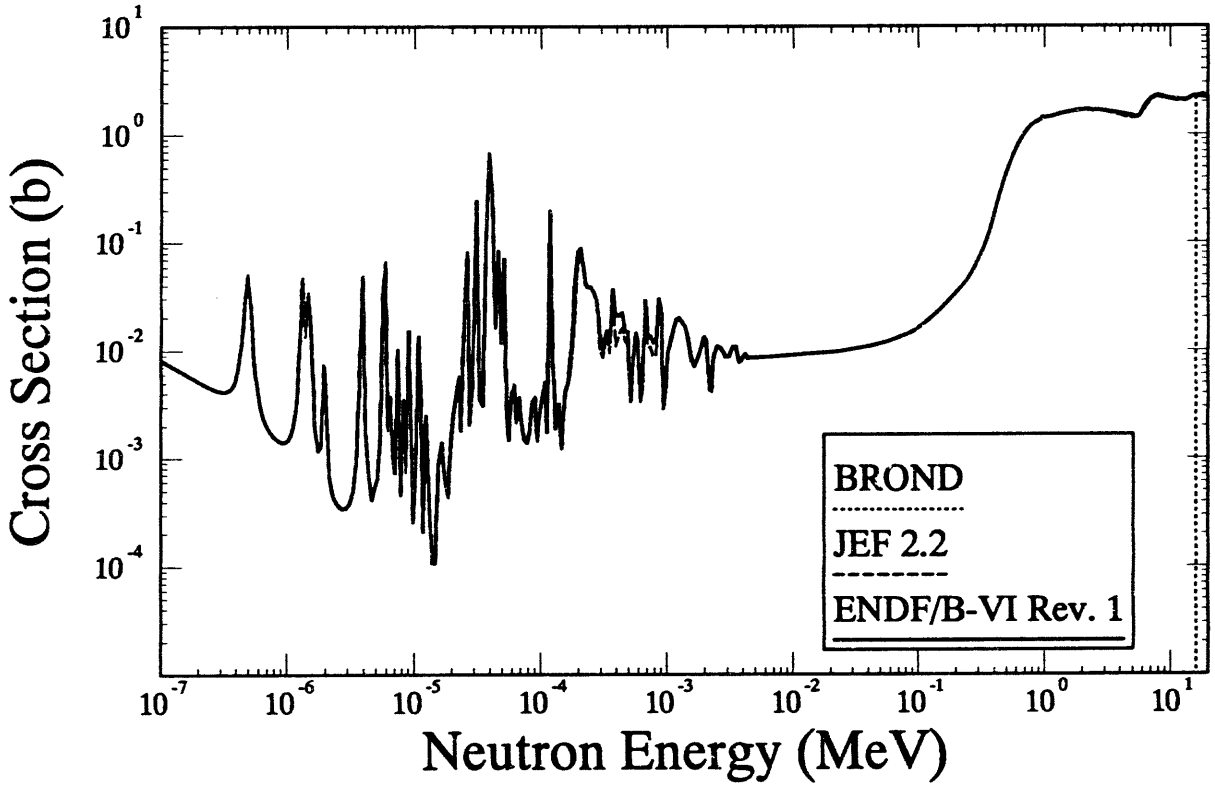

Figure A-63d: ^{237}Np(n,f)F.P. Cross Section

Table A-64a
Alternative Cross Section Sources for the ^{239}Pu(n,f)F.P. Reaction

^{239}Pu(n,f)F.P.			Comment
Cross Section Library	Material Number	Covariance Data	
ENDF/B-VI	9437	No	LANL, Eval. April 1989.
IRDF-90	9437	No	Taken from ENDF/B-VI.
ENDF/B-V	1399	Yes	LANL, Eval. June 1983, tape 563, revision 2.
ENDF/B-V	6399	Yes	GE-FBRD, Eval. Oct. 1976, Dosimetry Tape 531a.
JENDL-3	3943	No	NAIG, Eval. Mar. 1987, tape 28.
JENDL-3 Dos.	9431	Yes	Toshiba evaluation March 1987. Covariance data from IRDF-85.
BROND	9421	No	IHMT, Eval. Sept. 1980, tape ma242.51.
JEF 2.2	9437	No	CAD/ORNL, Eval. Sept.1990, tape jef-8.

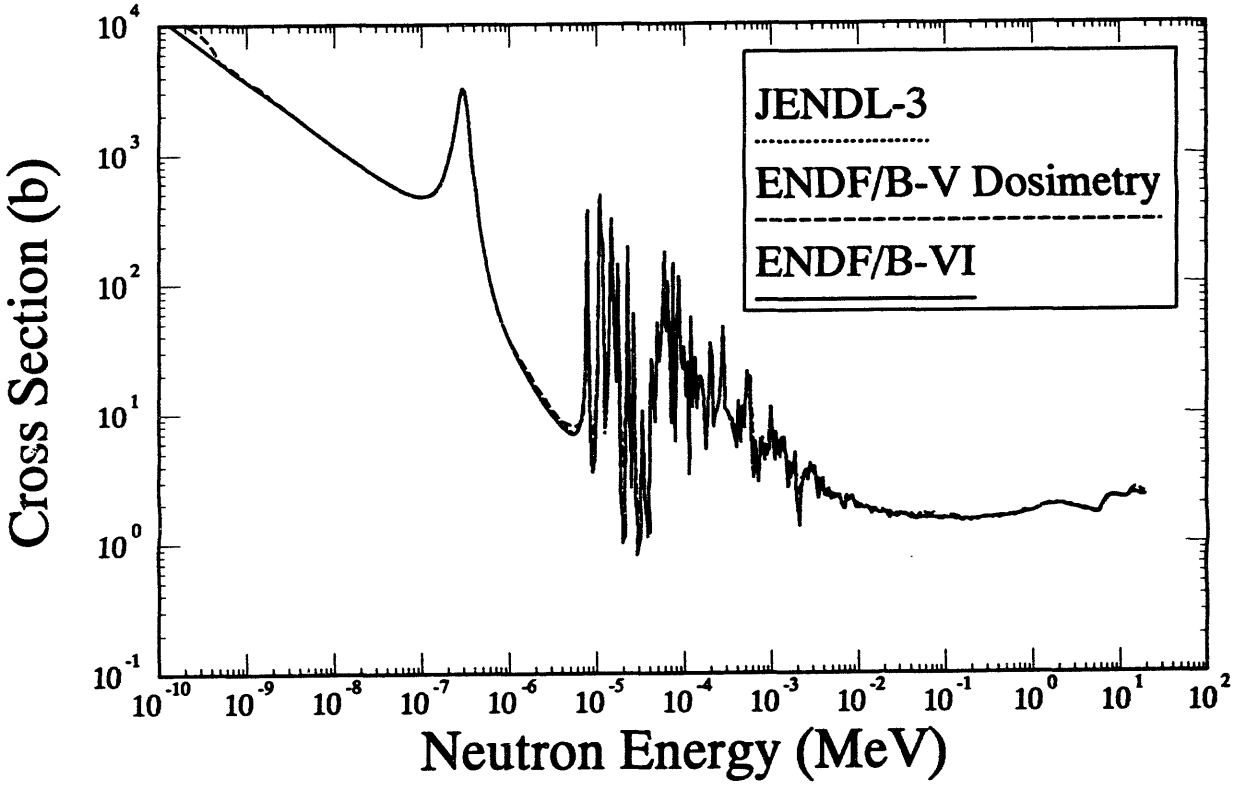

Figure A-64a: ^{239}Pu(n,f)F.P. Cross Section

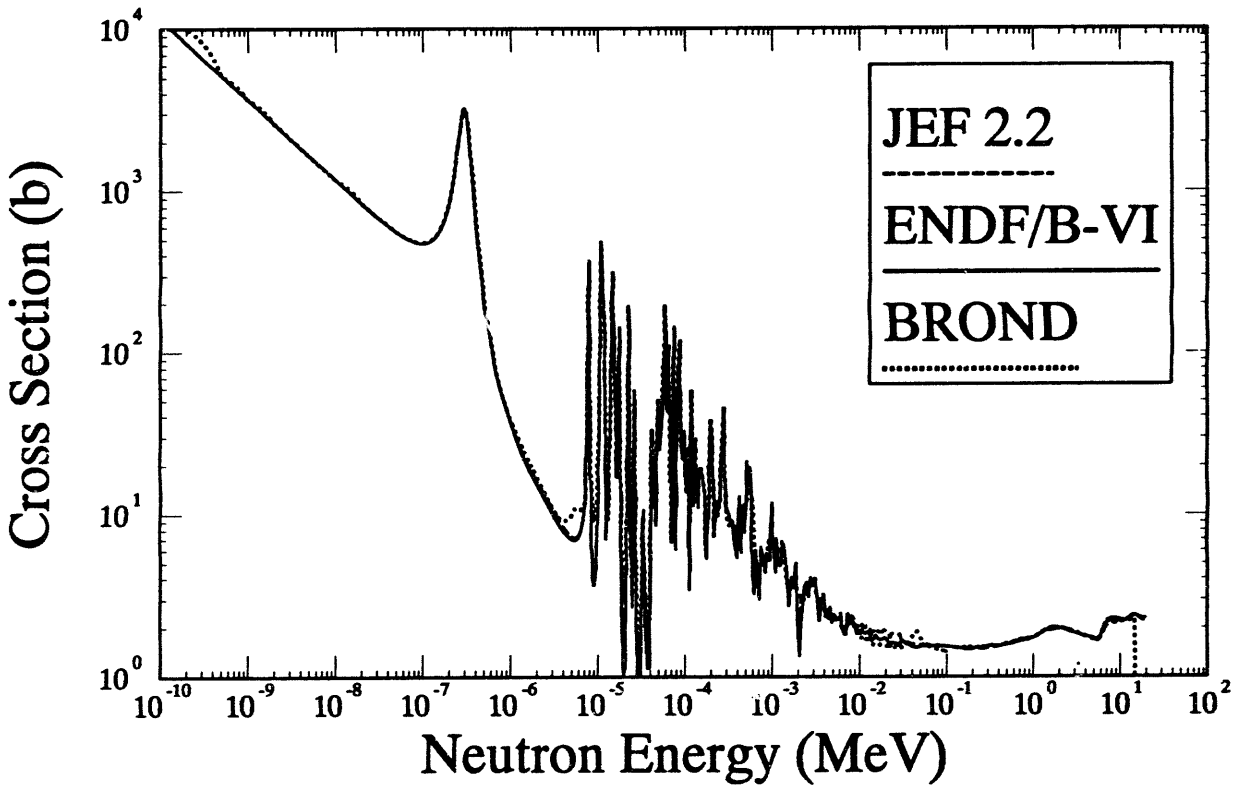

Figure A-64b: ^{239}Pu(n,f)F.P. Cross Section

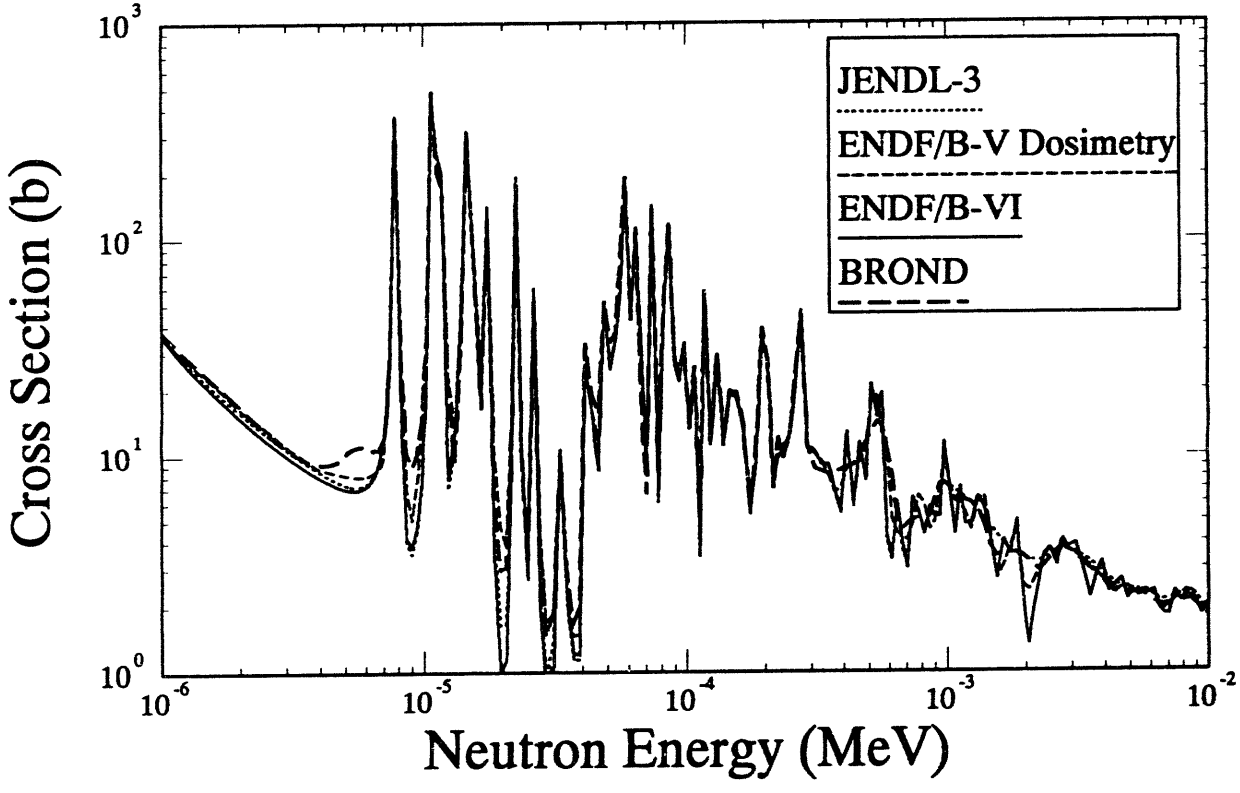

Figure A-64c: ^{239}Pu(n,f)F.P. Cross Section

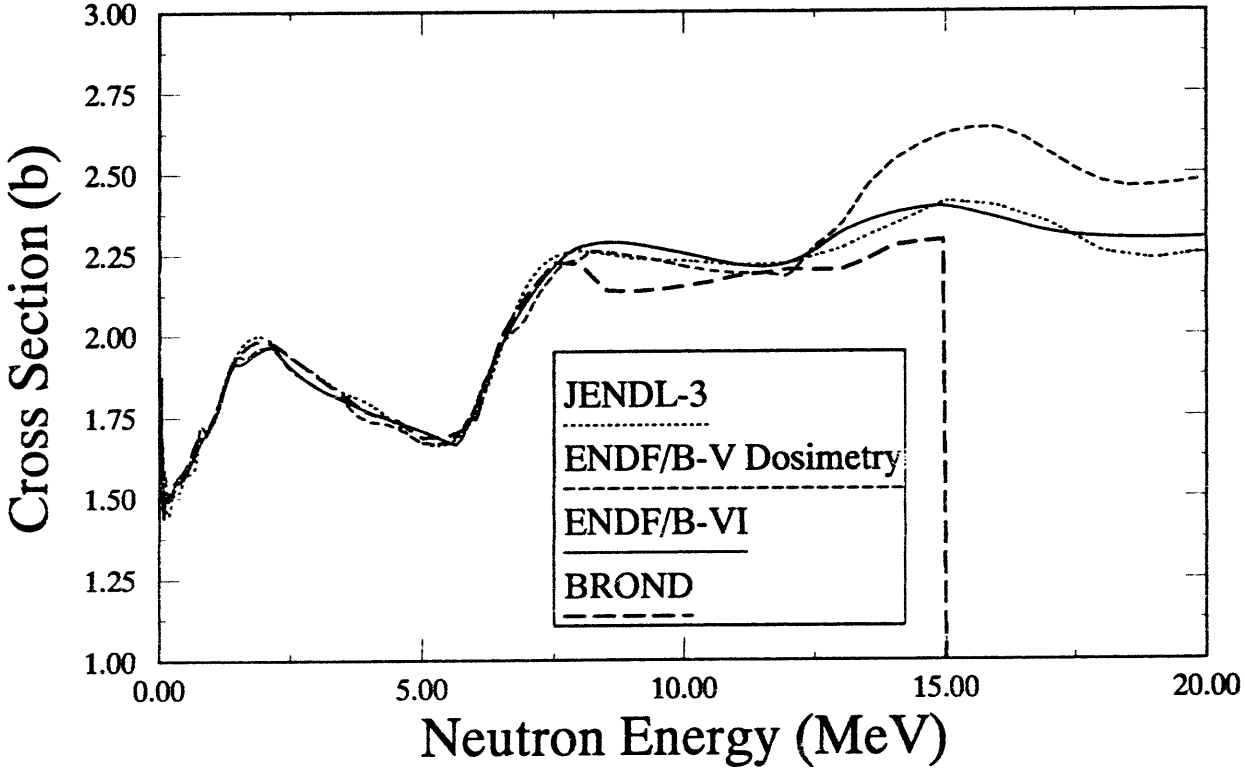

Figure A-64d: ^{239}Pu(n,f)F.P. Cross Section

Table A-65a
Alternative Cross Section Sources for the ^{241}Am(n,f)F.P. Reaction

^{241}Am(n,f)F.P.			Comment
Cross Section Library	Material Number	Covariance Data	
ENDF/B-VI	9543	Yes	CNDC, Eval. Feb. 1988.
ENDF/B-V	1361	Yes	HEDL, ORNL, Eval. April 1978, tape 560, revision 2, simple Maxwellian shape.
ENDF/B-V	NA -- 7951	---	HEDL, ORNL, Eval. April 1978, Activation Tape 532b. Only (n,γ) in evaluation.
JEF 2.2	9543	No	NEA, Rcom. June 1982, tape jef-9. Data taken from KEDAK-4.
JENDL-3	3951	No	JAERI, Eval. March 1988, tape ma257.28.
JENDL-3 Dos.	9531	Yes	Same as JENDL-3. Covariance from ENDF/B-VI.
BROND	9511	No	HAR, Eval. March 1980, revised Nov. 1983, tape ma242.51.
IRDF-82	1009	No	AERE, Eval. 1979.

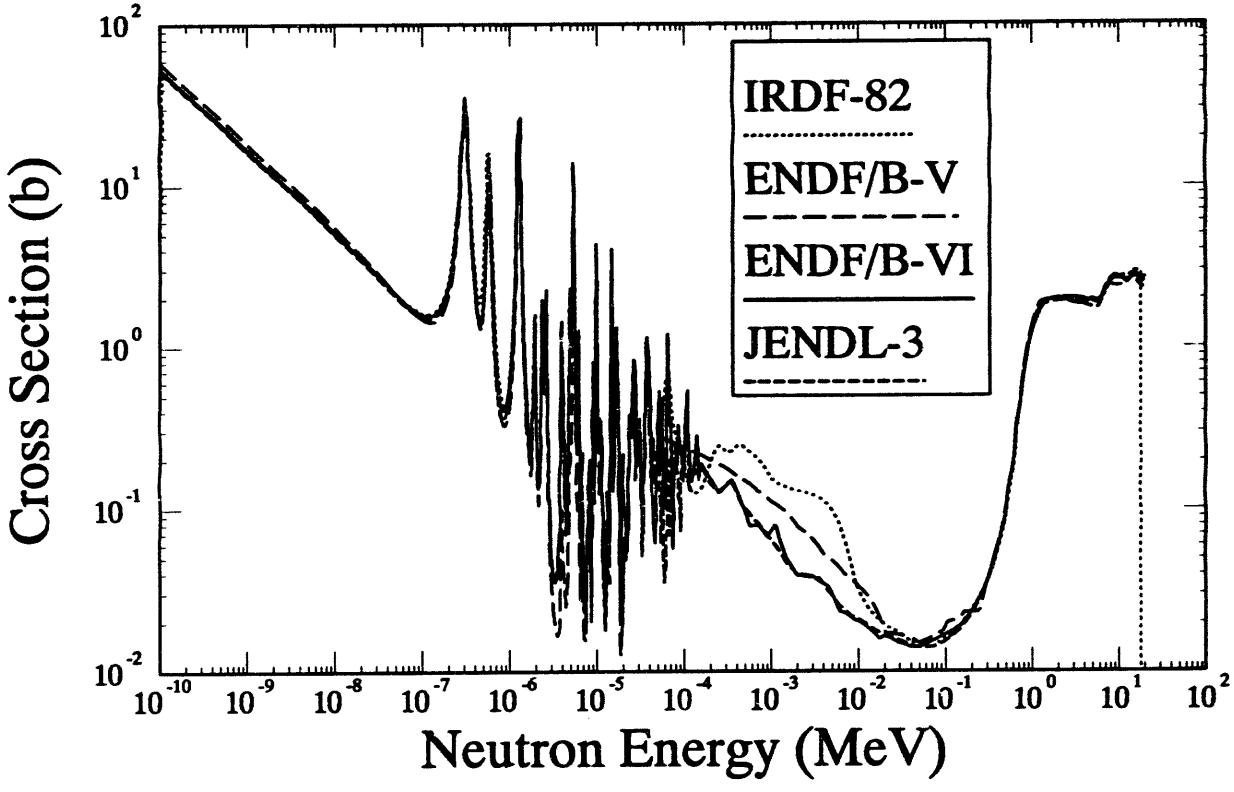

Figure A-65a: ^{241}Am(n,f)F.P. Cross Section

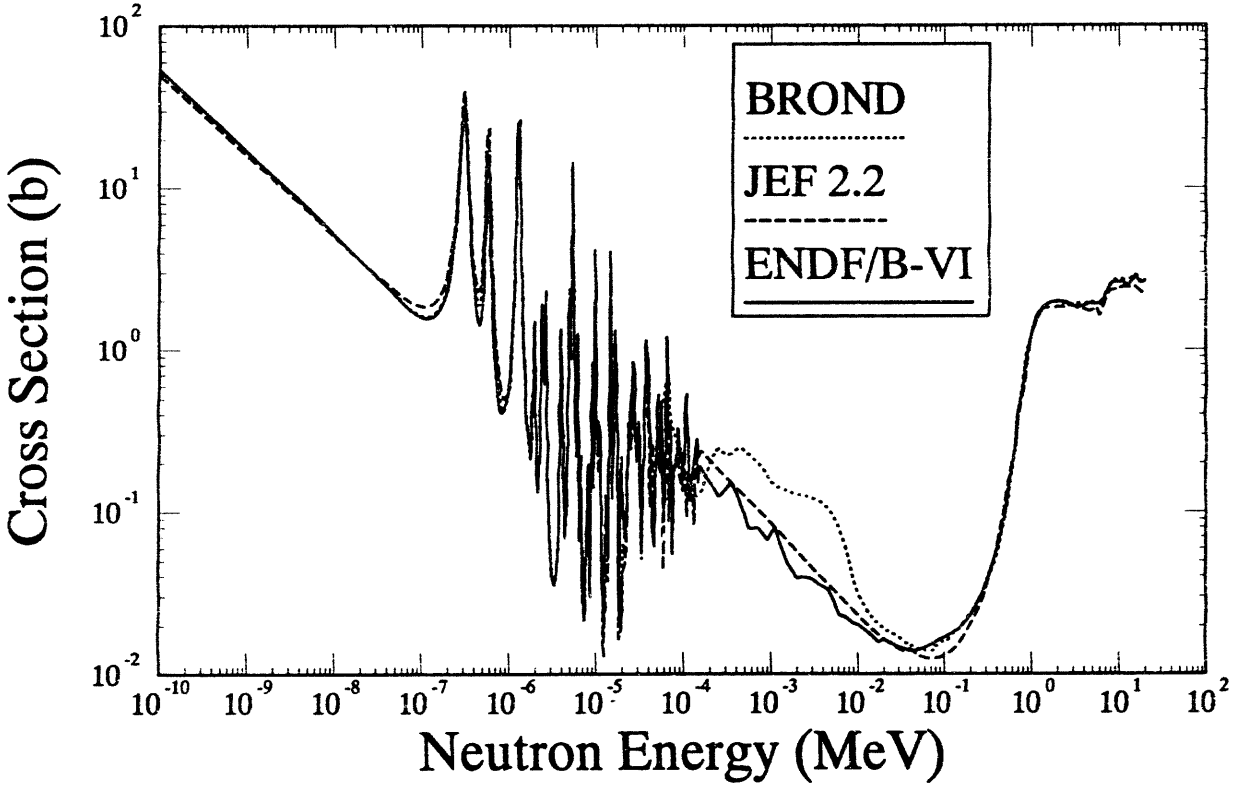

Figure A-65b: ^{241}Am(n,f)F.P. Cross Section

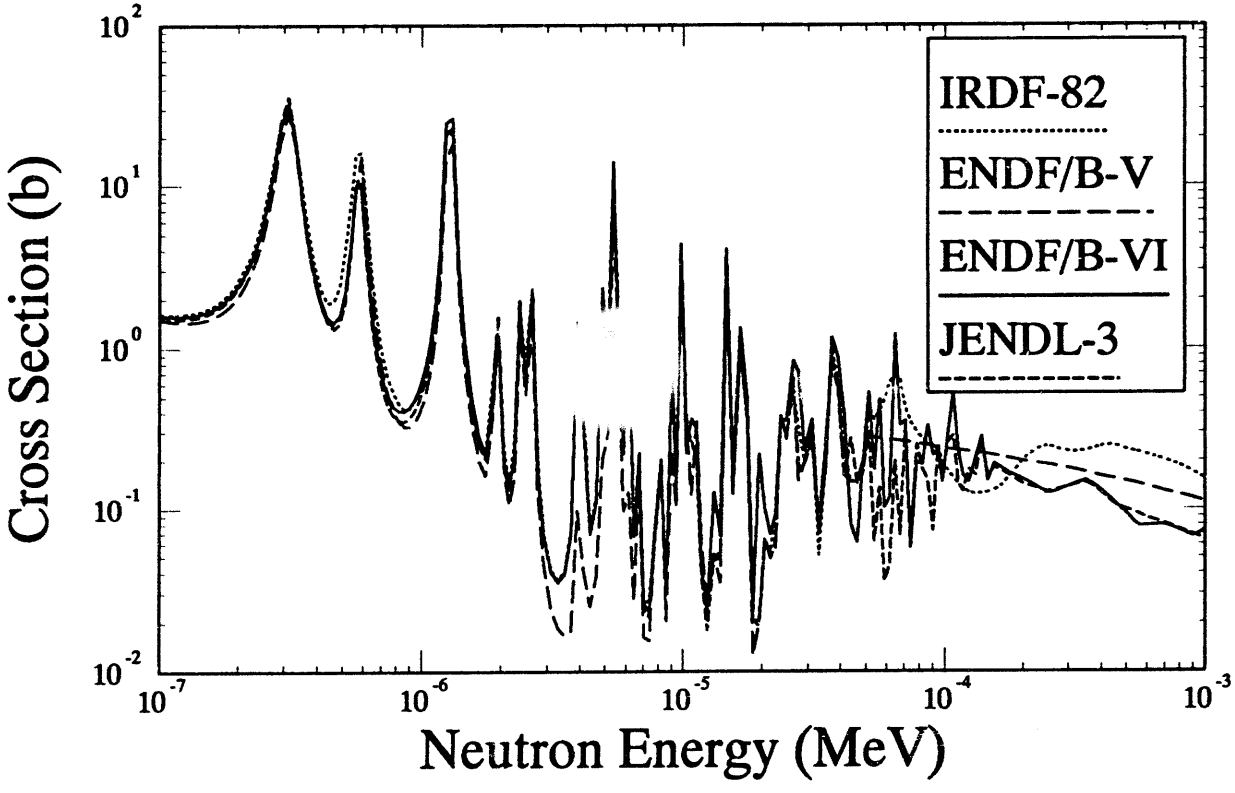

Figure A-65c: ^{241}Am(n,f)F.P. Cross Section

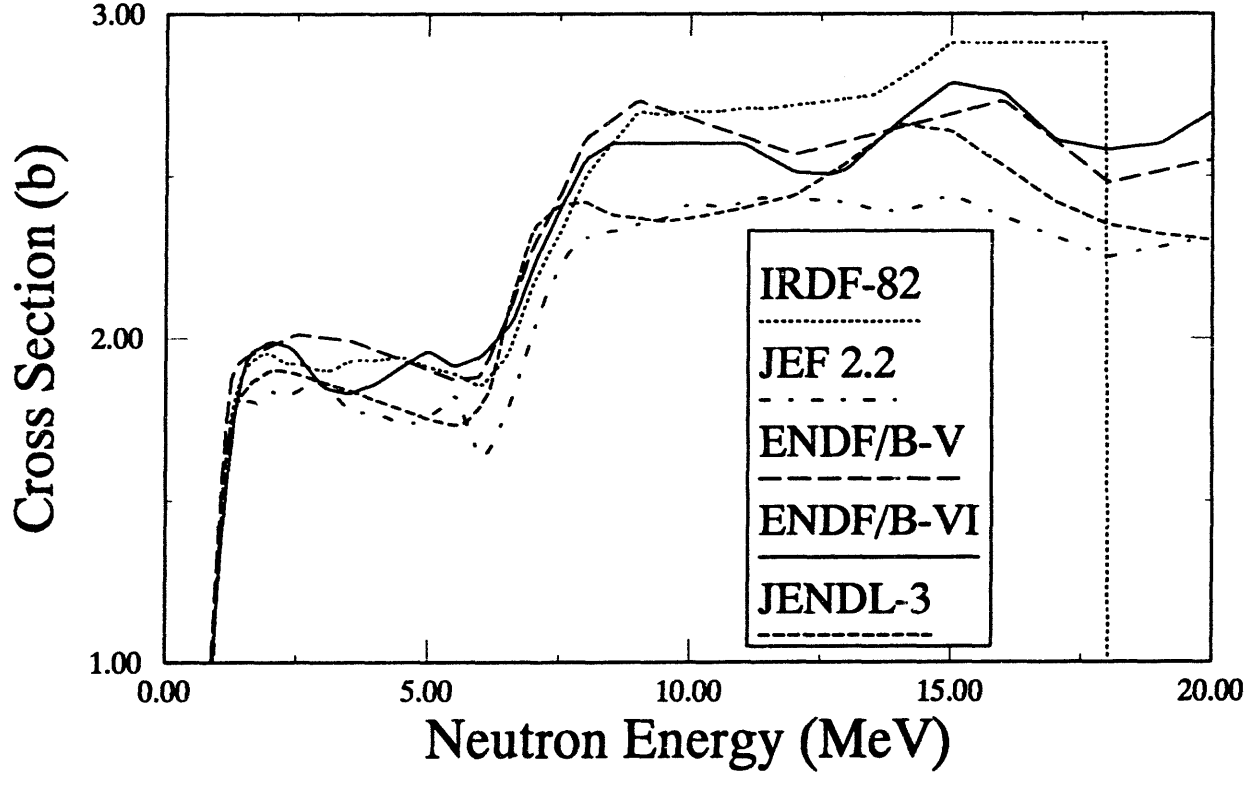

Figure A-65d: ^{241}Am(n,f)F.P. Cross Section

Table A-66a
Cross Sections for the RML Enriched Uranium Fission Foil

RML $^{enriched}U(n,f)F.P.$ Composition				Comment
Isotope	Cross Section Library	Material Number	Atom Fraction	
^{235}U	ENDF/B-VI	9228	0.9300	Baseline isotope.
^{234}U	ENDF/B-VI	9225	0.00981	
^{236}U	ENDF/B-VI	9231	0.00359	
^{238}U	ENDF/B-VI	9237	0.0566	
All material atom fractions normalized to one atom of prime sensor element.				

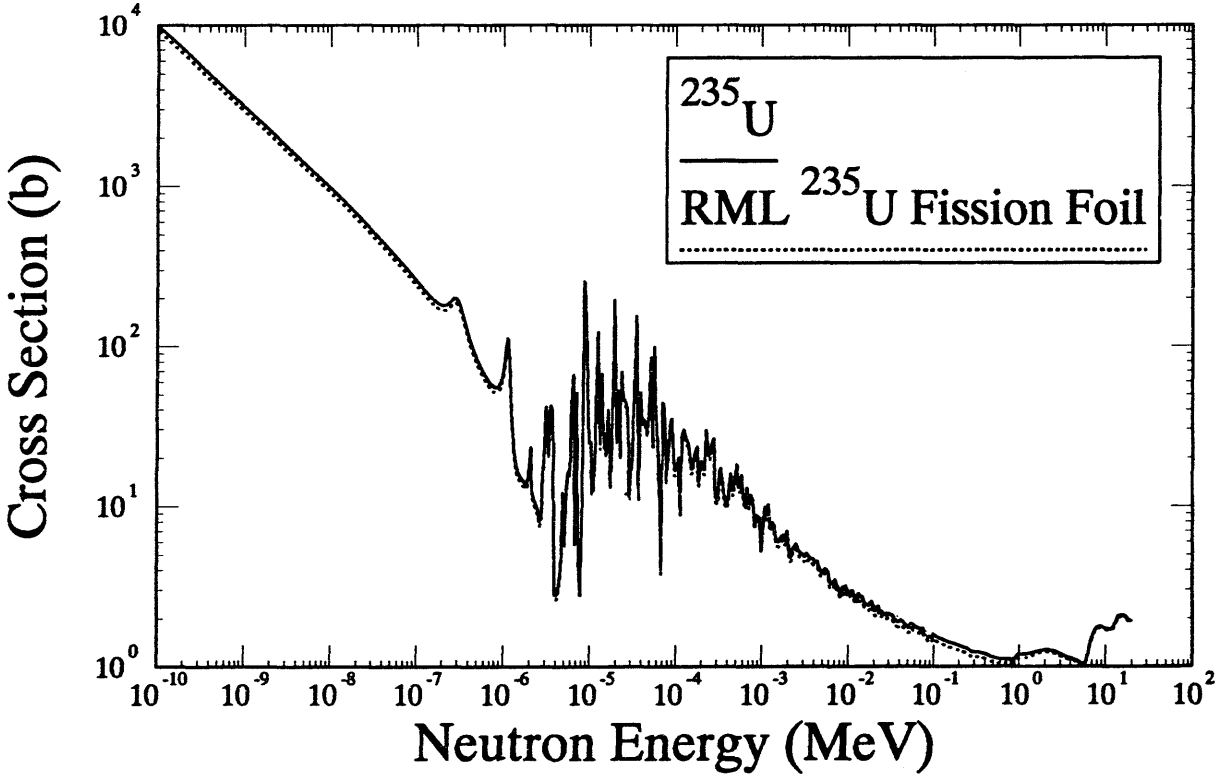

Figure A-66a: RML Enriched Uranium Fission Cross Section

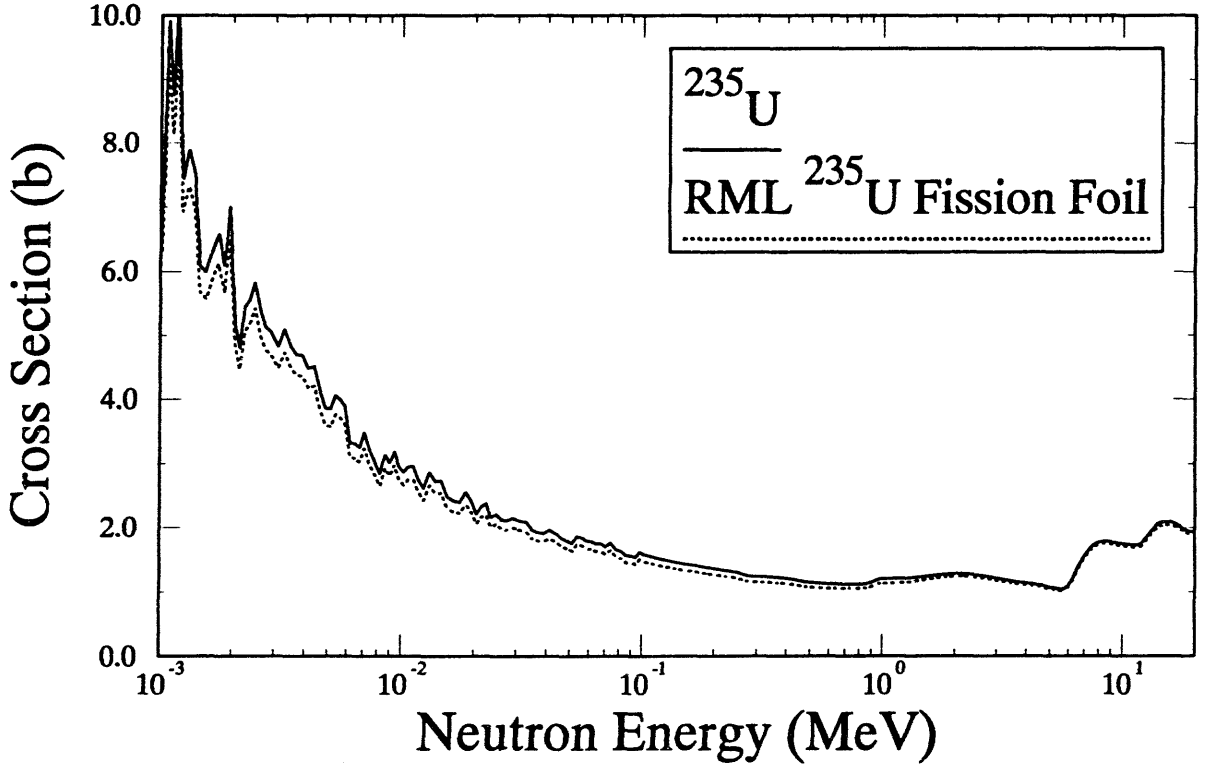

Figure A-66b: RML Enriched Uranium Fission Foil Cross Section

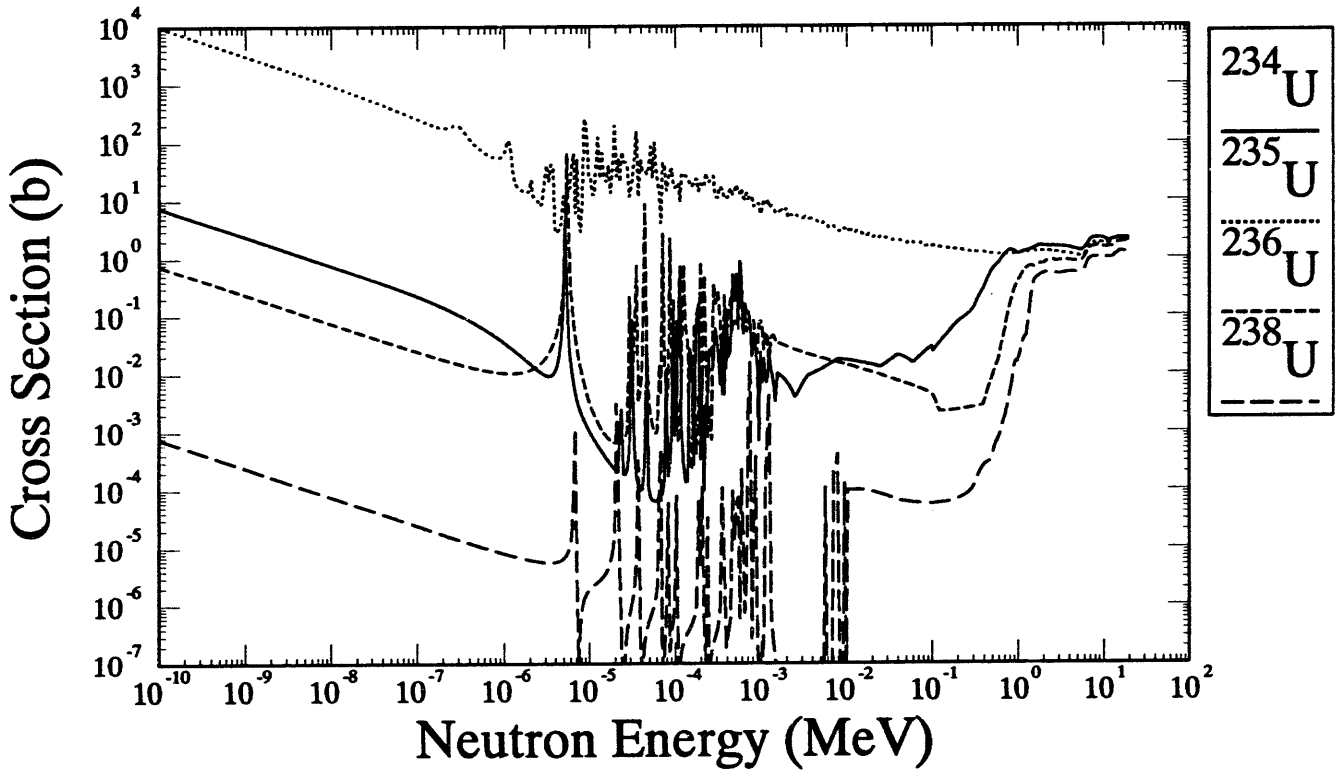

Figure A-66c: Comparison of Fission Cross Section for Uranium Isotopes

Table A-67a
Cross Section for the RML Depleted Uranium Fission Foil

RML ^{depleted}U(n,f)F.P. Composition				Comment
Isotope	Cross Section Library	Material Number	Atom Fraction	
^{238}U	ENDF/B-VI	9237	0.9979	Baseline Isotope.
^{234}U	ENDF/B-VI	9225	0.00001	
^{235}U	ENDF/B-VI	9228	0.00205	Major thermal cross section impurity.
^{236}U	ENDF/B-VI	9231	0.00004	
All material atom fractions normalized to one atom of prime sensor element.				

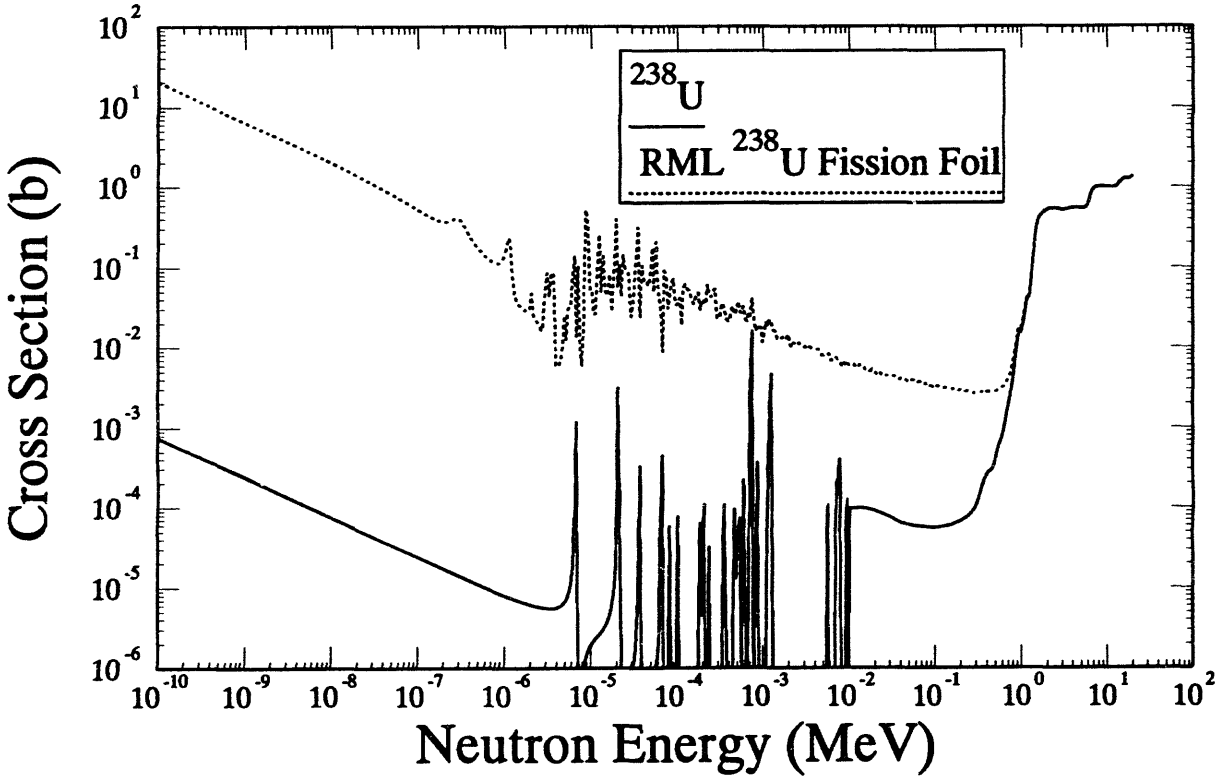

Figure A-67a: RML Depleted Uranium Fission Foil Cross Section

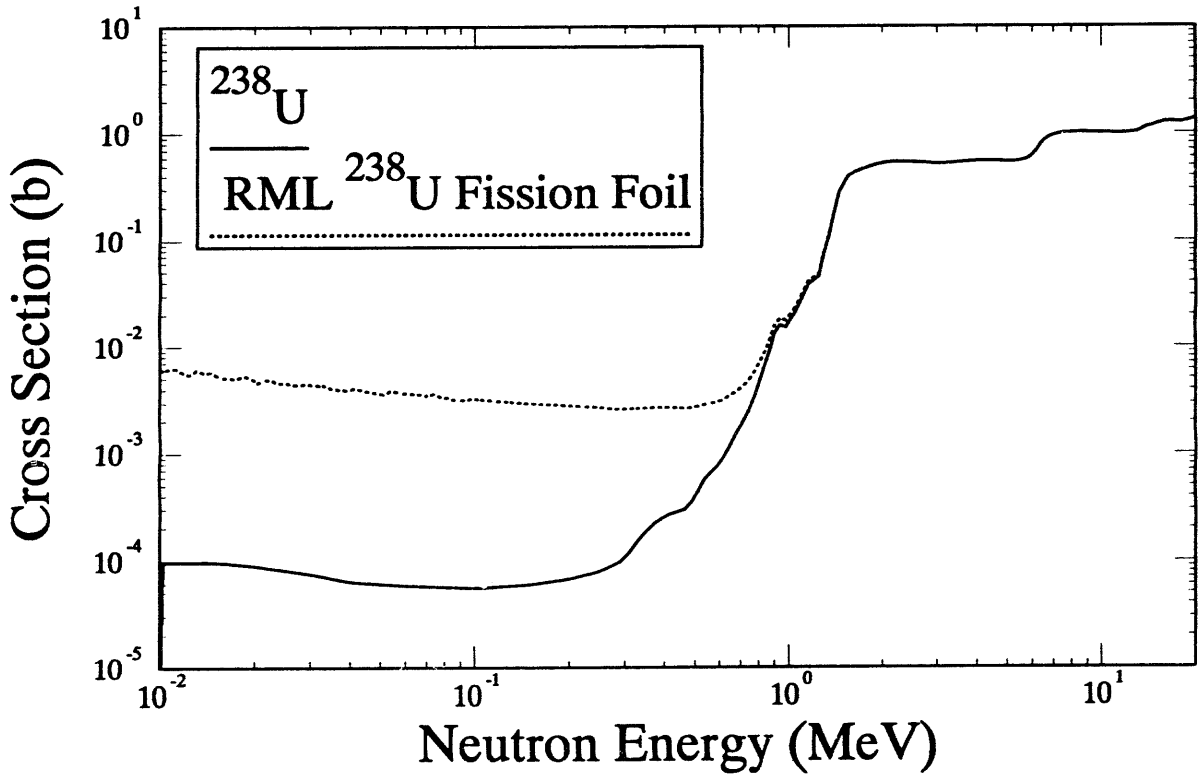

Figure A-67b: RML Depleted Uranium Fission Foil Cross Section

Table A-68a
Cross Sections for the RML Plutonium Fission Foil

RML Pu(n,f)F.P. Composition				Comment
Isotope	Cross Section Library	Material Number	Atom Fraction	
^{239}Pu	ENDF/B-VI	9437	0.869965	Baseline isotope.
^{238}Pu	ENDF/B-VI	9428	0.0006798	
^{240}Pu	ENDF/B-VI	9440	0.115968688	Component causes a shape change in dosimeter cross section.
^{241}Pu	ENDF/B-VI	9443	0.010797	
^{242}Pu	ENDF/B-VI	9446	0.00235936	
^{235}U	ENDF/B-VI	9228	0.000199946	
^{237}Np	ENDF/B-VI	9346	0.00002999	
All material atom fractions normalized to one atom of prime sensor element.				

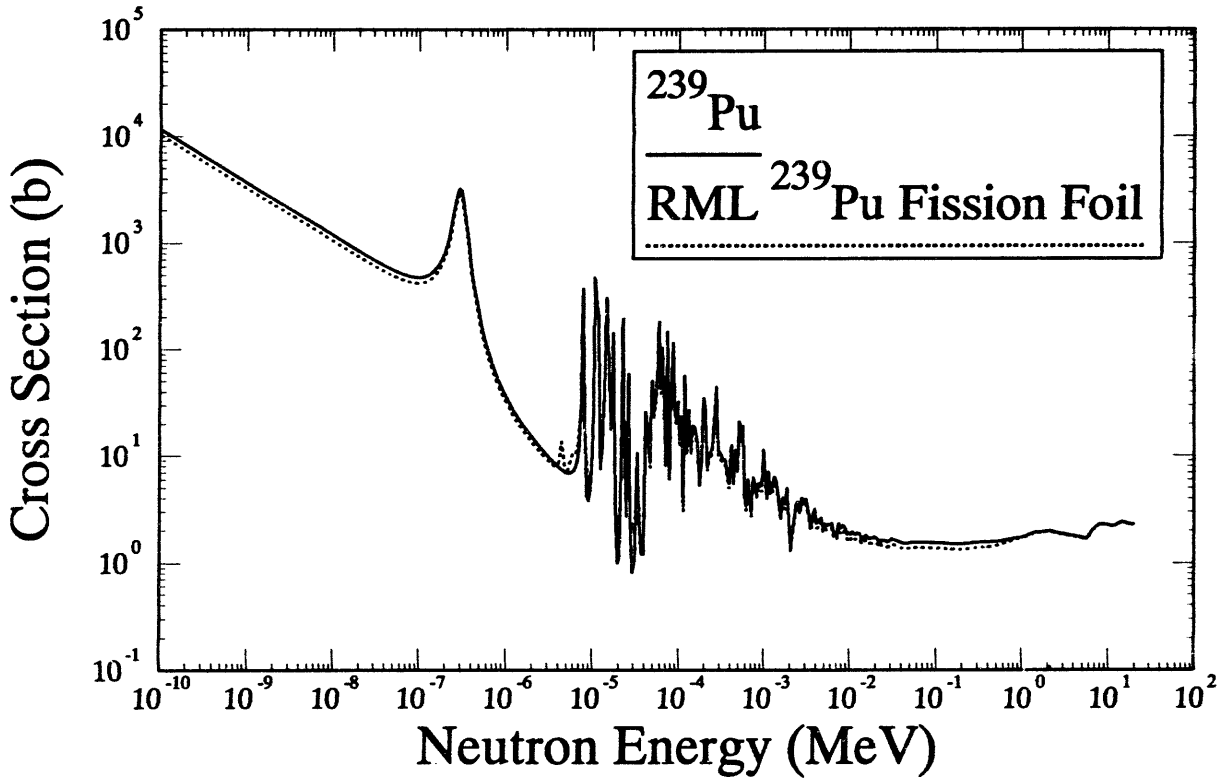

Figure A-68a: RML Plutonium Fission Foil Cross Section

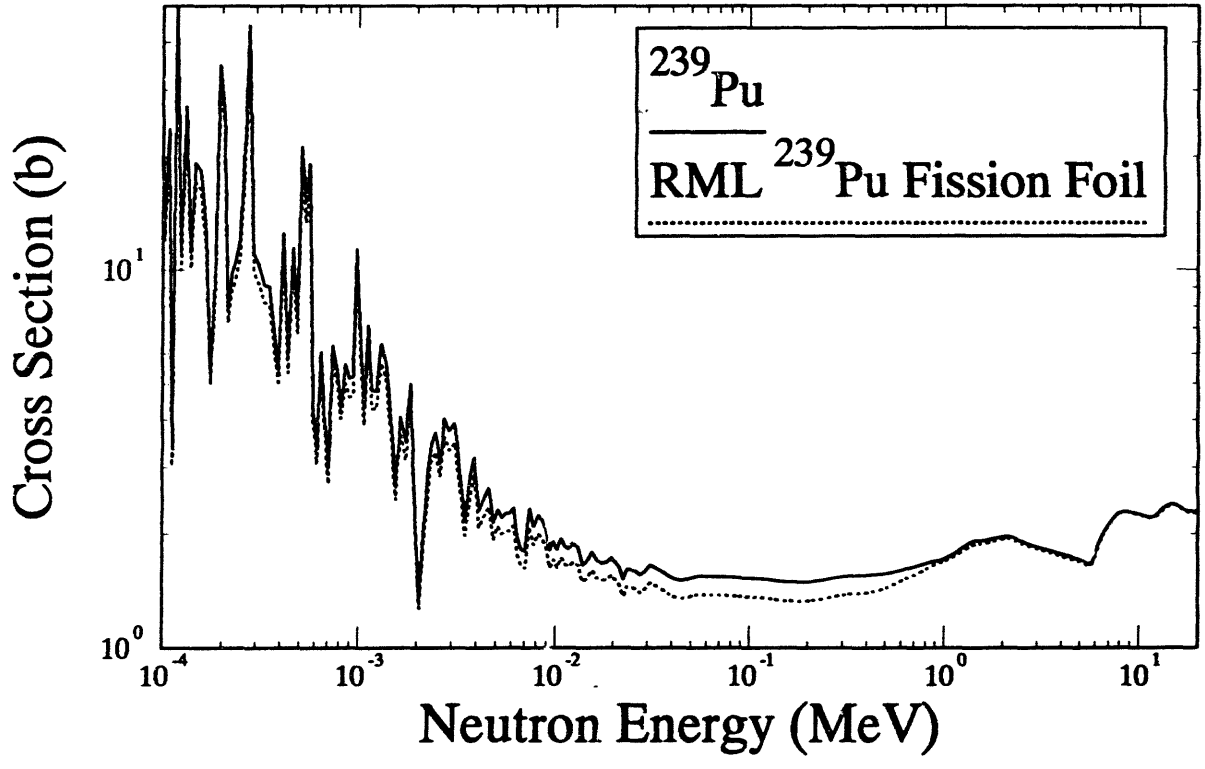

Figure A-68b: RML Plutonium Fission Foil Cross Section

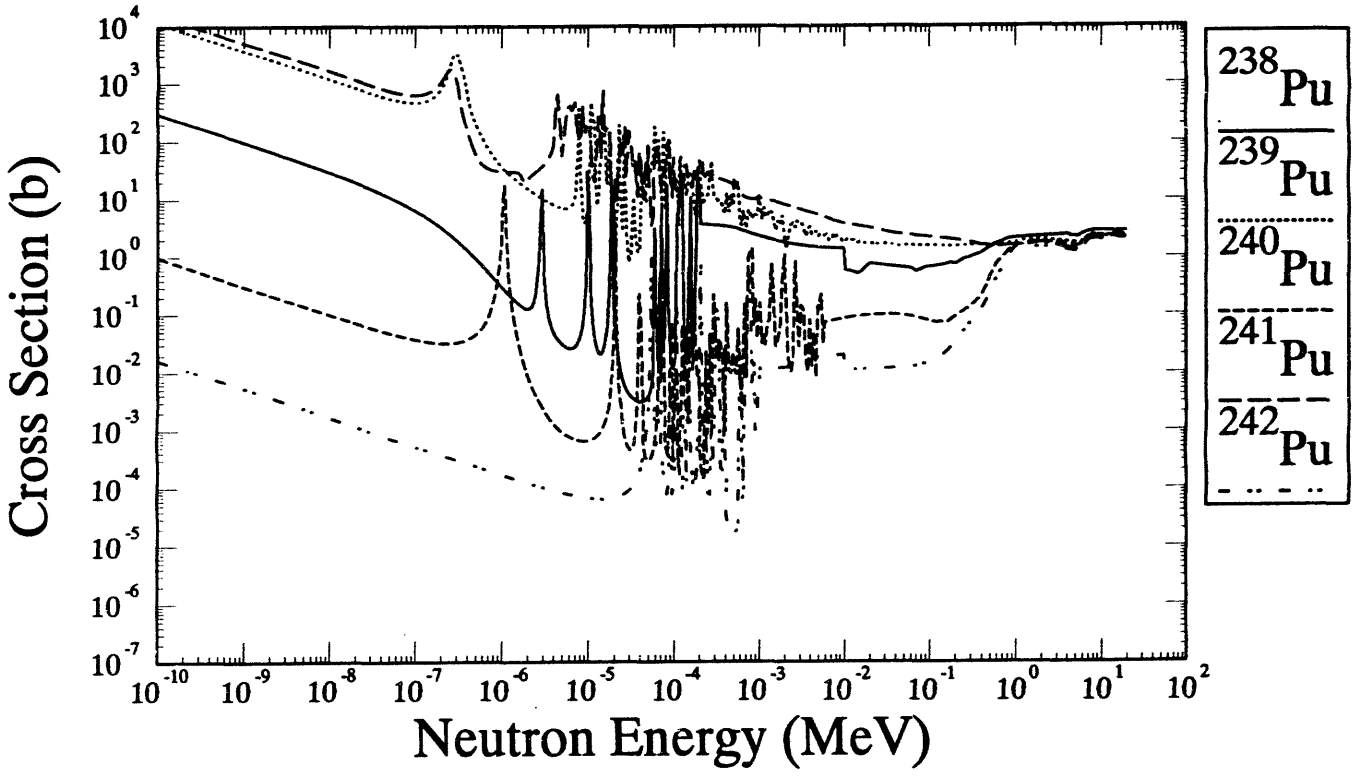

Figure A-68c: Comparison of Fission Cross Section for Plutonium Isotopes

Table A-69a
^{32}S-3-MeV Sensor as Calibrated in a ^{252}Cf Field

^{252}Cf(n,X) 3-MeV			Comment
Cross Section Library	Material Number	Covariance Data	
SNLRML	1625	Yes	Methodology requires this response and covariance to be identical to the ^{32}S(n,p)^{32}P sensor. If the ENDF/B-VI ^{252}Cf spectrum is assumed, then multiply the ^{32}S(n,p)^{32}P values by 3.3718 to get a ^{252}Cf 3-MeV fluence equivalent sensor.

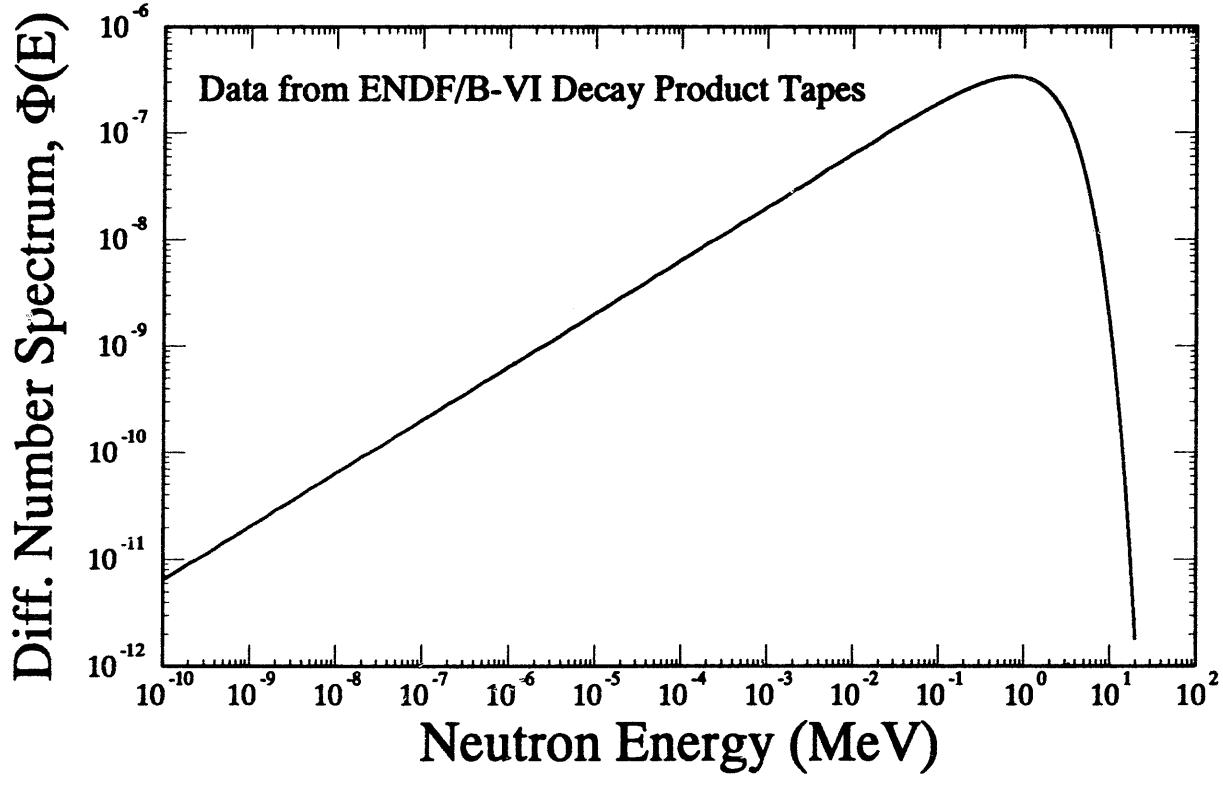

Figure A-69a: ENDF/B-VI ^{252}Cf fission Neutron Spectrum Recommended for Use with the ^{32}S-3MeV Dosimetry Sensor

Intentionally Left Blank

APPENDIX B

Cross Section Covariance Matrices

No current cross section library includes covariance data on ^{10}B. The $^{10}B(n,\alpha)$ covariance data is the best available input at this time. See Figure B-2 for the $^{10}B(n,\alpha)$ covariance matrix.

Figure B-1: ^{10}B(n,abs) Covariance Matrix

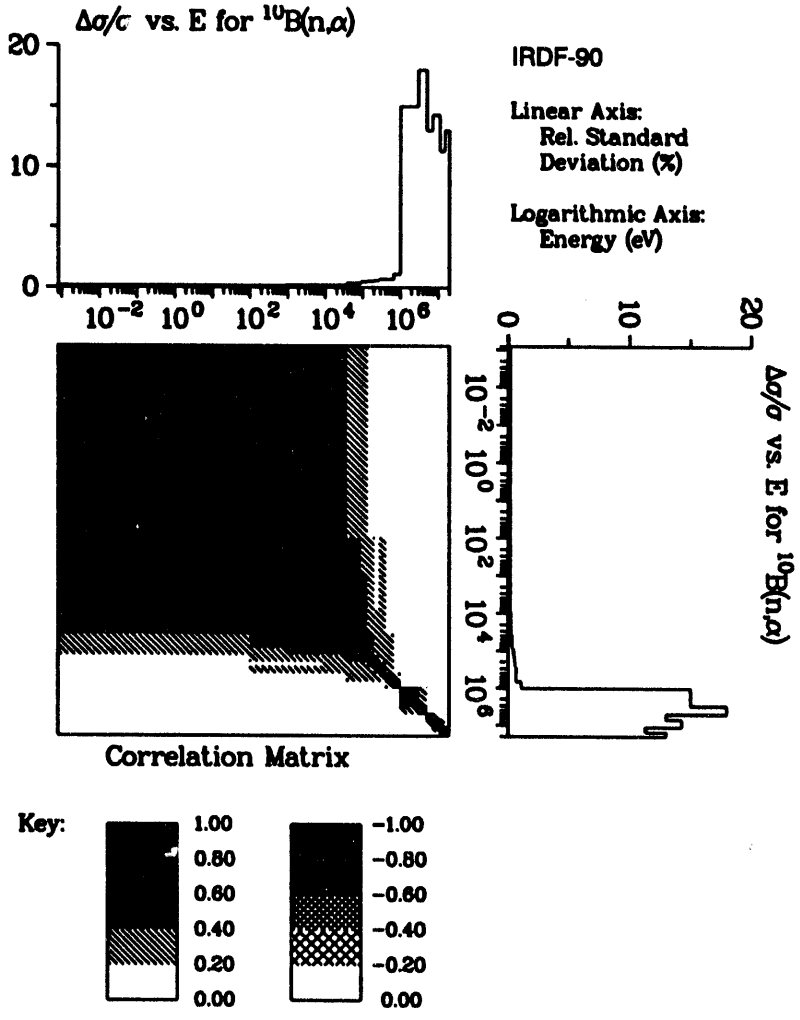

Figure B-2: $^{10}B(n,X)^{4}He$ Covariance Matrix

No current cross section library includes covariance data on ^{11}B.

Figure B-3: ^{11}B(n,abs) Covariance Matrix

No current cross section library includes covariance data on ^{10}B or ^{11}B. When this data is available to support Figures B-1 and B-3, the covariance data can be combined to provide a matrix for natural boron. Since the major component of the $^{Nat}B(n,abs)$ reaction is the $^{10}B(n,\alpha)$, the covariance matrix from Figure B-2 is the best available data.

Figure B-4: $^{Nat}B(n,abs)$ Covariance Matrix

No current cross section library includes covariance data on ^{10}B, ^{11}B, or ^{Nat}C. When this data is available the covariance data can be combined to provide a matrix for B_4C. Since the major component of the $^{Enriched}B_4C$(n,abs) reaction is the $^{10}B(n,\alpha)$, the covariance matrix from Figure B-2 is the best available data.

Figure B-5: $^{Enriched}B_4C$(n,abs) Covariance Matrix

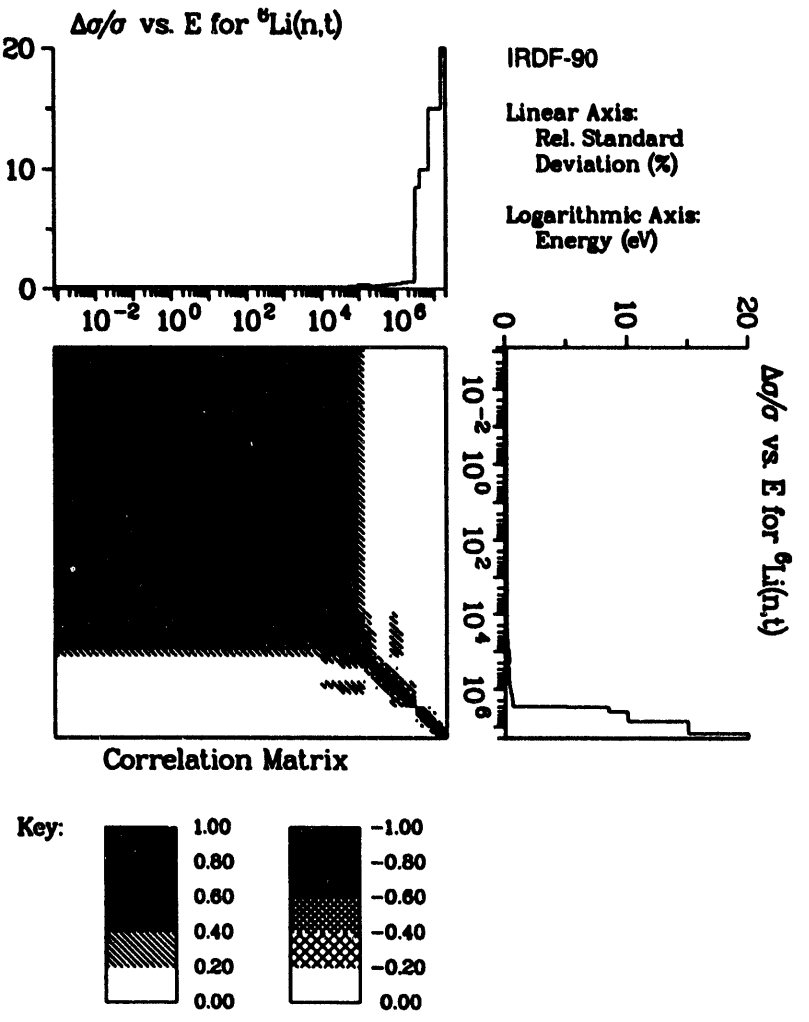

Covariance data for $^{6}Li(n,t)$ with $^{6}Li(n,t)$.

Figure B-6: $^{6}Li(n,X)^{4}He$ Covariance Matrix

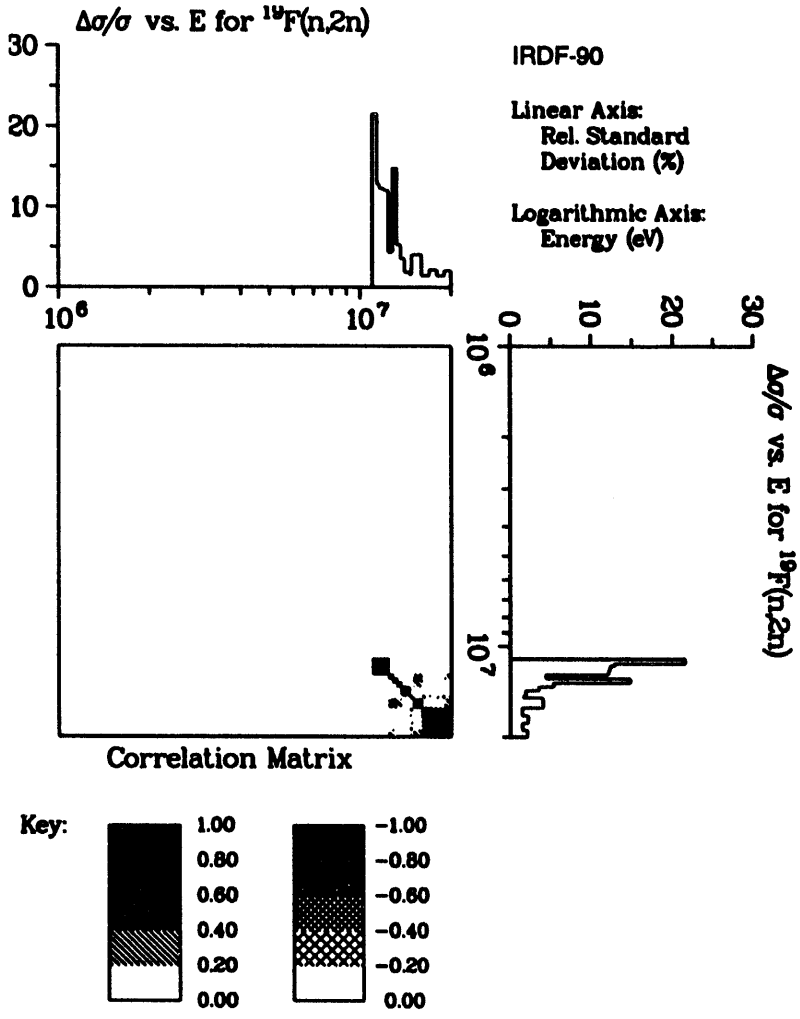

Covariance data for $^{19}F(n,2n)$ with $^{19}F(n,2n)$.

Figure B-7: $^{19}F(n,2n)^{18}F$ Covariance Matrix

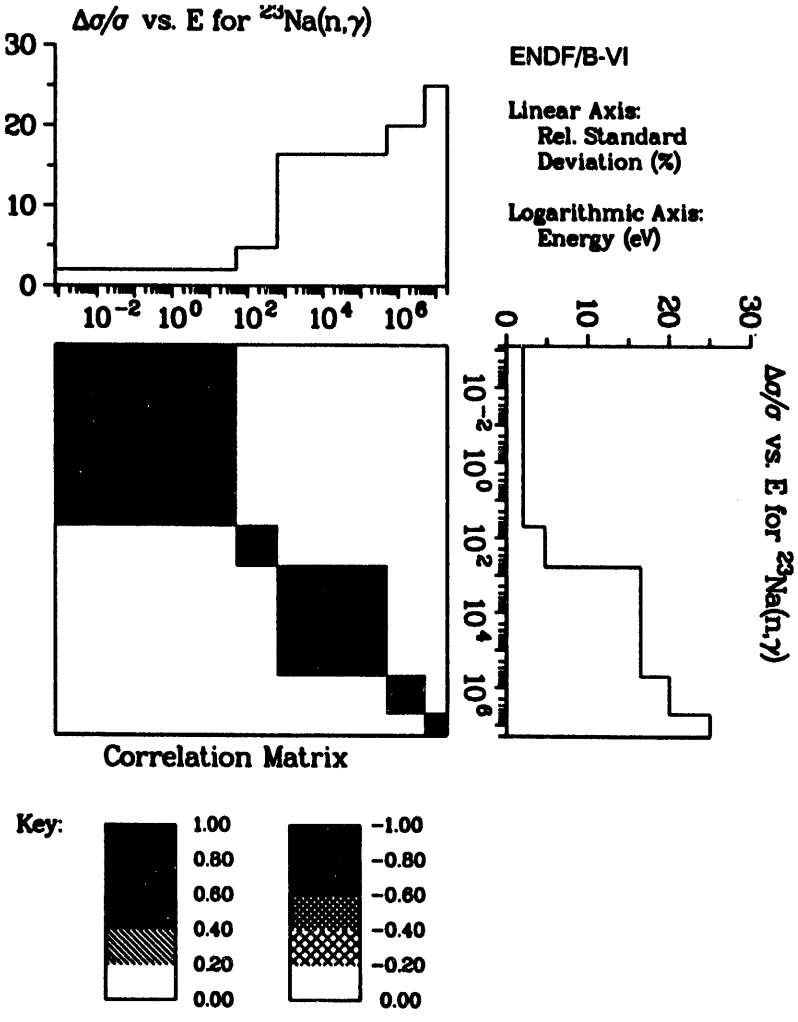

Covariance data for $^{23}Na(n,\gamma)$ with $^{23}Na(n,\gamma)$.

Figure B-8: $^{23}Na(n,\gamma)^{24}Na$ Covariance Matrix

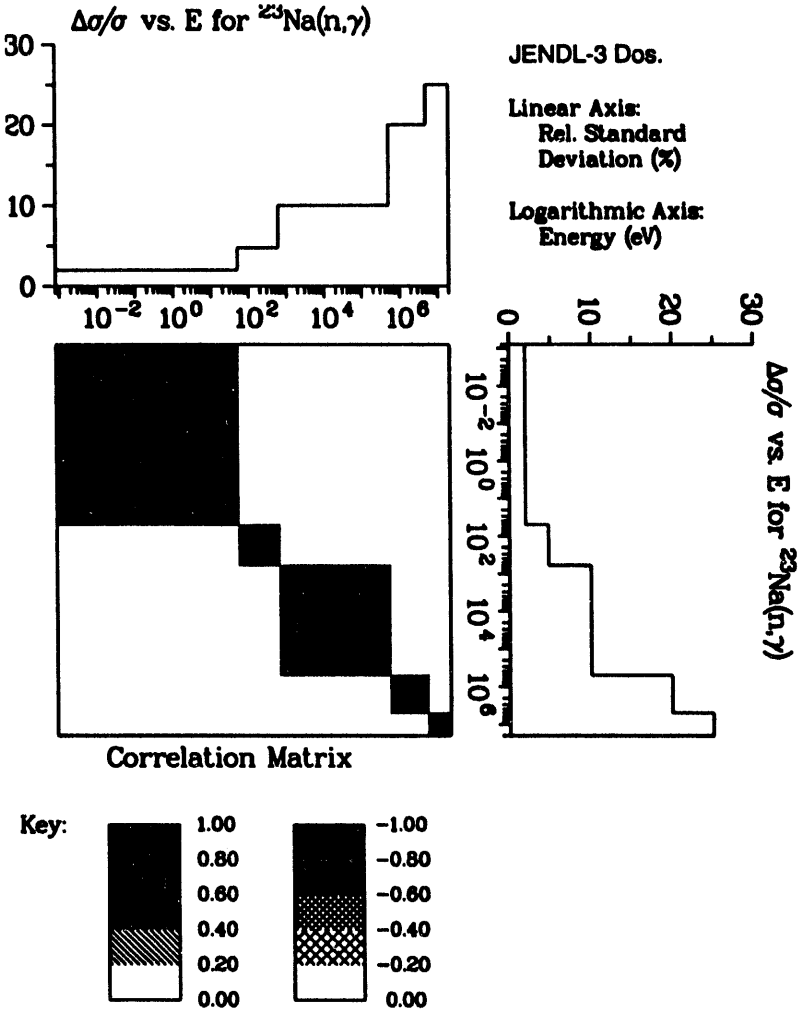

Covariance data for $^{23}Na(n,\gamma)$ with $^{23}Na(n,\gamma)$.

Figure B-8a: $^{23}Na(n,\gamma)^{24}Na$ Covariance Matrix

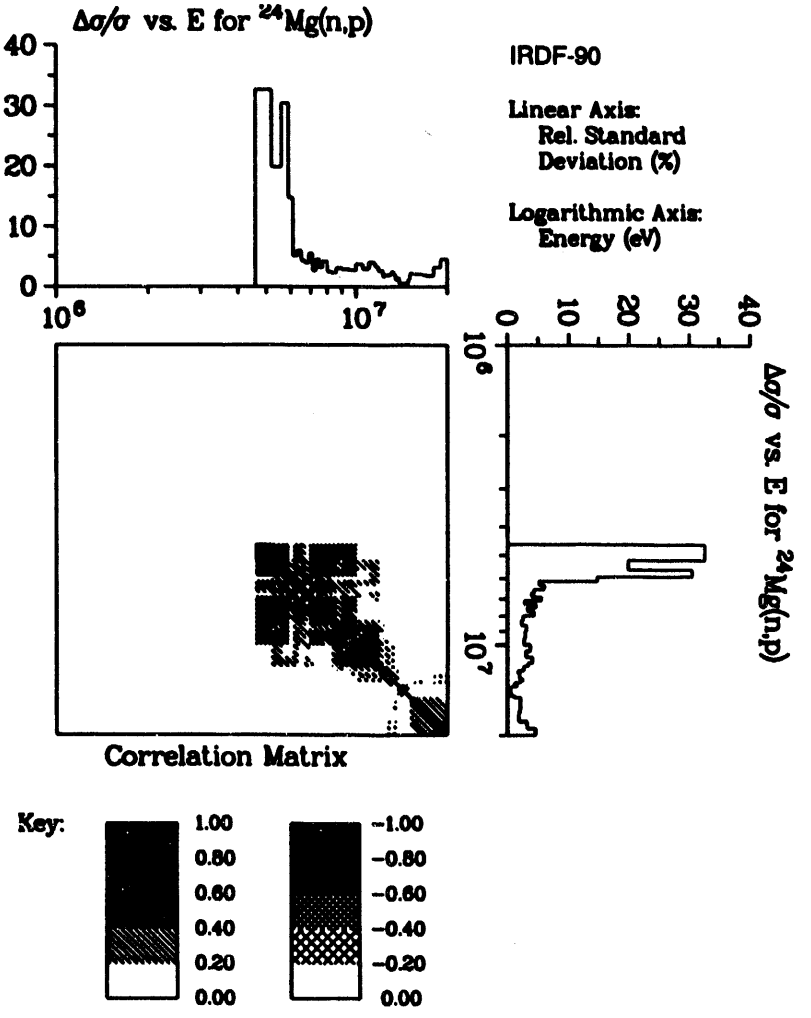

Covariance data for $^{24}Mg(n,p)$ with $^{24}Mg(n,p)$.

Figure B-9: $^{24}Mg(n,p)^{24}Na$ Covariance Matrix

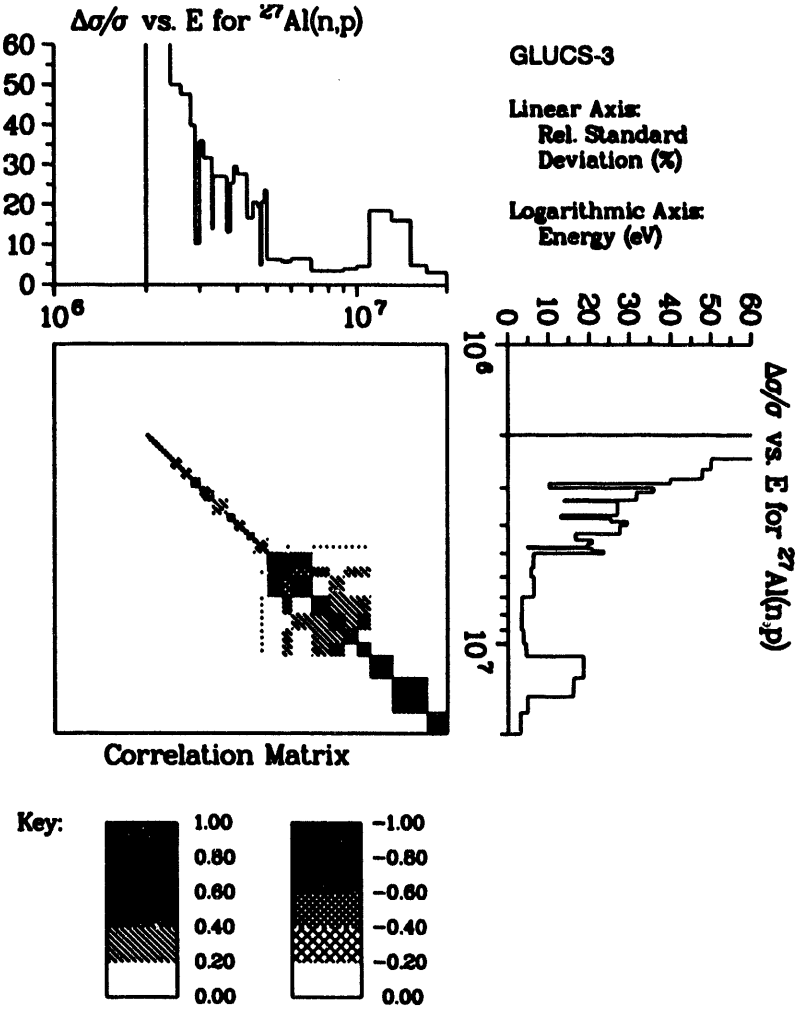

Covariance data for ^{27}Al(n,p) with ^{27}Al(n,p).

Figure B-10: ^{27}Al(n,p)^{27}Mg Covariance Matrix

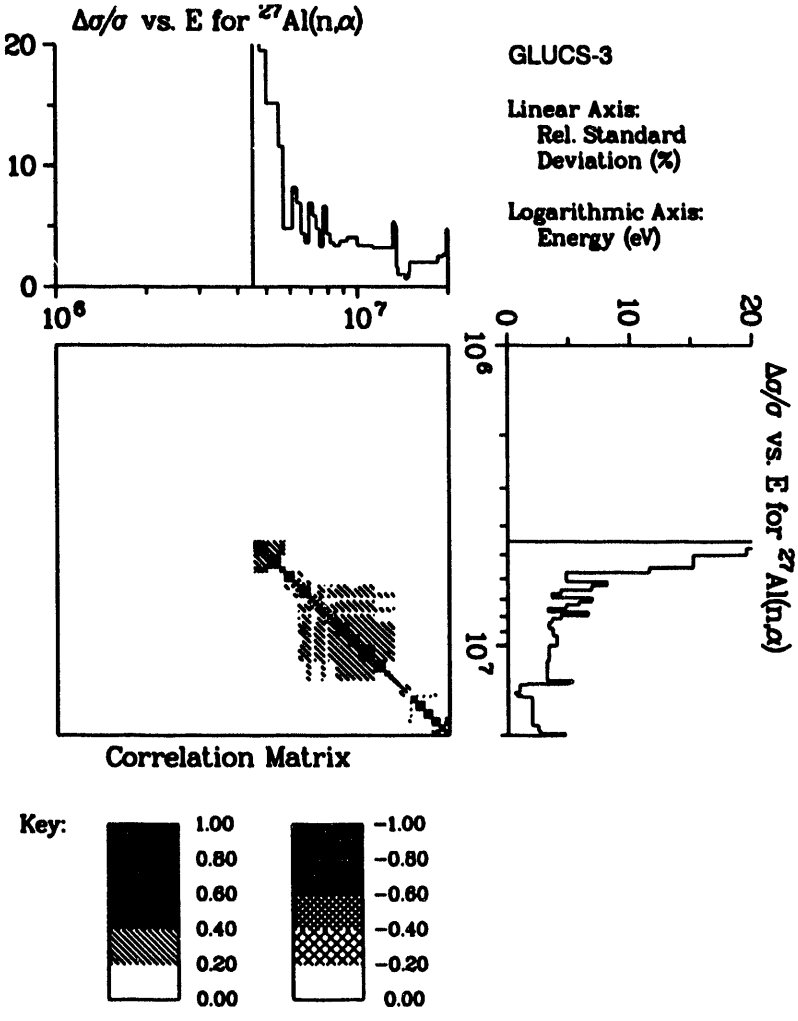

Covariance data for $^{27}Al(n,\alpha)$ with $^{27}Al(n,\alpha)$.

Figure B-11: $^{27}Al(n,\alpha)^{24}Na$ Covariance Matrix

No current cross section library includes covariance data all of the important displacement reactions on ^{Nat}Si. When the data becomes available, an attempt will be made to propagate the covariance information through the displacement kerma

Figure B-12: $^{Nat}Si(n,X)1MeV$ Covariance Matrix

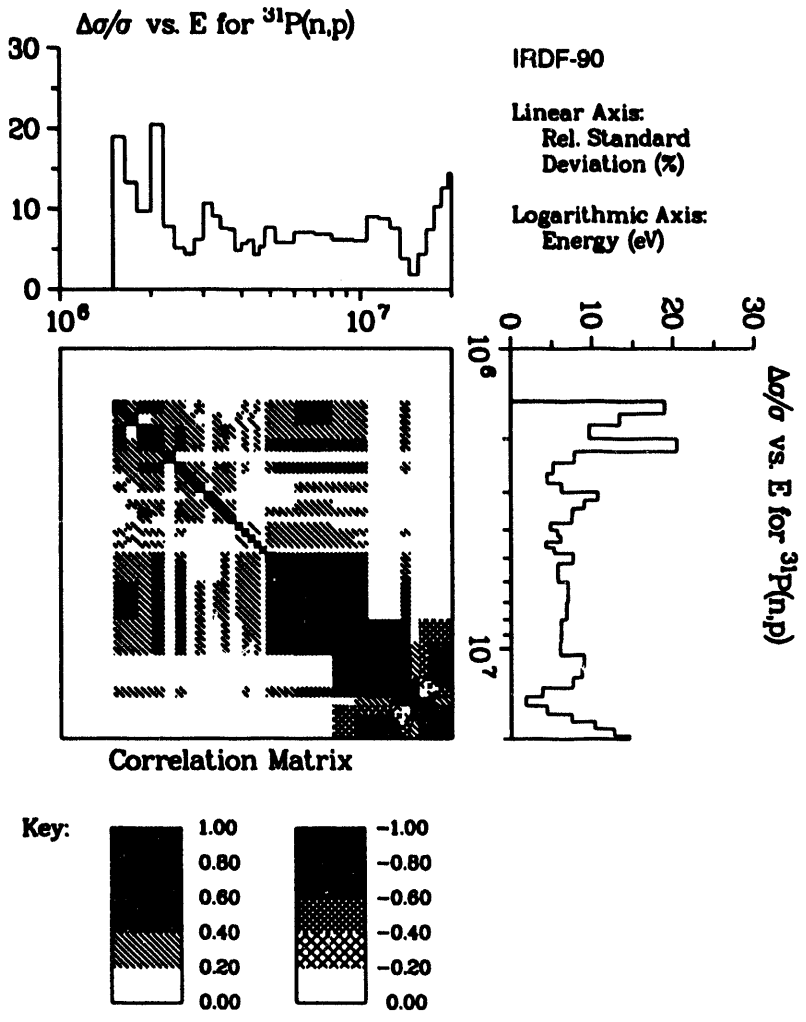

Covariance data for $^{31}P(n,p)$ with $^{31}P(n,p)$.

Figure B-13: $^{31}P(n,p)^{31}Si$ Covariance Matrix

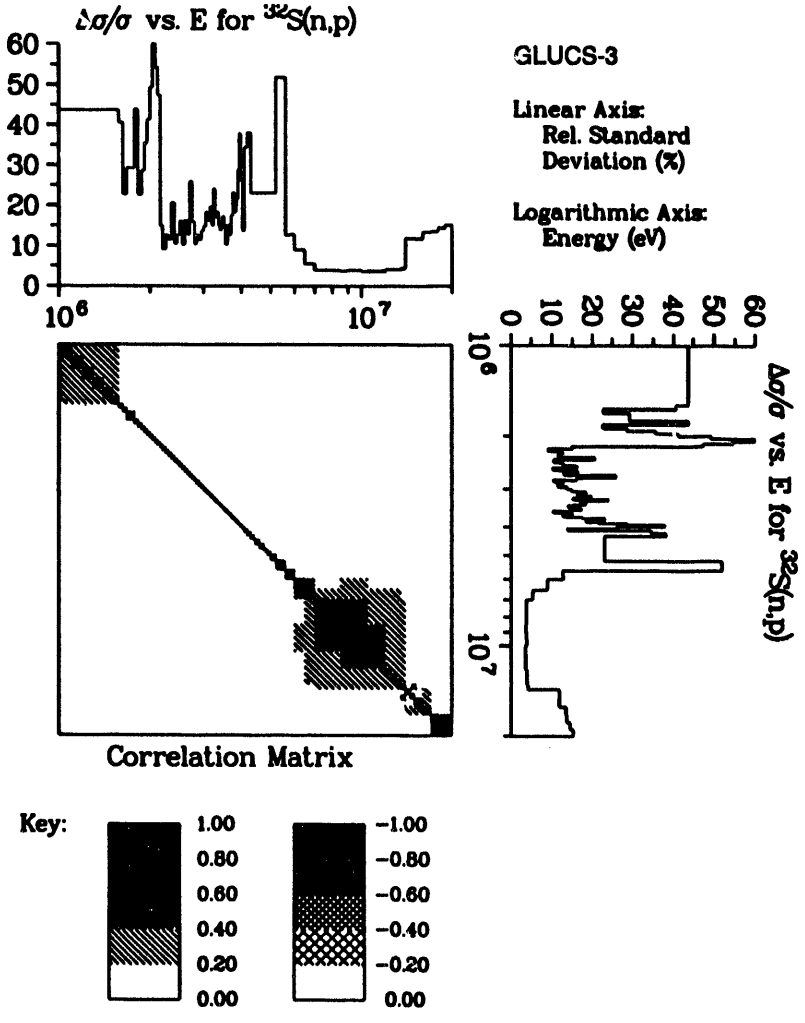

Covariance data for $^{32}S(n,p)$ with $^{32}S(n,p)$.

Figure B-14: $^{32}S(n,p)^{32}P$ Covariance Matrix

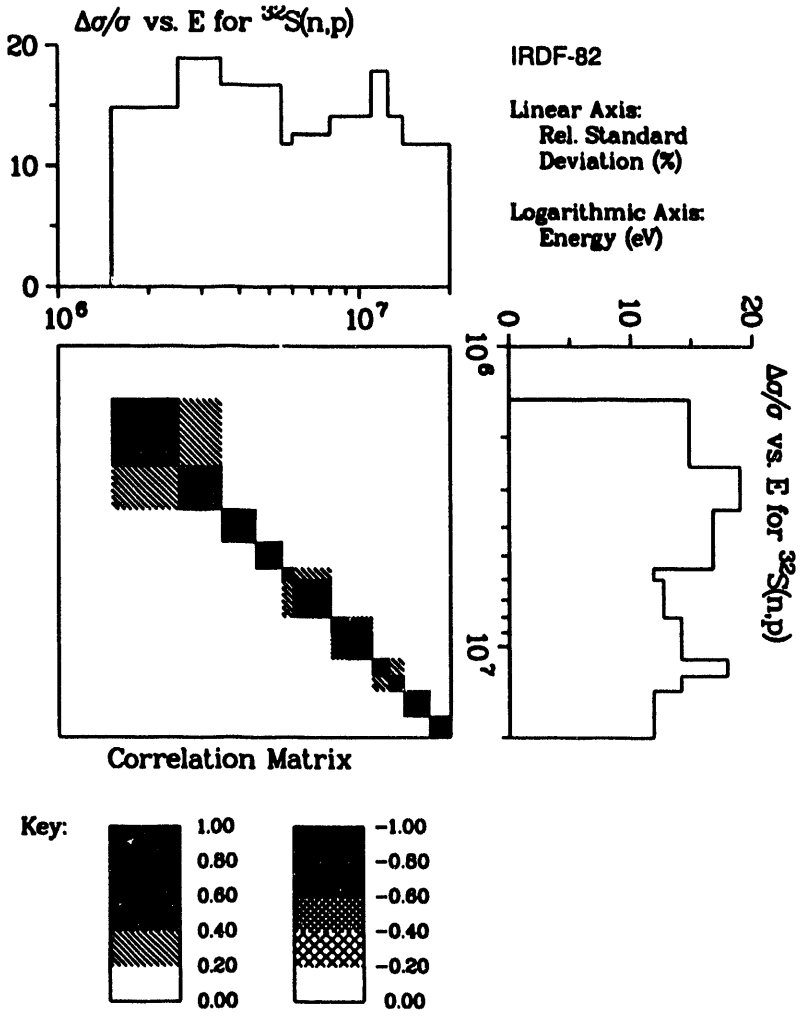

Covariance data for $^{32}S(n,p)$ with $^{32}S(n,p)$.

Figure B-14a: Previous $^{32}S(n,p)^{32}P$ Covariance Matrix

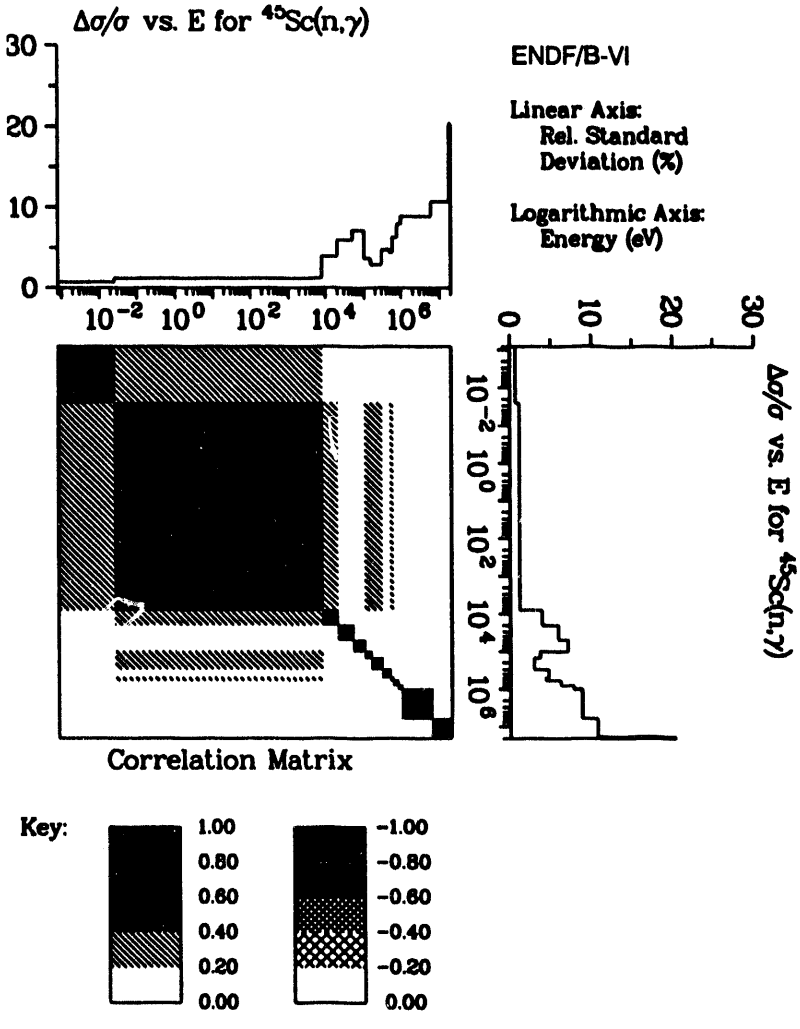

Covariance data for $^{45}Sc(n,\gamma)$ with $^{45}Sc(n,\gamma)$.

Figure B-15: $^{45}Sc(n,\gamma)^{46}Sc$ Covariance Matrix

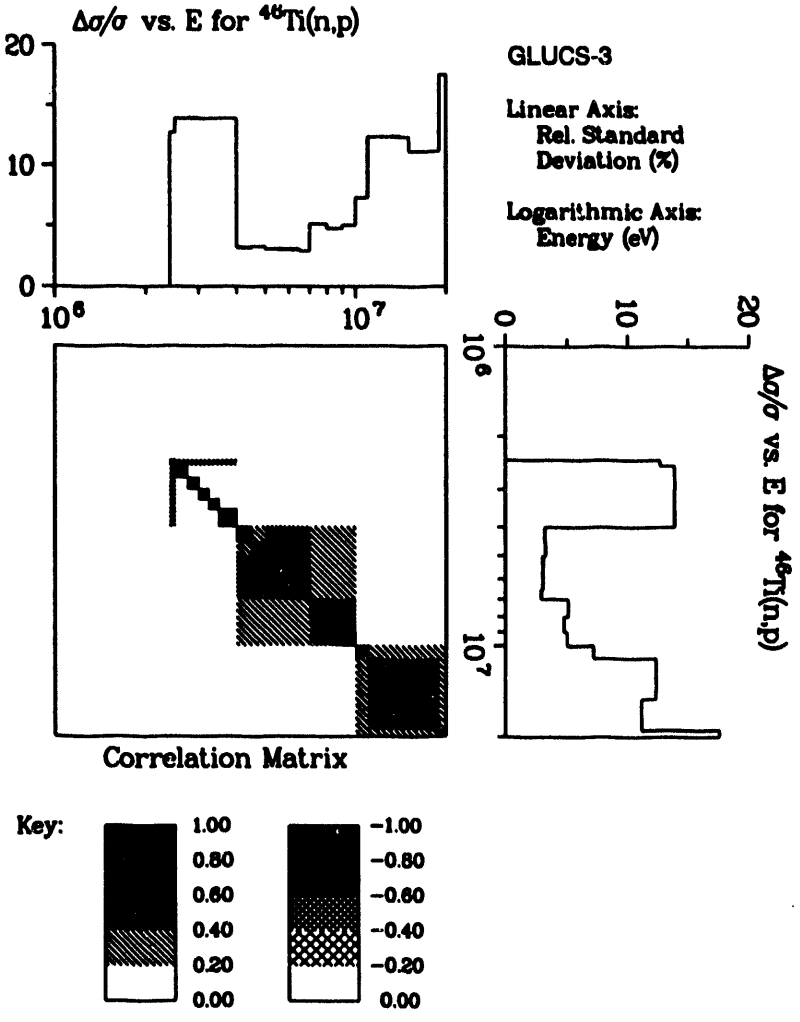

Covariance data for ^{46}Ti(n,p) with ^{46}Ti(n,p).

Figure B-16: ^{46}Ti(n,p)^{46}Sc Covariance Matrix

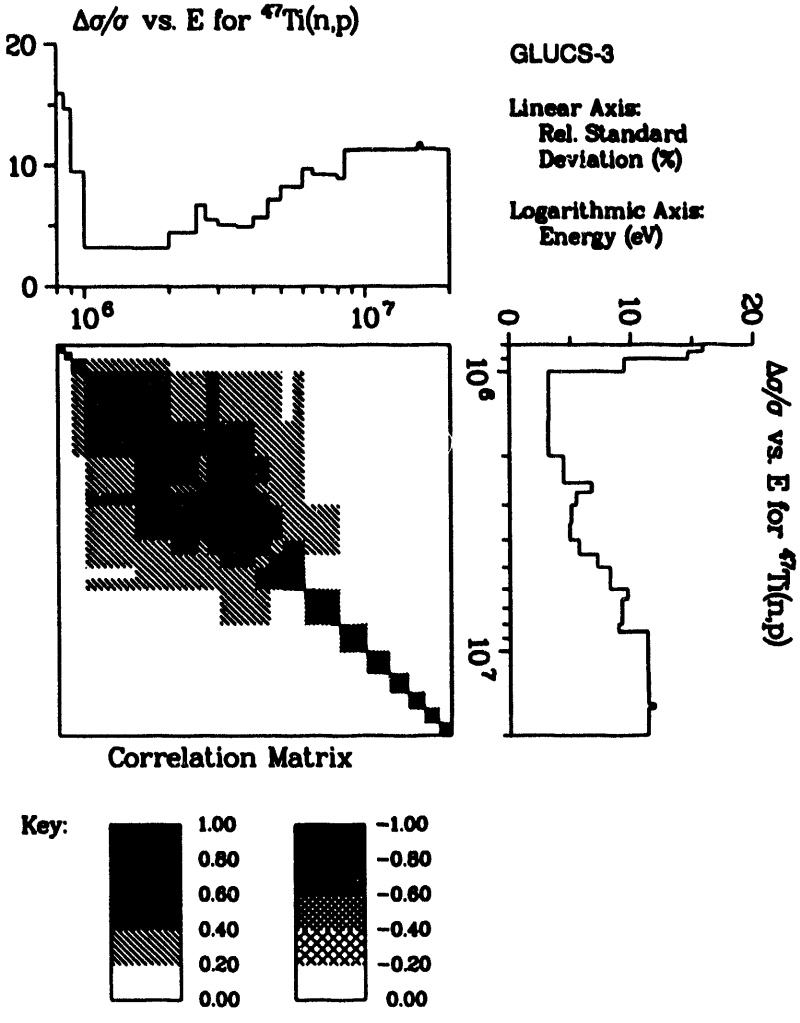

Covariance data for ^{47}Ti(n,p) with ^{47}Ti(n,p).

Figure B-17: ^{47}Ti(n,p)^{47}Sc Covariance Matrix

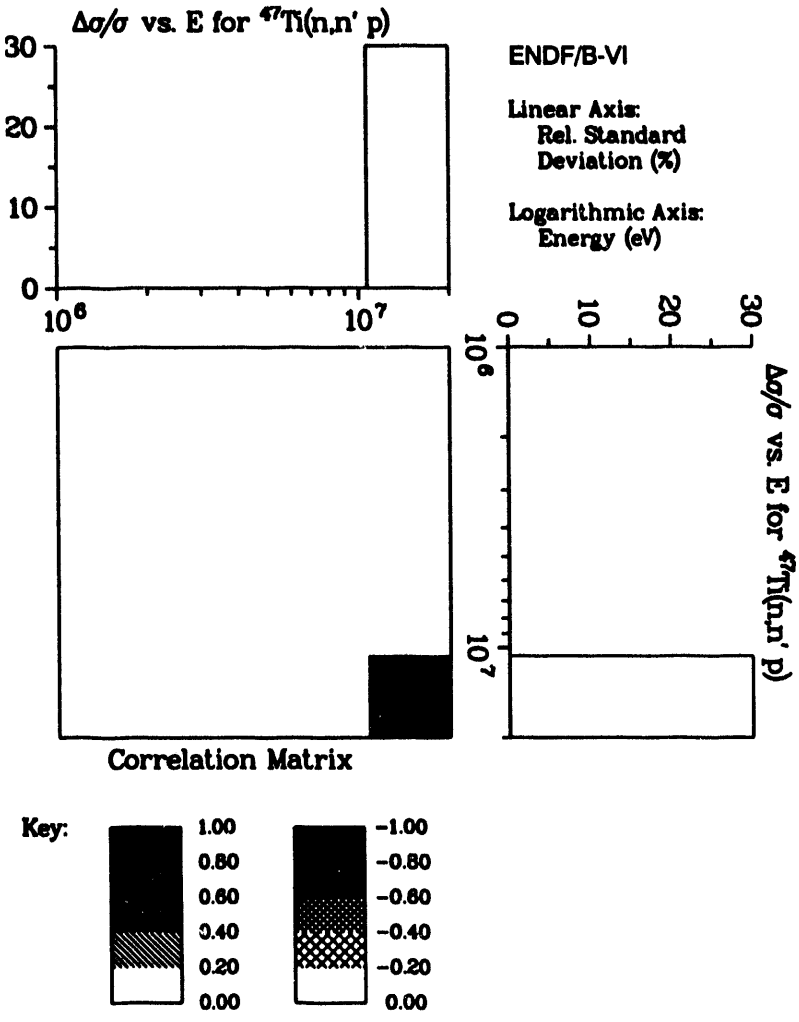

Covariance data for ^{47}Ti(n,n' p) with ^{47}Ti(n,n' p).

Figure B-18: ^{47}Ti(n,np)^{46}Sc Covariance Matrix

No current covariance data exists for this reaction. The covariance data for the separate titanium reaction can be combined (assuming no cross correlation in the reactions cross section evaluations) to obtain a $^{Nat}Ti(n,X)^{46}Sc$ covariance matrix. This will be done at a later time. The current version of the SNLRML cross section compendium leaves this covariance matrix empty.

Figure B-19: $^{Nat}Ti(n,X)^{46}Sc$ Covariance Matrix

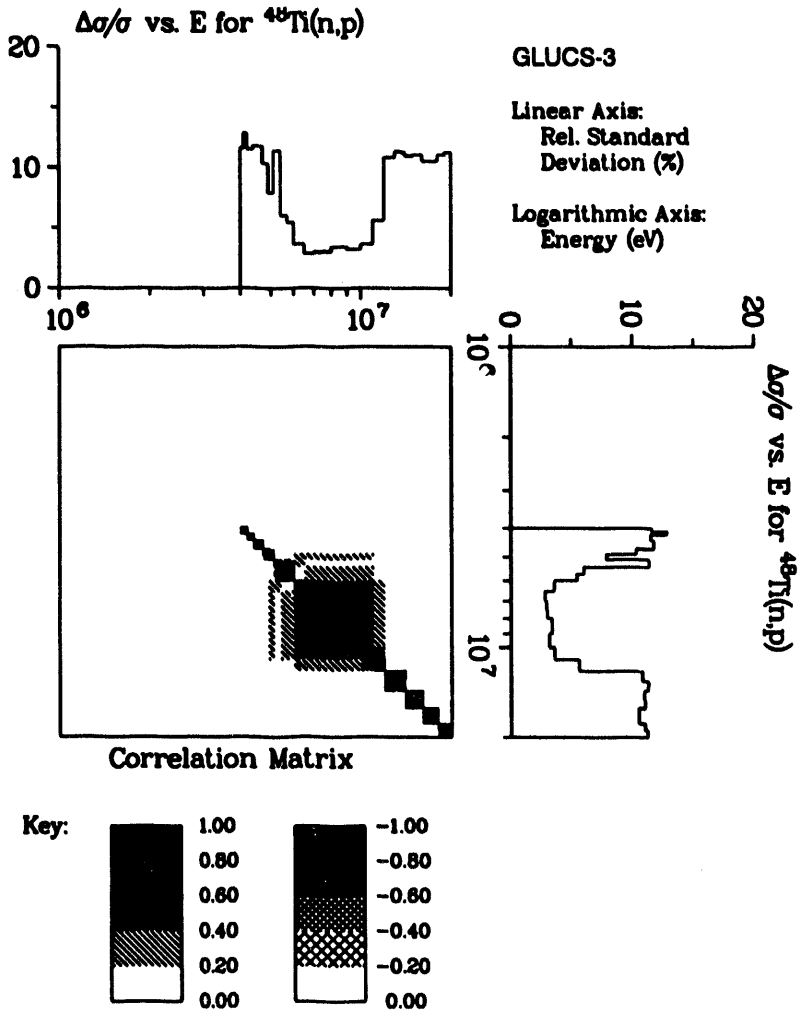

Covariance data for ^{48}Ti(n,p) with ^{48}Ti(n,p).

Figure B-20: ^{48}Ti(n,p)^{48}Sc Covariance Matrix

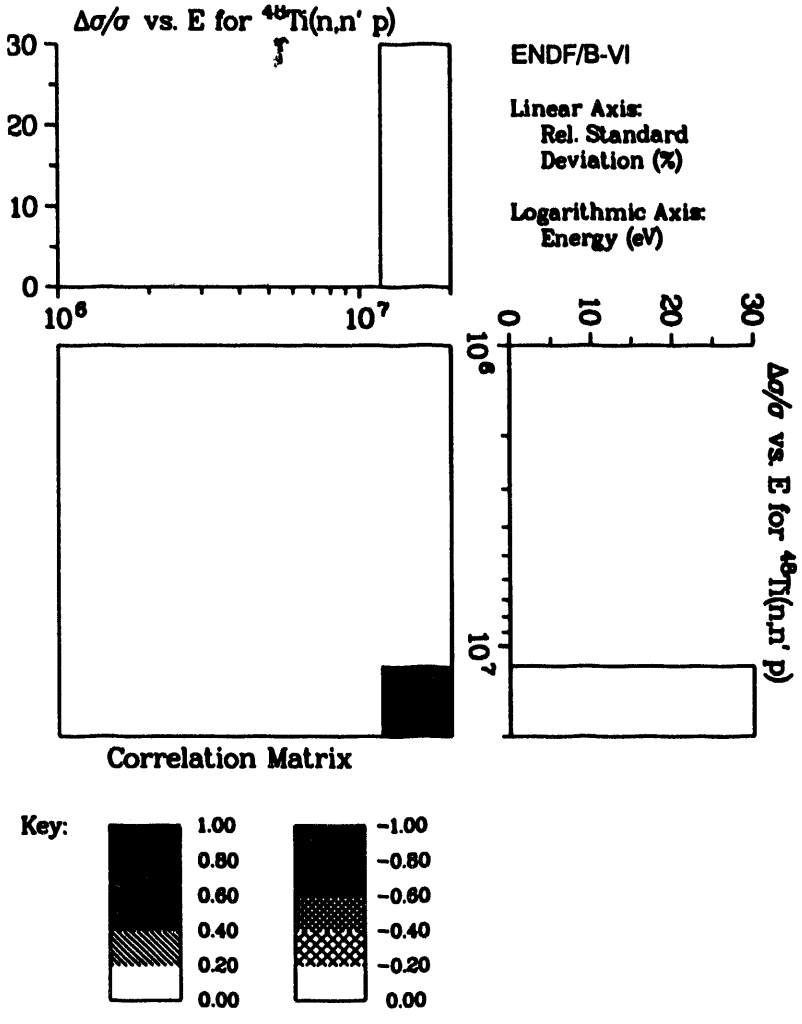

Covariance data for ^{48}Ti(n,n' p) with ^{48}Ti(n,n' p).

Figure B-21: ^{48}Ti(n,np)^{47}Sc Covariance Matrix

No current covariance data exists for this reaction. The covariance data for the separate titanium reaction can be combined (assuming no cross correlation in the reactions cross section evaluations) to obtain a $^{Nat}Ti(n,X)^{47}Sc$ covariance matrix. This will be done at a later time. The current version of the SNLRML cross section compendium leaves this covariance matrix empty.

Figure B-22: $^{Nat}Ti(n,X)^{47}Sc$ Covariance Matrix

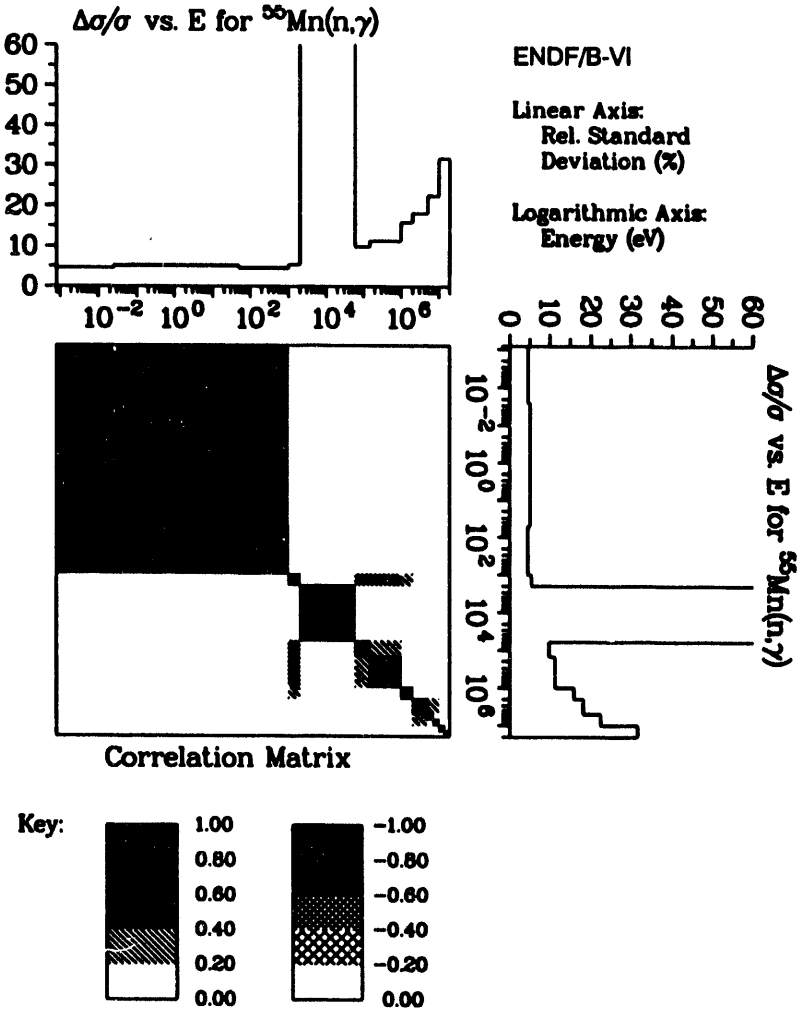

Covariance data for $^{55}Mn(n,\gamma)$ with $^{55}Mn(n,\gamma)$.

Figure B-23: $^{55}Mn(n,\gamma)^{56}Mn$ Covariance Matrix

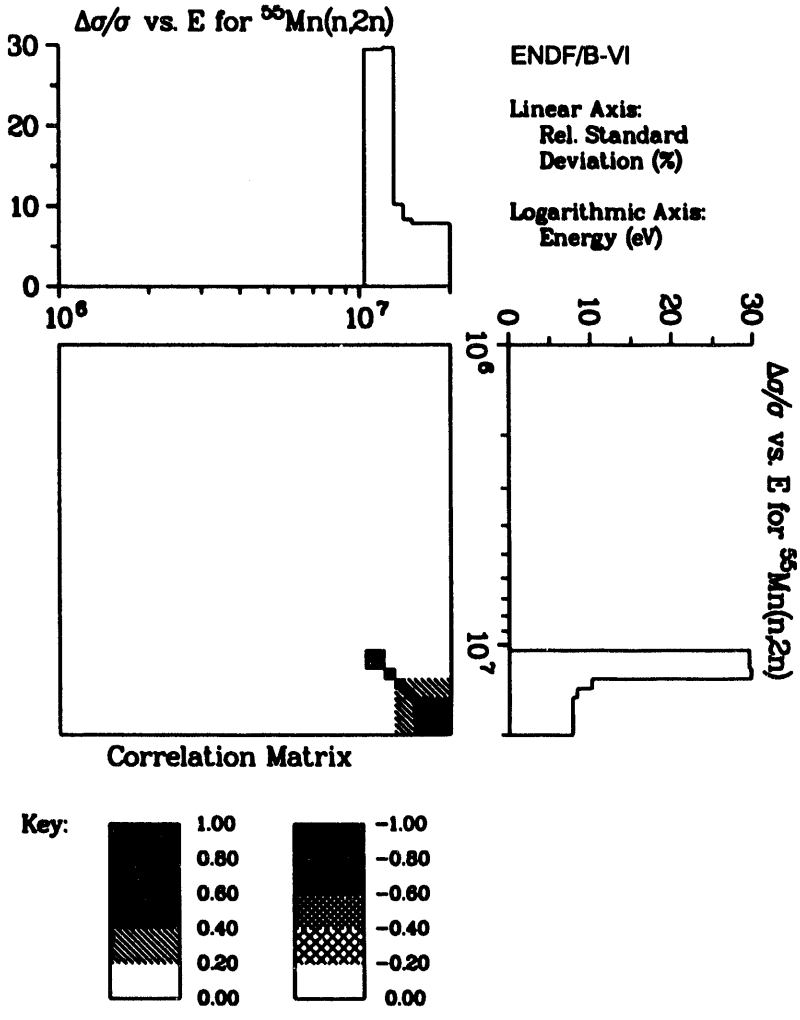

Covariance data for ^{55}Mn(n,2n) with ^{55}Mn(n,2n).

Figure B-24: ^{55}Mn(n,2n)^{54}Mn Covariance Matrix

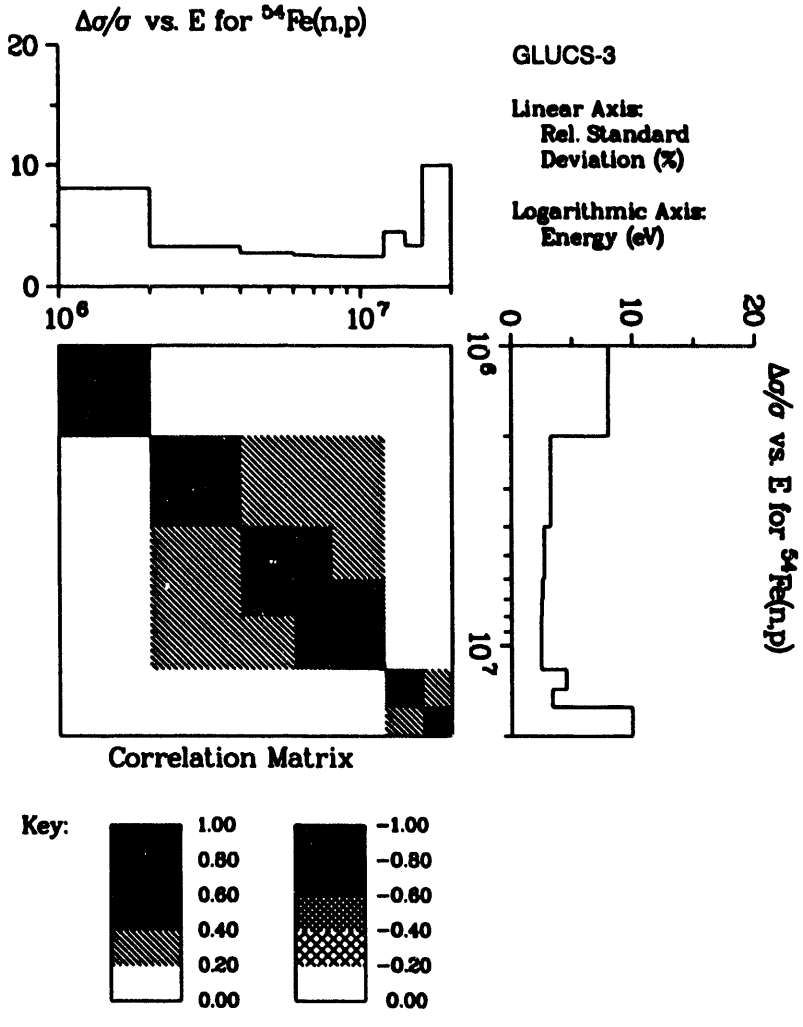

Covariance data for $^{54}Fe(n,p)$ with $^{54}Fe(n,p)$.

Figure B-25: $^{54}Fe(n,p)^{54}Mn$ Covariance Matrix

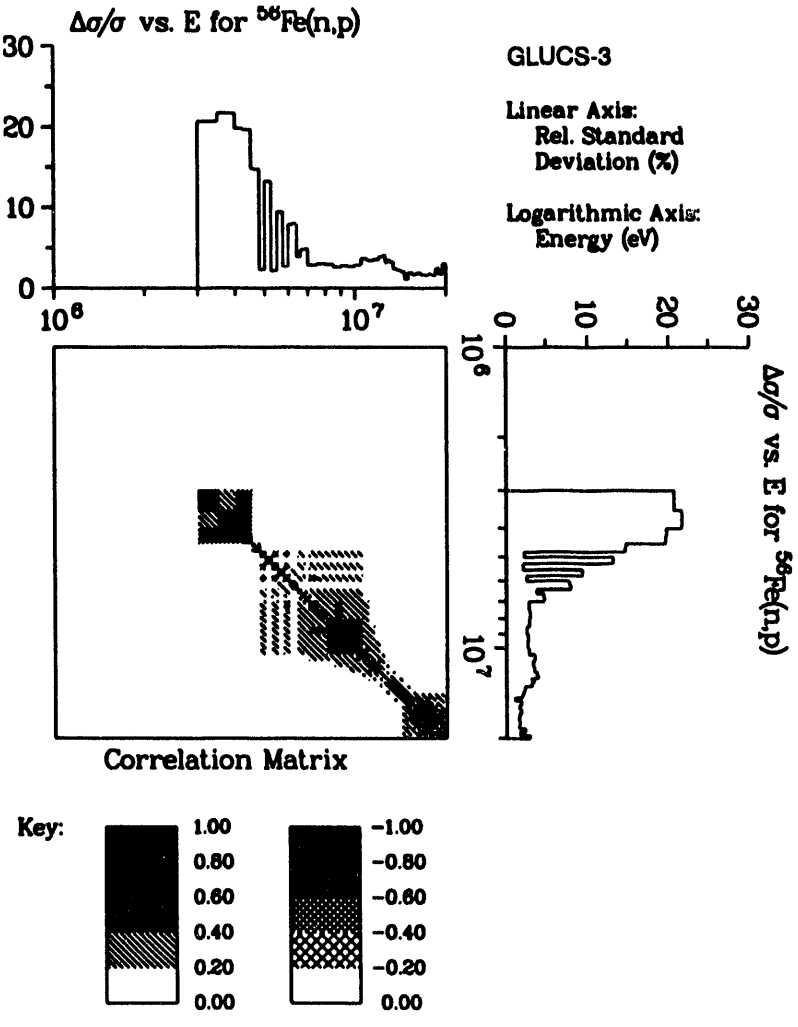

Covariance data for ^{56}Fe(n,p) with ^{56}Fe(n,p).

Figure B-26: ^{56}Fe(n,p)^{56}Mn Covariance Matrix

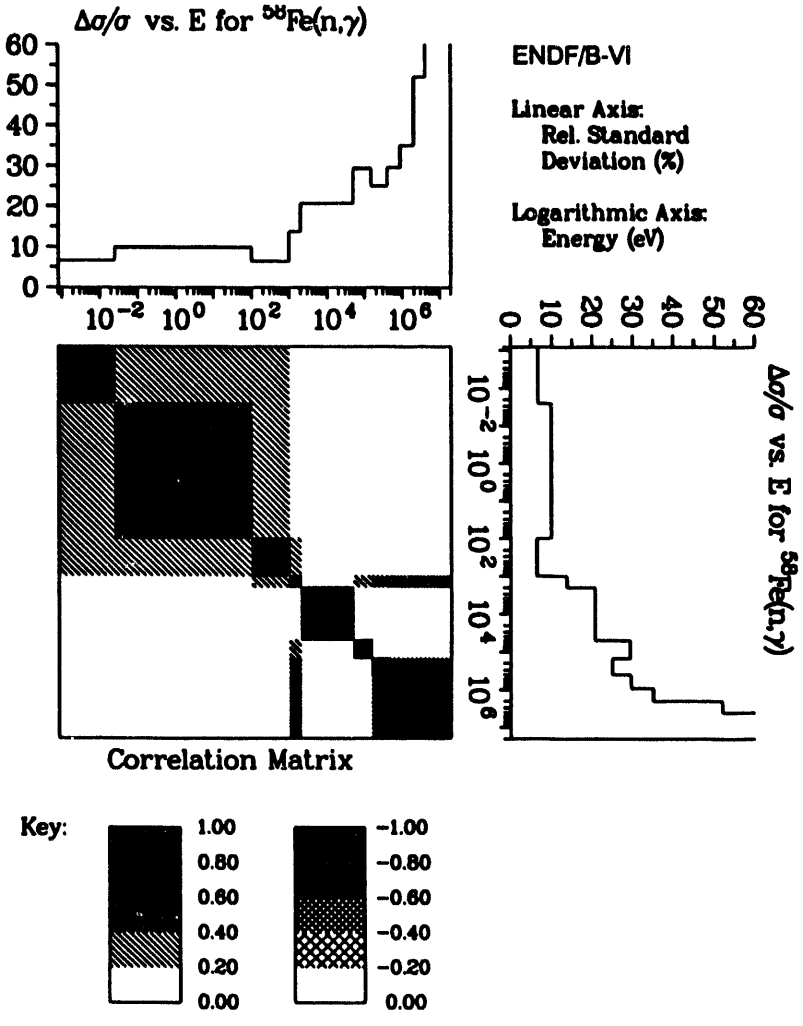

Covariance data for $^{58}Fe(n,\gamma)$ with $^{58}Fe(n,\gamma)$.

Figure B-27: $^{58}Fe(n,\gamma)^{59}Fe$ Covariance Matrix

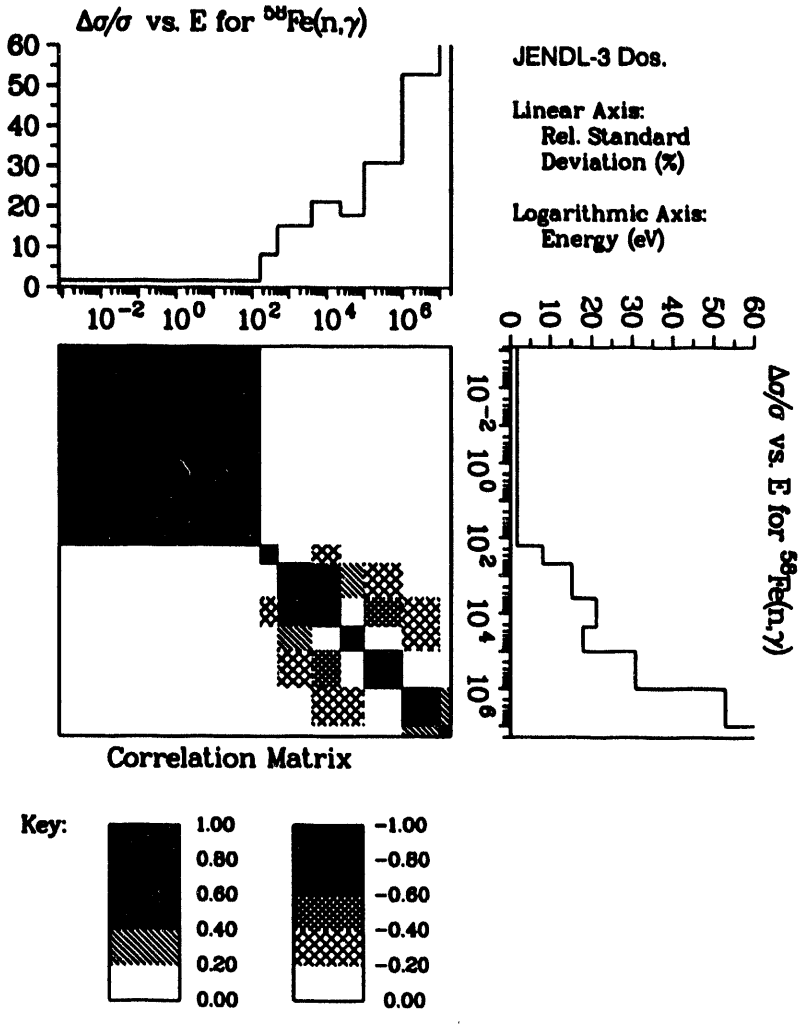

Covariance data for $^{58}Fe(n,\gamma)$ with $^{58}Fe(n,\gamma)$.

Figure B-27a: $^{58}Fe(n,\gamma)^{59}Fe$ Covariance Matrix

No current cross section library includes covariance data on ^{Nat}Fe(n,X)dpa. Since this quantity is generally treated as an exposure parameter, a covariance matrix is not appropriate. The covariance should relate the exposure parameter to a specific damage mechanism/measure.

Figure B-28: ^{Nat}Fe(n,X)dpa Covariance Matrix

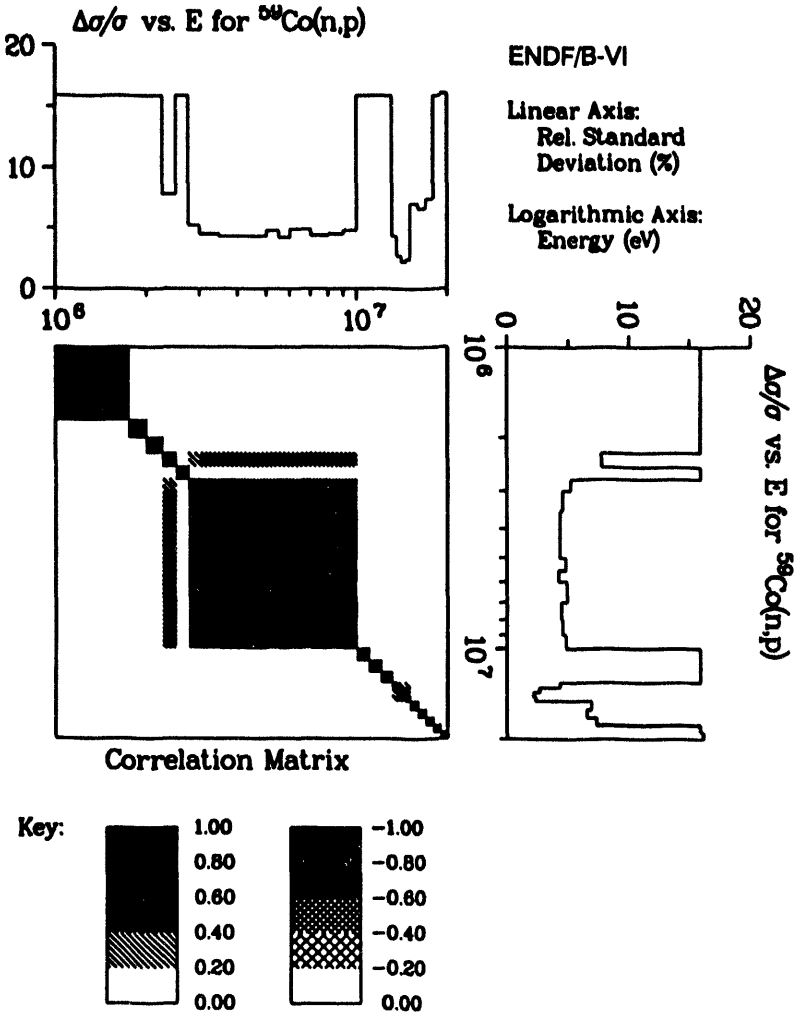

Covariance data for ^{59}Co(n,p) with ^{59}Co(n,p).

Figure B-29: ^{59}Co(n,p)^{59}Fe Covariance Matrix

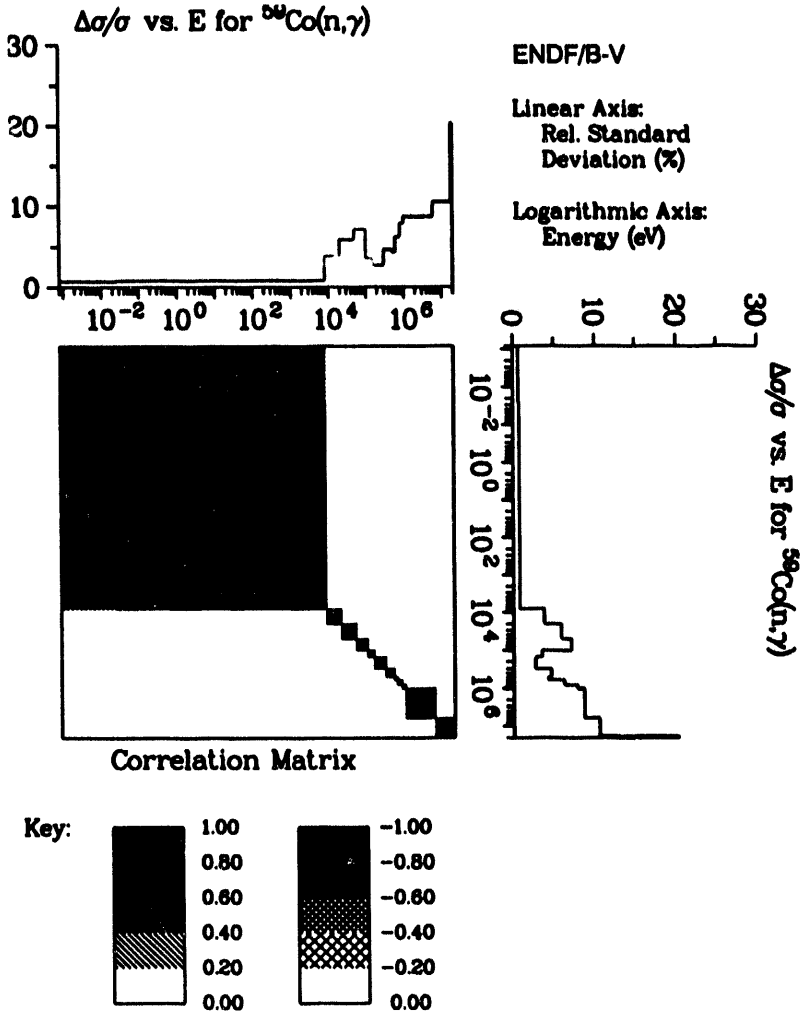

Covariance data for $^{59}Co(n,\gamma)$ with $^{59}Co(n,\gamma)$.

Figure B-30: $^{59}Co(n,\gamma)^{60}Co$ Covariance Matrix

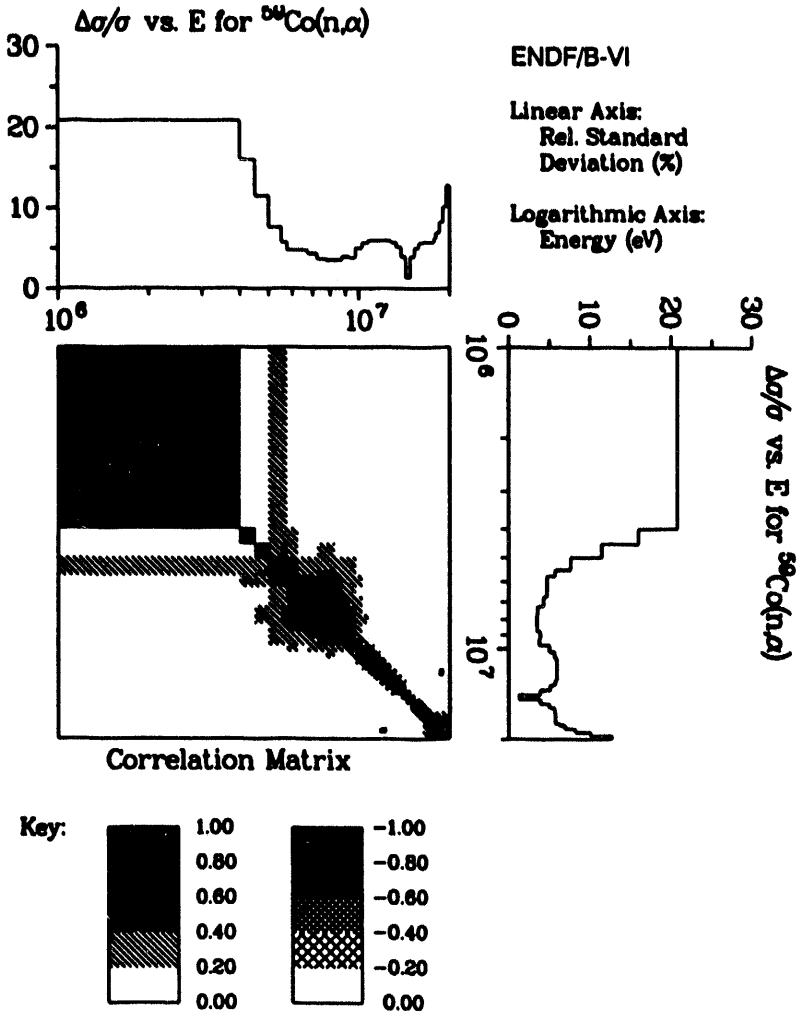

Covariance data for $^{59}Co(n,\alpha)$ with $^{59}Co(n,\alpha)$.

Figure B-31: $^{59}Co(n,\alpha)^{56}Mn$ Covariance Matrix

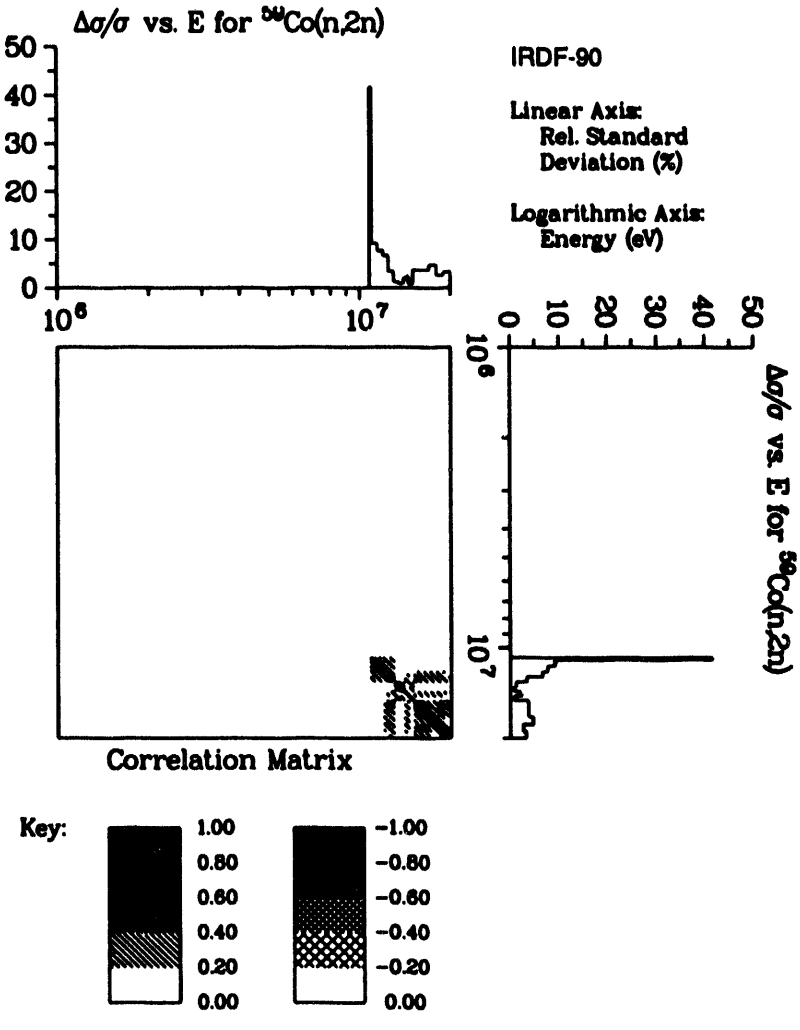

Covariance data for ^{59}Co(n,2n) with ^{59}Co(n,2n).

Figure B-32: ^{59}Co(n,2n)^{58}Co Covariance Matrix

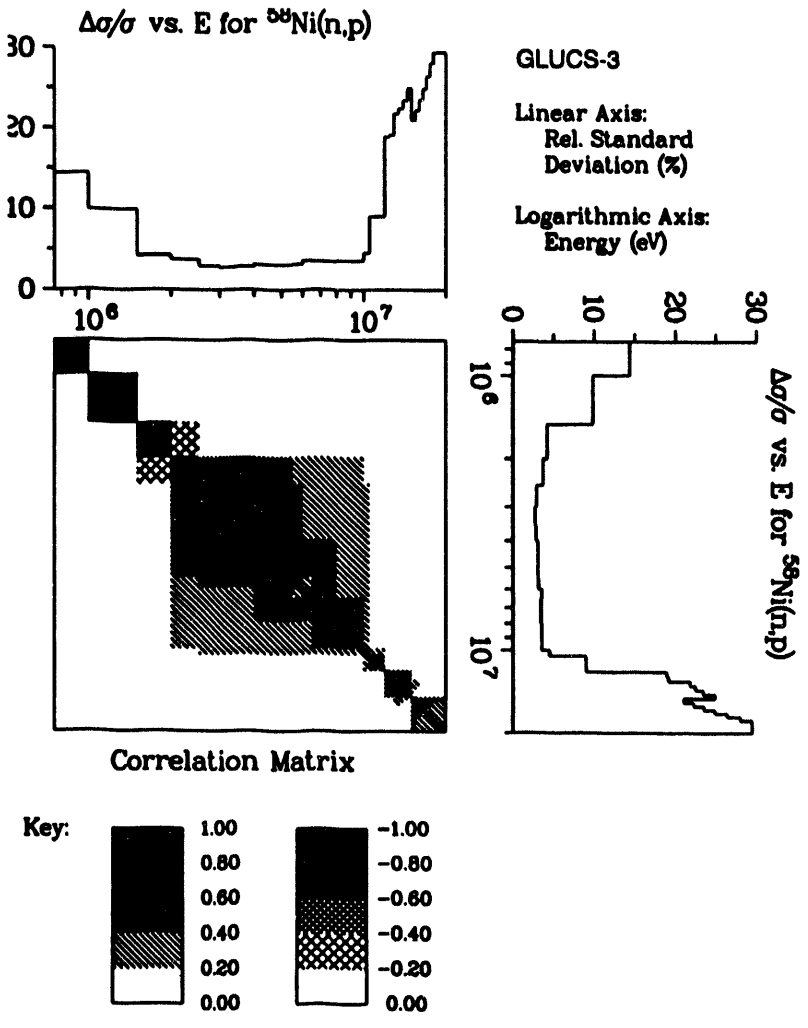

Covariance data for ^{58}Ni(n,p) with ^{58}Ni(n,p).

Figure B-33: ^{58}Ni(n,p)^{58}Co Covariance Matrix

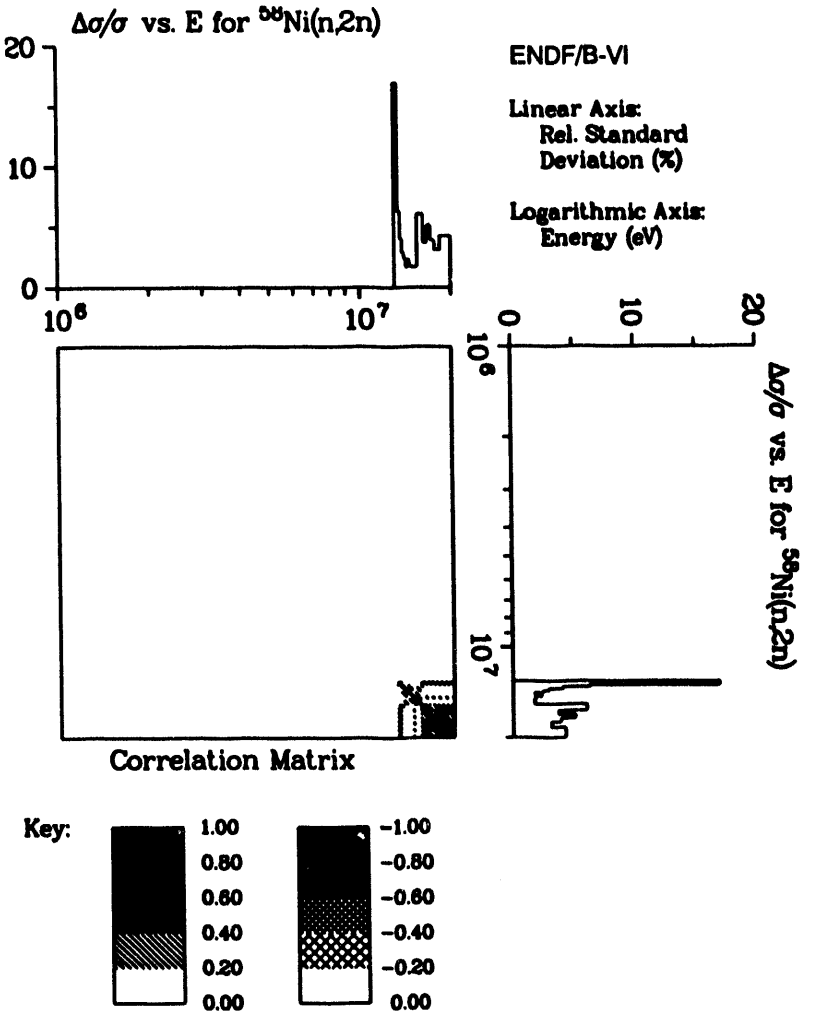

Covariance data for ^{58}Ni(n,2n) with ^{58}Ni(n,2n).

Figure B-34: ^{58}Ni(n,2n)^{57}Ni Covariance Matrix

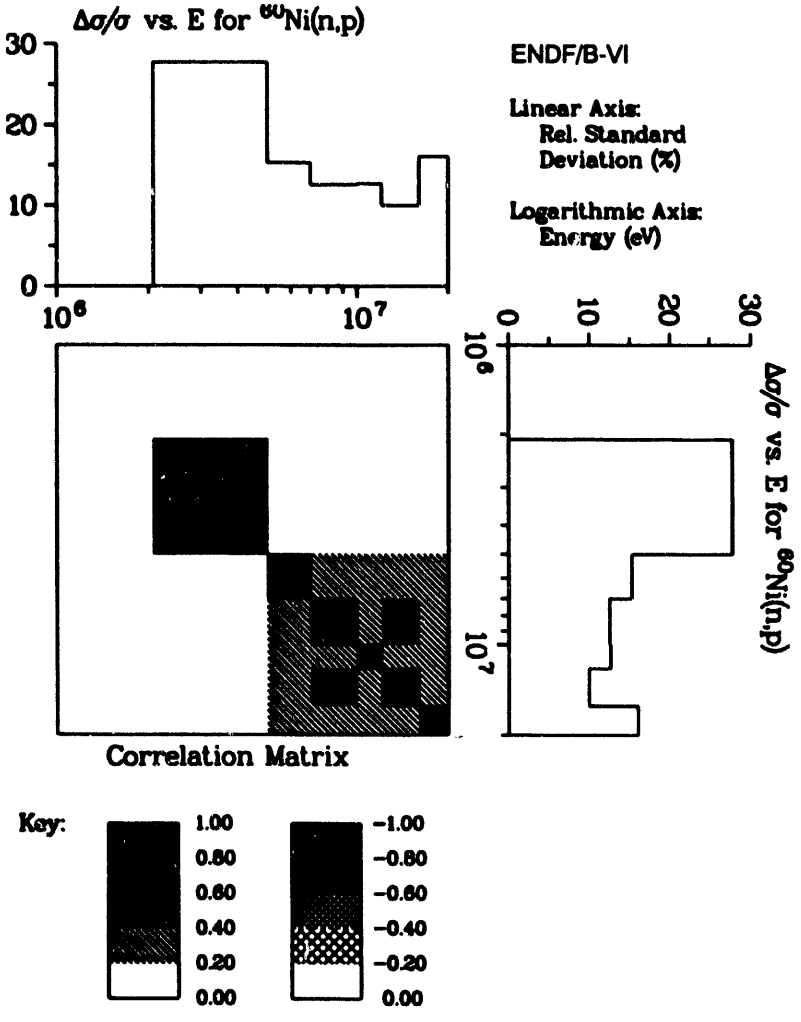

Covariance data for ^{60}Ni(n,p) with ^{60}Ni(n,p).

Figure B-35: ^{60}Ni(n,p)^{60}Co Covariance Matrix

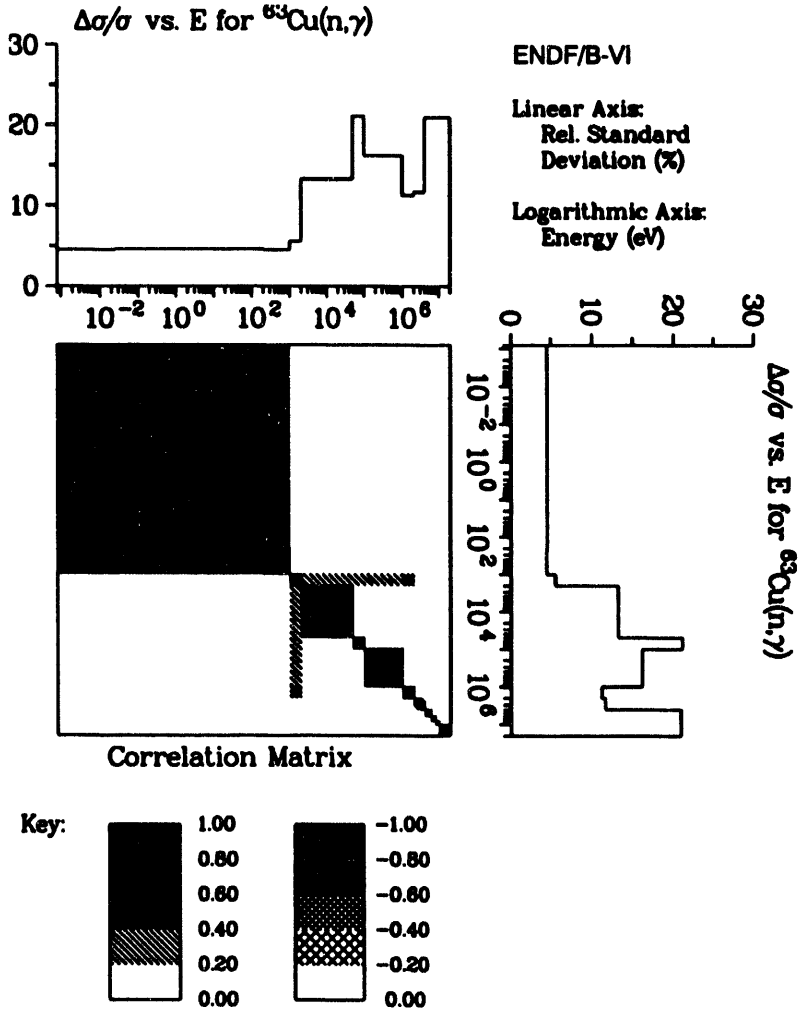

Covariance data for $^{63}Cu(n,\gamma)$ with $^{63}Cu(n,\gamma)$.

Figure B-36: $^{63}Cu(n,\gamma)^{64}Cu$ Covariance Matrix

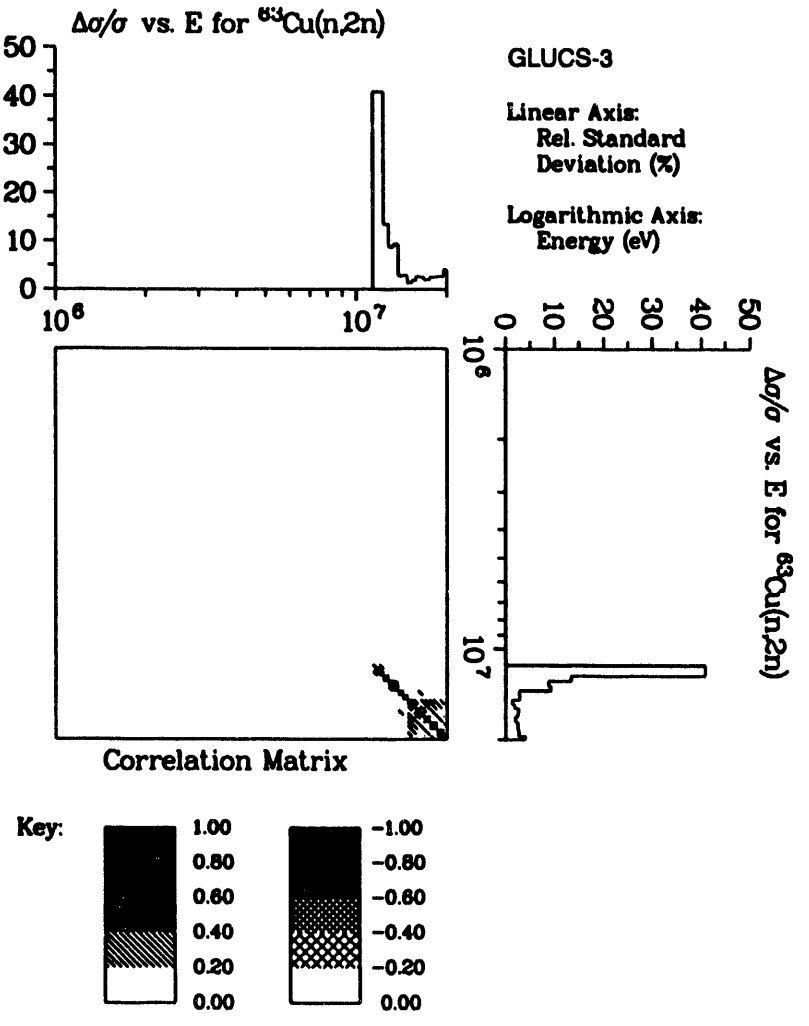

Covariance data for $^{63}Cu(n,2n)$ with $^{63}Cu(n,2n)$.

Figure B-37: $^{63}Cu(n,2n)^{62}Cu$ Covariance Matrix

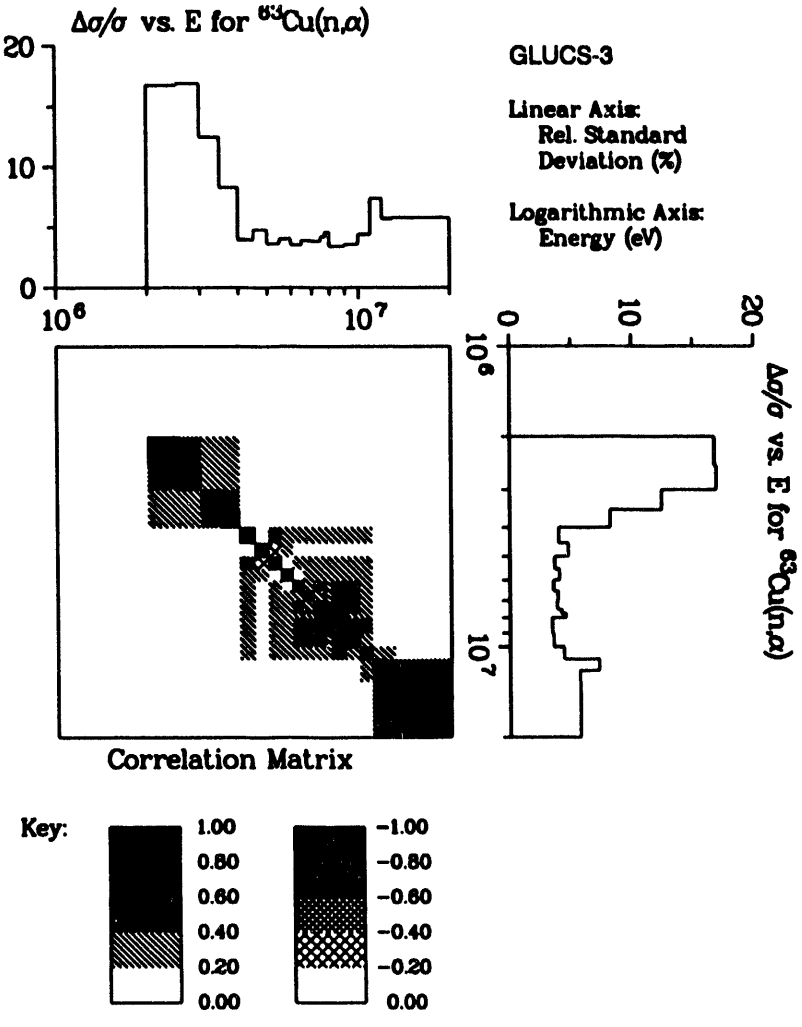

Covariance data for $^{63}Cu(n,\alpha)$ with $^{63}Cu(n,\alpha)$.

Figure B-38: $^{63}Cu(n,\alpha)^{60}Co$ Covariance Matrix

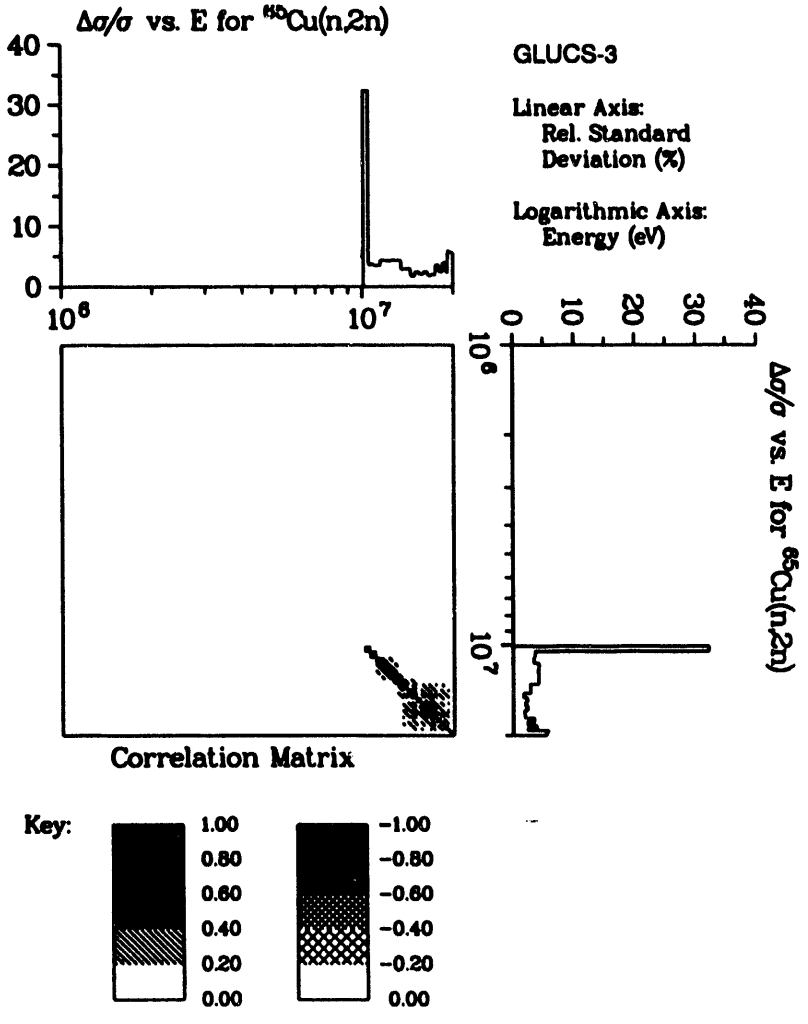

Covariance data for $^{65}Cu(n,2n)$ with $^{65}Cu(n,2n)$.

Figure B-39: $^{65}Cu(n,2n)^{64}Cu$ Covariance Matrix

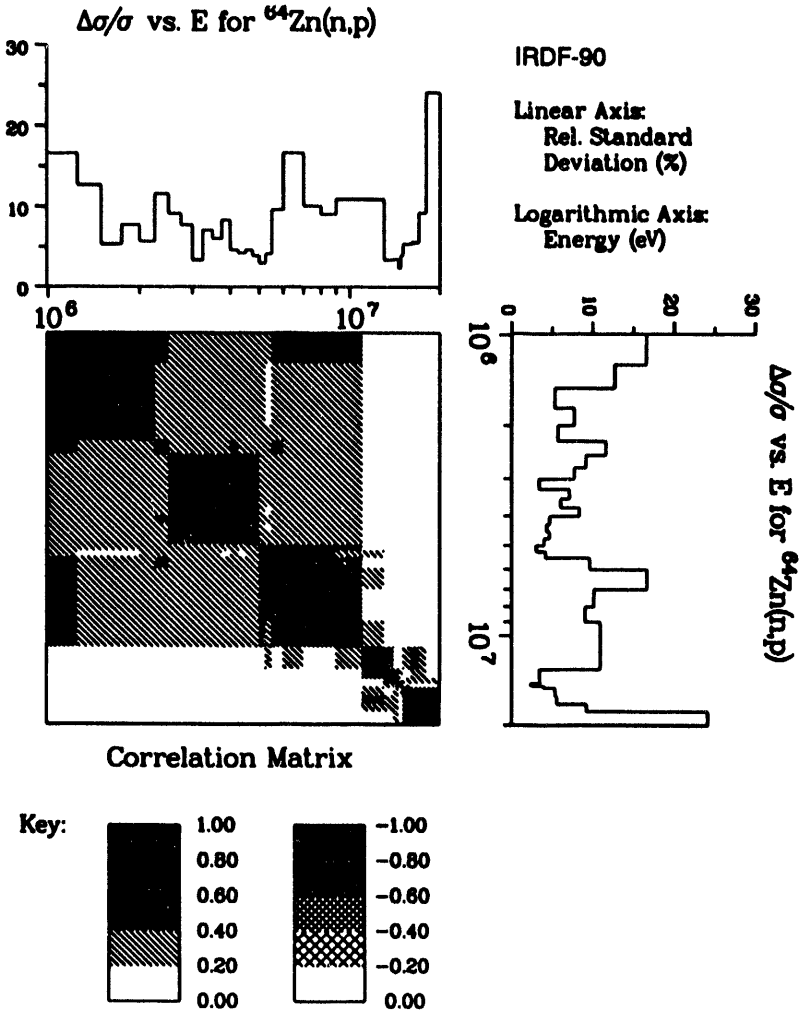

Covariance data for ^{64}Zn(n,p) with ^{64}Zn(n,p).

Figure B-40: ^{64}Zn(n,p)^{64}Cu Covariance Matrix

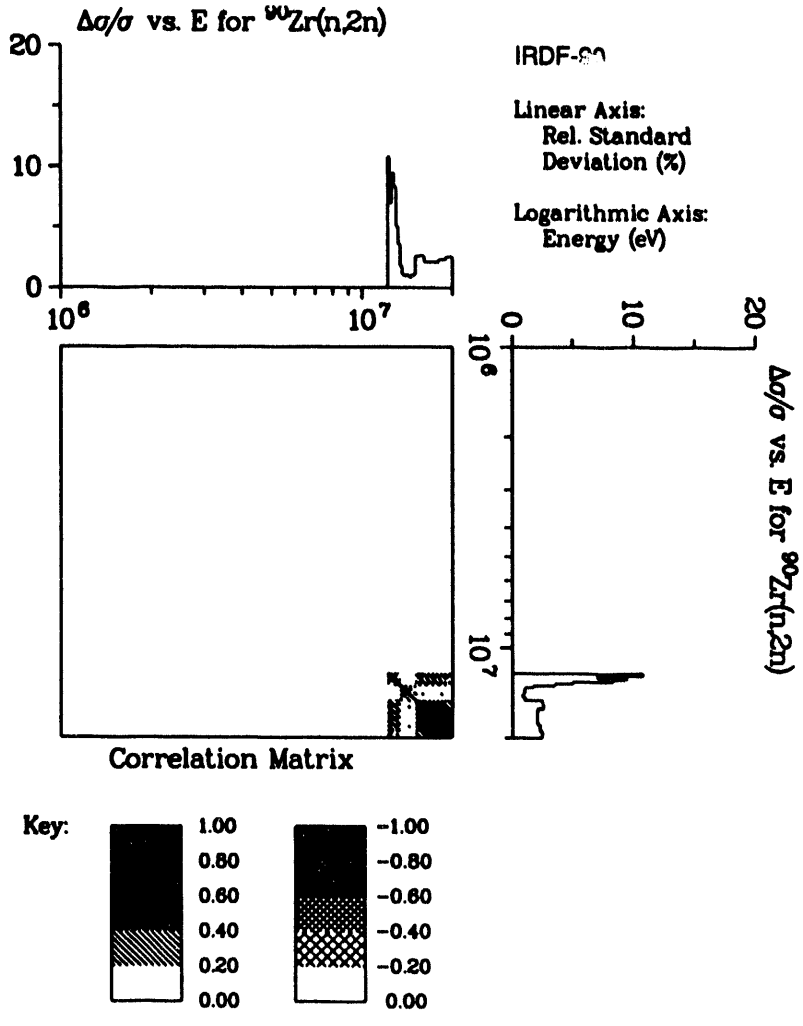

Covariance data for ^{90}Zr(n,2n) with ^{90}Zr(n,2n).

Figure B-41: ^{90}Zr(n,2n)^{89}Zr Covariance Matrix

No current cross section library includes covariance data all of the important displacement reactions on ^{Nat}Ga and ^{Nat}As. When the data becomes available, an attempt will be made to propagate the covariance information through the displacement damage function.

Figure B-42: GaAs(n,X)1MeV Covariance Matrix

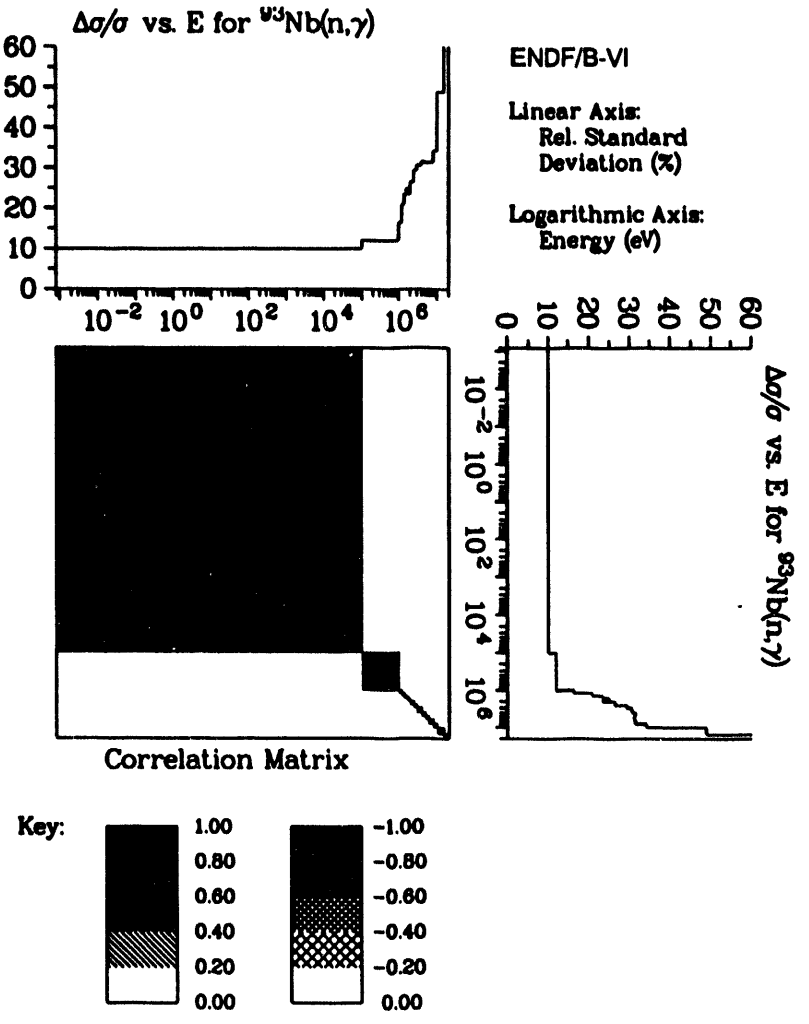

Covariance data for $^{93}Nb(n,\gamma)$ with $^{93}Nb(n,\gamma)$.

Figure B-43: $^{93}Nb(n,\gamma)^{94}Nb$ Covariance Matrix

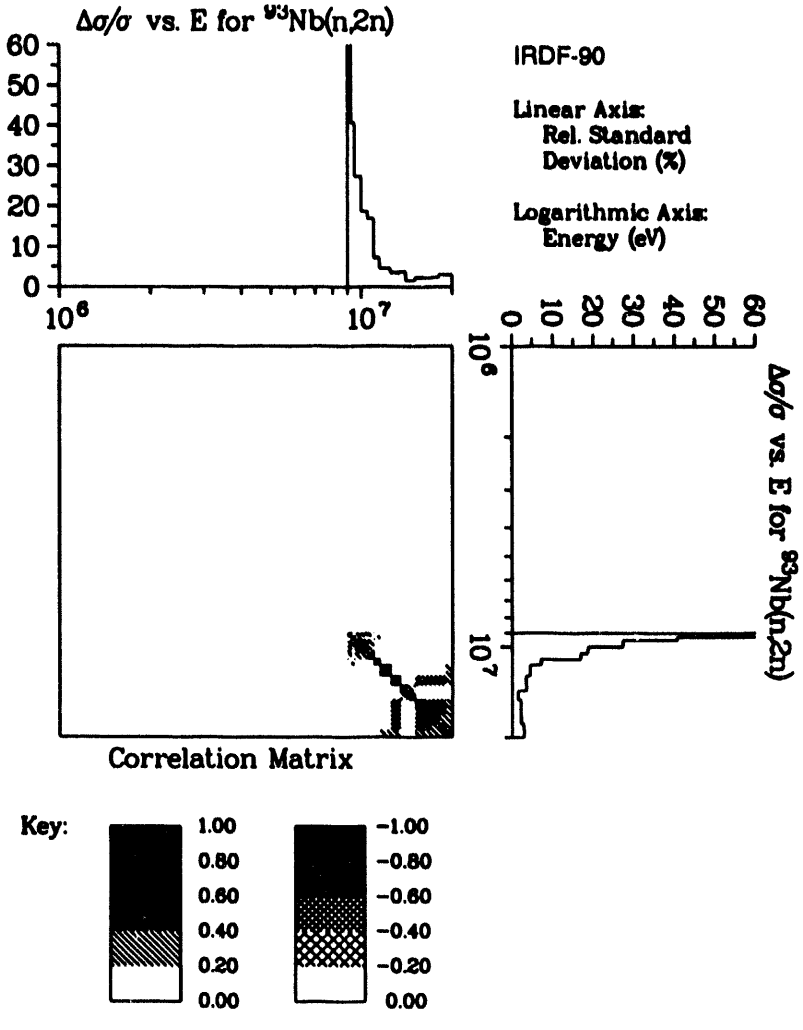

Covariance data for ^{93}Nb(n,2n) with ^{93}Nb(n,2n).

Figure B-44: ^{93}Nb(n,2n)^{92m}Nb Covariance Matrix

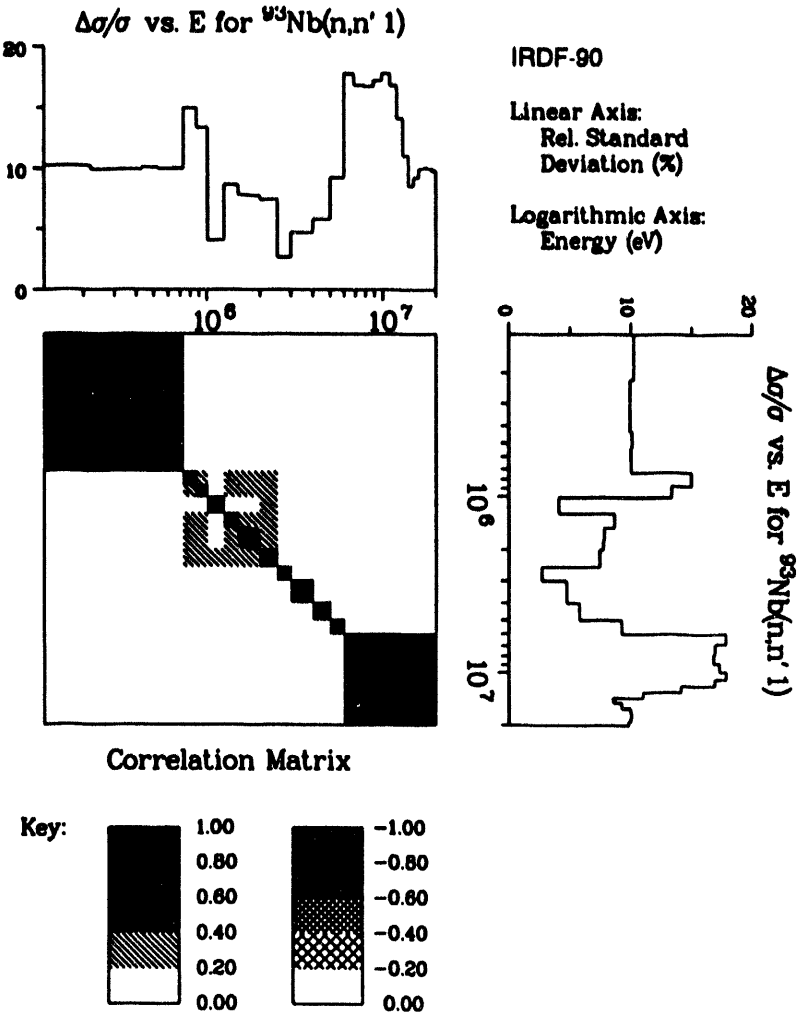

Covariance data for ^{93}Nb(n,n' 1) with ^{93}Nb(n,n' 1).

Figure B-45: ^{93}Nb(n,n')^{93m}Nb Covariance Matrix

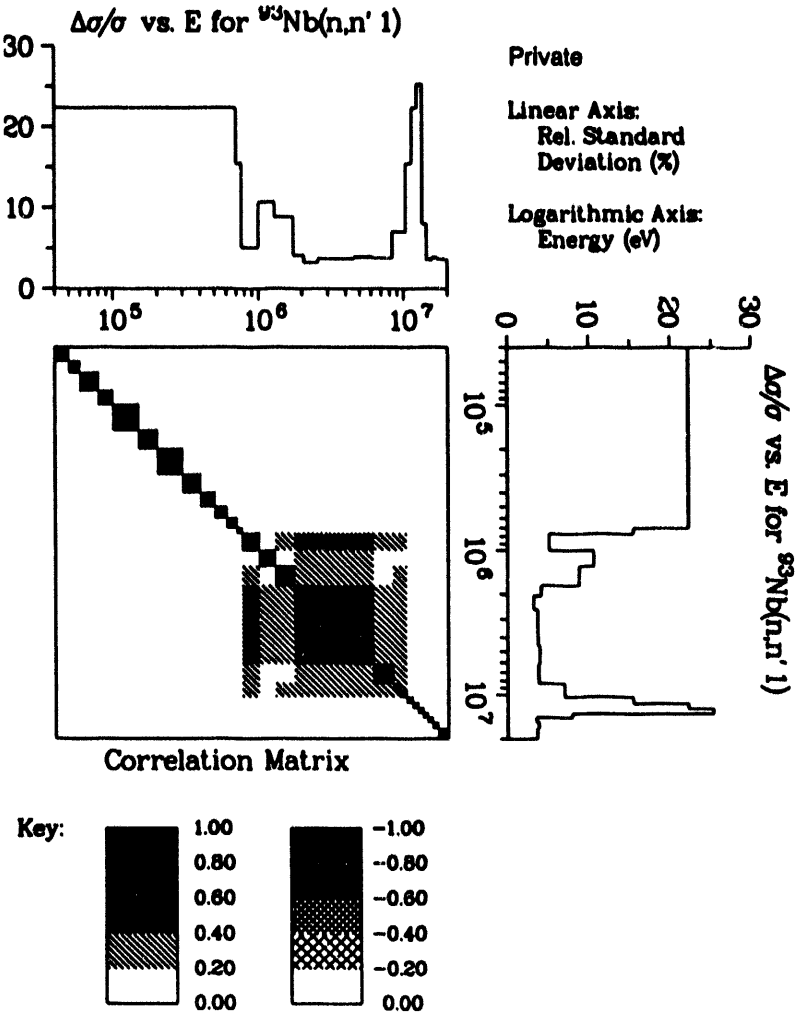

Covariance data for ^{93}Nb(n,n' 1) with ^{93}Nb(n,n' 1).

Figure B-45a: ^{93}Nb(n,n')^{93m}Nb Covariance Matrix

No current cross section library includes covariance data on $^{98}Mo(n,\gamma)^{99}Mo$. When the data becomes available, an attempt will be made to provide the covariance information in the SNLRML cross section library.

Figure B-46: $^{98}Mo(n,\gamma)^{99}Mo$ Covariance Matrix

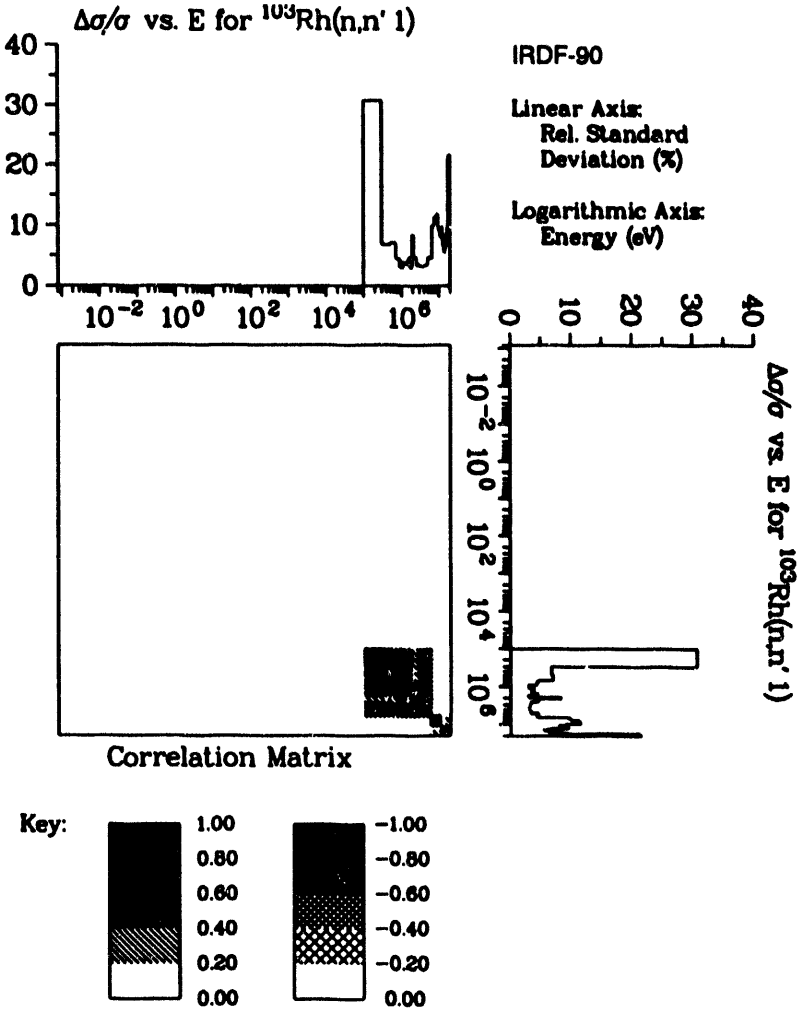

Covariance data for ^{103}Rh(n,n' 1) with ^{103}Rh(n,n' 1).

Figure B-47: ^{103}Rh(n,n')^{103m}Rh Covariance Matrix

No current cross section library includes covariance data on $^{109}Ag(n,\gamma)^{110m}Ag$. When the data becomes available, an attempt will be made to provide the covariance information in the SNLRML cross section library.

Figure B-48: $^{109}Ag(n,\gamma)^{110m}Ag$ Covariance Matrix

No current cross section library includes covariance data on any of the important absorption reactions on cadmium. When data becomes available, it will be included in the SNLRML library.

Figure B-49: ^{Nat}Cd(n,abs) Covariance Matrix

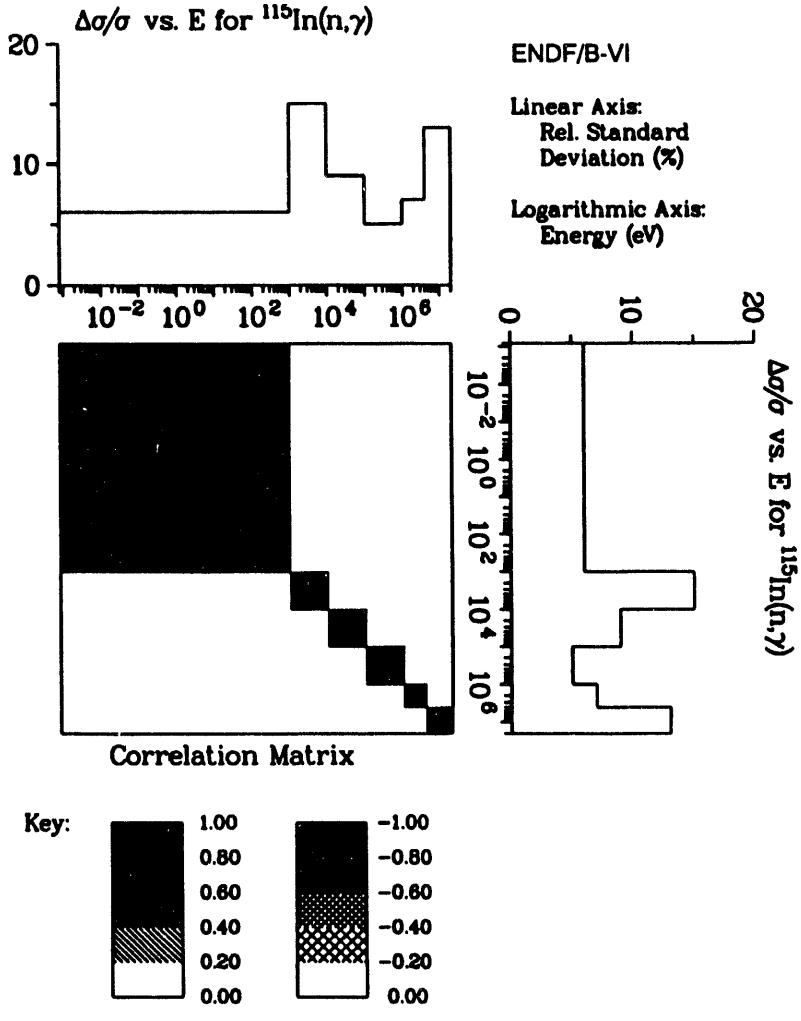

Covariance data for $^{115}In(n,\gamma)$ with $^{115}In(n,\gamma)$.

Figure B-50: $^{115}In(n,\gamma)^{116m}In$ Covariance Matrix

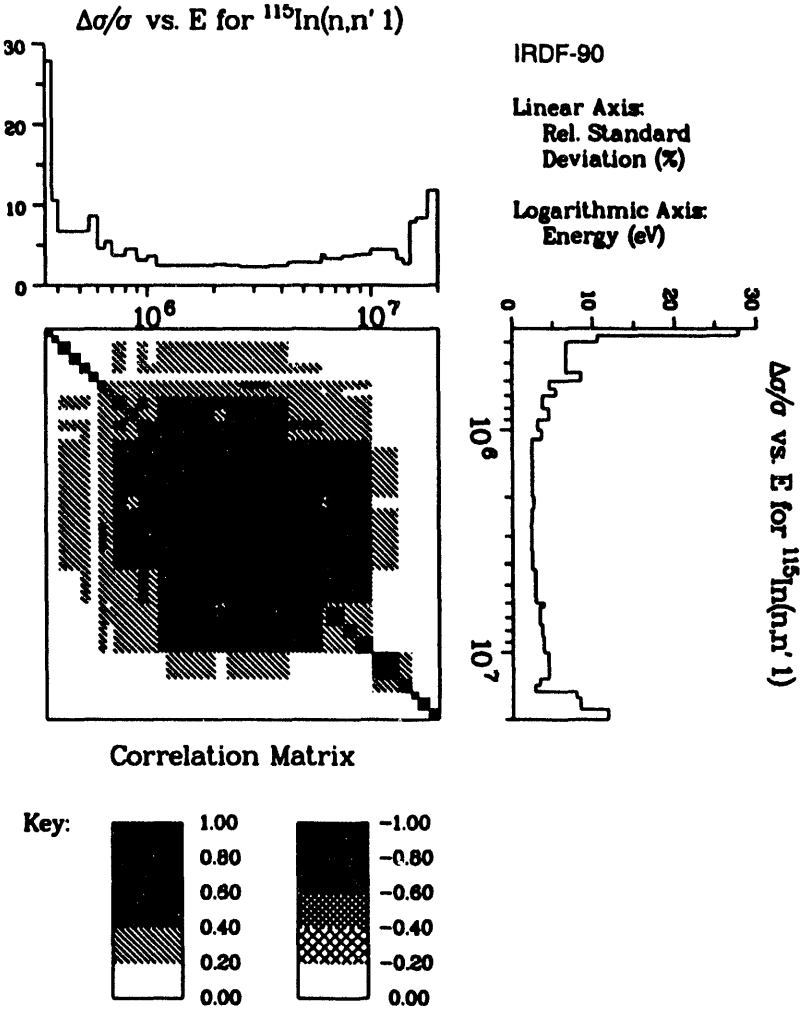

Covariance data for ^{115}In(n,n' 1) with ^{115}In(n,n' 1).

Figure B-51: ^{115}In(n,n')^{115m}In Covariance Matrix

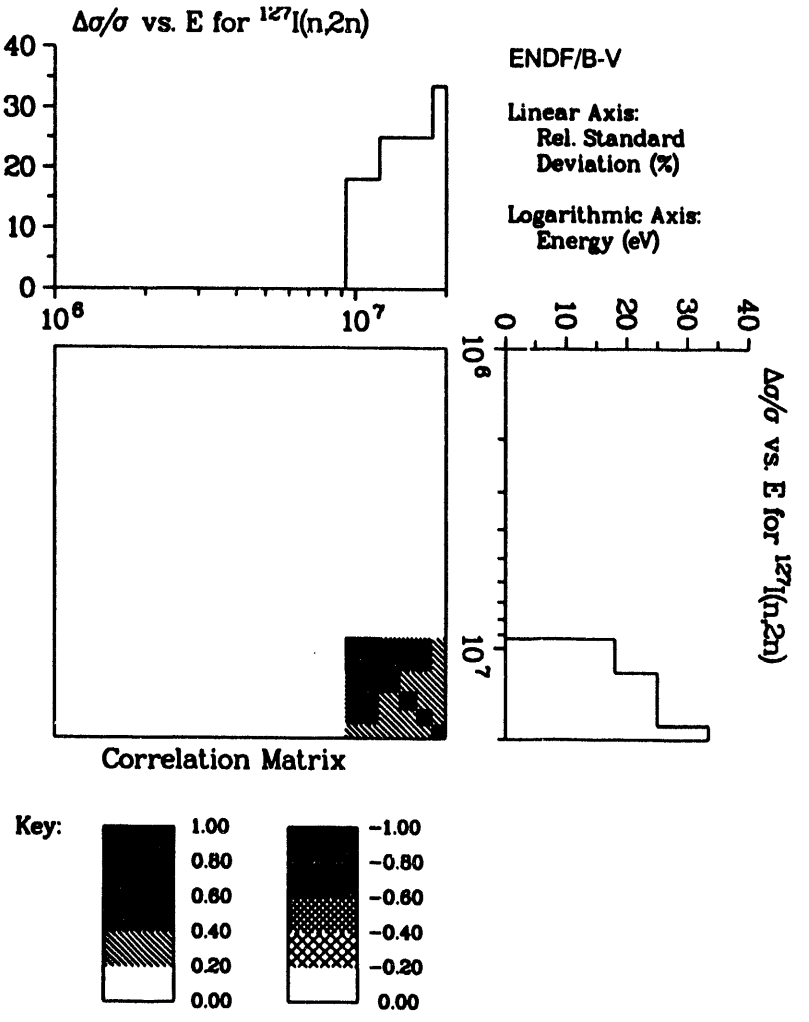

Covariance data for ^{127}I(n,2n) with ^{127}I(n,2n).

Figure B-52: ^{127}I(n,2n)^{126}I Covariance Matrix

No current cross section library includes covariance data on $^{197}Au(n,p)^{197}Pt$. When the data becomes available, an attempt will be made to provide the covariance information in the SNLRML cross section library.

Figure B-53: $^{197}Au(n,p)^{197}Pt$ Covariance Matrix

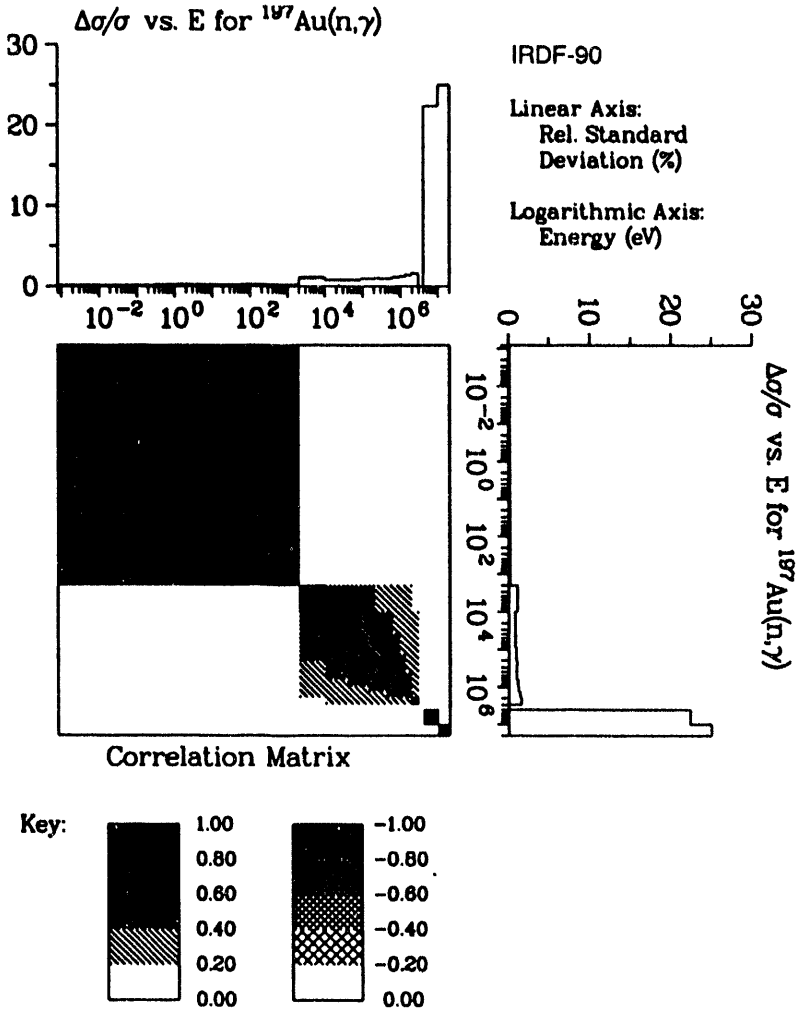

Covariance data for $^{197}Au(n,\gamma)$ with $^{197}Au(n,\gamma)$.

Figure B-54: $^{197}Au(n,\gamma)^{198}Au$ Covariance Matrix

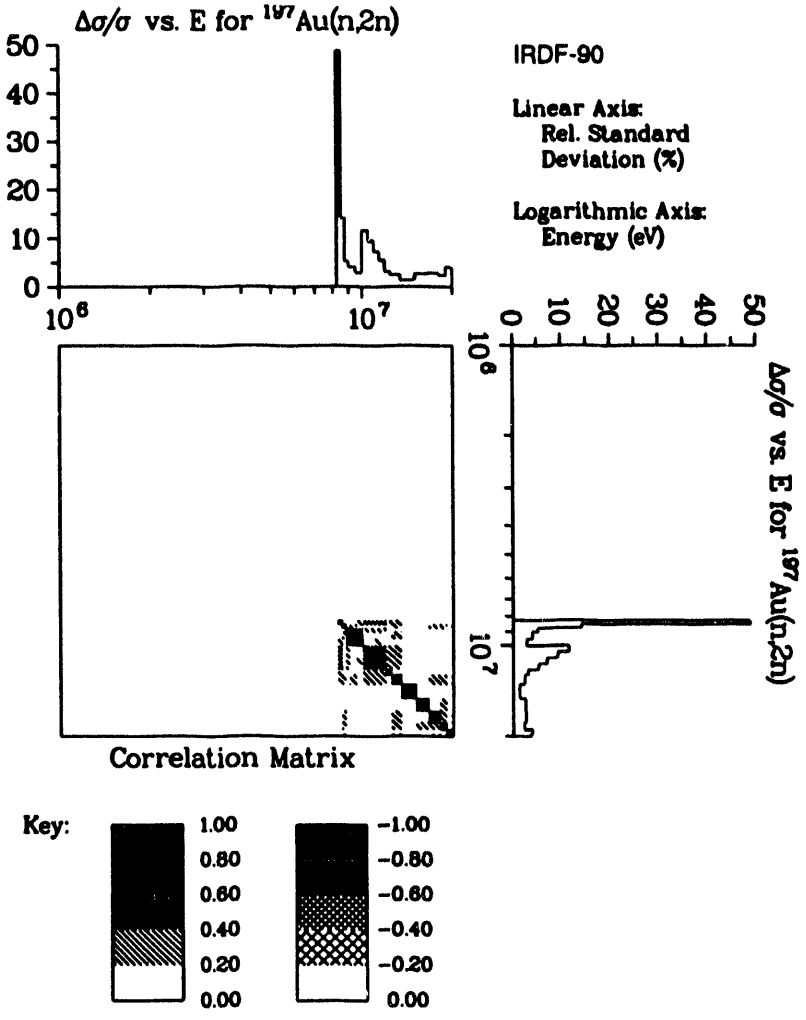

Covariance data for ^{197}Au(n,2n) with ^{197}Au(n,2n).

Figure B-55: ^{197}Au(n,2n)^{196}Au Covariance Matrix

No current cross section library includes covariance data on $^{197}Au(n,3n)^{195}Au$. When the data becomes available, an attempt will be made to provide the covariance information in the SNLRML cross section library.

Figure B-56: $^{197}Au(n,3n)^{195}Au$ Covariance Matrix

No current cross section library includes covariance data on all of the absorption reactions on gold. When data becomes available, it will be included in the SNL-RML library. Since the (n,γ) reaction is usually the dominant absorption process, the covariance data for this reaction should be used in most applications. The covariance matrix for the ^{Nat}Au(n,abs) cover cross section in the SNLRML library is deliberately left blank and NOT set to the ^{197}Au(n,γ)^{198}Au covariance matrix (available as reaction 54) to avoid misuse of the data for high energy neutron spectra that do not have a significant thermal component (such as DT and DD reactions).

Figure B-57: ^{Nat}Au(n,abs) Covariance Matrix

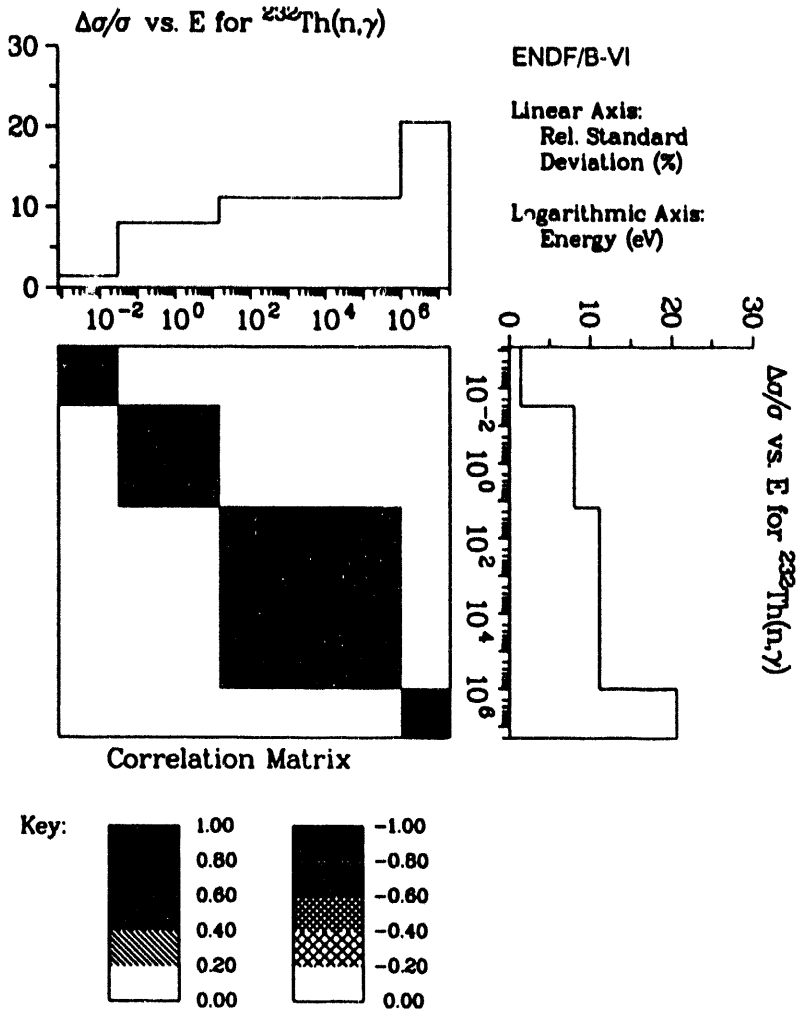

Covariance data for $^{232}Th(n,\gamma)$ with $^{232}Th(n,\gamma)$.

Figure B-58: $^{232}Th(n,\gamma)^{233}Th$ Covariance Matrix

No covariance data exists in any cross section library for the $^{232}Th(n,2n)^{231}Th$ reaction. If data becomes available, the SNLRML library will be updated.

Figure B-59: $^{232}Th(n,2n)^{231}Th$ Covariance Matrix

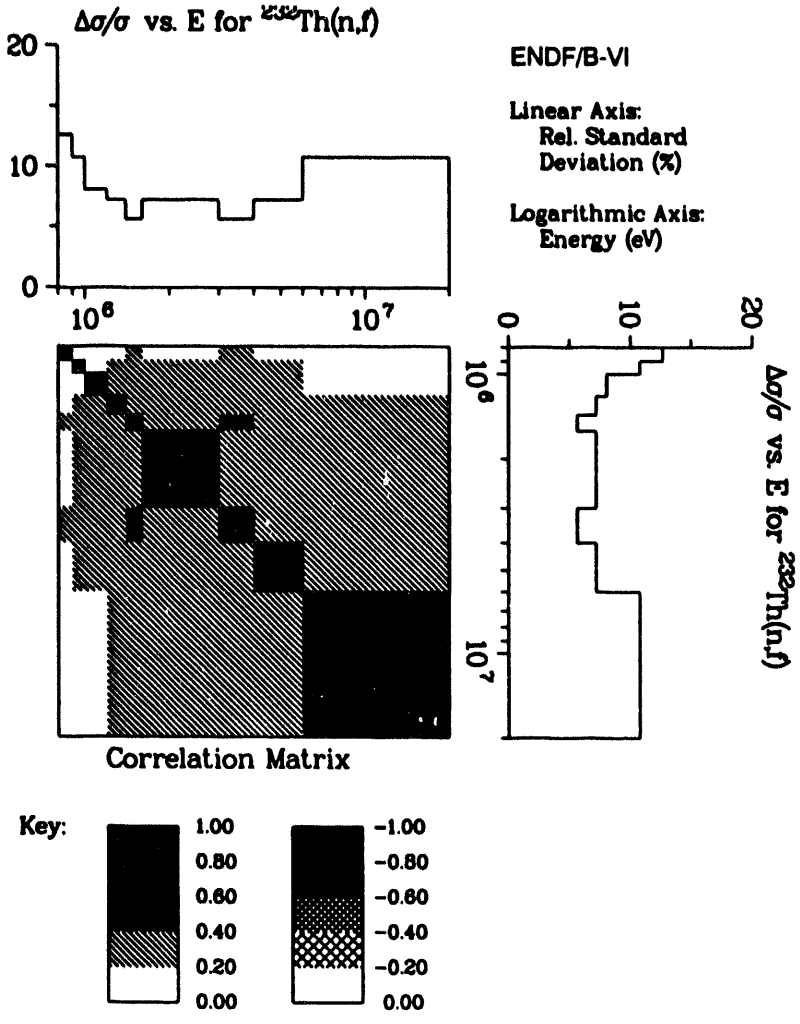

Covariance data for ^{232}Th(n,f) with ^{232}Th(n,f).

Figure B-60: ^{232}Th(n,f)FP Covariance Matrix

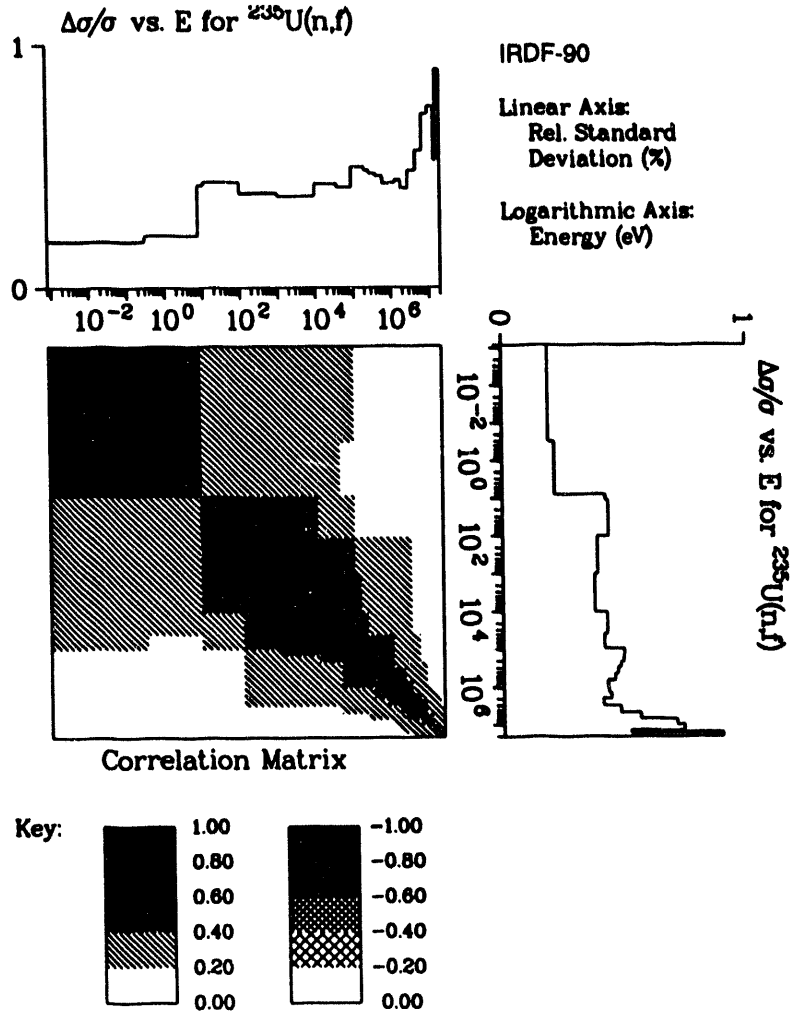

Covariance data for $^{235}U(n,f)$ with $^{235}U(n,f)$.

Figure B-61: $^{235}U(n,f)FP$ Covariance Matrix

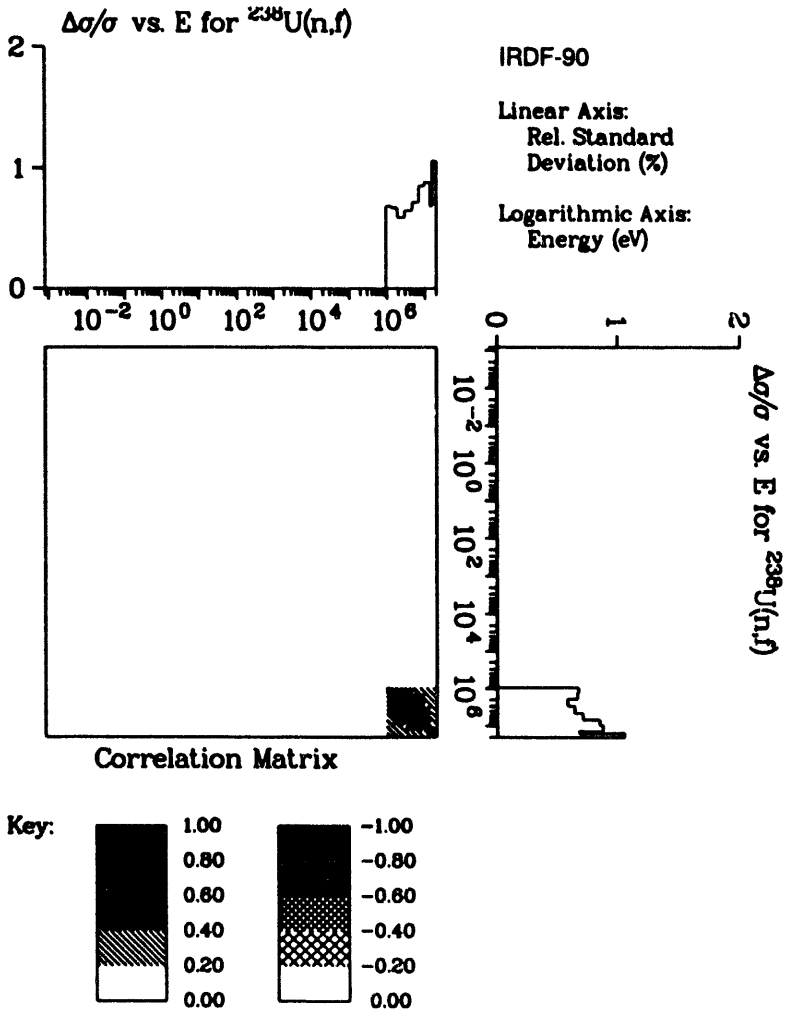

Covariance data for $^{238}U(n,f)$ with $^{238}U(n,f)$.

Figure B-62: $^{238}U(n,f)FP$ Covariance Matrix

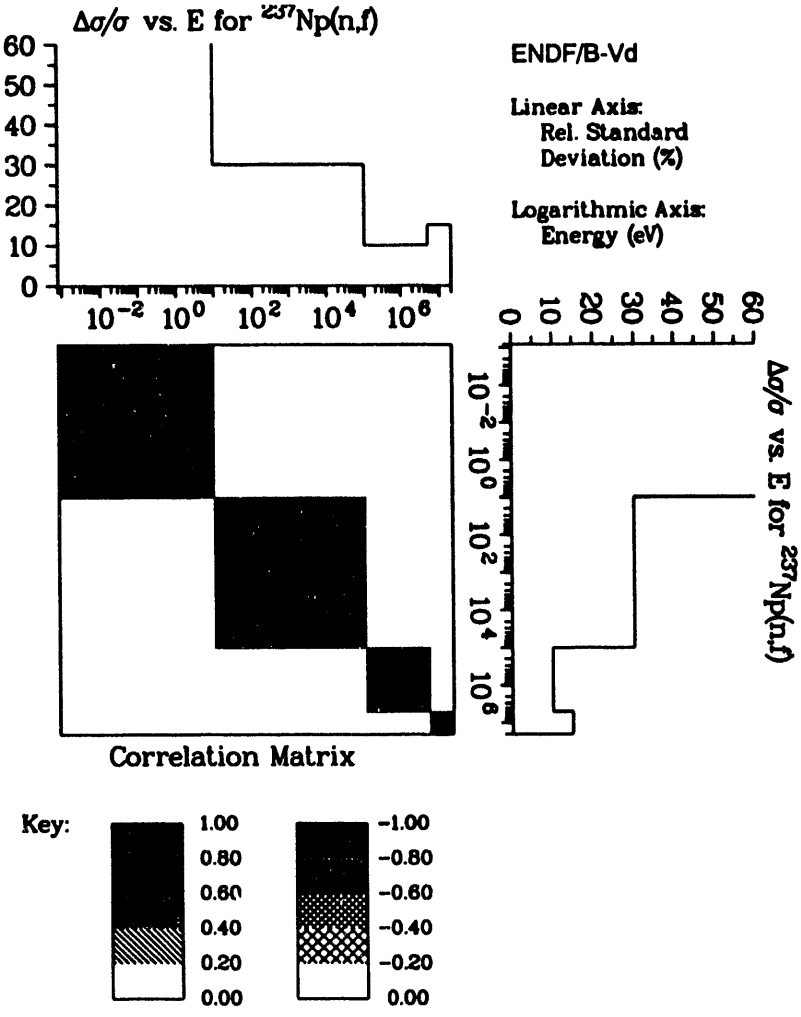

Covariance data for ^{237}Np(n,f) with ^{237}Np(n,f).

Figure B-63: ^{237}Np(n,f)FP Covariance Matrix

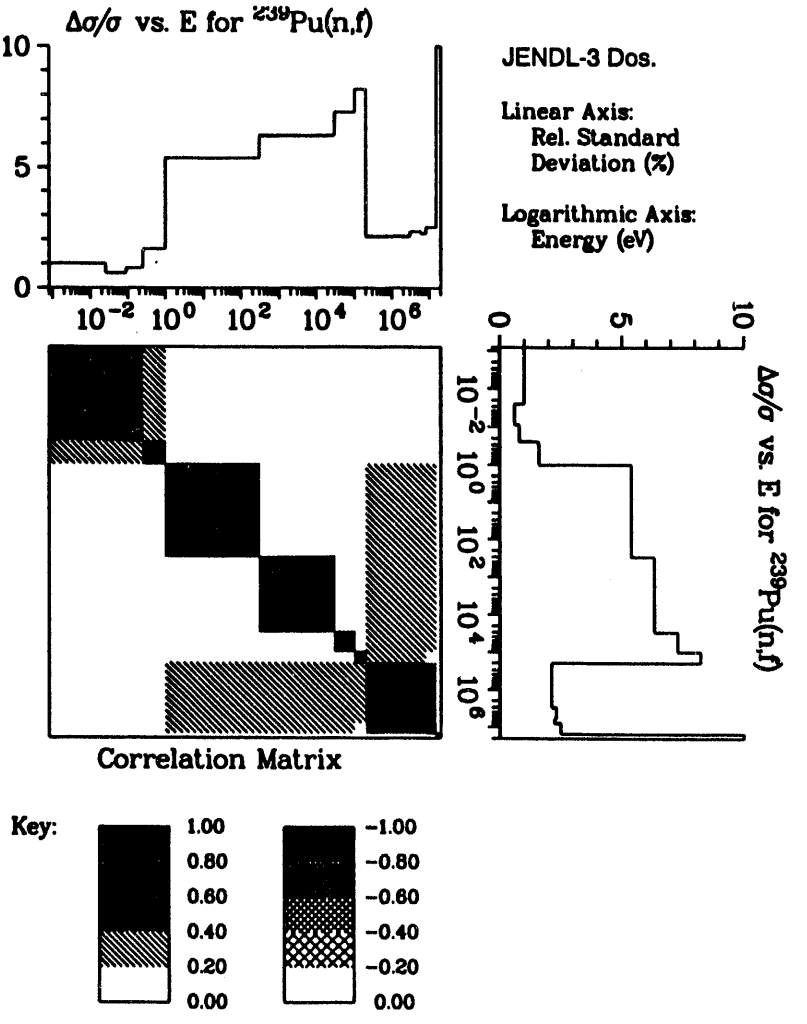

Covariance data for ^{239}Pu(n,f) with ^{239}Pu(n,f).

Figure B-64: ^{239}Pu(n,f)FP Covariance Matrix

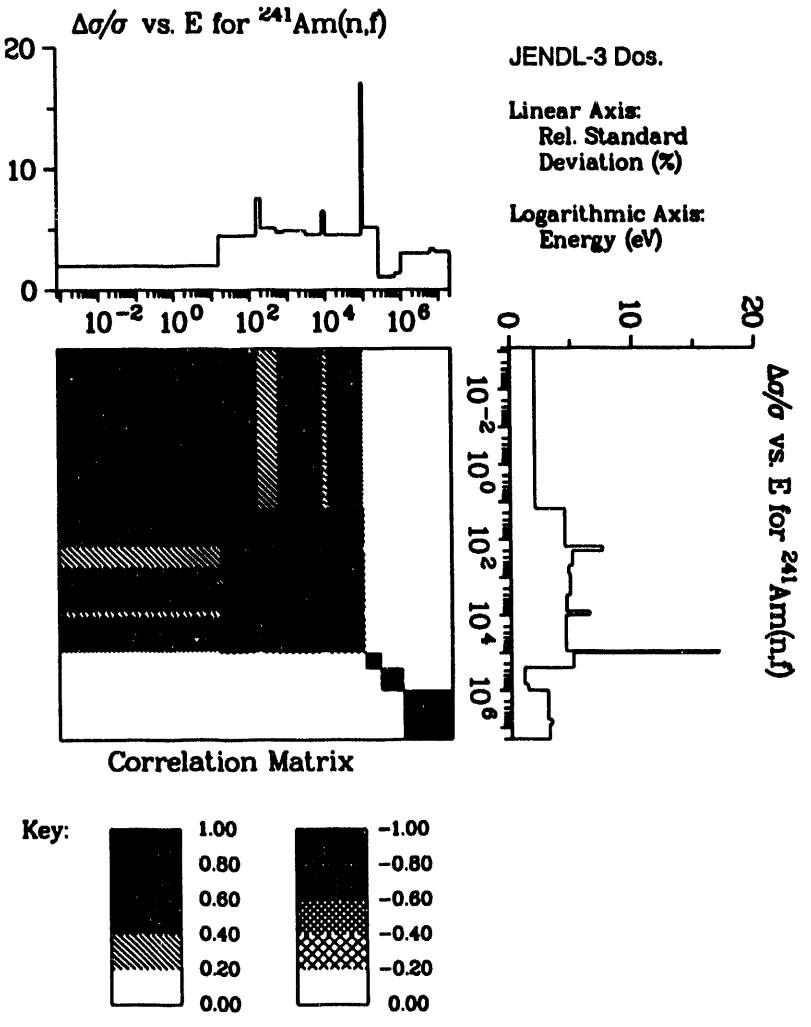

Covariance data for ^{241}Am(n,f) with ^{241}Am(n,f).

Figure B-65: ^{241}Am(n,f)FP Covariance Matrix

Covariance data was presented in this document for $^{235}U(n,f)FP$ reaction. Since it is the major responding reaction in this sensor it should be used for all uncertainty processing. The $^{235}U(n,f)FP$ covariance matrix appears in the SNLRML library for this sensor.

Figure B-66: RML Enriched Uranium Fission Covariance Matrix

Covariance data was presented in this document for $^{238}U(n,f)FP$ reaction. Since it is the major responding reaction in this sensor (if it is used correctly) it should be used for all uncertainty processing. The $^{238}U(n,f)FP$ covariance matrix appears in the SNLRML library for this sensor.

Figure B-67: RML Depleted Uranium Fission Foil Covariance Matrix

Covariance data was presented in this document for ^{239}Pu(n,f)FP reaction. Since it is the major responding reaction in this sensor it should be used for all uncertainty processing. The ^{239}Pu(n,f)FP covariance matrix appears in the SNLRML library for this sensor.

Figure B-68: RML Plutonium Fission Foil Covariance Matrix

Covariance data was presented in this document for $^{32}S(n,p)^{32}P$ reaction. This sensor is identical in shape to the $^{32}S(n,p)^{32}P$ sensor and varies only in a normalization that is attributable to the counting calibration methodology.

Figure B-69: ^{32}S-3MeV Covariance Matrix

APPENDIX C

SNLRML Dosimetry Reaction Constants

Table C-1
SNLRML Dosimetry Reaction Constants

	Dosimetry Reactions	Target Nucleus			Residual Nucleus		
		Elmental Atomic Weight	Isotopic Atomic Number Abundance (%)	Isotopic Mass Excess 1 amu = 931501.6 keV (keV)	Half-life	E_γ (keV)	Yield (%) γ/Reaction (fission yield %)
1.	$^{10}B(n,abs)$	10.81	19.9	+12050.8	----	----	----
2.	$^{10}B(n,^4He)X$	10.81	19.9	+12050.8	---	---	---
3.	$^{11}B(n,abs)$	10.81	80.1	+8668.0	----	----	----
4.	$^{Nat}B(n,abs)$	10.81	----	----	----	----	----
5.	$^{enriched}B_4C(n,abs)$	10.46835	---	---	---	---	---
6.	$^6Li(n,^4He)$	6.941	7.5	+14085.6	---	---	---
7.	$^{19}F(n,2n)^{18}F$	18.998403	100.0	-1487.40	1.8295 hr	$<E_{\beta+}>$=249.8	100.0
8.	$^{23}Na(n,\gamma)^{24}Na$	22.98977	100.0	-8419.5	0.62356 d	1368.633 2754.030	99.9936 99.855
9.	$^{24}Mg(n,p)^{24}Na$	24.305	78.99	-13933.1	0.62356 d	1368.633 2754.030	99.9936 99.855
10.	$^{27}Al(n,p)^{27}Mg$	26.98154	100.0	-17196.8	9.462 m	843.76 1014.44	71.8 28.0
11.	$^{27}Al(n,\alpha)^{24}Na$	26.98154	100.0	-17196.8	0.62356 d	1368.633 2754.030	99.9936 99.855
12.	$^{Nat}Si(n,X)1MEV$	28.0855	100.0	----	----	----	----

Table C-1 (Continued)
SNLRML Dosimetry Reaction Constants

	Dosimetry Reactions	Target Nucleus			Residual Nucleus		
		Elmental Atomic Weight	Isotopic Atomic Number Abundance (%)	Isotopic Mass Excess 1 amu = 931501.6 keV (keV)	Half-life	E_γ (keV)	Yield (%) γ/Reaction (fission yield %)
13.	$^{31}P(n,p)^{31}Si$	30.97376	100.0	-24440.7	157.3 m	1266.15 $<E_\beta>$=595.6	0.07 99.93
14.	$^{32}S(n,p)^{32}P$	32.06	95.02	-26016.18	14.26 d	$<E_\beta>$=694.9	100.
15.	$^{45}Sc(n,\gamma)^{46}Sc$	44.9559	100.0	-41069.9	83.79 d	889.277 1120.545	99.9844 99.9874
16.	$^{46}Ti(n,p)^{46}Sc$	47.88	8.0	-44125.7	83.79d	889.277 1120.545	99.9844 99.9874
17.	$^{47}Ti(n,p)^{47}Sc$	47.88	7.3	-44931.9	3.345 d	159.381	67.9
18.	$^{47}Ti(n,np)^{46}Sc$	47.88	7.3	-44931.9	83.79 d	889.277 1120.545	99.9844 99.9874
19.	$^{Nat}Ti(n,X)^{46}Sc$	47.88	100.0	----	83.79d	889.277 1120.545	tbd tbd
20.	$^{48}Ti(n,p)^{48}Sc$	47.88	73.8	-48487.1	43.67 h	983.524 1037.522 1312.102	100.0 97.5 100.0
21.	$^{48}Ti(n,np)^{47}Sc$	47.88	73.8	-48487.1	3.345 d	159.381	67.9
22.	$^{Nat}Ti(n,X)^{47}Sc$	47.88	100.0	----	3.345 d	159.381	tbd

Table C-1 (Continued)
SNLRML Dosimetry Reaction Constants

	Dosimetry Reactions	Target Nucleus			Residual Nucleus		
		Elmental Atomic Weight	Isotopic Atomic Number Abundance (%)	Isotopic Mass Excess 1 amu = 931501.6 keV (keV)	Half-life	E_γ (keV)	Yield (%) γ/Reaction (fission yield %)
23.	$^{55}Mn(n,\gamma)^{56}Mn$	54.93805	100.0	-57709.2	2.5785 hr	846.754 1810.72 2113.05	98.87 27.18925 14.33615
24.	$^{55}Mn(n,2n)^{54}Mn$	54.93805	100.0	-57709.2	312.3 d	834.843	99.9758
25.	$^{54}Fe(n,p)^{54}Mn$	55.847	5.9	-56250.8	312.3 d	834.843	99.9758
26.	$^{56}Fe(n,p)^{56}Mn$	55.847	91.72	-60604.1	2.5785 hr	846.754 1810.72 2113.05	98.87 27.18925 14.33615
27.	$^{58}Fe(n,\gamma)^{59}Fe$	55.847	0.28	-62152.2	44.496 d	1099.251 1291.596 1481.7	56.5 43.2 0.059
28.	$^{nat}Fe(n,X)dpa$	55.847	---	---	---	---	---
29.	$^{59}Co(n,p)^{59}Fe$	58.93320	100.0	-62226.5	44.496 d	1099.251 1291.596 1481.7	56.5 43.2 0.059

Table C-1 (Continued)
SNLRML Dosimetry Reaction Constants

	Dosimetry Reactions	Target Nucleus			Residual Nucleus		
		Elmental Atomic Weight	Isotopic Atomic Number Abundance (%)	Isotopic Mass Excess 1 amu = 931501.6 keV (keV)	Half-life	E_γ (keV)	Yield (%) γ/Reaction (fission yield %)
30.	$^{59}Co(n,\gamma)^{60}Co$	58.93320	100.0	-62226.5	1925.5 d	1173.238	99.857
						1332.502	99.983
					10.47 m	58.603	2.01
					(meta)	826.28	0.00768
						1332.501	0.24
						2158.77	0.00072
31.	$^{59}Co(n,\alpha)^{56}Mn$	58.93320	100.0	-62226.5	2.5785 h	846.754	98.87
						1810.72	27.18925
						2113.05	14.33615
32.	$^{59}Co(n,2n)^{58}Co$	58.93320	100.0	-62226.5	70.86 d	810.775	99.45
						863.959	0.69
						1674.730	0.519
					9.15 h (meta)	24.889	0.0369
33.	$^{58}Ni(n,p)^{58}Co$	58.6934	68.077	-60225.1	70.86 d	810.775	99.45
						863.959	0.69
						1674.730	0.519
					9.15 h (meta)	24.889	0.0369
34.	$^{58}Ni(n,2n)^{57}Ni$	58.6934	68.077	-60225.1	35.65 h	1377.63	81.7
						1919.52	12.255

Table C-1 (Continued)
SNLRML Dosimetry Reaction Constants

Dosimetry Reactions		Target Nucleus			Residual Nucleus		
		Elmental Atomic Weight	Isotopic Atomic Number Abundance (%)	Isotopic Mass Excess 1 amu = 931501.6 keV (keV)	Half-life	E_γ (keV)	Yield (%) γ/Reaction (fission yield %)
35.	$^{60}Ni(n,p)^{60}Co$	58.6934	26.223	-64470.7	1925.5 d 10.47 m (meta)	1173.238 1332.502 58.603 826.28 1332.501 2158.77	99.857 99.983 2.01 0.00768 0.24 0.00072
36.	$^{63}Cu(n,\gamma)^{64}Cu$	63.546	69.17	-65578.7	12.701 h	1345.77	0.47336
37.	$^{63}Cu(n,2n)^{62}Cu$	63.546	69.17	-65578.7	9.74 m	1173.02 875.71	0.335 0.147
38.	$^{63}Cu(n,\alpha)^{60}Co$	63.546	69.17	-65578.7	1925.5 10.47 m (meta)	1173.238 1332.502 58.603 826.33 1332.501 2158.86	99.857 99.983 2.01 0.0058 0.25 0.00088
39.	$^{65}Cu(n,2n)^{64}Cu$	63.546	30.83	-67261.0	12.701 h	1345.77	0.47336
40.	$^{64}Zn(n,p)^{64}Cu$	65.39	48.6	-66001.7	12.701 h	1345.77	0.47336

Table C-1 (Continued)
SNLRML Dosimetry Reaction Constants

	Dosimetry Reactions	Target Nucleus			Residual Nucleus		
		Elmental Atomic Weight	Isotopic Atomic Number Abundance (%)	Isotopic Mass Excess 1 amu = 931501.6 keV (keV)	Half-life	E_γ (keV)	Yield (%) γ/Reaction (fission yield %)
41.	$^{90}Zr(n,2n)^{89}Zr$	91.224	51.45	-88769.7	78.41 h 4.18 m (meta)	909.14 1712.8 1744.47 1507.3	99.871 0.763014 0.128833 6.075
42.	GaAs(n,X)1MeV	144.64459	----	----	----	----	----
43.	$^{93}Nb(n,\gamma)^{94m}Nb$	92.90638	100	-87209.8	6.26 m	702.645 871.119 992.75 1863.84	0.00315 0.50 0.00075 $6.6x10^{-5}$
44.	$^{93}Nb(n,2n)^{92m}Nb$	92.90638	100.0	-87209.8	10.15 d	934.44 912.6 1847.33	99.07 1.78326 0.852
45.	$^{93}Nb(n,n')^{93m}Nb$	92.90638	100.0	-87209.8	5.89×10^3 d	30.77 16.52 ($K_{\alpha 1,2}$)	0.000549 9.25
46.	$^{98}Mo(n,\gamma)^{99}Mo$	95.94	24.13	-88113.2	65.94 h	739.58 778.	12.13 4.34254
47.	$^{103}Rh(n,n')^{103m}Rh$	102.90550	100.0	-88027.0	56.12 m	39.	0.0684

Table C-1 (Continued)
SNLRML Dosimetry Reaction Constants

	Dosimetry Reactions	Target Nuclus			Residual Nucleus		
		Elmental Atomic Weight	Isotopic Atomic Number Abundance (%)	Isotopic Mass Excess 1 amu = 931501.6 keV (keV)	Half-life	E_γ (keV)	Yield (%) γ/Reaction (fission yield %)
48.	$^{109}Ag(n,\gamma)^{110m}Ag$	107.8682	48.161	-88720.0	249.76 d	116.48 884.684 937.493 1384.300 1505.040 1475.788	0.00799 72.7 34.1314 24.1204 12.9532 3.96868
49.	$^{nat}Cd(n,abs)$	112.411	----	----	----	----	----
50.	$^{115}In(n,\gamma)^{116m}In$	114.82	95.7	-89534.0	54.41 m	1293.54 1097.3 818.7 2112.1	84.4 56.2104 11.4784 15.5296
51.	$^{115}In(n,n')^{115m}In$	114.82	95.7	-89534.0	4.486 h	336.241 497.370	45.9 0.047
52.	$^{127}I(n,2n)^{126}I$	126.90447	100.0	-88984.0	13.02 d	753.819 388.633 666.331	4.1514 33.99 33.00
53.	$^{197}Au(n,p)^{197}Pt$	196.96654	100.0	-31165.0	18.3 h 95.41 m (meta)	268.78 191.437 ---	0.2331 3.7 ---

Table C-1 (Continued)
SNLRML Dosimetry Reaction Constants

	Dosimetry Reactions	Target Nuclus			Residual Nucleus		
		Elmental Atomic Weight	Isotopic Atomic Number Abundance (%)	Isotopic Mass Excess 1 amu = 931501.6 keV (keV)	Half-life	E_γ (keV)	Yield (%) γ/Reaction (fission yield %)
54.	$^{197}Au(n,\gamma)^{198}Au$	196.96654	100.0	-31165.0	2.6943 d	1087.6904 675.8874 411.8044	0.159045 0.8038278 95.57
55.	$^{197}Au(n,2n)^{196}Au$	196.96654	100.0	-31165.0	6.183 d	1091.4 1005.7 355.68	0.14877 0.002697 87.
56.	$^{197}Au(n,3n)^{195}Au$	196.96654	100.0	-31165.0	186.09 d	211.36 199.46 129.757	0.0109 0.008611 0.8175
57.	$^{Nat}Au(n,abs)$	196.96654	----	----	----	----	----
58.	$^{232}Th(n,\gamma)^{233}Th.$	232.0381	100.0	35444.4	22.3 m	890.1 490.80 499.02 669.901 764.4	0.14 0.17 0.21 0.68 0.120
59.	$^{232}Th(n,2n)^{231}Th$	232.0381	100.0	35444.4	25.52 h	311.00 217.94 102.270	0.0029 0.040 0.41

Table C-1 (Continued)
SNLRML Dosimetry Reaction Constants

Dosimetry Reactions		Target Nucleus			Residual Nucleus		
		Elmental Atomic Weight	Isotopic Atomic Number Abundance (%)	Isotopic Mass Excess 1 amu = 931501.6 keV (keV)	Half-life	E_γ (keV)	Yield (%) γ/Reaction (fission yield %)
60.	$^{232}Th(n,f)^{95}Zr$	232.0381	100.0	35444.4	---	---	5.67313 (RC)
	$^{232}Th(n,f)^{99}Mo$						3.84804E-3 (RI)
	$^{232}Th(n,f)^{140}Ba$						2.95528 (RC)
							1.09001E-4 (RI)
	$^{232}Th(n,f)^{141}Ce$						7.87647 (RC)
							4.82795E-2 (RI)
	$^{232}Th(n,f)^{140}La$						7.48275 (RC)
							2.4400E-7 (RI)
							7.87649 (RC)
							2.71003E-5 (RI)
61.	$^{235}U(n,f)^{95}Zr$	238.0289	0.720	40915.5	---	---	6.42554 (RC)
	$^{235}U(n,f)^{99}Mo$						2.93502E-2 (RI)
							5.91653 (RC)
	$^{235}U(n,f)^{140}Ba$						2.18602E-3 (RI)
							5.98741 (RC)
	$^{235}U(n,f)^{141}Ce$						4.72071E-1 (RI)
							5.94622 (RC)
	$^{235}U(n,f)^{140}La$						3.16002E-5 (RI)
							5.98872 (RC)
							1.31401E-3 (RI)

Table C-1 (Continued)
SNLRML Dosimetry Reaction Constants

	Dosimetry Reactions	Target Nucleus: Elmental Atomic Weight	Target Nucleus: Isotopic Atomic Number Abundance (%)	Target Nucleus: Isotopic Mass Excess 1 amu = 931501.6 keV (keV)	Residual Nucleus: Half-life	Residual Nucleus: E_γ (keV)	Residual Nucleus: Yield (%) γ/Reaction (fission yield %)
62.	$^{238}U(n,f)^{95}Zr$	238.0289	99.2745	47306.0	---	---	5.15126 (RC)
							7.88021E-4 (RI)
	$^{238}U(n,f)^{99}Mo$						6.18839 (RC)
							2.39006E-5 (RI)
	$^{238}U(n,f)^{140}Ba$						5.84596 (RC)
							2.57317E-2 (RI)
	$^{238}U(n,f)^{141}Ce$						5.37935 (RC)
							4.51012E-8 (RI)
	$^{238}U(n,f)^{140}La$						5.84597 (RC)
							1.38004E-5 (RI)
63.	$^{237}Np(n,f)^{95}Zr$	237.	----	44868.3	---	---	5.68896 (RC)
							6.1647E-2 (RI)
	$^{237}Np(n,f)^{99}Mo$						6.11547 (RC)
							6.54700E-3 (RI)
	$^{237}Np(n,f)^{140}Ba$						5.47246 (RC)
							5.83709E-1 (RI)
	$^{237}Np(n,f)^{141}Ce$						5.47689 (RC)
							8.6300E-5 (RI)
	$^{237}Np(n,f)^{140}La$						5.47688 (RC)
							4.4210E-5 (RI)

Table C-1 (Continued)
SNLRML Dosimetry Reaction Constants

Dosimetry Reactions		Target Nucleus			Residual Nucleus		
		Elmental Atomic Weight	Isotopic Atomic Number Abundance (%)	Isotopic Mass Excess 1 amu = 931501.6 keV (keV)	Half-life	E_γ (keV)	Yield (%) γ/Reaction (fission yield %)
64.	$^{239}Pu(n,f)^{95}Zr$	244.	----	48584.9	---	---	4.65413 (RC)
							7.94561E-2 (RI)
	$^{239}Pu(n,f)^{99}Mo$						5.95472 (RC)
							1.6212E-2 (RI)
	$^{239}Pu(n,f)^{140}Ba$						5.31538 (RC)
							9.4334E-1 (RI)
	$^{239}Pu(n,f)^{141}Ce$						5.15886 (RC)
							2.71004E-4 (RI)
	$^{239}Pu(n,f)^{140}La$						5.32713 (RC)
							1.17572E-2 (RI)
65.	$^{241}Am(n,f)^{95}Zr$	243.	----	52931.2	---	---	3.75501 (RC)
							1.04484E-1 (RI)
	$^{241}Am(n,f)^{99}Mo$						5.40483 (RC)
							1.98844E-2 (RI)
	$^{241}Am(n,f)^{140}Ba$						4.99172 (RC)
							1.10761 (RI)
	$^{241}Am(n,f)^{141}Ce$						4.75360 (RC)
							7.28014E-4 (RI)
	$^{241}Am(n,f)^{140}La$						5.01242 (RC)
							2.07034E-2 (RI)

Table C-1 (Continued)
SNLRML Dosimetry Reaction Constants

	Dosimetry Reactions	Target Nucius			Residual Nucleus		
		Elmental Atomic Weight	Isotopic Atomic Number Abundance (%)	Isotopic Mass Excess 1 amu = 931501.6 keV (keV)	Half-life	E_γ (keV)	Yield (%) γ/Reaction (fission yield %)
66.	RML $^{235}U(n,f)^{140}Ba$ (SPR3CAV18, B_4C) RML $^{235}U(n,f)^{140}Ba$ (ACF9, B_4C) RML $^{235}U(n,f)^{140}La$ (SPR3CAV18, B_4C) RML $^{235}U(n,f)^{140}La$ (ACF9, B_4C)	235.20787	---	---	---	---	5.98624 (RC) 0.468384 (RI) 5.98383 (RC) 0.471534 (RI) 5.98754 (RC) 1.30327E-3 (RI) 5.98514 (RC) 1.31248E-3 (RI)
67.	RML $^{238}U(n,f)^{140}Ba$ (SPR3CAV18, B_4C) RML $^{238}U(n,f)^{140}Ba$ (ACF9, B_4C) RML $^{238}U(n,f)^{140}La$ (SPR3CAV18, B_4C) RML $^{238}U(n,f)^{140}La$ (ACF9, B_4C)	238.0445	---	---	---	---	5.84729 (RC) 3.2321E-2 (RI) 5.84548 (RC) 2.66776E-2 (RI) 5.84732 (RC) 3.3002E-5 (RI) 5.845496 (RC) 1.6564E-5 (RI)

Table C-1 (Continued)
SNLRML Dosimetry Reaction Constants

Dosimetry Reactions		Target Nuclus			Residual Nucleus		
		Elmental Atomic Weight	Isotopic Atomic Number Abundance (%)	Isotopic Mass Excess 1 amu = 931501.6 keV (keV)	Half-life	E_γ (keV)	Yield (%) γ/Reaction (fission yield %)
68.	RML $^{239}Pu(n,f)^{140}Ba$ (SPR3CAV18, B_4C) RML $^{239}Pu(n,f)^{140}Ba$ (ACF9, B_4C) RML $^{239}Pu(n,f)^{140}La$ (SPR3CAV18, B_4C) RML $^{239}Pu(n,f)^{140}La$ (ACF9, B_4C)	238.688	---	---	---	---	5.29852 (RC) 9.21266E-1 (RI) 5.29617 (RC) 9.15152E-1 (RI) 5.29877 (RC) 1.11687E-2 (RI) 5.30728 (RC) 1.11167E-2 (RI)
69.	$^{32}S(n,X)$ 3MeV	32.06	95.02	-26016.18	14.26 d	$<E_\beta>$=694.9	100.

APPENDIX D

Dosimetry Sensor Sensitive Energy Region

Table D-1
Sensor Response Region for SPR-III Central Cavity
(SPR3CAV18 Spectrum)

Reaction	Bare Sensor			B_4C and Cadmium Covered Sensor		
	Calculated Activity (dps/nucleus)	90% Activity Limits		Calculated Activity (dps/nucleus)	90% Activity Limits	
		Lower Energy (MeV)	Upper Energy (MeV)		Lower Energy (MeV)	Upper Energy (MeV)
$^{10}B(n,\alpha)X$	1.212E-24	1.350E-08	2.900E+00	7.098E-25	5.000E-02	3.700E+00
$^{6}Li(n,\alpha)X$	7.846E-25	3.600E-08	4.200E+00	6.116E-25	1.000E-01	4.500E+00
$^{19}F(n,2n)^{18}F$	4.118E-34	1.190E+01	1.730E+01	4.017E-34	1.190E+01	1.730E+01
$^{23}Na(n,\gamma)^{24}Na$	6.360E-33	4.250E-08	2.600E+00	4.877E-33	5.250E-02	2.900E+00
$^{24}Mg(n,p)^{24Na}$	9.727E-33	6.500E+00	1.160E+01	9.386E-33	6.500E+00	1.160E+01
$^{27}Al(n,p)^{27}Mg$	2.517E-30	3.500E+00	9.100E+00	2.416E-30	3.500E+00	9.200E+00
$^{27}Al(n,\alpha)^{24}Na$	4.486E-33	6.400E+00	1.200E+01	4.332E-33	6.400E+00	1.200E+01
$^{28}Si(n,1MeV)X$	8.193E-01	2.000E-01	5.200E+00	7.707E-01	2.100E-01	5.300E+00
$^{31}P(n,p)^{31}Si$	1.080E-30	2.200E+00	7.100E+00	1.034E-30	2.200E+00	7.200E+00
$^{32}S(n,p)^{32}P$	1.862E-32	2.300E+00	7.200E+00	1.781E-32	2.300E+00	7.300E+00
$^{45}Sc(n,\gamma)^{46}Sc$	1.284E-33	2.100E-08	1.300E+00	8.683E-34	3.800E-02	1.500E+00
$^{46}Ti(n,p)^{46}Sc$	5.144E-34	3.800E+00	9.300E+00	4.937E-34	3.800E+00	9.300E+00
$^{47}Ti(n,p)^{47}Sc$	2.258E-32	1.700E+00	7.500E+00	2.161E-32	1.700E+00	7.500E+00
$^{47}Ti(n,np)^{46}Sc$	4.912E-37	1.150E+01	1.770E+01	4.795E-37	1.150E+01	1.780E+01
Standard sensor cover is 0.1481 $barn^{-1}$ enriched (91.67% ^{10}B) B_4C and 4.705×10^{-3} $barn^{-1}$ cadmium.						

Table D-1 (Continued)
Sensor Response Region for SPR-III Central Cavity
(SPR3CAV18 Spectrum)

Reaction	Bare Sensor			B_4C and Cadmium Covered Sensor		
	Calculated Activity (dps/nucleus)	90% Activity Limits		Calculated Activity (dps/nucleus)	90% Activity Limits	
		Lower Energy (MeV)	Upper Energy (MeV)		Lower Energy (MeV)	Upper Energy (MeV)
$^{nat}Ti(n,X)^{46}Sc$	5.147E-34	3.800E+00	9.300E+00	4.940E-34	3.800E+00	9.300E+00
$^{48}Ti(n,p)^{48}Sc$	6.029E-34	5.900E+00	1.230E+01	5.818E-34	5.900E+00	1.230E+01
$^{48}Ti(n,np)^{47}Sc$	2.090E-36	1.230E+01	1.840E+01	2.041E-36	1.230E+01	1.840E+01
$^{nat}Ti(n,X)^{47}Sc$	2.261E-32	1.700E+00	7.500E+00	2.163E-32	1.700E+00	7.500E+00
$^{55}Mn(n,\gamma)^{56}Mn$	5.416E-31	2.300E-08	1.800E+00	3.137E-31	3.000E-02	2.400E+00
$^{55}Mn(n,2n)^{54}Mn$	3.003E-36	1.100E+01	1.600E+01	2.926E-36	1.100E+01	1.600E+01
$^{54}Fe(n,p)^{54}Mn$	1.068E-33	2.300E+00	7.400E+00	1.022E-33	2.300E+00	7.400E+00
$^{56}Fe(n,p)^{56}Mn$	4.014E-32	5.500E+00	1.120E+01	3.867E-32	5.500E+00	1.120E+01
$^{58}Fe(n,\gamma)^{59}Fe$	7.347E-34	3.600E-04	2.300E+00	6.028E-34	4.250E-02	2.400E+00
Fe(n,X)dpa	5.880E-22	2.400E-01	6.000E+00	5.562E-22	2.700E-01	6.000E+00
$^{59}Co(n,p)^{59}Fe$	1.328E-34	3.500E+00	9.500E+00	1.274E-34	3.500E+00	9.500E+00
$^{59}Co(n,\gamma)^{60}Co$	6.549E-35	1.800E-08	1.400E+00	2.721E-35	5.500E-02	2.300E+00
$^{59}Co(n,\alpha)^{56}Mn$	5.728E-33	5.700E+00	1.200E+01	5.526E-33	5.700E+00	1.210E+01
$^{59}Co(n,2n)^{58}Co$	1.148E-35	1.130E+01	1.620E+01	1.118E-35	1.130E+01	1.620E+01
$^{58}Ni(n,p)^{58}Co$	6.233E-33	2.000E+00	7.400E+00	5.965E-33	2.000E+00	7.400E+00
Standard sensor cover is 0.1481 $barn^{-1}$ enriched (91.67% ^{10}B) B_4C and 4.705×10^{-3} $barn^{-1}$ cadmium.						

Table D-1 (Continued)
Sensor Response Region for SPR-III Central Cavity
(SPR3CAV18 Spectrum)

Reaction	Bare Sensor			B_4C and Cadmium Covered Sensor		
	Calculated Activity (dps/nucleus)	90% Activity Limits		Calculated Activity (dps/nucleus)	90% Activity Limits	
		Lower Energy (MeV)	Upper Energy (MeV)		Lower Energy (MeV)	Upper Energy (MeV)
$^{58}Ni(n,2n)^{59}Ni$	1.070E-35	1.310E+01	1.800E+01	1.045E-35	1.310E+01	1.800E+01
$^{60}Ni(n,p)^{60}Co$	4.226E-36	4.800E+00	1.070E+01	4.068E-36	4.800E+00	1.070E+01
$^{63}Cu(n,\gamma)^{64}Cu$	2.534E-31	4.250E-03	2.400E+00	2.122E-31	4.750E-02	2.600E+00
$^{63}Cu(n,2n)^{64}Cu$	5.697E-32	1.190E+01	1.700E+01	5.556E-32	1.190E+01	1.710E+01
$^{63}Cu(n,\alpha)^{60}Co$	1.127E-36	4.600E+00	1.090E+01	1.085E-36	4.600E+00	1.090E+01
$^{65}Cu(n,2n)^{64}Cu$	2.524E-33	1.080E+01	1.590E+01	2.458E-33	1.080E+01	1.590E+01
$^{64}Zn(n,p)^{64}Cu$	2.998E-31	2.400E+00	7.400E+00	2.869E-31	2.400E+00	7.400E+00
$^{90}Zr(n,2n)^{89}Zr$	1.198E-34	1.270E+01	1.750E+01	1.170E-34	1.270E+01	1.750E+01
GaAs(n,1MeV)X	4.233E-21	1.700E-01	5.200E+00	3.965E-21	1.800E-01	5.300E+00
$^{93}Nb(n,\gamma)^{94}Nb$	9.256E-29	2.100E-02	1.500E+00	7.872E-29	4.000E-02	1.600E+00
$^{93}Nb(n,2n)^{92m}Nb$	1.513E-34	9.900E+00	1.460E+01	1.470E-34	9.900E+00	1.460E+01
$^{93}Nb(n,n)^{93m}Nb$	1.0[illegible]3E-34	7.200E-01	5.800E+00	1.050E-34	7.200E-01	5.800E+00
$^{98}Mo(n,\gamma)^{99}Mo$	1.072E-31	4.250E-02	2.200E+00	9.495E-32	6.900E-02	2.300E+00
$^{103}Rh(n,n)^{103m}Rh$	9.283E-29	4.500E-01	5.600E+00	8.861E-29	4.750E-01	5.600E+00
$^{109}Ag(n,\gamma)^{110m}Ag$	3.979E-34	5.000E-06	1.800E+00	2.885E-34	4.250E-02	2.100E+00
Standard sensor cover is 0.1481 $barn^{-1}$ enriched (91.67% ^{10}B) B_4C and 4.705×10^{-3} $barn^{-1}$ cadmium.						

Table D-1 (Continued)
Sensor Response Region for SPR-III Central Cavity
(SPR3CAV18 Spectrum)

Reaction	Bare Sensor			B_4C and Cadmium Covered Sensor		
	Calculated Activity (dps/nucleus)	90% Activity Limits		Calculated Activity (dps/nucleus)	90% Activity Limits	
		Lower Energy (MeV)	Upper Energy (MeV)		Lower Energy (MeV)	Upper Energy (MeV)
$^{115}In(n,\gamma)^{116m}In$	5.801E-29	7.600E-08	2.100E+00	3.893E-29	5.750E-02	2.300E+00
$^{115}In(n,n)^{115m}In$	4.416E-30	1.000E+00	5.900E+00	4.228E-30	1.000E+00	5.900E+00
$^{127}I(n,2n)^{126}I$	3.804E-34	9.700E+00	1.480E+01	3.697E-34	9.800E+00	1.480E+01
$^{197}Au(n,p)^{197}Pt$	7.062E-36	6.600E+00	1.600E+01	6.845E-36	6.700E+00	1.600E+01
$^{197}Au(n,\gamma)^{198}Au$	5.216E-31	2.400E-07	1.600E+00	3.517E-31	4.750E-02	1.900E+00
$^{197}Au(n,2n)^{196}Au$	3.120E-25	8.800E+00	1.380E+01	3.026E-25	8.800E+00	1.380E+01
$^{197}Au(n,3n)^{195}Au$	4.013E-28	1.630E+01	1.970E+01	3.934E-28	1.630E+01	1.970E+01
$^{232}Th(n,\gamma)^{233}Th$	7.090E-29	1.600E-02	2.000E+00	6.073E-29	5.750E-02	2.100E+00
$^{232}Th(n,2n)^{231}Th$	1.683E-24	7.000E+00	1.150E+01	1.625E-24	7.000E+00	1.150E+01
$^{232}Th(n,f)fp$	4.009E-26	1.500E+00	7.100E+00	3.833E-26	1.500E+00	7.100E+00
$^{235}U(n,f)fp$	1.319E-24	1.050E-02	4.000E+00	1.145E-24	8.800E-02	4.200E+00
$^{238}U(n,f)fp$	1.641E-25	1.500E+00	6.600E+00	1.568E-25	1.500E+00	6.600E+00
$^{237}Np(n,f)fp$	8.757E-25	5.250E-01	5.300E+00	8.374E-25	5.250E-01	5.400E+00
$^{239}Pu(n,f)fp$	1.809E-24	2.800E-07	4.200E+00	1.556E-24	1.100E-01	4.400E+00
$^{241}Am(n,f)fp$	8.427E-25	7.200E-01	5.600E+00	8.067E-25	7.200E-01	5.600E+00
Standard sensor cover is 0.1481 $barn^{-1}$ enriched (91.67% ^{10}B) B_4C and 4.705×10^{-3} $barn^{-1}$ cadmium.						

Table D-1 (Continued)
Sensor Response Region for SPR-III Central Cavity
(SPR3CAV18 Spectrum)

Reaction	Bare Sensor			B_4C and Cadmium Covered Sensor		
	Calculated Activity (dps/nucleus)	90% Activity Limits		Calculated Activity (dps/nucleus)	90% Activity Limits	
		Lower Energy (MeV)	Upper Energy (MeV)		Lower Energy (MeV)	Upper Energy (MeV)
RML $^{enriched}U$	1.245E-24	1.275E-02	4.100E+00	1.083E-24	8.800E-02	4.300E+00
RML $^{depleted}U$	1.665E-25	1.400E+00	6.600E+00	1.588E-25	1.400E+00	6.600E+00
RML Pu	1.702E-24	3.000E-07	4.300E+00	1.473E-24	1.150E-01	4.500E+00
Standard sensor cover is 0.1481 $barn^{-1}$ enriched (91.67% ^{10}B) B_4C and $4.705x10^{-3}$ $barn^{-1}$ cadmium.						

Table D-2
Sensor Response Region for ACRR Central Cavity
(ACF9 Spectrum)

Reaction	Bare Sensor			B_4C and Cadmium Covered Sensor		
	Calculated Activity (dps/nucleus)	90% Activity Limits		Calculated Activity (dps/nucleus)	90% Activity Limits	
		Lower Energy (MeV)	Upper Energy (MeV)		Lower Energy (MeV)	Upper Energy (MeV)
$^{10}B(n,\alpha)X$	4.603E-22	6.300E-09	5.250E-06	1.471E-24	8.800E-04	2.100E+00
$^{6}Li(n,\alpha)X$	1.132E-22	6.300E-09	6.000E-06	7.114E-25	1.700E-03	3.800E+00
$^{19}F(n,2n)^{18}F$	3.332E-34	1.190E+01	1.730E+01	3.250E-34	1.190E+01	1.730E+01
$^{23}Na(n,\gamma)^{24}Na$	8.649E-31	6.600E-09	2.400E-03	1.874E-32	1.900E-03	8.800E-01
$^{24}Mg(n,p)^{24Na}$	7.069E-33	6.500E+00	1.170E+01	6.824E-33	6.500E+00	1.170E+01
$^{27}Al(n,p)^{27}Mg$	1.741E-30	3.400E+00	9.400E+00	1.670E-30	3.400E+00	9.400E+00
$^{27}Al(n,\alpha)^{24}Na$	3.359E-33	6.500E+00	1.210E+01	3.245E-33	6.600E+00	1.210E+01
$^{28}Si(n,1MeV)X$	6.804E-01	1.900E-01	4.800E+00	6.390E-01	2.000E-01	4.900E+00
$^{31}P(n,p)^{31}Si$	8.736E-31	2.200E+00	7.100E+00	8.355E-31	2.200E+00	7.100E+00
$^{32}S(n,p)^{32}P$	1.512E-32	2.300E+00	7.200E+00	B4CCd	1.446E-32	2.300E+00
$^{45}Sc(n,\gamma)^{46}Sc$	3.124E-31	6.300E-09	5.750E-06	2.351E-33	3.200E-03	8.400E-01
$^{46}Ti(n,p)^{46}Sc$	3.547E-34	3.700E+00	9.600E+00	3.403E-34	3.700E+00	9.600E+00
$^{47}Ti(n,p)^{47}Sc$	1.850E-32	1.600E+00	7.500E+00	1.770E-32	1.600E+00	7.500E+00
$^{47}Ti(n,np)^{46}Sc$	3.966E-37	1.150E+01	1.770E+01	3.871E-37	1.150E+01	1.770E+01
$^{nat}Ti(n,X)^{46}Sc$	3.550E-34	3.700E+00	9.600E+00	3.406E-34	3.700E+00	9.600E+00
Standard sensor cover is 0.1481 $barn^{-1}$ enriched (91.67% ^{10}B) B_4C and 4.705×10^{-3} $barn^{-1}$ cadmium.						

Table D-2 (Continued)
Sensor Response Region for ACRR Central Cavity
(ACF9 Spectrum)

Reaction	Bare Sensor			B_4C and Cadmium Covered Sensor		
	Calculated Activity (dps/nucleus)	90% Activity Limits		Calculated Activity (dps/nucleus)	90% Activity Limits	
		Lower Energy (MeV)	Upper Energy (MeV)		Lower Energy (MeV)	Upper Energy (MeV)
$^{48}Ti(n,p)^{48}Sc$	4.304E-34	6.000E+00	1.250E+01	4.156E-34	6.000E+00	1.250E+01
$^{48}Ti(n,np)^{47}Sc$	1.679E-36	1.230E+01	1.840E+01	1.640E-36	1.230E+01	1.840E+01
$^{nat}Ti(n,X)^{47}Sc$	1.852E-32	1.600E+00	7.500E+00	1.772E-32	1.600E+00	7.500E+00
$^{55}Mn(n,\gamma)^{56}Mn$	1.405E-28	7.200E-09	3.600E-04	1.730E-30	3.200E-04	4.750E-01
$^{55}Mn(n,2n)^{54}Mn$	2.483E-36	1.100E+01	1.600E+01	2.419E-36	1.100E+01	1.600E+01
$^{54}Fe(n,p)^{54}Mn$	8.435E-34	2.200E+00	7.400E+00	8.069E-34	2.200E+00	7.400E+00
$^{56}Fe(n,p)^{56}Mn$	2.659E-32	5.500E+00	1.160E+01	2.564E-32	5.500E+00	1.160E+01
$^{58}Fe(n,\gamma)^{59}Fe$	3.187E-32	7.600E-09	6.900E-03	1.377E-33	3.400E-04	1.600E+00
Fe(n,X)dpa	5.062E-22	1.350E-01	5.500E+00	4.743E-22	1.800E-01	5.600E+00
$^{59}Co(n,p)^{59}Fe$	9.346E-35	3.400E+00	9.800E+00	8.964E-35	3.400E+00	9.800E+00
$^{59}Co(n,\gamma)^{60}Co$	2.662E-32	8.400E-09	1.350E-04	7.784E-35	1.275E-04	1.200E+00
$^{59}Co(n,\alpha)^{56}Mn$	4.103E-33	5.800E+00	1.220E+01	3.961E-33	5.800E+00	1.220E+01
$^{59}Co(n,2n)^{58}Co$	9.451E-36	1.130E+01	1.620E+01	9.208E-36	1.130E+01	1.620E+01
$^{58}Ni(n,p)^{58}Co$	4.990E-33	1.900E+00	7.400E+00	4.773E-33	1.900E+00	7.400E+00
$^{58}Ni(n,2n)^{59}Ni$	8.543E-36	1.310E+01	1.800E+01	8.344E-36	1.310E+01	1.800E+01
$^{60}Ni(n,p)^{60}Co$	2.806E-36	4.700E+00	1.100E+01	2.702E-36	4.700E+00	1.100E+01
Standard sensor cover is 0.1481 $barn^{-1}$ enriched (91.67% ^{10}B) B_4C and 4.705×10^{-3} $barn^{-1}$ cadmium.						

Table D-2 (Continued)
Sensor Response Region for ACRR Central Cavity
(ACF9 Spectrum)

Reaction	Bare Sensor			B_4C and Cadmium Covered Sensor		
	Calculated Activity (dps/nucleus)	90% Activity Limits		Calculated Activity (dps/nucleus)	90% Activity Limits	
		Lower Energy (MeV)	Upper Energy (MeV)		Lower Energy (MeV)	Upper Energy (MeV)
$^{63}Cu(n,\gamma)^{64}Cu$	1.038E-29	7.600E-09	5.750E-03	5.870E-31	5.750E-04	1.300E+00
$^{63}Cu(n,2n)^{64}Cu$	4.621E-32	1.190E+01	1.700E+01	4.506E-32	1.190E+01	1.700E+01
$^{63}Cu(n,\alpha)^{60}Co$	7.620E-37	4.500E+00	1.120E+01	7.337E-37	4.500E+00	1.120E+01
$^{65}Cu(n,2n)^{64}Cu$	2.094E-33	1.080E+01	1.580E+01	2.039E-33	1.080E+01	1.580E+01
$^{64}Zn(n,p)^{64}Cu$	2.401E-31	2.400E+00	7.400E+00	2.296E-31	2.400E+00	7.400E+00
$^{90}Zr(n,2n)^{89}Zr$	9.601E-35	1.270E+01	1.750E+01	9.371E-35	1.270E+01	1.750E+01
GaAs(n,1MeV)X	3.679E-21	6.300E-02	4.700E+00	3.357E-21	1.100E-01	4.800E+00
$^{93}Nb(n,\gamma)^{94}Nb$	1.054E-27	2.000E-08	1.275E-01	2.131E-28	1.000E-03	8.800E-01
$^{93}Nb(n,2n)^{92m}Nb$	1.275E-34	9.900E+00	1.450E+01	1.239E-34	9.900E+00	1.450E+01
$^{93}Nb(n,n)^{93m}Nb$	9.503E-35	7.600E-01	5.300E+00	9.089E-35	8.000E-01	5.300E+00
$^{98}Mo(n,\gamma)^{99}Mo$	9.239E-31	1.000E-05	4.000E-01	1.678E-31	4.500E-04	1.700E+00
$^{103}Rh(n,n)^{103m}Rh$	7.911E-29	4.750E-01	5.100E+00	7.555E-29	5.000E-01	5.100E+00
$^{109}Ag(n,\gamma)^{110m}Ag$	1.416E-31	3.800E-08	6.600E-06	6.522E-34	8.000E-04	1.200E+00
$^{115}In(n,\gamma)^{116m}In$	3.822E-26	3.600E-08	1.800E-06	6.563E-29	1.275E-03	1.900E+00
$^{115}In(n,n)^{115m}In$	3.866E-30	1.000E+00	5.400E+00	3.701E-30	1.000E+00	5.400E+00
$^{127}I(n,2n)^{126}I$	3.202E-34	9.700E+00	1.470E+01	3.112E-34	9.700E+00	1.470E+01
Standard sensor cover is 0.1481 $barn^{-1}$ enriched (91.67% ^{10}B) B_4C and 4.705×10^{-3} $barn^{-1}$ cadmium.						

Table D-2 (Continued)
Sensor Response Region for ACRR Central Cavity
(ACF9 Spectrum)

Reaction	Bare Sensor			B_4C and Cadmium Covered Sensor		
	Calculated Activity (dps/nucleus)	90% Activity Limits		Calculated Activity (dps/nucleus)	90% Activity Limits	
		Lower Energy (MeV)	Upper Energy (MeV)		Lower Energy (MeV)	Upper Energy (MeV)
$^{197}Au(n,p)^{197}Pt$	5.523E-36	6.800E+00	1.600E+01	5.355E-36	6.800E+00	1.610E+01
$^{197}Au(n,\gamma)^{198}Au$	2.657E-28	3.800E-08	5.500E-06	9.181E-31	5.500E-04	1.000E+00
$^{197}Au(n,2n)^{196}Au$	2.635E-25	8.800E+00	1.370E+01	2.556E-25	8.800E+00	1.370E+01
$^{197}Au(n,3n)^{195}Au$	3.188E-28	1.630E+01	1.970E+01	3.125E-28	1.630E+01	1.970E+01
$^{232}Th(n,\gamma)^{233}Th$	2.159E-27	2.200E-08	6.900E-03	1.108E-28	6.900E-04	1.500E+00
$^{232}Th(n,2n)^{231}Th$	1.313E-24	7.100E+00	1.160E+01	1.268E-24	7.100E+00	1.160E+01
$^{232}Th(n,f)fp$	3.456E-26	1.500E+00	6.900E+00	3.303E-26	1.500E+00	6.900E+00
$^{235}U(n,f)fp$	6.833E-23	6.000E-09	8.800E-05	1.417E-24	1.800E-03	3.400E+00
$^{238}U(n,f)fp$	1.430E-25	1.400E+00	6.200E+00	1.365E-25	1.400E+00	6.200E+00
$^{237}Np(n,f)fp$	7.576E-25	5.000E-01	4.800E+00	7.161E-25	5.500E-01	4.800E+00
$^{239}Pu(n,f)fp$	1.502E-22	9.600E-09	1.100E-05	1.618E-24	3.800E-03	3.800E+00
$^{241}Am(n,f)fp$	1.767E-24	2.100E-08	3.900E+00	7.135E-25	7.600E-01	5.100E+00
RML $^{enriched}U$	6.356E-23	6.000E-09	8.800E-05	1.334E-24	1.800E-03	3.500E+00
RML $^{depleted}U$	2.828E-25	1.000E-08	4.900E+00	1.392E-25	1.400E+00	6.200E+00
RML Pu	1.326E-22	9.600E-09	1.150E-05	1.519E-24	4.250E-03	3.900E+00

Standard sensor cover is 0.1481 $barn^{-1}$ enriched (91.67% ^{10}B) B_4C and 4.705×10^{-3} $barn^{-1}$ cadmium.

APPENDIX E

Uncertainty in Dosimetry Sensor Cross Sections

Table E-1
Uncertainty for SNLRML Spectrum-Averaged Dosimetry Sensor Cross Sections

Reaction	Fission Spectrum-Averaged Uncertainty					
	SPR3CAV28			ACF9		
	Bare	Cd	B4C-Cd	Bare	Cd	B4C-Cd
$^{10}B(n,\alpha)X$	2.30 %	3.43 %	3.91 %	0.16 %	0.19 %	1.79 %
$^{6}Li(n,\alpha)X$	1.19 %	1.35 %	1.46 %	0.15 %	0.18 %	1.04 %
$^{19}F(n,2n)^{18}F$	5.78 %	5.78 %	5.77 %	5.84 %	5.84 %	5.83 %
$^{23}Na(n,\gamma)^{24}Na$	15.55 %	17.40 %	17.70 %	2.94 %	6.05 %	16.64 %
$^{24}Mg(n,p)^{24Na}$	3.72 %	3.72 %	3.71 %	3.54 %	3.54 %	3.54 %
$^{27}Al(n,p)^{27}Mg$	10.83 %	10.83 %	10.81 %	12.10 %	12.10 %	12.07 %
$^{27}Al(n,\alpha)^{24}Na$	2.61 %	2.61 %	2.61 %	2.50 %	2.50 %	2.49 %
$^{28}Si(n,X)1MeV$	----	----	----	----	----	----
$^{31}P(n,p)^{31}Si$	7.03 %	7.03 %	7.03 %	7.10 %	7.10 %	7.10 %
$^{32}S(n,p)^{32}P$	19.41 %	19.41 %	19.38 %	19.61 %	19.61 %	19.59 %
$^{45}Sc(n,\gamma)^{46}Sc$	4.20 %	5.31 %	5.29 %	1.05 %	1.31 %	4.12 %
$^{46}Ti(n,p)^{46}Sc$	4.51 %	4.51 %	4.50 %	4.87 %	4.87 %	4.86 %
$^{47}Ti(n,p)^{47}Sc$	6.19 %	6.19 %	6.20 %	5.94 %	5.94 %	5.94 %
$^{47}Ti(n,np)^{46}Sc$	30.00 %	30.00 %	30.00 %	30.00 %	30.00 %	30.00 %
$^{Nat}Ti(n,X)^{46}Sc$	4.51 %	4.51 %	4.51 %	4.87 %	4.87 %	4.87 %

Standard B_4C sensor cover is 0.1481 $barn^{-1}$ enriched (91.67% ^{10}B) B_4C and 4.705×10^{-3} $barn^{-1}$ cadmium.
Standard Cd cover is 2.587×10^{-3} $barn^{-1}$ cadmium

Table E-1 (Continued)
Uncertainty for SNLRML Spectrum-Averaged Dosimetry Sensor Cross Sections

Reaction	Fission Spectrum-Averaged Uncertainty					
	SPR3CAV28			ACF9		
	Bare	Cd	B4C-Cd	Bare	Cd	B4C-Cd
$^{48}Ti(n,p)^{48}Sc$	4.04 %	4.04 %	4.05 %	4.12 %	4.12 %	4.12 %
$^{48}Ti(n,np)^{47}Sc$	30.00 %	30.00 %	30.00 %	30.00 %	30.00 %	30.00 %
$^{Nat}Ti(n,X)^{47}Sc$	6.20 %	6.20 %	6.21 %	5.94 %	5.94 %	5.95 %
$^{55}Mn(n,\gamma)^{56}Mn$	14.75 %	17.48 %	17.65 %	5.51 %	6.83 %	26.59 %
$^{55}Mn(n,2n)^{54}Mn$	20.98 %	20.98 %	20.97 %	21.21 %	21.21 %	21.19 %
$^{54}Fe(n,p)^{54}Mn$	3.05 %	3.05 %	3.05 %	3.11 %	3.11 %	3.11 %
$^{56}Fe(n,p)^{56}Mn$	4.29 %	4.29 %	4.29 %	4.08 %	4.08 %	4.08 %
$^{58}Fe(n,\gamma)^{59}Fe$	29.21 %	29.92 %	30.89 %	9.44 %	10.56 %	23.64 %
$^{Nat}Fe(n,X)dpa$	----	----	----	----	----	----
$^{59}Co(n,p)^{59}Fe$	4.96 %	4.96 %	4.96 %	5.02 %	5.02 %	5.03 %
$^{59}Co(n,\gamma)^{60}Co$	2.80 %	3.59 %	5.34 %	0.76 %	0.79 %	2.97 %
$^{59}Co(n,\alpha)^{56}Mn$	4.46 %	4.46 %	4.46 %	4.44 %	4.44 %	4.45 %
$^{59}Co(n,2n)^{58}Co$	4.60 %	4.60 %	4.60 %	4.67 %	4.68 %	4.67 %
$^{58}Ni(n,p)^{58}Co$	4.49 %	4.49 %	4.49 %	4.56 %	4.56 %	4.56 %
$^{58}Ni(n,2n)^{59}Ni$	4.18 %	4.18 %	4.18 %	4.18 %	4.18 %	4.18 %
$^{60}Ni(n,p)^{60}Co$	15.02 %	15.02 %	15.01 %	15.03 %	15.03 %	15.01 %

Standard B_4C sensor cover is 0.1481 $barn^{-1}$ enriched (91.67% ^{10}B) B_4C and 4.705×10^{-3} $barn^{-1}$ cadmium.
Standard Cd cover is 2.587×10^{-3} $barn^{-1}$ cadmium

Table E-1 (Continued)
Uncertainty for SNLRML Spectrum-Averaged Dosimetry Sensor Cross Sections

Reaction	Fission Spectrum-Averaged Uncertainty					
	SPR3CAV28			ACF9		
	Bare	Cd	B4C-Cd	Bare	Cd	B4C-Cd
$^{63}Cu(n,\gamma)^{64}Cu$	15.06 %	15.41 %	15.51 %	5.34 %	6.75 %	12.57 %
$^{63}Cu(n,2n)^{64}Cu$	3.63 %	3.63 %	3.63 %	3.67 %	3.67 %	3.67 %
$^{63}Cu(n,\alpha)^{60}Co$	4.08 %	4.08 %	4.08 %	4.16 %	4.16 %	4.16 %
$^{65}Cu(n,2n)^{64}Cu$	3.97 %	3.97 %	3.96 %	3.99 %	3.98 %	3.98 %
$^{64}Zn(n,p)^{64}Cu$	7.41 %	7.41 %	7.41 %	7.07 %	7.07 %	7.07 %
$^{90}Zr(n,2n)^{89}Zr$	2.72 %	2.72 %	2.72 %	2.74 %	2.74 %	2.74 %
GaAs(n,X)1MeV	----	----	----	----	----	----
$^{93}Nb(n,\gamma)^{94}Nb$	12.59 %	12.60 %	12.83 %	10.20 %	10.25 %	10.91 %
$^{93}Nb(n,2n)^{92m}Nb$	10.00 %	10.00 %	9.98 %	10.07 %	10.07 %	10.05 %
$^{93}Nb(n,n')^{93m}Nb$	7.22 %	7.23 %	7.23 %	6.96 %	6.96 %	6.97 %
$^{98}Mo(n,\gamma)^{99}Mo$	----	----	----	----	----	----
$^{103}Rh(n,n')^{103m}Rh$	4.99 %	4.99 %	4.93 %	4.85 %	4.85 %	4.80 %
$^{109}Ag(n,\gamma)^{110m}Ag$	----	----	----	----	----	----
$^{115}In(n,\gamma)^{116m}In$	6.15 %	6.17 %	6.11 %	6.01 %	6.01 %	8.55 %
$^{115}In(n,n')^{115m}In$	2.60 %	2.60 %	2.60 %	2.57 %	2.57 %	2.57 %
$^{127}I(n,2n)^{126}I$	20.45 %	20.44 %	20.45 %	20.38 %	20.38 %	20.39 %
Standard B_4C sensor cover is 0.1481 $barn^{-1}$ enriched (91.67% ^{10}B) B_4C and 4.705×10^{-3} $barn^{-1}$ cadmium. Standard Cd cover is 2.587×10^{-3} $barn^{-1}$ cadmium						

Table E-1 (Continued)
Uncertainty for SNLRML Spectrum-Averaged Dosimetry Sensor Cross Sections

Reaction	Fission Spectrum-Averaged Uncertainty					
	SPR3CAV28			ACF9		
	Bare	Cd	B4C-Cd	Bare	Cd	B4C-Cd
$^{197}Au(n,p)^{197}Pt$	----	----	----	----	----	----
$^{197}Au(n,\gamma)^{198}Au$	0.84 %	0.89 %	1.05 %	0.17 %	0.18 %	0.78 %
$^{197}Au(n,2n)^{196}Au$	6.65 %	6.65 %	6.65 %	6.68 %	6.68 %	6.67 %
$^{197}Au(n,3n)^{195}Au$	----	----	----	----	----	----
$^{232}Th(n,\gamma)^{233}Th$	12.90 %	12.95 %	13.16 %	10.21 %	11.15 %	12.19 %
$^{232}Th(n,2n)^{231}Th$	----	----	----	----	----	----
$^{232}Th(n,f)F.P.$	7.21 %	7.21 %	7.22 %	7.08 %	7.08 %	7.08 %
$^{235}U(n,f)F.P.$	0.44 %	0.46 %	0.46 %	0.22 %	0.34 %	0.44 %
$^{238}U(n,f)F.P.$	0.64 %	0.64 %	0.64 %	0.33 %	0.54 %	0.63 %
$^{237}Np(n,f)F.P.$	10.31 %	10.32 %	10.31 %	11.79 %	10.97 %	10.28 %
$^{239}Pu(n,f)F.P.$	2.82 %	2.97 %	2.96 %	1.39 %	3.61 %	3.72 %
$^{241}Am(n,f)F.P.$	2.81 %	2.81 %	2.81 %	2.42 %	2.65 %	2.84 %
RML $^{Enriched}U$	0.44 %	0.46 %	0.46 %	0.22 %	0.34 %	0.44 %
RML $^{Depleted}U$	0.64 %	0.64 %	0.64 %	0.33 %	0.54 %	0.63 %
RML Pu	2.79 %	2.93 %	2.82 %	1.40 %	3.63 %	3.64 %

Standard B_4C sensor cover is 0.1481 $barn^{-1}$ enriched (91.67% ^{10}B) B_4C and 4.705×10^{-3} $barn^{-1}$ cadmium.
Standard Cd cover is 2.587×10^{-3} $barn^{-1}$ cadmium

Intentionally Left Blank

DISTRIBUTION:

1 Air Force Space Technology Center
Attn.: J. F. Janni
Kirtland Air Force Base
Albuquerque, NM 87117-6008

2 Aberdeen Proving Grounds
Attn.: C. Heimbach
M. Oliver
Bldg. 960 STECS-NE
Aberdeen Proving Ground, MD
21005-5059

1 AFRRI
Attn.: H. Gerstenberg
Bethesda, MD 20889

1 Arkansas Tech. University
Attn.: S. C. Apple
#2 Black Oak Court
Russellville, AR 72801

2 Army Pulsed Radiation Facility
Attn.: A. H. Kazi
STECS-NE
Aberdeen, MD 21005-5059

1 Babcock and Wilcox Nuclear Service Company
Attn.: A. L. Lowe, Jr.
3315 Old Forest Road
P. O. Box 10935
Lynchburg, VA 24506-0935

2 Battelle Pacific Northwest Laboratories
Attn.: L. R. Greenwood
J. H. Reeves
Mail Stop P7-22
P. O. Box 999
Richland, WA 99352

1 C.E.A.
Attn.: J. Chevallier
Is Sur Tille
21120
FRANCE

1 Columbia University
Attn.: J. Helm
202 Mudd Bldg.
New York, NY 10027

1 Defense Electronics Supply Ctr.
Attn.: J. E. Nicklaus
1507 Wilmington Pike, ECC
Dayton, OH 45444-5279

1 Dr. H. Farrar IV
18 Flintlock Lane
Bell Canyon, CA 91307

1 EFC/JRC ISPRA
Attn.: R. Dierckx
I-21020 Ispra
ITALY

1 Energy Science and Technology Software Center
P. O. Box 1020
Oak Ridge, TN 37831

1 General Electric Co.
Attn.: G. Martin
Vallecitos Nuclear Center
M/C Vo4
Pleasanton, CA 94566

1 Harry Diamond Laboratories
Attn.: H. A. Eisen
SLCHD-NW-TS
2800 Powder Mill Rd.
Aldelphi, MD 20783-1197

2 International Atomic Energy Agency
Nuclear Data Section
Attn.: N. P. Kocherov
A. Pashchenko
Wagramerstrasse 5
P. O. Box 100
A-1400, Vienna
AUSTRIA

2 Kaman Sciences Corp.
Attn.: R. Ponzini
R. Zombola
P. O. Box 7463
Colorado Springs, CO 80933

1 Kaman Sciences Corp.
Attn.: W. A. Alfonte, Jr.
2550 Huntington Ave., Suite 500
Alexandria, VA 22503

1 Kyoto University
Attn.: I. Kimura
Kyota
606-01
JAPAN

1 Kyoto University
Research Reactor Institute
Attn.: K. Kobayshi
Kumatori-cho, Sennan-gun, Osaka
590-04
JAPAN

1 Los Alamos National Laboratory
Attn.: P. G. Young, T-2
P. O. Box 1663
Los Alamos, NM 87545

1 W. N. McElroy
113 Thayer Drive
Richland, WA 99352

1 Messenger & Assoc.
Attn.: G. C. Messenger
3111 Bel Air, 7F
Las Vegas, NV 89109

1 Naval Research Laboratory
Attn: A. I. Namenson
Code 4653
Washington, DC 20375

1 Nagoya University
Attn.: H. Toyokawa
Dept. of Nuclear Engineering
Nagoya 964-01
Nagoya
464-01
JAPAN

3 National Institute of Standards and Technology
Attn.: A. Carlson
C. Eisenhauer
J. Grundl
RADP C311
Gaitherburg, MD 20899

1 Northrop Corp.
Attn.: B. Ahlport
Org. 3020/N3
2301 West 20th Street
Hawthorne, CA 90250

3 Nuclear Effects Laboratory
Attn.: M. T. Flanders
M. H. Sparks
W. Sallee
STEWS-NE-T
White Sands Missile Range, NM
88002

4 Oak Ridge National Laboratory
Attn.: C. Y. Fu
D. M. Hetrick
F. B. K. Kam
D. Larson
Building 3001 MS-028
P. O. Box X
Oak Ridge, TN 37831-6028

1 Paul Scherrer Institute
Attn.: F. Hegedus
Villigen PSI
5332
SWITZERLAND

1 Physikalish Technische
Bundesanstalt
Attn.: A. V. Alevra
Bundesalle 100
D-38116 Braunschweig
GERMANY

1 Radiation Experiments & Monitors
Attn.: A. Holmes-Siedle
64A Acre End Street
Eynsham
Oxford OX8 1PD
ENGLAND

1 Radiation Shielding Information
Center
Attn.: R. W. Roussin
Oak Ridge National Laboratory
Oak Ridge, TN 37831-6362

1 Rome Laboratory
Attn.: J. C. Garth
RI/ESR
Hanscom A.F.B., MA 01731

1 Russian Nuclear Data Center
Attn.: K. Zolotarev
Institute of Physics and Power
Engineering
Ploschad Bondarenko
209020 Obinsk
THE RUSSIAN FEDERATION

1 S-Cubed Division of Maxwell
Laboratory
Attn.: R. Braasch
3020 Callan Rd.
San Diego, CA 92121-1095

2 Science Applications Int'l Corp.
Attn.: R. Weitz
M. S. Lazo
2109 Air Park Rd. SE
Albuquerque, NM 87111

1 Spire Corp.
Attn.: E. Burke
One Patriots Park
Bedford, MA 01730

2 The Netherlands Energy Research
Foundation, ECN
Attn.: H. J. Nolthenius
W. P. Voorbraak
B. U. Nuclear Energy
Westerduinweg 3
Postbus 1
1755 ZG Petten
THE NETHERLANDS

1 Tohoku University
Attn.: S. Iwasaki
Aobaku-aza-aoba
Sendai
980
JAPAN

1 Pennsylvania State University
Attn.: M. P. Manahan Sr.
Dept. of Nuclear Engineering
231 Sackett Building
University Park, PA 16802

1 University of Birmingham
Attn.: D. R. Weaver
Edgbaston Birmingham B15 2TT
UNITED KINGDOM

1 University of Arizona
Attn.: J. G. Williams
Nuclear Reactor Laboratory
Dept. of Nuclear & Energy
Engineering
Tucson, AZ 85721

2 University of New Mexico
Dept. of Nuclear Engineering
Attn.: A. Prinja
J. VanDenburg
Albuquerque, NM 87131

1 United Kingdom Atomic Energy
Authority
Atomic Energy Research
Establishment
Attn.: A. J. Fudge
Harwell, Didcot
Oxfordshire OX11 ORA
UNITED KINGDOM

1 U. S. Army Combat Sys. Test Act.
Attn.: J. W. Gerdes
Bldg. 860 STE CS-NE
Aberdeen, MD 21005-5059

1 Westinghouse Electric Corporation
Attn.: E. P. Lippincott
Mail Stop E4-33
Westinghouse Energy Center
P. O. Box 355
Pittsburgh, PA 15230-0355

1 Westinghouse - Bettis
Attn.: R. Amato
P.O. Box 79
Pittsburgh, PA 15122

1 Wolicki Associates, Inc.
Attn.: E. A. Wolicki
1310 Gatewood Drive
Alexandria, VA 22307

1	1277	R. J. Leeper
1	4341	Neutron Lab
1	6400	N. R. Ortiz
1	6500	J. K. Rice
1	6501	J. V. Walker
1	6501	T. F. Luera
1	6502	T. R. Schmidt
1	6514	P. S. Pickard
1	6514	R. L. Coats
15	6514	P. J. Griffin
1	6514	G. A. Harms
10	6514	J. G. Kelly
1	6514	M. S. Lazo
1	6514	J. VanDenburg
1	6521	J. W. Bryson
1	6521	D. T. Berry
1	6521	C. V. Holm
1	6521	F. M. McCrory
	6521	M. F. Morris
1	6521	D. W. Vehar
1	7715	D. J. Thompson
1	9301	J. D. Plimpton
1	9303	W. Beezhold
1	9312	F. Biggs
1	9352	C. R. Drumm
1	9352	W. C. Fan
5	7141	Technical Library
1	7151	Technical Publications
10	7613	Document Processing for DOE/OSTI
1	8523-2	Technical Library

Dist. 4

• U.S. GOVERNMENT PRINTING OFFICE 1993-0-573-026/80012

END

DATE
FILMED
2/23/94